SCAPHITID AMMONITES OF THE UPPER CRETACEOUS (MAASTRICHTIAN) FOX HILLS FORMATION IN SOUTH DAKOTA AND WYOMING

NEIL H. LANDMAN AND KARL M. WAAGE

BULLETIN
OF THE
AMERICAN MUSEUM OF NATURAL HISTORY
NUMBER 215 NEW YORK : 1993

SCAPHITID AMMONITES OF THE UPPER CRETACEOUS (MAASTRICHTIAN) FOX HILLS FORMATION IN SOUTH DAKOTA AND WYOMING

NEIL H. LANDMAN
Associate Curator and Chairman
Department of Invertebrates
American Museum of Natural History

KARL M. WAAGE
Professor Emeritus
Department of Geology and Geophysics
Curator Emeritus
Peabody Museum of Natural History
Yale University
New Haven, CT 06511

BULLETIN OF THE AMERICAN MUSEUM OF NATURAL HISTORY
Number 215, 257 pages, 189 figures, 21 tables, 3 appendices
Issued April 5, 1993
Price: $29.00 a copy

ISSN 0003-0090

Sample of scaphite species from the Fox Hills Formation in its type area showing the excellent preservation with many specimens retaining original shell. These species are arranged in a clockwise spiral starting from the upper right, as follows: *Jeletzkytes nebrascensis* microconch, *Discoscaphites conradi* macroconch, *D. gulosus* macroconch, *J. spedeni,* n.sp. microconch, *D. conradi* macroconch, *D. gulosus* macroconch, *J. nebrascensis* macroconch, *Hoploscaphites nicolletii* macroconch, *J. spedeni,* n.sp. macroconch, *D. gulosus* microconch, *D. gulosus* microconch, *D. conradi* microconch, *J. spedeni,* n.sp. microconch, and *H. nicolletii* microconch. Note the consistent difference in form between macroconchs and microconchs.

CONTENTS

ABSTRACT

Well-preserved scaphitid ammonites from the type area of the Upper Cretaceous Fox Hills Formation in north-central South Dakota are the primary focus of this study; also included are scaphites from the uppermost Pierre Shale in this area and from the Fox Hills Formation in the Lance Creek–Red Bird area of eastern Wyoming. The Fox Hills beds represent the marginal marine phase of the progradational sequence marking the final withdrawal of the Cretaceous sea from the Western Interior. Within this marine sequence, which lies above the *Baculites clinolobatus* Range Zone, the following three range zones based on scaphites are recognized:

Jeletzkytes nebrascensis Range Zone
Hoploscaphites nicolletii Range Zone
Hoploscaphites birkelundi Range Zone

Based on recent correlation studies using macro- and microfossils, the *H. nicolletii* and *J. nebrascensis* zones equate with the lower Upper Maastrichtian of the European boreal province; the *H. birkelundi* Zone is either uppermost Lower Maastrichtian or possibly lowermost Upper Maastrichtian.

More than 2500 adults and several hundred juveniles were examined in this study. These specimens fall into three genera: *Hoploscaphites* Nowak, 1911, *Jeletzkytes* Riccardi, 1983, and *Discoscaphites* Meek, 1876. *Hoploscaphites* includes *H. nicolletii* (Morton, 1842), *H. comprimus* (Owen, 1852), *H. melloi,* n. sp., and *H. birkelundi,* n. sp. This genus consists of compressed shells with or without ventrolateral tubercles, and less commonly, umbilical tubercles or bullae. *Jeletzkytes* includes *J. spedeni,* n. sp., *J. nebrascensis* (Owen, 1852), and *J. dorfi,* n. sp. and is characterized by medium to large shells with conspicuous ventrolateral and umbilicolateral tubercles. *Discoscaphites* includes *D. conradi* (Morton, 1834), *D. gulosus* (Morton, 1834), and a micromorphic species, *D. rossi,* n. sp. This genus consists of small to medium shells with multiple rows of tubercles. A cladistic analysis using the genus *Scaphites* Parkinson, 1811 as an outgroup indicates that *Hoploscaphites* and *Jeletzkytes* are more closely related to each other than either is to *Discoscaphites.*

The excellent preservation of these scaphites permits study of their ontogeny. The embryonic shell or ammonitella is approximately 700 μm in diameter and exhibits a tuberculate micro-ornamentation. The ammonitella is spheroidal in *Hoploscaphites* and *Jeletzkytes* and ellipsoidal in *Discoscaphites.* The juvenile shell is closely coiled and expands gradually in whorl width and whorl height. There is a slight change at approximately 5 mm shell diameter, coincident with the first appearance of ornament in the form of ribs. Ventrolateral tubercles appear as early as 10–15 mm shell diameter followed by the development of flank tubercles in species of *Discoscaphites* and *Jeletzkytes.* Rows of flank tubercles develop in succession from the ventrolateral margin toward the umbilicus. The angular length of the juvenile body chamber averages approximately 240°.

The mature shell is not as tightly coiled as that of the juvenile. The body chamber consists of an elongate shaft and recurved hook terminating in a constricted aperture. The change in the shape of the body chamber coincides with a change in the pattern of ornamentation. Large ventrolateral tubercles occur on the shaft in species of *Jeletzkytes* and in some species of *Hoploscaphites.* Muscle attachment areas on the body chamber are indicated by thin layers of myostracum preserved on steinkerns.

All species are strongly dimorphic at maturity. The average size of macroconchs is significantly larger than that of microconchs, but dimorphs are primarily distinguished on the basis of shape. The body chamber of macroconchs increases abruptly in height, resulting in a nearly straight umbilical shoulder and a relatively small umbilicus whereas the body chamber of microconchs expands only gradually in size; the umbilical shoulder parallels the curve of the venter and the umbilicus is relatively broad. Macroconchs tend to be more sharply differentiated morphologically between species than are microconchs. In species of *Hoploscaphites* and *Discoscaphites,* septal approximation occurs over more chambers and is more marked in macroconchs than in microconchs. Macroconchs are more abundant than microconchs in most species.

Remains of upper and lower mandibles are associated with all three scaphite genera. The lower mandible is composed of paired, externally convex plates that lie opposite one another, their ventral commissure aligned along the plane of bilateral symmetry. The plates are chitinous with an outer layer of calcite. The upper mandible, which is composed only of chitin, is a single element with two vertical, winglike, lateral parts that converge anteriorly to form a beaklike structure. Like the plates of the lower mandible, wings of the upper mandible are ornamented with concentric ribs that follow finer growth lines. Commonly occurring with mandible remains are hollow chitinous structures consisting of an inverted cup-shaped base 2–5 mm in diameter from which two hornlike projections taper upward to sharp points. Their identification is uncertain but, based on their uniform shape, they may represent hooklike structures rather than radular elements.

INTRODUCTION

The youngest marine Cretaceous strata in the Western Interior of the United States, those lying above the *Baculites clinolobatus* Range Zone, are restricted in area of outcrop to a relatively small part of the northern Great Plains. Here they border major and minor basins and uplifts and consist chiefly of silty clay, silt, and sand in progradational sequences that comprise the uppermost Pierre Shale and overlying Fox Hills Formation. Fossils are only locally common and well-preserved marine faunas of any appreciable diversity are scarce. The richly fossiliferous strata found within the type area of the Fox Hills Formation, lying just west of the Missouri River (Lake Oahe) in north-central South Dakota, represent a remarkable exception. Here an unusually complete fossil record of the marine-continental gradation includes, in its marine part (lower Fox Hills Formation), a dominantly molluscan fauna consisting of about 20 genera of gastropods, 49 genera of bivalves, and 9 genera of cephalopods. Among the latter are an abundance of beautifully preserved scaphites that are the primary basis for this study.

The excellent preservation of the scaphites is due to their mode of occurrence. The scaphites and associated invertebrates occur mostly in concretions of calcite-cemented sediment. Concretion formation took place early in postdepositional history, before compaction of the surrounding sediment could crush the shells; consequently, most shells retain their original form. Scaphites commonly break free of the concretions as entire specimens, many preserving the nacreous layer of the shell with its colorful iridescence; the outer prismatic shell layer usually adheres to the concretion. Internal structures such as the septa, siphuncle, and caecum are commonly preserved, permitting study of these important features.

Most of the fossils on which taxonomic descriptions are based are adults. However, juveniles are also abundant although not always in the same concretions. Juveniles permitted measurements of the angular length of the body chamber during growth. Identification of juveniles was possible by comparing them to ontogenetic suites of specimens prepared from known adults and checking for the presence of complete, or nearly complete, body chambers on their normally coiled shells.

Altogether, we have examined approximately 2700 scaphite specimens from the Fox Hills Formation representing three genera. Most are from the type area of the formation in Corson, Dewey, and Ziebach counties, South Dakota; a few specimens are from the uppermost Pierre Shale. Other specimens are from the Fox Hills Formation of the Lance Creek–Red Bird area in Niobrara County, Wyoming. The specimens were collected by K.M.W. and his students largely in the period from 1957 to 1965 but also intermittently since that period. This is the third monograph resulting from the studies of the type area of the Fox Hills Formation. The first (Waage, 1968) covered stratigraphy and paleoenvironments; the second (Speden, 1970a), systematics of the bivalve fauna. The present study on the scaphitid ammonites is primarily systematic and attempts to take advantage of the abundance and quality of the specimens by expanding the analysis to include intraspecific variation, ontogeny, associated structures, and distributional features. It differs from the first two monographs in the inclusion of material outside the type area in order to present a biostratigraphy of the youngest marine Upper Cretaceous beds in the Western Interior, that is, those lying above the *Baculites clinolobatus* Range Zone.

ACKNOWLEDGMENTS

Support for fieldwork during 1957 to 1965 came from National Science Foundation grants G-5657 and G18674 and the Charles Schuchert Fund, Division of Invertebrate Paleontology, Yale Peabody Museum. Field personnel and other assistants are acknowledged in Waage (1968) and Speden (1970a).

Additions to the collection were made from the Fox Hills Formation in its type area and from the Fox Hills Formation in the Lance Creek–Red Bird area of Wyoming by Waage in 1967 and by Landman and Waage in 1977, 1981, 1983, 1985, and 1988. This work was supported by NSF grant GP-4467 to Yale

University, NSF collaborative grants EAR 8211959 and EAR 8302093 to Yale University and the American Museum of Natural History, respectively, National Geographic Society grant 3851-88 to AMNH, and the Charles Schuchert Fund. During this later collecting, we were ably assisted in the field for part or most of a summer by David Schindel, then a colleague at Yale; Yale graduate students Charles Thayer, Charles Byers, David Jablonski, Susan Kidwell, Danita Brandt, Ellen Wright, and Marcus Key; Collection Manager Russell White (Division I.P., YPM); Yale undergraduate John Kurtz; VPI graduate students Brett Bennington and David Jacobs; and Susan Klofak, Dept. Invertebrates, AMNH. We are indebted also to the landowners in the Lance Creek–Red Bird area for access to their properties, in particular to H. Wasserburger and J. Meng for their interest and help.

Staff members at both of our museums have greatly assisted in curation of the collection and in study of the specimens and preparation of the manuscript. At AMNH, Susan Klofak skillfully prepared the specimens for study and made suture drawings. Andrew Modell did the photography for all specimens except where noted in the figure captions, Peling Fong assisted in scanning electron microscopy, Stephanie Crooms and Barbara Worcester handled the word processing of the manuscript, and Kathy Sarg and the staff of the Department of Exhibition and Graphics prepared the line drawings.

At YPM, Copeland MacClintock and Russell White produced a detailed locality catalog of the collection, integrating geographic, stratigraphic, and biostratigraphic data referenced to original fieldnotes and maps and are presently preparing this catalog for entry into YPM's new Argus computing system for collections. Jean Lawless, Virginia Starquist, and student assistant Lori Osmundson did bibliographic work and traced sutures and Marian Emons performed the clerical work. We are most grateful to all of these people for their assistance and patience.

The scaphite collection was augmented by loans and gifts from other institutions and individuals. We thank the following for loans of scaphites critical to our work: William A. Cobban, U.S. Geological Survey, for Fox Hills material at the Denver Federal Center; Fred Collier, Collection Manager, Dept. Paleontology, USNM, for Meek's and Owen's types; Elana Benamy, Collection Manager, Invertebrate Paleontology, Academy of Natural Sciences, Philadelphia, for Morton's types; Mary Carman, Collection Manager, Dept. Paleontology, Field Museum of Natural History, Chicago, for Owen's types; Ralph Johnson, Monmouth Amateur Paleontologist's Society, for scaphites from the Severn Formation of Maryland in the MAPS collections; Peter and Neal Larson, Black Hills Institute, Hill City, SD, for Fox Hills fossils; Don Parsons, collector, Rapid City, SD for Fox Hills material; and Brad and Helen Ross, collectors, Timber Lake, SD, for Fox Hills fossils. The Larsons, Parsons, and the Ross' have generously donated specimens to us for study. Our particular thanks to Helen Ross for making special collecting trips for us that contributed to our sparse collections of Upper Pierre Shale scaphites, for tracking down and collecting the rare and unusual siderite concretion fauna in the Elk Butte Member of the Pierre Shale, and for much other assistance and kindness to us, in and out of the field.

We have gained much from discussions with and help from colleagues. Ellis Yochelson, USGS, contributed substantially to our study of scaphite mandibles and gave us the photographs of the unique Meek and Hayden specimen. Norman F. Sohl, USGS, kindly gave us the benefit of his knowledge of the Prairie Bluff Formation and its biostratigraphy. The late George (Jurij) Jeletzky, Geol. Survey of Canada, discussed scaphite genera and biogeography with us. Bruce Lieberman and Melanie Stiassny, AMNH, provided help with the cladistic analysis. John Arnold, University of Hawaii, and David Jacobs, AMNH, discussed the nature of the hooklike structures. Kazushige Tanabe, University of Tokyo, reviewed the chapter on mandibles, and Richard Davis, Cincinnati Museum of Natural History, and David Jacobs reviewed the chapter on ontogeny. We are especially grateful to William A. Cobban, USGS, and W. J. Kennedy, Oxford University, for their most helpful reviews of the entire manuscript and for discussions prior to its completion.

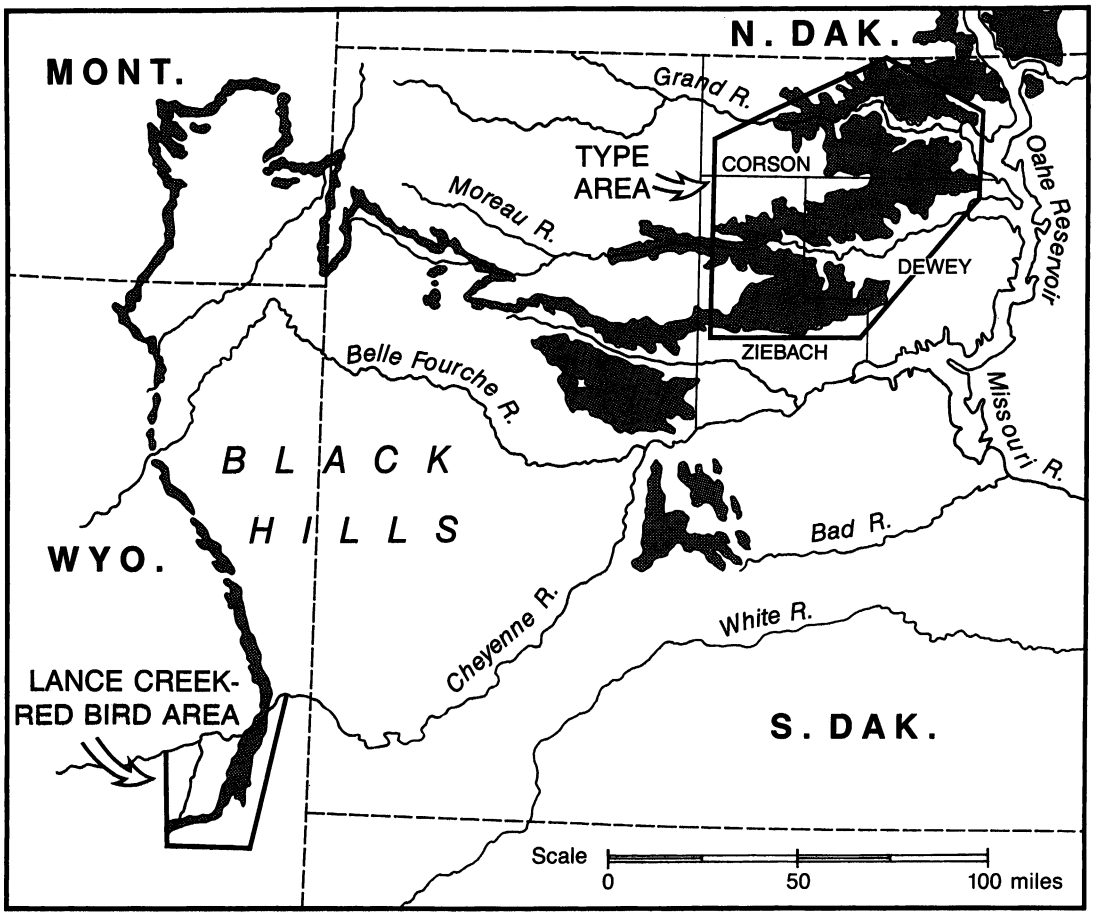

Fig. 1. Outcrop area of the Fox Hills Formation around the Black Hills in the northern Great Plains of the United States.

FOSSIL DISTRIBUTION AND BIOSTRATIGRAPHY

TYPE AREA OF THE FOX HILLS FORMATION

Most of the ammonites described here are from the large outcrop area of the Fox Hills Formation lying west of the Missouri River in parts of Corson, Dewey, and Ziebach counties, north-central South Dakota (fig. 1). It is referred to as the type area of the Fox Hills Formation because it includes the locality cited by Meek and Hayden (1861: 427) in applying the name Fox Hills to what they previously had called "Formation No. 5" in the initial classification (Hall and Meek, 1856: 405; Meek and Hayden, 1856a: 63) of the Western Interior Cretaceous. Here the formation includes 250–350 ft of dominantly silty to sandy strata gradational downward into the Pierre Shale and upward into the nonmarine beds of the Hell Creek Formation (fig. 2). The Fox Hills Formation constitutes the marginal marine phase of a progradational sequence representing the final episode of withdrawal of the Cretaceous seaway from the Western Interior, and contains the youngest Cretaceous marine faunas known from the Interior region.

The internal stratigraphy of the Fox Hills Formation is not the same everywhere within the type area. Detailed stratigraphic study and

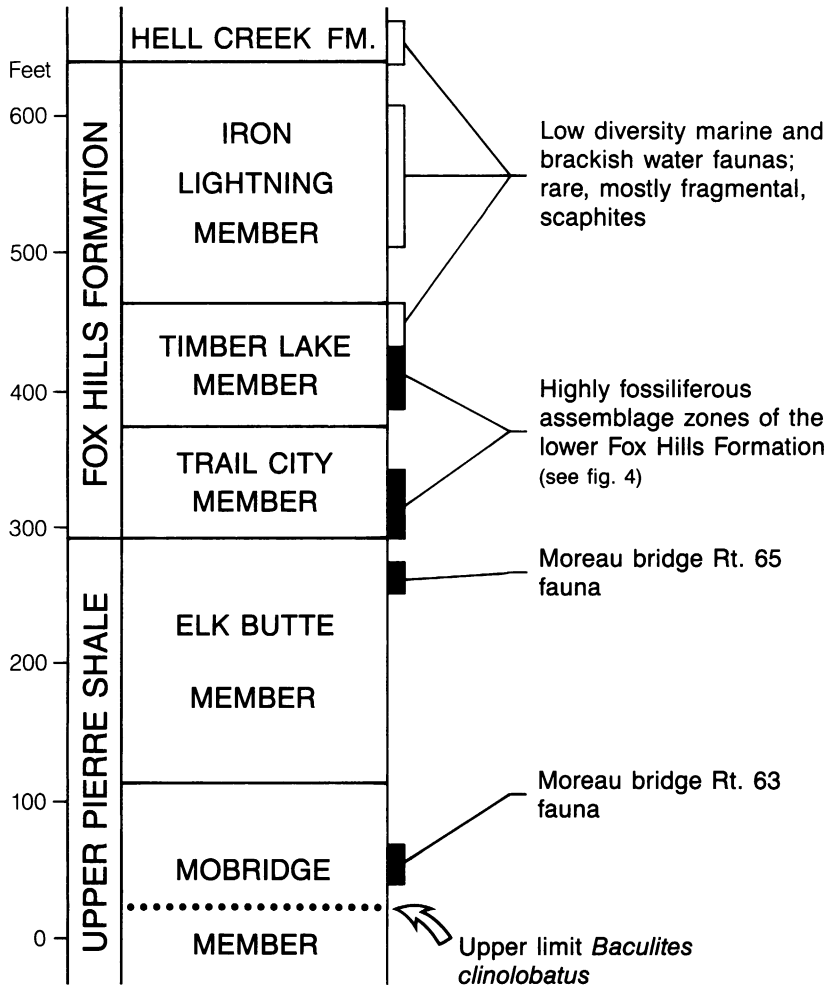

Fig. 2. Stratigraphic units exposed in the type area of the Fox Hills Formation showing positions of the principal scaphite-bearing fossil accumulations (solid bars) and other fossiliferous intervals (open bars).

environmental reconstruction (Waage, 1968) reveal that the formation has distinctive lower and upper parts, products of different depositional regimes. Within each part, there is pronounced lateral change in facies. Sediments of the lower part of the Fox Hills were deposited in dominantly subtidal environments on and around a barrier sand body that grew into the area from the northeast. Clayey silts that preceded the bar complex and eventually flanked it constitute the Trail City Member and the sandy bar complex itself is called the Timber Lake Member. Sediments of the upper part of the formation and immediately succeeding beds of the overlying Hell Creek Formation were part of a deltaic front which moved into the area from the west or northwest, first filling in the area behind the Timber Lake barrier, then overstepping it. The deltaic sediments constitute the Iron Lightning Member. Two distinctive facies are found in this member. A conspicuously layered unit of thin bedded to laminated silt, sand, and clay (Bullhead lithofacies), representing proximal subaqueous delta front deposits, is intercalated with and succeeded by fine to medium-grained, dirty, clayey sands of a distributary system (Colgate lithofacies), which weather to friable, grayish-white on outcrop except where locally in-

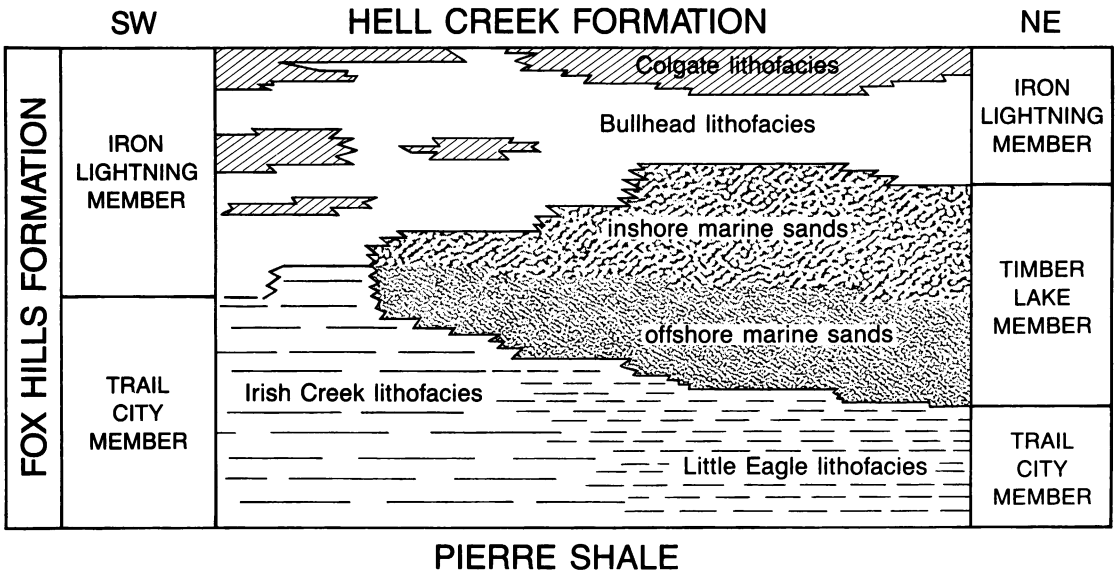

Fig. 3. Relationships of the facies within the Fox Hills Formation in its type area.

durated. Overlying deposits of the subaerial delta constitute the basal Hell Creek Formation, which contains a few local bodies of sand or clay with shell beds of dominantly brackish water bivalves. These probably mark local embayments or estuaries. The Breien Member of the Hell Creek Formation (Laird and Mitchell, 1942) in south-central North Dakota is the only local deposit of this kind bearing a formal name.

The relationships of the facies within the type Fox Hills are shown diagramatically in figure 3. Fossils are at least locally common in all these facies. In the Iron Lightning Member the invertebrate faunas are of low diversity; collectively, they include marine, brackish, and freshwater elements. The latter were transported and are found mostly in the distributary system (Colgate lithofacies) mixed with a distinctive brackish water fauna dominated by *Corbicula* and *Crassostrea.* A sparse, specialized, dominantly infaunal marine assemblage is found locally in the Bullhead lithofacies. Ammonites are rare in the Iron Lightning Member but fragments of scaphites have been found in both of its facies. Some just above the disconformable base of the Iron Lightning are obviously reworked from the lower Fox Hills. But fragments can be found in most of the *Crassostrea* shell beds whether in the Iron Lightning Member or basal Hell Creek; identifiable fragments are mostly *Jeletzkytes nebrascensis* micro- and macroconchs.

The lower part of the Fox Hills Formation contains the source beds of most of the scaphites here described. Within the Trail City Member, the clayey silts present two intergrading lithofacies (fig. 3). In the eastern two-thirds of the type area where the Trail City underlies the sands of the Timber Lake Member, the clayey silts have been mixed by bioturbation and generally lack any trace of bedding. This is the Little Eagle lithofacies. It contains numerous layers of calcitic concretions, those in its lower half abundantly fossiliferous. In the western third of the type area, the Trail City consists of thinly interbedded clay and silt and largely lacks fossiliferous concretion layers. This is the Irish Creek lithofacies and it grades laterally into both the Little Eagle lithofacies and the sands of the Timber Lake Member, occupying the entire lower part of the Fox Hills Formation (fig. 3). Fossils are not common in the Irish Creek except in the uppermost, sandier beds where fossiliferous concretion layers from the Timber Lake Member persist into this lithofacies.

In the eastern two-thirds of the type area,

the Little Eagle lithofacies becomes increasingly sandy upward and grades into the Timber Lake Member. This complex sand body contains in its lower part several layers of concretions with abundant marine fossils in very fine-grained dirty (subgraywacke), bioturbated sand that weathers yellowish-orange on the outcrop. Its upper part is generally current-bedded, cleaner, fine-grained sand containing a much less diverse, shallow marine fauna characterized by the callianasid burrow "*Ophiomorpha*" and the thick-shelled, shallow-infaunal bivalve *Tancredia americana.* Ammonite remains are few and fragmental.

Most of the marine fossils in the lower Fox Hills occur in calcitic concretions. The best preservation of scaphites probably occurs in concretions of calcareous siltstone in the basal Trail City Member of the Fox Hills Formation. The scaphites are undeformed and many specimens retain exquisite ornamental details. The chambers in the phragmocones are usually filled with yellow calcite that reinforces the shell, permitting recovery of entire specimens. Throughout this member numerous specimens show evidence of muscle attachment areas on steinkerns and jaw parts are not uncommon in body chambers and loose in concretions. Scaphites in the dominantly sandy Timber Lake Member, which overlies the Trail City, are generally less well preserved although they commonly retain the original shell structure. The shell typically has a brassy luster and many show postmortem breakage and cracking. Cross sections reveal that the internal whorls may be absent or distorted even in shells that appear whole on the outside. The higher current and wave energy in the shoreface sand environment of the Timber Lake Member may account for shell damage prior to final burial. Not uncommon in the Timber Lake concretions are phragmocones internally free of matrix. Although these provide excellent views of septa and siphuncles they rarely can be freed of the matrix without shattering.

The fossiliferous concretion layers, either individually or in groups of several closely spaced layers, contain distinctive assemblages of fossils; each of these assemblages apparently formed simultaneously throughout its extent (Waage, 1964: 554). One or two species of bivalves commonly dominate a particular assemblage; less commonly an ammonite is a dominant or conspicuous subdominant. A succession of assemblage zones based on these distinctive associations and named for their dominant fossils is recognized within the lower Fox Hills (Waage, 1964, 1968; Speden, 1970a); these are shown in figure 4. The striking faunal difference apparent from one assemblage zone to the next results only from a change in the numerically dominant bivalve species. Most of these bivalves range throughout the marine lower part of the formation (Speden, 1970a: 19). In the two assemblage zones named for *Hoploscaphites nicolletii,* this species is exceptionally abundant and conspicuous because of its size, but the actual dominant species by count is usually a bivalve.

The four assemblage zones of the lower Trail City Member are concentrated within a lobate northeast-southwest trending region of about 2500 square miles within the type area (Waage, 1968: fig. 19). They apparently represent successive, temporary communities that flourished off the down-current end of the advancing Timber Lake sand body, which subsequently overspread the lobate area. The comparable *Cucullaea* Assemblage Zone (CAZ) in the Timber Lake Member represents a younger subtidal community that extended over the basal sands of the barrier complex and also spread south and southwestward during deposition of the upper Irish Creek lithofacies of the Trail City Member. Limits of an assemblage zone may be marked by the termination of individual concretion layers or a gradual to abrupt change to barren concretions.

In addition to the major accumulations of the assemblage zones, fossils also occur in more locally distributed concretions and concretion layers in the type Fox Hills Formation. Two of these occurrences have also furnished scaphites for the present study. Scattered concretions in the uppermost part of the Trail City and lowermost Timber Lake Members locally contain an assemblage dominated by *Phelopteria,* nuculid bivalves, juvenile scaphites, microconchs of *Hoploscaphites comprimus,* and rare specimens of *H. nicoletti.* Previously called *abyssinus* concretions (Waage, 1968: 71), they are now re-

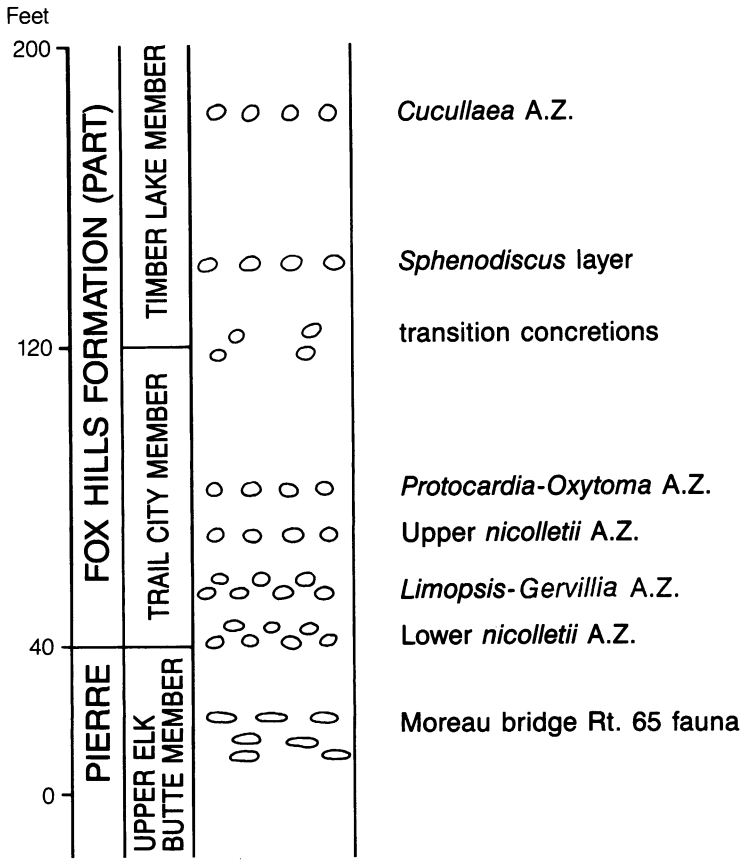

Fig. 4. Assemblage zones (AZ) and associated scaphite-bearing beds in the Fox Hills Formation in its type area.

ferred to as "transition concretions" because of their apparent restriction to the interval of change from Trail City to Timber Lake lithology. The second occurrence of locally fossiliferous concretions is in the *Sphenodiscus* layer, one or two layers of red-brown weathering concretions 15–30 ft above the base of the Timber Lake Member. Locally these carry single large specimens of *Sphenodiscus lenticularis* and frequently *Jeletzkytes nebrascensis* and other scaphites.

The base of the Fox Hills Formation in its type area lies approximately 250 ft above the highest occurrence of *Baculites clinolobatus,* presumably the top of its range zone, in the upper Mobridge Member of the Pierre Shale and is separated from it by mostly unfossiliferous dark gray shale of the uppermost Mobridge and Elk Butte Members of the Pierre (fig. 2). Two intervals with scaphite-bearing concretions occur in this sequence. One of these, near the top of the dominantly calcareous shale of the Mobridge Member, consists of about 25 ft of shale containing two or three layers of hard, flat to ovoid, small but locally ledge-forming calcitic concretions, very few of which bear scaphites distinct from those in the overlying Fox Hills Formation. The scaphites are poorly preserved and although shell is retained in many, specimens are commonly incomplete or have crushed phragmocones. Mello (1969) studied the Upper Pierre Shale in this area and used two thin bentonite beds for correlation of the upper Mobridge Member, recognizing that the lower of these marked the highest local occurrence of *Baculites clinolobatus* (Mello, pp. 15, 38). The concretion layers occur in an interval from about 35 to 60 ft above the lower bentonite, i.e., above the top of the *B. cli-*

nolobatus Range Zone. Our specimens of this fauna are all from Moreau Bridge Rt. 63 loc. 32 (fig. 2; p. 113).

The second locality, brought to our attention by Helen Ross, lies just below the base of the Trail City Member in the uppermost Elk Butte Member of the Pierre Shale. The fossils occur sparingly in small, flat-oval, rusty-weathering sideritic concretions. The plane of symmetry of the shells lies in the plane of the flattened concretions, and the specimens suffered lateral compaction and cracking, but most retain their lateral aspect without distortion. They are preserved with a flaky covering of nacreous shell. The scaphites are those of the Trail City fauna and are remarkable for their relatively large size, which is not simply a matter of their compaction. The only bivalve found to date, *Spyridoceramus tegulatus,* is nearly three times its normal size. The fauna appears restricted to exposures of the uppermost Elk Butte Member on either side of the State Highway Route 65 bridge over the Moreau River in Ziebach and Dewey counties, South Dakota (loc. 307, figs. 2, 4).

LANCE CREEK–RED BIRD AREA

Scaphites from a second area of Fox Hills outcrop, the Lance Creek–Red Bird area in Niobrara County, Wyoming (fig. 1), are included in this study because of their close relationship to the fauna in the type Fox Hills. The Fox Hills Formation in the Lance Creek–Red Bird area (fig. 5) is divided into four lithologically distinctive units and exhibits many similarities with the type Fox Hills sequence. It is twice as thick as the latter, its parts totaling about 600 ft, but it is far less fossiliferous and no detailed stratigraphic study comparable to that on the type Fox Hills has been made.

The Lance Creek–Red Bird Fox Hills marks a somewhat older progradation of the Cretaceous sea than does the type Fox Hills. Its dominantly sandy strata are gradational downward into the Pierre Shale and upward into the Lance Formation, which has its type in the area. The lower, marine part of the Fox Hills consists of offshore silts transitional to the Pierre Shale, overlain by subtidal bioturbated sands of a bar complex—units analogous respectively to the Trail City and Timber Lake Members in the type area, but not formally named here. The lower silt unit is poorly exposed and has yielded very few fossils. In the Red Bird section of the Pierre Shale, Gill and Cobban (1966: A50) have included these siltstones (units 112–115) in their description and noted a distinctive glauconitic sand bed (unit 112) that marks the base of the Fox Hills Formation in this area. Our measurement of the lower silt unit (130 ft) is taken from their section.

The lower silts change either gradually or abruptly upward into the second unit of the Fox Hills, the marine sands. These form a conspicuous bluff in many parts of the Fox Hills outcrop, appearing as yellowish-gray to light tan massive sand studded with reddish-brown calcareous concretions. The massive nature of the sand results from bioturbation, and both the sand and concretions are locally fossiliferous. Fossil distribution is uneven, both vertically within the unit and geographically over the outcrop area. Unlike the fossiliferous concretions in the type area, no patterns of fossil associations mark specific concretion layers and we could discern no persistent faunal subdivisions within the unit. The concretions vary from small, hard, rounded to ovoid, lime-cemented, gray to reddish-gray weathering and 1 ft or less in diameter, to large masses 3 or 4 ft or more in long diameter consisting of hard, red-brown weathering lime-cemented cores with thick, loosely cemented punky gray-weathering jackets. Fossils may or may not occur in the smaller concretions and in both the cores and jackets of the larger concretions. Scaphites are not as well preserved as those of the type area. Even in the hard concretionary material, ammonite shells are mostly broken or partially crushed and the shell material mostly chalky; entire specimens are uncommon. Ammonites in concretion jackets or in the sand invariably are crushed or partly crushed.

The massive sand unit, which is about 100 ft thick, terminates abruptly at a nearly plane surface of disconformity that extends throughout the Lance Creek–Red Bird area. At a number of localities accumulations of phosphatic nodules and phosphatized fossils, reworked from the underlying sand, occur in a red-brown concretionary sand bed lying on

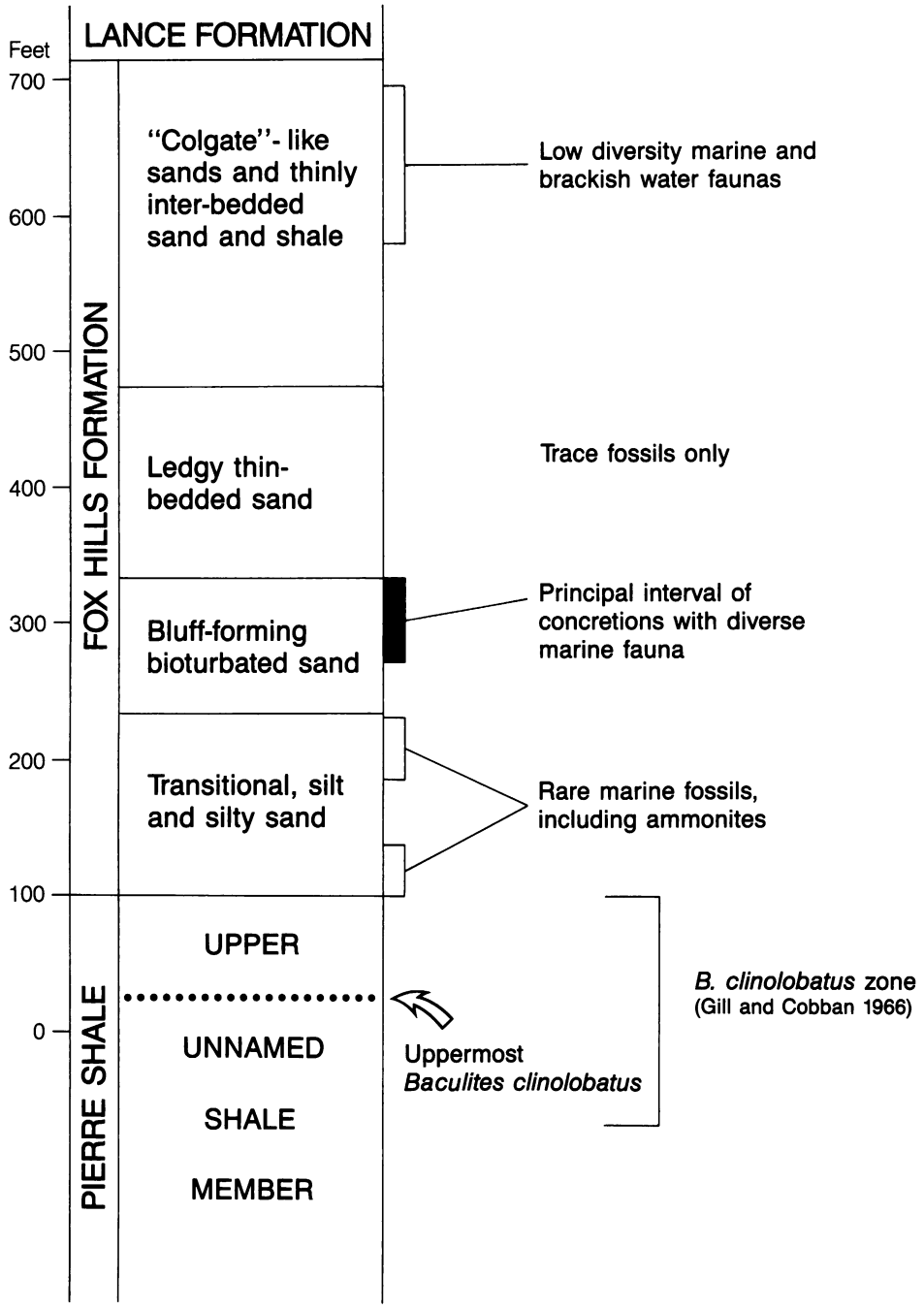

Fig. 5. Stratigraphy of the Fox Hills Formation and underlying Pierre Shale in the Lance Creek–Red Bird area.

the massive sand. Elsewhere the disconformity is evidenced only by the conspicuous change from massive, bluff-forming, yellowish-gray sands below to thin-bedded, ledgy, somewhat darker brown sands above. The latter, which are locally as much as 140 ft thick, are a persistent, if variable, part of the Fox Hills sequence in this area and constitute

its third subdivision. Sands of this well-stratified unit occur in beds from an inch to a foot and a half thick interbedded with partings and very thin beds of sandy bluish-gray shale. This unit is most conspicuous in the southern part of the outcrop area but to the north along the outcrop that parallels U.S. Highway 85 on the west (shown on USGS 7½ minute Redbird quadrangle) the shaley interbeds increase at the expense of the sand beds and the unit disappears as a topographical feature, underlying flat lands west of the bluff on the underlying massive sand. Body fossils have not been found in this unit but it is locally rich in trace fossils.

Above the ledgy sandstone lies the fourth unit of the Fox Hills, a conspicuous sequence of very light gray to white sandstone bodies weathering to billowy outcrop, and interbedded with thin-bedded blue-gray sandy shale and gray sandstone. In the one complete section measured of the upper Fox Hills, this unit was 240 ft thick to the base of the first lignite in the sequence which, as in the type area, is used to mark the base of the Lance Formation (Hell Creek lithogenetic equivalent). This top unit resembles the Iron Lightning Member of the type area. As in that area, the white-weathering sandstones have long been called the "Colgate" (Calvert, 1912). The shaley interbeds of the "Colgate" locally contain a *Crassostrea, Anomia, Corbicula* association in the Lance Creek–Red Bird area and like their Iron Lightning equivalent in the Dakotas are a part of the marginal marine sequence and an integral part of the Fox Hills Formation. The "Colgate" sands dominate this upper unit in outcrops north and east of Lance Creek but where the outcrop line turns northward along U.S. Highway 85 the shale interbeds thicken and at least the lower part of the unit changes to a lithofacies identical to that of the Bullhead lithofacies of the type area. It is likely that most of the third unit, the thin-bedded sands, also become part of this Bullhead-like lithofacies, which is partially well exposed west and north of Red Bird.

No ammonite fossils have yet been recovered from the upper two units of the Fox Hills. Except for one specimen, the scaphites described herein all come from the upper 60 ft of the massive sandstone unit and as far as we can judge constitute a single fauna. This interval lies about 160 ft above the beds included in the *Baculites clinolobatus* Range Zone of the Red Bird section of the Pierre Shale by Gill and Cobban (1966: A34).

ZONATION

The scaphites treated in this study all come from marine latest Cretaceous strata lying above the *Baculites clinolobatus* Range Zone. They fall within the range zone of *Sphenodiscus,* which, in the northern part of the Western Interior, only slightly overlaps the upper part of the range of *B. clinolobatus* (Scott and Cobban, 1965: 3). Older reports of the association of *Sphenodiscus* with *Baculites grandis* (Dane et al., 1937: 229; Cobban and Reeside, 1952: 1020, among others) precede the zonal separation of *B. clinolobatus* from *B. grandis* by Cobban (1958a: 114).

Subdivision of the post-*B. clinolobatus* beds, or *Sphenodiscus* Zone, was effectively done by Cobban and Reeside (1952: 1020–1021), based to a considerable extent on Cobban's unpublished biostratigraphic studies in the Missouri Valley area of the Dakotas, including the type Fox Hills. The zone of "*Discoscaphites nicolletii* (Morton)" in the lower part of the Trail City Member of the Fox Hills and the zone of "*Discoscaphites nebrascensis* (Owen)" in the overlying "Timber Lake Member and the upper part of the Trail City Member" were recognized (ibid., p. 1021). In addition, an "undetermined zone" was indicated embracing the nearly barren Elk Butte Member of the Pierre Shale just beneath the Fox Hills, and between it and the Mobridge Member of the Pierre Shale containing *Baculites clinolobatus.*

Subsequently, the "undetermined zone" was understood to include the fossiliferous lower Fox Hills beds of the Lance Creek–Red Bird area of eastern Wyoming. Here the Fox Hills includes a variety of forms of *Sphenodiscus* including *Sphenodiscus* (*Coahuilites*). These constitute a lower part of the range zone of *Sphenodiscus*; the upper part, in the type Fox Hills, contains only *S. lenticularis* (Owen). *Sphenodiscus* (*Coahuilites*) became a zonal marker for the "undetermined zone" (Scott and Cobban, 1965; Gill and Cobban, 1966). Other names have also been employed

for each of the three zones established by Cobban and Reeside (1952). Obradovich and Cobban (1975: 36) employed the following markers for the three zones:

Discoscaphites cheyenensis, Discoscaphites nebrascense
Discoscaphites roanensis, Hoploscaphites nicolleti
Hoploscaphites aff. *H. nicolleti, Spenodiscus (Coahuilites)*

Our work supports the threefold zonation of the post-*B. clinolobatus* beds and can contribute some precision to local zonal boundaries, and help stabilize the fossil nomenclature.

In the type area of the Fox Hills Formation each of the three genera of scaphites shows morphologic change across the Trail City–Timber Lake transition. Least apparent are the changes in *Discoscaphites,* probably owing to the relative rarity of *D. conradi* and *D. gulosus* specimens in our Timber Lake collections. Nevertheless, only these latter collections contain occasional specimens of *D. gulosus* with mid-ventral tubercles on the body chamber. In the *Hoploscaphites* and *Jeletzkytes* lineages, morphologic change is explicit and reflected in changes in taxa, which clearly define two zones within the type Fox Hills.

The *Hoploscaphites nicolletii* Range Zone includes the fauna of the Trail City Member. It makes its first appearance in the area of the type Fox Hills in the local concentration of sideritic concretions in the uppermost beds of the Elk Butte Member of the Pierre Shale at loc. 307, indicated on figures 2 and 4 as the Moreau bridge Rt. 65 fauna. The local top of the zone is in the irregularly distributed concretions at the top of the Trail City Member referred to previously (p. 13) as the transition concretions. These occur mostly in the clayey silts just below the silt-sand transition that marks the boundary between members. Here *H. nicolletii* occurs with *H. comprimus* and rare *Jeletzkytes nebrascensis,* the latter two making their first appearance.

Other useful fossils commonly found in the *Hoploscaphites nicolletii* Range Zone include:

Discoscaphites conradi
D. gulosus
Jeletzkytes spedeni, n. sp.
Sphenodiscus lenticularis
Spyridoceramus tegulatus (formerly *Tenuipteria fibrosa*) with concentric sculpture, variety 2

Of these, *J. spedeni* appears to be restricted to the zone. *Hoploscaphites nicolletii* is the appropriate name-bearer because its macroconchs are by far the most abundant individuals and they occur at all known ammonitiferous horizons within the zone.

The *Jeletzkytes nebrascensis* Range Zone, the youngest ammonite zone in the Western Interior, includes the fauna of the Timber Lake Member and equivalent strata in the Irish Creek lithofacies. It begins with the first appearance of *J. nebrascensis* in the "transition concretions" in the uppermost Trail City Member and extends through the Iron Lightning Member of the upper Fox Hills, where fragments of its key ammonites occur locally in both the Bullhead and Colgate lithofacies. It also includes locally the lowermost Hell Creek Formation in which fragmental ammonite material occurs in local oyster beds above the basal lignite or lignitic clay that marks the base of the formation.

In addition to *Jeletzkytes nebrascensis,* the ammonite fauna of this zone commonly includes:

Hoploscaphites comprimus
Discoscaphites gulosus
D. conradi
Sphenodiscus lenticularis
Baculites columna
B. larsoni

Of these, *H. comprimus* and the rare *B. larsoni* (Cobban and Kennedy, 1992) appear to be restricted to this zone.

About 230 ft of dark gray shale of the Elk Butte and uppermost Mobridge Members of the Pierre Shale lie between the lowest occurrence of fossils in the *H. nicolletii* Range Zone (Moreau Bridge Rt. 65 fauna) and the Range Zone of *Baculites clinolobatus* (fig. 2). Most of this interval is unfossiliferous except for sparingly fossiliferous, scattered, flat, dense limestone concretions between 35 and 60 ft above the local highest occurrence of *B. clinolobatus.* This is the Moreau Bridge Rt. 63 fauna noted on p. 13 and figure 2. It con-

tains (fig. 6) *Hoploscaphites melloi,* n. sp., *Jeletzkytes* sp., and *Spyridoceramus tegulatus* (radially ribbed form, variety 1). *H. melloi* may extend downward into the *B. clinolobatus* Range Zone in the area of the type Fox Hills; however, the few specimens of *Hoploscaphites* crushed flat in the shale of the *B. clinolobatus* Zone are too poorly preserved to identify as *H. melloi* with certainty.

In the Lance Creek–Red Bird area of eastern Wyoming, the Fox Hills Formation contains *Hoploscaphites birkelundi,* n. sp., formerly referred to as "*H.* aff. *nicolleti.*" We use this scaphite as name-bearer for the zone represented by the fauna of the marine lower Fox Hills Formation in this area. This fauna occurs chiefly in concretions in the bluff-forming, bioturbated sandstone of the formation (fig. 5); the underlying 130 ft of the formation are poorly fossiliferous and the lower limit of the *H. birkelundi* Range Zone is not established.

In addition to *H. birkelundi,* its Range Zone includes:

Sphenodiscus (*Coahuilites*) spp.
Sphenodiscus ?lenticularis
Jeletzkytes dorfi, n. sp.
Spyridoceramus tegulatus (with concentric sculpture, variety 2)

CORRELATION

Correlation of post-*Baculites clinolobatus* beds in the type area of the Fox Hills with those in the Lance Creek–Red Bird area is not clear-cut. The *Hoploscaphites nicolletii* and *Jeletzkytes nebrascensis* faunas are absent in the Lance Creek–Red Bird area; they are considered equivalent to the upper brackish part of the Fox Hills and lower part of the overlying Lance Formations (Cobban and Reeside, 1952: 1021). The *Hoploscaphites birkelundi* Zone of the Lance Creek–Red Bird area most likely follows as the next zone beneath the *H. nicolletii* Zone; it is absent in the type area and is probably represented in that area by part or most of the unfossiliferous portion of the Elk Butte Member.

The *H. melloi* fauna in the upper Mobridge Member of the Pierre Shale in north-central South Dakota as yet has no known equivalent in the Lance Creek–Red Bird area. Landman and Waage (in press) suggested that certain morphologic features in *Hoploscaphites,* namely, greater compression, smaller umbilicus, and increased ornamentation, characterize shells from nearshore, sandy bottom environments compared with those from more offshore, silty bottom environments. This is shown in a comparison of *H. comprimus* from the sandy Timber Lake Member and *H. nicolletii* from the underlying silty clay of the Trail City Member. A similar relationship may exist between *H. birkelundi,* which occurs in a nearshore environment, and *H. melloi,* which occurs in an offshore environment. Indeed, a number of morphological features such as whorl compression suggest this relationship. However, there are many other differences between *H. birkelundi* and *H. melloi* in addition to the apparent morphological indicators of environment, and these two species are not as closely related to each other as are *H. nicolletii* and *H. comprimus.*

Thin-shelled inoceramids of the variable species *Spyridoceramus tegulatus* (formerly *Tenuipteria fibrosa*) occur with *Hoploscaphites* throughout the post-*B. clinolobatus* marine beds in both areas and extend back at least to the *Baculites baculus* Range Zone. Where associated with *H. melloi* and throughout the *B. clinolobatus* Zone, the shell sculpture of *S. tegulatus* mainly consists of radial ribs. Where associated with *H. birkelundi* and with the faunas of the *H. nicolletii* and *Jeletzkytes nebrascensis* zones of the type Fox Hills, *S. tegulatus* shell ornament is dominated by concentric rugae. We concur with others (Cobban, 1964; Kauffman, 1971, personal commun.; Wright, 1981: 47) that the changes in the *S. tegulatus* lineage based on dominant ornament are successional and of biostratigraphic value; Wright's (1981) careful study presents the most convincing case. It is not likely that the ornament change in *Spyridoceramus* is an environmental response. If that were the case, one might expect a return to radial ribbing instead of a continuation of concentric rugae on the Trail City specimens. These are in a matrix of silty to sandy clay like that of the *B. clinolobatus* Zone of the Red Bird section and occupy a similar position on the marginal marine gradient. Once established, concentric ornamentation dominated throughout the remaining

life span of *Spyridoceramus* in the Western Interior.

The biostratigraphy of the two variants of *Spyridoceramus* help clarify the relative stratigraphic positions of *H. birkelundi* and *H. melloi.* The latter, occurring with radially ribbed *Spyridoceramus,* is the older fauna in the post-*B. clinolobatus* beds, and is possibly associated wtih part of the *B. clinolobatus* Zone. *H. birkelundi,* associated with the initial *Spyridoceramus* showing dominant concentric ornament, is younger than *H. melloi,* and older than the *H. nicolletii* fauna, which contains the earliest *Discoscaphites.* Our interpretation of the correlation of the post-*B. clinolobatus* marine beds in the Lance Creek–Red Bird area and the type area of the Fox Hills is shown in figure 6.

AGE

The post-*Baculites clinolobatus* marine sequence in the Western Interior is Maastrichtian in age, and lies stratigraphically well above any of the numerous and varied interpretations of the base of the stage in the Western Interior succession of zones. Recently, the base of the Maastrichtian has been clarified by the work of Kennedy et al. (1992) who have established the presence of the North American species *Nostoceras* (*N.*) *hyatti* and *Jeletzkytes nodosus* in the Vistula Valley sequence of Poland. Here these species occur in the uppermost Campanian but are gone before the first appearance of *Belemnella lanceolata,* which is commonly used as a marker for the base of the Maastrichtian in the European boreal Cretaceous. In the Western Interior *Nostoceras* (*N.*) *hyatti* occurs in the *Baculites jenseni* Zone along with the last-occurring specimens of *Jeletzkytes nodosus.* On this basis and supportive evidence on the range of *N.* (*N.*) *hyatti* in equivalent strata in Arkansas, Kennedy et al. (ibid., fig. 1) placed the base of the Maastrichtian at the base of the succeeding *Baculites eliasi* Zone in the Western Interior.

Uncertainty exists as to just what parts of the European Maastrichtian are represented by the post-*Baculites clinolobatus* marine sequence. No generally accepted subdivision of the Maastrichtian into substages exists in either Europe or North America. On both continents a twofold subdivision is employed in the boreal province and a threefold subdivision in the tethyan province, but there is as yet no agreement upon either interprovincial or intercontinental correlations. Jeletzky (1960: 29; 1962: 1006) argued that the type Fox Hills is late Early Maastrichtian, placing the boundary between Early and Late Maastrichtian age in the Western Interior at the top of the *Jeletzkytes nebrascensis* Range Zone. This correlation with the Eurasian Maastrichtian was based largely on his interpretation of *Tenuipteria* lineages in Europe and North America prior to the clarification of *Tenuipteria* systematics by Speden (1970b) and Dhondt (1983a), and also on his misidentification of an ammonite fragment from the Maastrichtian of Hemmoor, northwest Germany, as *Hoploscaphites nicolletii* (see p. 99). However, in a diagram, Jeletzky (1968: fig. 2) later showed a downward shift in the boundary to the top of the *H. nicolletii* Zone, leaving the *J. nebrascensis* Zone in the earliest Late Maastrichtian.

Because of the lack of definitive microfossils and the largely endemic nature of its ammonite faunas, the type Fox Hills cannot be correlated directly with divisions of the European Maastrichtian. However, it can be correlated on the basis of its ammonites with the Prairie Bluff Chalf of the East Gulf Coastal Plain and the Severn Formation of the Atlantic Coastal Plain. The strongest tie is with the Prairie Bluff Chalk, which contains abundant *Discoscaphites conradi* and *D. gulosus* (Jeletzky and Waage, 1978). In addition, the type Fox Hills has rare *Baculites columna,* which is also present in the Prairie Bluff Chalk (Stephenson and Monroe, 1940). The relatively short-lived genus *Discoscaphites* is not known from strata older than the Prairie Bluff and its equivalents in the Gulf Coastal Plain; in the Western Interior it appears to be confined to the Fox Hills and uppermost Pierre Shale in and immediately adjacent to the type area of the Fox Hills, occurring in abundance in the *Hoploscaphites nicolletii* Zone and commonly in the *Jeletzkytes nebrascensis* Zone. In the Atlantic Coastal Plain, *Discoscaphites conradi* occurs in the Severn Formation of Maryland (Sohl and Mello, 1970) together with *Jeletzkytes nebrascensis* (see fig. 133).

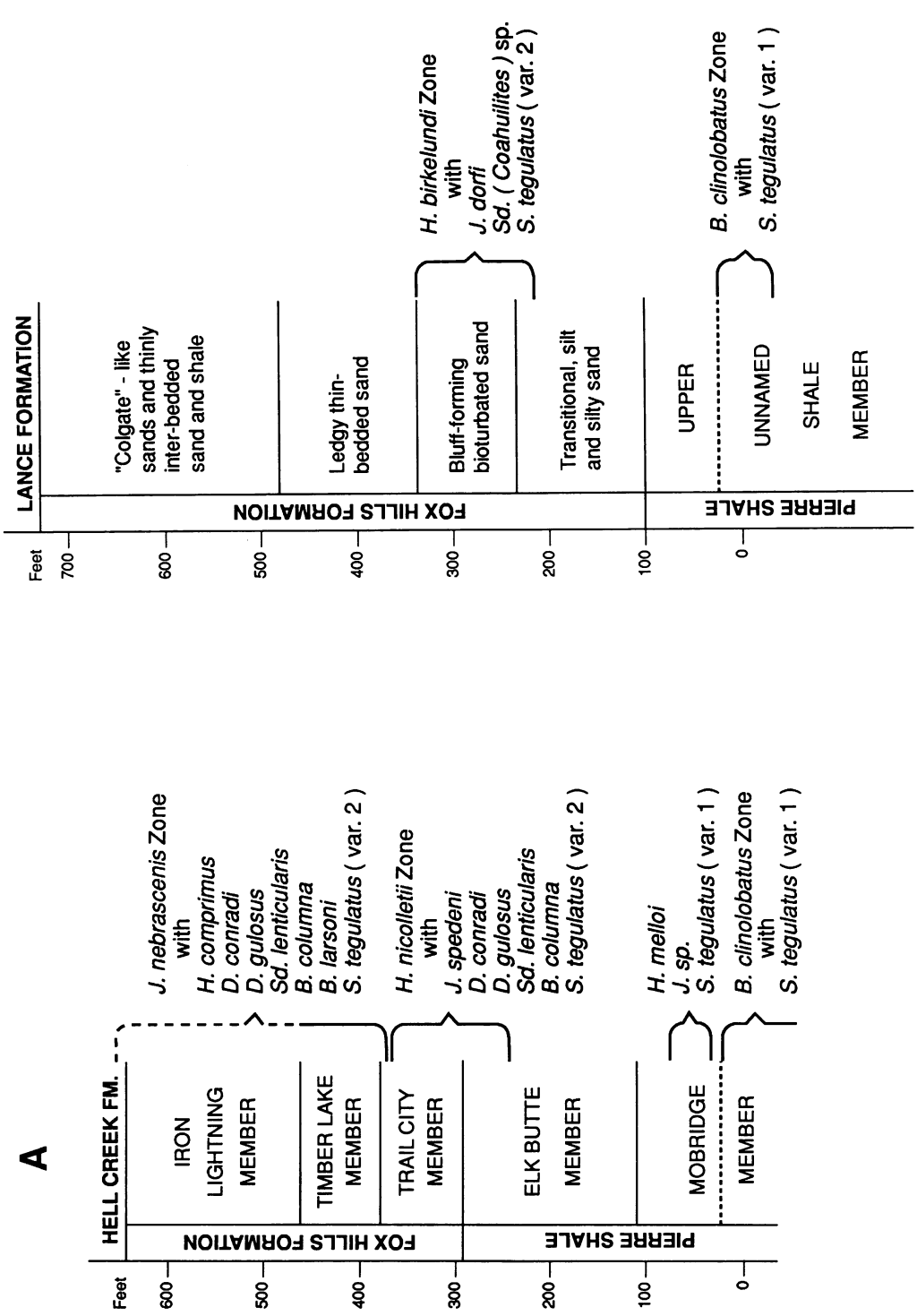
A
Feet
600
500
400
300
200
100
0
HELL CREEK FM.
FOX HILLS FORMATION
PIERRE SHALE
IRON LIGHTNING MEMBER
TIMBER LAKE MEMBER
TRAIL CITY MEMBER
ELK BUTTE MEMBER
MOBRIDGE MEMBER
J. nebrascenis Zone with
H. comprimus
D. conradi
D. gulosus
Sd. lenticularis
B. columna
B. larsoni
S. tegulatus (var. 2)
H. nicolletii Zone with
J. spedeni
D. conradi
D. gulosus
Sd. lenticularis
B. columna
S. tegulatus (var. 2)
H. melloi
J. sp.
S. tegulatus (var. 1)
B. clinolobatus Zone with
S. tegulatus (var. 1)
B
Feet
700
600
500
400
300
200
100
0
LANCE FORMATION
FOX HILLS FORMATION
PIERRE SHALE
"Colgate" - like sands and thinly inter-bedded sand and shale
Ledgy thin-bedded sand
Bluff-forming bioturbated sand
Transitional, silt and silty sand
UPPER SHALE MEMBER
UNNAMED
H. birkelundi Zone with
J. dorfi
Sd. (Coahuilites) sp.
S. tegulatus (var. 2)
B. clinolobatus Zone with
S. tegulatus (var. 1)

On the basis of planktonic foraminifera, nannoflora, and dinoflagellates, both the Prairie Bluff Chalk and Severn Formation are widely considered to be Middle Maastrichtian (May, 1980; Brouwers and Hazel, 1978; Smith and Mancini, 1987: 26; Whitney, 1984). Middle Maastrichtian in the Atlantic and Gulf Coastal Plain is generally taken as equivalent to the *Globotruncana gansseri* Zone following Pessagno (1969). The Severn Formation is considered to be lower Middle Maastrichtian (Brouwers and Hazel, 1978) but the Prairie Bluff Chalk is lower Middle Maastrichtian in its lower part and upper Middle Maastrichtian in its upper part, according to Smith and Mancini (1983). A tripartite subdivision of the Maastrichtian is not recognized in the boreal Cretaceous of northwestern Europe. Here the Middle Maastrichtian (sensu Pessagno, 1969) would straddle the boundary between Lower and Upper Maastrichtian and include, approximately, the European belemnoid zone of *Belemnella occidentalis,* in part, and the lower part of the *Belemnitella junior* Zone, and fall within the nannofossil zone of *Lithraphidites quadratus.* The age of the Prairie Bluff Chalk, under this bipartite classification, which we follow herein, would appear to be late Early to early Late Maastrichtian.

Additional support for the presence of Upper Maastrichtian fossils in the Prairie Bluff Chalk is provided by the work of Dhondt (1979, 1983a, 1983b) on thin-shelled inoceramids of the genus *Tenuipteria* (s.l.) Stephenson. This complex includes both equivalved and inequivalved species (Speden, 1970b) distributed throughout the boreal Maastrichtian strata of the Northern Hemisphere (Dhondt, 1983a). Of the North American representatives included in the genus *Tenuipteria* Stephenson, *Tenuipteria fibrosa,* an equivalved species, occurs in the North American Western Interior where it ranges from the *Baculites baculus* Zone of the Pierre Shale to the *Jeletzkytes nebrascensis* Zone of the type Fox Hills (Speden, 1970b: 18). *Tenuipteria argentea,* an inequivalved species, occurs in the Upper Cretaceous Owl Creek, Prairie Bluff Chalk, and Kemp Clay of the Gulf Coastal Plain. Dhondt (1983a, 1983b) considered the northern European equivalved and inequivalved forms to be conspecific with the respective North American species. In the resultant taxonomic adjustments, *Tenuipteria argentea* was retained for the inequivalved form and the equivalved form (*Tenuipteria fibrosa*) became *Spyridoceramus tegulatus* (Dhondt, 1983a, 1983b).

In northern Europe, *Tenuipteria argentea* is restricted in range to the Upper Maastrichtian and *Spyridoceramus tegulatus* occurs in the Lower Maastrichtian and extends into the basal Upper Maastrichtian where it overlaps the earliest *T. argentea* (Dhondt, 1983a: 49, 50; 1983b: fig. 1) within the lower part of the *Belemnitella junior* Zone. In North America, the two inoceramids are geographically separated: *S. tegulatus* in the Western Interior extends from the *Baculites baculus* Zone into the range zone of *Discoscaphites* in the type Fox Hills, and *T. argentea* in the Gulf Coastal Plain occurs with *Discoscaphites* in the Prairie Bluff Chalk. This suggests that the two formations, the marine type Fox Hills and at least part of the Prairie Bluff Chalk, fall within the overlap interval of *S. tegulatus* and *T. argentea* and are therefore earliest Late Maastrichtian in age. Brouwers and Hazel (1978: 4) noted that "There is no evidence that any outcropping rocks of the Atlantic and Gulf Coastal Province (assigned to the Navarroan Provincial Stage) are as young as the [Late Maastrichtian] *Abathomphalus mayaroensis* Subzone." But this is in reference to the threefold subdivision of the Maastrichtian in which the upper part of the Middle Maastrichtian *Globotruncana gansseri* Subzone supposedly correlates with the lower part of the Upper Maastrichtian of the Eu-

←

Fig. 6. Key fossils of the post-*Baculites clinolobatus* marine strata as they occur in local sections at the type area of the Fox Hills Formation, South Dakota **(A)** and at the Lance Creek–Red Bird area, Wyoming **(B)**. H = *Hoploscaphites,* J = *Jeletzkytes,* D = *Discoscaphites,* Sd = *Sphenodiscus,* B = *Baculites,* and S = *Spyridoceramus* in which variety 1 has radial ribs dominant, variety 2 concentric rugae dominant. The *H. birkelundi* Zone in section B most likely correlates with the lower part of the Elk Butte Member in section A.

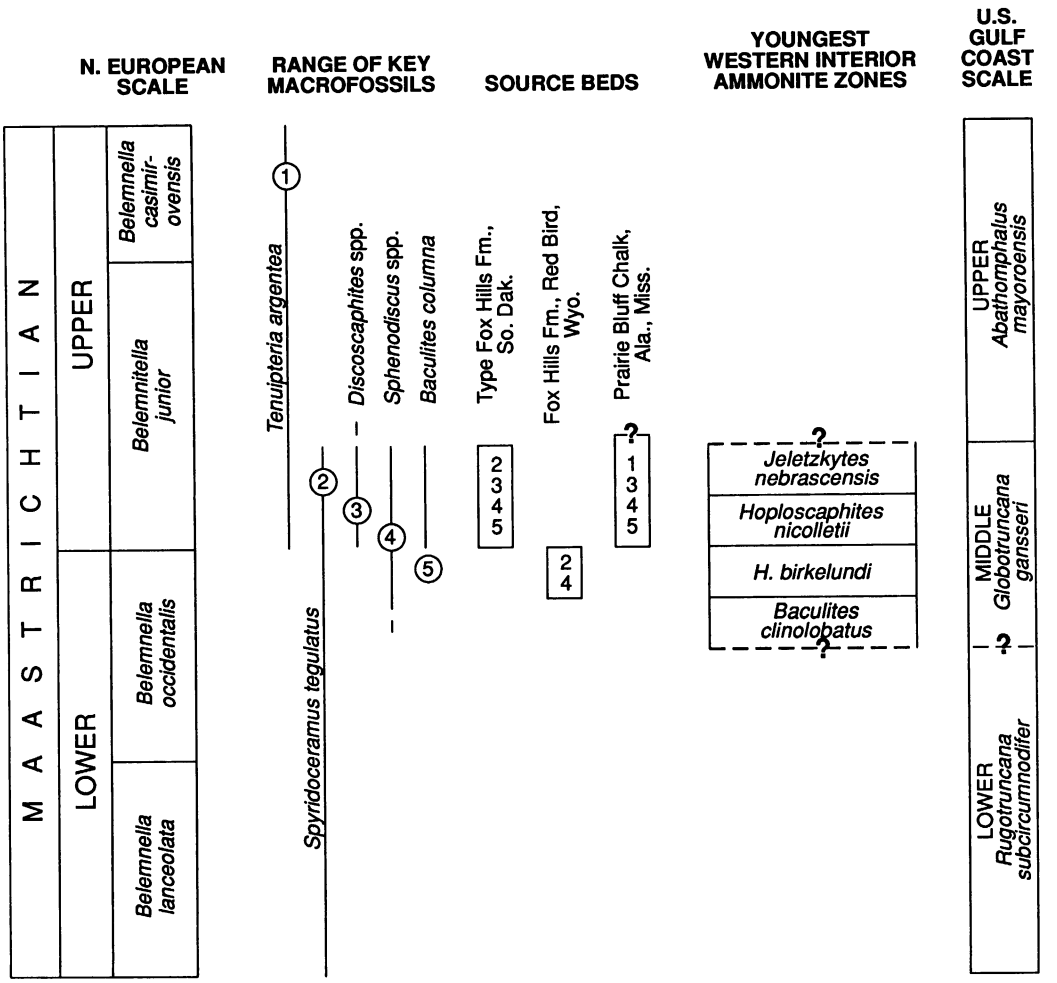

Fig. 7. Age relationships and correlation of the youngest ammonite zones of the Western Interior, based on European tegulated inoceramid ranges (1, 2) after Dhondt (1983a: 45) and North American key ammonite ranges (3, 4, 5). The North European belemnite zones are from Christensen (1979), the Gulf Coast pelagic foram zones from Pessagno (1969).

ropean twofold subdivision. This is precisely the interval in which the *Discoscaphites*-bearing *Hoploscaphites nicolletii* and *Jeletzkytes nebrascensis* zones of the type Fox Hills and the *Discoscaphites* fauna of the Prairie Bluff Chalk appear to occupy, as shown in figure 7.

Recently, Schönfeld and Burnett (1991) have attempted correlation of tethyan Campanian-Maastrichtian sequences in DSDP sites in the eastern North Atlantic with well-known boreal Campanian-Maastrichtian localities in northwest Germany, using benthic and planktonic foraminifera and nannoplankton. In relating the tripartite Maastrichtian standard of the tethyan sequence with its planktonic foraminiferal zones to the bipartite boreal standard belemnite zones, they concluded that the Middle Maastrichtian of the tethyan sequence, which they equated with the *Globotruncana gansseri* Zone, together with the tethyan Upper Maastrichian, are probably equivalent to the entire boreal Upper Maastrichtian.

In summary, the intercontinental distribution of tegulated inoceramids and their association with *Discoscaphites* in North America support an early Late Maastrichtian

age for the type Fox Hills zones of *Hoploscaphites nicolletii* and *Jeletzkytes nebrascensis*. In terms of the prevalent Gulf Coast subdivision of the Maastrichtian, all three zones of the post-*Baculites clinolobatus* marine beds in the Western Interior fall within the *Globotruncana gansseri* Zone as recognized in the Gulf and Atlantic Coastal Plains. The correlation of the entire *G. gansseri* Zone with the boreal lower Upper Maastrichtian (Schönfeld and Burnett, 1991) needs additional corroboration, but raises the possibility that all three scaphite zones of the post-*B. clinolobatus* sequence are early Late Maastrichtian in age.

PATTERNS OF DISTRIBUTION

The characteristics of fossil assemblages in the type Fox Hills Formation are described in previous publications, principally, Waage (1964, 1968), Speden (1970a), and Rhoads et al. (1972). These studies interpreted the accumulations in the assemblage zones as the results of recurrent mass mortalities with little postmortem disturbance before burial. We still find this interpretation tenable after many years of continued study. The marked resemblance to modern marine bottom communities is indicated by the distribution of bivalves and the dominance of one epifaunal and one or more infaunal species in each assemblage (Waage, 1964). Trophic group analysis of the bivalve assemblages (Rhoads et al., 1972) has added depth of detail to this resemblance. Within the context of this interpretation, some aspects of scaphite distribution are noteworthy.

The three genera *Hoploscaphites, Discoscaphites,* and *Jeletzkytes* occur together throughout the marine part of the type Fox Hills Formation and constitute its total scaphite fauna. They have in common the typical scaphitid form and suture as well as a marked sexual dimorphism. They differ in morphologic details and in the pattern of variation among species, as described in the systematic section. They also differ with respect to their geographic, environmental, and stratigraphic patterns of distribution.

The relative abundance of the three genera in the principal assemblage zones LNAZ, LGAZ, UNAZ, and POAZ of the lower Trail City Member and CAZ of the Timber Lake Member was determined based on a sample of approxiately 2700 scaphite specimens, both entire and broken, of known provenance, species, and dimorph. Of these, 16 percent were *Jeletzkytes,* 23 percent *Discoscaphites,* and 61 percent *Hoploscaphites.* Collection bias, while undoubtedly present to some degree, is probably not significant here. The numerical dominance of *Hoploscaphites* is a function of its unique occurrence in dense clusters of macroconchs of *H. nicolletii* in the two assemblage zones LNAZ and UNAZ that bear its name. The geographic distribution of concretions with UNAZ assemblages covers only one-fourth the area of that of concretions from other Trail City assemblage zones; if this were not so the disproportion of *H. nicolletii* macroconchs would be even greater.

Figure 8 shows the relative abundances of the three scaphite genera. *Jeletzkytes,* the large, robust member of the scaphite fauna, is rather remarkably evenly represented throughout the principal layers of accumulation. The low point in UNAZ is misleading; as already noted, the area covered by this assemblage is only about one-fourth the size of that of the other assemblages from the Trail City Member. If corrected for this, the distribution of *Jeletzkytes* in the Trail City assemblage zones varies at most by no more than 30 specimens. The Timber Lake assemblages cover a slightly larger area and have a slightly larger count of *Jeletzkytes* than the Trail City assemblages.

Discoscaphites, consisting of small to medium size, multituberculate scaphites, is far more abundant in LGAZ and POAZ concretions than elsewhere in the Trail City Member and is not well represented in the Timber Lake Member.

Hoploscaphites, morphologically the most conservative of the three genera, has gracile, compressed shells with subdued ornament and is by far the most abundant kind of scaphite in the type Fox Hills. As previously noted, this genus is exceptionally abundant in LNAZ and UNAZ concretions. Only in LGAZ is it the least common scaphite. In POAZ, it shares dominance with *Discoscaphites* and it is the dominant scaphite in the Timber Lake fauna. Macroconchs of *H. nicolletii* in LGAZ and POAZ are slightly larger

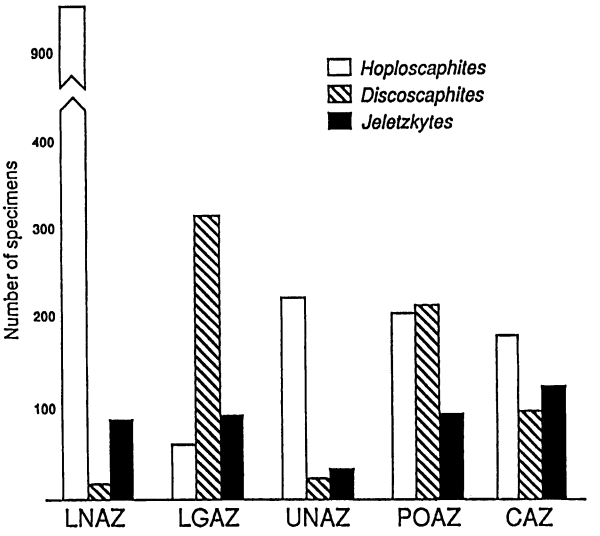

Fig. 8. Relative abundance of scaphite genera by assemblage zone in the Fox Hills Formation in its type area based on approximately 2700 specimens.

in average size than those in LNAZ and UNAZ. Large specimens of *H. nicolletii* (see p. 89), present sparingly throughout the marine Fox Hills Formation, appear to be most common on or just outside the edge of the area covered by the Trail City assemblages.

Only 5 percent of *H. nicolletii* specimens in the Trail City assemblage zones are microconchs. In the Timber Lake Member (CAZ and adjacent concretions), we have found only one concretion with a cluster of small macroconchs of *H. comprimus*. Otherwise, the distribution of specimens of *H. comprimus* in the Timber Lake Member is scattered and the ratio of the number of macroconchs to microconchs averages 3:2.

The phenomenon of clusters of macroconchs does not appear among species of the other two scaphite genera in the type Fox Hills Formation. In light of the interpretation of the assemblages as relatively undisturbed mass killings of bottom communities, the clusters of *H. nicolletii* macroconchs suggest some behavioral rite such as egg laying. Simple geographic separation of adult dimorphs would not entirely account for the great numbers of macroconchs. Within the known geographic extent of the Lower *nicolletii* Assemblage Zone, macroconch specimens of this species are estimated to be in the hundreds of millions (Waage, 1964: 549).

Some indication of geographic separation of *H. nicolletii* and *H. comprimus* dimorphs is found in the transition concretions of the uppermost Trail City and lower Timber Lake Members. These concretions occur in a shallower part of the inshore-offshore gradient than the lower Trail City assemblage zones, probably at the base of the lower shoreface. They contain an unusual assemblage of numerous juvenile scaphites, protobranch bivalves, abundant comminuted plant fragments, and a few adult scaphites, most of which are microconchs of *H. nicolletii* and/or *H. comprimus*. Although microconchs of one or the other of these two species occur throughout the marine part of the type Fox Hills, they are relatively more abundant in these transition concretions and in some faunally similar concretions scattered within the sand body of the Timber Lake Member.

Unfortunately, the lower Trail City assemblages rich in *H. nicolletii* macroconchs grade laterally into a largely unfossiliferous sequence and dip beneath the surface to the west and northwest (shoreward) before reaching an inshore transition. Consequently, we do not know whether we are dealing with an obscured record of geographically separated microconchs of *H. nicolletii* in shallower water or a dramatically unbalanced sex ratio within the species.

The distribution of juvenile scaphites also appears to be concentrated in the transition concretions although juveniles occur in small numbers in concretions from all assemblage zones. Transition concretions are small, usually about 20–30 cm in diameter. Three concretions were analyzed and found to contain 300–400 juveniles each, the majority of which were species of *Hoploscaphites*. Most juveniles were 2–4 mm in phragmocone diameter, which probably corresponds to 3.5–6 mm maximum shell diameter. Above this size, the number of juveniles steadily decreased. No ammonitellas were present. Many of the juveniles had broken apertures but a fair number of specimens showed little breakage. Among the larger juveniles were specimens of *Jeletzkytes* and *Discoscaphites*. The dominance of protobranchs among the bivalves and the abundant plant hash suggest a rather unfavorable environment but one that would afford some protection for juvenile scaphites.

An associational feature of species of *Hoploscaphites* is their frequent co-occurrence with the inoceramid *Spyridoceramus* (= *Tenuipteria*) *tegulatus*. This epifaunal bivalve is most abundant in LNAZ where it is a dominant in one of several bivalve associations. It is also present in UNAZ, but rare in other parts of the marine Fox Hills. Within the area of the type Fox Hills, *Spyridoceramus* also occurs with species of *Hoploscaphites* in sparsely fossiliferous, small concretions in the upper part of the Mobridge Member of the Pierre Shale. Species of the other two scaphite genera, *Jeletzkytes* and *Discoscaphites*, also share this association with *Spyridoceramus* but not to as great a degree.

That the association of scaphites and substrate-dwelling inoceramids was a living association and not entirely a thanatocoenose is suggested by oxygen and carbon isotopic analyses by Whittaker et al. (1987) on fossils from the Lea Park Formation (Campanian) of south-central Saskatchewan. They noted (ibid., pp. 980–981) that "Compared with baculitids, scaphitids generally have oxygen and carbon isotopic compositions more similar to those of inoceramids, which implies that scaphitids generally lived lower in the water column. Indeed, the considerable overlap in $\delta^{18}O$ and $\delta^{13}C$ values between inoceramids and scaphitids suggests that scaphitids lived close to the substrate . . . they probably spent much more time hovering over or sitting on the seabed than they did floating or swimming in the higher reaches of the water column." These conclusions are predicated on the presence of an isotopically stratified water column. Wright (1987) has presented evidence for such stratification in the Western Interior seaway during the early Maastrichtian.

Some morphological differences, chiefly among species of *Hoploscaphites* and *Jeletzkytes*, appear to be ecophenotypic. We have described these elsewhere (Landman and Waage, in press) and summarize them briefly here to complete our observations on patterns of distribution. In the genera noted, and less conspicuously in *Discoscaphites*, species from sandy inshore environments commonly show a greater degree of whorl compression, a relatively smaller umbilicus, and more extensive tuberculation. This is shown in *Hoploscaphites comprimus* in the Timber Lake Member in contrast to *H. nicolletii* from the underlying, offshore Trail City Member in the type Fox Hills and by *H. birkelundi* in the Fox Hills sands of the Lance Creek–Red Bird area in contrast to *H. melloi* in the uppermost Mobridge Member of the Pierre Shale in north-central South Dakota. *Jeletzkytes nebrascensis* from the Timber Lake Member of the type Fox Hills strongly shows these same features in contrast to its predecessor *J. spedeni* from the underlying Trail City Member.

SCAPHITE PALEONTOLOGY

REPOSITORIES

Most of the specimens used in this study are reposited in the Yale Peabody Museum of Natural History (YPM). They were supplemented by specimens from the American Museum of Natural History (AMNH), the Academy of Natural Sciences, Philadelphia (ANSP), the U.S. National Museum (USNM), the University of Chicago collection in the

Field Museum of Natural History (UC), the Black Hills Institute (BHI), the Monmouth Amateur Paleontologist's Society (MAPS), and individuals mentioned in the acknowledgments.

Fieldnotes and maps (USGS 7½ minute quadrangle sheets) and a catalog of the collection are reposited in the Peabody Museum of Natural History, Yale University. Also at that institution is a detailed register of localities.

TERMS AND METHODS

In systematic descriptions, we first describe the adult morphology of a species and subsequently its ontogenetic development. The qualitative terms used to describe the adult morphology of scaphites are found widely in the literature (e.g., Cobban, 1969; Kennedy, 1986a, 1986b). We also use the terms adoral, adapertural, anterior, and forwards to indicate in the direction of the aperture; the antonyms are adapical, posterior, and backwards. The adult shell consists of a closely coiled phragmocone and slightly to strongly uncoiled body chamber. The early whorls of the phragmocone are concealed; the point at which the phragmocone is exposed is called the point of exposure. The exposed portion of the phragmocone of an adult shell is called the adult phragmocone. The adult body chamber consists of a shaft adoral of the last (ultimate) septum followed by a hook terminating at the aperture. The point at which the hook recurves is called the point of recurvature. As in all recent studies of scaphites (Cobban, 1951; Birkelund, 1965), the change in the coiling of the final body chamber coincident with changes in the pattern of ornamentation, approximation of the last few septa, and formation of a constriction at the apertural margin are interpreted as marking the attainment of maturity.

There are two kinds of shell projections at the aperture of scaphites. An anterior projection of the ventral margin of the aperture may or may not be present; when present, it occurs in both dimorphs of a species and is a useful identifying character (figs. 48A, E). A strong anterior projection of the ventral margin produces a rostrum at the aperture. An anterior projection of the dorsal margin of the aperture is also present on both dimorphs of all species described herein (figs. 26D, 49E–G). Although sometimes referred to as a lappet (Cobban and Jeletzky, 1965), it differs from the sense in which this term is used generally (Arkell, 1957), i.e., for lateral projections on both sides of the aperture in microconchs (males) of some Jurassic and Cretaceous ammonites. Rather, the anterior projection of the dorsal margin of the aperture of scaphites, called here the dorsal projection, consists of the protruding end of the plate of shell that forms the dorsal wall of the body chamber where the latter is not in contact with the phragmocone. At the aperture, the projection usually thins and is reflexed against, and more or less annealed to, the phragmocone. It commonly shows subdued transverse ribbing and growth lines.

A number of terms are used to describe ornamentation. Ribs may be referred to by their location on the shell, for example, dorsal ribs (dorsals), flank ribs (flanks), and ventral ribs (ventrals). These are composed of either primary ribs (primaries) or secondary ribs (secondaries), or both; these terms refer to the relative length of the rib on the shell. Primaries extend the full whorl height from umbilicus to venter. Secondaries extend only part of the distance from umbilicus to venter. Depending on its length, a secondary may be long or short; for example, a long secondary arises near the umbilicus and extends to the venter. Secondaries branch off primaries or off other secondaries or are intercalated between primaries or other secondaries (referred to as intercalaries in Arkell, 1957). Rib spacing is expressed by the number of ventral ribs/cm. In addition to ribs, there are tubercles, bullae, and clavi, which are defined according to standard usage (Arkell, 1957).

Mature or submature external sutures of all of the species studied are illustrated. Wedekind's terminology as elaborated by Wiedmann and Kullmann (1981) is employed. In general, however, sutures are not diagnostic for scaphite species, or even genera, and we do not discuss them in detail.

Several measurements were made of adult shells and the results were analyzed using standard statistical tests (F-tests and Student's t-tests evaluated at the 0.05 level of confidence). A complete analysis was per-

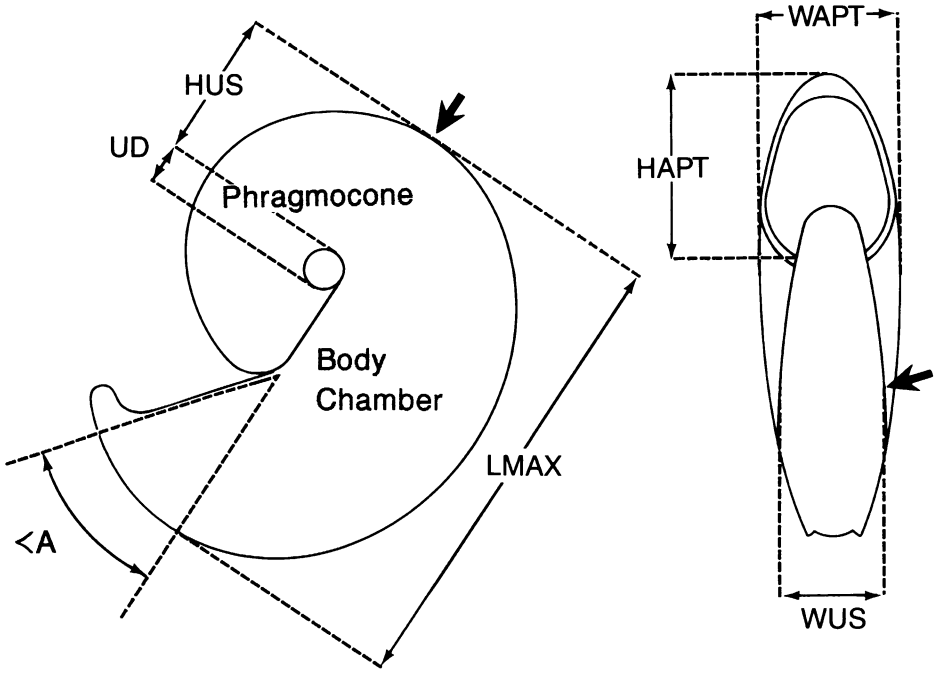

Fig. 9. Measurements of adult shells. The arrow indicates the base of the body chamber. Abbreviations: LMAX = maximum length (shell diameter), WUS = whorl width at the ultimate septum, HUS = whorl height at the ultimate septum, WAPT = whorl width at the aperture, HAPT = whorl height at the aperture, UD = umbilical diameter, A = apertural angle, WUS/HUS = ratio of whorl width to whorl height at the ultimate septum, WAPT/HAPT = ratio of whorl width to whorl height at the aperture; UD/LMAX = ratio of umbilical diameter to maximum length (this ratio only applies to adult shells and differs from UD/D used in ontogentic studies; see figure 9).

formed only on species with sample sizes of more than about 20 specimens. Most of our measurements are those commonly employed in ammonite studies; they are illustrated and defined in figure 9. The general categories used to describe the size of adult shells are: small, LMAX under 50 mm; medium, LMAX 50 to 100 mm; and large, LMAX over 100 mm.

As in other studies of scaphitid ammonites (e.g., Riccardi, 1983), the umbilical diameter of the adult (UD) is measured parallel to the line of LMAX (fig. 9). This measurement is equivalent to the umbilical diameter of the adult phragmocone if the line of the ultimate septum also parallels that of LMAX and the umbilicus of the coil lies on the umbilical shoulder of the final body chamber. However, in *H. melloi* the line of the last septum almost never parallels that of LMAX and the umbilicus of the coil usually lies above the umbilical shoulder of the final body chamber. As a result, UD may underestimate the umbilical diameter of the adult phragmocone by as much as 20 percent in this species, but the difference is generally less than 5 percent in all other species.

The apertural angle of the mature body chamber (A) is measured with respect to the long axis of the shell. This measurement also was used by Birkelund (1965) and Riccardi (1983). It is a useful indication of the degree of recurvature or deflection of the hook of the mature body chamber. We modified the original measurement in two ways. First, we restricted its use to macroconchs where this angle can be determined with some accuracy because the straight umbilical shoulder of the mature body chamber is coincident with the long axis of the shell. In microconchs, on the other hand, the curved umbilical shoulder of the mature body chamber does not coincide with the long axis of the shell, and, as a result, this angle is more difficult to measure. Sec-

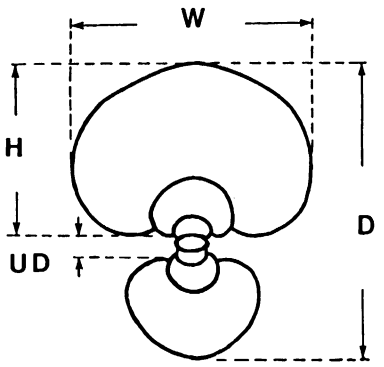

Fig. 10. Measurements on a dorsoventral cross section of a juvenile specimen. Abbreviations: D = diameter, H = whorl height, W = whorl width, UD = umbilical diameter, W/H = ratio of whorl width to whorl height, UD/D = ratio of umbilical diameter to shell diameter (at base of mature body chamber, D = adult phragmocone diameter).

ond, we defined our angle as the degree of deflection of the hook from the long axis of the shell. A higher angle, therefore, indicates a greater degree of deflection or recurvature. This angular measurement is labeled Ω in Riccardi (1983: fig. 1). Riccardi (1983) and Birkelund (1965) defined their apertural angle as 180° − Ω, so that lower angles indicate higher degrees of deflection. This seems an unnecessary complication, and we prefer our more straightforward measurement (fig. 9).

In addition to the description of adult morphology and variation, we also describe the ontogenetic development of most of the principal species. The ontogenetic description of each species studied is included in the systematic section. A comparison of the ontogeny of all of the Fox Hills scaphites appears in the Ontogeny section.

The study of ontogeny was approached in a number of ways. Adult shells were sequentially broken back to expose earlier and earlier whorls. Specimens were photographed at each stage of this process to document the ontogenetic changes in the whorl shape and pattern of ornamentation. The specimens and photographs provided an ontogenetic record to help identify specimens preserved at a juvenile stage of development. Two kinds of oriented cross sections were also made through juvenile and adult specimens: (1) median cross sections coincident with the plane of symmetry and (2) dorsoventral cross sections perpendicular to the plane of symmetry and passing through the axis of coiling (fig. 10). Using median sections, we measured the size of the ammonitella and the angular length of the juvenile body chamber. Using dorsoventral sections, we recorded the growth of umbilical diameter, whorl width, and whorl height versus shell diameter (fig. 10). Isometry was tested according to the procedure described by Imbrie (1956) and Hayami and Matsukuma (1970). Other methods such as those used to measure protoconch angle, ammonitella angle, number of chambers, number of whorls, and septal spacing, are described in the Ontogeny section.

Photographs of adult specimens are natural size unless otherwise indicated whereas photographs of juveniles and early whorls are almost always enlarged. Arrows on photographs indicate the base of the body chamber. The orientations in which specimens were photographed are shown in figure 11.

Specimens are referred to by number with a prefix indicating their repository. Locality numbers are listed in Appendix III. The stratigraphic position of specimens is indicated by formation (e.g., Fox Hills Formation), or member, e.g., Trail City Member (TCM), Timber Lake Member (TLM), or assemblage zone. The principal assemblage zones of the Fox Hills Formation in its type area are listed in stratigraphic sequence below; they are described on p. 12 and figure 4.

Cucullaea Assemblage Zone (CAZ)
Protocardia-Oxytoma Assemblage Zone (POAZ)
Upper *nicolletii* Assemblage Zone (UNAZ)
Limopsis-Gervillia Assemblage Zone (LGAZ)
Lower *nicolletii* Assemblage Zone (LNAZ)

ONTOGENY

Scaphites, like other accretionary organisms, retain a record of their growth in their shells. Changes in the morphology of the shell may indicate major changes in the ontogenetic development of the animal. In this section, we present a general overview of the ontogeny of all the Fox Hills scaphites. The ontogenies of individual species are given in the systematic descriptions.

In order to study ontogeny, we dissected a number of adult shells to expose their early

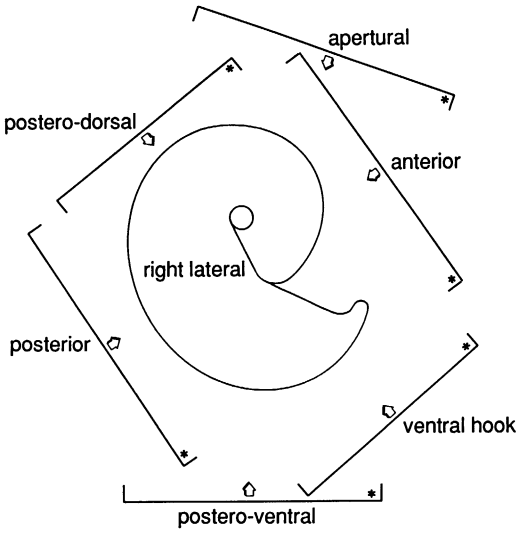

Fig. 11. Adult specimens are photographed from several directions as shown. Asterisks indicate the up position in each direction. The shell is oriented following our interpretation of the probable floating position when the animal was withdrawn into its body chamber. Specimens are identified by museum number, locality number, and assemblage zone and/or stratigraphic unit.

whorls. We also prepared median and dorsoventral cross sections. Changes in the size, shape, and ornament of the shell allow recognition of embryonic, juvenile, and mature stages of growth, each of which is discussed in turn. Dimorphism is discussed under a separate section at the end.

Embryonic Stage

Definition: The early whorls of scaphites and all other Mesozoic ammonites are similar in morphology and are called the ammonitella (Druschits and Khiami, 1970; Druschits et al., 1977; Tanabe et al., 1981). The ammonitella in scaphites consists of an initial chamber (the protoconch) followed by 0.75 whorls (fig. 12). It ends in a constriction (primary constriction) just adoral of a local thickening of the shell wall (primary varix). The ammonitella is interpreted as the embryonic shell; hatching probably occurred after the formation of the primary constriction (Druschits et al., 1977; Tanabe et al., 1981). [In the course of subsequent development, 8 to 12 chambers filled the shell up to the primary constriction (fig. 12)].

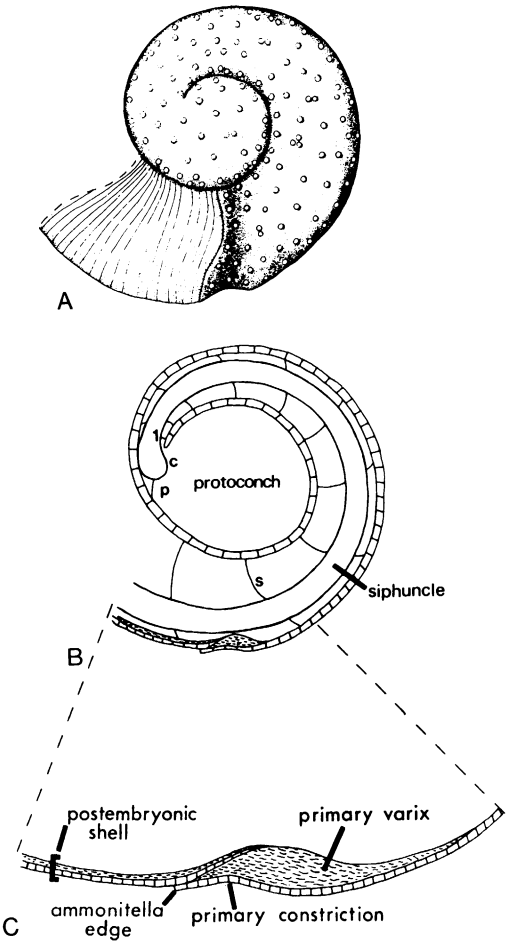

Fig. 12. Ammonitella and part of the succeeding whorl of an adult scaphite. **A.** Outer view showing the tubercles on the ammonitella. **B.** Median cross section showing protoconch, siphuncle, septa (s), proseptum or first septum (1), caecum (c), and prosiphon (p). **C.** Close-up of primary constriction and accompanying varix.

External Surface: In the Fox Hills scaphites, the ammonitella bears a tuberculate micro-ornamentation similar to that in other scaphites and more distantly related ammonites (figs. 13, 14; Bandel et al., 1982). Such tubercles were first observed in scaphites from the Western Interior by Smith (1905). The tubercles are approximately 3 μm in diameter. Commonly, they are irregularly distributed over the exposed surfaces of the ammonitella, but sometimes they appear in spiral rows. In cross section, the tubercles display a spherulitic microstructure. As in

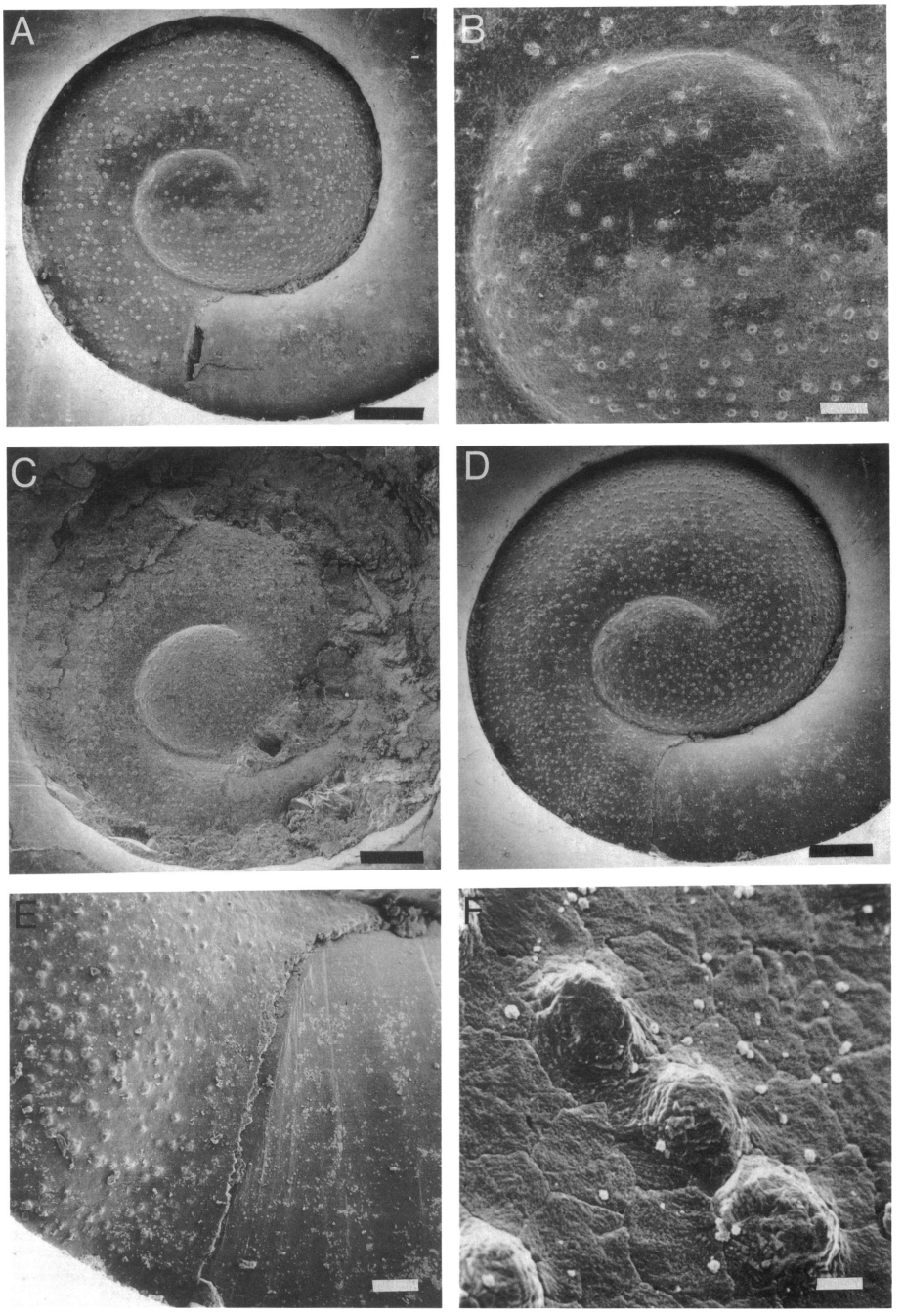

Fig. 13. Ammonitellas of *Hoploscaphites* and *Jeletzkytes*. **A.** *H. nicolletii* (Morton), YPM 34111, loc. 69, UNAZ. Scale bar = 100 μm. **B.** Close-up of protoconch of specimen in A. Scale bar = 20 μm. **C.** *J. nebrascensis* (Owen), YPM 34112, loc. 33, TLM float. Scale bar = 100 μm. **D.** Species of *Hoploscaphites* or *Jeletzkytes,* YPM 34113, loc. 242, LNAZ. Scale bar = 100 μm. **E.** Close-up of primary constriction of specimen in D. Scale bar = 20 μm. **F.** Close-up of tubercles of specimen in D. Scale bar = 2 μm.

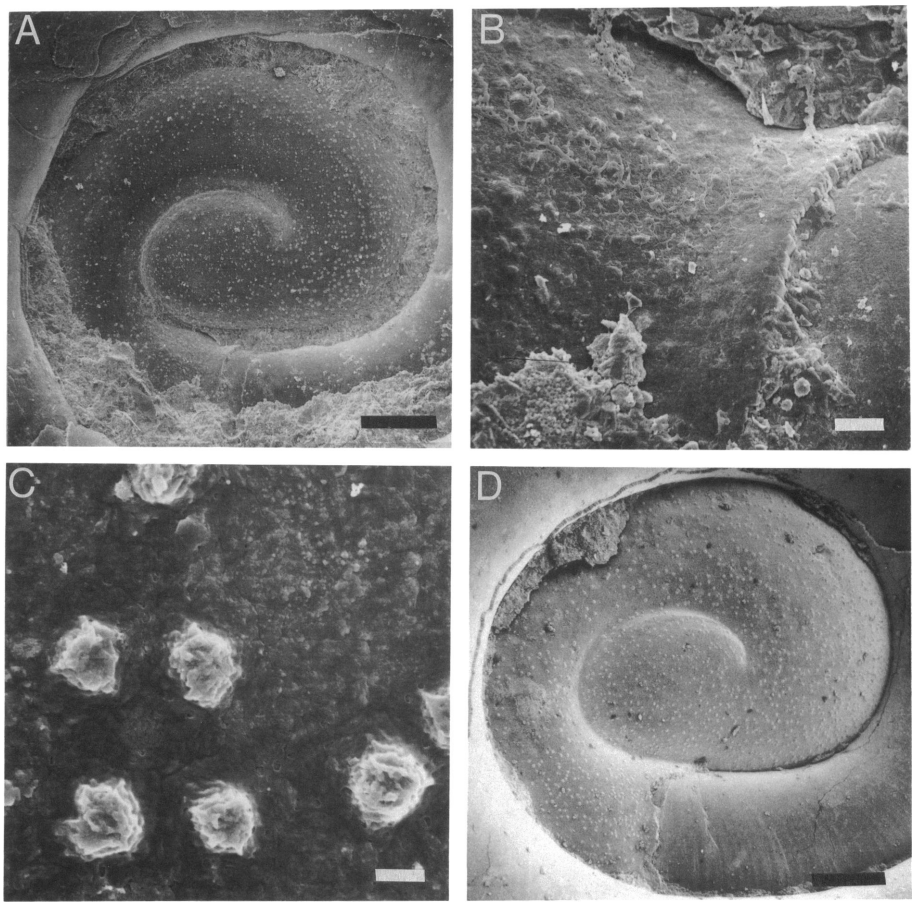

Fig. 14. Ammonitellas of *Discoscaphites*. **A.** *D. rossi,* n. sp., AMNH 44672, loc. 3161, TLM. Scale bar = 100 μm. **B.** Close-up of primary constriction of specimen in A. Scale bar = 10 μm. **C.** Close-up of tubercles of specimen in A. Scale bar = 2 μm. **D.** Species of *Discoscaphites,* YPM 34114, loc. 242, LNAZ. Scale bar = 100 μm.

other ammonites, the tubercles die out in the primary constriction, just beyond which the postembryonic shell begins (figs. 13E, 14B).

SHELL STRUCTURE: The wall of the protoconch is prismatic in microstructure. It passes into the wall of the first whorl, which thickens gradually and terminates in the primary varix (fig. 15); the primary varix consists of nacre. As in other scaphites, the primary varix parallels the primary constriction and lies close to its adapical side. The postembryonic shell is initially composed of an outer prismatic and an inner nacreous layer, but at approximately two whorls after the primary constriction another prismatic layer develops inside the nacreous layer.

PROTOCONCH SIZE AND SHAPE: The protoconch in the Fox Hills scaphites resembles an oblate ellipsoid in shape. In order to accurately describe its size and shape, we measured it in median cross section (fig. 16). The maximum diameter of the protoconch (PD_1) was measured from the ventral edge of the proseptum to the opposite side of the protoconch and did not include the thickness of the outer shell walls. The minimum diameter of the protoconch (PD_2) was defined as the distance perpendicular to the maximum diameter through the center of the protoconch. The angle formed by a line joining the center of the protoconch and the ventral position of the proseptum and the line tangent to that

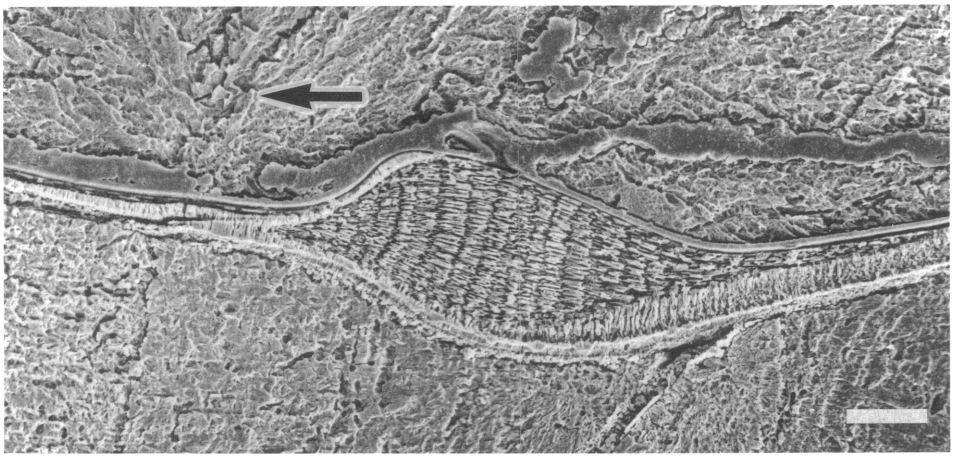

Fig. 15. Median cross section through the ammonitella of *Hoploscaphites comprimus* (Owen) showing the primary constriction and accompanying varix, AMNH 44673, loc. 3161, TLM. Arrow indicates adoral direction. Scale bar = 20 μm.

point on the protoconch surface was defined as the protoconch angle (PA). This new parameter provided a measure of the curvature of the distal part of the protoconch.

The maximum diameter of the protoconch

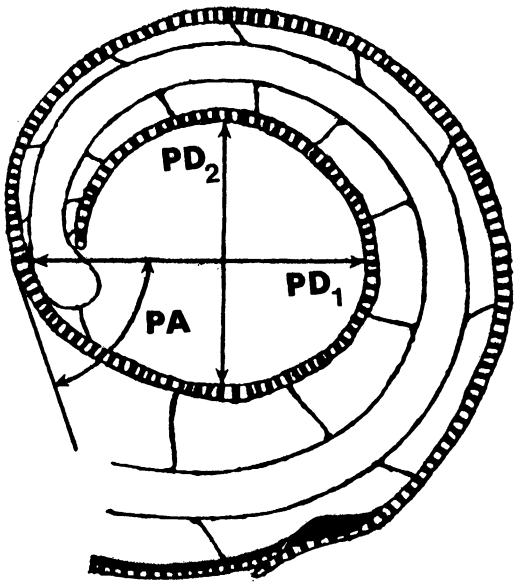

Fig. 16. Diagrammatic median cross section through the ammonitella of an adult specimen showing measurements of the maximum and minimum diameter of the protoconch (PD_1 and PD_2, respectively) and protoconch angle (PA).

(PD_1) is very similar among *H. nicolletii, J. spedeni,* and *J. nebrascensis* as well as between dimorphs within each species (tables 1, 2). The averages of the samples for each of these three species vary from 407 to 414 μm and the measurements within each species range from 390 to 462 μm. The maximum protoconch diameter is generally smaller in species of *Discoscaphites* than in species of *Hoploscaphites* and *Jeletzkytes* (table 3). PD_1 averages 398 μm in *D. conradi,* 364 μm in *D. gulosus,* and 336 μm in *D. rossi,* the smallest value among all the Fox Hills scaphites.

The minimum diameter of the protoconch (PD_2) is similar among all the Fox Hills scaphites except *D. rossi* (tables 1–3). It varies from an average of 355 μm in *D. gulosus* to an average of 389 μm in *H. nicolletii.* In *D. rossi,* it averages 318 μm and ranges from 301 to 330 μm. The ratio of the maximum to minimum diameter of the protoconch averages as little as 1.02 in *D. gulosus* and as much as 1.14 in *J. nebrascensis.* These values indicate that the protoconch is nearly equidimensional in median cross section with respect to these two measurements.

The protoconch angle (PA) permits an unequivocal separation of *Discoscaphites* from *Jeletzkytes* and *Hoploscaphites* (tables 1–3, fig. 17). In *H. nicolletii* and *J. spedeni,* PA averages 66° and 67°, respectively. In contrast, this angle averages 54° in *D. conradi,*

TABLE 1
Ammonitella Measurements of *H. nicolletii* and *H. comprimus*[a]

Species	Dimorph		AD (μm)	AA (°)	PD_1 (μm)	PD_2 (μm)	PA (°)
H. nicolletii	M	N	13	8	8	8	8
		$\bar{x}$	769	302	413	390	67
		SD	27.39	8.76	21.03	22.45	2.75
		Range	718–806	288–316	390–462	361–436	63–72
	m	N	1	1	1	1	1
		$\bar{x}$	762	305	418	382	65
		SD	0.00	0.00	0.00	0.00	0.00
		Range	—	—	—	—	—
	M, m	N	14	9	9	9	9
		$\bar{x}$	768	302	414	389	67
		SD	26.37	8.26	19.74	21.16	2.67
		Range	718–806	288–316	390–462	361–436	63–72
H. comprimus	M	N	1				
		$\bar{x}$	671				
		SD	0.00				
		Range	—				
	m	N	1				
		$\bar{x}$	648				
		SD	0.00				
		Range	—				
	M, m	N	2				
		$\bar{x}$	660				
		SD	16.26				
		Range	648–671				

[a] Abbreviations: M = macroconch; m = microconch; AD = ammonitella diameter; AA = ammonitella angle; PD_1 = maximum protoconch diameter; PD_2 = minimum protoconch diameter; PA = protoconch angle; N = number of specimens; $\bar{x}$ = mean, SD = standard deviation.

52° in *D. gulosus,* and 57° in *D. rossi.* These low values indicate that the protoconch is more depressed in *Discoscaphites* than in *Hoploscaphites* and *Jeletzkytes.* The shape of the protoconch in *Hoploscaphites* and *Jeletzkytes* is more similar to that in other scaphites (see Landman, 1987) and may represent the primitive condition.

AMMONITELLA SIZE AND SHAPE: The ammonitella was measured in median cross section in two ways (fig. 18). The diameter of the ammonitella (AD) was defined as the distance from the adoral end of the primary constriction through the protoconch to the opposite side of the ammonitella. The angle of the ammonitella (AA) was defined as the angle formed by a line extending from the center of the protoconch through the ventral position of the proseptum and a line extending from the center of the protoconch through the adoral end of the primary constriction.

The ammonitella diameter varies slightly among the Fox Hills scaphites. In *H. nicolletii,* the ammonitella diameter ranges from 718 to 806 μm and averages 768 μm (table 1). No conspicuous stratigraphic variation in ammonitella diameter is apparent (table 4). The ammonitella diameter in *J. spedeni* averages 771 μm and is similar to that in *H. nicolletii* (table 2). In contrast, the ammonitella diameter is smaller in species of *Discoscaphites.* AD averages 747 μm in *D. conradi,* 705 μm in *D. gulosus,* and 683 μm in *D. rossi,* the lowest value among all the Fox Hills scaphites (table 3).

A scatter plot of protoconch angle versus ammonitella diameter reveals a clear separation between species of *Discoscaphites,* on the one hand, and species of *Hoploscaphites* and *Jeletzkytes,* on the other (fig. 19). This separation is mainly due to a difference in protoconch angle, which reflects the de-

TABLE 2
Ammonitella Measurements of *J. spedeni* and *J. nebrascensis*[a]

Species	Di-morph		AD (μm)	AA (°)	PD_1 (μm)	PD_2 (μm)	PA (°)
J. spedeni	m	N	5	3	3	3	2
		$\bar{x}$	771	297	408	367	66
		SD	30.66	5.03	11.24	27.54	2.12
		Range	720–803	292–302	396–418	335–385	65–68
J. nebrascensis	m	N	1	1	1	1	1
		$\bar{x}$	678	310	407	358	61
		SD	0.00	0.00	0.00	0.00	0.00
		Range	—	—	—	—	—

[a] Abbreviations: see table 1.

TABLE 3
Ammonitella Measurements of *D. conradi*, *D. gulosus*, and *D. rossi*[a]

Species	Dimorph		AD (μm)	AA (°)	PD_1 (μm)	PD_2 (μm)	PA (°)
D. conradi	M	N	5	3	3	3	3
		$\bar{x}$	738	303	397	389	55
		SD	34.71	4.04	32.32	27.68	3.06
		Range	715–798	299–307	373–434	363–418	52–58
	m	N	2	2	2	2	2
		$\bar{x}$	746	316	400	380	54
		SD	33.23	6.36	25.46	23.34	1.41
		Range	723–770	311–320	382–418	363–396	53–55
	M, m[b]	N	9	6	6	6	6
		$\bar{x}$	747	308	402	386	54
		SD	31.08	7.14	24.90	21.01	2.07
		Range	715–798	299–320	373–434	363–418	52–58
D. gulosus	M	N	4	3	3	3	3
		$\bar{x}$	695	302	358	356	51
		SD	29.71	9.71	13.50	7.02	1.16
		Range	670–737	294–313	344–371	349–363	50–52
	m	N	2	2	2	2	2
		$\bar{x}$	692	306	372	355	54
		SD	7.07	7.78	6.36	12.73	6.36
		Range	687–697	301–312	368–377	346–364	49–58
	M, m[b]	N	7	5	5	5	5
		$\bar{x}$	705	304	364	355	52
		SD	35.78	8.22	12.93	8.08	3.63
		Range	670–770	294–313	344–377	346–364	49–58
D. rossi	M, m	N	6	6	6	6	5
		$\bar{x}$	683	305	336	318	58
		SD	24.94	7.16	20.95	11.65	1.10
		Range	649–717	296–314	308–366	301–330	57–60

[a] Abbreviations: see table 1.

[b] The number of specimens (N) is greater than the total number of specimens for M and m because this category includes undifferentiated specimens that were sectioned before determining which dimorphs they represented.

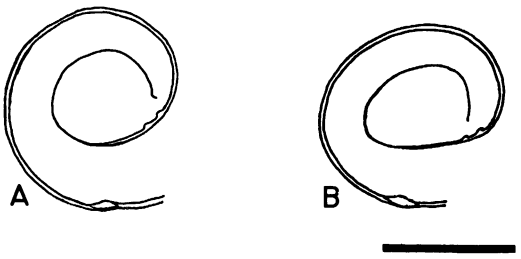

Fig. 17. Comparison of the shape in median cross section of the ammonitellas of *Hoploscaphites* and *Discoscaphites*. **A.** *H. nicolletii* (Morton), YPM 34119, loc. 44, LNAZ. **B.** *D. gulosus* (Morton), YPM 23045, loc. 25, LGAZ. Scale bar = 500 μm.

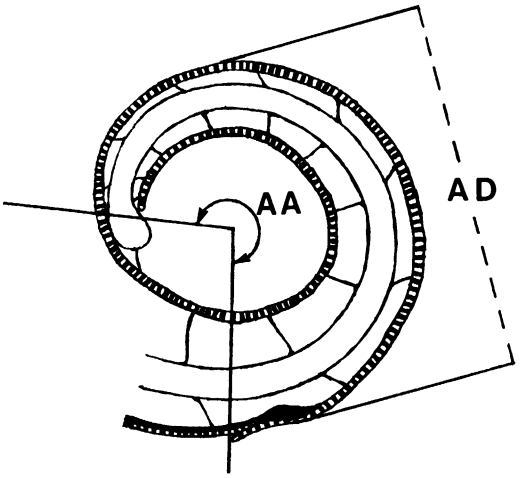

Fig. 18. Diagrammatic median cross section through the ammonitella of an adult specimen showing measurements of the ammonitella diameter (AD) and ammonitella angle (AA).

pressed protoconch and ellipsoidal ammonitella characteristic of *Discoscaphites* (compare figs. 13 and 14).

The ammonitella diameter in the Fox Hills scaphites is generally larger than that in older scaphites from the Western Interior. Landman (1987) reported a range in ammonitella diameter from 582 to 755 μm in a variety of Turonian to Santonian species. However, most values were less than 700 μm. Tanabe et al. (1979) reported slightly higher values ranging from 641 to 949 μm in four Turonian species of *Scaphites* from Japan.

The ammonitella angle is similar among all the Fox Hills scaphites. In *H. nicolletii,* it averages 302° and ranges from 288 to 316° (table 1). In *J. spedeni,* it averages 297° and ranges from 292 to 302° (table 2). In a single microconch of *J. nebrascensis,* it equals 310° (table 2). Among species of *Discoscaphites,* it averages 308° in *D. conradi,* 304° in *D. gulosus,* and 305° in *D. rossi* (table 3). These values of the ammonitella angle are slightly higher than those in other scaphites. Landman (1987) reported a range from 267 to 289° for a variety of Turonian to Santonian species from the Western Interior and Tanabe et al. (1979) reported a similar range (280–295°) for four species from Japan.

The angle of the ammonitella does not covary with the diameter of the ammonitella. For example, the coefficient of correlation between ammonitella angle and ammonitella diameter in six specimens of *D. conradi* is 0.084. The coefficient of correlation is equally low among species; in a sample of 30 specimens of *H. nicolletii, J. spedeni, J. nebrascensis, D. conradi, D. gulosus,* and *D. rossi* the coefficient of correlation is −0.110 (fig. 20). Low correlations have also been reported in older scaphite species (Landman, 1987) as well as in many other ammonites (Tanabe and Ohtsuka, 1985).

In contrast, there is a stronger relationship between protoconch diameter and ammonitella diameter. For example, in the same six specimens of *D. conradi* the coefficient of correlation between ammonitella diameter and protoconch diameter is 0.974. Protoconch diameter and ammonitella diameter are also strongly correlated among species. The coefficient of correlation in the same sample of 30 specimens described above is 0.857 (fig. 21). Similar positive correlations have been documented within and among many other

TABLE 4
Ammonitella Diameter (μm) of *H. nicolletii* by Assemblage Zone (AZ)[a]

AZ	N	$\bar{x}$	SD	Range
LNAZ	7	775	23.56	737–806
LGAZ	2	756	7.78	751–762
UNAZ	—	—	—	—
POAZ	3	769	44.98	718–803

[a] Abbreviations: see table 1 and description of assemblage zones in the text.

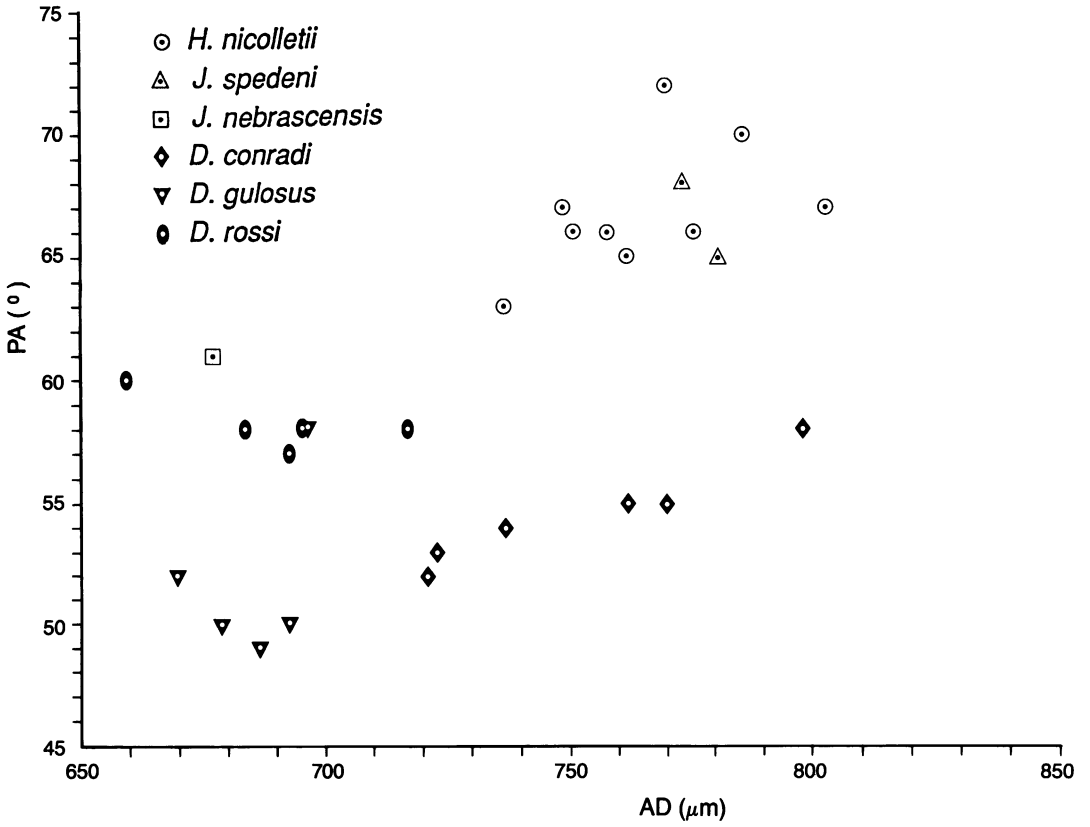

Fig. 19. Plot of protoconch angle (PA) versus ammonitella diameter (AD) in six species of scaphites.

ammonite species (Tanabe et al., 1979; Tanabe and Ohtsuka, 1985; Landman, 1987).

INTERNAL STRUCTURES: The first septum, the proseptum, as in all other ammonites, is prismatic in microstructure. A prismatic necklike attachment of the proseptum is also present (figs. 22, 23). This structure was previously documented in the Turonian to Santonian genera *Scaphites, Clioscaphites,* and *Pteroscaphites* by Landman (1987). It may represent a unique derived character for all scaphites. The necklike attachment of the proseptum appears on the surface of steinkerns as a saddle superimposed on the ventral saddle of the prosuture (Landman and Bandel, 1985). All subsequent septa are nacreous in microstructure and are characterized by short prochoanitic necks with poorly developed cuffs and auxiliary deposits (fig. 22E, F; Smith, 1905).

The bulblike beginning of the siphuncle is called the caecum and is located in the protoconch. It has the same shape and structure in all of the Fox Hills scaphites. In median cross section, it is semicircular in outline (fig. 23A). Birkelund and Hansen (1968) illustrated a similar cross section of a caecum from a Maastrichtian scaphite from Greenland. The caecum is similar in older scaphite species as well as in other members of the suborder Ancyloceratina (Tanabe et al., 1979; Tanabe and Ohtsuka, 1985; Landman, 1987).

The prosiphon consists of several bands or folds that extend from the caecum to the interior surface of the protoconch wall (fig. 23A). Such short, adorally convex prosiphons are common in scaphites as in other species within the suborder Ancyloceratina.

JUVENILE STAGE

The juvenile stage is defined as all postembryonic growth prior to the onset of maturity, that is, prior to the formation of the final body chamber.

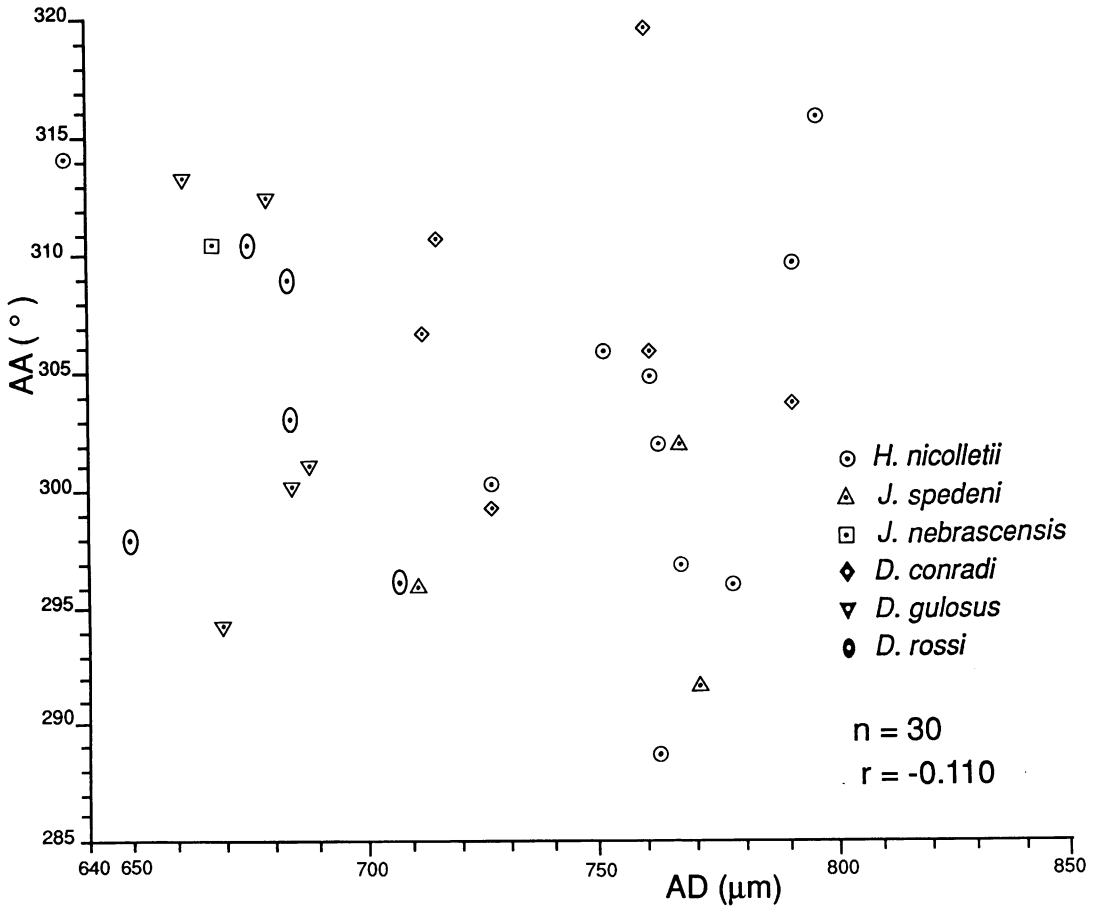

Fig. 20. Plot of ammonitella angle (AA) versus ammonitella diameter (AD) in six species of scaphites.

SHAPE: The juvenile shell is planispirally coiled and expands both in whorl width and whorl height. We examined the allometric growth of whorl width and whorl height versus shell diameter.

The growth of whorl width shows a marked increase at the end of the embryonic stage. This abrupt increase has been documented in many other ammonites (Landman, 1987; Kulicki, 1974, 1979). Thereafter, the growth of whorl width is isometric or, more commonly, negatively allometric. It is relatively constant throughout ontogeny although some species show a change at approximately 5 mm shell diameter. A similar change in whorl width was observed in *Jeletzkytes plenus* by Smith (1905) and in several species of Turonian to Santonian scaphites by Landman (1987) and may reflect a change in the mode of life of these animals at this diameter (Landman, 1987).

The growth of whorl width is approximately the same in dimorphs within the same species. However, in juveniles of *H. nicolletii,* macroconchs are slightly wider than microconchs at comparable shell diameters. Closely related species within the same genus may also differ in whorl width at comparable shell diameters. For example, *J. spedeni* is wider than *J. nebrascensis,* and *D. gulosus* is wider than *D. conradi* for most of juvenile growth.

In contrast to the negatively allometric or isometric growth of whorl width, the growth of whorl height is positively allometric in all species. Whorl height increases constantly throughout ontogeny and the rate of increase is more or less the same in dimorphs within the same species. However, in *H. comprimus,*

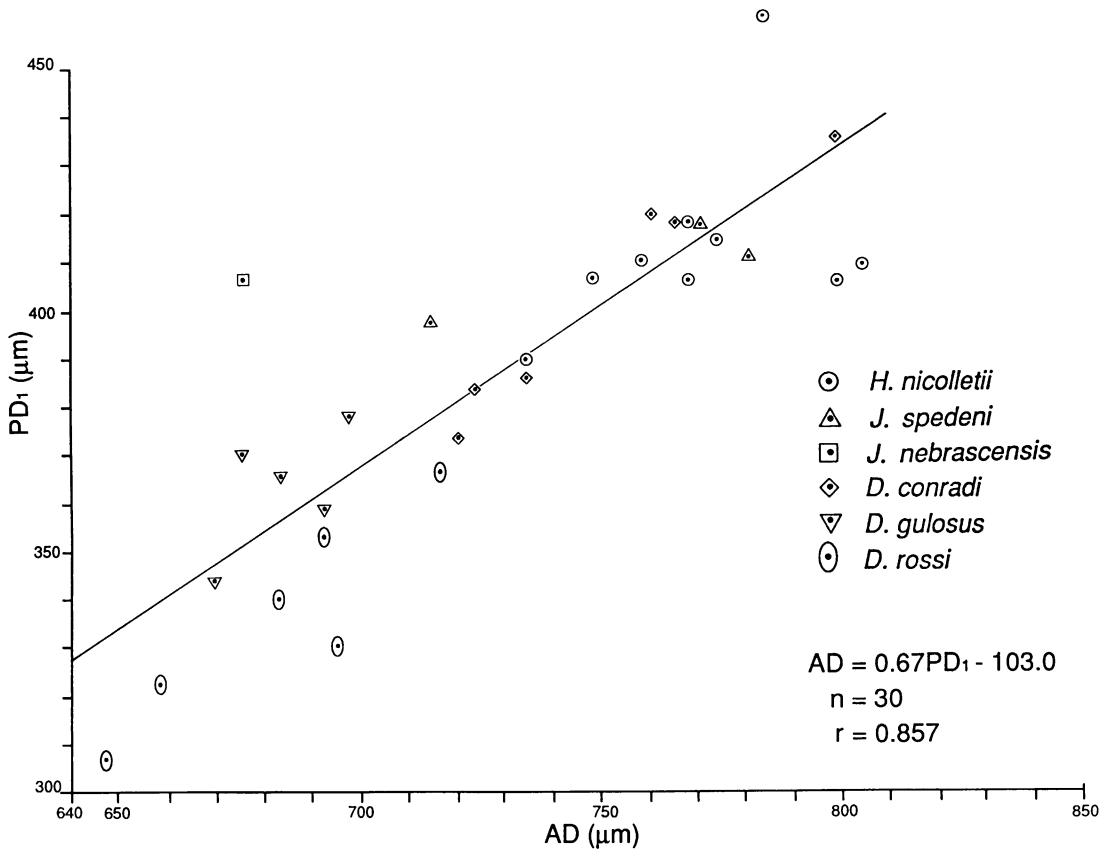

Fig. 21. Plot of maximum diameter of the protoconch (PD_1) versus ammonitella diameter (AD) in six species of scaphites.

macroconchs have consistently higher whorl heights than microconchs at comparable shell diameters.

As a result of the allometric growth of whorl width and whorl height, the shell whorls up to about 5 mm shell diameter are depressed with the ratio of whorl width to whorl height ranging from 1.0 to 2.0. The whorls become increasingly more compressed during ontogeny with the ratio of whorl width to whorl height reaching a minimum of 0.5–0.7 at the base of the mature body chamber in most species except in *J. spedeni* and in *D. gulosus,* which retain a more nearly equidimensional whorl section. The ratio of whorl width to whorl height is approximately the same in juveniles of dimorphs within the same species except in *H. nicolletii* in which microconchs tend to be slightly more compressed than macroconchs at comparable shell diameters. Closely related species within the same genus may also differ in the ratio of whorl width to whorl height at comparable shell diameters. For example, *D. conradi* is more compressed than *D. gulosus,* and *J. nebrascensis* is more compressed than *J. spedeni* throughout ontogeny. *H. comprimus* macroconchs are also more compressed than those of *H. nicolletii,* whereas the microconchs of these two species are less distinct in this respect.

In addition to changes in whorl width and whorl height, the whorl shape may also change during development. In *D. rossi* and *D. conradi* the flanks are flat and tend to slope inward toward the umbilicus in early ontogeny. *D. rossi* also forms a bevel between the flanks and narrow venter. Species with multiple rows of flank tubercles, for example, *D. gulosus,* develop an angular profile in costal cross sec-

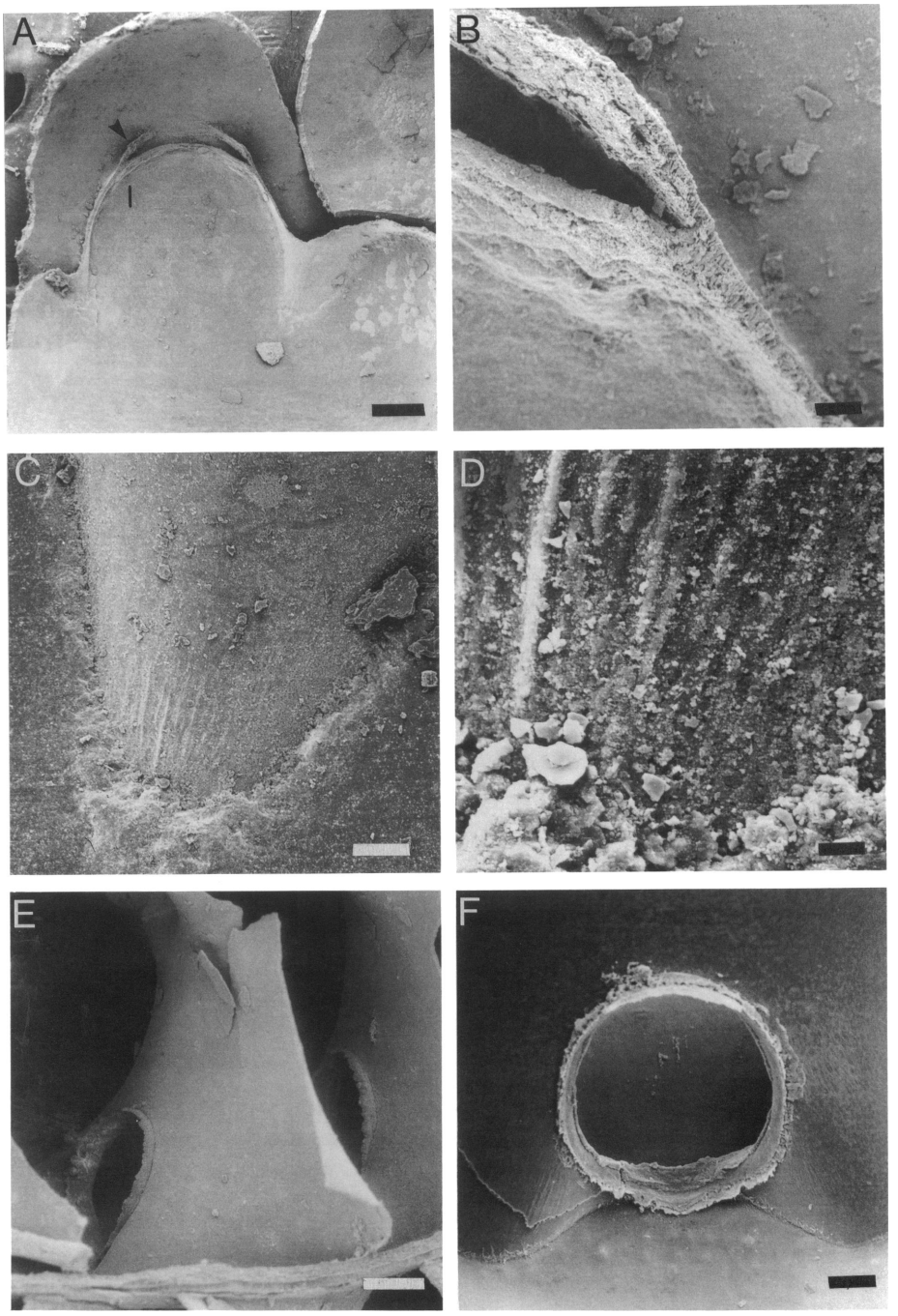

Fig. 22. Internal structures in Fox Hills scaphite specimens free of matrix. **A–D.** YPM 34115, loc. 100, CAZ. **A.** View into the interior of the protoconch showing the proseptum (1) and its necklike attachment (arrow). Scale bar = 50 μm. **B.** Close-up of proseptum and its necklike attachment. Scale bar = 5 μm. **C.** Wrinkles are visible on the proseptum. Scale bar = 10 μm. **D.** Close-up of wrinkles on the proseptum. Scale bar = 2 μm. **E.** Septa with prochoanitic septal necks, YPM 34116, loc. 195, TLM. Adoral direction toward left. Scale bar = 50 μm. **F.** Close-up of prochoanitic neck and cuff, YPM 34117, loc. 100, CAZ. Adoral direction out of page. Scale bar = 20 μm.

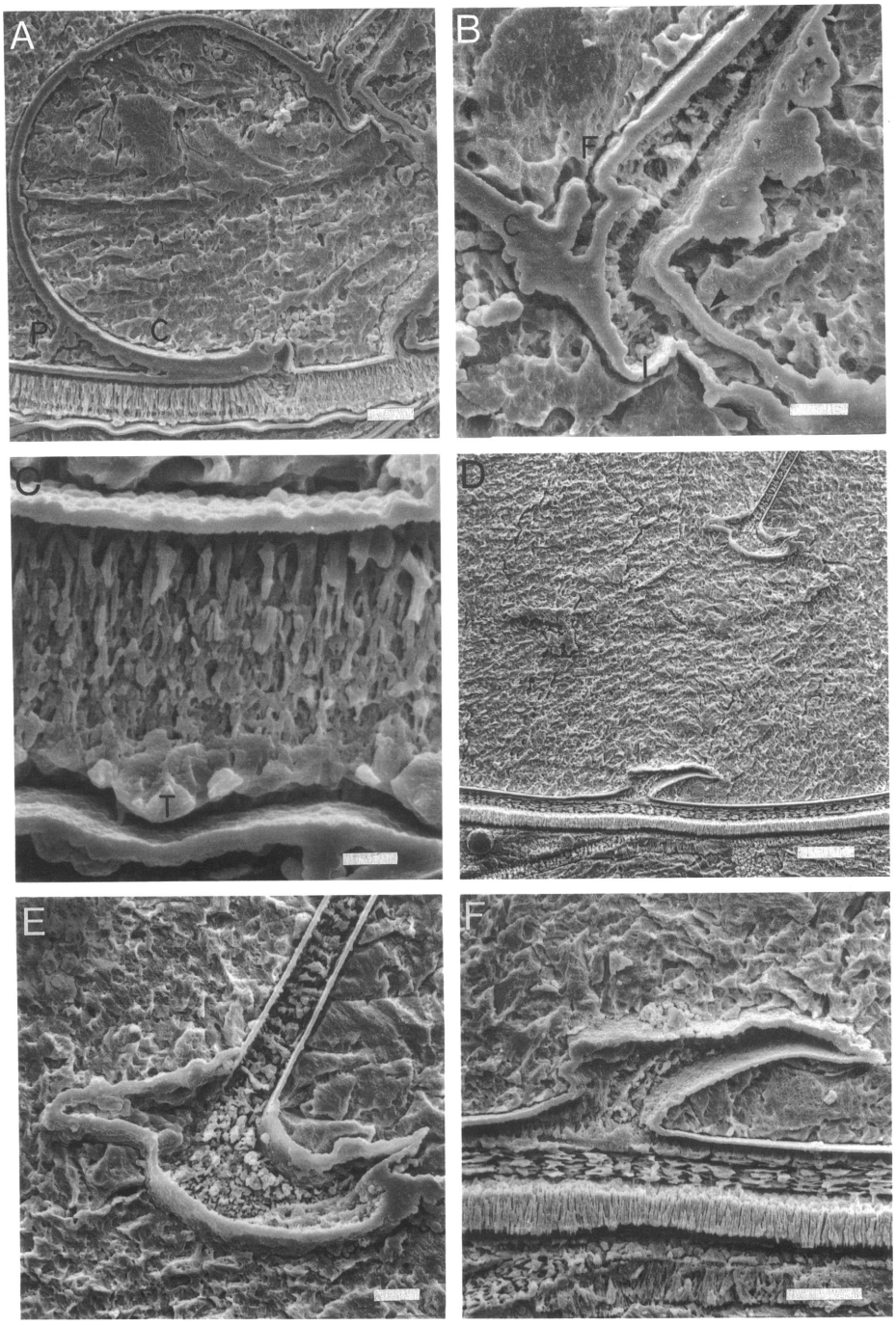

Fig. 23. Median cross section of *Hoploscaphites comprimus* (Owen) showing internal structures, AMNH 44674, loc. 3161, TLM. **A.** Caecum (C) with prosiphon (P). Scale bar = 10 μm. **B.** Close-up of the proseptum (1), its necklike attachment (arrow), caecum (C), and flange (F). Scale bar = 5 μm. **C.** Close-up of the wall of the protoconch showing a tubercle (T). Scale bar = 2 μm. **D.** Prochoanitic septal neck at approximately one whorl from the primary constriction. Adoral direction toward right. Scale bar = 20 μm. **E.** Close-up of dorsal side of septal neck. Adoral direction toward right. Scale bar = 5 μm. **F.** Close-up of ventral side of septal neck and shell wall. Adoral direction toward right. Scale bar = 10 μm.

tion at the appearance of these tubercles. The umbilicus is initially relatively shallow in all species, but deepens during ontogeny.

Differences in whorl shape between closely related species may manifest themselves early on, for example, in the more robust form of *D. gulosus* versus *D. conradi.* Such differences may also appear within the same species, e.g., in coarsely ornamented versus less coarsely ornamented specimens of *J. spedeni.* The whorl shape is more or less the same in dimorphs within the same species except in *H. comprimus,* in which microconchs develop a flatter venter coincident with the appearance of ventrolateral tubercles.

The growth of umbilical diameter during most of juvenile development is isometric to negatively allometric. The rate of increase of the umbilical diameter is more or less the same in dimorphs within the same species, although in *H. comprimus* microconchs are more widely umbilicate than macroconchs. Closely related species may also differ in umbilical diameter. For example, at the onset of maturity, macroconchs of *H. nicolletii* are more widely umbilicate than those of *H. comprimus* although the umbilical diameters of the microconchs of these two species are identical.

The most marked change in the growth of umbilical diameter occurs at the onset of maturity. Dimorphs within the same species start to diverge at approximately one whorl before the base of the mature body chamber. The umbilical diameter begins to increase more slowly or not at all in macroconchs whereas it continues to increase at the same rate in microconchs.

The ontogenetic changes in the growth of umbilical diameter are echoed in changes in the ratio of umbilical diameter to shell diameter, or, in other words, the relative umbilical diameter. This ratio decreases throughout most of postembryonic growth. The rate of decrease is more or less the same until the onset of maturity in dimorphs within the same species, except in *H. comprimus* in which the umbilicus is relatively wider in microconchs than in macroconchs at comparable shell diameters. The umbilicus is relatively small throughout the ontogeny of most of the Fox Hills scaphites although there are slight differences among species. For example, *J. spedeni* has a relatively larger umbilicus throughout growth than does the co-occurring coarsely ornamented species *D. gulosus.*

At the onset of maturity, the ratio of umbilical diameter to shell diameter decreases more steeply in macroconchs than in microconchs reaching a minimum value in both dimorphs at the base of the mature body chamber. The ratio at the base of the mature body chamber is lower in microconchs than in macroconchs. This difference is most pronounced within species of *Hoploscaphites.* For example, the ratio at the base of the mature body chamber averages 0.10 in macroconchs of *H. comprimus* versus 0.22 in microconchs. In *D. gulosus,* this ratio averages 0.10 in macroconchs and 0.15 in microconchs. In *J. nebrascensis* this ratio averages 0.12 in macroconchs and 0.18 in microconchs.

ORNAMENT: The juvenile shell is involute and, therefore, the ornament on earlier whorls is covered over by later whorls. (For illustrations of the ornament on juvenile shells, see the systematic descriptions.) The juvenile shell bears fine growth lines that parallel the ornamentation. Ribs first appear at approximately 4–5 mm shell diameter. They cross the venter with a forward projection, which is most marked in species of *Hoploscaphites.* This projection may persist through ontogeny or weaken at the appearance of ventrolateral tubercles. Primary ribs are straight to slightly sinuous and rectiradiate to prorsiradiate. They are accompanied by long, flexuous lirae in species of *Discoscaphites.* The ratio of the number of dorsal to ventral ribs ranges from 1:2 to 1:3 in all species up to the point of exposure. Secondaries develop by both branching and intercalation. Initially, they originate near the ventral margin, but as whorl height increases, the point of origin migrates to dorsal of mid-flank. Some shells, such as coarsely ornamented specimens of *J. spedeni,* show a bundling pattern of secondaries branching from a single row of tubercles.

In species of *Jeletzkytes* and *Discoscaphites,* ventrolateral tubercles appear as early as one whorl before the point of exposure (15–20 mm shell diameter in *Jeletzkytes,* 10–15 mm shell diameter in *Discoscaphites*), whereas in species of *Hoploscaphites,* they appear at the point of exposure. Ventrolateral tubercles initially occur on every rib or, more

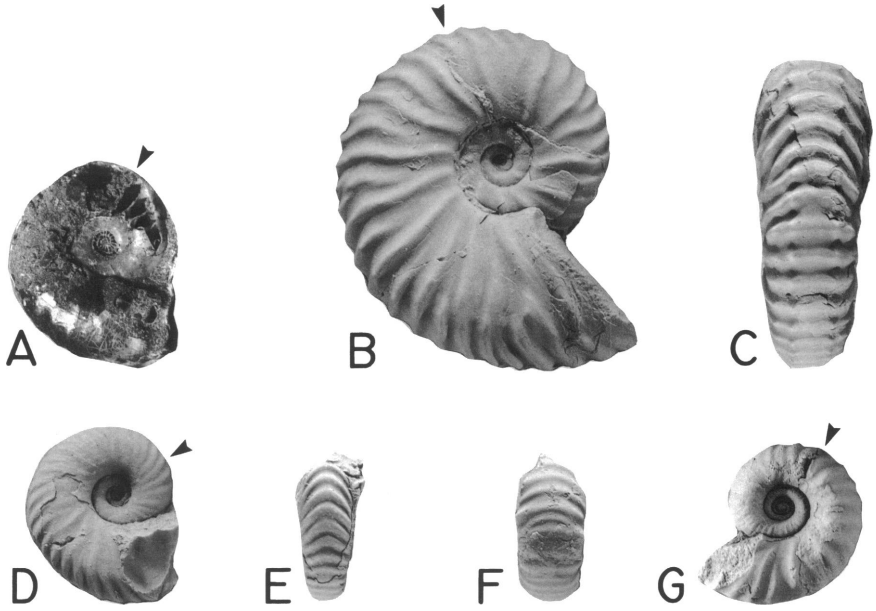

Fig. 24. Juveniles of *Hoploscaphites, Discoscaphites,* and *Jeletzkytes* with complete or nearly complete body chambers. **A,** Right lateral, uncoated view of juvenile of *H. nicolletii* (Morton) with some chambers free of matrix, ×2, YPM 33189, loc. 89, POAZ. **B, C.** Juvenile of *J. nebrascensis* (Owen), ×1.5, YPM 33190, loc. 312, Fox Hills Fm. **B,** Right lateral; **C,** ventral. **D, E.** Juvenile of *H. nicolletii,* ×2, YPM 34127, loc. 27, upper TCM, transition concretions. **D,** Right lateral; **E,** ventral. **F, G.** Juvenile of *D. gulosus* (Morton), ×3, YPM 34126, loc. 27, upper TCM, transition concretions. **F,** Ventral; **G,** left lateral.

rarely, on every other rib. On the exposed phragmocone of species of *Jeletzkytes,* they commonly occur at the junction of two or three flank ribs.

At the appearance of ventrolateral tubercles, the forward projection of the ventral ribs diminishes. Commonly, two ventral ribs loop between pairs of ventrolateral tubercles on either side of the venter. Ventrolateral tubercles generally lie opposite each other although occasionally a few are offset. The distance between pairs of ventrolateral tubercles on either side of the venter is smaller in species of *Discoscaphites* than in species of the other two genera.

Additional rows of tubercles commonly develop on the flanks and near the umbilicus in species of *Jeletzkytes* and *Discoscaphites.* These rows appear in succession from the ventrolateral margin toward the umbilicus. Flank tubercles occur on primaries and stronger secondaries. The tubercles of the first flank row are initially only slightly smaller than those of the ventrolateral row but this difference becomes stronger through ontogeny in species of *Jeletzkytes.*

The number of ribs is higher on the exposed phragmocone than on earlier whorls. The ratio of the number of dorsal to ventral ribs generally increases throughout ontogeny although in some forms, e.g., microconchs of *D. rossi* and *H. nicolletii,* this ratio is nearly constant. In those species bearing tubercles, more rows of tubercles are present on the exposed phragmocone than on any previous whorl (a maximum of six rows of flank tubercles and one row of umbilical tubercles in *J. nebrascensis*). The number of tubercles usually diminishes on the mature body chamber, with generally only the ventrolateral, umbilical, and some flank tubercles persisting.

The pattern of ornamentation is generally similar in dimorphs within the same species. The only significant difference is that the ratio of the number of dorsal to ventral ribs in later ontogeny is higher in macroconchs than in microconchs. However, dimorphs of *H. ni-*

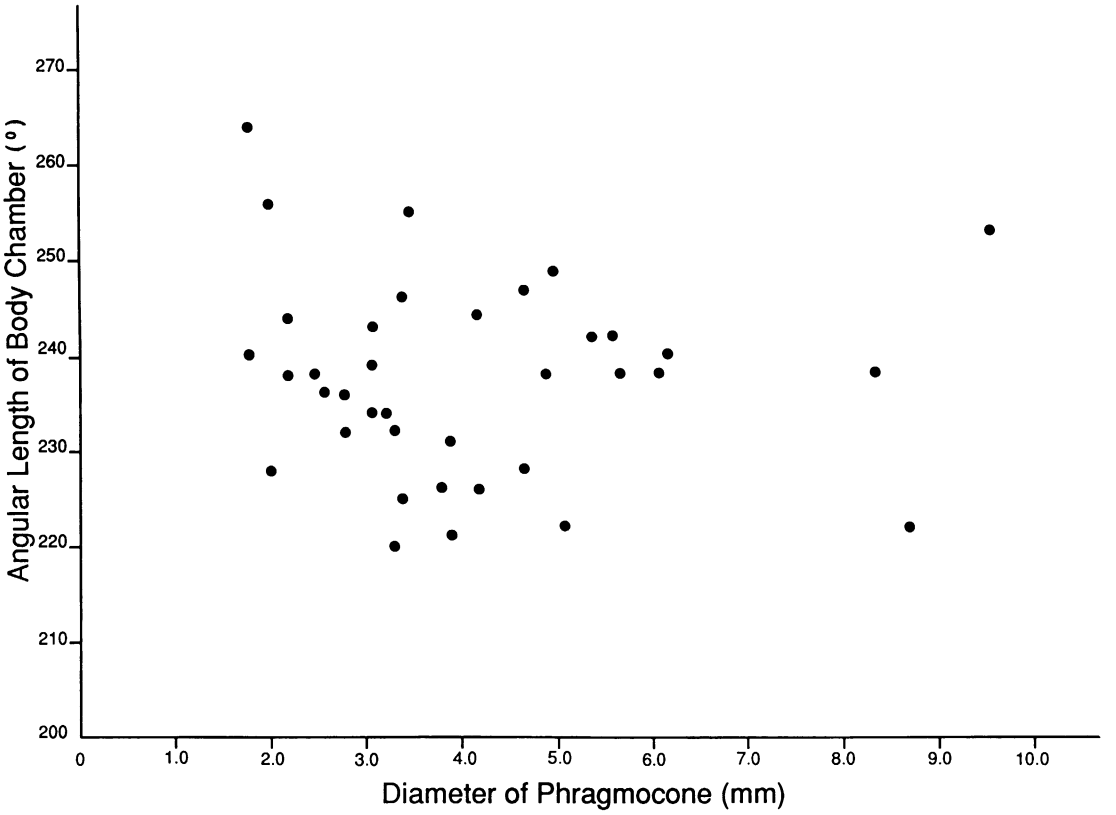

Fig. 25. Plot of angular length of body chamber versus diameter of phragmocone in 37 juveniles of *Hoploscaphites comprimus* (Owen).

colletii show an additional difference. Because the whorls of microconchs are more compressed than those of macroconchs, the ventral ribs, starting at approximately 10 mm shell diameter, are coarser and stubbier in microconchs than in macroconchs.

ANGULAR LENGTH OF THE BODY CHAMBER: The apertural lip in juvenile shells is unmodified and very thin and, consequently, commonly broken (fig. 24). The angular length of the body chamber was measured in a sample of 37 well-preserved juveniles of *H. comprimus* ranging from 1.8 to 9.6 mm in phragmocone diameter. The angular length averaged 237° and ranged from 220 to 264° (fig. 25). The angular length of the body chamber did not co-vary with phragmocone diameter. Variation in the angular length of the body chamber may reflect differences in the point during chamber formation at which each animal died. Specimens just having formed a septum presumably would have had shorter body chambers than those that were just about to form a septum. (The angular length between any two septa averages approximately 20°.) Variation in the angular length of the body chamber may also indicate that some of the specimens were, in fact, broken.

MATURE STAGE

SHAPE: The mature shell is more loosely coiled than that of the juvenile. However, the degree of coiling of the mature shell varies among the Fox Hills scaphites. Species of *Discoscaphites* are more tightly coiled than those of the other two genera. They have a short shaft, which is arcuate in side view, and a hook in contact with the phragmocone. For example, in *D. conradi* macroconchs the dorsal lip of the aperture is pressed tightly against

the venter of the adjacent phragmocone overlapping it as far as the first row of flank tubercles. Species of *Hoploscaphites* and *Jeletzkytes,* on the other hand, are more loosely coiled and show a separation between the phragmocone and reflexed hook. This separation is larger in microconchs than in macroconchs. Even within the same dimorph this gap is usually wider in larger specimens with longer shafts.

The body chambers of macroconchs fall into two general shape categories: compressed or robust. They are compressed in *Hoploscaphites,* robust in *Jeletzkytes,* and compressed or robust in *Discoscaphites.* In both shape categories, the whorl section is significantly more compressed at the ultimate septum than at the aperture.

ORNAMENT: The development of ornament on the adult shell varies among the Fox Hills scaphites, but some general patterns emerge. In macroconchs of all three genera, the ornament on the phragmocone changes and weakens on the posterior part of the final body chamber. This weakening of ornament is most pronounced in macroconchs of *H. nicolletii* in which it may be accompanied by attenuation of the shell whorl and thinning of the outer wall. This feature has been called the stretch zone (Landman and Waage, 1986). Another common feature in macroconchs and microconchs of all three genera is a change in the direction of ribbing in passing from the normally coiled phragmocone to the scaphitoid body chamber. The ribs change from relatively rectiradiate to relatively prorsiradiate. Because ribs approximately parallel growth lines, this change in ribbing may indicate a change in the position of the aperture during formation of the final body chamber.

Ribbing on the mature body chamber also tends to become finer and more closely spaced toward the aperture. This is especially well expressed in species of *Hoploscaphites* and *Jeletzkytes.* For example, in macroconchs of *H. nicolletii,* the number of ventral ribs increases from approximately 10/cm on the shaft to 20/cm on the anterior portion of the body chamber. In macroconchs of *J. nebrascensis,* the number of ventral ribs increases from 5 to 10/cm on the posterior part of the body chamber to 7 to 14/cm on the hook. The forward projection of ventral ribs is most conspicuous in the region of fine, closely spaced ribbing near the aperture.

The most prominent features in all genera, but especially in *Hoploscaphites* and *Jeletzkytes,* are the ventrolateral tubercles on the shaft. In *H. nicolletii,* the strongest primary ribs coincide with the largest ventrolateral tubercles, which are sometimes clavate in shape. These ventrolateral tubercles diminish in size or disappear altogether toward the aperture. In macroconchs of *J. nebrascensis,* the largest ventrolateral tubercles also occur on the shaft and diminish in size on the hook.

The presence of large ventrolateral tubercles may affect the shape of the venter. In macroconchs of *J. nebrascensis,* the venter is narrow, flat, and bicarinate in costal cross section on the middle of the shaft but broadens and rounds on the hook coincident with the disappearance of ventrolateral tubercles. In macroconchs of *H. comprimus,* large ventrolateral tubercles are also associated with a flattening of the venter. These tubercles are usually clavate with larger ones directed outward, a feature present but less pronounced in other species of *Hoploscaphites* and in *Jeletzkytes.*

The pattern of ornamentation in many species almost suggests a mutual exclusion between coarse tubercles and fine, closely spaced ribbing. For example, in *J. nebrascensis,* strong ventrolateral and flank tubercles on the shaft of the body chamber are associated with very weak ribs on the venter. The disappearance of these tubercles toward the aperture coincides with the reappearance of fine, closely spaced ventral ribs. In *H. comprimus,* the region of very fine ribbing is shifted forward relative to that in *H. nicolletii.* As a result, large ventrolateral tubercles extend farther forward in *H. comprimus* and in some specimens may even extend to the aperture.

APERTURE: The outer wall of the shell turns abruptly inward at the apertural margin, then reflexes, creating a constriction (fig. 26A). The reflexed portion may extend as much as 3 mm. This constriction is well developed on the venter and sides of the aperture. It shallows toward the dorsum where the shell ends in an adoral projection. The constriction is present on the sides of this projection but weakens toward the middle. The constriction is clearly visible on steinkerns.

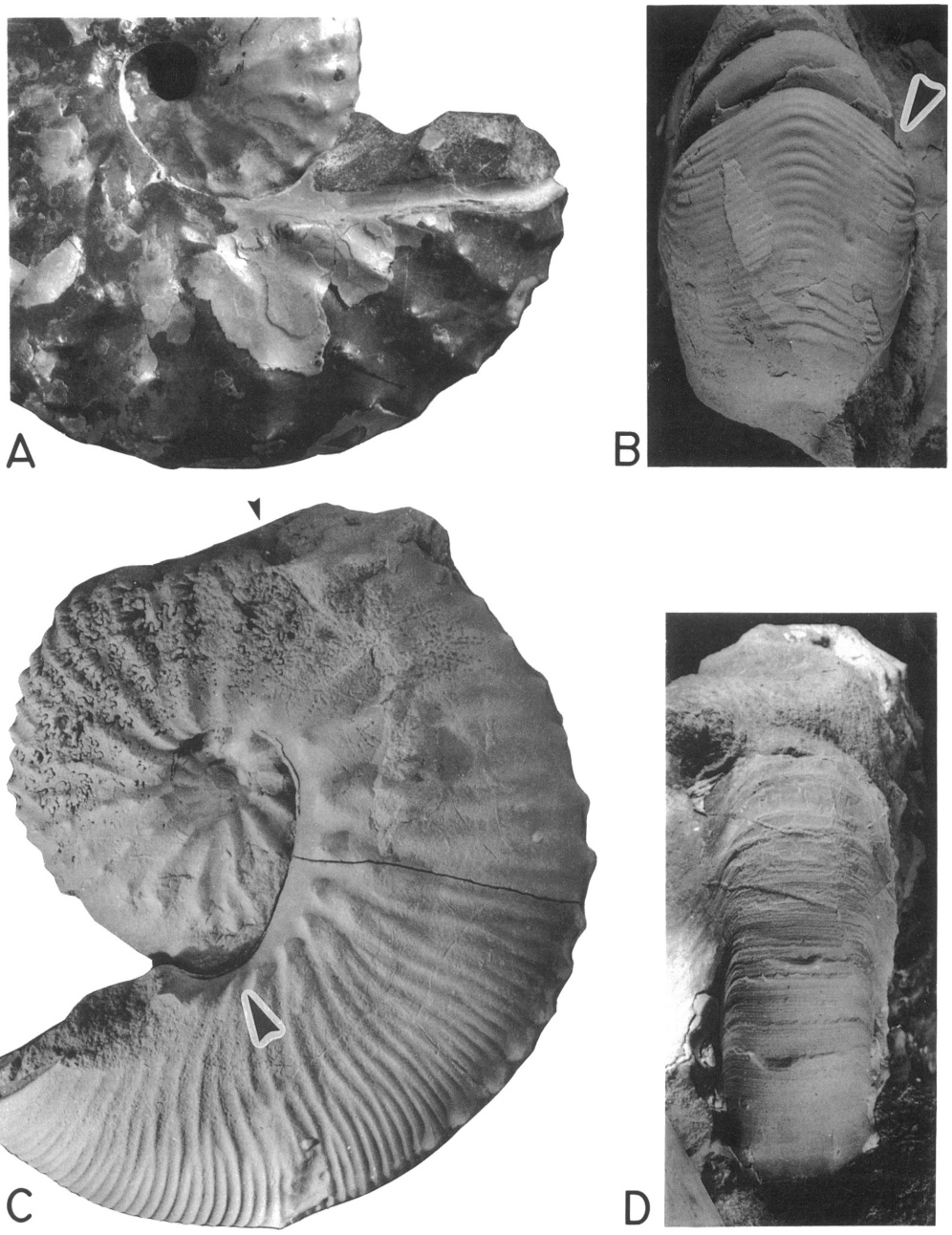

Fig. 26. Apertural margin at maturity. **A.** *Discoscaphites gulosus* (Morton) microconch, right lateral, uncoated close-up showing constriction at apertural margin, ×2, YPM 27204, loc. 110, POAZ. **B.** Ventral view of presumably pathologic specimen of *Jeletzkytes nebrascensis* (Owen) showing maturelike apertural constriction (arrow) adapical of constriction at final aperture, ×1.5, YPM 32534, loc. 34, TLM. **C, D.** *J. nebrascensis* microconch, YPM 32826, loc. 73, TLM. **C.** Left lateral, arrow indicates location of view shown in D. **D.** Natural cast of the outer surface of the impressed zone of the body chamber developed against the venter of the phragmocone. The actual shell is retained on the body chamber. The shell is covered with numerous transverse ribs and growth lines, as shown on the cast, and extends as a projection at the aperture, ×2.

There are very few shells in our collections that represent intermediate stages in the formation of the final body chamber. All such shells lack a well-defined aperture and are probably broken. We have a fragment of an anterior portion of a body chamber of a presumably pathologic specimen in which two maturelike apertural constrictions occur before the final aperture (only one of these constrictions is visible in fig. 26B).

In species of *Hoploscaphites* from the type area, and to a lesser extent in co-occurring species of *Jeletzkytes,* the ventral part of the apertural margin is extended as a projection that conforms to the anterior projection of the ventral ribbing. In *H. nicolletii* and *H. comprimus,* the venter ends in a short, rapidly tapering, blunt rostrum (fig. 48A, E). The dorsal part of the apertural margin is also extended as a projection in all genera. As explained on p. 26, the dorsal projection represents the protruding end of the dorsal wall of the body chamber and is reflexed against the phragmocone (fig. 26C, D). The inner surface of this projection is, of course, smooth but the outer surface is marked by transverse ribbing and growth lines.

MUSCLE ATTACHMENT AREAS: Muscle attachment areas are indicated by very thin layers of myostracum preserved on steinkerns of the mature body chamber. The ventral muscle attachment area occurs on the mid-venter a few millimeters in front of the ultimate suture. It is oval to teardrop in shape with its blunt end forward in species of *Hoploscaphites* (see fig. 53D). It ranges in maximum length from 2 to 5 mm depending on adult size. In species of *Jeletzkytes* the ventral muscle attachment area is similar in shape but more rounded and ranges from 6 to 7 mm in maximum length (see fig. 145H). In contrast, in species of *Discoscaphites* the ventral muscle attachment area is narrow and elongate with bluntly rounded ends and averages 5 mm in maximum length (see fig. 152E).

The dorsal muscle attachment areas are rarely preserved and have been noted on only a few macroconchs of *H. nicolletii* (see fig. 53E). They extend several millimeters in front of the last suture; they are wedge-shaped and drape over the umbilical shoulder on each side of the shell.

Internal molds of the mature body chamber of all three genera, but especially *Discoscaphites,* also bear a very faint, low rounded ridge that runs along the mid-venter from the ventral muscle attachment area nearly to the aperture (see fig. 153G). This ridge is commonly tripartite and probably represents an imprint of an internal structure and not a muscle as it lacks any indication of myostracum.

CHAMBER AND WHORL NUMBER: We investigated the relationship among number of chambers, number of whorls, and maximum length (LMAX) in adult specimens of *H. nicolletii.* In 23 macroconchs of *H. nicolletii* ranging in maximum length from 44.0 to 69.0 mm, the number of chambers, excluding the protoconch, averaged 90 and ranged from 71 to 105. Number of chambers did not covary with adult size; the coefficient of correlation was 0.237 (fig. 27). We also measured the number of whorls, with a precision of ⅛ whorl, from the first septum to the aperture in another sample of 30 macroconchs of the same species ranging in maximum length from 42.5 to 69.0 mm. The number of whorls averaged 5.6 and ranged from 4.5 to 6.0. As with number of chambers, number of whorls did not covary with adult size; the coefficient of correlation was 0.195 (fig. 28).

SEXUAL DIMORPHISM

DEFINITION: Dimorphism is sometimes apparent in juveniles but is most clearly expressed at maturity. Dimorphs are referred to as macroconchs and microconchs. They are interpreted as sexual in nature, the macroconch, the female and the microconch, the male, following the interpretation in most other ammonite studies (e.g., Makowski, 1962; Lehmann, 1981b).

SHAPE: Dimorphs are easily distinguished at maturity by differences in the shape of the body chamber. In macroconchs the body chamber increases gradually in width but abruptly in height, reaching its maximum size in the middle or anterior portion of the shaft. Thereafter, width either remains the same or gradually decreases, while height rapidly decreases to the aperture. In microconchs, on the other hand, the body chamber increases

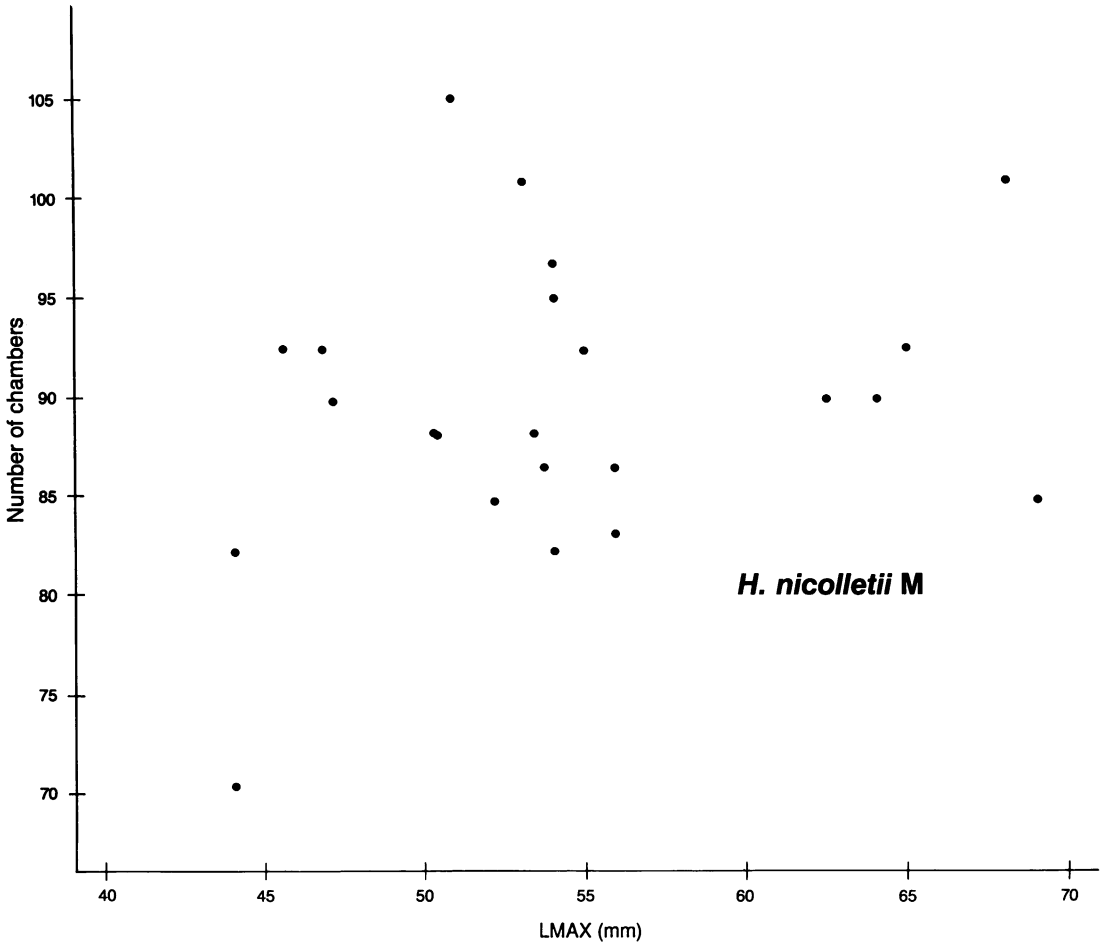

Fig. 27. Plot of number of chambers versus maximum length (LMAX) in 23 adult macroconchs of *Hoploscaphites nicolletii* (Morton).

only gradually in size through the shaft and then decreases very slightly toward the aperture.

The whorl dimensions at the ultimate septum and at the aperture are generally larger in macroconchs than in microconchs. The whorl proportions at these points may also differ. For example, in *H. nicolletii,* the whorl section at the ultimate septum is more compressed in macroconchs than in microconchs. On the other hand, in species of *Jeletzkytes* and *Discoscaphites,* whorl proportions at the ultimate septum and at the aperture are more or less the same in dimorphs within the same species. This is due to the fact that the relationships between whorl dimensions at each of these points and adult size are isometric and nearly identical in both dimorphs. For example, in *D. gulosus* the relationship between whorl width at the ultimate septum and adult size is isometric and similar in both macroconchs and microconchs (fig. 29). The relationship between whorl height at the ultimate septum and adult size is also isometric and similar in both dimorphs (fig. 30). As a result, the ratio of whorl width to whorl height at this point is more or less the same in the two morphs (fig. 31). Such arguments also explain the similarity in whorl proportions at the aperture in dimorphs within this species (figs. 32–34).

Two important differences between dimorphs involve the shape of the umbilical shoulder and the diameter of the umbilicus.

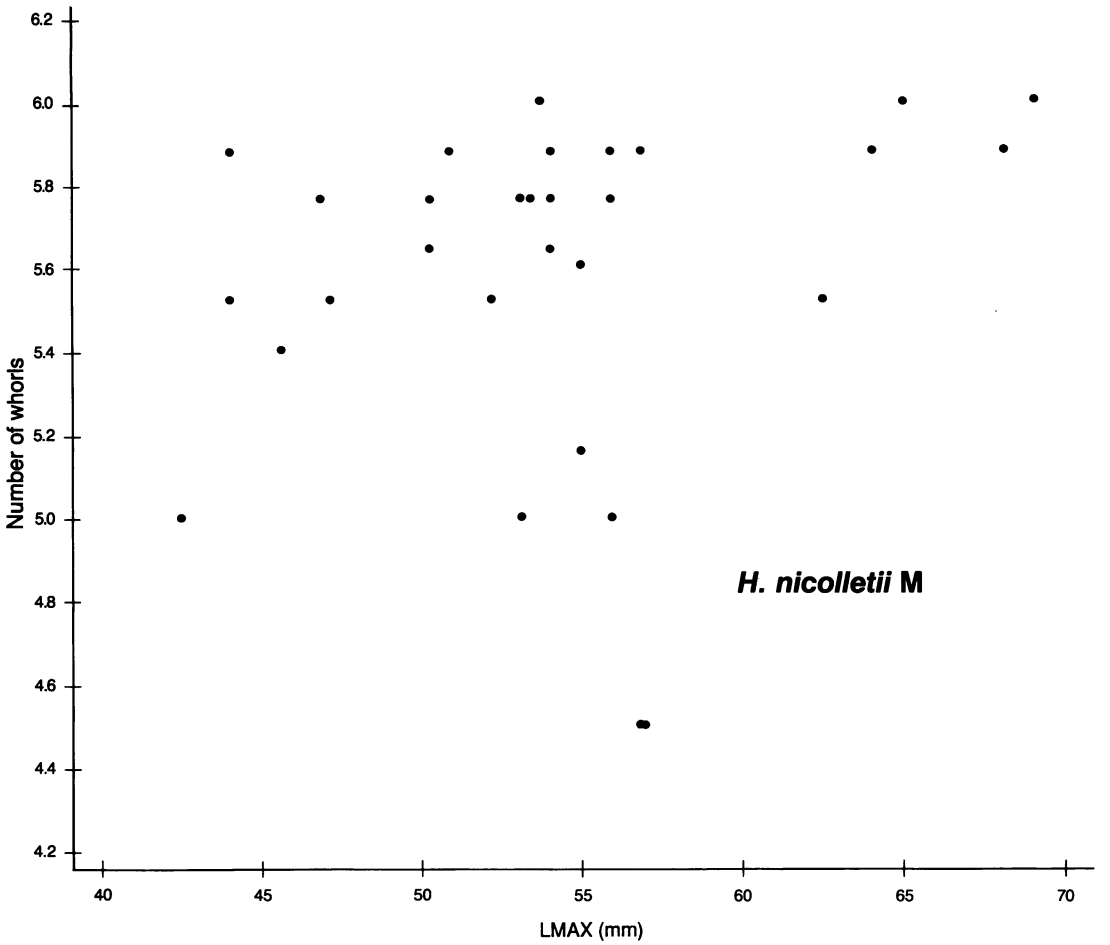

Fig. 28. Plot of number of whorls versus maximum length (LMAX) in 30 adult macroconchs of *Hoploscaphites nicolletii* (Morton).

In macroconchs the umbilical shoulder is straight in side view. A dorsal swelling develops along the shoulder in some specimens. In microconchs, on the other hand, the umbilical shoulder parallels the curve of the venter, forming a flat, broad dorsal shelf that slopes gently outward at a right or obtuse angle to the flanks. In species of *Hoploscaphites,* the average umbilical diameter (UD) and the average ratio of umbilical diameter to maximum length (UD/LMAX, relative umbilical diameter) are significantly larger in microconchs than in macroconchs. In species of *Jeletzkytes* and *Discoscaphites,* the average relative umbilical diameter, but not necessarily the average umbilical diameter, is significantly larger in microconchs than in macroconchs. For example, in *D. gulosus,* the average umbilical diameter in microconchs is approximately the same as that in macroconchs (fig. 35), but the average relative umbilical diameter is significantly larger.

SIZE: The average size of adult macroconchs is significantly larger than that of adult microconchs. The average size of macroconchs is 1.2 to 1.6 times that of microconchs or, in other words, macroconchs are, on average, 20 to 60 percent larger than microconchs. Size histograms of many species, such as *D. gulosus,* show a bimodal distribution representing the two morphs. However, the size ranges of dimorphs commonly overlap. In *D. conradi* and *D. gulosus,* the extent of overlap ranges from 20 to 30 percent of the

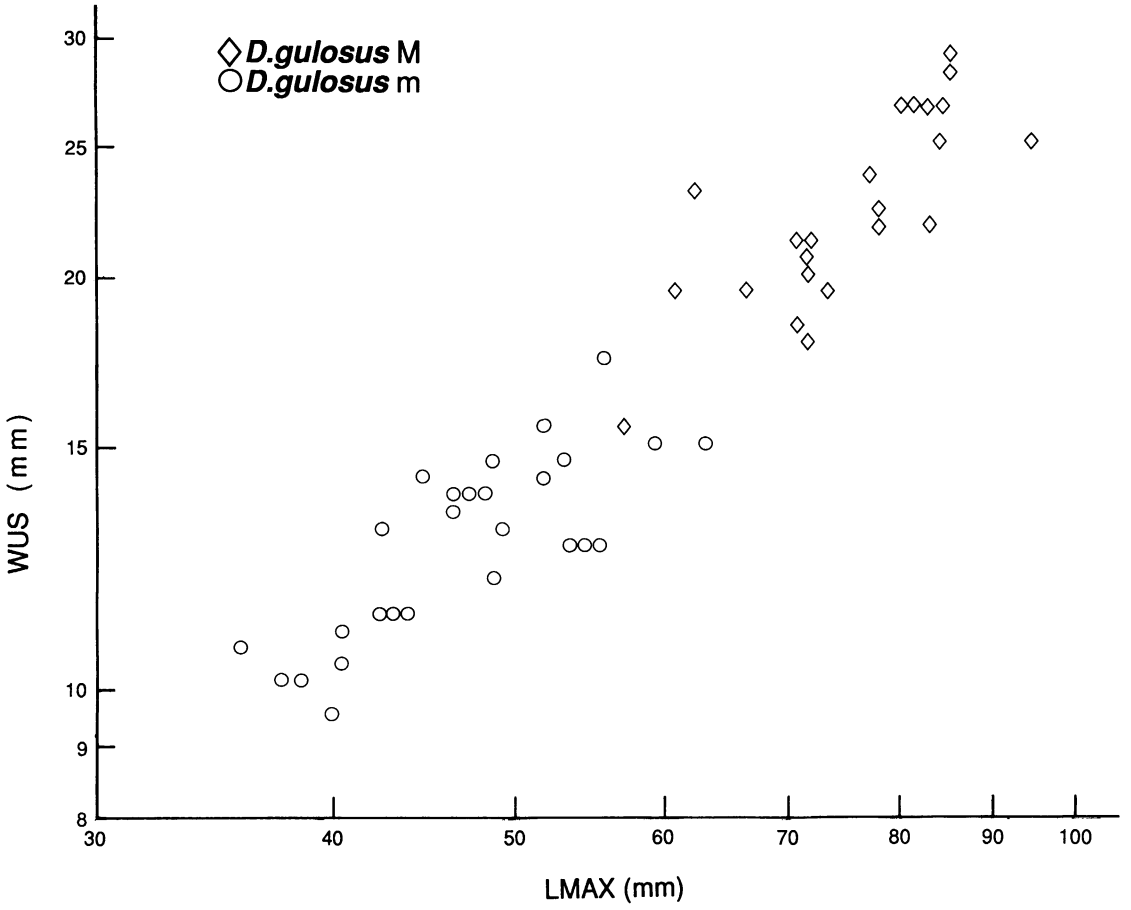

Fig. 29. Plot of whorl width at the ultimate septum (WUS) versus maximum length (LMAX) in macro- and microconchs of *Discoscaphites gulosus* (Morton).

total combined size range of both dimorphs whereas in *H. nicolletii, H. comprimus, J. spedeni,* and *J. nebrascensis* it ranges from 30 to 40 percent.

Comparable amounts of size overlap between dimorphs have been observed in other scaphite species. Based on data provided by Cobban (1969), the extent of size overlap is approximately 20 percent in *Scaphites leei* III and 50 to 60 percent in *S. hippocrepis* I and *S. hippocrepis* III. In *S. whitfieldi,* the extent of size overlap is approximately 50 percent (Landman, 1987). In contrast, no size overlap has been reported between dimorphs in *H. constrictus* from either Poland or the Cotentin Peninsula (Makowski, 1962; Kennedy, 1986a).

The size range within dimorphs is expressed as the ratio of the size of the largest specimen to that of the smallest. In macroconchs of *Hoploscaphites* and *Jeletzkytes,* this ratio ranges from 1.6 to 2.2, whereas in macroconchs of *Discoscaphites,* it ranges from 1.6 to 2.6. The largest macroconch is at least 1.6 times larger than the smallest macroconch in all species. The ratio of the size of the largest specimen to that of the smallest in microconchs of *Hoploscaphites* and *Jeletzkytes* ranges from 1.5 to 1.6, whereas in microconchs of *Discoscaphites* it ranges from 1.7 to 2.1. The largest microconch is at least 1.5 times larger than the smallest microconch in all species.

These ratios of maximum to minimum size within dimorphs in the Fox Hills scaphites are similar to those within dimorphs in other

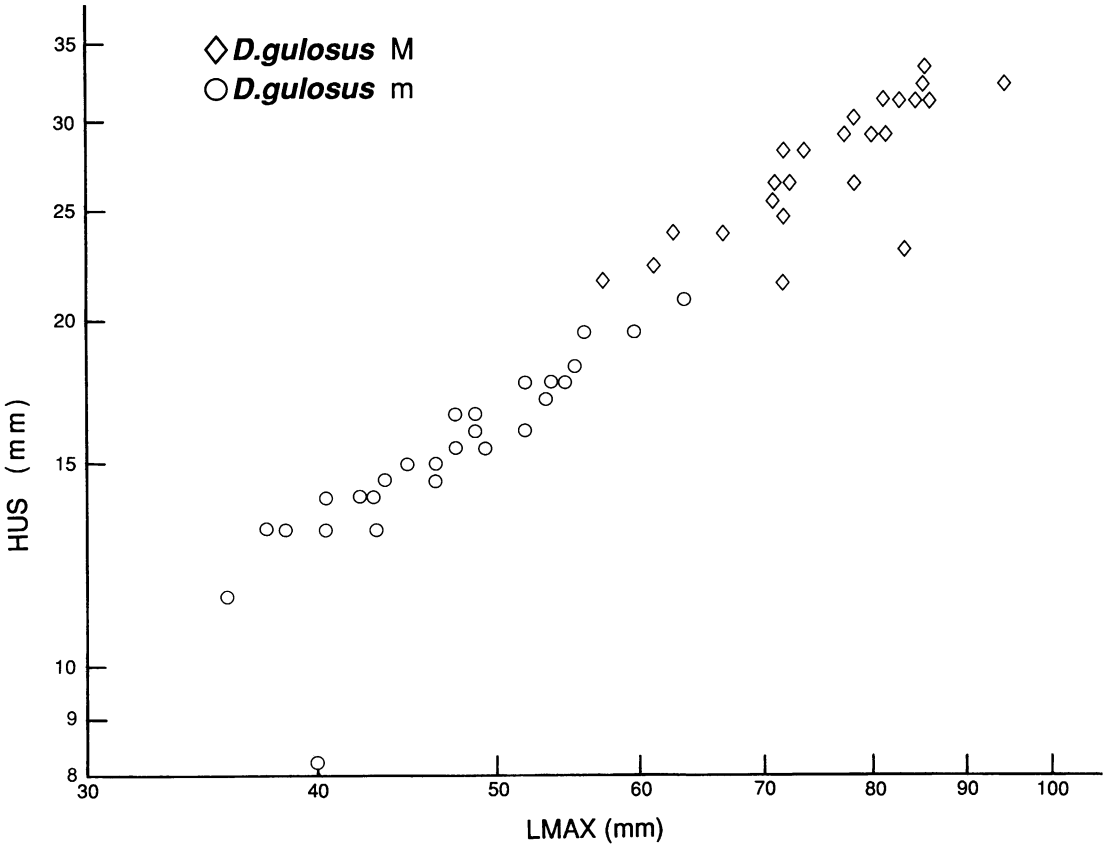

Fig. 30. Plot of whorl height at the ultimate septum (HUS) versus maximum length (LMAX) in macro- and microconchs of *Discoscaphites gulosus* (Morton).

scaphite species. In collections of *H. constrictus* from various European localities, the ratio of the size of the largest specimen to that of the smallest within each dimorph ranges from 1.4 to 1.6 (Makowski, 1962; Birkelund, 1982; Kennedy, 1986b). In *Scaphites whitfieldi,* this ratio equals 1.9 in macroconchs and 1.6 in microconchs (Landman, 1987). The ratio of the size of the largest specimen to that of the smallest within dimorphs of *S. leei* II and *S. leei* III ranges from 1.5 to 1.6 and 1.3 to 1.7 in macroconchs and microconchs, respectively (Cobban, 1969). This ratio is generally higher in *S. hippocrepis* I, II, and III and ranges from 1.5 to 2.5 in both dimorphs. However, as Cobban (1969) noted, there are rare individuals of very large and very small size within dimorphs of these species so that the actual size ratio may approach 4.0.

ORNAMENT: The pattern of ornamentation on the mature body chamber is similar in dimorphs within the same species, although it is commonly better developed in macroconchs. For example, the distinctive pattern of fine ribbing in macroconchs of *H. nicolletii* is only weakly echoed in the corresponding microconchs. Similarly, in *H. comprimus,* restriction of fine ribbing to the anterior portion of the body chamber is present in macroconchs but not in all microconchs. Because the species-specific features of the ornamentation are generally not as well developed in microconchs as in macroconchs, microconchs of closely related species are sometimes difficult to distinguish except by their direct association with the corresponding macroconchs.

There are several other minor differences in ornamentation between dimorphs. Be-

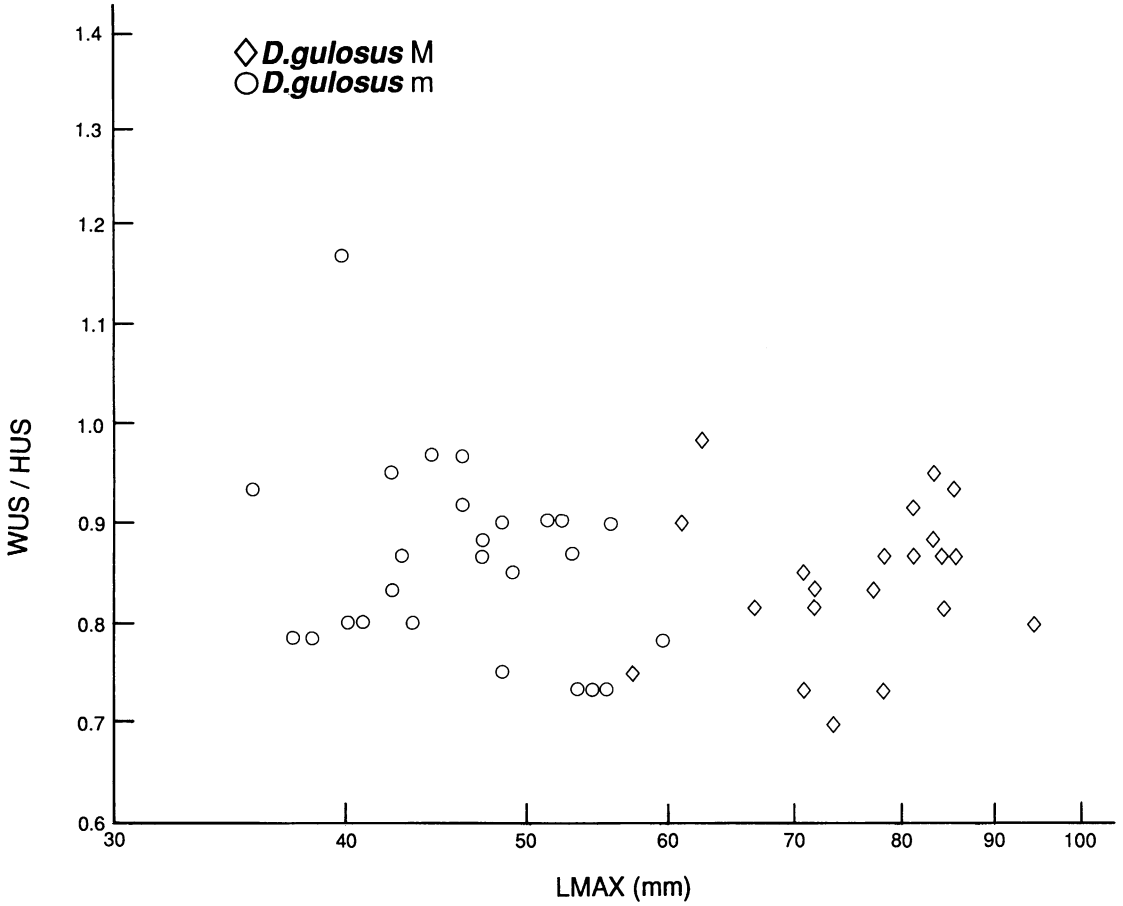

Fig. 31. Plot of the ratio of whorl width to whorl height at the ultimate septum (WUS/HUS) versus maximum length (LMAX) in macro- and microconchs of *Discoscaphites gulosus* (Morton).

cause of the difference in the whorl height of the adult body chamber, the number of rows of flank tubercles is generally larger in macroconchs than in microconchs in those species that bear flank tubercles. For example, in macroconchs of *D. gulosus* there are three or four rows of flank tubercles, whereas there are only two or three in microconchs. This disparity is greater if the difference in the whorl height of the body chamber is larger. For example, the number of rows of flank tubercles in macroconchs of *J. nebrascensis* ranges from five to seven, whereas it ranges from two to four in the corresponding microconchs.

Coincident with the larger shell size and expanded whorl height of macroconchs, the number of ribs, especially secondary ribs, is commonly higher in macroconchs than in microconchs, resulting in equivalent coverage of the shell surface by ornamentation. In other words, the ratio of the number of dorsal to ventral ribs is generally higher in macroconchs than in microconchs. For example, on the mature phragmocone of *J. nebrascensis* this ratio averages 1:5 in macroconchs and 1:3 in microconchs. In *H. nicolletii,* the ratio at the end of the mature phragmocone ranges from 1:4 to 1:6 in macroconchs and from 1:2 to 1:3 in microconchs.

Umbilical bullae are present on the mature body chambers of microconchs even if these features are absent on the corresponding macroconchs. For example, in *H. nicolletii,* microconchs bear umbilical bullae, whereas they are rare or absent on macroconchs. Sim-

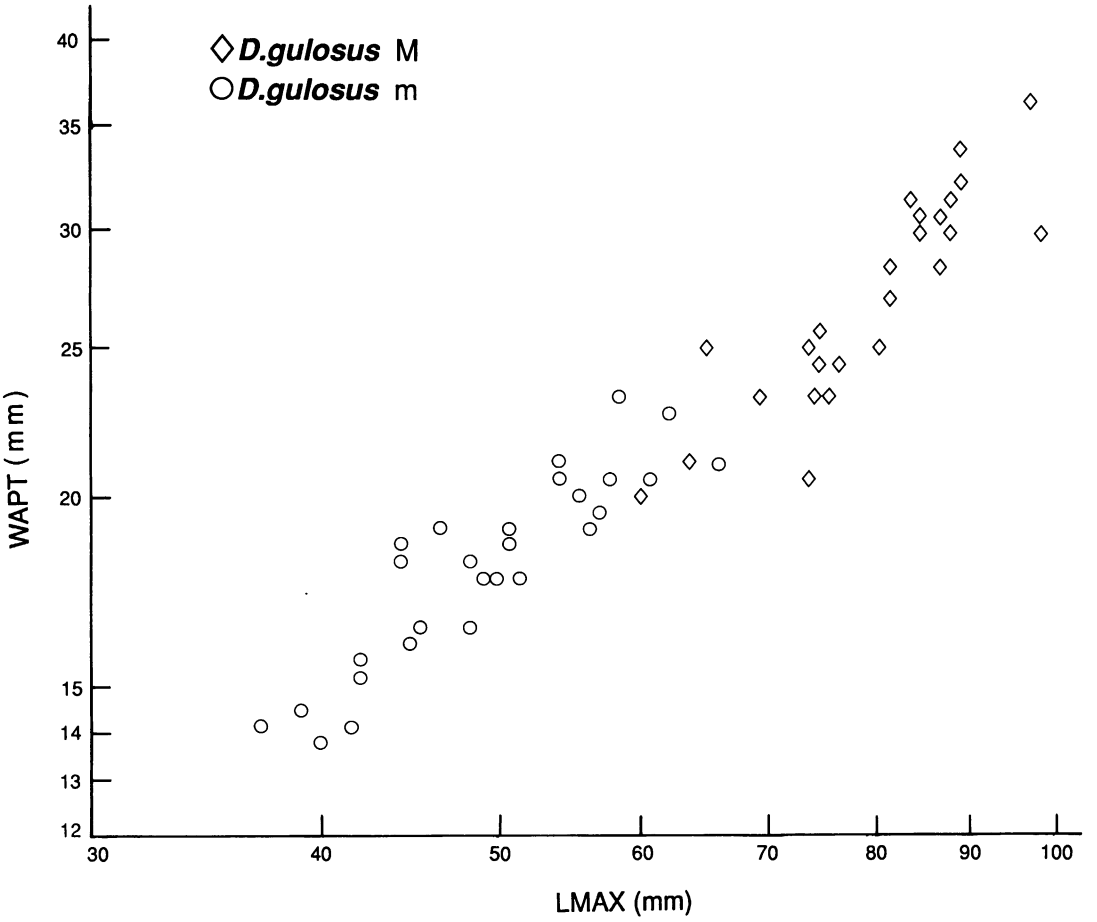

Fig. 32. Plot of whorl width at the aperture (WAPT) versus maximum length (LMAX) in macro- and microconchs of *Discoscaphites gulosus* (Morton).

ilarly, in *J. spedeni,* umbilical bullae generally persist to the aperture in microconchs, whereas in macroconchs, they may fade out on the posterior portion of the body chamber. In microconchs of *J. nebrascensis* umbilical tubercles are more prominent than flank tubercles, whereas in the corresponding macroconchs, umbilical tubercles are less prominent than flank tubercles. The ubiquity and relatively large size of umbilical tubercles in microconchs is probably related to the fact that the umbilical shoulder is curved in microconchs and straight in macroconchs.

SEPTAL APPROXIMATION: Closer spacing or approximation of the last few septa is common in both dimorphs. The pattern of septal approximation was examined in dimorphs of four species. Phragmocone chambers were counted starting from the last, most recently formed chamber (1). Interseptal distances to the nearest 0.5 mm were measured along the venter. In using length as a measure of septal spacing rather than angle, it is not possible to compare actual values among specimens of different shell diameter, only patterns. In addition, use of length tends to underestimate the degree of approximation, because intervals of equal length along the venter actually mark off progressively smaller angular increments with increasing shell diameter.

The number of chambers over which septal approximation occurred was recorded as well as the magnitude of septal approximation. To determine the number of chambers over which septal approximation occurred, we first had to locate the changeover point from ear-

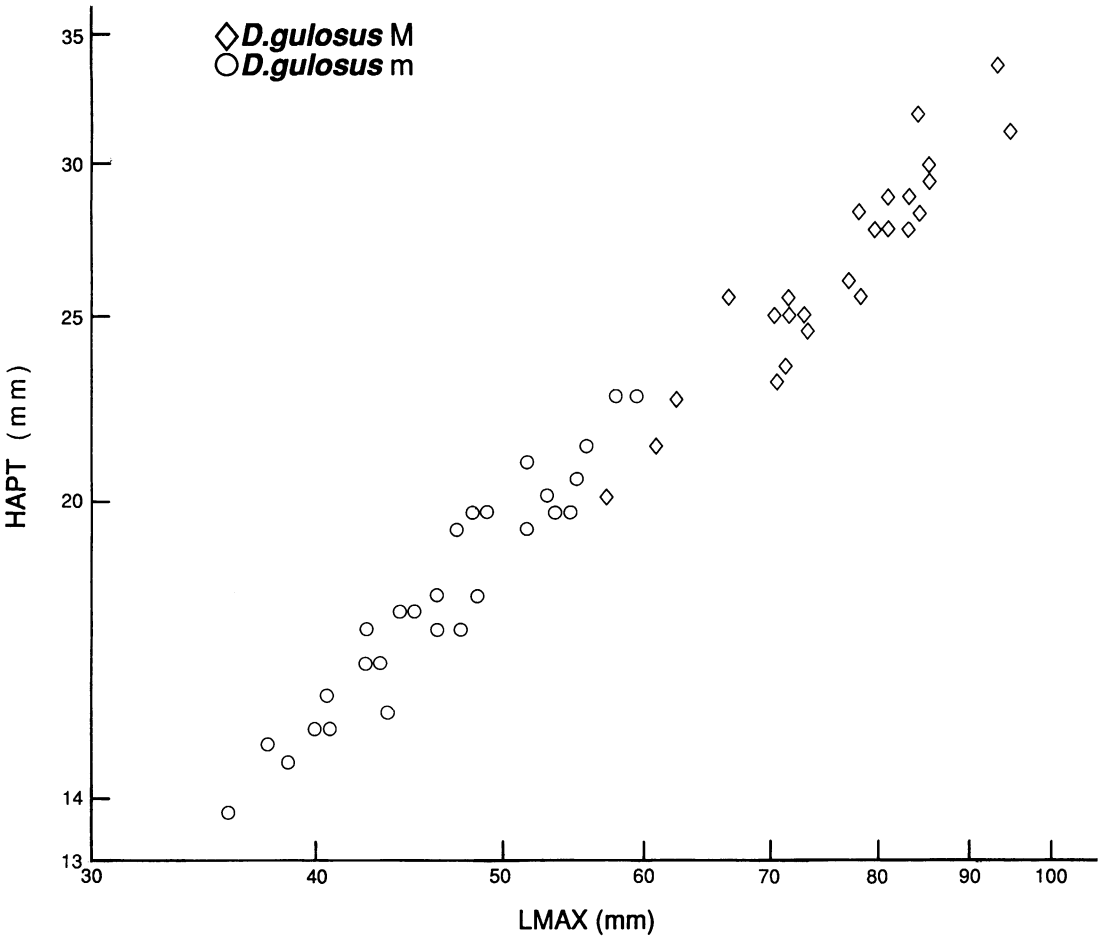

Fig. 33. Plot of whorl height at the aperture (HAPT) versus maximum length (LMAX) in macro- and microconchs of *Discoscaphites gulosus* (Morton).

lier "normal" chambers with interseptal distances characteristic of juvenile or submature growth to later chambers marked by progressively reduced distances. Interseptal distances of as many as the last eight chambers of the phragmocone were measured in each specimen. Specimens in which interseptal distances of fewer than four chambers were measurable were excluded unless these measurements revealed a definite changeover from "normal" to reduced septal spacing. To assess the magnitude of septal approximation, the interseptal distance of the last chamber was compared with that of the last "normal" chamber.

The patterns of septal approximation are clearly different in dimorphs of *H. nicolletii,* which represents the largest sample of specimens examined (fig. 36). Septal approximation occurs over more chambers and is more marked in macroconchs than in microconchs. In macroconchs septal approximation occurs over as many as the last five chambers or over as few as the last two chambers with most specimens showing approximation over the last three chambers. The decrease in septal spacing is generally monotonic. The interseptal distance of the last chamber averages less than half that of the last "normal" chamber. In contrast, septal approximation in microconchs occurs over the last two chambers or more commonly in only the last chamber. The interseptal distance of the last chamber averages approximately 70 percent of that of the last "normal" chamber.

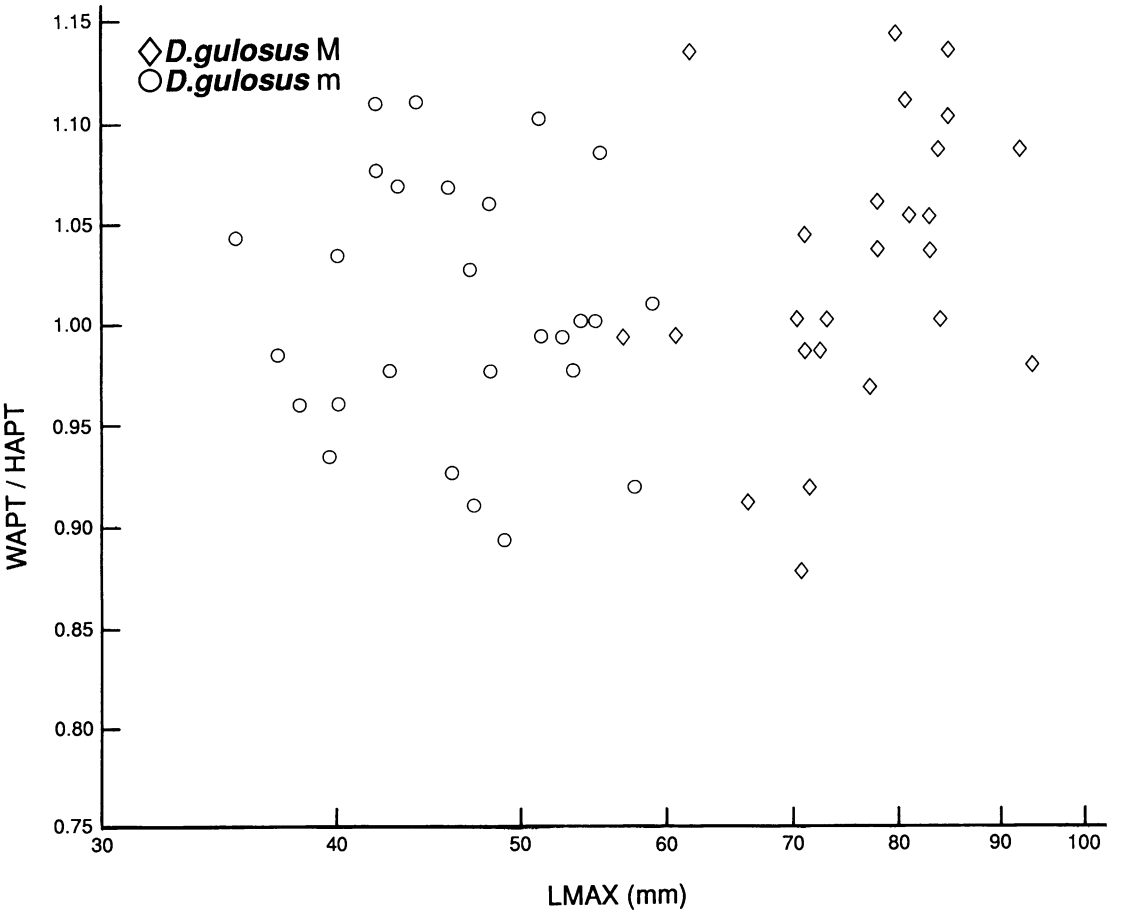

Fig. 34. Plot of the ratio of whorl width to whorl height at the aperture (WAPT/HAPT) versus maximum length (LMAX) in macro- and microconchs of *Discoscaphites gulosus* (Morton).

D. gulosus and *D. conradi* are similar to *H. nicolletii* in that septal approximation occurs over more chambers in macroconchs than in microconchs (fig. 36). In macroconchs of *D. gulosus,* septal approximation occurs over as many as the last five chambers or more commonly over the last four chambers. In the corresponding microconchs septal approximation occurs over as many as the last four chambers or more commonly over only the last three chambers. The decrease in septal spacing is generally monotonic in both dimorphs. In macroconchs of *D. conradi,* septal approximation occurs over as many as the last four chambers with most specimens showing it over the last three chambers. In the corresponding microconchs septal approximation occurs over as many as the last four chambers with most specimens showing it over only the last two chambers. In contrast to *H. nicolletii,* the magnitude of septal approximation in *D. gulosus* and *D. conradi* is nearly the same in macroconchs and microconchs. The interseptal distance of the last chamber averages a little less than half that of the last "normal" chamber in dimorphs of both species.

There is no difference in the pattern of septal approximation between dimorphs of *J. spedeni* (fig. 36). The majority of specimens in both dimorphs shows approximation over the last four or five chambers. In addition, both dimorphs experience a similar reduction in septal spacing of approximately half

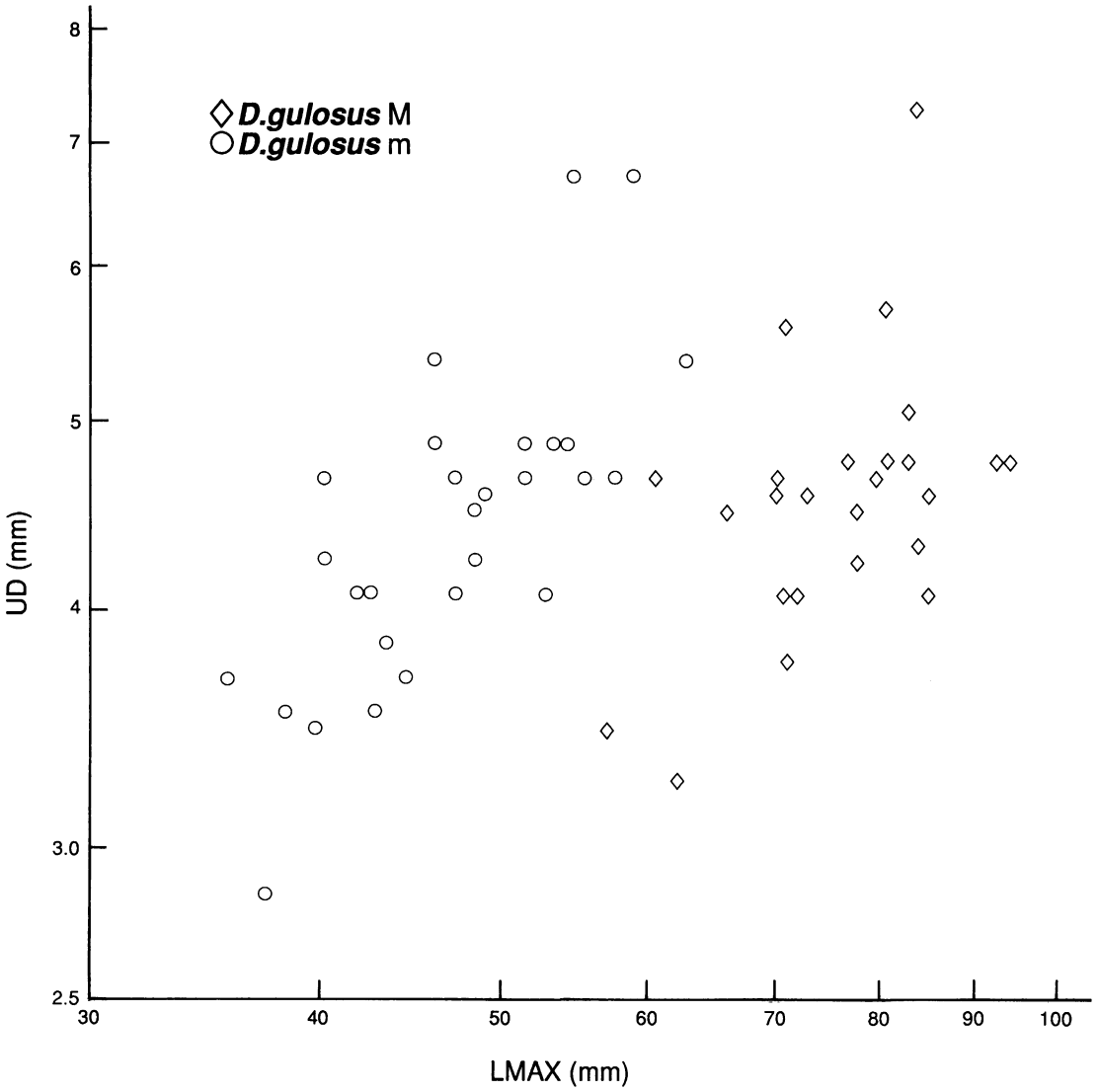

Fig. 35. Plot of umbilical diameter (UD) versus maximum length (LMAX) in macro- and microconchs of *Discoscaphites gulosus* (Morton).

relative to the septal spacing of the last "normal" chamber.

In other ammonites in which septal spacing has been recorded, there is, in general, a difference in the pattern of septal approximation between dimorphs. Microconchs show septal approximation in the last one or over the last two chambers whereas macroconchs show progressively reduced septal spacing over many more chambers (Makowski, 1962; Crick, 1978; Lehmann, 1981b).

ASSOCIATED STRUCTURES

Mandibles

Remains of mandibles are associated with the body chambers of all three scaphite genera in the type Fox Hills Formation. They are common with *Hoploscaphites* and *Jeletzkytes*. Mandible form and composition are the same in all three genera.

The lower mandible in ammonites is usually larger and thicker than the upper man-

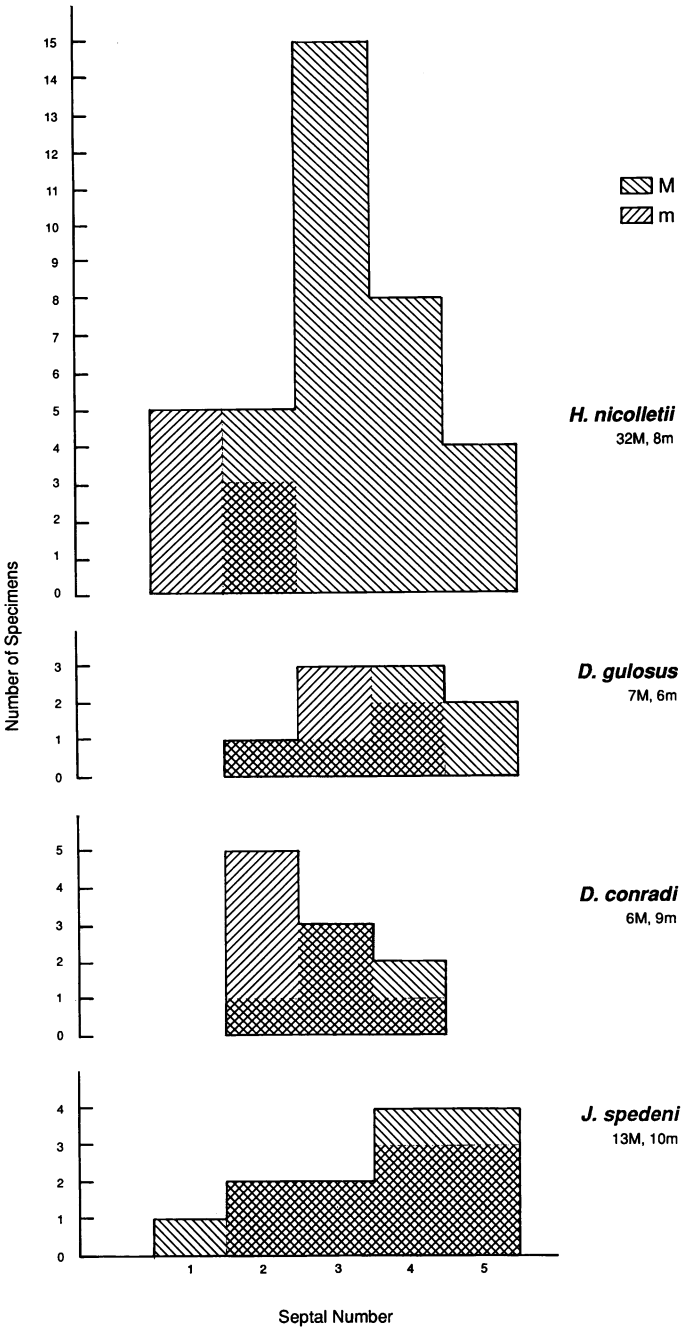

Fig. 36. Histogram of number of specimens versus number of chambers over which septal approximation occurs in macro- and microconchs of *Hoploscaphites nicolletii* (Morton), *Discoscaphites gulosus* (Morton), *D. conradi* (Morton), and *Jeletzkytes spedeni,* n. sp. Chambers are numbered starting with the last, most recently formed chamber of the phragmocone (1).

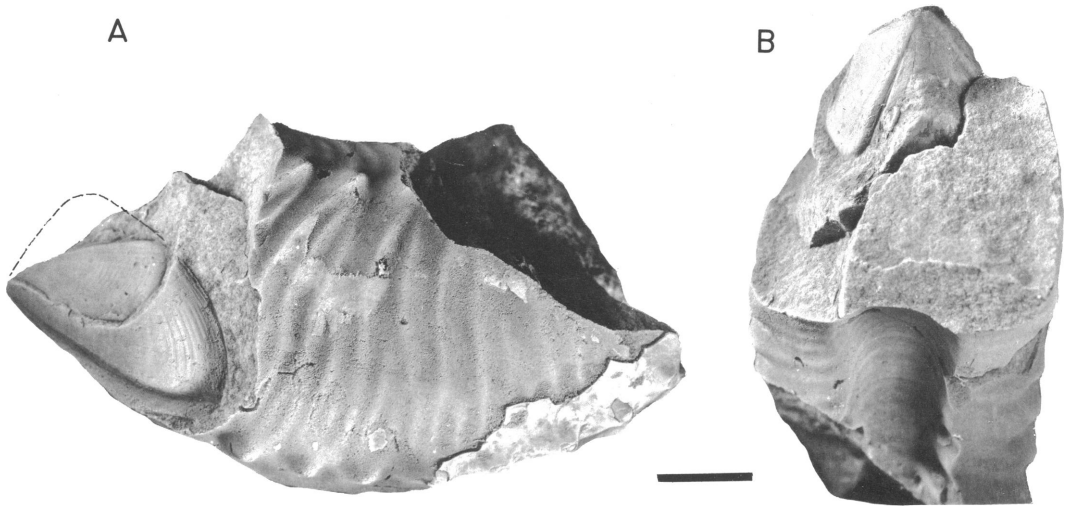

Fig. 37. Specimen of scaphite mandibles illustrated and described by Meek and Hayden, USNM 386. **A.** Left lateral view of upper mandible nested within gape of lower mandible. **B.** Dorsal view of upper mandible. Scale bar = 1 cm. (Photos courtesy of E. Yochelson)

dible and most lower mandibles are reinforced with an outer layer of calcite; consequently, they are by far the most commonly preserved mandibular element. In size and configuration, the lower mandible is very similar to the body chamber cross section at or near the aperture, a feature which early on led to their interpretation as ammonite opercula. Called "aptychi" or "anaptychi," depending on whether they had the calcitic layer or not, a whole terminology based on form and structure evolved around the many variations found. Within the last 25 years increased study of both lower and upper structures, stimulated primarily by the work of Lehmann (1972, 1981a, and other papers), has demonstrated conclusively that these are buccal structures homologous with the jaws of living cephalopods, but not necessarily analogous to them in function. Their considerable variation in form among the different ammonite groups strongly suggests diversity in function of the buccal apparatus.

In the 1850s, F. V. Hayden collected from the Fox Hills Formation along the Moreau River a remarkable specimen (USNM 386, fig. 37) showing an upper mandible nested within the gape of the lower mandible plates, the entire structure lodged in the anterior end of a body chamber fragment of a microconch of *Jeletzkytes nebrascensis* [= *Scaphites* (*Discoscaphites*) *cheyennensis* of Meek]. Meek (Meek and Hayden, 1864: 118–121; Meek, 1876: 438–441, 416–418) described the specimen and, against prevailing opinion, interpreted it as the remains of jaws. The Meek and Hayden specimen is cited frequently in the more recent literature on aptychi and ammonite mandibles and has played a significant role in revealing their true nature and relationships (Lehmann, 1971). Our larger collections from the type Fox Hills have no specimen to match it, although they include examples of both lower and upper mandibles and six specimens with the upper mandible lying within the plates of the lower mandible (figs. 38, 39).

The lower mandible of the Fox Hills scaphites consists of paired, externally convex plates, the mirror image of one another, that meet along the plane of bilateral symmetry (fig. 38B). The commissure of the plates is ventral in position and straight for most of the length of the lower mandible (fig. 40). The commissure meets the straight anterior edge of the plates at right angles; the apex of this juncture is homologous with the beak of the lower mandible in modern cephalopods. Modifications around the apex of the plates in Fox Hills scaphites consist of some thickening of the chitinous material and the development of a small narrow fold whose sides

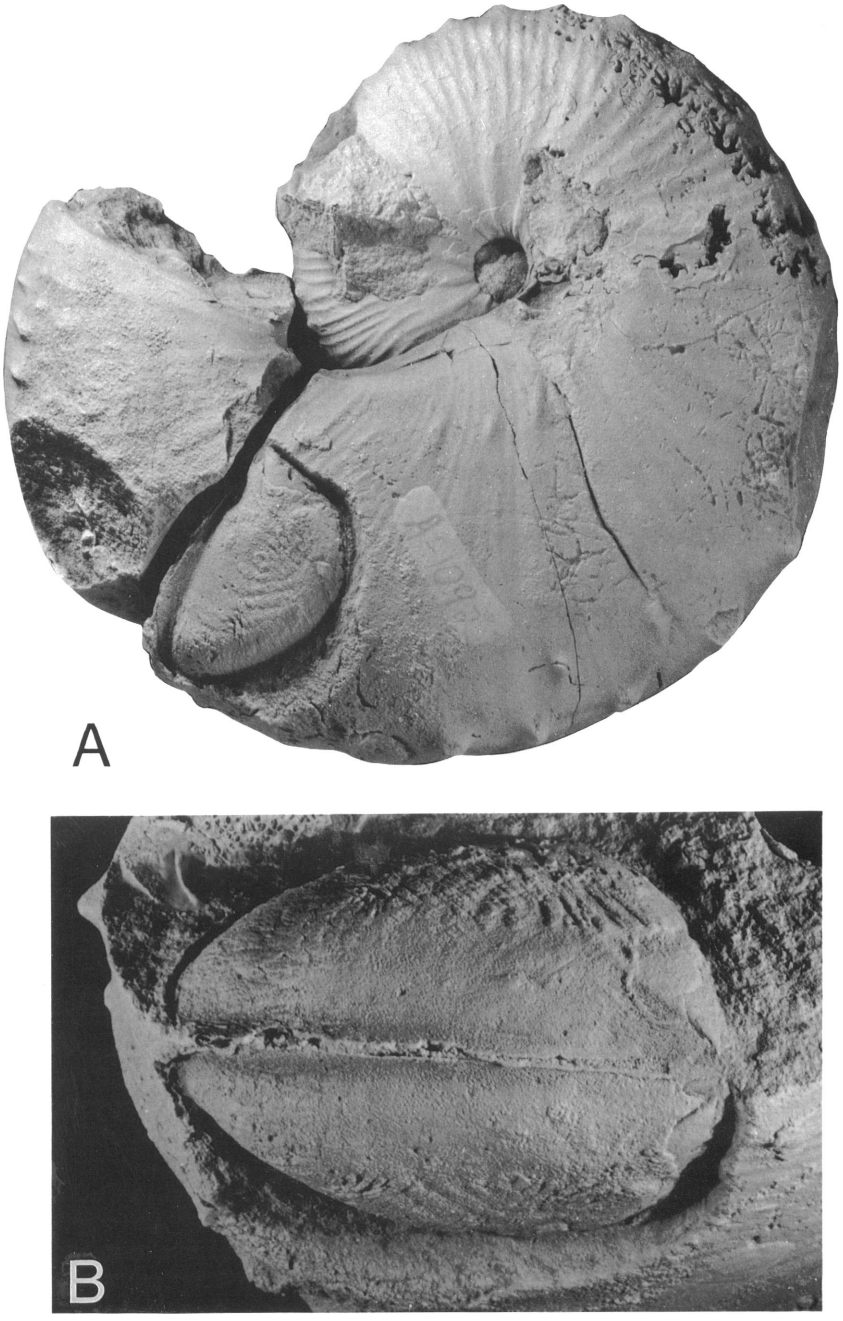

Fig. 38. Macroconch of *Jeletzkytes spedeni,* n. sp., with lower mandible preserved in body chamber, YPM 23220, loc. 248, POAZ. **A.** Left lateral. **B.** Close-up of ventral side of lower mandible after removal of the anterior part of the body chamber, ×2. Note converging ridges. Anterior direction toward right.

converge toward the apex. This fold is the anterior end of the arcuate area of greatest convexity that extends diagonally upward across the body of the plates. On smaller, flatter plates the fold is slight and its position marked by small grooves on the internal mold that flank it and converge toward the apex. On larger mandible plates, such as those of

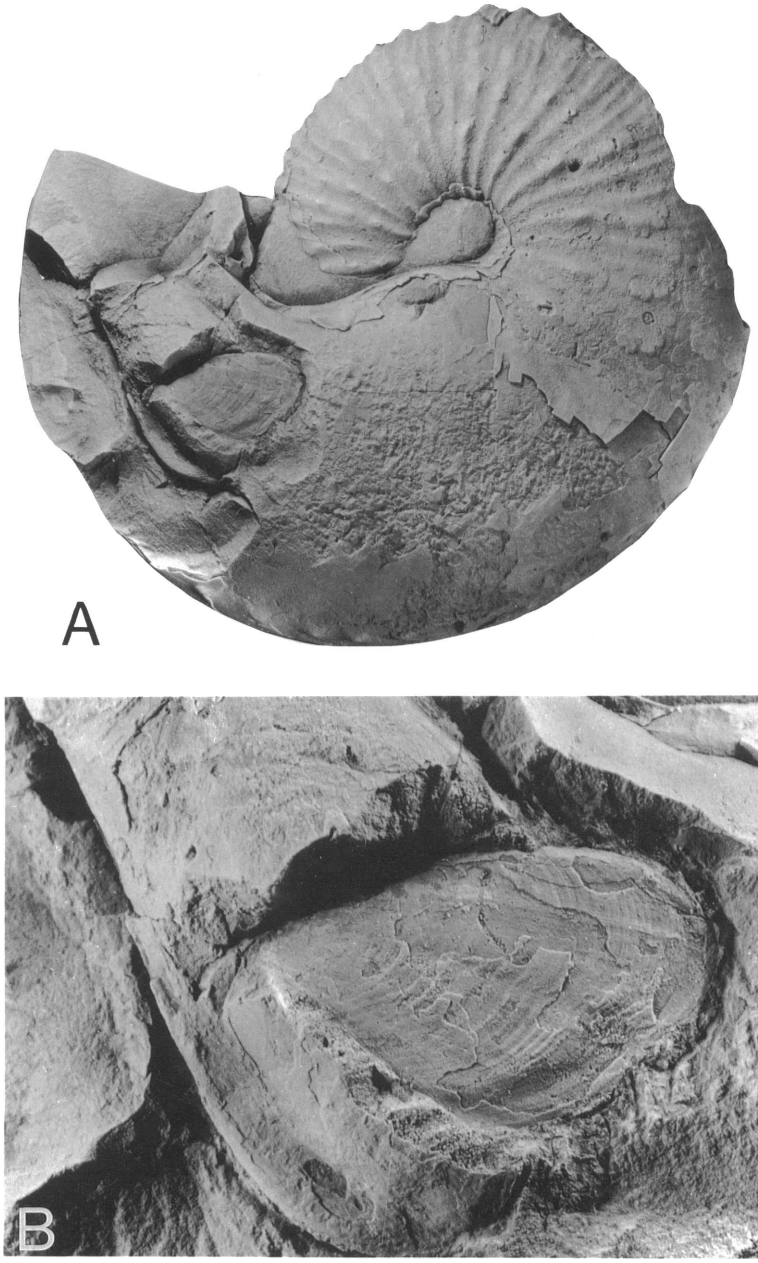

Fig. 39. Macroconch of *Jeletzkytes dorfi,* n. sp., with upper and lower mandibles in the anterior part of the body chamber, BHI 2038, Pierre Shale, north of Wall, South Dakota. **A.** Left lateral. **B.** Close-up of the left wing of the upper mandible exposed where part of the left plate of the lower mandible is missing, ×3.

Jeletzkytes (fig. 41A) the fold is prominent up to 10 or 12 mm from the apex and projects slightly forward, toothlike, beyond the apex. A short distance posterior to the apex a flat flange appears bordering the commissure; it increases gradually in width as the margin of plate convexity rises dorsally away from the commissure (fig. 40A). The flange narrows and disappears where the commissure ends and the plate edge curves upward around the posterior end of the plate. From this point the plate edge rises gradually forward, the

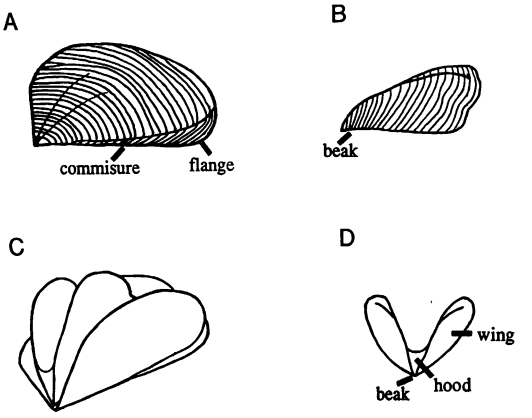

Fig. 40. Morphology of scaphite mandibles. **A.** Lower mandible, external view of left plate. Anterior direction toward left, dorsal direction toward top. **B.** Upper mandible, external view of left side. Anterior direction toward left, dorsal direction toward top. **C.** Oblique view of mandibles in approximate life position. Anterior direction toward lower left, dorsal direction toward top. **D.** Upper mandible, anterior view. Dorsal direction toward top.

plate reaching its maximum width at about one-third of its length from the straight anterior edge, which it curves ventrally to join.

Plates of the lower mandible consist of a thin, laminated, inner layer of chitinous material and an outer layer of prismatic calcite (figs. 41, 42). This calcite is presumed to be the original composition of the outer layer as the Fox Hills concretions preserve the aragonitic shell of the ammonites as well as both calcitic and aragonitic shell layers of associated bivalves. The calcitic layer is usually absent on even slightly weathered surfaces, and in freshly exposed specimens it may be partly or entirely absent as a result of removal prior to formation of the enclosing concretion. On the Meek and Hayden specimen, a 0.75 mm thick layer of prismatic calcite is preserved on only one of the small pieces broken away from the lower mandible (fig. 37); it is absent elsewhere on the specimen, its former presence indicated by a gap in the matrix above the chitinous layer. The calcitic layer varies in thickness with specimen size, but rarely exceeds a millimeter in our specimens. Around the outer periphery of the plates, the calcitic layer is rimmed by the upturned edges of the underlying chitinous material; toward the commissure the calcitic layer crosses the flange and thins out around its reflexed edge (fig. 42). One of our specimens shows the layer on the apex of the plates; it appears to be slightly thicker there in association with the slightly thicker layer of chitin.

Well-preserved lower mandible specimens show that where the flange along the commissure is present the plates are distinctly separate. In sections across the flange, the chitinous layer can be seen to be reflexed sharply back under the plate for several millimeters before it terminates (fig. 42); the calcitic layer thins out on the bend of the chitinous layer. The flange commonly occupies about $\frac{5}{6}$ of the length of the plate along the commissure. Along the remaining $\frac{1}{6}$, the plates meet along a sharply defined straight edge that shows a thin line on specimens in which the apices of the right and left plates abut. Many of our specimens occur as single plates; on these, the commissure at the apex is always sharp and straight with no indication that the opposite plate was broken from it. Frequently, specimens show both plates essentially in their correct relative position but separated from one another by matrix. Also common are juxtaposed plates that have rotated slightly relative to one another so that their apices overlap. These relationships point to plates free to react individually to postmortem influences, i.e., plates which interfaced along the commissure at the apex but whose chitinous layer in that area was not continuous between plates.

The plates of the lower mandible are ornamented with concentric ribbing that follows much finer growth lines, which are visible only on the surfaces of very well-preserved plates (figs. 40, 41A, C). On the latter, a pattern of very fine striations radiates out from the apex over the convex part of the plate. On the flange, ribs and growth lines slant diagonally forward to the commissure (fig. 41C). Where the lower mandible plates are directly associated with a scaphite specimen, maximum length of the plates consistently approximates the height of the aperture. The mandibles of juveniles are more delicate and less common than those of adults. On these smaller plates, we have been unable to find the calcitic layer; whether it was added only

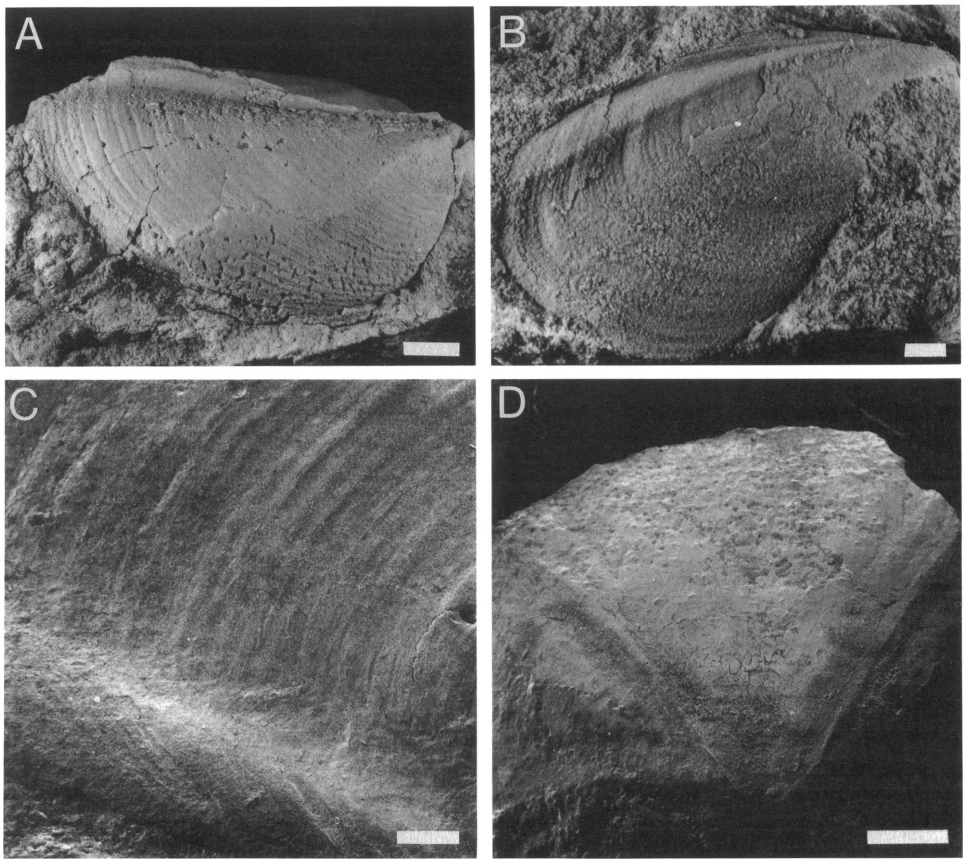

Fig. 41. Scaphite mandibles. **A.** Lower mandible of *Jeletzkytes spedeni,* n. sp., YPM 23224, loc. 21, LNAZ. Anterior direction toward right, dorsal direction toward bottom. Scale bar = 5 mm. **B.** Upper mandible, YPM 23213, loc. 222, LNAZ. Anterior direction toward right, dorsal direction toward top. Scale bar = 1 mm. **C.** Close-up of lower mandible showing ribs reflexed along the flange, YPM 32370, loc. 104, LNAZ. Anterior direction toward lower right. Scale bar = 500 μm. **D.** Anterior view of upper mandible of *J. nebrascensis* (Owen) showing its beaklike structure, YPM 23215, loc. 73, TLM. Dorsal direction toward top. Scale bar = 1 mm.

in the adult stage or removed by postmortem dissolution remains to be determined. Warping, bending, and rolling of small plates is common, but could have happened after decalcification. Even large plates were apparently somewhat flexible and show warping.

The upper mandible (figs. 37, 39, 40B–D, 41B, D) is a single piece of chitinous material thinner overall than that of the lower mandible plates except at its beaklike apex. The upper mandible consists of two vertical, winglike, lateral parts that converge as they narrow anteriorly and join to form the beaklike structure (figs. 40D, 41B, D). The maximum length of the upper mandible is approximately two-thirds that of the lower mandible in the Fox Hills scaphites. The thin wings of the upper mandible are rarely preserved entire and are commonly crumpled and often separated from the thicker beaklike anterior end. Like the plates of the lower mandible, the wings of the upper mandible are ornamented by concentric ribs that follow finer growth lines (figs. 40B, 41B). An indentation low on the rounded posterior margin of the wing imparts a slightly bilobate aspect rather butterflylike in outline, the upper lobe the larger (figs. 40B, D, 41B). Close to the dorsal edge of the wings, beginning near their posterior end, a ridge forms which becomes narrower and more pronounced forward, as its flanks become more tightly infolded. The

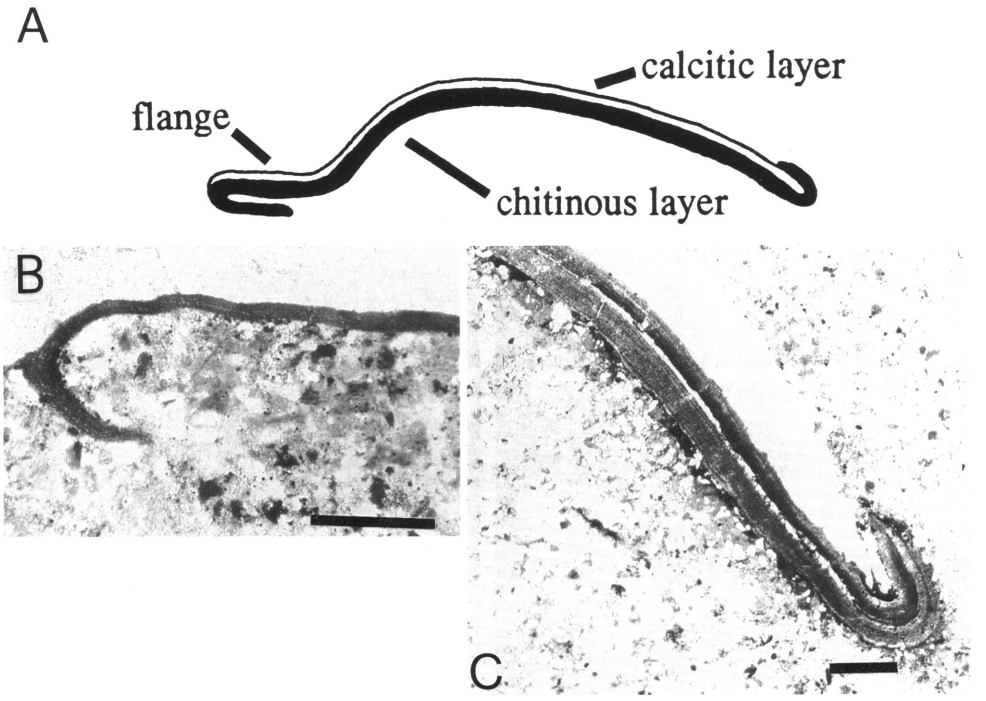

Fig. 42. Morphology of lower mandible. **A.** Schematic cross section through one of the plates of the lower mandible. Dorsal direction toward right. **B.** Cross section showing the reflexed chitinous layer of the flange, YPM 23221, loc. 4, TCM float. Scale bar = 0.5 mm. **C.** Cross section showing the upturned edge of the chitinous layer, YPM 23223, loc. 33, TLM. Scale bar = 0.5 mm.

ridges join at the apex usually subtending an angle between 40 and 70°. The wings terminate laterally against the ridges on the beak and the triangular space between the ridges is filled for a short distance behind the apex by a bridge of chitinous material (fig. 41D; "hood" of Tanabe, 1983: 678). Thickening of the chitinous material begins about where the wings are first joined anteriorly by the hood. The beaklike part of the upper mandible is formed primarily by the thickened anterior portions of the wing ridges, which curve centrally as they converge, the point of convergence extending slightly beyond the flanking anterior ends of the wings to form the point of the beak.

In general form, the upper mandible is quite similar to the upper mandible of desmoceratids illustrated by Tanabe (ibid., p. 679). The scaphite upper mandible may also be similar to it in structure. Tanabe (ibid., p. 678) interpreted the desmoceratid upper mandible as consisting of inner and outer lamellae as in modern cephalopod beaks. The outer lamella comprises the hood, the inner lamella the lateral wall—what we refer to here as the "wings" of the scaphite upper mandible. Preservation of our specimens is such that distinct inner and outer lamellae are indistinguishable in the thickened chitinous material around the beak. If the scaphite upper mandible had inner and outer lamellae they were most likely joined together in life, for if separate as in modern cephalopods, one would expect sediment to be preserved between the lamellae.

The mandibles of the scaphites included herein were certainly usable to some degree as jaws, although obviously not for biting and tearing as are the more specialized beaks of *Nautilus,* some other ammonoids, and coleoids. They are unusual in having separate plates in the lower mandible, each with its apex thickened and pointed. These parts of the lower mandible, together with the beak of the upper mandible, could have performed

a plucking or grasping function with enhanced manipulation if the separate lower mandible plates could have operated somewhat independently. Lehmann's (1981a: 150) proposition that the lower mandible acted as a scoop to gather sediment might apply to some ammonites with univalved lower mandibles, but scaphites with separate "toothed" lower mandible plates do not seem adapted for this function and more likely gathered their food directly from the substrate or bottom flora.

The secondary use of the lower mandible as an operculum is no longer a popular hypothesis (Morton, 1981), although Lehmann and Kulicki (1990) recently revived the concept of a "double function." Lower mandibles of the Fox Hills scaphites do conform closely to the aperture in size and shape, except for a bit of a gape on the ventral midline at the presumed position of the funnel. Unlike the illustration of a scaphite aperture shown in Lehmann and Kulicki (1990: fig. 1, p. 326), the aperture of the Fox Hills scaphites has rounded dorsal shoulders and only a slight, if any, impression of younger whorls. The uncoiling of the body chamber commonly brings the aperture free of the phragmocone and the anterior projection of the dorsal margin of the aperture tends to partially fill the impressed zone. Additionally, the chitinous inner layer of the lower mandible, the "organic sublayer" of Lehmann and Kulicki (ibid., p. 326), does not extend as an organic fringe beyond the outer calcitic layer as shown on their illustration; but as we have shown (fig. 42) it reflexes back over the edge of the calcitic layer for a short distance and terminates. Without a flexible fringe of chitinous material to provide adjustments, the scaphite lower mandible would have to have been a rather precise fit of the aperture to act effectively as an operculum. If the life position of the buccal mass was such that the commissure of the plates of the lower mandible was perpendicular to the plane of the aperture, it would have taken a 90° rotation of the buccal mass to bring the lower mandible into position as an operculum, and would also have necessitated a flattening of the ventral side of the buccal mass to bring the plates into the same plane. Such a maneuver is scarcely credible. The example is the extreme possibility; more likely, the commissure of the lower mandible plate was at a less than 90° angle to the plane of the aperture and the buccal mass more rounded as in living cephalopods. The apices of the plates of the lower mandible could still have met effectively with the beak of the upper mandible if the long axes of the plates diverged and slanted ventrally backward, but it still would have taken a considerable rotation of the buccal mass, not likely less than 60°. Lehmann and Kulicki (1990: 330) suggested that the retractor muscle, which pulled the animal into the shell, may have been inserted in the cephalic complex so as to bring about its rotation "almost automatically" on retraction. They estimated that the lower mandible could have been brought into place as an operculum by a rotation of as little as 45°.

In the Fox Hills scaphites, there is a constriction at the aperture and in some species, an overall slight narrowing through the hook. Placement of the lower mandible in the aperture would have been a very snug fit, whereas if it were held behind the constriction, or somewhat within the body chamber, or slanted backward from the dorsal edge, it could have been better accommodated and the slant would have further reduced the necessary degree of buccal rotation. This is as conjectural as previous attempts to maintain the secondary opercular function of the lower mandible. Convincing evidence of the position in life of the lower mandible is not likely to be found because even the best fossil mandibles, including the Meek and Hayden specimen, have undergone shifts and rotations of parts after decomposition of the enclosing tissues, obscuring the true position of the upper mandible relative to the lower. We do not agree with Morton (1981: 61) that "—the ventral position inside the body chamber is likely to have been closest to the position in life,"; more likely this position is where the buccal mass collapsed during decomposition. We do agree with him (ibid.) that "some problems remain," enough, we believe, to hold open the possibility of the secondary opercular function.

Hooklike Structures

Another structure found associated with the scaphites from the type Fox Hills Formation

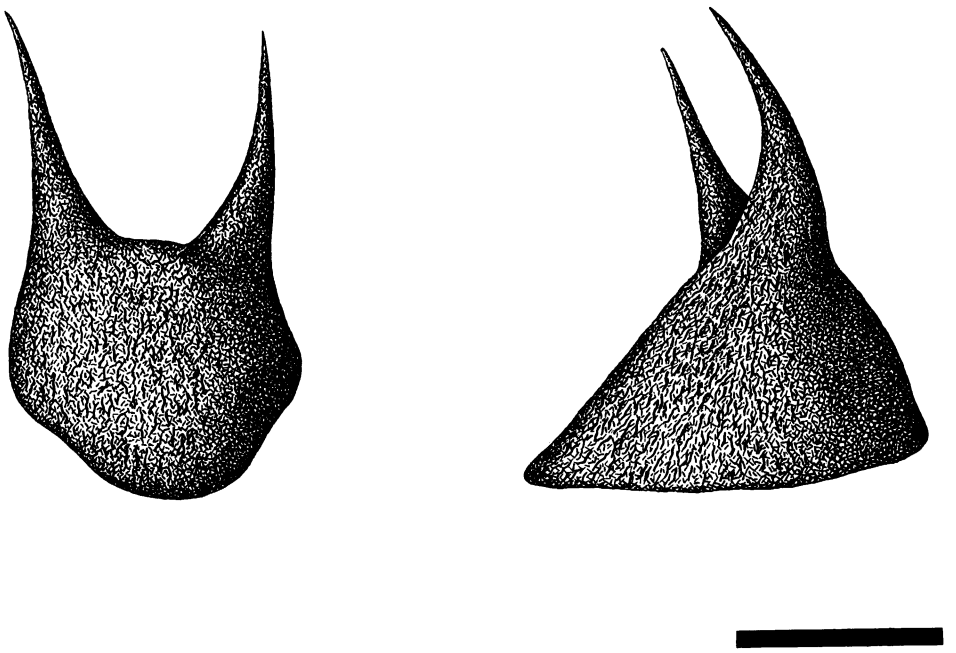

Fig. 43. Sketch of hooklike structures. The base of the hooklike structures appears to have a long dimension; the two horns arise opposite each other on either side of a long axis of symmetry and closer to one end. The horns diverge slightly away from the axis and bend toward the larger end. Scale bar = 1 mm. Drawing by Carl Wester.

is preserved, like the mandibles, as thin dark crusts, presumably of altered chitinous material. This structure consists of an inverted cup-shaped base 2 to 5 mm in diameter from which two hornlike processes taper upward to sharp points (fig. 43). The entire structure to the points of the "horns" is hollow. These structures commonly occur with ammonites where mandibles are also preserved, often in the body chambers and around the aperture. As the drawing (fig. 43) and scanning electron micrographs (fig. 44) show, the bases appear to have a long dimension; the two "horns" arise opposite each other on either side of a long axis of symmetry and closer to one end. The "horns" diverge slightly away from the axis and bend toward the longer end of the base. The base curves slightly inward forming a subcircular opening.

That the structures are indeed parts of the scaphites is indicated by their close association with shells of *Hoploscaphites* and *Jeletzkytes* in which they frequently occur in the body chamber or near the aperture (fig. 45). They are most numerous in the concretions of the Lower and Upper *nicolletii* Assemblage Zones where *Hoploscaphites nicolletii* is particularly abundant. They are preserved of the same material as the mandibles whereas the preservation of crustaceans, beetles, plant material, and fish parts in these concretions is recognizably different. Particularly convincing is the occurrence of smaller specimens with the smaller genus *Hoploscaphites* and larger specimens with the larger genus *Jeletzkytes*. All are consistently identical in shape no matter what the size.

The structures may occur singly or more than one in a body chamber. One microconch of *Jeletzkytes nebrascensis* has 16 individual structures scattered within the posterior part of the body chamber (fig. 46). Because the material is very thin and the tips of the "horns" are very delicate, recovery of whole specimens is difficult.

Somewhat similar structures have been found in the Upper Cretaceous ammonite *Rhaeboceras* but no study of them has yet been published. We have seen specimens of these; their preservation is generally like the structures in *Hoploscaphites* and *Jeletzkytes* and, not unexpectedly, they are larger in size

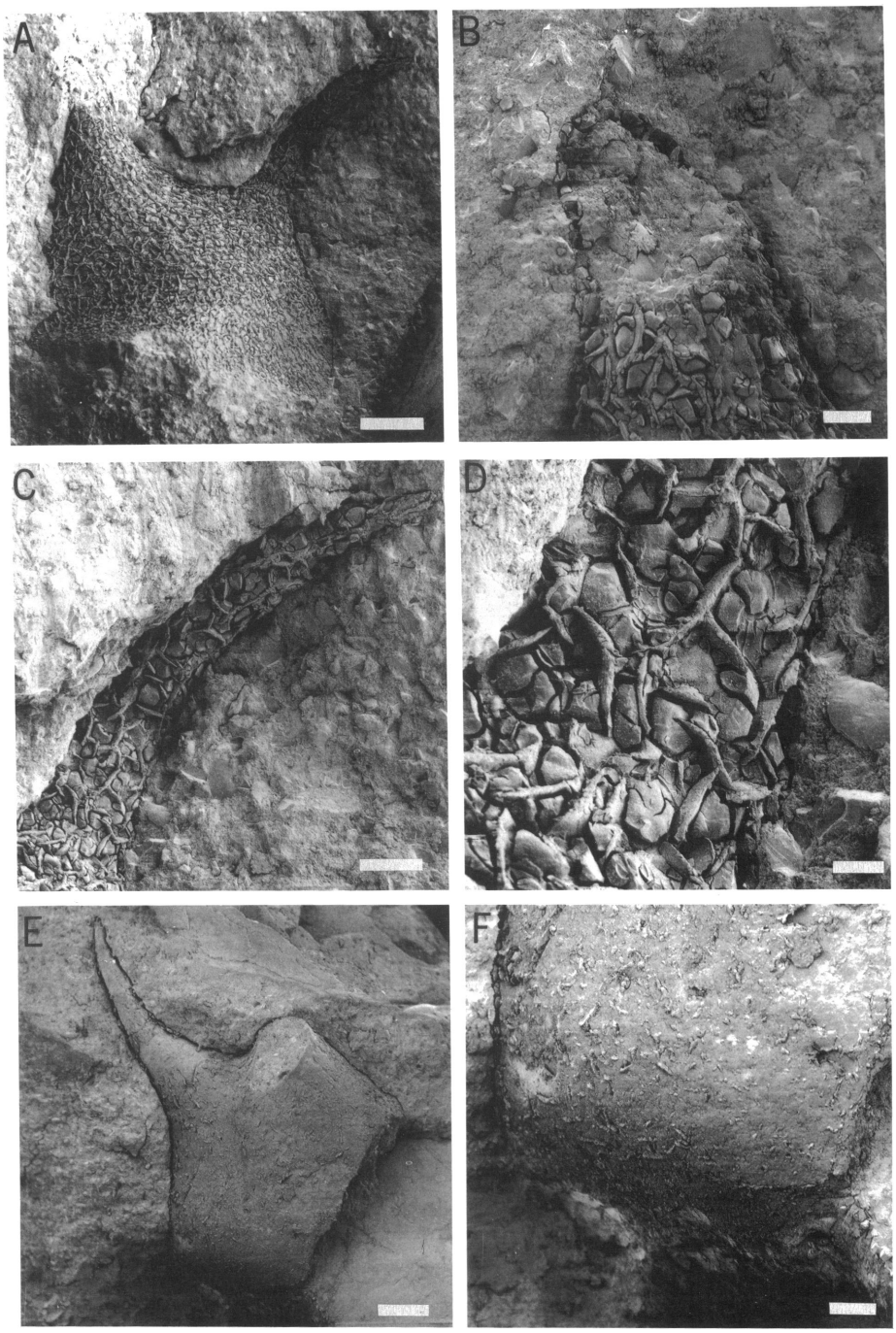

Fig. 44. Morphology of hooklike structures. **A–D.** Specimen partially embedded in matrix, YPM 34110, loc. 21, LNAZ. **A.** Overview showing that one of the "horns" is broken. Scale bar = 500 μm. **B.** Close-up of the broken "horn" revealing that it was originally hollow although it is now filled with matrix. Scale bar = 100 μm. **C.** Other "horn" tapers to a sharp point. Scale bar = 200 μm. **D.** Close-up showing the outer surface. Scale bar = 50 μm. **E, F.** Specimen partially embedded in matrix, YPM 34118, loc. 312, Fox Hills Fm. **E.** Overview. Scale bar = 500 μm. **F.** Close-up of recurved base. Scale bar = 200 μm.

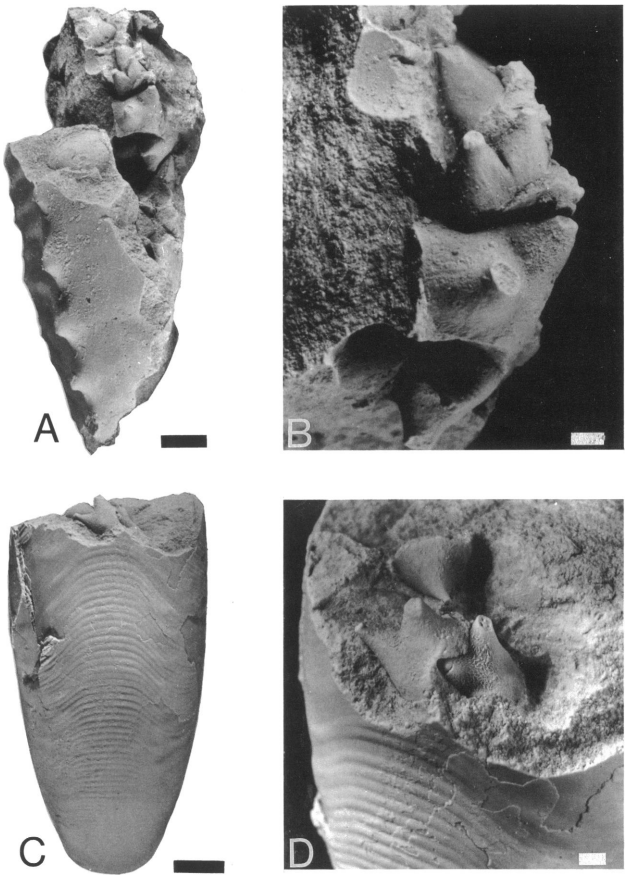

Fig. 45. Hooklike structures preserved in mature body chambers. **A, B.** Body chamber fragment of *Jeletzkytes nebrascensis* (Owen) with 16 hooklike structures, YPM 34109, loc. 73, TLM. **A.** Ventral view (shown in lateral view as a sketch in fig. 46). Scale bar = 5 mm. **B.** Close-up of four hooks. Scale bar = 1 mm. **C, D.** Body chamber fragment of *Hoploscaphites nicolletii* (Morton) with hooklike structures near aperture, YPM 32337, loc. 303, LNAZ. **C.** Ventral view. Scale bar = 5 mm. **D.** Close-up of hooklike structures. Scale bar = 1 mm.

since they are associated with larger ammonites. They also vary considerably in shape and in one example are clearly aligned together, some with interlocking bases, forming a battery of variously shaped elements between the upper and lower mandibles. That the structures in *Rhaeboceras* are radular elements is apparent; those in *Hoploscaphites* and *Jeletzkytes* differ in some significant features and their function is open to question.

The fact that the structures found associated with *Hoploscaphites* and *Jeletzkytes* are all identical in shape poses a problem for their interpretation as radular elements although it is conceivable that scaphites had a highly modified, reduced radula with a single central element. The bases of the bicornate, bilaterally symmetrical structures show no indentations or asymmetry that would suggest basal impingement on, or interlocking with, other elements of a radular row. In the one specimen of *Jeletzkytes* with 16 individual structures in the body chamber, all are the same size and shape and are scattered, showing no significant linear arrangement. Moreover, they are large relative to the size of the adjacent lower mandible plate in the specimen and it is difficult to envision how all of them could possibly have been enclosed within the space between the mandibles.

An alternative possibility is that these were external hooklike structures. While not ac-

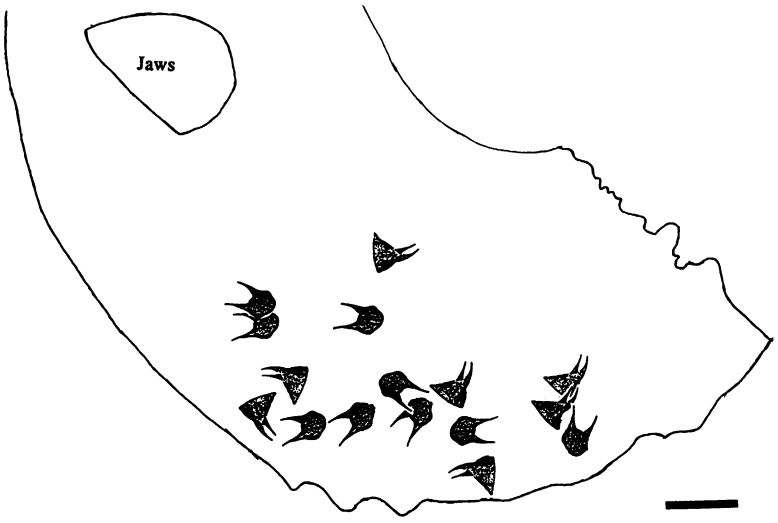

Fig. 46. Sketch showing 16 hooklike structures scattered within the posterior portion of the body chamber of a mature microconch of *Jeletzkytes nebrascensis* (Owen), YPM 34109, loc. 73, TLM. Scale bar = 1 cm. Drawing by Susan Klofak.

tually hook-shaped, the slender "horns" with their sharp points both curve in the same direction, more or less parallel to the plane of symmetry that passes between them. If arrayed along a tentacle or arm with "horns" directed orad, they could have functioned well as grasping organs. From the evidence available these structures are not comparable to those of the *Rhaeboceras* radula; whether they represent elements of a significantly reduced radula or are external hooklike structures remains to be discovered.

GENERA OF FOX HILLS SCAPHITES

The three groups of scaphites in the type Fox Hills Formation are assigned to the genera *Discoscaphites, Hoploscaphites,* and *Jeletzkytes.* The taxonomic history of these three genera is reviewed here in support of our usage and interpretations.

The name *Discoscaphites* was first introduced by Meek (1876: 415) to designate a multituberculate subgenus of *Scaphites.* He included in it all species of scaphites then known from the type Fox Hills Formation, recognizing divisions *a* and *b* based on the gross form of the adult shell. These divisions are now understood to represent the typical scaphitid dimorphs: *a* the macroconch and *b* the microconch. Meek (1870: 429, footnote) based the subgenus *Discoscaphites* on *Ammonites conradi* Morton, 1834 from the Prairie Bluff Chalk of Alabama. Morton's *conradi* comprised a variable group of small, multituberculate scaphites and Meek (1870) relied on his own identification of a specimen from the Fox Hills beds on Fountain Creek, Colorado, to establish the presence of *conradi* in the Western Interior.

Most of Meek's specimens from the type Fox Hills Formation are from the fauna of the Timber Lake Member, a conclusion based on their sandstone matrix, locality data, associated bivalve taxa, and the particular scaphite species present. F. V. Hayden, who made the collections in question, apparently never collected from the equally fossiliferous beds in the underlying Trail City Member (Waage, 1968: 33). Had he done so, Meek would have had sufficient specimens to realize that the small, very involute, multituberculate scaphites representative of Morton's *conradi,* were clearly distinct from the larger, less involute, multituberculate forms Meek illustrated as *conradi* (1876: pl. 36, fig. 2) and recognized as identical with *Ammonites nebrascensis* Owen, 1852. Meek also included in *Discoscaphites* two species that did not conform to his own definition of the sub-

genus, *Scaphites* (*Discoscaphites*) *nicolletii* (Morton) and *S.* (*D.*) *mandanensis* (Morton), neither of which has rows of flank tubercules.

Discoscaphites Meek, 1876 thus included three distinct stocks of Fox Hills scaphites; these correspond to the three groups presently recognized. In a study of Polish Late Cretaceous scaphites, Nowak (1911: 55) introduced the new genus *Hoploscaphites,* which he based primarily on *Scaphites constrictus* (Sowerby). Subsequently, Nowak (1916) assigned to this genus all of the North American species that Meek had placed in *Discoscaphites.* Diener (1916: 527) noted that Meek's name had nomenclatural priority and Reeside (1927: 26), in his review paper on the scaphites, considered *Hoploscaphites* a junior subjective synonym of *Discoscaphites.*

In his diagnosis of *Hoploscaphites,* Nowak (1911: 565) emphasized the compressed, involute form, flexuous ribs, and suture but mentioned neither size of specimens nor presence of tubercles. But in his description (ibid., p. 580) of the type species *constrictus* and its variations he noted both nontuberculate forms and those with ventrolateral and umbilical tubercles on the mature body chamber. His inclusion of the American "*Discoscaphites*" necessarily broadened the scope of the genus and Reeside (1927: 26) emended Nowak's diagnosis to include multituberculate forms while reestablishing Meek's name *Discoscaphites.*

Reeside's diagnosis was not generally followed by Eurasian students of scaphites who adopted *Hoploscaphites,* either as a genus or subgenus, which they defined rather strictly on the basis of the type species *constrictus.* More recent usage (Jeletzky and Waage, 1978; Blaszkiewicz, 1980; Riccardi, 1983; Kennedy, 1986a, 1986b) treats *Hoploscaphites* as a genus. In a discussion of Campanian-Maastrichtian biostratigraphy Jeletzky (1952: 1027) applied this interpretation to "the more or less typical forms of *Scaphites* (*Hoploscaphites*) *nicolletii* Morton" in the Western Interior of North America. Subsequently, Cobban and Jeletzky (1965) in their description of *Scaphites* (*Hoploscaphites*) *gilli* (Cobban and Jeletzky, 1965) clearly limited *Hoploscaphites* to scaphites "that have a compressed adult living chamber which is ordinarily well-ribbed but may be nodeless or may possess a row of ventrolateral nodes with or without an additional row of umbilicolateral nodes" (p. 794). Somewhat expanded but basically similar diagnoses by Birkelund (1965: 102) and Kennedy (1986b: 197) have served to stabilize the genus *Hoploscaphites* in the restricted sense of Nowak's (1911) original description.

In the Western Interior, *Hoploscaphites gilli* marks the first appearance (in the *Baculites perplexus* Zone) of this genus in North America.[1] Between *H. gilli* and *H. nicolletii* of the type Fox Hills Formation, closely related compressed species with fine flexuous ribbing occur, such as *H. landesi* Riccardi, 1983, *H. birkelundi,* n. sp., and *H. melloi,* n. sp., as well as other undescribed species. These species mark a persistent lineage in the Campanian-Maastrichtian strata of the Western Interior (Jeletzky, 1962; Cobban, personal commun., 1963; Waage, 1968: 146). These species are distinguished by differences in their pattern of ribbing, development of tubercles, and tightness of coiling; geologically younger, more derived species are more tightly coiled with a smaller apertural angle. Younger species from the Western Interior also develop a stronger adoral projection of the ventral margin of the aperture than do any of the Eurasian species of this genus. This feature is probably a biogeographical variation peculiar to endemic species of *Hoploscaphites* from the Western Interior; interestingly, the same feature also shows up in geologically younger species of *Jeletzkytes.*

Restudy by Jeletzky and Waage (1978) of the type suite and other specimens of *Ammonites conradi* Morton from the Prairie Bluff Chalk of Alabama and Mississippi, led to the restriction of *Discoscaphites* to small to medium size, highly involute, multituberculate scaphites. Morton's *conradi* is a very distinctive complex of forms whose marked difference from other scaphites in the Fox Hills Formation even extends to the ammonitella (see p. 33). It comprises both very com-

[1] We question the identification as *Hoploscaphites* of a single scaphite microconch from the Turonian Blue Hill Shale Member of the Carlile Shale in Kansas by Crick (1978: 18), and consider *H. gilli* as marking the first appearance of *Hoploscaphites* in the North American Western Interior.

pressed and very inflated species, which co-occur. It is the youngest lineage of scaphites to appear in North America; in the Western Interior region, as far as we know, it is restricted to the type Fox Hills. Its geographic distribution outside the Western Interior includes both the Atlantic and Gulf Coastal Plains but it is most common in the Prairie Bluff Chalk of the Mississippi embayment.

The third group of scaphites originally placed by Meek under *Discoscaphites* consists of the large multituberculate species of the type Fox Hills. These include Owen's *nebrascensis* and *cheyennensis* of the Timber Lake Member, their more varied predecessors in the Trail City Member, which apparently were unknown to Meek, and older related species. Birkelund (1965) also utilized *Discoscaphites* as a subgenus to describe two species from the Upper Cretaceous of West Greenland, *waagei* and *angmartussutensis,* which she related to the Fox Hills species *cheyennensis* and *nebrascensis,* respectively.

Owen's *nebrascensis* and *cheyennensis* have commonly been considered to be end-members of the "*nodosus* group" of scaphites (Jeletzky, 1952: 1027; Birkelund, 1965: 123; Jeletzky and Waage, 1978: 1121; Riccardi, 1983: 15; Cobban and Kennedy, in press; W. J. Kennedy, personal commun., 1991). The concept of the "*nodosus* group" began with Meek (1876: 414), who originated it as a subsection of *Scaphites* Parkinson based on *Scaphites* (*Ammonites*?) *nodosus* Owen, 1852. In it he included a complex of mostly medium to large size, robust scaphites with strong ventrolateral and subumbilical nodes. He excluded from it similar Eurasian forms possessing a ventral row of nodes on which Nowak (1916) subsequently based his genus *Acanthoscaphites.* Meek also excluded the large multituberculate scaphites of the type Fox Hills, which he made a part of his subgenus *Discoscaphites.*

Riccardi (1983: 14) has reviewed the subsequent nomenclatural history of the "*nodosus* group," which has fluctuated in generic assignment among *Scaphites, Acanthoscaphites,* and *Hoploscaphites.* In his study of the scaphites from the Bearpaw Formation of western Canada, Riccardi (1983: 14) introduced the genus *Jeletzkytes,* type species *Scaphites* (*Ammonites*?) *nodosus* Owen, 1852, to include the species of the "*nodosus* group." He (ibid., p. 15) echoed Jeletzky and Waage (1978) in writing that "the latest representatives of the '*nodosus* group' are probably transitional to some of these multituberculate scaphitids [such as *nebrascensis*] which bloomed in the same area during Maastrichtian time." Riccardi (ibid., p. 29) also noted that his new species, *J. criptonodosus,* in the *Baculites baculus* Zone, has some features in common with the older species, *J. brevis* and *J. plenus,* as well as with "certain Western Interior scaphitids usually included in *Discoscaphites* Meek, e.g., *D. cheyennensis* (Owen)."

We agree that the larger multituberculate scaphites in the type Fox Hills are end-members of the "*nodosus* group" and we include them provisionally in the genus *Jeletzkytes.* Nevertheless, species within this genus show considerable variation in ornament and shell shape. *Jeletzkytes nodosus,* as represented by its type specimen (Owen, 1852: pl. 8, fig. 4; Riccardi, 1983: pl. 2, fig. 1), is characterized by relatively few, very prominent ventrolateral and umbilicolateral tubercles on the last part of the phragmocone and mature body chamber. The shell is loosely coiled; the mature body chamber is depressed and gradually increases in size through the shaft, reaching its maximum height and width at the point of recurvature and thereafter decreasing through the hook to the aperture.

In contrast, the species in the Fox Hills Formation have a short shaft and tightly recurved hook. The mature body chamber is compressed to quadrate in whorl section and increases rapidly in size reaching a maximum at about midshaft. Ribbing is finer and more sinuous in the Fox Hills species and is characterized by closer spacing on the anterior shaft and hook. Ventrolateral and umbilicolateral tubercles are smaller, more numerous, and much more closely spaced than those on *J. nodosus,* and several rows of flank tubercles commonly appear on the phragmocone, some or all of which may persist onto the mature body chamber. In side view, the final body chamber is more evenly arcuate in the Fox Hills species, whereas it presents a more elongate aspect in *J. nodosus.* The umbilical shoulder is straight or, more commonly, arched in macroconchs of the Fox

Hills species, but may parallel the venter in *J. nodosus.*

Riccardi (1983) acknowledged this breadth of variation in his original generic diagnosis of *Jeletzkytes* and distinguished two subgroups: "earlier representatives with stronger and sparser ribbing and bearing prominent lateral and ventrolateral tubercles on the body chamber [and] younger representatives with relatively finer and denser ribbing and 2–3 rows of lateral nodes on the phragmocone which tend to fade away on the flanks of the body chamber." The difference in tightness of shell coiling, noted above, is another important distinction.

Further clarification of the phylogenetic relationships among these species must await the taxonomic revision of the "*nodosus* group" from the Pierre Shale currently in preparation by W. A. Cobban and W. J. Kennedy. By provisionally adopting *Jeletzkytes* for the Fox Hills species, we express our suspicion that *Jeletzkytes* is more diverse taxonomically than is presently understood.

Although the species-level relationships within *Hoploscaphites* and *Jeletzkytes* are unclear, we constructed a phylogenetic hypothesis of the relationships among the genera *Hoploscaphites, Jeletzkytes,* and *Discoscaphites* to serve as a baseline for future studies. The genus *Scaphites* was chosen as an outgroup based on previous hypotheses of scaphite phylogeny (Birkelund, 1965; Riccardi, 1983). Evaluation of the relationships among these genera was complicated, however, by the presence of widespread homoplasy (convergence) among the most derived species of *Hoploscaphites* and *Jeletzkytes* (Birkelund, 1965: 72; Landman and Waage, in press). For example, geologically younger species of both these genera inhabited shallow nearshore environments and developed flank tubercles on the mature body chamber. In addition, a large number of species of *Hoploscaphites* and *Jeletzkytes,* except for some of the most primitive and most derived, have not yet been described. To circumvent these difficulties, we confined our analysis to a comparison of the most primitive species within each of these genera. Several primitive species were examined to establish the character states within each genus following the methodology of Maddison et al. (1984). We believe this approach provides a first approximation of the phylogenetic relationships among these scaphite genera, which requires further testing in the future.

The four genera were represented by the following species: *Scaphites* by *S. hugardianus* d'Orbigny, 1840 and related species (reviewed by Cooper, 1990); *Jeletzkytes* by *J. nodosus* and related species (reviewed by Riccardi, 1983; Cobban and Kennedy, in press); *Hoploscaphites* by *H. ikorfatensis* (Birkelund, 1965), *H. ravni* (Birkelund, 1965), *H. greenlandicus* (Donovan, 1953), and *H. gilli* (Cobban and Jeletzky, 1965); and *Discoscaphites* by *D. conradi* and *D. gulosus.*

Thirteen characters were used to construct the cladogram (table 5). Most characters apply to both macroconchs and microconchs unless otherwise noted. Characters are described below. Zero indicates the primitive condition.

1. Degree of recurvature of the final hook in macroconchs (apertural angle): 0, loosely recurved (apertural angle > 100°); 1, moderately recurved (70° < apertural angle < 90°); 2, tightly recurved (30° < apertural angle < 50°).

2. Curvature of the shaft of the mature body chamber of macroconchs in side view: 0, gently curved; 1, more tightly curved; 2, very tightly curved.

3. Whorl section (degree of inflation) of the mature body chamber: 0, very depressed; 1, moderately depressed; 2, compressed; (1, 2), moderately depressed or compressed (treated as a polymorphism).

4. Distance between pairs of ventrolateral tubercles on either side of the venter of the mature body chamber: 0, very distant; 1, moderately distant; 2, close.

5. Area of prominence of the ventrolateral tubercles on the mature body chamber: 0, no preferred area; 1, along the shaft.

6. Ventrolateral tubercles on the mature body chamber locally clavate; 0, no; 1, yes.

7. Umbilical/subumbilical bullae (tubercles) on the mature body chamber, at least in microconchs: 0, absent; 1, present.

8. Umbilical/subumbilical bullae (tubercles) on the mature body chamber very prominent: ?, unknown; 1, yes; 2, no.

TABLE 5
Matrix of Character States Used to Construct Cladogram in Figure 47

	Characters[a]												
Genus	1	2	3	4	5	6	7	8	9	10	11	12	13
Scaphites	0	0	0	0	0	0	0	?	0	0	0	0	0
Jeletzkytes	1	1	1	1	1	1	1	1	0	1	0	1	0
Hoploscaphites	1	1	2	1	1	0	1	2	0	2	0	1	0
Discoscaphites	2	2	1, 2	2	0	0	1	2	1	1	1	1	1

[a] Defined in text.

9. Flank tubercles (as distinct from subumbilical or ventrolateral tubercles) on the mature body chamber: 0, absent; 1, present.

10. Degree of sinuosity of ribbing on the flanks of the mature body chamber: 0, straight; 1, weakly flexuous; 2, very flexuous.

11. Fine lirae on shell whorls: 0, absent; 1, present.

12. Projection of ribs on the venter of the mature body chamber: 0, projected backward; 1, weakly projected forward.

13. Ammonitella shape: 0, spheroidal; 1, ellipsoidal.

According to the cladogram (fig. 47), *Hoploscaphites* and *Jeletzkytes* are sister taxa. They are more closely related to each other than either is to *Discoscaphites*. This relationship is supported by characters related to the tightness of coiling of the adult shell and the distribution of ventrolateral tubercles on the mature body chamber.

In summary, the three groups of scaphites in the type Fox Hills Formation are assigned to three different genera. This assignment conforms with the current classification and is logically consistent with the proposed phylogeny. The three genera are briefly reviewed below.

Discoscaphites Meek s.s., as restricted by Jeletzky and Waage (1978) to the characters of its type species *Ammonites conradi* Morton, includes small to medium size, consistently multituberculate scaphites with an ellipsoidal ammonitella. It is the youngest

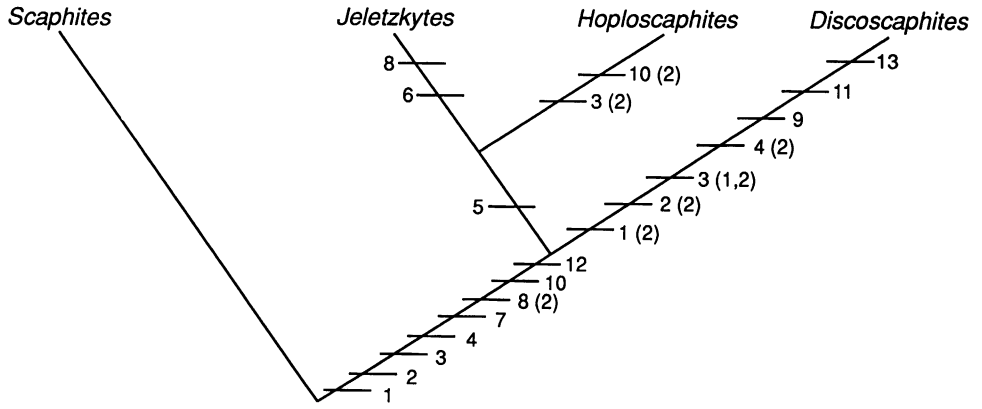

Fig. 47. Minimum-length cladogram illustrating the relationships among *Hoploscaphites, Jeletzkytes,* and *Discoscaphites* (length = 19, CI = 1.0) constructed from character data in table 5. The outgroup is represented by primitive species of *Scaphites*. Numerals refer to characters in table 5; transformations are to state 1 unless otherwise indicated in parentheses. Data were analyzed using the Branch and Bound option of PAUP version 3.0 (Phylogenetic Analysis Using Parsimony; Swofford, 1990). Multistate characters were coded as unordered. Character 3 was treated as polymorphic. Distribution of character states is consistent with ACCTRAN (Swofford and Maddison, 1987).

scaphite genus in the Western Interior where it is known from the type Fox Hills Formation of the Missouri Valley region.

Hoploscaphites includes *H. nicolletii* and related species, which differ in some details from the Eurasian type species *H. constrictus* but fall within the commonly accepted diagnosis of the genus (Cobban and Jeletzky, 1965; Birkelund, 1965; Riccardi, 1983). This genus consists of compressed forms with or without ventrolateral tubercles, and, less commonly, umbilical tubercles or bullae, largely on the body chamber. All species are marked by fine, flexuous ribs. The oldest recorded species in the Western Interior is *H. gilli* from the Late Campanian *Baculites perplexus* Zone (Cobban and Jeletzky, 1965). Other species include *H. landesi* Riccardi, 1983 and *Discoscaphites nicolleti* var. *saltgrassensis* Elias, 1933.

Jeletzkytes includes medium to large size, robust scaphites that bear prominent ventrolateral tubercles that are locally clavate and prominent subumbilical tubercles or bullae. More derived species, e.g., *J. nebrascensis* of the Timber Lake Member and *J. spedeni,* n. sp., of the Trail City Member, show multiple rows of flank tubercles on the exposed phragmocone that may extend onto the mature body chamber. The oldest described species of this genus is *J. nodosus* from the Pierre Shale and Bearpaw Formation.

TAXONOMY OF SCAPHITE DIMORPHISM

The taxonomic treatment of dimorphism in ammonites has varied (see Westermann, 1969), but studies of scaphites that have considered dimorphism have consistently included both dimorphs in the same species. Although this implies acceptance of dimorphism as sexual in nature, two methods of indicating the individual dimorphs are in use by students of scaphites. The obvious and more interpretative practice uses the terms female and male and their conventional zoological symbols (Makowski, 1962; Cobban, 1969; Riccardi, 1983); the other practice uses the descriptive terms macroconch (M) and microconch (m) for the supposed female and male forms, respectively (Crick, 1978; Jeletzky and Waage, 1978; Kennedy, 1986a, 1986b; Landman, 1987). We follow the latter method.

Systematic revisions recognizing dimorphism commonly involve synonymy of one of the dimorphs. Studies of scaphites show a strong consensus for the macroconch (female) as name-bearer (see all references in preceding paragraph). We favor this practice not simply because it seems well established for scaphites but because we find, in the Fox Hills scaphites, that macroconchs tend to be more sharply differentiated morphologically between species than are microconchs. Riccardi (1983: 14) also found this to be true, observing that "microconchs of different, but clearly related species are usually more difficult to discriminate than the corresponding macroconchs." The widespread preference for the macroconch as name-bearer in taxonomic revisions to accommodate dimorphism may not be an option under the rule of priority. However, because many forms now recognized as dimorphs of the same species were initially described as separate species in a single article (same date of publication), both names have equal priority, allowing the revising author to choose between them (ICZN, 1985: 53, Rec. 24A). Accordingly, we have selected the macroconch as name-bearer of *Hoploscaphites nicolletii* over the microconch *mandanensis* in revising Morton's (1834) initial descriptions. On the other hand, we have designated the microconch *Discoscaphites gulosus* as name-bearer because the available macroconch, Morton's variety *petechialis,* is a fragment lacking the body chamber whereas his *gulosus* is an entire specimen.

In our systematic revisions, we designate a specimen of one of the dimorphs, usually the macroconch, as a type specimen, and employ the term allotype to describe a representative specimen of the other dimorph. The ICZN does not recommend using this term for specimens other than paratypes (ICZN, 1985: 141, Rec. 72.4). However, with the sexual dimorphs as clearly defined as they are in the Fox Hills scaphites, it seems justifiable to us to take advantage of this unregulated but most useful term in dealing with these strongly dimorphic ammonites.

SYSTEMATIC DESCRIPTIONS

CLASS CEPHALOPODA

ORDER AMMONOIDEA ZITTEL, 1884

SUPERFAMILY SCAPHITACEAE WRIGHT & WRIGHT, 1951

FAMILY SCAPHITIDAE GILL, 1871

SUBFAMILY SCAPHITINAE WRIGHT, 1953

Genus *HOPLOSCAPHITES* Nowak, 1911

TYPE SPECIES: *Ammonites constrictus* Sowerby, 1817: 189, pl. 184A, fig. 1, by original designation.

DIAGNOSIS: Small to medium size, compressed, strongly dimorphic scaphites with very involute phragmocone; body chamber with short, arcuate shaft and slightly recurved hook; peristome with weak to strong adoral projection on venter; ribs become finer, more flexuous forward with weak adoral projection on flanks and weak to strong adoral projection on venter; body chamber with or without ventrolateral tubercles (or clavi) and umbilical bullae, which may appear on younger part of otherwise nontuberculate phragmocone. Mid-ventral tubercles uncommon. Ventral muscle attachment area ovoid. (See also Birkelund, 1965: 102 and Kennedy, 1986b: 197.)

OCCURRENCE: Upper Campanian to Upper Maastrichtian, France, northern Spain, Ireland, Belgium, The Netherlands, Germany, Switzerland, Denmark, Sweden, Poland, Russia, Ukraine, Israel, Canada, U.S. Western Interior, Greenland, Chile, Grahamland, Zululand (Kennedy, 1986b: 197; Kennedy and Summesberger, 1987).

Hoploscaphites nicolletii (Morton, 1842)

Figures 48–68

Macroconch Synonymy:

Ammonites nicolletii Morton, 1842: 209, pl. 10, fig. 3.

Ammonites nicolletii Morton, Owen, 1852: pl. 8, fig. 1.

?*Scaphites nicolletii* (Morton), Meek and Hayden, 1856b: 281.

Discoscaphites nicolleti (Morton) Meek, Reeside, 1927: 27, 31, pl. 9, figs. 5–7.

Scaphites (*Hoploscaphites*) *nicolletii* (Morton), Jeletzky, 1952, *in* Cobban and Reeside, 1952: 1027.

Scaphites (*Hoploscaphites*) *nicolletii* (Morton, 1842?) Meek, 1876, Jeletzky, 1962: 1014, pl. 141, fig. 1 (not fig. 2).

Scaphites (*Hoploscaphites*) *nicolleti* (Morton), Waage, 1964: 548, fig. 8.

Scaphites (*Hoploscaphites*) *nicolleti* (Morton), Waage, 1968: 145, 146, pl. 2, B.

Hoploscaphites nicolletii (Morton), Riccardi, 1983: 12, 13.

Hoploscaphites nicolleti (Morton), Landman and Waage, 1986: 217, fig. 4A–D.

Microconch Synonymy:

Note: Specimens until now called *mandanensis* include microconchs of both *Hoploscaphites nicolletii* (Morton) and *H. comprimus* (Owen) and are exceedingly difficult to identify as belonging to one or the other species. This is particularly true of specimens of *mandanensis* cited in the older literature. Because *H. nicolletii* is by far the most abundant scaphite in the Fox Hills Formation, specimens of *mandanensis* cited in the older literature for which no evidence exists to unequivocably identify them as *H. comprimus* instead of *H. nicolletii* are preceded by a query and listed under *H. nicolletii.*

?*Ammonites mandanensis* Morton, 1842: 208, pl. 10, fig. 2.

?*Ammonites abyssinus* Morton, 1842: 209, pl. 10, fig. 5.

?*Scaphites mandanensis* (Morton), Meek and Hayden, 1856b: 281.

DIAGNOSIS: Macroconchs with fine, dense ribbing on anterior two-thirds of body chamber, ribs, and peristome with strong adoral projection on venter; ventrolateral tubercles mostly on posterior part of body chamber may or may not appear on adjacent part of phragmocone. Microconch body chamber more compressed with broad flat umbilical shoulder bordered by bullae; ventrolateral tubercles as on macroconch.

NAME: Under the Code (Article 24 [a]), *nicolletii* and *mandanesis* are deemed to have been established simultaneously. As first revising authors we select *nicolletii* as the name of the species.

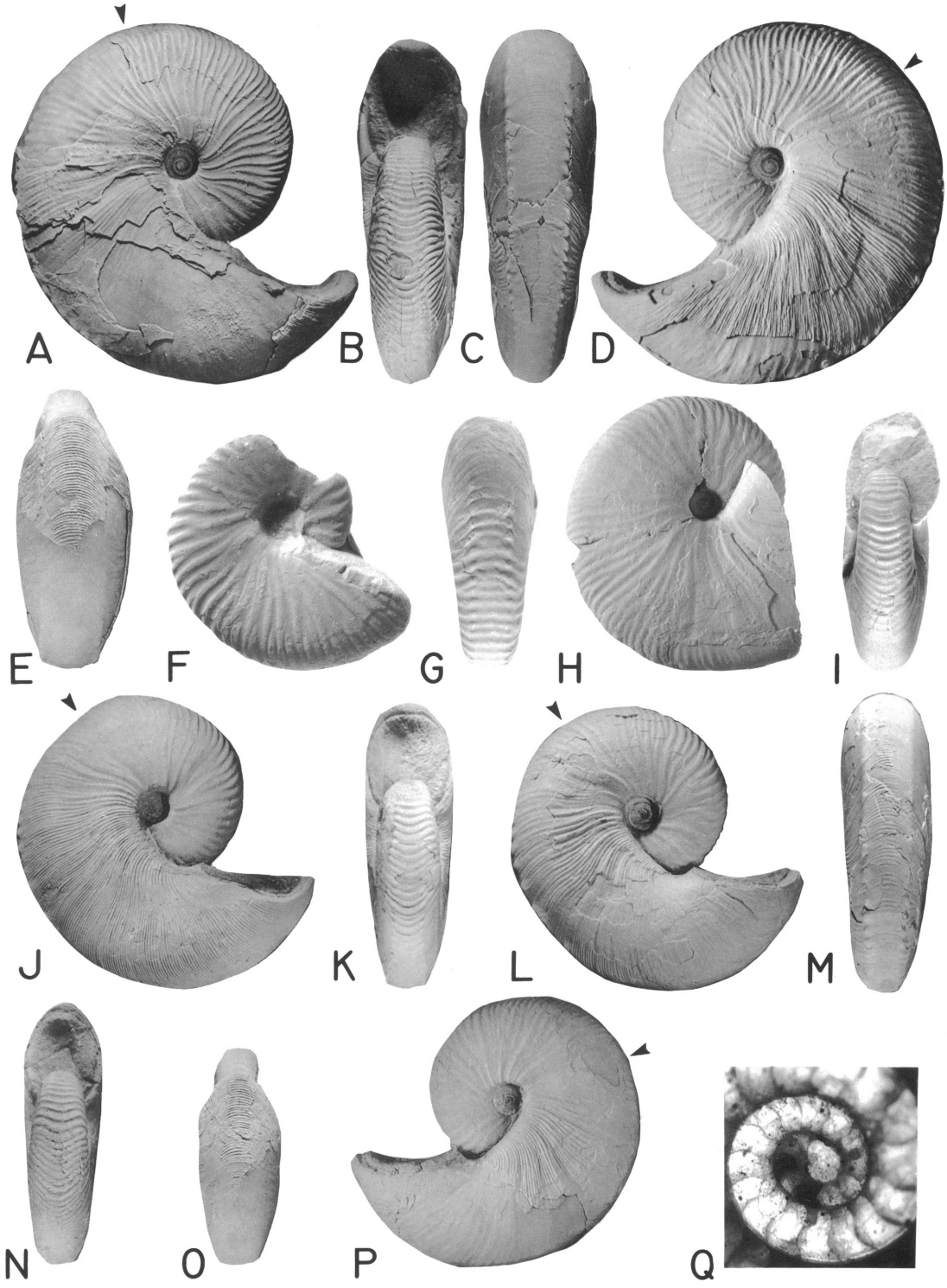
A
B
C
D
E
F
G
H
I
J
K
L
M
N
O
P
Q

TYPES: Neotype, YPM 27222, loc. 54, LNAZ, fig. 48A–E.

Allotype, YPM 27235, loc. 177, LNAZ, fig. 52H–L.

REMARKS: The two specimens on which Morton (1842) based his species *Ammonites nicolletii* (a macroconch) and *Ammonites mandanensis* (a microconch) were brought to him by the geographer Joseph N. Nicollet. In 1839 Nicollet went up the Missouri River as far as Fort Pierre with the Corps of Topographical Engineers, subsequently traveling to the northeast, well east of the Missouri River and any area of outcrop of the Fox Hills Formation (Goetzman, 1959: 70–71). The anomaly of Nicollet's possession of Fox Hills fossils when he never saw the Fox Hills outcrop was explained by Hayden (1862: 3), who noted that Nicollet "saw nothing of No. 5 [the Fox Hills Formation] though he obtained some of its characteristic fossils, which may have been presented to him by members of the American Fur Company." These specimens of indefinite locality were deposited by Morton in the collections of the Academy of Natural Sciences of Philadelphia and subsequently lost, although painted plaster casts of both are still in the ANSP collections. One of us (KMW) searched the invertebrate collections at ANSP in the late 1950s with then Curator Horace Richards, who was convinced these types and other missing voucher specimens had been discarded by mistake many years ago.

The cast labeled as the type of *nicolletii* (fig. 48F, G) conforms in both size and the profile of its anterior edge to Morton's crude illustration, which lacks details such as the piece missing from the periphery. The cast indicates a partial specimen lacking all of the body chamber except, possibly, the adapical few millimeters. It doesn't show any sutures. We find no reason to doubt that this cast, as its label states, is a cast of Morton's type of *Ammonites nicolletii*. Subsequent studies have perpetuated the use of the name to the present; the more significant of these are reviewed briefly here.

The specimen Owen (1852: pl. 8, fig. 7) figured as *Ammonites nicolletii* Morton is better illustrated than Morton's type but it too lacks the body chamber and the specimen itself is lost. Of the Cretaceous specimens described by Owen (1852), a few are in the Gurley collection of the University of Chicago (now in the Field Museum) and a few are in the National Museum (USNM); these are the only repositories we know of with Owen's specimens and his *nicolletii* fragment is not at either place. Owen's illustration shows a lateral view of the outer whorl of a phragmocone similar to the cast of Morton's type.

Meek's (1876: 435) description of *Scaphites* (*Discoscaphites*) *nicolletii* is based on the two specimens he illustrated. Both of these are in the USNM collection; one (ibid., pl. 34, fig. 2) lacks the body chamber but the other (ibid., pl. 34, fig. 4) preserves the shaft and part of the hook. The latter specimen (USNM 407), refigured here on figure 70A, B, is identifiable by its very compressed form and rib pattern on the body chamber as the Timber Lake species *H. comprimus* (Owen, 1852). Meek (1876: 435) placed Owen's *Scaphites comprimus* in synonymy under *Scaphites* (*Discoscaphites*) *nicolletii,* but his own two specimens of the latter are clearly Owen's *comprimus.* We reinstate *comprimus* as a valid species (p. 100).

Reeside (1927: pl. 9, figs. 5–7) illustrated a specimen of *Discoscaphites nicolleti* that lacks almost all of the body chamber. It is listed (ibid., pl. 9 legend) as coming "from the top of the Pierre Shale half a mile north of Linton, N. Dak." The "top of the Pierre Shale" became the Trail City Member of the Fox Hills Formation in later stratigraphic revisions (Morgan and Petsch, 1945; Waage,

←

Fig. 48. *Hoploscaphites nicolletii* (Morton) macroconchs. **A–E.** Neotype, YPM 27222, loc. 54, LNAZ. **A,** Right lateral; **B,** apertural; **C,** posterior; **D,** left lateral; **E,** ventral hook. **F, G.** Plaster cast of Morton's type of *Ammonites nicolletii,* ANSP 51563, locality unknown. **F,** Right lateral; **G,** ventral. **H, I.** Incomplete specimen illustrated by Reeside (1927: pl. 9, figs. 5, 6), near Linton, North Dakota. **H,** Right lateral; **I,** apertural. **J, K.** YPM 27221, loc. 51, UNAZ. **J,** Right lateral; **K,** apertural. **L–P.** Small adult, YPM 27224, loc. 44, LNAZ. **L,** Right lateral; **M,** posterior; **N,** apertural; **O,** ventral hook; **P,** left lateral. **Q.** Early whorls in transmitted light, ×30, YPM 27250, loc. 44, LNAZ.

1968: 43). Around Linton only the lower part of the typical Trail City Member is present due to facies change, but it includes the abundantly fossiliferous Lower *nicolletii* Assemblage Zone (Waage, 1968: 62). Reeside's specimen of *nicolletii* from the Linton area (our fig. 48H, I) is too incomplete to show the characteristic shape and ornamentation of the body chamber of this species.

Jeletzky (1962: 1014, pl. 141, fig. 1) illustrated for the first time an entire specimen of what we call *Hoploscaphites nicolletii* from the Trail City Member of the type Fox Hills Formation at a locality (our loc. 21) in which the Lower *nicolletii* Assemblage Zone is exposed and abundantly fossiliferous. Jeletzky (ibid.) identified this specimen as *Scaphites (Hoploscaphites) nicolletii* (Morton, 1842?) Meek, 1876 (changing Meek's subgeneric designation from *Discoscaphites* to *Hoploscaphites*). The purpose of his study was to support his identification of a specimen from Hemmoor, Germany, as *H nicolletii* and his correlation of the Hemmoor beds with the type Fox Hills of the U.S. Western Interior. His identification of the German specimen has not been generally accepted, as noted later, but he included a significant discussion of Morton's type *nicolletii* that is pertinent here. Jeletzky stated (ibid., p. 1015):

> It should be stressed that the Hemmoor specimen is similar only with the Meek's (1876) specimens of *S. H. nicolletii* but not with its type specimen figured and described by Morton (1842, synonymy). The latter specimen is a much more heavily built, coarsely ribbed form, with tubercles occurring on each of the secondary ribs and extending back to the beginning of the last whorl. Morton's (1842) type specimen could thus be an extreme variety of *Scaphites (Hoploscaphites) nicolletii* Meek, an older form closely allied to *S. H. nicolletii* Meek . . . or an entirely different *Scaphites* species. This problem, and that of the proper name for *S. H. nicolletii* Meek is, however, beyond the scope of this paper . . .

The solution to the problem of the identity of *Hoploscaphites nicolletii* (Morton) is critical for the present study of the Fox Hills scaphites. *Scaphites (Hoploscaphites) nicolletii* Meek is unquestionably Owen's (1852) *H. comprimus,* as reinstated herein, and not the *H. nicolletii* specimen figured by Jeletzky (1962: pl. 141, fig. 1). Moreover, Jeletzky's characterization of Morton's type *nicolletii* was based on comparison with a single specimen of *H. nicolletii* as presently understood, not with a suite of specimens showing the full range of variation within this species. Among the several hundred specimens we have examined are stout individuals with coarse ribs and ventrolateral tubercles on the phragmocone, features very similar to those on Morton's type. In addition, many specimens show a change in rib pattern on the terminal phragmocone identical to that on Morton's type. This close similarity cannot be found with any other species of *Hoploscaphites* described in this study nor with any species of the two associated scaphite genera. Nevertheless, the definitive morphological characters used to identify species of *Hoploscaphites* are those found on the body chamber,

→

Fig. 49. *Hoploscaphites nicolletii* (Morton) macroconchs. **A–D.** Large adult with umbilical bulge, YPM 23704, loc. 44, LNAZ. **A,** Right lateral; **B,** apertural; **C,** left lateral; **D,** left lateral, uncoated, showing septal approximation. **E–G.** Incomplete adult with broken hook showing dorsal projection preserved as a cast developed against the venter of the phragmocone, YPM 27226, loc. 17, LNAZ. **E,** Oblique view, ×3; **F,** right lateral; **G,** anterior, ×3.

Fig. 50. *Hoploscaphites nicolletii* (Morton) macroconchs. **A–D.** Large adult, YPM 27247, loc. 62, POAZ. **A,** Right lateral; **B,** ventral hook; **C,** apertural; **D,** left lateral. **E–H.** Pathologic adult, injury inflicted on right umbilical shoulder at juvenile stage, YPM 23041, loc. 209, LNAZ. **E,** Right lateral, spiral furrow marks damage to mantle; **F, G,** posteroventral and apertural showing asymmetry; **H,** left lateral.

Fig. 51. *Hoploscaphites nicolletii* (Morton) macroconchs. **A–C.** Adult with typical rib pattern, YPM 27244, loc. 82, UNAZ. **A,** Posteroventral; **B,** apertural; **C,** left lateral. **D, E.** Large adult with umbilical bulge, atypical grooves on hook may mark apertural positions, YPM 27248, loc. 77, UNAZ. **D,** Posterodorsal showing ventrolateral tubercles; **E,** left lateral. **F, G.** Large adult, YPM 27225, loc. 44, LNAZ. **F,** Left lateral; **G,** apertural. **H–J.** Adult with variation in ribbing at phragmocone-body chamber juncture, YPM 27246, loc. 54, LNAZ. **H,** Apertural; **I,** posteroventral; **J,** left lateral.

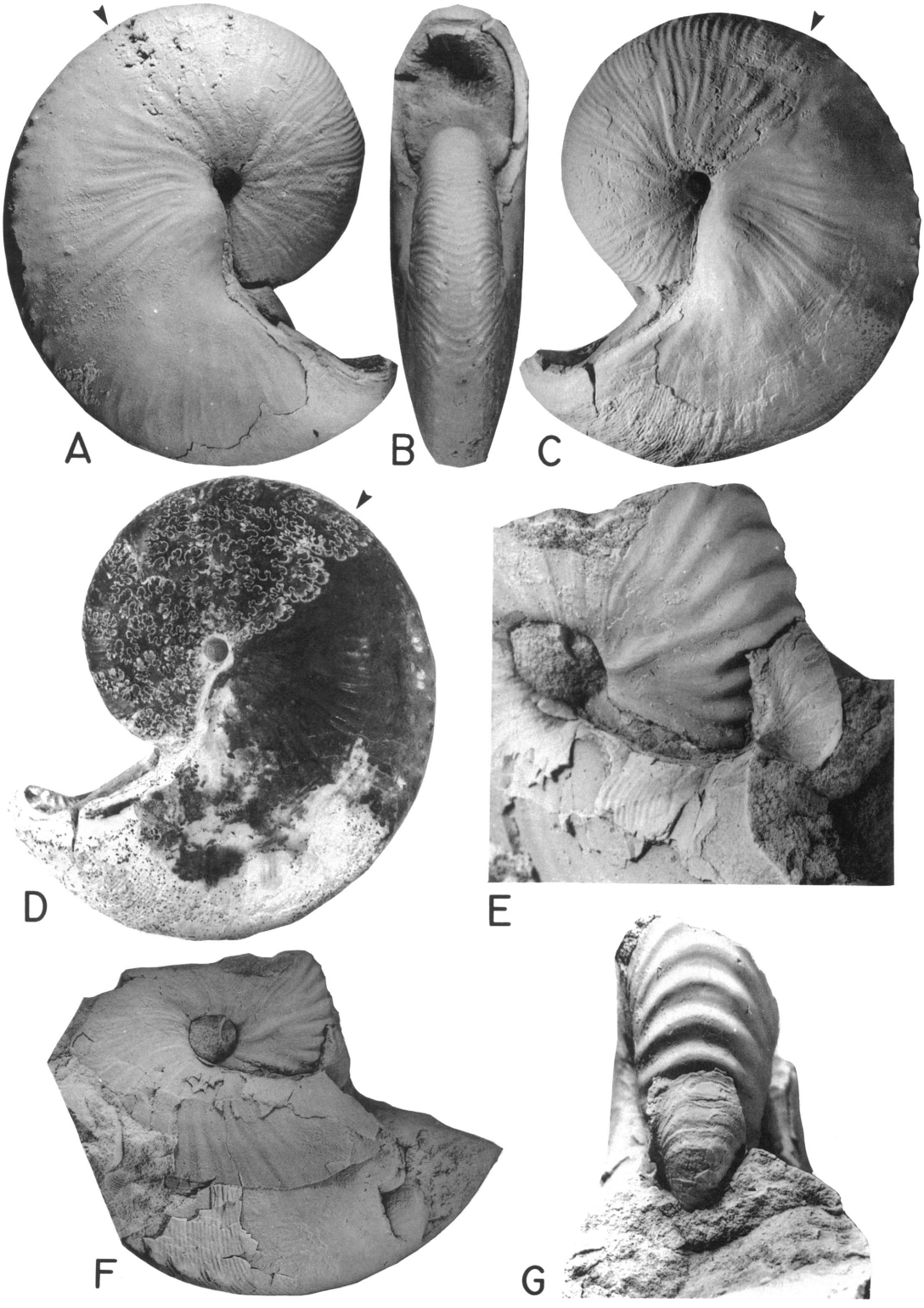
A
B
C
D
E
F
G

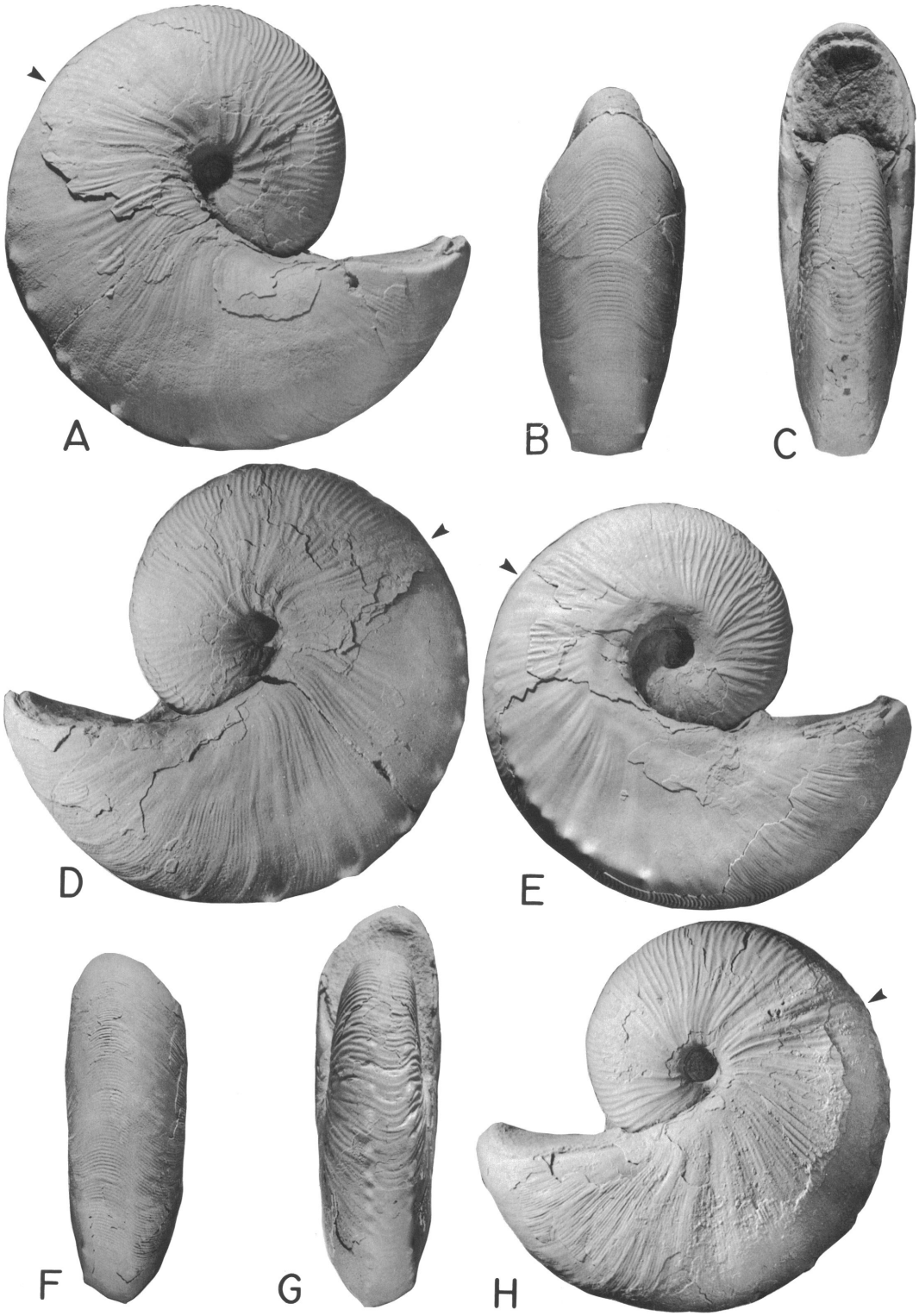

Fig. 50

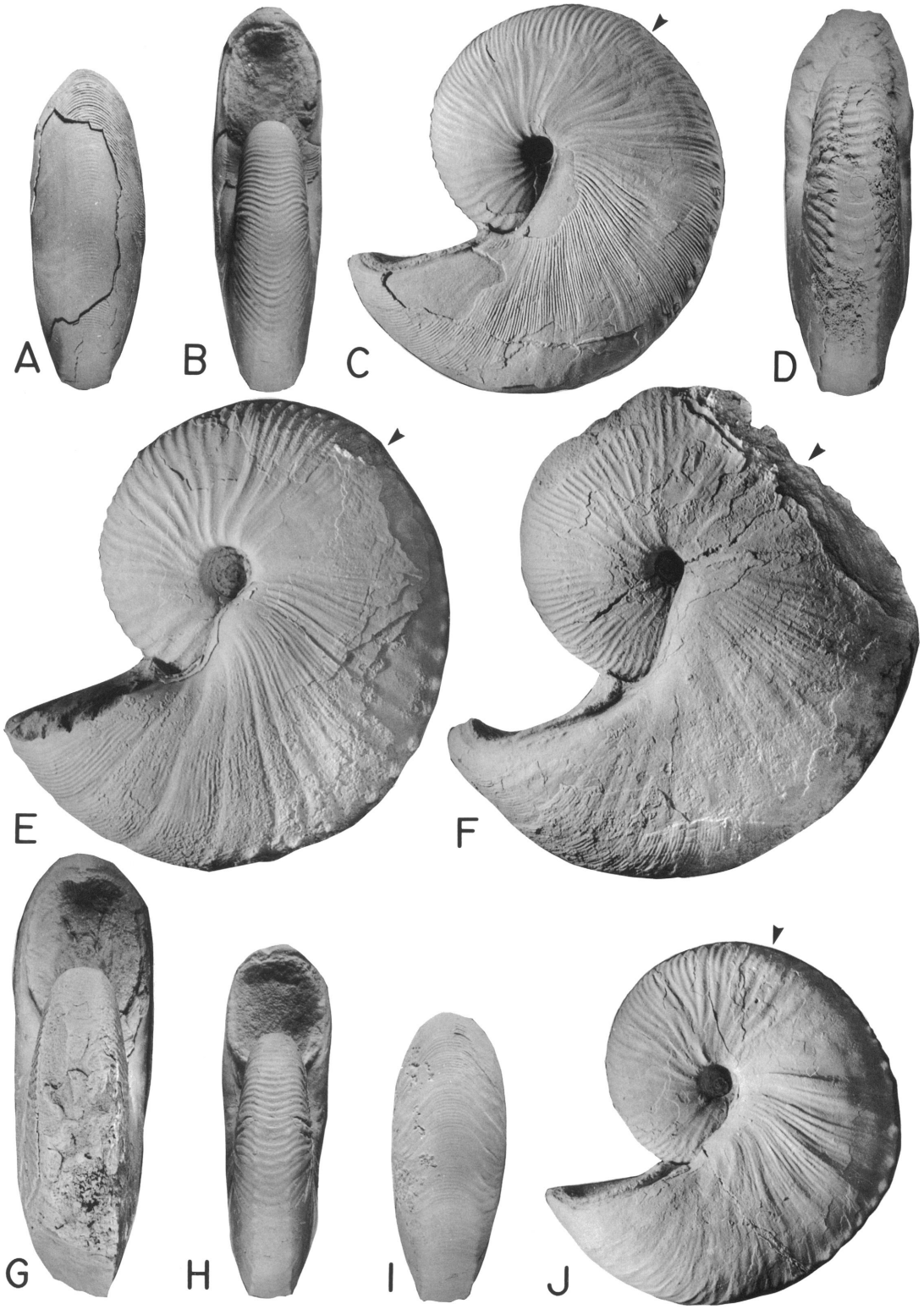

Fig. 51

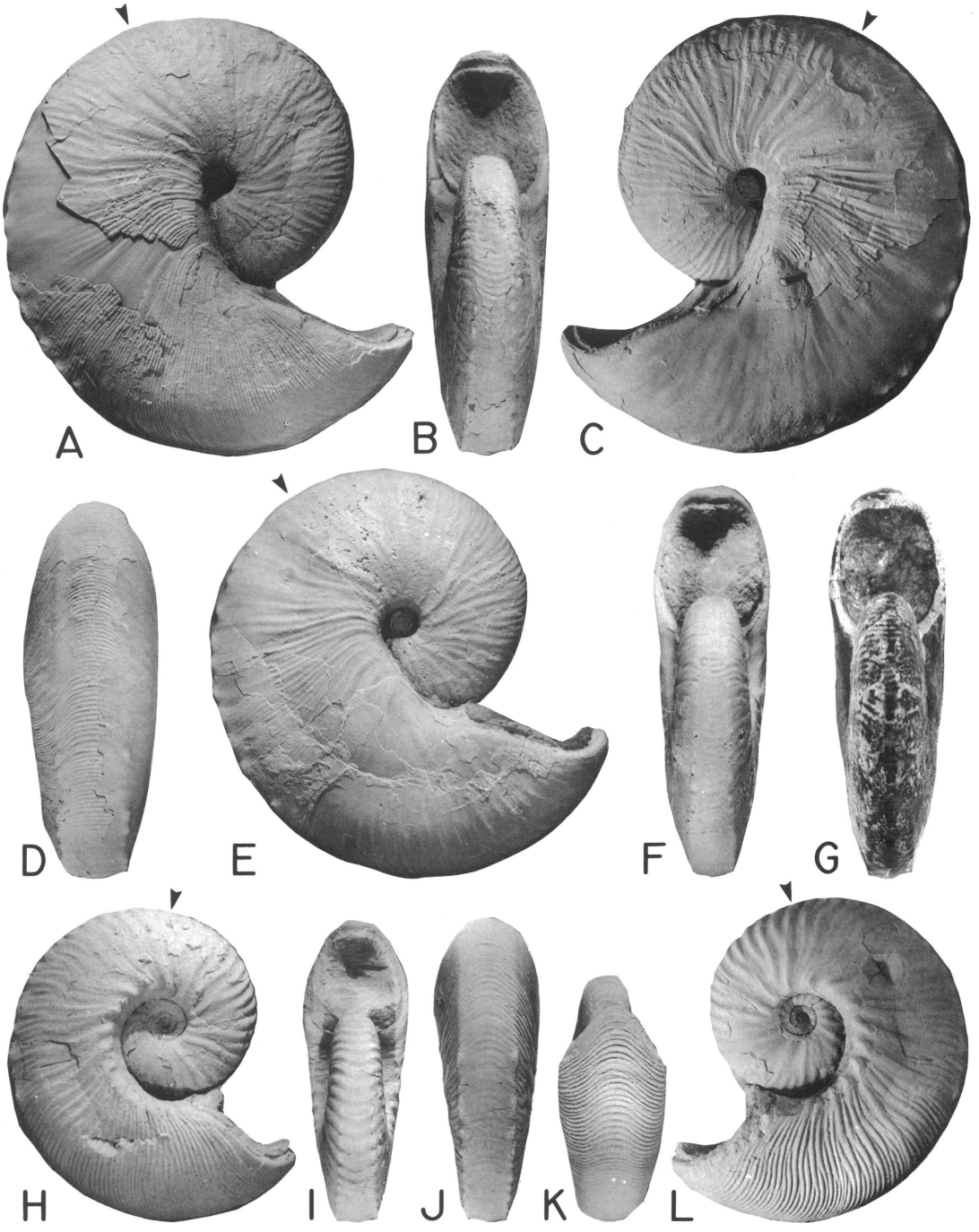

Fig. 52. *Hoploscaphites nicolletii* (Morton) macroconchs and microconch. **A–D.** Adult macroconch, YPM 27223, loc. 209, LNAZ. **A,** Right lateral; **B,** apertural; **C,** left lateral; **D,** posteroventral. **E–G.** Adult macroconch, YPM 27245, loc. 44, LNAZ. **E,** Right lateral; **F,** apertural; **G,** apertural, uncoated, showing trace of siphuncle. **H–L.** Allotype, adult microconch, YPM 27235, loc. 177, LNAZ. **H,** Right lateral; **I,** apertural; **J,** posterior; **K,** ventral hook; **L,** left lateral.

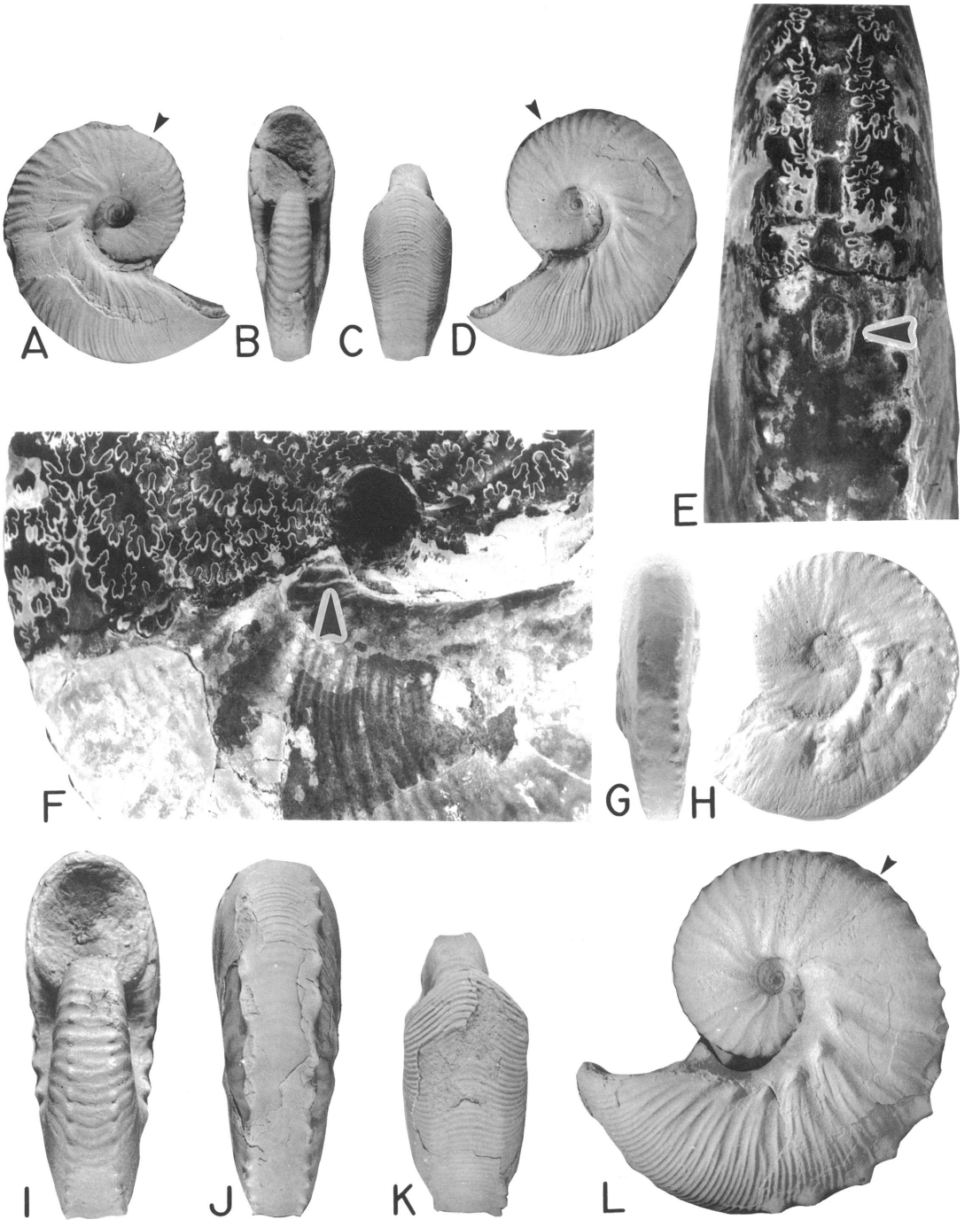

Fig. 53. *Hoploscaphites nicolletii* (Morton) macroconch and microconchs. **A–D.** Microconch, YPM 23707, loc. 52, UNAZ. **A,** Right lateral; **B,** apertural; **C,** ventral hook; **D,** left lateral. **E, F.** Macroconch, YPM 23742, loc. 25, LGAZ float. **E,** Uncoated venter, showing ventral muscle attachment area (arrow), ×2.5; **F,** uncoated umbilical shoulder showing dorsal muscle attachment area (arrow), ×2.3. **G, H.** Microconch, plaster cast of missing holotype of ?*Ammonites mandanensis* Morton, ANSP 51562, locality unknown. **G,** Posterior; **H,** left lateral. **I–L.** Robust microconch, YPM 27243, loc. 52, UNAZ. **I,** Apertural; **J,** posterior; **K,** ventral hook; **L,** left lateral.

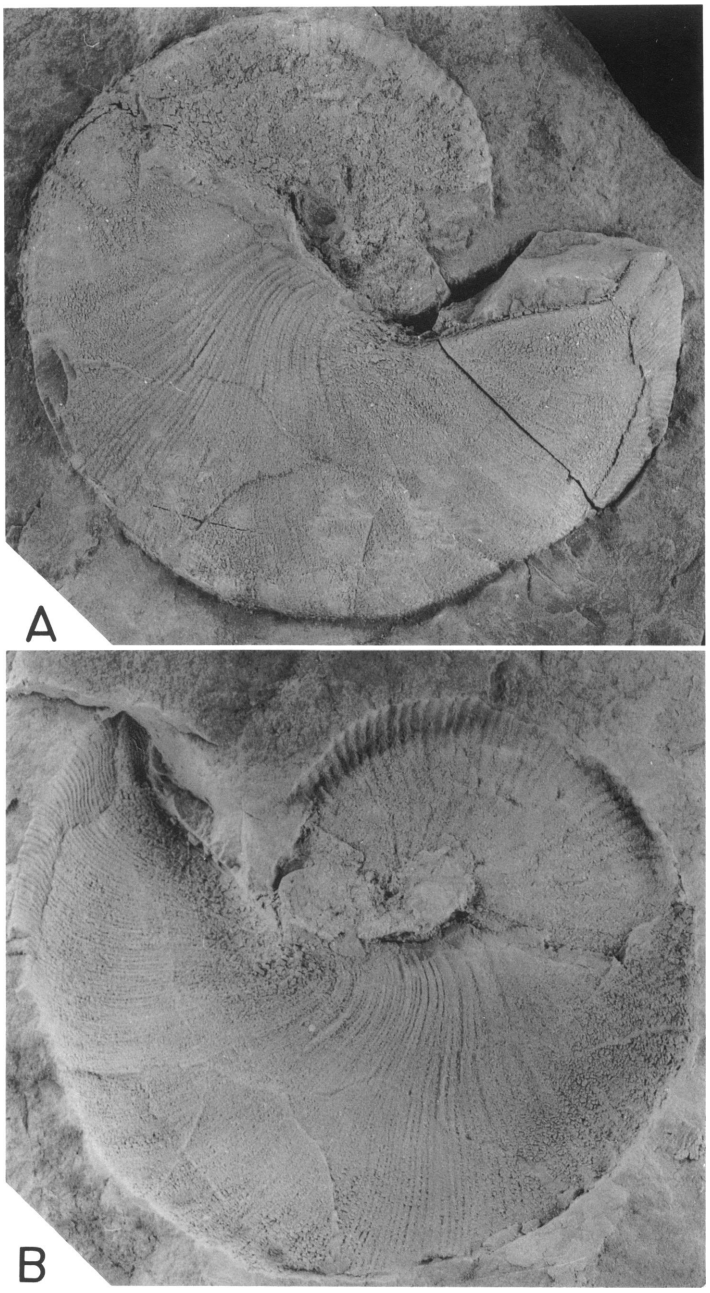

Fig. 54. *Hoploscaphites nicolletii* (Morton), large macroconch in sideritic concretion, YPM 27227, loc. 307, uppermost Elk Butte Member, Pierre Shale. **A,** Right lateral; **B,** right lateral mold in concretion.

and Morton's *nicolletii* remains a nomen dubium.

Selection of a complete specimen of *H. nicolletii* from the Trail City Member of the type Fox Hills Formation as neotype affirms present usage and stabilizes the nomenclature among the closely related species of *Hoploscaphites* in the Maastrichtian faunas of the North American Western Interior. Recognition of these closely related species is crit-

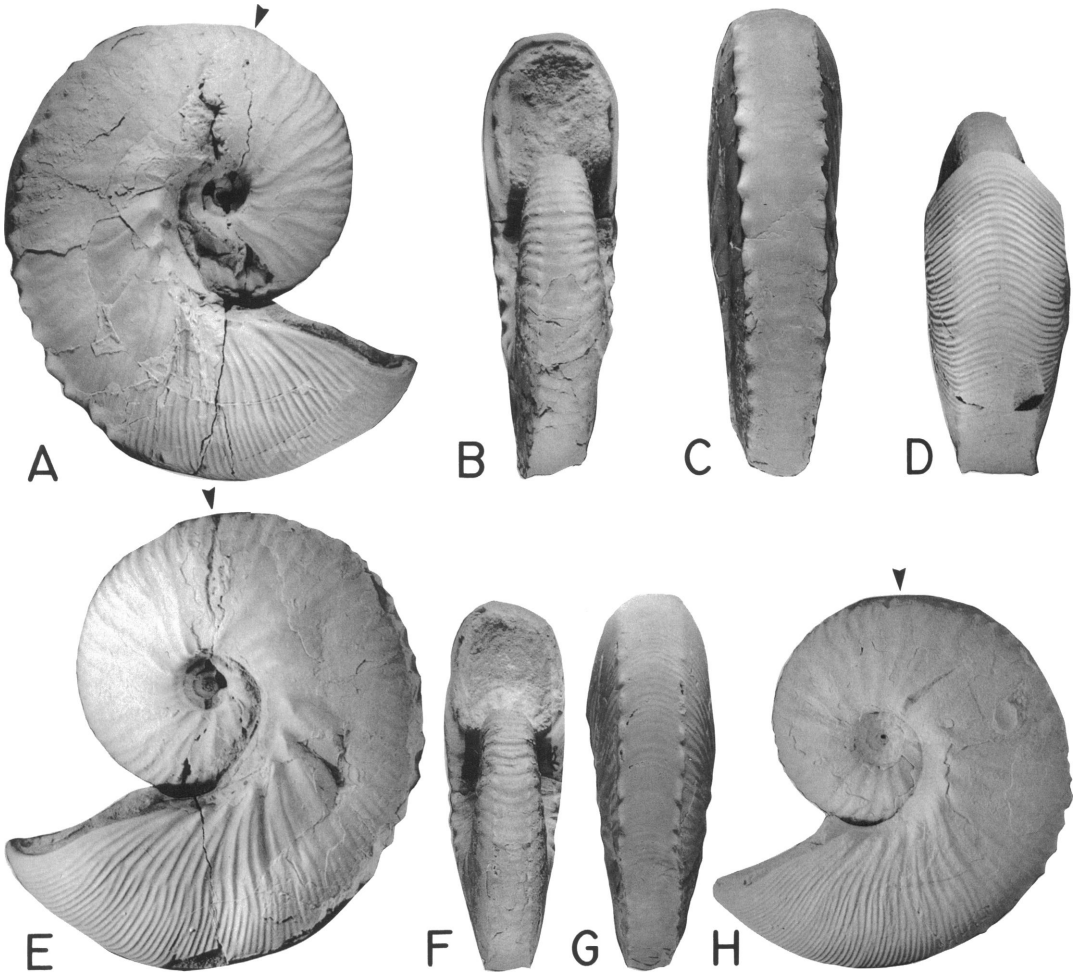

Fig. 55. *Hoploscaphites nicolletii* (Morton) microconchs. **A–E.** YPM 27238, loc. 85, POAZ. **A,** Right lateral; **B,** apertural; **C,** posterior; **D,** ventral hook; **E,** left lateral. **F–H.** YPM 27237, loc. 241, LGAZ. **F,** Apertural; **G,** posterior; **H,** left lateral.

ical in order to reveal the evolutionary patterns during the later history of the genus *Hoploscaphites.*

The neotype is from the general area in which Morton's holotype most probably was found: in or closely adjacent to the type area of the Fox Hills Formation. The specimens figured by Owen (1852), Meek (1876), Reeside (1927), and Jeletzky (1962) are undoubtedly from this area and the latter two are from the same horizon in the Trail City Member.

Selection of the allotype of *H. nicolletii* involves the synonymy of two other microconch species of Morton's (1842), *mandanensis* and *abyssinus.* Morton's original specimens of *mandanensis* (1842: 208, pl. 10, fig. 2) and *abyssinus* (1842: 209, pl. 10, fig. 5) are both lost although plaster casts of *mandanensis* are in the ANSP collections. However, even had we chosen to retain separate names for the macroconch and microconch of the strongly dimorphic Fox Hills scaphites, *abyssinus* would have been synonymized under *mandanensis.* Morton's specimen of *abyssinus* consisted only of inner whorls with the center broken out and would not have been distinguishable from inner whorls of related species. Meek (1876: 441–444, pl. 35, figs. 2 and 4) redescribed *abyssinus* and *mandanensis* in considerably more detail based

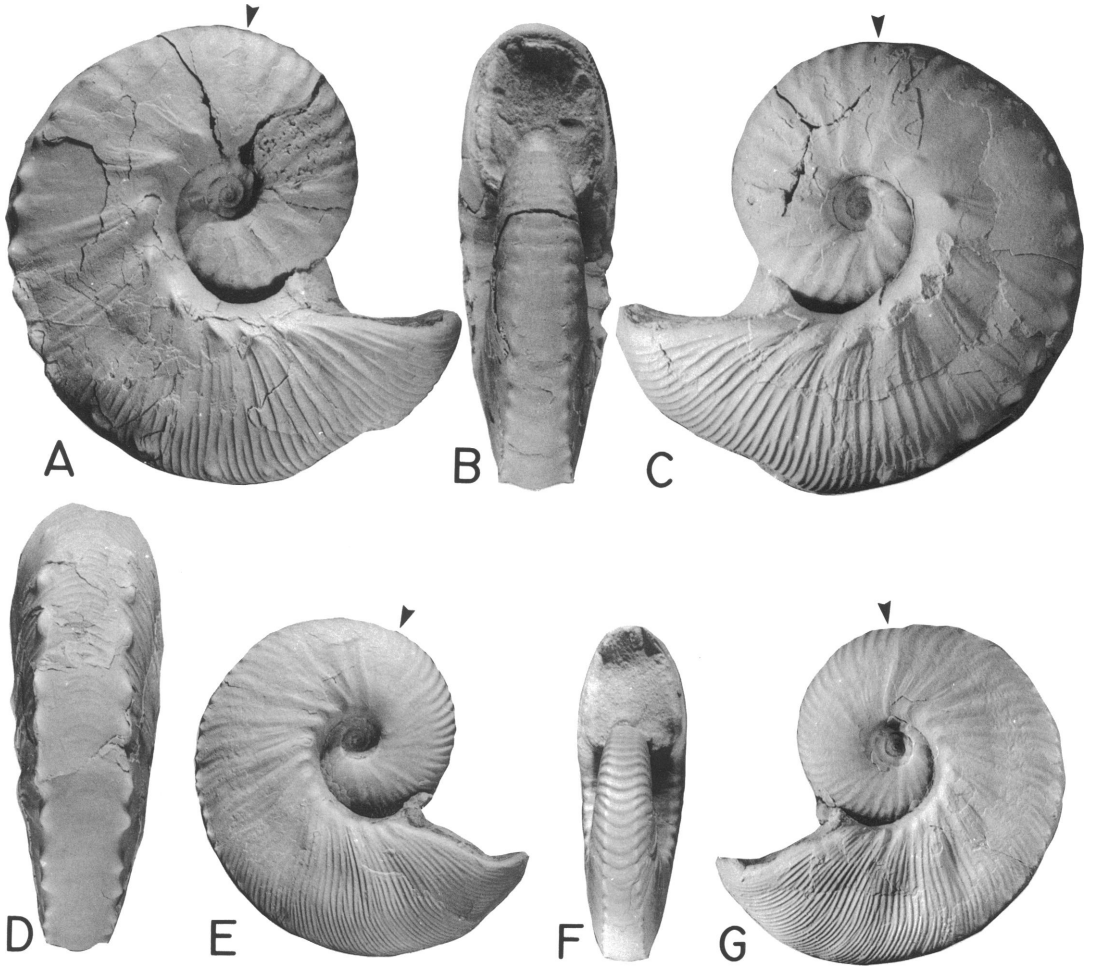

Fig. 56. *Hoploscaphites nicolletii* (Morton) microconchs. **A–D.** Specimen with injury on hook, YPM 27144, loc. 25, POAZ float. **A,** Right lateral; **B,** apertural; **C,** left lateral; **D,** posterior. **E–G.** YPM 27236, loc. 17, UNAZ. **E,** Right lateral; **F,** apertural; **G,** left lateral.

on adult specimens and questioned whether *abyssinus* might not be only a variant of *mandanensis*. Meek's figure 2a of *abyssinus* (USNM 409, refigured in our fig. 74J) is clearly a larger and more coarsely ornamented specimen of his *mandanensis,* a form whose general morphology is defined by the cast of Morton's missing type (fig. 53G, H). Meek's figure 4 of *abyssinus* does not closely resemble his figure 2 nor any other species of *Hoploscaphites* microconch in the Fox Hills, but is suggestive of the microconch of *Discoscaphites conradi* (sensu Jeletzky and Waage, 1978) in its very small umbilicus, rows of flank tubercles on its phragmocone, and persistence of the ventrolateral tubercles to the aperture. Unfortunately, Meek's specimen is missing and his figure 4 is essentially unidentifiable; thus, no basis remains for recognizing a species *abyssinus.*

Our restudy of these Fox Hills scaphites reveals that *mandanesis* specimens figured by Owen (1852: pl. 7, fig. 5; USNM 20243), Meek (1876: pl. 35, fig. 1; USNM 410), as well as Meek's *abyssinus* (1876: pl. 35, fig. 2a; USNM 409) are not microconchs of *H. nicolletii* but of *H. comprimus* (Owen, 1852). All of these specimens are refigured herein on figure 74 under the latter species. The cast of Morton's missing type is not good enough to determine

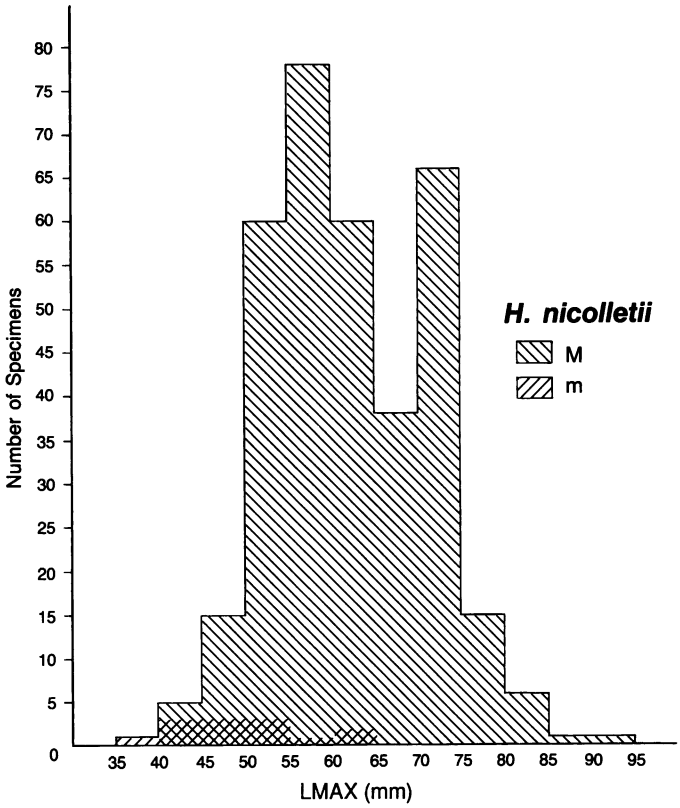

Fig. 57. Size frequency histogram of a sample of *Hoploscaphites nicolletii* (Morton) from the Fox Hills Formation in its type area.

whether it is a microconch of *H. comprimus* or *H. nicolletii* (see note under microconch synonymy, p. 73). Consequently, an allotype for *H. nicolletii* was selected from Trail City microconchs of the same assemblage zone (LNAZ) as the macroconch neotype.

OCCURRENCE: *Hoploscaphites nicolletii* is common to abundant in the Trail City Member throughout its extent in the Missouri Valley area of north-central South Dakota and adjacent North Dakota. It is largely restricted to the four assemblage zones in the lower part of this member. The species *H. comprimus* apparently succeeds it beginning in the uppermost part of the Trail City where a few scattered concretions at a single locality just a foot or two below the contact with the Timber Lake Member contain both *H. nicolletii* and *H. comprimus*. In the type area *H. nicolletii* is also present in sideritic concretions in the upper Elk Butte Member of the Pierre Shale at the Rt. 65 Moreau Bridge locality (loc. 307), where specimens of this species are exceptionally large. The total stratigraphic range of this species is from the uppermost Elk Butte Member of the Pierre Shale to the top of the Trail City Member of the Fox Hills Formation. It appears to be geographically restricted to these occurrences in the Missouri Valley region. Reports of *H. nicolletii* from other areas are discussed on p. 96.

MATERIAL: Over 1400 adult specimens of *Hoploscaphites nicolletii* were collected from the Trail City Member in the type area of the Fox Hills and adjacent areas in Corson and Dewey counties, South Dakota, and Emmons County, North Dakota. Of these specimens, 345 macroconchs and 13 microconchs, all complete or nearly complete, comprise the group of measured specimens (table 6). These 345 macroconchs are distributed among the four assemblage zones of the Trail City Mem-

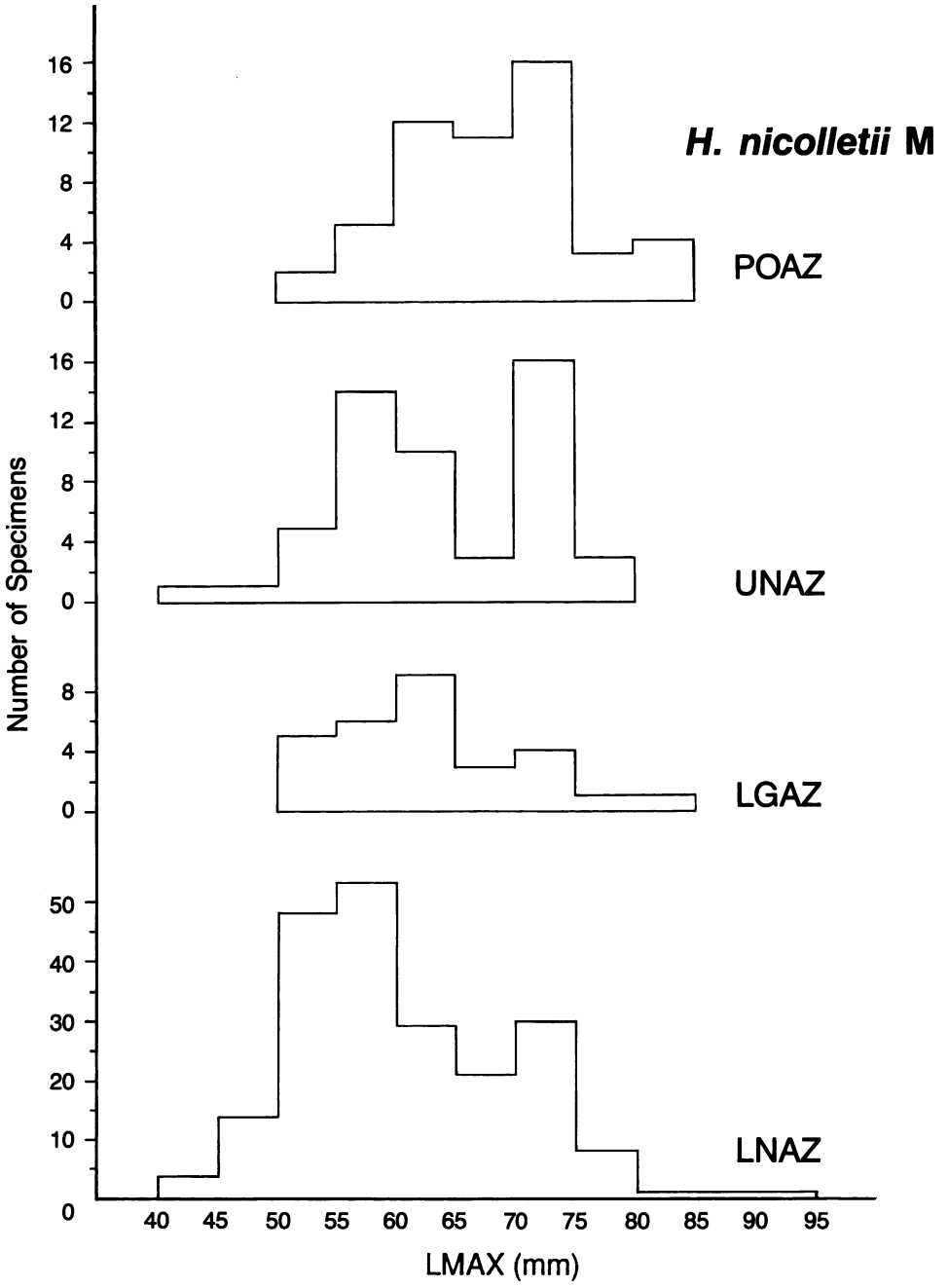

Fig. 58. Size frequency histogram of samples of *Hoploscaphites nicolletii* (Morton) macroconchs from four assemblage zones in the Fox Hills Formation in its type area.

ber as follows: LNAZ 210, LGAZ 29, UNAZ 53, and POAZ 53 (table 7). Specimens of the rarer microconch are about equally divided among the four assemblage zones. In addition, several hundred complete or nearly complete juveniles were collected.

MACROCONCH DESCRIPTION: The adult macroconch of *H. nicolletii* is tightly coiled

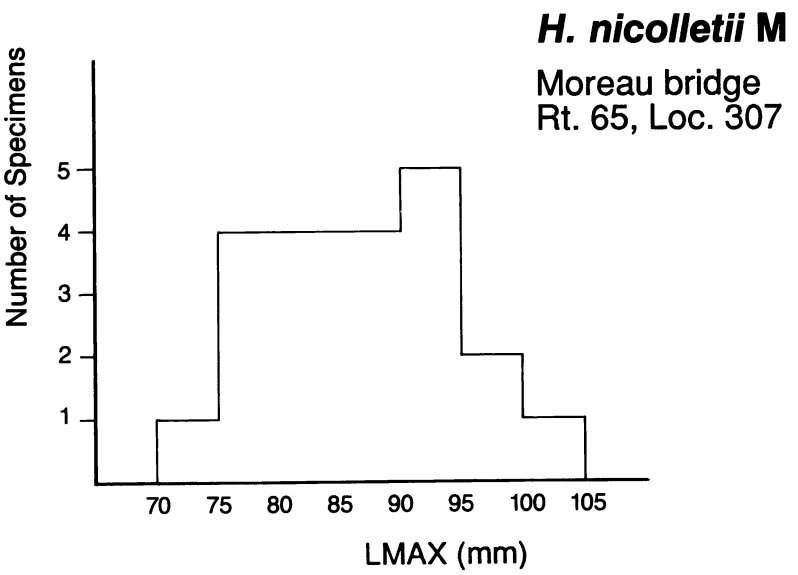

Fig. 59. Size frequency histogram of a sample of *Hoploscaphites nicolletii* (Morton) macroconchs from the uppermost Elk Butte Member of the Pierre Shale at Moreau bridge, Rt. 65, loc. 307.

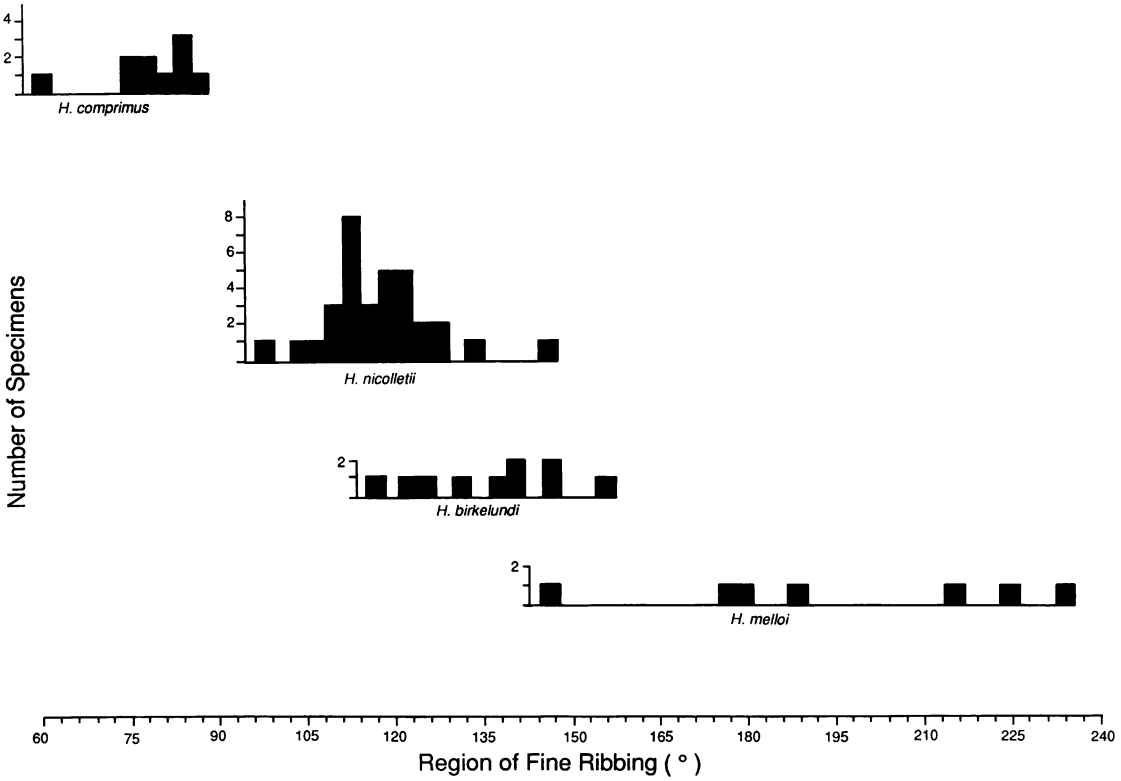

Fig. 60. Region of fine ribbing on the mature body chamber, demarcated in angular length, versus specimen number in samples of *Hoploscaphites melloi,* n. sp., *H. birkelundi,* n. sp., *H. nicolletii* (Morton), and *H. comprimus* (Owen). Species are stacked in stratigraphic order showing progressive restriction of fine ribbing on shell in successively younger forms.

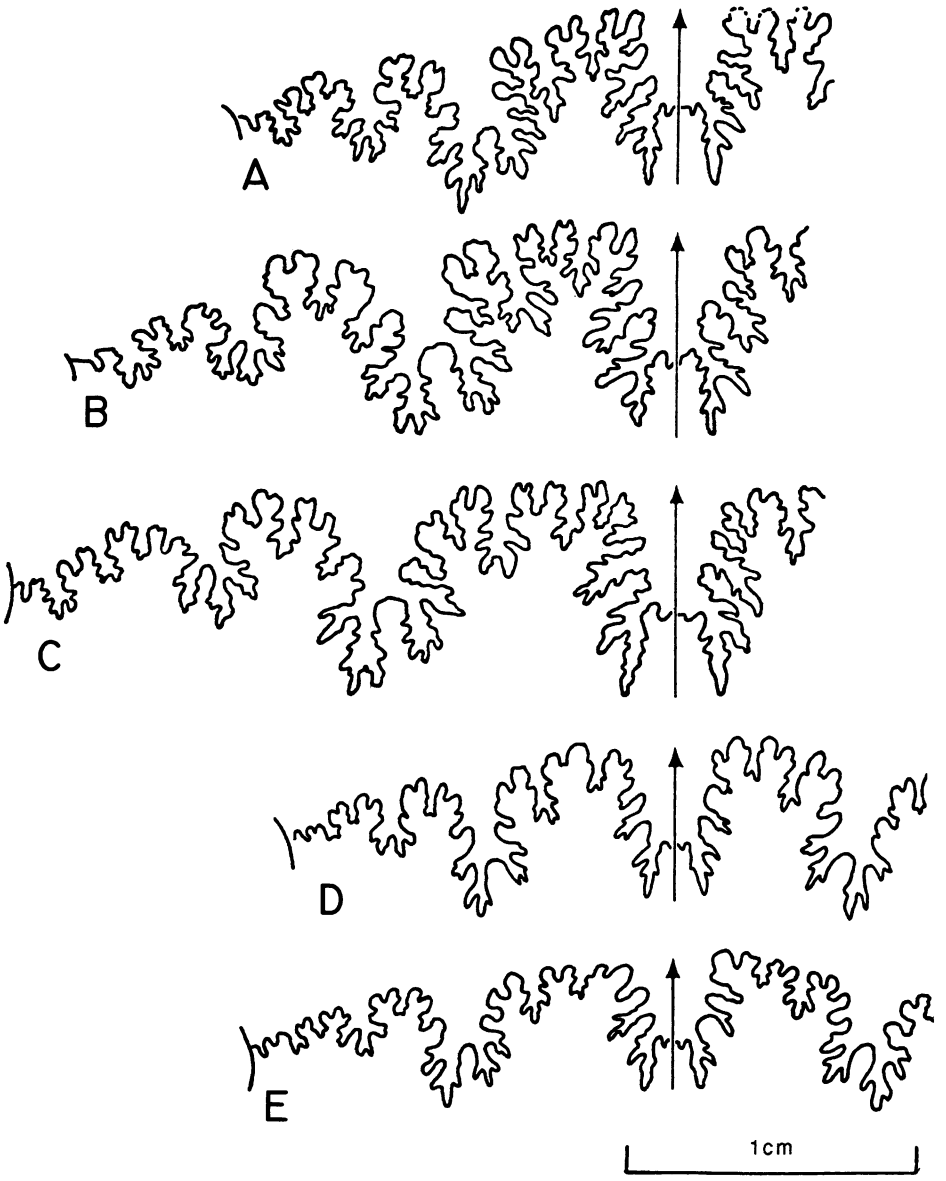

Fig. 61. Sutures of *Hoploscaphites nicolletii* (Morton) macroconchs and microconchs. **A.** Seventh from last suture of an adult macroconch, YPM 34692, loc. 21, LNAZ. **B.** Fifth from last suture of an adult macroconch, YPM 34693, loc. 44, LNAZ. **C.** Third from last suture of an adult macroconch, YPM 23742, loc. 25, LGAZ. **D.** Fifth from last suture of an adult microconch, YPM 34694, loc. 302, UNAZ. **E.** Third from last suture of an adult microconch, YPM 34695, loc. 50, LGAZ.

with a small umbilicus. The shaft of the body chamber is short; it is arcuate on the venter and straight along the dorsal shoulder. The hook is usually in contact with the phragmocone, or very slightly separated from it along the dorsal rim of the aperture; the short dorsal projection is reflexed against the venter of the phragmocone. The venter of the aperture has a short, rapidly tapering, blunt rostrumlike projection.

The dimensions of the measured specimens are listed in table 6. LMAX averages

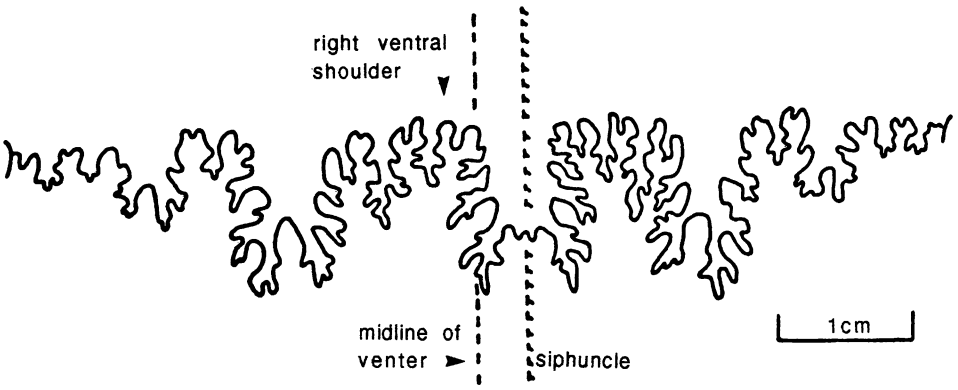

Fig. 62. Fourth from last suture of an adult macroconch of *Hoploscaphites nicolletii* (Morton), YPM 23751, loc. 44, LNAZ, showing asymmetry.

61.8 mm and ranges from 42.4 to 91.5 mm. The ratio of the size of the largest specimen to that of the smallest is 2.2. The size distribution is bimodal with a dominant peak at 55–60 mm and a smaller peak at 70–75 mm (fig. 57). It is illustrated by assemblage zone in figure 58. The average size of the specimens in POAZ (67.5 mm) is higher than that of the specimens in any of the other assemblage zones (table 7). In contrast, the size of the exceptionally large specimens of *H. nicolletii* from the top of the Elk Butte Member of the Pierre Shale, described on p. 14, averages 86.3 mm and ranges from 73.0 mm to 101.6 mm (N = 26; figs. 54A, B, 59). The ratio of the average size of these specimens to that of the specimens from the Trail City Member is 1.4.

The exposed phragmocone of the macroconch is approximately 0.5 whorls in angular length and is strongly compressed. It expands gradually in width but rapidly in height in the last quarter whorl before the ultimate septum. The ratio of whorl width to whorl height at the ultimate septum averages 0.59 with larger specimens having slightly more compressed whorl sections at this point than do smaller specimens (table 6).

The body chamber, slightly more than 0.5 whorls in angular length, increases in width at a slightly greater rate than in the phragmocone, reaching a maximum value at the anterior end of the shaft. Thereafter, width remains more or less the same through the hook to the aperture. Whorl height increases markedly in the body chamber, attaining its

TABLE 6
Adult Measurements of *H. nicolletii*[a]

	Macroconch				Microconch			
	N	$\bar{x}$	SD	Range	N	$\bar{x}$	SD	Range
LMAX (mm)	345	61.8	8.73	42.4–91.5	13	49.7	7.39	39.2–62.1
WUS (mm)	288	13.4	2.21	6.5–22.8	13	9.9	1.99	7.2–13.0
HUS (mm)	289	22.4	3.38	15.5–36.2	13	14.7	3.09	11.2–20.2
WUS/HUS	286	0.59	0.060	0.33–0.92	13	0.68	0.048	0.63–0.80
WAPT (mm)	277	18.6	2.60	13.5–28.6	12	17.1	2.09	13.2–19.9
HAPT (mm)	269	22.4	2.87	15.3–32.1	12	19.7	2.35	16.1–24.0
WAPT/HAPT	266	0.83	0.065	0.61–1.45	11	0.86	0.060	0.76–0.99
UD (mm)	277	4.9	0.67	3.3–7.3	13	6.2	1.14	4.5–8.6
UD/LMAX	277	0.08	0.015	0.04–0.12	13	0.12	0.011	0.10–0.14
A (°)	54	45.6	6.52	32.0–61.5				

[a] Abbreviations: see table 1 and figure 9.

TABLE 7
Maximum Length (mm) of *H. nicollettii* by Assemblage Zone (AZ)[a]

	Macroconch				Microconch			
AZ	N	$\bar{x}$	SD	Range	N	$\bar{x}$	SD	Range
POAZ	53	67.5	6.89	50.7–80.4	3	54.8	10.88	42.3–62.1
UNAZ	53	63.0	8.06	42.6–77.0	3	44.6	4.68	39.2–47.4
LGAZ	29	62.5	7.26	50.2–81.0	3	52.3	8.11	43.7–59.8
LNAZ	210	59.9	8.84	42.4–91.5	4	47.9	4.27	41.8–51.4

[a] Abbreviations: see table 1 and description of assemblage zones in the text.

maximum about midlength, then decreases through the rest of the shaft and the hook to the aperture, reaching the same value there as at the ultimate septum. The ratio of whorl width to whorl height at the aperture averages 0.83 (table 6), with larger specimens having slightly more depressed apertures than do smaller specimens. The whorl section at the aperture is significantly more depressed than that at the ultimate septum (0.59).

The umbilical diameter averages 4.9 mm (table 6), with larger specimens having relatively smaller umbilical diameters than do smaller specimens. The ratio of umbilical diameter to shell diameter averages 0.08 (table 6). Variation in umbilical diameter reflects the tightness of the coil in the last whorl of the adult shell; commonly it is the same or even less than that of the preceding whorl; sometimes it is greater. The umbilical edge of the coil passes directly into the straight umbilical shoulder of the body chamber in most adult macroconchs. Some specimens, mostly very small adults, have a sagging rather than straight umbilical shoulder. Dorsal swelling along the shoulder is sometimes present, especially in larger shells, and restricts the size of the umbilicus (fig. 49A, C, D).

The pattern of ribbing in adult macroconchs is the same for all specimens, regardless of size. Ribbing is prorsiradiate throughout, dominantly fine, with primaries and long secondaries very gently biconcave. Increase is by both intercalation and branching. Ribs become finer and more closely approximated forward from the point of exposure, and the anterior two-thirds of the body chamber is typically covered with very fine, closely spaced ribs. All of the ribs on the venter show an adoral projection.

The overall fining-forward rib pattern is not a simple gradation but includes several fairly distinct developmental stages or zones (figs. 51C, 52A), some of which coincide with changes in the shape of the shell as it passes into its scaphitid form. The first stage includes the exposed phragmocone, which at its first appearance, has relatively low, broad ribs (see ontogeny of *H. nicolletii,* p. 92, for a more complete description of the phragmocone). The ratio of the number of dorsal to ventral ribs is 1:2 or less commonly 1:3; forward near the end of the phragmocone this ratio is about 1:4 to 1:6. Intercalation and branching are mostly on the ventral half of the flanks; the number of ribs crossing the venter of the phragmocone is commonly 8–10/cm.

The second stage begins approximately at the end of the phragmocone and includes a small area of the posterior body chamber, usually about 40° measured along the venter from the ultimate septum. This area, referred to as the "stretch zone" (Landman and Waage, 1986), is marked by weakening of the ribbing, which in some specimens renders the shell nearly smooth on the flanks and to some extent even on the venter.

Stage 3 covers the posterior part of the shaft, which shows narrow but strong, slightly biconcave primaries with intercalated secondaries. On most shells, the primaries of stage 3 are the most conspicuous ribs on the body chamber but they are neither as regularly spaced nor sized as those of stage 1. There are commonly 9–10 ribs/cm on the venter and the ratio of the number of dorsal to ventral ribs is about 1:4, very similar to the rib density at the end of the phragmocone in stage 1.

Stage 4 occupies the anterior shaft and hook of the body chamber, featuring very fine, closely approximated ribbing (fig. 60). The number of ventral ribs increases abruptly from

about 10–13/cm on the shaft to as many as 20–22/cm on the anterior body chamber. Details of shell ribbing are muted on the innermost shell layers and are, therefore, absent on steinkerns. For example, steinkerns may show only a few broad undulations on the flanks of the body chamber and the fine ribbing on the venter may be barely visible.

Only ventrolateral tubercles are present on *H. nicolletii* macroconchs; these are most common on the posterior two-thirds of the body chamber. They increase in size within stage 2 of the ribbing pattern, reach their maximum size within stage 3, and disappear within stage 4. Ventrolateral tubercles may or may not occur on part of the exposed phragmocone. Only on exceptionally large, robust macroconchs or those with uncommonly coarse ornament do ventrolateral tubercles extend to the aperture and occur over most or all of the exposed phragmocone. On such specimens, a few faint bullate rib swellings may also appear on the body chamber just below the umbilical shoulder.

The ventrolateral tubercles first appear as rib swellings where the ribs bend forward near the ventral margin. Commonly, the tubercles become clavate as they increase in size (fig. 52A, C, D). Where tubercles fade out on the body chamber they may revert to bullate rib swellings. Tubercle spacing is as variable as tubercle number and shows no preferred pattern; the distribution of tubercles on the two ventrolateral rows may or may not match.

The external suture of macroconchs (figs. 16A–C, 62) is typically scaphitid and does not differ significantly from that of macroconchs of other Campanian and Maastrichtian species of *Hoploscaphites.* The ventral and lateral lobes are subequal in size and the latter is asymmetrical owing to the relative enlargement of its inner branch. The lateral lobe is consistently bifid; the first auxillary lobe, which is half or less than half the size of the lateral, may be bifid or trifid. The folioles on the saddles are somewhat more delicate, or finely divided, than the blunter folioles of species of *Discoscaphites,* but no definitive differences in sutures were detected among the genera and species of Fox Hills scaphites.

The ventral muscle attachment area is ovoid in shape (fig. 53E). The dorsal attachment areas, which are generally not preserved, appear as small saddles across the umbilical shoulder just adoral of the ultimate septum (fig. 53F).

MICROCONCH DESCRIPTION: The average size of microconchs is significantly smaller than that of macroconchs (fig. 57, table 6). The ratio of the size of the largest microconch to that of the smallest microconch is 1.48. As is typical for scaphitid microconchs, the whorl height expands gradually through the arcuate shaft of the body chamber and then decreases very slightly through the hook. Departure of the shell from the normal coil is slight and begins at about the position of the ultimate septum. In larger specimens there may be a slight gap between the phragmocone and body chamber about where the shaft turns into the hook, whereas this gap is not evident in smaller specimens, the coil of the phragmocone remaining partially within the impressed zone of the body chamber. The presence of such a small gap between the phragmocone and body chamber led both Morton (1842) and Owen (1852) to refer this microconch (then the species *mandanensis*) to the genus *Ammonites* and Meek (1876: 444) to suggest that it "may be regarded as forming a transition from *Scaphites* to *Ammonites.*" In all specimens, the microconch hook is reflexed back so that its dorsal projection lies against the phragmocone.

The adult shell is strongly compressed and the nearly flattened flanks converge slightly toward the venter. Larger specimens show the same degree of compression as smaller specimens. The ratio of whorl width to whorl height at the ultimate septum averages 0.68, which is significantly higher than that in macroconchs (0.59; table 6). The ratio of whorl width to whorl height at the aperture averages 0.86, which is not significantly different from that in macroconchs (0.83; table 6). As in macroconchs, the whorl section is significantly more depressed at the aperture than at the ultimate septum.

The umbilical diameter averages 6.2 mm, which is significantly larger than that in macroconchs (4.9 mm; table 6). The ratio of umbilical diameter to shell diameter averages 0.12, which is also significantly higher than that in macroconchs (0.08). Larger microconchs have approximately the same relative umbilical diameter as smaller microconchs. All whorls including the protoconch are par-

tially visible within the umbilicus of the adult. The umbilical shoulder of the body chamber is broad and flat and it slopes gently outward to form a sharp, slightly obtuse angle with the flanks. On many specimens, the shell width of the body chamber increases more rapidly on the dorsal than on the ventral part of the shell so that the whorl section and aperture become subchordate to chordate in outline.

Ribbing on the mature shell is similar to that on the macroconch. The ribs are prorsiradiate and show an adoral projection on the venter. They become finer and more closely approximated on the anterior half of the body chamber. However, the distinctive changes in ribbing observed on macroconchs are not as obvious on microconchs. Most of the exposed phragmocone has relatively broad ribs that increase by intercalation and branching, which occurs most conspicuously near the venter; the ratio of the number of dorsal to ventral ribs ranges from 1:2 to 1:3. Pronounced bullae appear on the edge of the umbilical shoulder on the posterior part of the body chamber or somewhat earlier in larger shells. These bullae give rise to primary ribs that increase by intercalation and branching; the ratio of the number of dorsal to ventral ribs in this area is about 1:4. Ribbing is weak on the posterior half of the body chamber but becomes more clearly defined, at least on outermost shell layers, on the anterior half, where ribs increase markedly in number and approximation, reaching a density of about 20/cm on the venter.

Ventrolateral tubercles occur on the posterior two-thirds of the body chamber, usually on every rib, and commonly are also present on the phragmocone. On larger, more coarsely ornamented specimens these tubercles may occur on the entire exposed phragmocone. Where the ventrolateral tubercles are present, the venter of the shell tends to become more flattened and the ventral ribs fainter, only returning after the disappearance of the ventrolateral tubercles.

The suture of microconchs is similar to that of macroconchs (fig. 61D, E). The saddles and lobes are not as deep or as intricately divided but these differences result from closer septal spacing in the smaller microconchs.

ONTOGENY: The protoconch and ammonitella are similar in size and shape to those of other scaphite species (table 1). The diameter of the ammonitella averages 769 μm in macroconchs, which is similar to that in microconchs (762 μm). Comparison of the average ammonitella diameter in both dimorphs by assemblage zone, listed in table 4, indicates that there is no significant stratigraphic variation. The ammonitella angle averages 302° in macroconchs and 305° in microconchs; these averages are slightly larger than those in other scaphites. The protoconch angle averages 67° and 65° in macroconchs and microconchs, respectively.

Dorsoventral, intercostal cross sections through an adult macroconch and an adult microconch are illustrated in figure 63. The growth of whorl width is negatively allometric in both dimorphs (slopes range from 0.8102 to 0.8557; fig. 64) in contrast to that of whorl height, which is positively allometric in both dimorphs (slopes range from 1.064 to 1.110; fig. 65). At comparable shell diameters, whorl width is slightly larger in macroconchs than in microconchs whereas whorl height is approximately the same in both dimorphs. The shell whorls up to about 5 mm diameter are depressed with the ratio of whorl width to whorl height ranging from 1.0 to 2.0. The whorls become increasingly more compressed during ontogeny with the ratio of whorl width to height reaching a minimum of 0.6 to 0.7 at the base of the mature body chamber. Microconchs tend to be slightly more compressed than macroconchs at comparable shell diameters.

The growth of umbilical diameter is approximately isometric (fig. 66). The rate of increase of the umbilical diameter is more or less the same in both dimorphs until maturity although microconchs tend to be slightly more widely umbilicate than macroconchs. At approximately one whorl before the base of the mature body chamber, the umbilical diameter begins to increase more slowly or not at all in macroconchs whereas it continues to increase at the same rate in microconchs. The ratio of umbilical diameter to shell diameter decreases through most of postembryonic growth. At comparable shell diameters microconchs tend to have higher ratios than macroconchs. The ratio decreases more steeply in macroconchs than in microconchs starting at approximately one whorl before the base of the mature body chamber. It

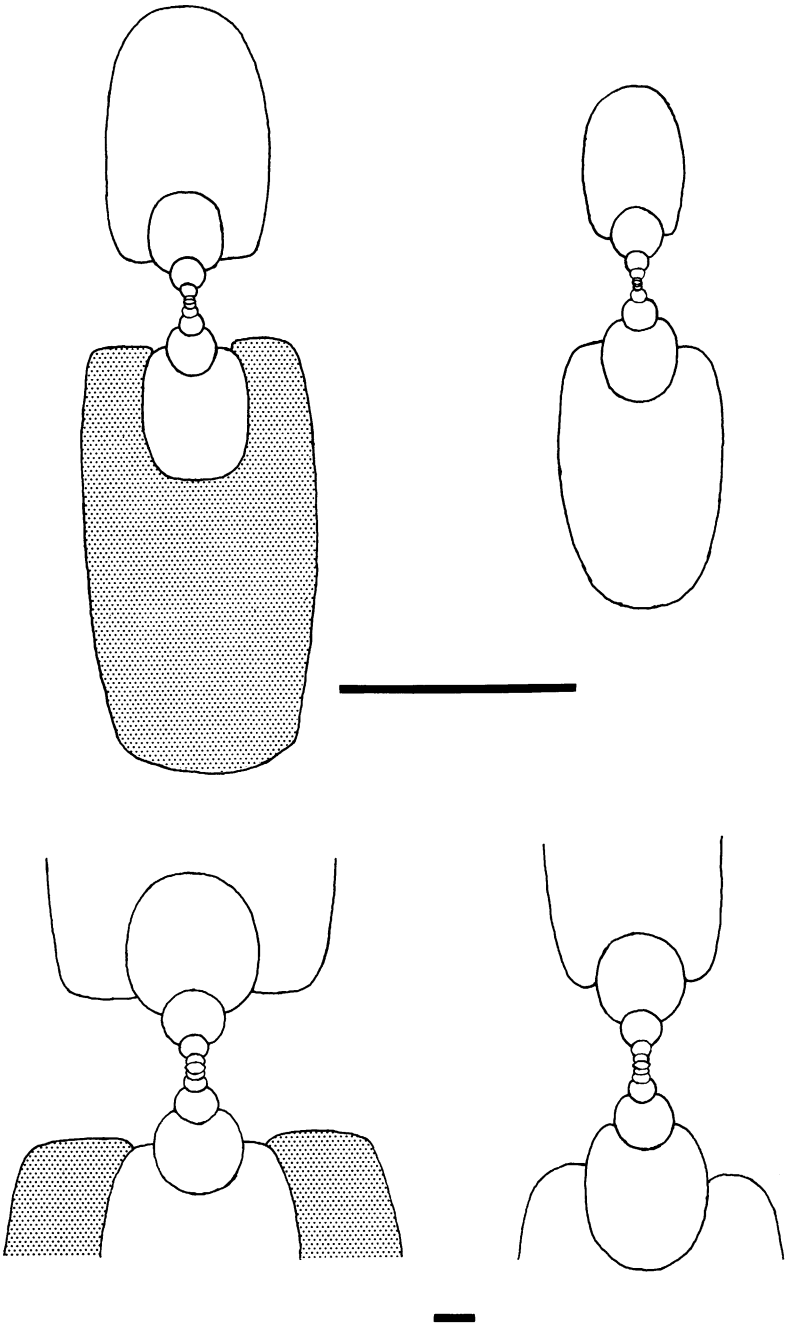

Fig. 63. Dorsoventral, intercostal cross sections through adult dimorphs of *Hoploscaphites nicolletii* (Morton). **Left.** Macroconch, YPM 23053, loc. 44, LNAZ. **Right.** Microconch, AMNH 44226, loc. 3157, TCM. Shaded area demarcates mature body chamber. Upper scale bar = 1 cm; lower scale bar = 1 mm.

reaches a minimum value near the base of the body chamber of 0.21–0.23 in microconchs and 0.10–0.17 in macroconchs.

The development of ornamentation in macroconchs is illustrated in figure 67. At approximately 4 mm shell diameter ribs appear on the venter with a forward projection and prorsiradiate ribs (primaries) appear on

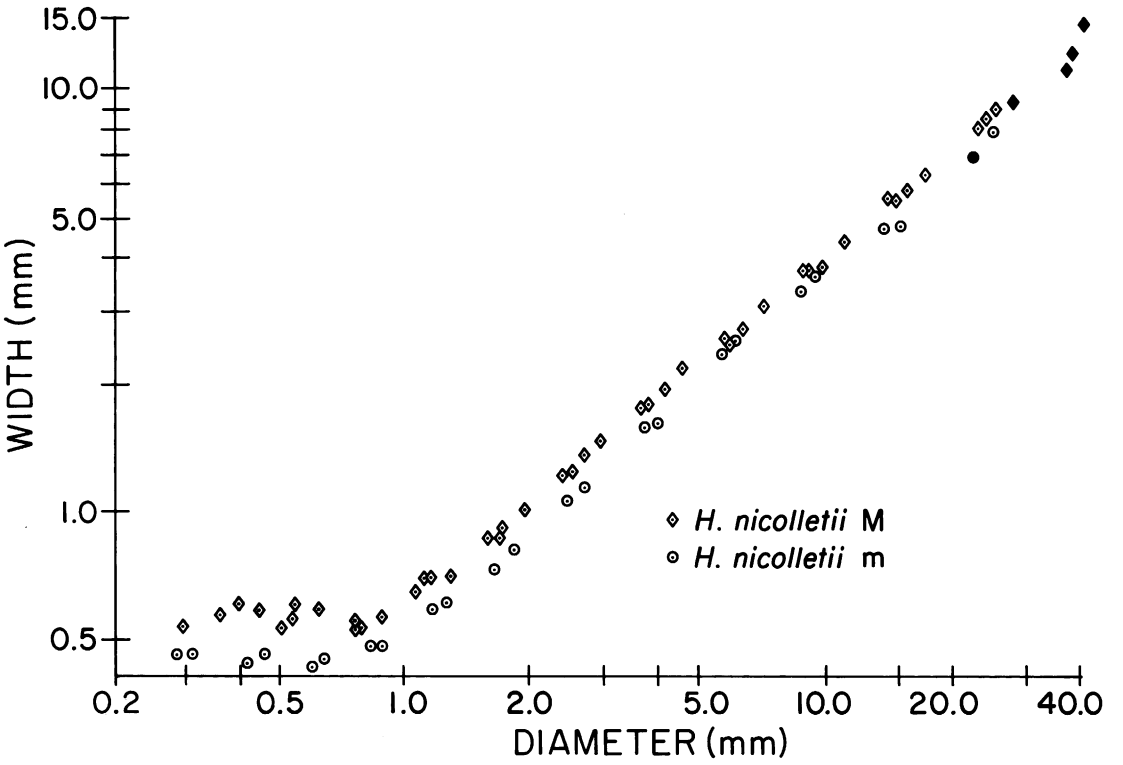

Fig. 64. Plot of whorl width versus shell diameter through the ontogeny of six adults (four macroconchs and two microconchs) of *Hoploscaphites nicolletii* (Morton). Black symbols indicate measurements near the base of or in the mature body chamber. Measurements listed in Appendix II.

the flanks. The ventral ribs maintain their forward projection throughout ontogeny and the primaries become weakly flexuous. Initially, secondaries develop mostly by intercalation and are short, originating near the ventral margin, leaving the upper third of the flanks smooth except for the primary ribs. Gradually, the secondaries become longer, developing by both branching and intercalation. Up to the point of exposure, the ratio of the number of dorsal to ventral ribs is 1:2 or, less commonly, 1:3.

Midway on the exposed phragmocone, the primaries become sharper and more biconcave in many specimens and develop slight bullae on the upper one-third of the flanks; the primaries weaken at the end of the phragmocone. The ventral ribs become sharper along with the primaries. Very long secondaries may appear, which develop by both branching and intercalation. At the end of the phragmocone, the ratio of the number of dorsal to ventral ribs may reach a maximum of 1:4 to 1:6. Ventrolateral tubercles appear on the exposed phragmocone, especially on larger specimens, occurring on every rib or every second or third rib.

The development of ornamentation in microconchs is basically similar to that in macroconchs (fig. 67). Ventral ribs show a forward projection as soon as they appear in ontogeny. However, because the whorls of microconchs tend to be slightly more compressed than those of macroconchs, the ventral ribs, starting at approximately 10 mm shell diameter (approximately 0.5 whorls before the point of exposure), are coarser and stubbier than those in macroconchs. They also tend to broaden along the mid-venter. Primaries on the juvenile shell are prominent, prorsiradiate, and weakly flexuous. They are perhaps slightly coarser than those in

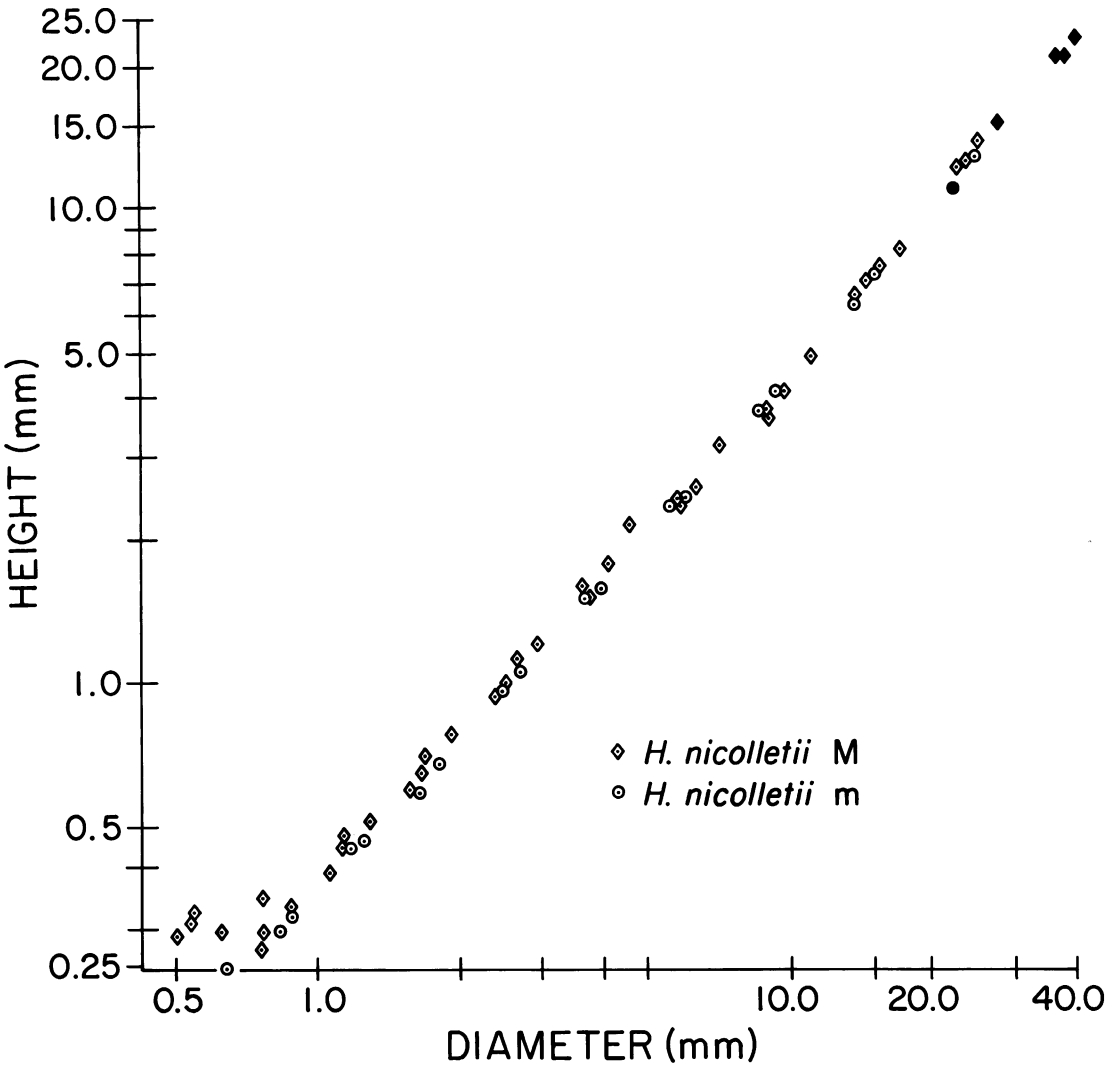

Fig. 65. Plot of whorl height versus shell diameter through the ontogeny of six adults (four macroconchs and two microconchs) of *Hoploscaphites nicolletii* (Morton). Black symbols indicate measurements near the base of or in the mature body chamber. Measurements listed in Appendix II.

macroconchs. The ratio of the number of dorsal to ventral ribs is 1:2 or 1:3 up to the point of exposure, similar to that in macroconchs. On the exposed phragmocone, the primaries sometimes become slightly more biconcave. However, the ratio of the number of dorsal to ventral ribs remains the same. Ventrolateral tubercles first appear on the exposed phragmocone, occurring on every rib. As a result, the forward projection of the ventral ribs gradually diminishes and the venter becomes flatter in costal cross section.

Both dimorphs show septal approximation at maturity. To establish the patterns of septal approximation, 32 macroconchs and eight microconchs were examined. Interseptal distances of as many as the last eight chambers in macroconchs and of as many as the last seven chambers in microconchs were measured.

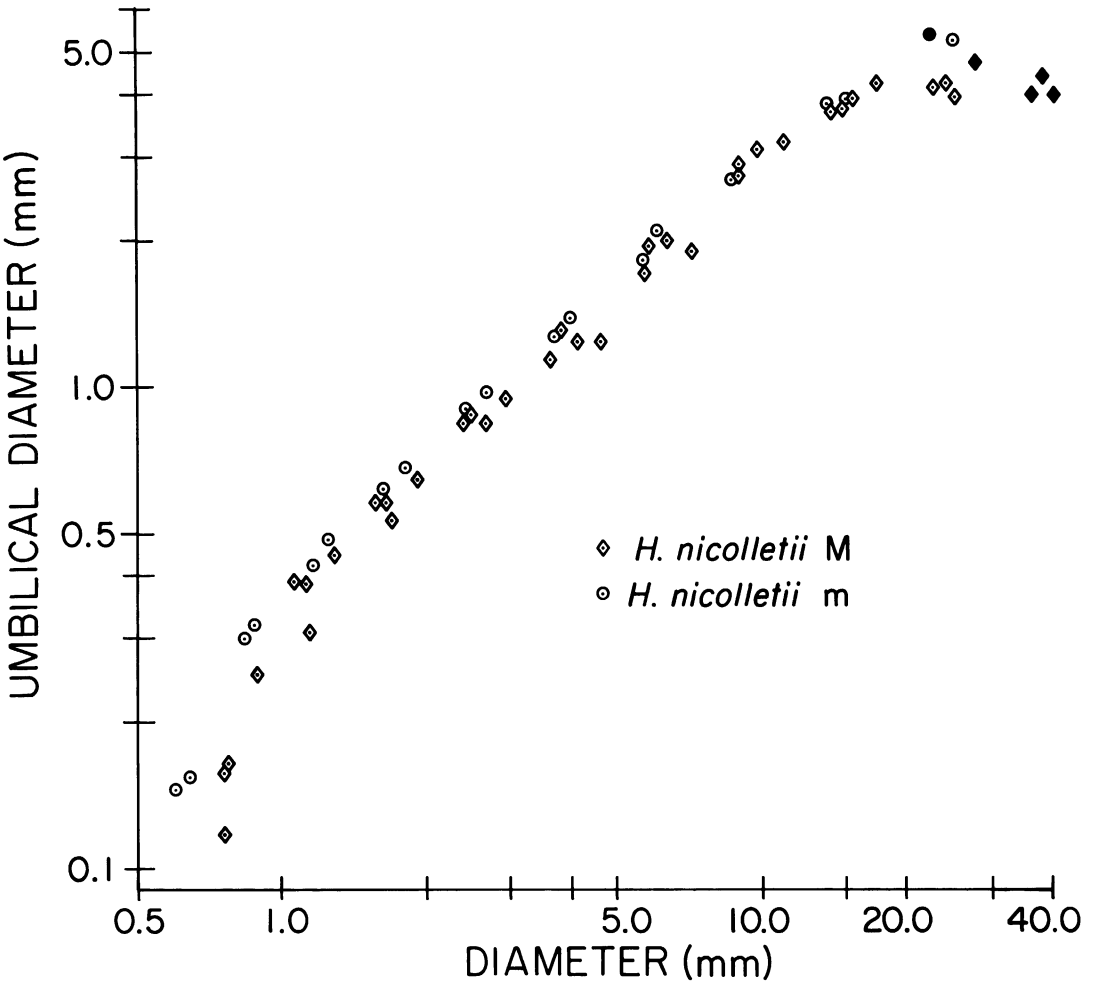

Fig. 66. Plot of umbilical diameter versus shell diameter through the ontogeny of six adults (four macroconchs and two microconchs) of *Hoploscaphites nicolletii* (Morton). Black symbols indicate measurements near the base of or in the mature body chamber. Measurements listed in Appendix II.

Septal approximation in macroconchs occurs over many more chambers and is more dramatic than that in microconchs (table 8, fig. 68). Septal approximation in macroconchs most commonly occurs over the last three chambers although it may occur over as many as the last five chambers or over as few as the last two chambers. The decrease in septal spacing is generally monotonic. The interseptal distance of the last chamber averages 44 percent of that of the last "normal" chamber, indicating an average reduction in septal spacing of more than one-half. Septal approximation in microconchs most commonly occurs in only the last chamber or over the last two chambers. The interseptal distance of the last chamber averages approximately 70 percent of that of the last "normal" chamber, indicating a much lower average reduction in septal spacing than in macroconchs.

DISCUSSION: References to *Hoploscaphites* (or *Discoscaphites*) *nicolletii,* or to *H. nicolletii*-like scaphites and the microconchs *mandanensis* and *abyssinus,* occur in a number of reports on the Cretaceous of the northern Great Plains. Review of these occurrences reveals that *H. nicolletii,* as defined herein, is apparently restricted in its distribution to the type area of the Fox Hills Formation and contiguous outcrops in the Missouri Valley of the central Dakotas.

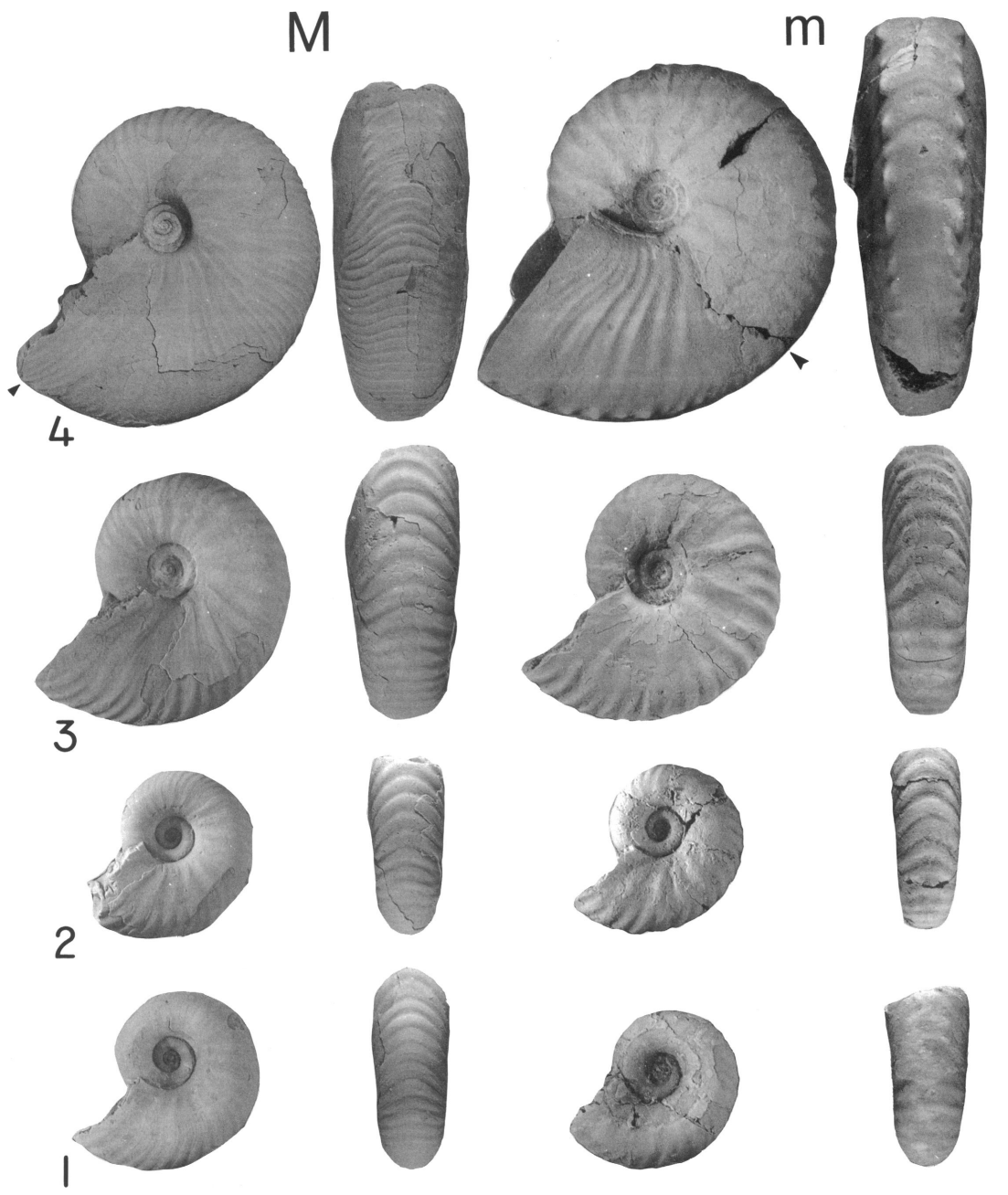

Fig. 67. Dissections of adult dimorphs (macroconch, YPM 30648, loc. 55, LNAZ, and microconch, AMNH 44675, loc. 3159, TCM) of *Hoploscaphites nicolletii* (Morton) showing four sizes through ontogeny in lateral and ventral view. 1. ×3. 2. ×2. 3. ×2. 4. ×1.5. Arrows indicate base of mature body chamber.

Kellum (1962: 55) listed *Discoscaphites nicolleti* (Morton) in a tally of the marine fauna of the Fox Hills Formation in the Lance Creek–Red Bird area of eastern Wyoming and this species also appears on other faunal lists from this area. The form of *Hoploscaphites* in the Lance Creek–Red Bird area resembles *H. nicolletii* superficially but is specifically

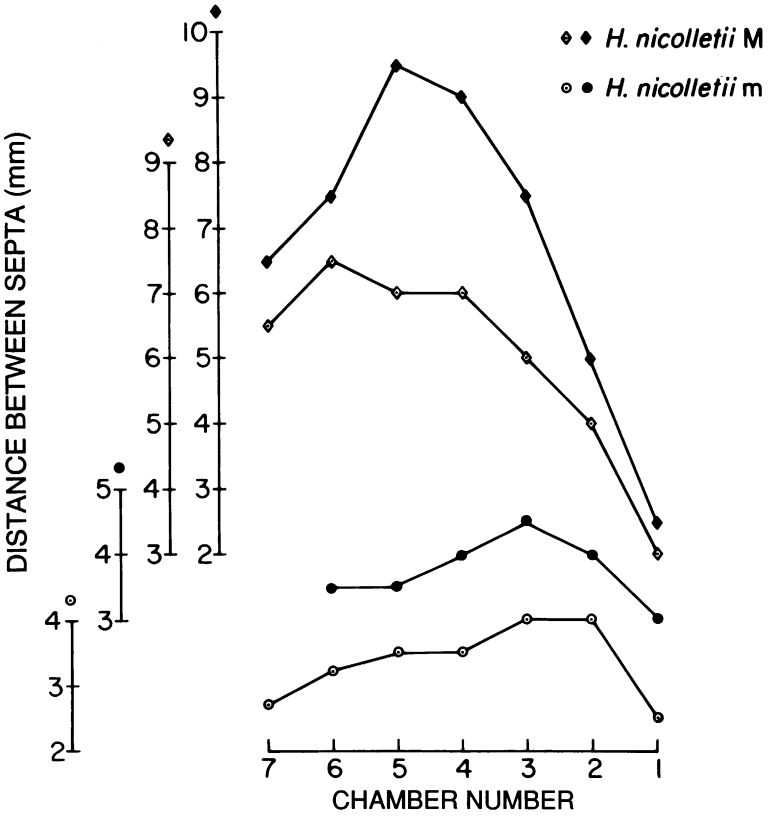

Fig. 68. Distance between septa versus chamber number, counting from the last, most recently formed, chamber of the phragmocone (1), in two macro- and two microconchs of *Hoploscaphites nicolletii* (Morton). Septal approximation occurs over more chambers and is more marked in macroconchs than in microconchs.

distinct and we describe it here (p. 119) as *Hoploscaphites birkelundi,* n. sp.

Elias (1933: 326) described *Discoscaphites nicolletii* var. *saltgrassensis* from the Salt Grass Member of the Pierre Shale in Wallace County, Kansas, suggesting (p. 327) that this marked the first appearance of the species in the central High Plains Cretaceous. Elias' specimen, a macroconch, lacks the strong adoral projection of ribbing on the venter characteristic of *H. nicolletii* (ibid., pl. 36, fig. 3b, 3c). It is a *Hoploscaphites* and probably a member of the clade including *H. nicolletii.* Elias' specimen comes from the upper part of the Salt Grass Member (ibid., p. 327, the legend on pl. 36, fig. 3, indicating the base of the member, is in error). *Baculites pseudovatus* var. A described by Elias from the lower and middle parts of the Salt Grass Member was subsequently redescribed as *B. eliasi* by Cobban (1958b: 663). This places Elias' *nicolletii* var. *saltgrassensis* just above the *B. eliasi* Range Zone and either still within that zone or in the *B. baculus* Range Zone that succeeds it.

TABLE 8
Pattern of Septal Approximation in *H. nicolletii*[a]

Di-morph	N	Number of chambers				
		1	2	3	4	5
M	32	—	5	15	8	4
m	8	5	3	—	—	—

[a] This table compares the number of chambers over which septal approximation occurs in a specimen versus the number of specimens within each dimorph. "N" equals the total number of specimens in which septal spacing was measured. Chambers are numbered starting with the last, most recently formed, chamber of the phragmocone (1).

Elias (1933: 328, pl. 39, figs. 2 to 8) also described and figured under the name *Discoscaphites abyssinus* four *Hoploscaphites* microconchs (figs. 2, 4, 6, 8), one *Hoploscaphites* macroconch (fig. 3), and two unidentifiable fragments. All are from the Beecher Island Shale Member of the Pierre Shale. On the basis of the baculites that Elias listed from this member they could be from either the *B. grandis* or *B. clinolobatus* Range Zone. The macroconch was refigured by Jeletzky (1962: 1015, pl. 141, fig. 3) under the name *Scaphites* (*Hoploscaphites*) aff. *nicolletii*. He pointed out its differences from the typcial *nicolletii* of the Missouri Valley Fox Hills, and its similarities to an undescribed species of *Hoploscaphites* in the *Baculites grandis* Range Zone. We have collected specimens very similar to this macroconch in concretions with *B. grandis* in the upper Pierre Shale of the Lance Creek–Red Bird area; they differ from *H. nicolletii* in being smaller and stouter, in having umbilical bullae on the body chamber and more numerous ventrolateral tubercles, and in lacking an adoral projection of the ventral ribs. The microconchs described by Elias, by association, most likely belong with this undescribed *Hoploscaphites* macroconch.

Landes (Russell and Landes, 1940: 179) identified *Discoscaphites abyssinus* from the Eastend Formation in Medicine Lodge Coulee, Alberta. Riccardi (1983: 13, pl. 1, figs. 23, 24) subsequently figured and described under *Hoploscaphites* sp. indet. one of Landes' specimens and a second specimen (ibid., pl. 1, figs. 25, 26) from the Belanger Member of the Bearpaw Formation, Cypress Hills, Saskatchewan. Both are partial specimens, mostly body chambers, of small microconchs and, as Riccardi (ibid., p. 13) observed, too few and poorly preserved for specific assignment. They differ from *H. nicolletii* microconchs in a number of features but appear similar to microconchs described by Elias (1933: pl. 39, figs. 2, 4, 6, 8) from the Beecher Island Shale Member of the Pierre Shale. Riccardi (ibid., p. 6) placed *Hoploscaphites* sp. indet. in the *Baculites baculus* Range Zone on his range chart and illustrated (ibid., pl. 26, figs. 6–10) a specimen of that baculite from the Belanger Member.

Riccardi (1983: 13, pl. 1, figs. 27–29) also described a small incomplete scaphite, *Hoploscaphites* sp. β, from the *Baculites baculus* Zone, noting that "In all the features present in the last available growth stages this material resembles *Hoploscaphites mandanensis* (Morton) and *H. nicolletii* (Morton)." The specimen figured retains only a small fraction of body chamber, but even if fully restored the specimen would be smaller than the smallest known *H. nicolletii*. Moreover, the ribbing shows only a very slight forward arching on the venter, whereas the stronger forward projection of the ventral ribbing on *H. nicolletii* shows up as soon as the ribs appear in ontogeny (p. 94). Riccardi (ibid., p. 13) pointed out additional differences; his *H.* sp. β may well belong with the *gilli-nicolletii* clade but it is not *H. nicolletii*.

Outside North America, the superficial resemblance of *Hoploscaphites nicolletii* to some members of the *H. constrictus* group scaphites has long been recognized (Frech, 1915; Nowak, 1916) but formal identification of foreign specimens as *H. nicolletii* are few. Ravn (1918: 363) described as *Scaphites nicolletii* a specimen from the Upper Campanian of Niagornat, Nûgssuaq peninsula, West Greenland. Subsequently, Rosenkrantz (1942: 40) showed this identification to be incorrect and Donovan (1953: 121) redescribed Ravn's scaphite as a new species, *Scaphites greenlandicus*. In his discussion of the distribution of *S. greenlandicus*, Donovan (ibid., p. 123) noted that "It may be represented in North America by the larger of the two examples figured by Meek (1876: pl. 34, fig. 4) as *S. nicolleti*, but figured North America material is not adequate to establish the occurrence of the species there beyond doubt." Indeed, Meek's figure does not clearly show the differentiated rib pattern of the actual specimen, illustrated in our figure 70A, B, which is diagnostic of *Hoploscaphites comprimus* (Owen), described herein. *H. nicolletii* and *H. comprimus* are both Maastrichtian and are younger forms than the Upper Campanian *S. greenlandicus*.

Jeletzky (1962: 1014) described a single fragmentary specimen from the Portland Cement Factory chalk pit at Hemmoor, Niederelbe, Germany, and assigned it to *Scaphites* (*Hoploscaphites*) *nicolletii* (Morton, 1842?) Meek, 1876. He noted specifically (ibid., p.

1015) that the Hemmoor specimen is similar only to Meek's (1876) specimens, which are *H. comprimus* (see p. 76), and not with Morton's (1842) type. He then compared the specimen directly (ibid., p. 1015, pl. 141, figs. 1a, b, c, d) with a complete specimen of *H. nicolletii* as redefined herein. Birkelund (1965: 158) believed the Hemmoor specimen "too poorly preserved for a certain identification," and Waage (1968: 145) agreed, adding that what ornament the Hemmoor specimen does show does not correspond with the distinctive ribbing pattern of *H. nicolletii*. Further study of the illustration of the somewhat distorted Hemmoor specimen (Jeletzky, 1962: pl. 141, fig. 2b) reveals that ventral ribbing on the periphery, if corrected for the distortion, lacks the strong anterior projection typical of *H. nicolletii*.

Of the European Maastrichtian scaphites *Hoploscaphites nicolletii* resembles most those variants of *H. constrictus* that possess both fine ribbing and ventrolateral tubercles on the body chamber. Nowak (1911: pl. 33, fig. 14) illustrated a specimen possessing these characters as *H. constrictus-tenuistriatus* Kner. Both Birkelund (1982) and Kennedy (1986a, b) treated *H. tenuistriatus* as a separate species including only nodeless forms with finely ribbed body chambers, referring Nowak's nodose form to *H. constrictus*. Nowak (ibid., pl. 33, figs. 9–11) also included several specimens with finely ribbed and tuberculate body chambers in his variety *H. constrictus-vulgaris*, which Kennedy (1986a, b) has synonymized under *H. constrictus*. Jeletzky (1962: 1015) tentatively referred Nowak's tuberculate *H. constrictus-tenuistriatus* to *Hoploscaphites nicolletii* but the smaller umbilicus of the former and lack of the strong anterior projection of the ventral ribbing and apertural lip preclude the possibility that it is conspecific with *H. nicolletii*.

To date there is no evidence that the endemic *H. nicolletii* ever got beyond the Dakotas, let alone North America.

Hoploscaphites comprimus (Owen, 1852)

Figures 60, 69–81

Macroconch Synonymy:

Scaphites (*Ammonites*?) *comprimus* Owen, 1852: 580, pl. 7, fig. 4.

Scaphites (*Discoscaphites*) *conradi* var. *intermedius* (Morton), Meek, 1876: 433, pl. 34, fig. 3.

Scaphites (*Discoscaphites*) *nicolletii* (Morton), Meek, 1876: 435–436, pl. 34, figs. 2a, b and 4a, b.

Microconch Synonymy:

(See note under microconch synonymy of *H. nicolletii*, p. 73).

Ammonites (?) *mandanensis* Morton, Owen, 1852: pl. 7, fig. 5.

Scaphites (*Discoscaphites*) *mandanensis* (Morton), Meek, 1876: pl. 35, fig. 1.

Scaphites (*Discoscaphites*) *abyssinus* (Morton), Meek, 1876: 441, pl. 35, fig. 2 (not fig. 4).

DIAGNOSIS: Macroconchs strongly compressed with very small umbilicus and narrow venter; fine, dense ribbing confined to anterior one-third of body chamber; ventrolateral tubercles may or may not extend over most or all of outer whorl, bullae common below umbilical shoulder, additional flank tubercles present or not. Microconchs more compressed with broad flat umbilical shoulder bordered by bullae; fine ribbing on anterior one-third of body chamber.

TYPES: Holotype, by monotypy, UC6380, Gurley Collection, University of Chicago, in Field Museum of Natural History (fig. 69D, E). Owen gave the locality as "Fox Hills, Nebraska." The route taken by John Evans, who collected the Cretaceous fossils described by Owen, is fairly well known (Waage, 1968: 21). It crossed the central part of the type area and the holotype most likely came from exposures of the Timber Lake Member on the Cheyenne-Moreau divide.

Allotype, YPM 27240, loc. 88, Timber Lake Member, Fox Hills Formation (fig. 73E–I).

OCCURRENCE: *Hoploscaphites comprimus* is known to date only from the Timber Lake and uppermost Trail City Members of the Fox Hills Formation and equivalent strata in and adjacent to the type area.

MATERIAL: A total of 105 adult specimens, of which about 40 are entire, and numerous juveniles from the type area of the Fox Hills Formation in Corson, Dewey, and Ziebach counties, South Dakota.

MACROCONCH DESCRIPTION: Specimens of *Hoploscaphites comprimus* in the Timber Lake Member and its lateral equivalents are

TABLE 9
Adult Measurements of *H. comprimus*[a]

	Macroconch				Microconch			
	N	$\bar{x}$	SD	Range	N	$\bar{x}$	SD	Range
LMAX (mm)	41	63.2	12.35	40.7–90.4	14	48.1	6.46	33.4–55.0
WUS (mm)	40	12.9	2.58	8.4–20.7	14	9.2	1.89	5.2–11.9
HUS (mm)	40	24.2	5.05	15.1–36.4	14	14.9	2.74	9.8–17.7
WUS/HUS	40	0.54	0.041	0.45–0.62	14	0.61	0.056	0.50–0.69
WAPT (mm)	38	17.2	3.67	7.3–24.6	13	15.7	1.77	12.6–18.5
HAPT (mm)	40	21.1	4.49	9.0–30.3	14	19.2	2.52	14.4–22.2
WAPT/HAPT	38	0.82	0.082	0.62–0.92	13	0.80	0.062	0.68–0.91
UD (mm)	40	3.8	0.59	3.0–5.6	13	6.2	1.01	4.0–8.0
UD/LMAX	40	0.06	0.014	0.03–0.09	13	0.13	0.020	0.11–0.16
A (°)	21	40.6	5.08	32.0–48.0				

[a] Abbreviations: see table 1 and figure 9.

distinct from *H. nicolletii* in the Trail City Member (table 9). The shells of *H. comprimus* are more compressed, with a narrower and more acutely rounded venter and a smaller umbilicus. The apertural angle averages 40.6°, which is significantly smaller than that in *H. nicolletii*. LMAX averages 63.2 mm and ranges from 40.7 to 90.4 mm. The ratio of the size of the largest specimen to that of the smallest is 2.2. The size distribution is trimodal (fig. 75); the relatively large representation of small specimens (40–45 mm) appears as one of the three peaks. No trace of a comparable peak appears on any of the size histograms of *H. nicolletii* from the individual assemblage zones of the Trail City Member or from the entire member itself. In contrast, the other two peaks, at 55–60 and 65–75 mm, are also present in all populations of *H. nicolletii*.

The ratio of whorl width to whorl height at the ultimate septum averages 0.54, which is significantly smaller than that in *H. nicolletii* (0.60). Larger specimens have slightly more compressed whorl sections at this point than smaller specimens. The ratio of whorl width to whorl height at the aperture averages 0.82, which is similar to that in *H. nicolletii* (0.83). The whorl section at the aperture is significantly more depressed than that at the ultimate septum.

The umbilical diameter averages 3.8 mm, which is significantly smaller than that in *H. nicolletii* (4.9 mm). Larger specimens have relatively smaller umbilical diameters than smaller specimens. The ratio of umbilical diameter to shell diameter averages 0.06, which is significantly smaller than that in *H. nicolletii* (0.08).

The ribs on the body chamber of *H. comprimus* are similar to those on the body chamber of *H. nicolletii* but the rib pattern is shifted forward, reducing the area of very fine ribbing on the anterior portion of the body chamber (rib zone 4; fig. 60). This displacement also affects the distribution of the larger ventrolateral tubercles, which also extend farther forward than they do on *H. nicolletii*. The ventral ribs of *H. comprimus* are strongly projected forward but the rostrum-like projection of the venter at the aperture is less acute, more rounded than on *H. nicolletii*.

Ventrolateral tubercles are more extensive on *H. comprimus*, extending throughout the exposed shell up to the lip on many of the larger or more coarsely ornamented specimens; on the body chamber these tubercles are usually clavate with larger ones directed outward (figs. 70E, F; 71C, E). On smaller, smoother shells tubercles may be restricted to the body chamber where they lie close together and extend outward nearly at right angles to the plane of symmetry (figs. 69F–I; 71H–J). Here the venter tends to be flattened and a specimen will sit upright on this surface without assistance.

Small bullae just below the umbilical shoulder occur much more commonly on shells of *H. comprimus* and may be found on all size specimens as compared with *H. nicolletii* where such bullae occur rarely and

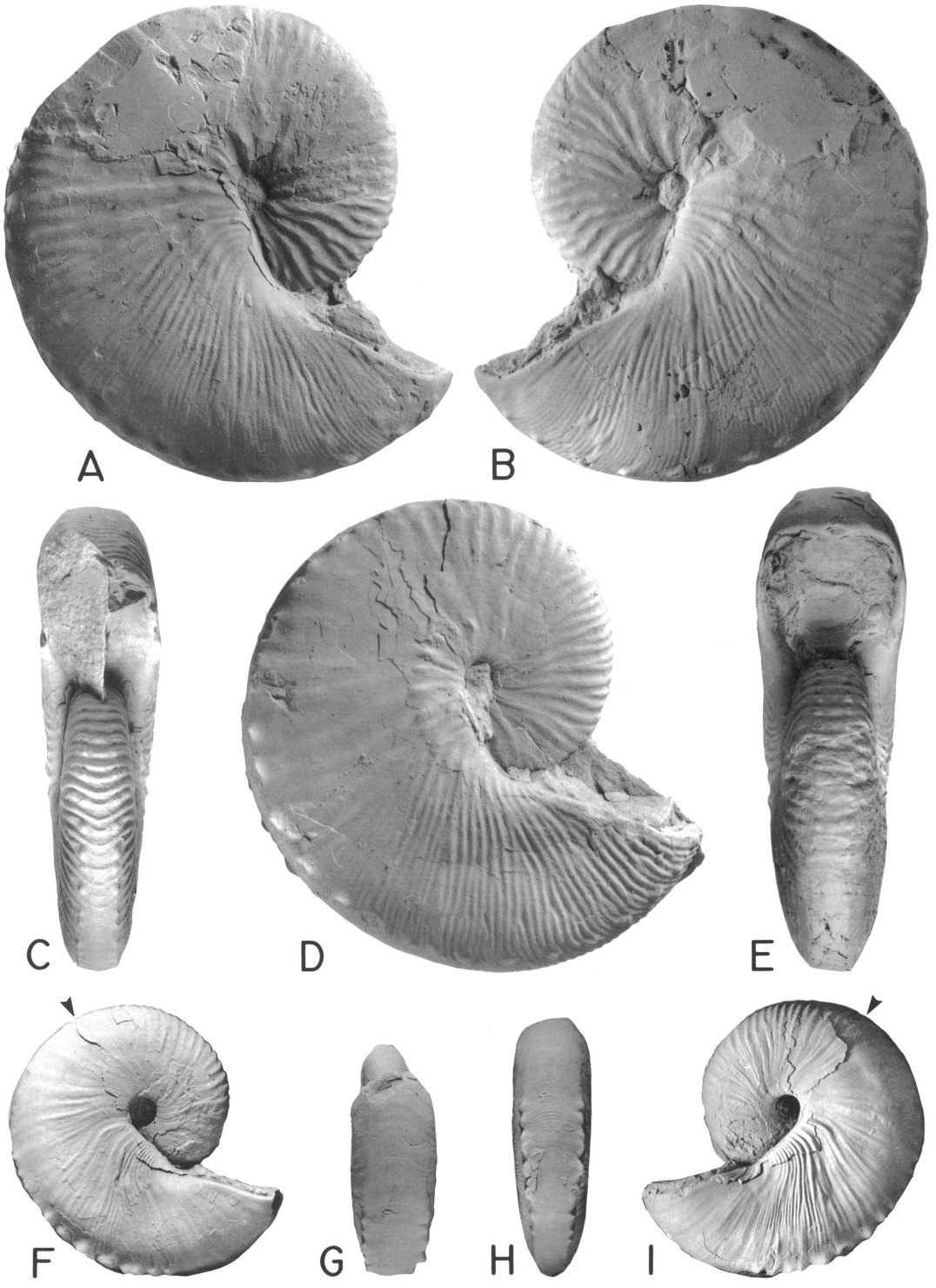

Fig. 69. *Hoploscaphites comprimus* (Owen) macroconchs. **A–C.** Meek's (1876: pl. 34, fig. 3a, b) *Scaphites conradi* var. *intermedius,* USNM 408, Fox Hills Fm., "Moreau River, Dakota" (ibid., p. 435). **A,** Right lateral; **B,** left lateral; **C,** apertural. **D, E.** Holotype, Owen's (1852: table 7, fig. 4) *Scaphites comprimus,* UC 6380, "Fox Hills, Nebraska" (ibid., p. 580). **D,** Right lateral; **E,** apertural. **F–I.** Small form, YPM 27233, loc. 37, TLM float. **F,** Right lateral; **G,** ventral hook; **H,** posterior; **I,** left lateral.

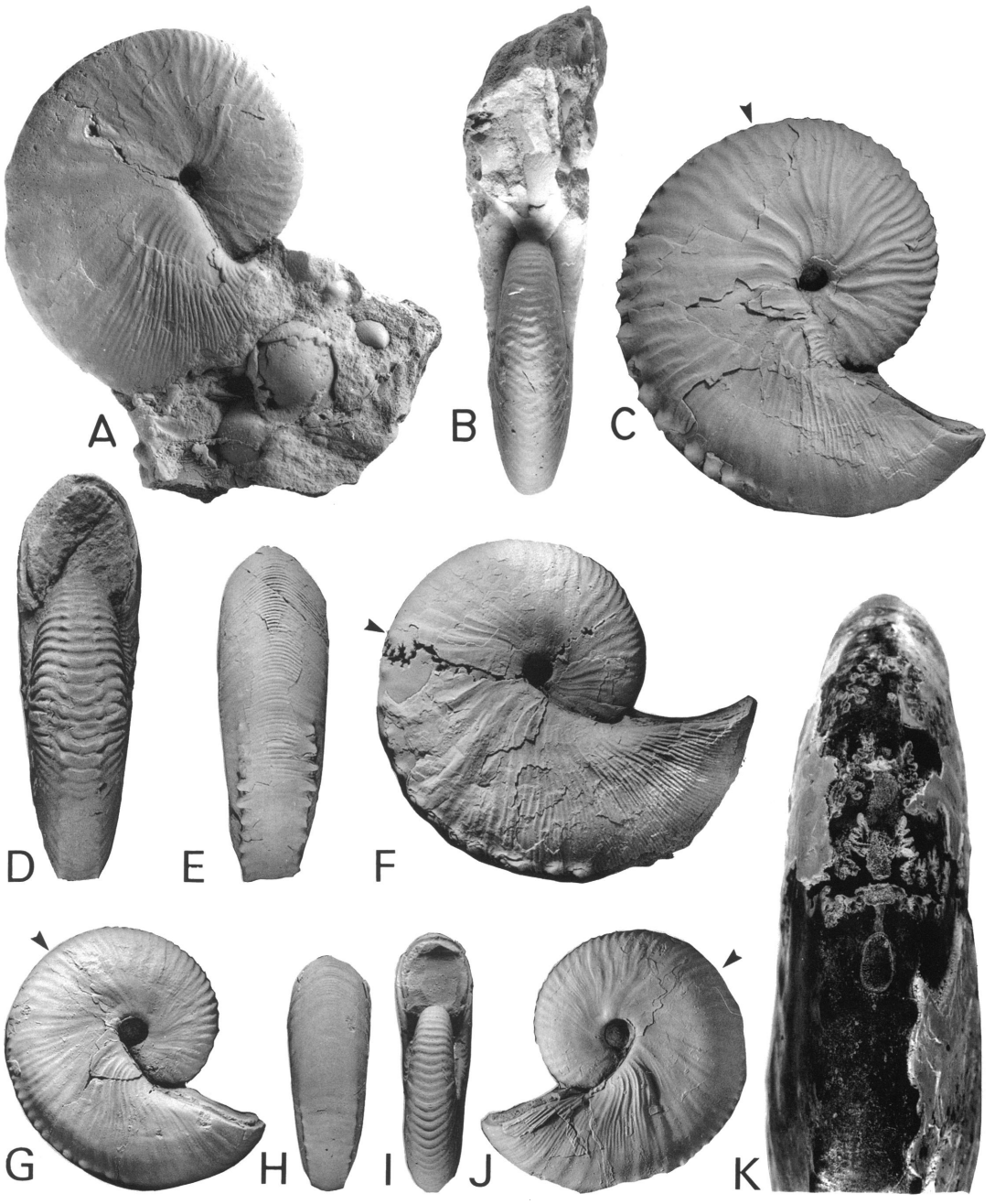

Fig. 70. *Hoploscaphites comprimus* (Owen) macroconchs. **A, B.** Meek's (1876: pl. 34, fig. 4a, b) *Scaphites* (*Discoscaphites*) *nicolletii,* USNM 407, Fox Hills Fm., "Moreau River, Fox Hills, Long Lake, &c., Dakota" (ibid., p. 436). **A,** Right lateral; **B,** apertural. **C–E.** YPM 27230, loc. 37, TLM float. **C,** Right lateral; **D,** apertural; **E,** posteroventral. **F, K.** YPM 23741, loc. 282, TLM. **F,** Right lateral; **K,** uncoated venter showing ventral muscle attachment area, ×2.5. **G–J.** Small form, YPM 27229, loc. 37, TLM float. **G,** Right lateral; **H,** posteroventral; **I,** apertural; **J,** left lateral.

only on very large specimens. They occur mostly on ribs of rib zone 3 but they may also be present on the exposed phragmocone. Additional tubercles or bullae may appear on the flanks, either scattered on the hook or forming a partial row just above the ventrolaterals (fig. 71A, E).

Small specimens of *H. comprimus* appear superficially distinct from larger specimens because of their subdued ornament. However, they clearly form part of a gradational series. Weak ornament is not restricted to small specimens and may occur throughout the size range but it is much more common in small specimens. The basic diagnostic features of *H. comprimus,* namely, the very compressed whorl section, narrow venter, small umbilicus, and dense ribbing confined to the anterior one-third of the body chamber are present in all size specimens.

The suture of *H. comprimus* macroconchs is like that of *H. nicolletii* macroconchs (fig. 76A, B); on some specimens the minor elements appear more deeply incised than those on *H. nicolletii* but this is not a consistent feature. In very small macroconchs of *H. comprimus* (40 mm < LMAX < 45 mm) the sutural elements are blunter and less incised than in larger macroconchs.

The muscle attachment area on the venter just adoral of the ultimate septum is ovoid, as in *H. nicolletii,* with its blunter end forward.

MICROCONCH DESCRIPTION: Adult microconchs of *H. comprimus* are generally difficult to distinguish from those of *H. nicolletii* except by their direct association with the macroconch of the species. However, *H. comprimus* microconchs tend to be more compressed. In addition, many *H. comprimus* microconchs show a more restricted area of very fine ribbing on the anterior body chamber compared with *H. nicolletii* microconchs of comparable size, although the differences may be slight and the fining of the ribs so gradual as to obscure the cutoff point.

The average size of microconchs (48.1 mm) is significantly smaller than that of macroconchs (63.2 mm; table 9). The size distribution of the microconchs is unimodal with the peak skewed to the right (fig. 75). The ratio of the size of the largest specimen to that of the smallest specimen is 1.65. The ratio of whorl width to whorl height at the ultimate septum averages 0.61, which is significantly higher than that in the corresponding macroconchs (0.54) but significantly lower than that in microconchs of *H. nicolletii* (0.68). The ratio of whorl width to whorl height at the aperture averages 0.80, which is approximately the same as that in the corresponding macroconchs (0.82) but significantly lower than that in microconchs of *H. nicolletii* (0.86).

The umbilical diameter averages 6.2 mm, which is significantly larger than that in the corresponding macroconchs (3.8 mm) but the same as that in microconchs of *H. nicolletii.* The ratio of umbilical diameter to shell diameter averages 0.13, which is significantly larger than that in the corresponding macroconchs (0.06) but the same as that in microconchs of *H. nicolletii.* Larger microconchs of *H. comprimus* have approximately the same relative umbilical diameter as smaller microconchs of this species.

→

Fig. 71. *Hoploscaphites comprimus* (Owen) macroconchs. **A–E.** Large ornate specimen, YPM 27232, loc. 34, TLM float. **A,** Right lateral; **B,** apertural; **C,** posterodorsal; **D,** ventral hook; **E,** left lateral. **F–J.** YPM 27228, loc. 90, TLM float. **F,** Right lateral; **G,** apertural; **H,** ventral hook; **I,** posterior; **J,** left lateral.

Fig. 72. *Hoploscaphites comprimus* (Owen) macroconchs and microconch. **A–C.** Large weakly ornamented macroconch, YPM 27066, loc. 67, TLM float. **A,** Right lateral; **B,** posteroventral; **C,** apertural. **D–H.** Macroconch, YPM 27231, loc. 41, TLM. **D,** Right lateral; **E,** apertural; **F,** posteroventral; **G,** ventral hook; **H,** left lateral. **I.** Microconch, left lateral, YPM 27242, loc. 88, TLM.

Fig. 73. *Hoploscaphites comprimus* (Owen) macroconch and microconchs. **A–D.** Macroconch, YPM 27234, loc. 37, TLM float. **A,** Right lateral; **B,** left lateral; **C,** apertural; **D,** posteroventral. **E–I.** Allotype, microconch, YPM 27240, loc. 88, TLM float. **E,** Right lateral; **F,** posterior; **G,** apertural; **H,** ventral hook; **I,** left lateral. **J–L.** Microconch, YPM 27239, loc. 37, TLM float. **J,** Right lateral; **K,** posteroventral; **L,** apertural.

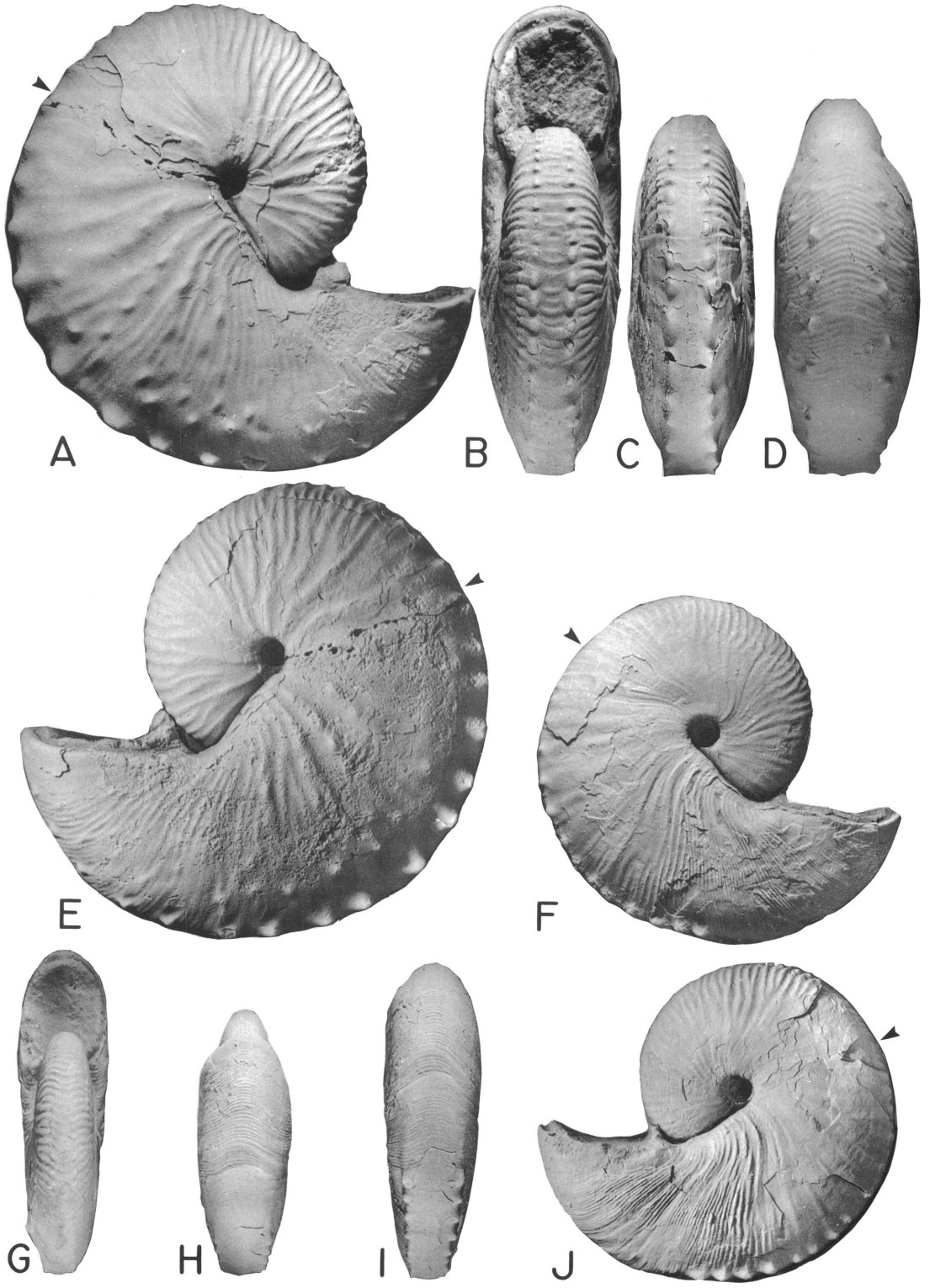
A
B
C
D
E
F
G
H
I
J

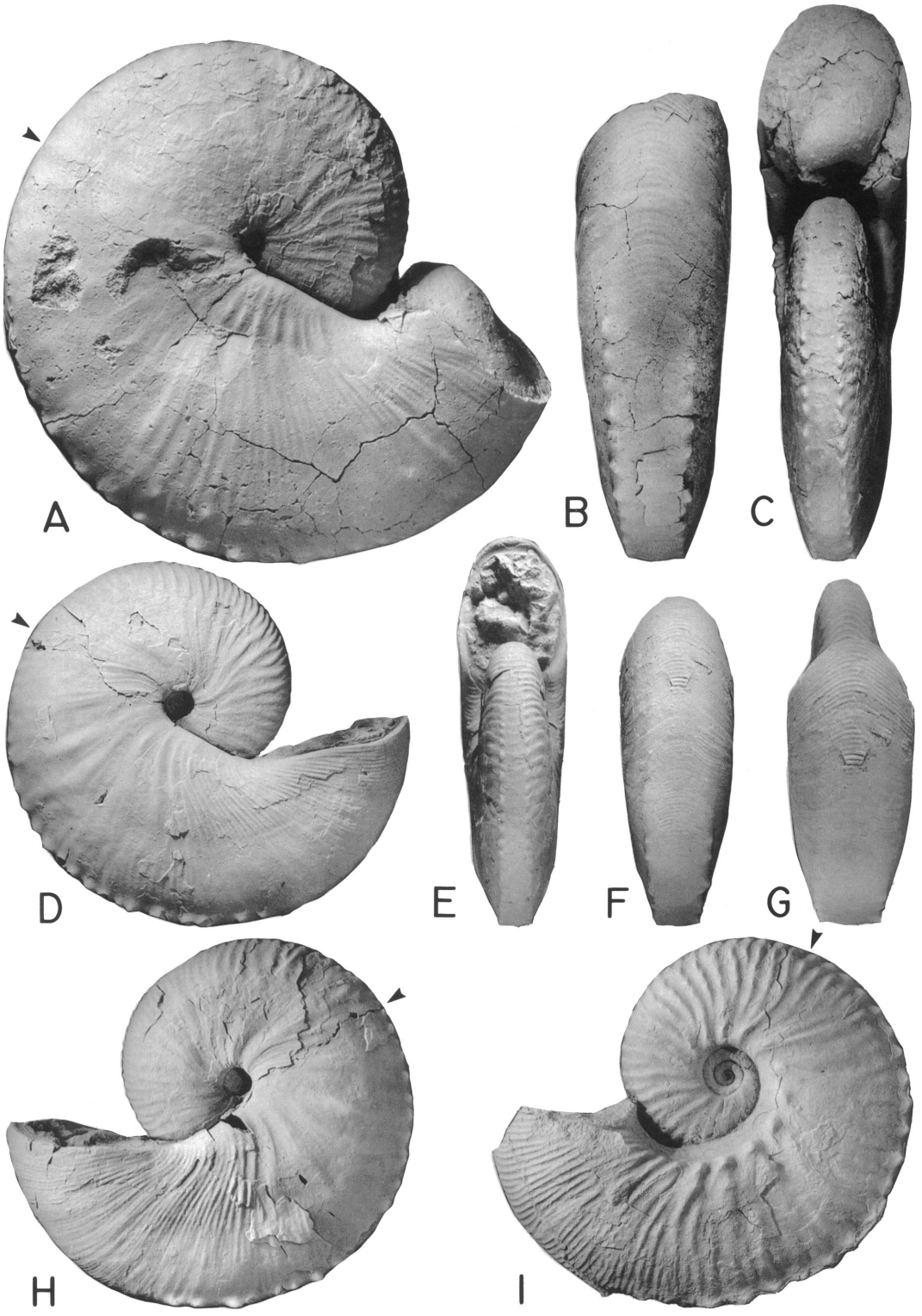

Fig. 72

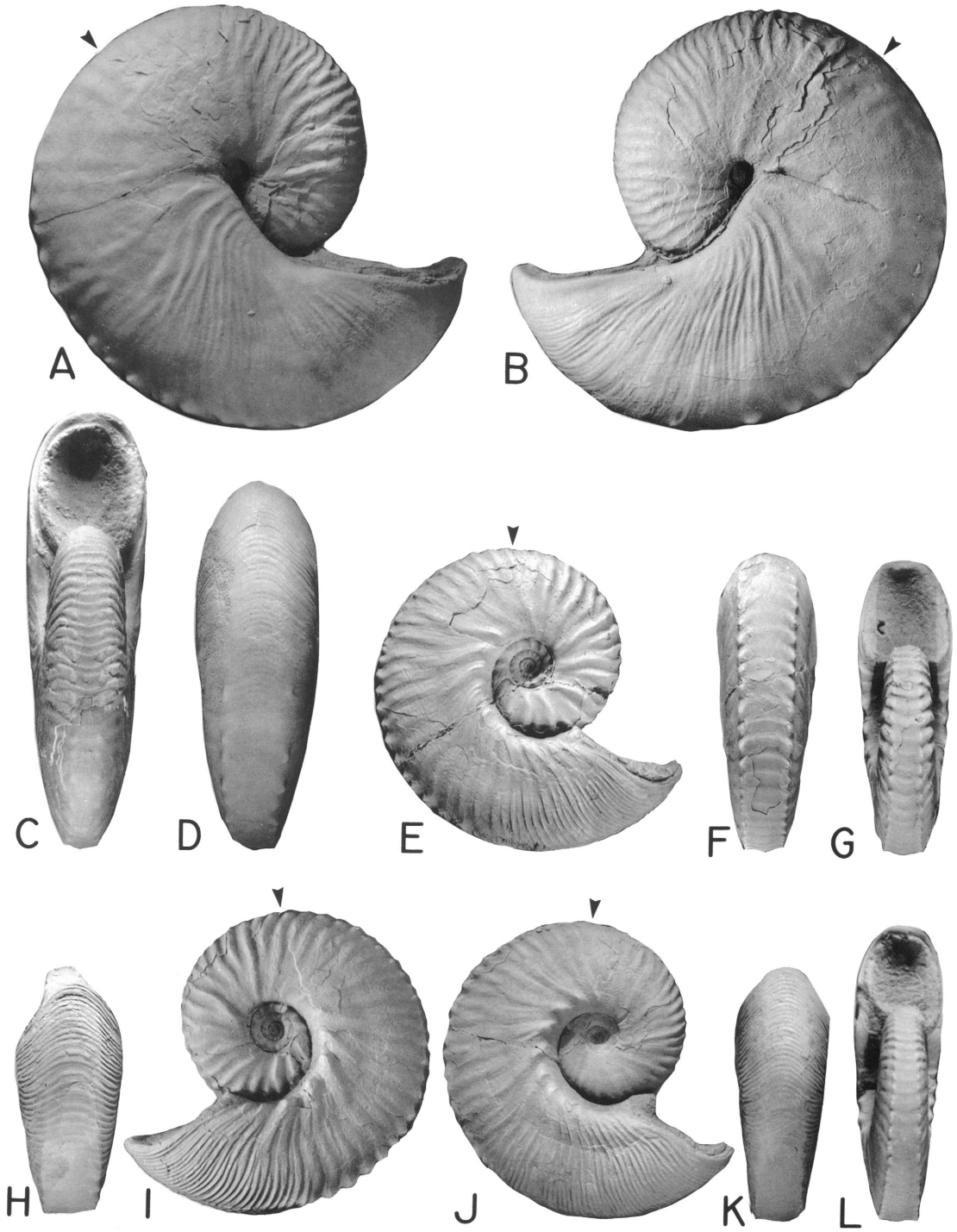

Fig. 73

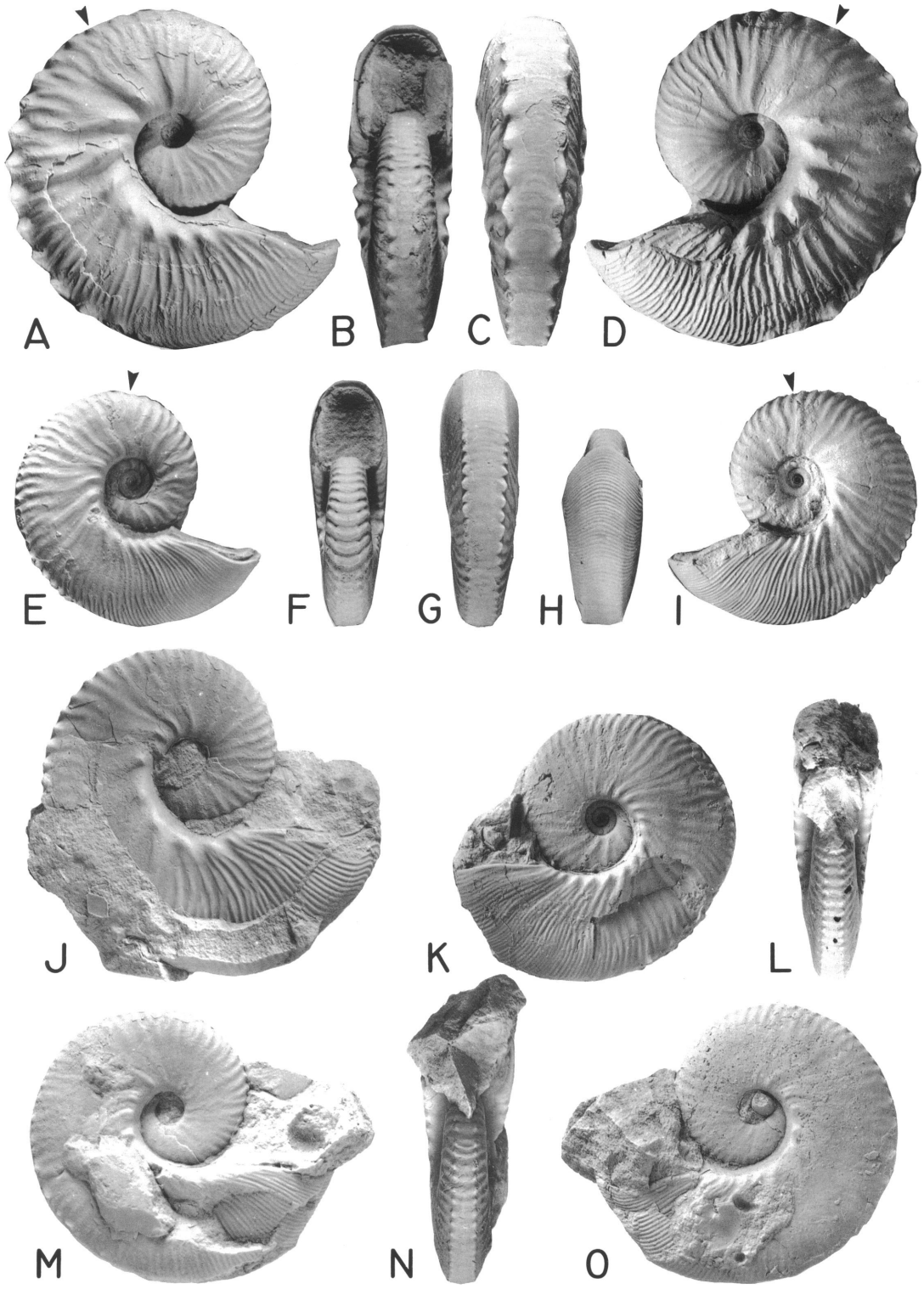
A
B
C
D
E
F
G
H
I
J
K
L
M
N
O

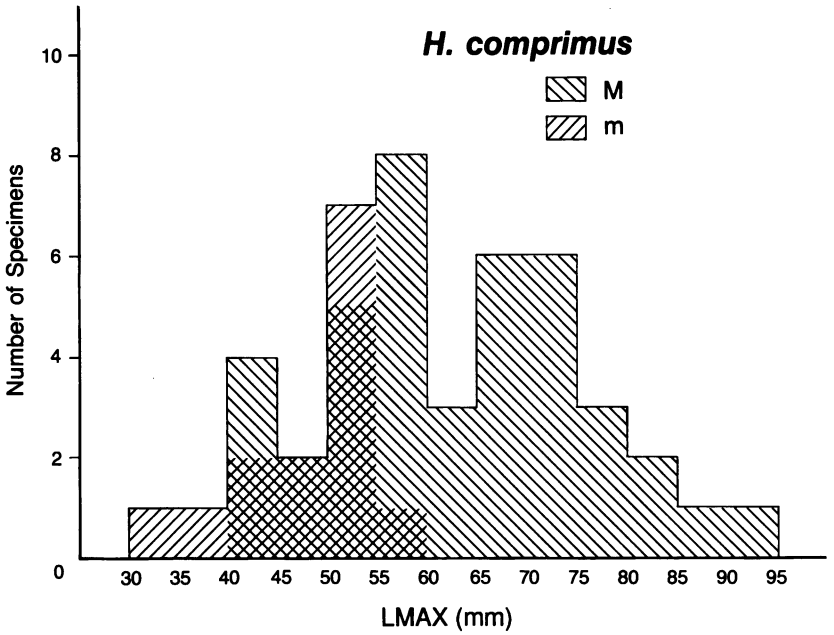

Fig. 75. Size frequency histogram of a sample of *Hoploscaphites comprimus* (Owen) from the Timber Lake Member of the Fox Hills Formation in its type area.

The suture of *H. comprimus* microconchs is nearly identical to that of the corresponding macroconchs (fig. 76C, D).

ONTOGENY: The protoconch and ammonitella of macroconchs are similar to those of microconchs (table 1). Dorsoventral, mostly intercostal cross sections through an adult macroconch and an adult microconch are illustrated in figure 77. The growth of whorl width is negatively allometric in both dimorphs (slopes range from 0.8311 to 0.8771; fig. 78) whereas that of whorl height is positively allometric in both dimorphs (slopes range from 1.0872 to 1.1247; fig. 79). At comparable shell diameters, whorl height is consistently higher in macroconchs than in microconchs whereas whorl width is approximately the same in both dimorphs. The shell whorls become increasingly more compressed throughout ontogeny in both dimorphs. The ratio of whorl width to height decreases from more than 1.00 at 5 mm shell diameter to 0.4–0.6 and 0.5–0.7 near the base of the mature body chamber in macroconchs and microconchs, respectively. *H. comprimus* macroconchs are consistently more compressed throughout ontogeny than *H. nicolletii* macroconchs whereas microconchs of the two species are less distinct in this respect.

The growth of umbilical diameter is slightly negatively allometric (fig. 80). The rate of increase of the umbilical diameter is more or less the same in both dimorphs until maturity although microconchs are generally more

←

Fig. 74. *Hoploscaphites comprimus* (Owen) microconchs. **A–D.** YPM 27241, loc. 37, TLM float. **A,** Right lateral; **B,** apertural; **C,** posterior; **D,** left lateral. **E–I.** YPM 27146, loc. 37, TLM float. **E,** Right lateral; **F,** apertural; **G,** posterior; **H,** ventral hook; **I,** left lateral. **J.** Meek's (1876: pl. 35, fig. 2a) *Scaphites abyssinus,* USNM 409, Fox Hills Fm., "Moreau River, Dakota" (ibid., p. 443), right lateral. **K, L.** Meek's (1876: pl. 35, fig. 1a) *Scaphites mandanensis,* USNM 410, Fox Hills Fm., "Moreau River, Dakota" (ibid., p. 444). **K,** Left lateral; **L,** apertural. **M–O.** Owen's (1852: pl. 7, fig. 5) *Ammonites*(?) *mandanensis* Morton, USNM 20243, "Fox Hills, between the Cheyenne and Moreau Rivers, Nebraska." **M,** Right lateral; **N,** apertural; **O,** left lateral.

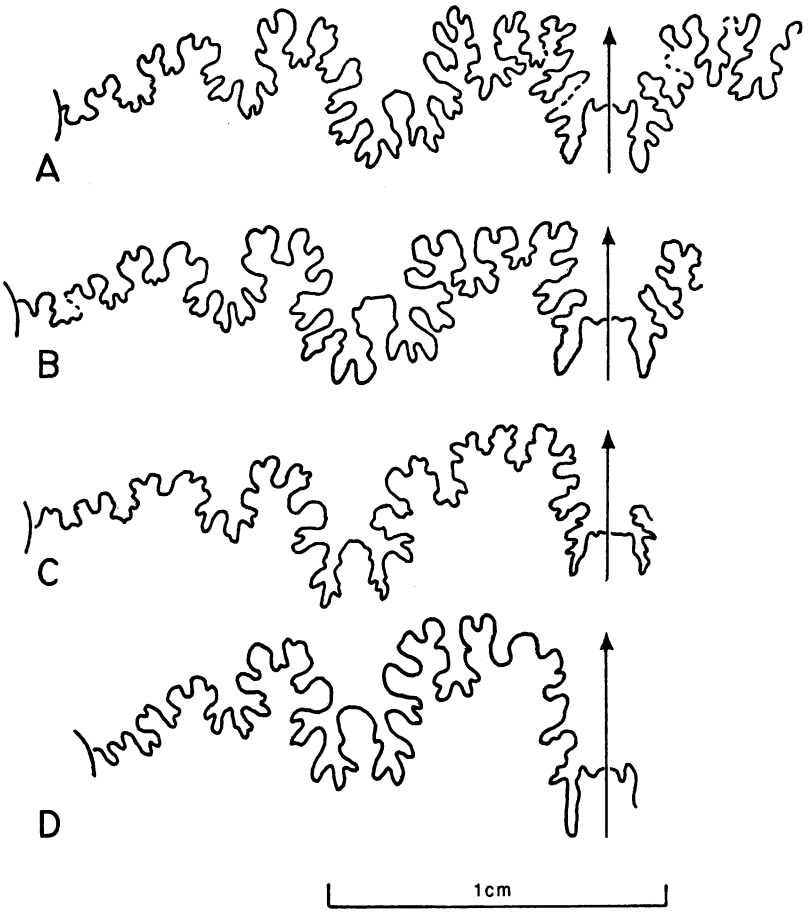

Fig. 76. Sutures of *Hoploscaphites comprimus* (Owen) macroconchs and microconchs. **A.** Eighth from last suture of an adult macroconch, YPM 23741, loc. 282, CAZ. **B.** Seventh from last suture of an adult macroconch, YPM 23744, loc. 34, TLM. **C.** Next to last suture of an adult microconch, YPM 34696, loc. 34, CAZ. **D.** Fifth from last suture of an adult microconch, YPM 34697, loc. 34, CAZ. This suture has been reversed to facilitate comparison with the other sutures.

widely umbilicate than macroconchs. This discrepancy is more pronounced than in *H. nicolletii*. At approximately one whorl before the base of the mature body chamber, the umbilical diameter begins to increase more slowly or not at all in macroconchs whereas it continues to increase at the same rate in microconchs. Near maturity, *H. comprimus* macroconchs are more narrowly umbilicate than *H. nicolletii* macroconchs whereas the microconchs of the two species are similar in this respect. The ratio of umbilical diameter to shell diameter decreases through most of postembryonic growth and reaches a minimum value near the base of the body chamber of 0.20–0.24 in microconchs and 0.09–0.11 in macroconchs. The ratio decreases more steeply in macroconchs than in microconchs starting at approximately one whorl before the base of the mature body chamber. At comparable shell diameters, microconchs maintain higher ratios than macroconchs, a discrepancy much more pronounced in *H. comprimus* than in *H. nicolletii*. The development of ornamentation in *H. comprimus* macroconchs and microconchs is similar to that in *H. nicolletii* macroconchs and microconchs, respectively (fig. 81).

DISCUSSION: The original specimens of *Scaphites comprimus* Owen (1852: pl. 6, fig. 4, refigured here as fig. 69D, E) and of *Discoscaphites conradi* var. *intermedius* Meek

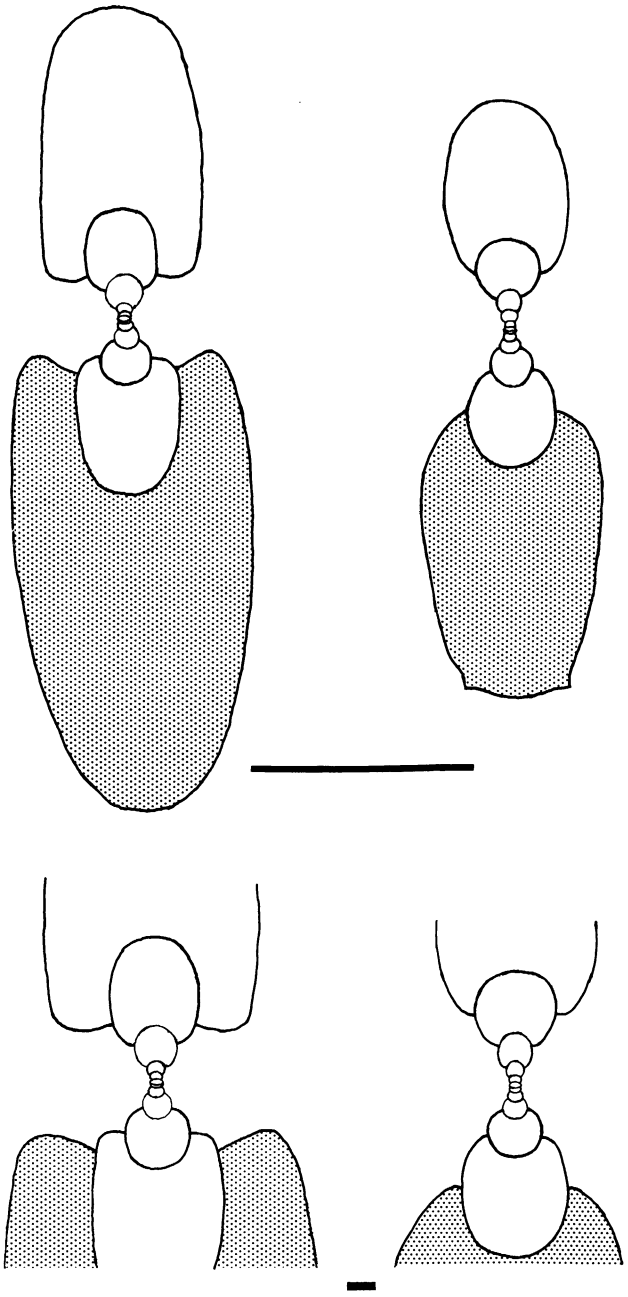

Fig. 77. Dorsoventral, mostly intercostal cross sections through adult dimorphs of *Hoploscaphites comprimus* (Owen). **Left.** Macroconch, YPM 23058, loc. 37, TLM. **Right.** Microconch, AMNH 44228, loc. 3160, TLM. Shaded area demarcates mature body chamber. Upper scale bar = 1 cm; lower scale bar = 1 mm.

(1876: pl. 34, fig. 3, refigured here as fig. 69A–C) clearly show the narrow venter, compressed form, and restricted area of fine ribbing characteristic of *H. comprimus*; both are large specimens with small bullae near the umbilical shoulder as well as some flank tubercles. Meek's (1876: pl. 34, figs. 2, 4) specimens of *Scaphites nicolletii* also belong to

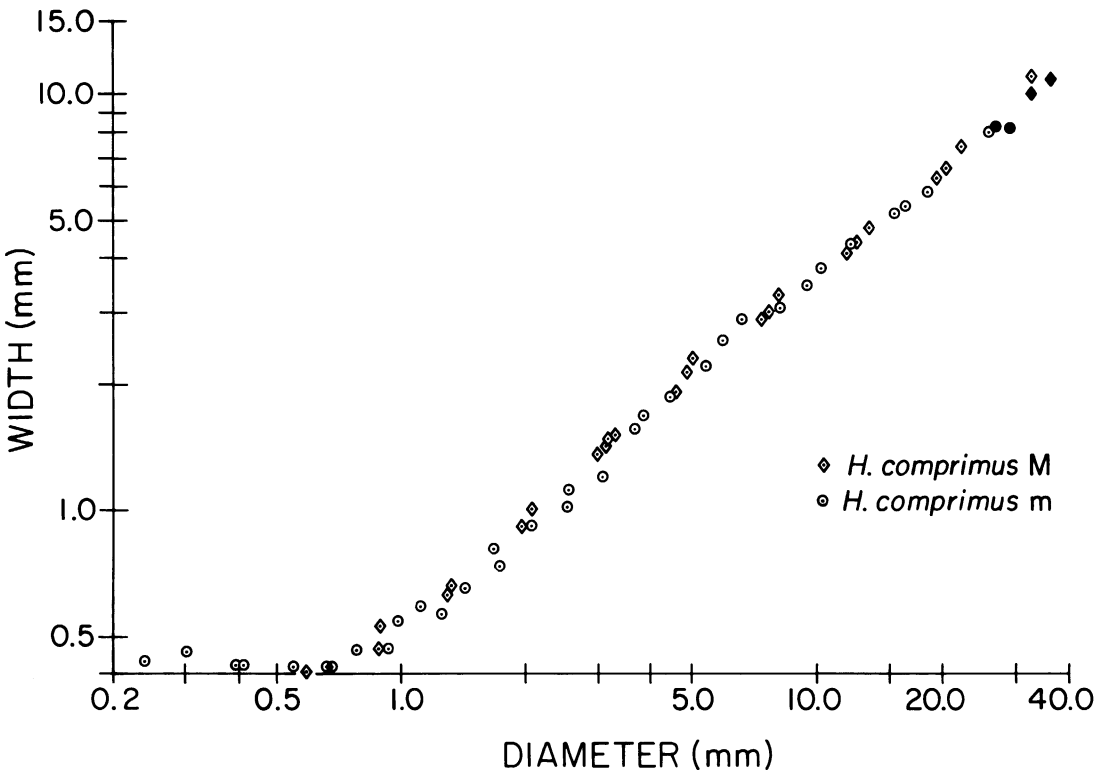

Fig. 78. Plot of whorl width versus shell diameter through the ontogeny of six adults (three macroconchs and three microconchs) of *Hoploscaphites comprimus* (Owen). Black symbols indicate measurements near the base of or in the mature body chamber. Measurements listed in Appendix II.

H. comprimus; both these specimens are strongly compressed with narrow venters and the one in figure 4 clearly shows fine, dense ribbing restricted to the anterior one-third of the body chamber (fig. 70A). Owen's (1852: pl. 8, fig. 1) illustration of *H. nicolletii* lacks diagnostic features; the specimen is lost. None of the microconchs illustrated by these authors can be attributed to *H. comprimus* with complete certainty but Meek's (1876: pl.35, fig. 1) *mandanensis* shown on figure 74K, L is probably *H. comprimus* on the strength of its ornament, its degree of compression, and its sandy matrix. Matrix, however, is not in itself supportive because POAZ concretions of the Trail City Member also have a sandy matrix in the eastern part of the type area. Meek's (1876: pl. 35, fig. 2) *abyssinus* is a large microconch of *H. comprimus* (fig. 74J). Owen's (1852: pl. 7, fig. 5) *mandanensis* also has a sandy matrix and restricted fine ribbing and is probably *H. comprimus* (fig. 74M–O).

Kellum (1962: 67, pl. 4, figs. 1, 2; pl. 6, figs. 3–7) described under *Scaphites* (*Discoscaphites*) *conradi* var. *intermedius* Meek three fragments from the Fox Hills Formation in the Lance Creek–Red Bird area, eastern Wyoming. One fragment (ibid., pl. 4, figs. 1, 2) consists of indeterminate inner whorls insufficiently compressed to be Meek's *intermedius*. The largest piece, most of a body chamber, shows a rather spectacular healed shell injury; it is a stout macroconch body chamber with coarser ornament than is characteristic of *intermedius*. It is assignable to our new species *Jeletzkytes dorfi* (p. 184). The third fragment is the tip of a hook insufficient for identification.

Hoploscaphites melloi, new species
Figures 60, 82–84

DIAGNOSIS: Macroconchs with fine, dense ribbing on all or most of body chamber; ventral ribs and peristome with very slight anterior projection. Few or no ventrolateral tu-

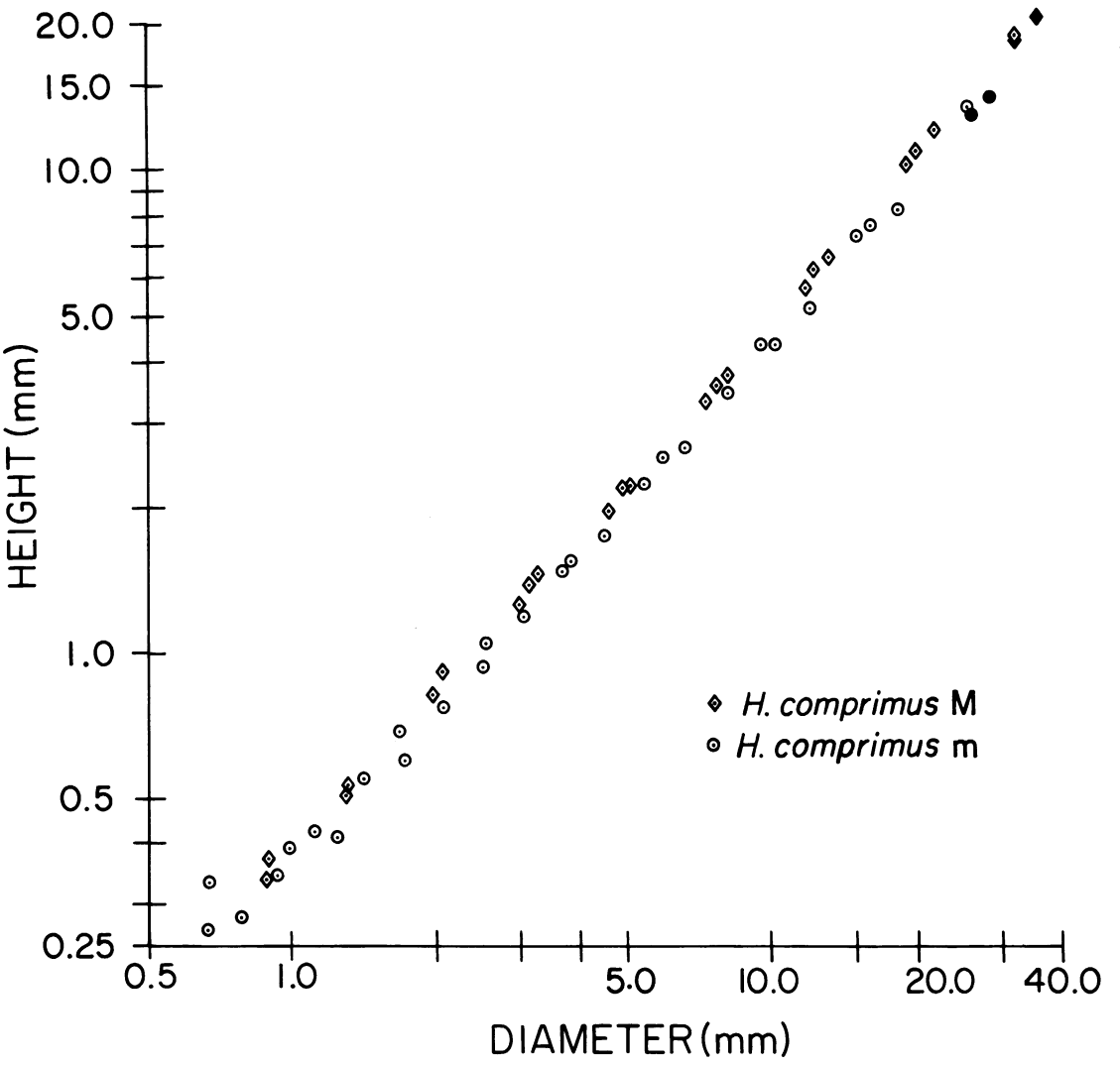

Fig. 79. Plot of whorl height versus shell diameter through the ontogeny of six adults (three macroconchs and three microconchs) of *Hoploscaphites comprimus* (Owen). Black symbols indicate measurements near the base of or in the mature body chamber. Measurements listed in Appendix II.

bercles on body chamber. Small umbilicus of coil lies above umbilical shoulder of body chamber. Microconch unknown.

TYPES: Holotype, macroconch, YPM 23044, loc. 31, upper Mobridge Member, Pierre Shale, figure 82A–C.

NAME: This species is named for James F. Mello, micropaleontologist at the U.S. National Museum, who studied the foraminifera of the upper Pierre Shale and the Fox Hills Formation in the type area (Mello, 1969) and found the initial specimens of this species.

OCCURRENCE: All specimens are from the upper part of the Mobridge Member of the Pierre Shale exposed on the inner bluffs of the Moreau River, northeast of the village of Green Grass and one mile west of the S.D. Rt. 63 bridge, locs. 31 and 32. Locality 32 is the Moreau Bridge Rt. 63 locality indicated on figure 2. The source concretions lie about 40 ft above the local last occurrence of *Baculites clinolobatus.* The sparse fauna consists chiefly of macroconchs of *Hoploscaphites melloi,* a species of *Jeletzkytes* of which we have too few specimens for adequate study, and the bivalve *Spyridoceramus* (sensu

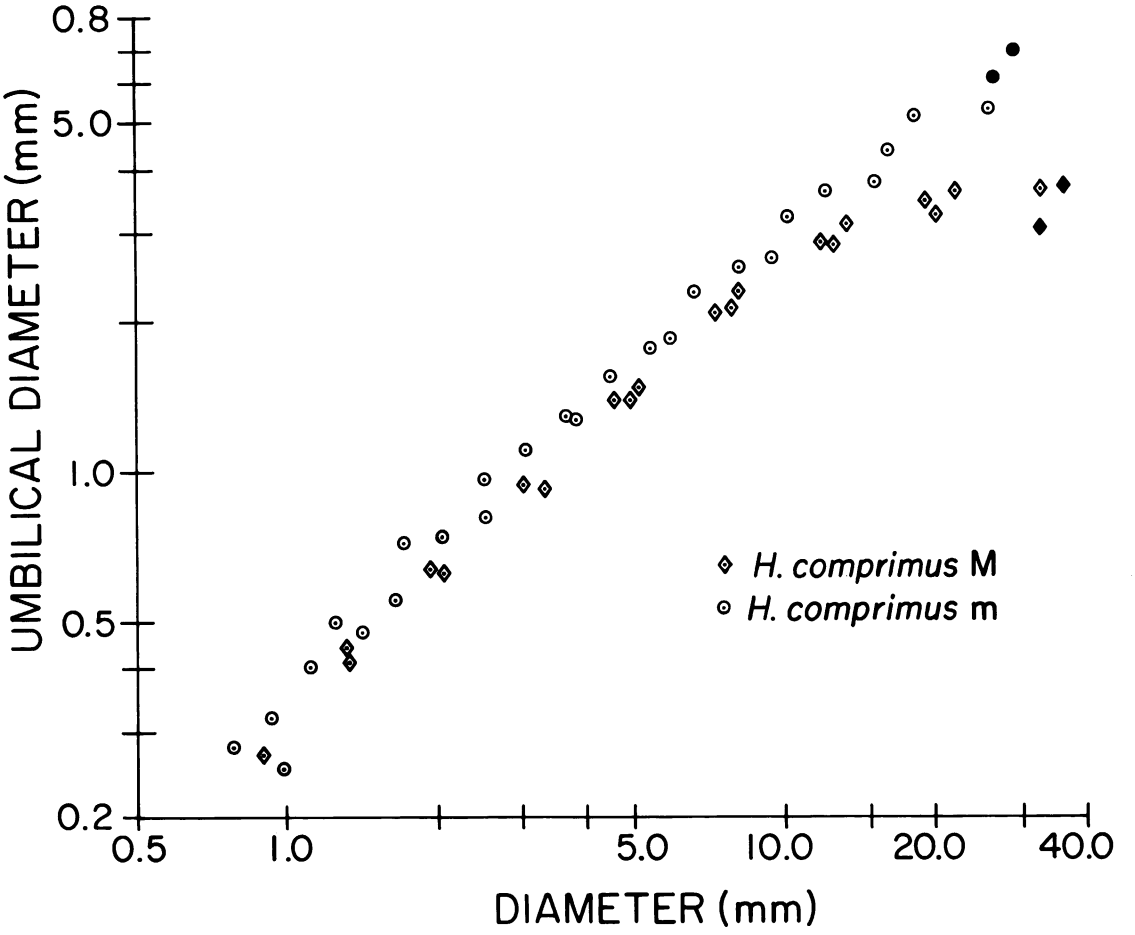

Fig. 80. Plot of umbilical diameter versus shell diameter through the ontogeny of six adults (three macroconchs and three microconchs) of *Hoploscaphites comprimus* (Owen). Black symbols indicate measurements near the base of or in the mature body chamber. Measurements listed in Appendix II.

Dhondt, 1983a) *fibrosus* (formerly *Tenuipteria fibrosa,* see Speden, 1970b).

MATERIAL: Twenty imperfect specimens, all macroconchs. Some shells are partly crushed; some appear to have been partly dissolved before concretion solidification; a few are relatively entire.

MACROCONCH DESCRIPTION: Macroconchs of *H. melloi* whole enough to measure cluster around the average size of *H. nicolletii* (61.8 mm; table 10). The ratios of whorl width to whorl height at the ultimate septum and at the aperture average 0.55 and 0.84, respectively, which are similar to the averages of the corresponding ratios in *H. nicolletii,* indicating a similarly compressed whorl shape. The umbilical diameter in *H. melloi* averages 3.9 mm, which conforms more closely to that of *H. comprimus* (3.8 mm) than to that of *H. nicolletii* (4.9 mm). The umbilicus of the coiled phragmocone usually lies 2 mm to as much as 4 mm above the line of the umbilical shoulder of the final body chamber, a result of a somewhat gradual uncoiling of the shell into the shaft (figs. 82D, E, 83D, F, I). This contrasts with most shells of *H. nicolletii* and *H. comprimus* in which there is a more abrupt uncoiling of the shell into the shaft near the base of the final body chamber. The umbilical shoulder of the body chamber may be straight (N = 9) or may sag gently (N = 6), the latter accentuating the "looser" coiling of the last

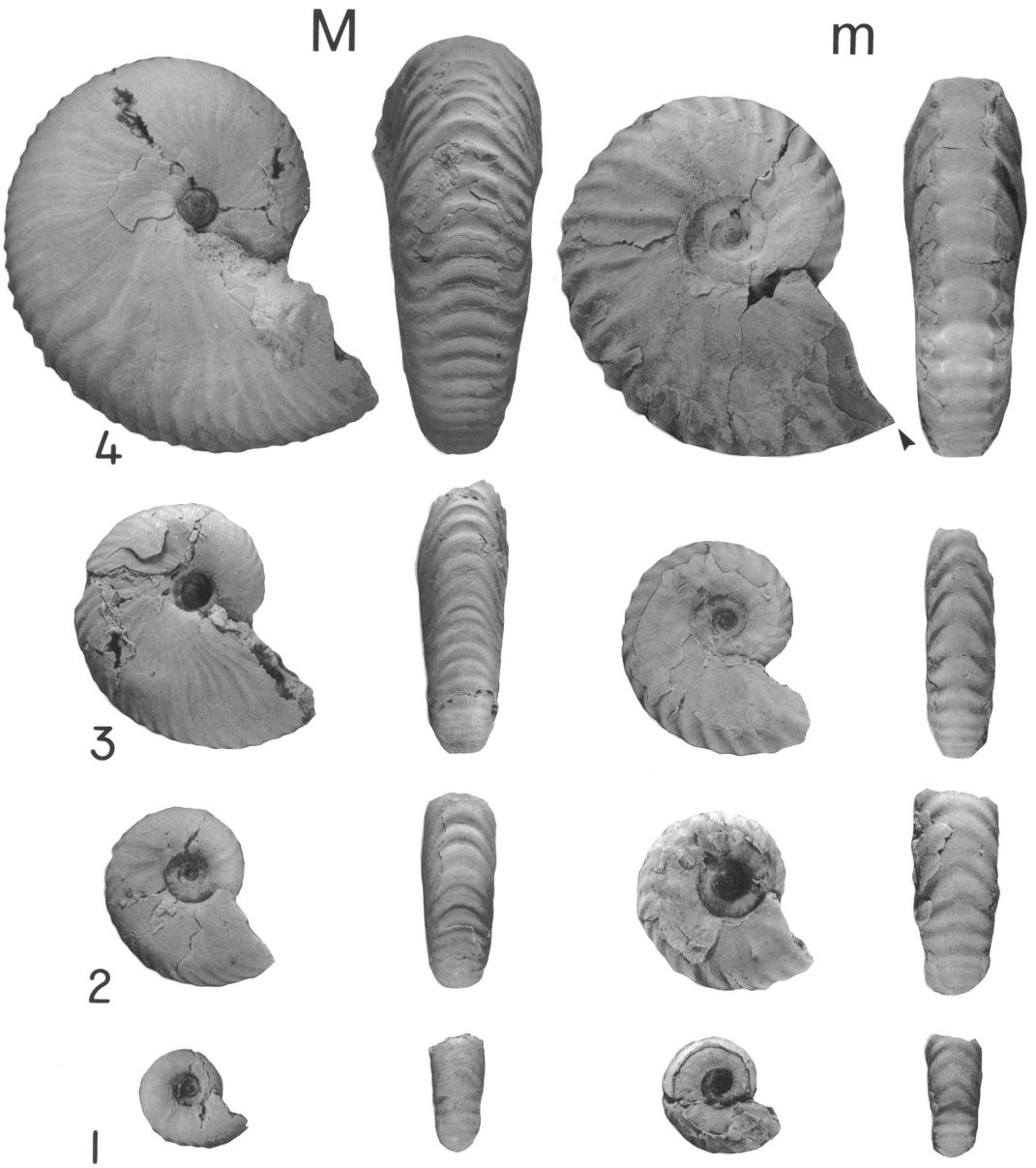

Fig. 81. Dissections of adult dimorphs (macroconch, YPM 23046, loc. 36, TLM float, and microconch, AMNH 44676, loc. 3160, TLM) of *Hoploscaphites comprimus* (Owen) showing four sizes through ontogeny in lateral and ventral view. 1. ×3. 2. ×3. 3. ×2. 4. ×2. Arrow indicates base of mature body chamber.

whorl. The hook is reflexed, as in *H. nicolletii,* leaving a slight gap or no gap between the dorsum of the hook, with its dorsal projection, and the phragmocone. The apertural angle in *H. melloi* ranges from 42 to 58°, which conforms to the upper two-thirds of the range in *H. nicolletii.*

Fine ribbing in *H. melloi* covers most of the body chamber and part of the phragmocone (fig. 60). The spacing of ribs on the body chamber varies; most of our specimens with shell preserved show 13–16 ventral ribs/cm on most of the body chamber, but at least one attains the closer spacing of 20–22 ribs/

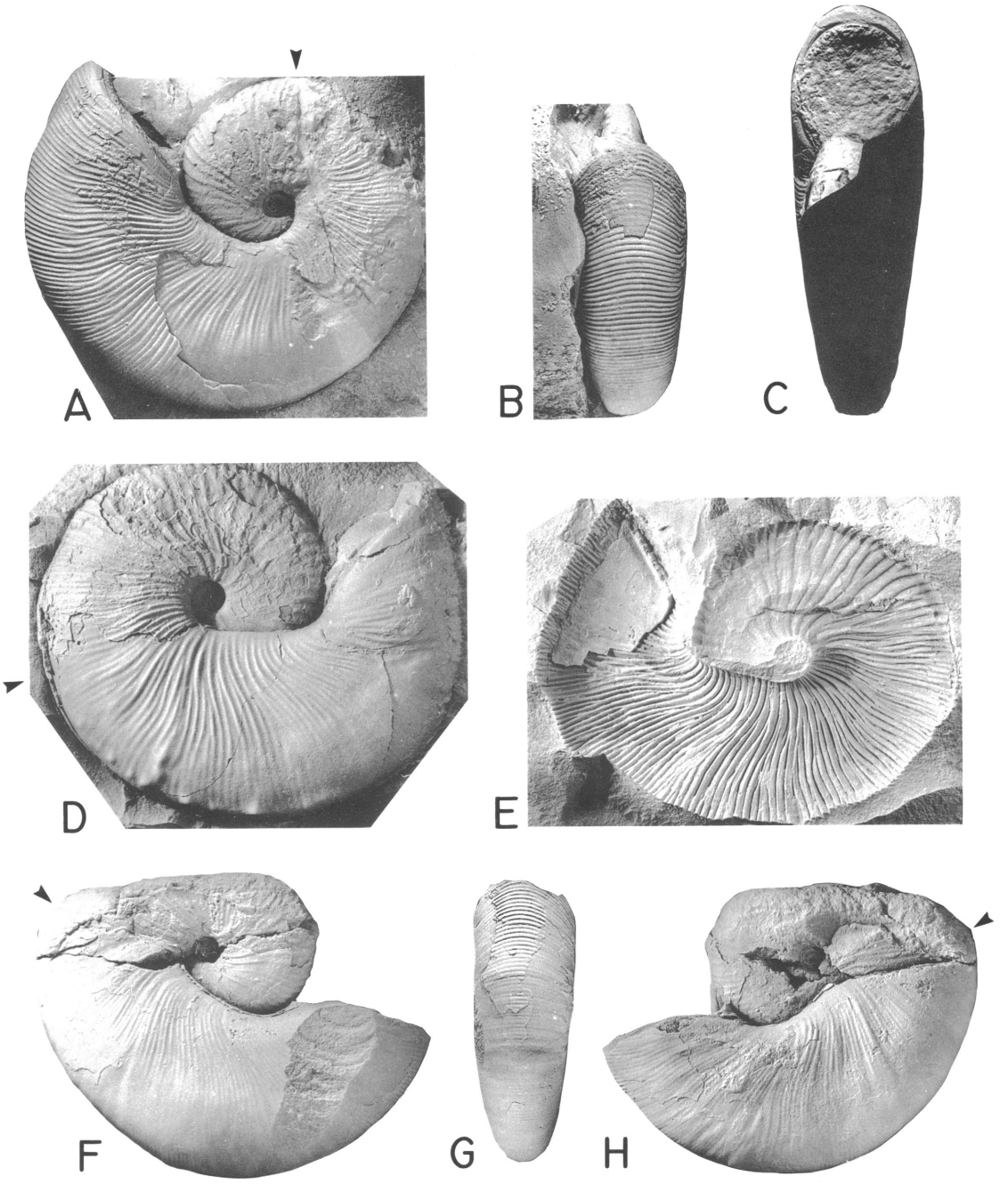

Fig. 82. *Hoploscaphites melloi,* n. sp., macroconchs. **A–C.** Holotype, YPM 23044, loc. 31, upper Mobridge Member, Pierre Shale. **A,** Left lateral; **B,** ventral hook; **C,** apertural, reconstructed. **D, E.** Specimen showing a few ventrolateral tubercles on body chamber, YPM 23043, loc. 32, upper Mobridge Member, Pierre Shale. **D,** Right lateral; **E,** partial right lateral mold in concretion. **F–H.** YPM 23071, loc. 32, upper Mobridge Member, Pierre Shale. **F,** Right lateral; **G,** posteroventral; **H,** left lateral.

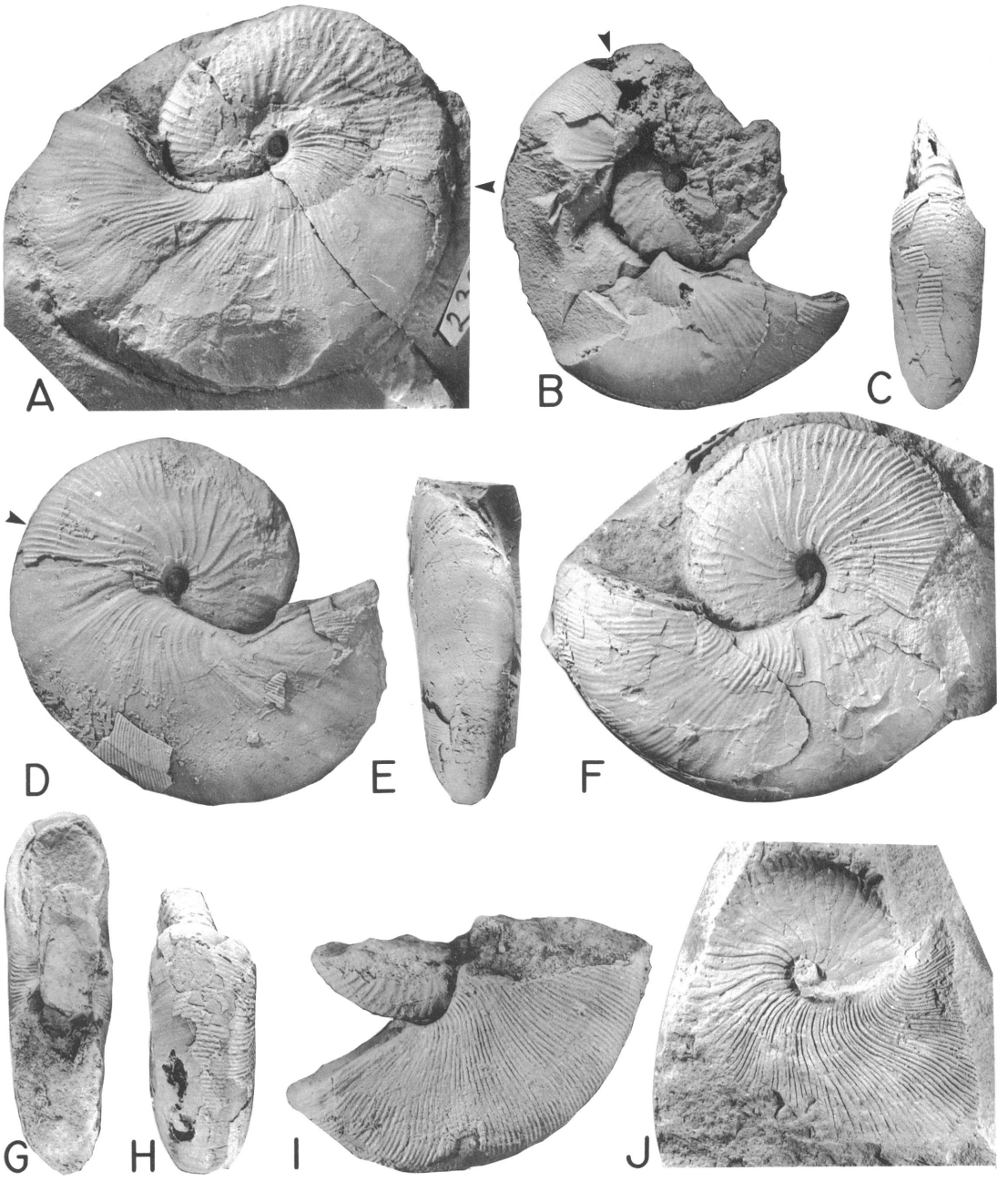

Fig. 83. *Hoploscaphites melloi,* n. sp., macroconchs. **A.** Left lateral, partially crushed specimen, YPM 23066, loc. 32, upper Mobridge Member, Pierre Shale. **B, C.** YPM 23067, loc. 32, upper Mobridge Member, Pierre Shale. **B,** Right lateral; **C,** ventral hook. **D, E.** YPM 23042, loc. 32, upper Mobridge Member, Pierre Shale. **D,** Right lateral; **E,** posteroventral. **F.** Left lateral, YPM 23068, loc. 32, upper Mobridge Member, Pierre Shale. **G–I.** Incomplete specimen, YPM 23074, loc. 32, upper Mobridge Member, Pierre Shale. **G,** Apertural; **H,** ventral hook; **I,** left lateral. **J.** Left lateral mold in concretion, YPM 23077, loc. 32, upper Mobridge Member, Pierre Shale.

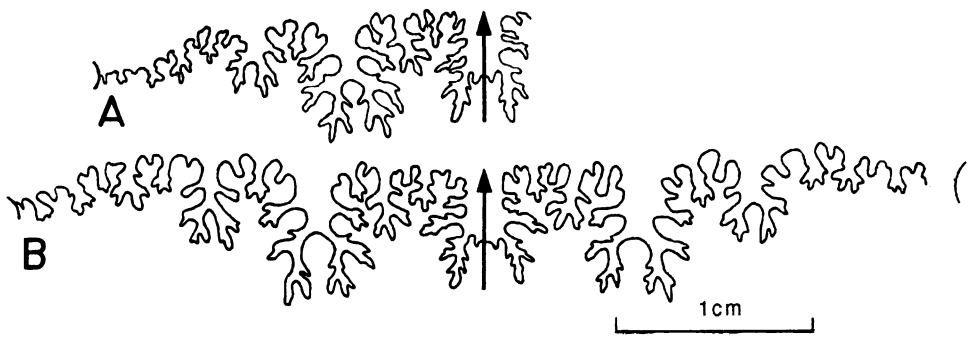

Fig. 84. Sutures of macroconchs of *Hoploscaphites melloi,* n. sp. **A.** Submature suture at approximately the point of exposure, YPM 23070, loc. 32, upper Mobridge Member, Pierre Shale. **B.** Submature suture at approximately 36 mm shell diameter of a broken specimen, YPM 23072, loc. 32, upper Mobridge Member, Pierre Shale.

cm that characterizes the fine ribbing in *H. nicolletii* and *H. comprimus.* The broad extent of fine ribbing on *H. melloi* over the last half whorl, or more, is a conspicuous feature that distinguishes this species from other species of *Hoploscaphites* described herein. The fine ribbing begins abruptly at or very close to the base of the mature body chamber, at the last or next to last septum of the phragmocone. In contrast, there are 7–10 ventral ribs/cm on most of the exposed phragmocone.

The ribs, as in *H. nicolletii,* are prorsiradiate and sinuous, but, unlike those in *H. nicolletii,* they have only a very slight adoral projection on the venter and, consequently, the ventral lip of the shell is only slightly protruding.

Of six specimens preserving the ventral periphery of the body chamber, four show no tubercles whatsoever, one has a few widely spaced ventrolateral tubercles on the midbody chamber, and one has a few weak ventrolateral tubercles at the juncture of the body chamber and phragmocone (fig. 82D).

The suture is visible on two specimens. It is similar to that of *H. nicolletii* (fig. 84) except that the lateral lobe appears slightly narrower and not as asymmetrical and the lateral saddle more rectangular in outline (fig. 84).

DISCUSSION: *Hoploscaphites melloi* differs from *H. nicolletii* and *H. comprimus* in the greater extent of fine ribbing on the body chamber, the much less pronounced adoral projection of the ventral ribs and ventral margin of the aperture, the offset of the umbilicus of the coil above the umbilical shoulder of the body chamber, and the paucity or total absence of ventrolateral tubercles.

In its greater extent of fine ribbing, *H. melloi* approaches the considerably older *Hoploscaphites gilli* Cobban and Jeletzky, 1965. In the latter, the finer ribbing begins "on the last quarter of the final septate whorl" (Cobban and Jeletzky, 1965: 797–798). *H. gilli* comprises "a variation series ranging from a tightly coiled moderately involute form to a smaller more loosely coiled less involute form" (ibid., p. 796). The specimens illustrated suggest that the more tightly coiled form (i.e., the one with the higher body chamber) is the macroconch and the loosely coiled form, the microconch. It is the macroconch that resembles *H. melloi* in its general form and ribbing pattern. However, *H. melloi* macroconchs differ conspicuously in being larger and having

TABLE 10
Adult Measurements of *H. melloi* Macroconchs[a]

	N	$\bar{x}$	SD	Range
LMAX (mm)	10	60.2	4.33	52.6–68.0
WUS (mm)	4	11.8	1.24	10.5–13.5
HUS (mm)	7	22.5	2.40	18.0–25.0
WUS/HUS	4	0.55	0.025	0.52–0.58
WAPT (mm)	4	17.9	2.44	14.4–20.1
HAPT (mm)	5	21.3	1.77	18.5–23.3
WAPT/HAPT	3	0.84	0.050	0.78–0.87
UD (mm)	14	3.9	0.70	2.8–5.2
UD/LMAX	8	0.06	0.012	0.04–0.08
A (°)	10	48.8	5.33	42.0–58.0

[a] Abbreviations: see table 1 and figure 9.

the umbilicus of the coil offset above the umbilical shoulder of the final body chamber. These same features also distinguish *H. melloi* from *Hoploscaphites landesi* Riccardi, 1983. *H. melloi* is probably most closely related to *H. nicolletii.*

Hoploscaphites birkelundi, new species
Figures 60, 85–90

Macroconch Synonymy:

Discoscaphites nicolleti (Morton), Dobbin and Reeside, 1929: 20.
Discoscaphites nicolleti (Morton), Kellum, 1962: 55.
Hoploscaphites aff. *H. nicolleti,* Obradovich and Cobban, 1975: 36, table 1; 48.

DIAGNOSIS: Macroconchs compressed with very small umbilicus, relatively long hook slightly separated from phragmocone. Anterior one-half to two-thirds of body chamber with very fine ribs showing moderate adoral projection on venter. Ventrolateral tubercles on much of body chamber and exposed phragmocone; umbilical bullae present or not. Microconchs small, compressed, with strong, widely spaced ribs bearing ventrolateral tubercles; ribbing becomes finer near aperture; incipient row of flank tubercles may appear near ultimate septum. Suture of both dimorphs with broad saddles, very narrow lobes.

TYPES: Holotype, YPM 27172, loc. RB 120, 50 to 60 ft below top of bluff-forming bioturbated sandstone, Fox Hills Formation, figure 85G–K.

Allotype, YPM 27210, loc. RB 106, bluff-forming bioturbated sandstone, Fox Hills Formation, figure 88F–H.

NAME: This species is named in honor of the late Dr. Tove Birkelund of the University of Copenhagen, Denmark.

OCCURRENCE: All specimens occur in gray to red-brown weathering concretions within a 60-ft interval of massive bioturbated sandstone in about the middle of the Fox Hills Formation (fig. 5). Collecting localities are distributed along the outcrop of this sandstone in the Redbird and Bowen Flat 7½ minute series quadrangles, Niobrara County, Wyoming.

MATERIAL: The suite of specimens studied includes 71 from the YPM collections and 5 from the AMNH collections. Of the YPM specimens, 40 are macroconchs and 31 microconchs; six macroconchs and eight microconchs are complete or nearly so, the remainder are fragmental or crushed; these include a number of well-preserved body chambers. The AMNH material includes three macroconchs and two microconchs.

MACROCONCH DESCRIPTION: Mostly medium size, compressed shells similar to *H. nicolletii* but with a slightly longer shaft and more reflexed hook that is not in contact with the phragmocone except in large specimens. The apertural angle averages 63.5°, which is significantly larger than that in *H. nicolletii* (45.6°; table 1). The gap between the hook and phragmocone in *H. birkelundi* is slight and although some specimens of *H. nicolletii* also show a similar gap, the reflexion of the body chamber in *H. birkelundi* is, in general, not as tight as in *H. nicolletii.* This difference may result in part from an apparent tapering of the hook not generally seen in *H. nicolletii,* but it may also simply reflect the longer hook of *H. birkelundi.* A more persistent difference in the shells of these two species is the smaller umbilical diameter of *H. birkelundi,* which averages 3.1 mm versus 4.9 mm in *H. nicolletii,* and the more compressed whorl section of *H. birkelundi,* notably at the ultimate septum. The ratio of whorl width to whorl height at this point averages 0.53 in *H. birkelundi* versus 0.59 in *H. nicolletii. H. birkelundi* is similar to *H. comprimus* in its degree of compression but tends to have a smaller umbilical diameter. The umbilical diameter averages 3.1 mm in *H. birkelundi* versus 3.8 mm in *H. comprimus.*

The size distribution of *H. birkelundi* macroconchs is illustrated in figure 89. As in *H. nicolletii* macroconchs, there are two well-defined peaks, a smaller one at 70–75 mm and a larger one at 60–65 mm. A less conspicuous third peak includes very small specimens at 45–50 mm. This apparent trimodality needs to be tested with a larger sample of specimens. The ratio of the size of the largest specimen to that of the smallest is 1.57.

Larger specimens tend to have slightly more compressed whorl sections at the the ultimate septum and at the aperture than smaller specimens. In addition, larger specimens have rel-

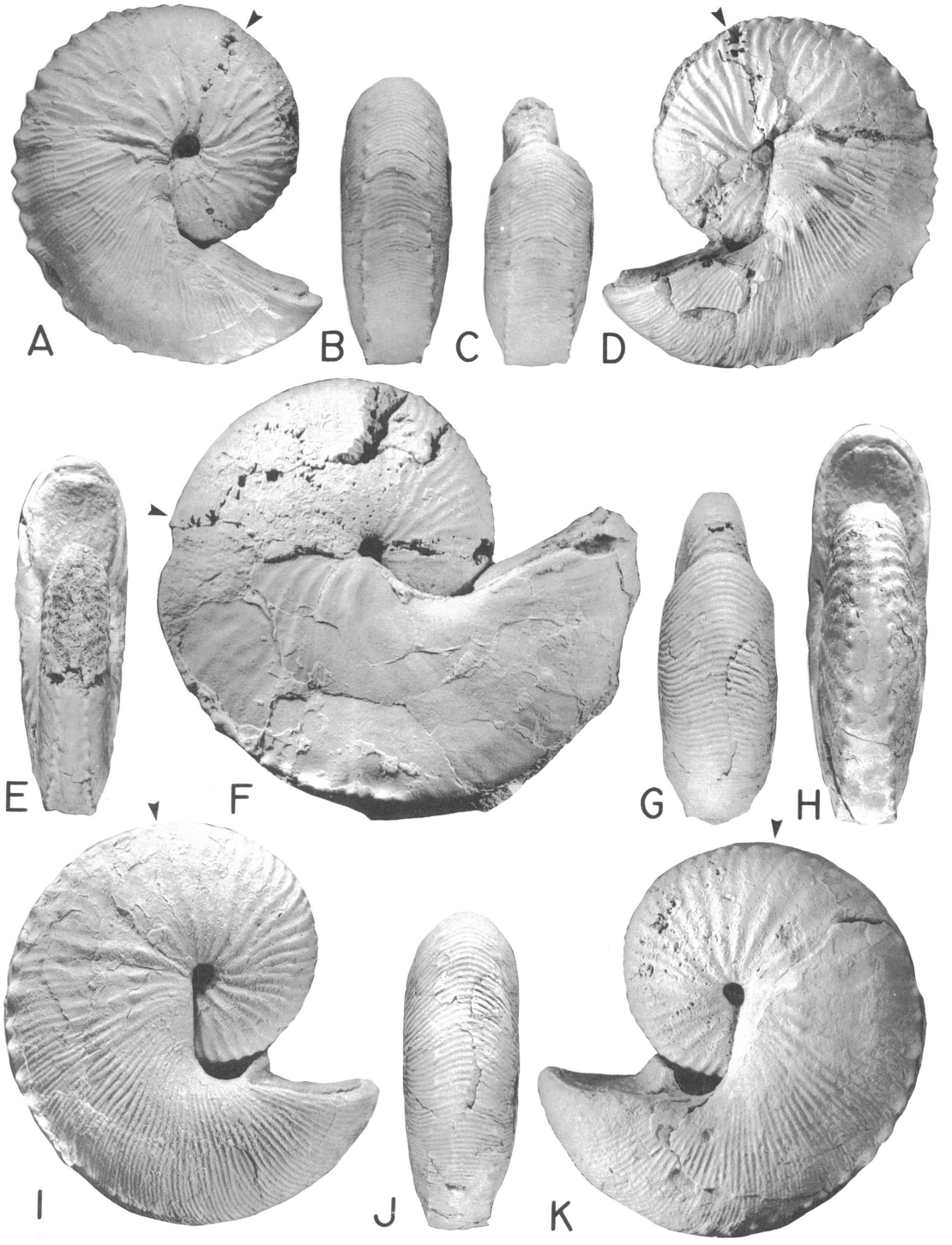

Fig. 85. *Hoploscaphites birkelundi,* n. sp., macroconchs. **A–E.** YPM 27170, loc. RB 104, bioturbated sand unit, lower Fox Hills Fm. **A,** Right lateral; **B,** posteroventral; **C,** ventral hook; **D,** left lateral; **E,** apertural. **F.** Large variant, right lateral, YPM 27181, loc. RB 103, bioturbated sand unit, lower Fox Hills Fm. **G–K.** Holotype, YPM 27172, loc. RB 120, bioturbated sand unit, lower Fox Hills Fm. **G,** Ventral hook; **H,** apertural; **I,** right lateral; **J,** posteroventral; **K,** left lateral.

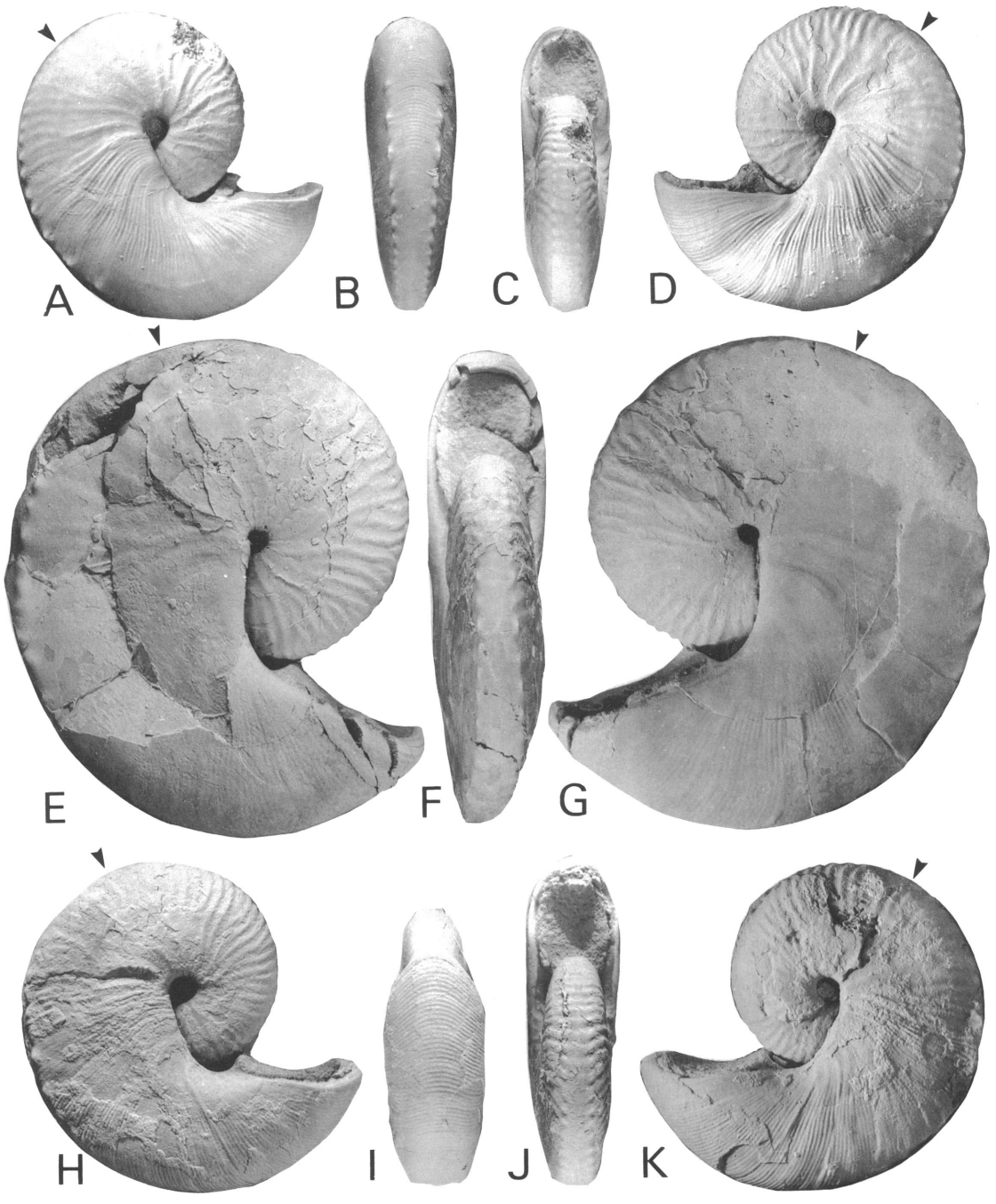

Fig. 86. *Hoploscaphites birkelundi,* n. sp., macroconchs. **A–D.** AMNH 44225, loc. 3156, bioturbated sand unit, lower Fox Hills Fm. **A,** Right lateral; **B,** posterior; **C,** apertural; **D,** left lateral. **E–G.** Large variant with small umbilicus, YPM 27180, loc. RB 114, bioturbated sand unit, lower Fox Hills Fm. **E,** Right lateral; **F,** apertural; **G,** left lateral. **H–K.** YPM 27169, loc. RB 107, bioturbated sand unit, lower Fox Hills Fm. **H,** Right lateral; **I,** ventral hook; **J,** apertural; **K,** left lateral.

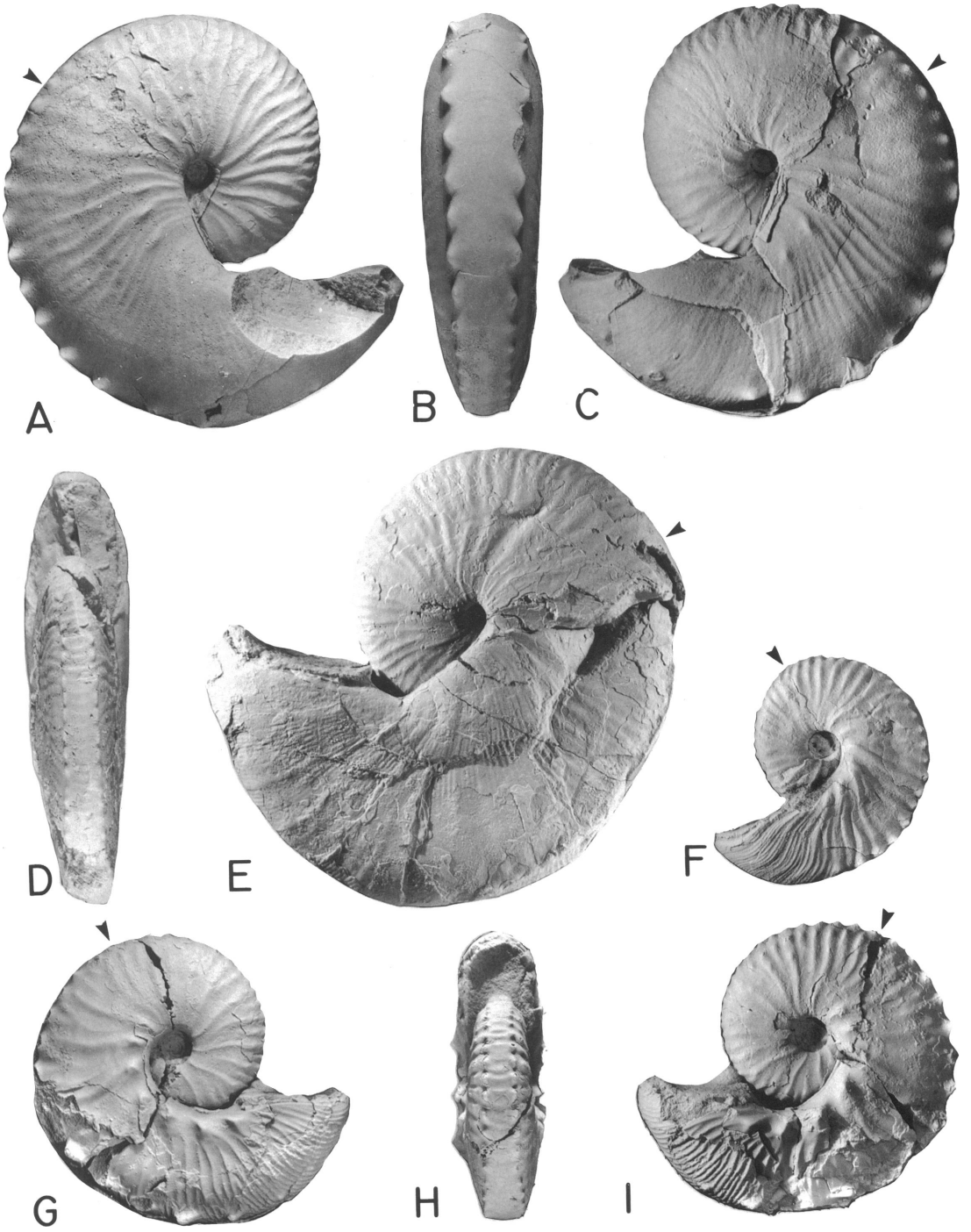

Fig. 87. *Hoploscaphites birkelundi,* n. sp., macroconchs and microconchs. **A–C.** Macroconch, YPM 27177, loc. RB 121, bioturbated sand unit, lower Fox Hills Fm. **A,** Right lateral; **B,** posterior; **C,** left lateral. **D, E.** Large compressed macroconch, YPM 27179, loc. RB 104, bioturbated sand unit, lower Fox Hills Fm. **D,** Apertural; **E,** left lateral. **F.** Microconch, left lateral, YPM 27211, loc. RB 120, bioturbated sand unit, lower Fox Hills Fm. **G–I.** Microconch, YPM 27218, RB 103, bioturbated sand unit, lower Fox Hills Fm. **G,** Right lateral; **H,** apertural; **I,** left lateral.

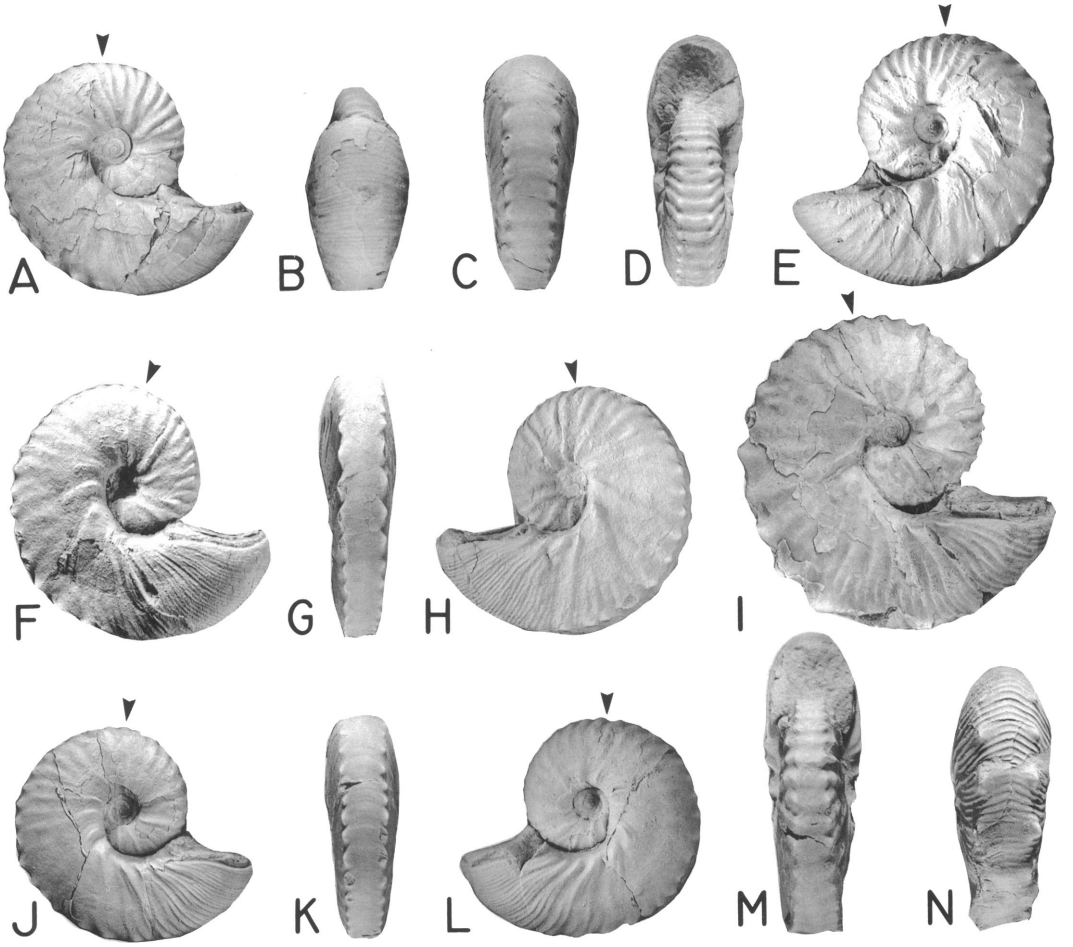

Fig. 88. *Hoploscaphites birkelundi,* n. sp., microconchs. **A–E.** YPM 27209, loc. RB 116, bioturbated sand unit, lower Fox Hills Fm. **A,** Right lateral; **B,** ventral hook; **C,** posterior; **D,** apertural; **E,** left lateral. **F–H.** Allotype, YPM 27210, loc. RB 106, bioturbated sand unit, lower Fox Hills Fm. **F,** Right lateral; **G,** posterior; **H,** left lateral. **I, M, N.** Coarsely ornamented specimen, YPM 27207, loc. RB 104, bioturbated sand unit, lower Fox Hills Fm. **I,** Right lateral; **M,** apertural; **N,** posteroventral. **J–L.** YPM 27208, loc. RB 118, bioturbated sand unit, lower Fox Hills Fm. **J,** Right lateral; **K,** posterior; **L,** left lateral.

atively smaller umbilical diameters than smaller specimens (compare fig. 86A and E). This same variation in shape with respect to adult size also occurs in *H. nicolletii* and *H. comprimus,* with larger specimens having higher, more compressed whorls and relatively smaller umbilical diameters than smaller specimens.

The ornament on *H. birkelundi* is similar among all specimens, regardless of size. Ribs have a moderate adoral projection on the venter and there is a short, blunt projection of the ventral lip at the aperture. The ribbing shows a pattern similar to that in *H. nicolletii* but not as clearly defined. The appearance of fine ribs, approximately 17/cm on the venter, is abrupt. The point at which fine ribs appear on the body chamber is earlier in some specimens than in *H. nicolletii* but the range of variation overlaps in the two species (fig. 60). In contrast, ribs are more widely spaced on the phragmocone with approximately 6 ventral ribs/cm at the point of exposure.

Ventrolateral tubercles are present on the body chamber and most of the phragmocone. They may or may not appear on the entire

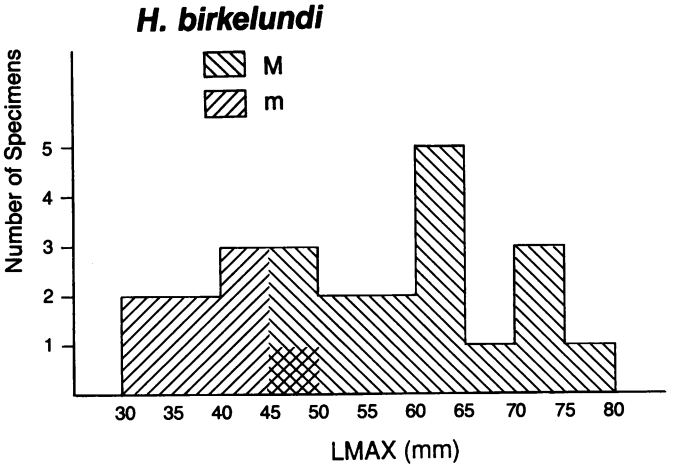

Fig. 89. Size frequency histogram of a sample of *Hoploscaphites birkelundi,* n. sp., from the Fox Hills Formation in the Lance Creek–Red Bird area, Wyoming.

exposed shell. In addition, bullae may or may not appear on ribs just below the umbilical shoulder on the younger part of the phragmocone and on the body chamber. On a few specimens some additional tubercles may appear above the ventrolaterals on the younger part of the phragmocone.

The suture of *H. birkelundi* macroconchs is similar to that in macroconchs of other species of *Hoploscaphites* (fig. 90A–C). However, the broad saddles and narrow lobes of *H. birkelundi* are more rectangular in outline than those of *H. nicolletii* and *H. comprimus* and are more like those of *H. melloi.* The lateral lobe is consistently narrower than the external (ventral lobe).

MICROCONCH DESCRIPTION: Small, compressed microconchs and medium size, stouter microconchs are associated with *H. birkelundi* macroconchs. On the basis of size and compression, the former are taken as microconchs of *H. birkelundi,* the latter as microconchs of the co-occurring larger, robust scaphites here included in *Jeletzkytes dorfi,* n. sp. (p. 188).

The dimensions of the measured specimens are listed in table 11. LMAX ranges from 31.4 to 49.4 mm and averages 39.9 mm (fig. 89). The average size is significantly smaller than that in macroconchs (61.4 mm). The ratio of the size of the largest microconch to that of the smallest microconch is 1.57. The adult shell is compressed and tightly coiled; the dorsal surface of the hook lies against the phragmocone or shows only a very slight separation. The ratio of whorl width to whorl height at the ultimate septum averages 0.72, which is significantly higher than that in macroconchs (0.53). The average is similar to that in *H. nicolletii* microconchs (0.68) but significantly higher than that in *H. comprimus* microconchs (0.61). The ratio of whorl width to whorl height at the aperture averages 0.86, which is not significantly different from that in the corresponding macroconchs (0.79) or that in microconchs of *H. nicolletii* (0.86) and *H. comprimus* (0.80). The umbilical diameter averages 4.7 mm, which is significantly higher than that in the corresponding macroconchs (3.1 mm) but significantly lower than that in microconchs of *H. nicolletii* and *H. comprimus* (both 6.2 mm). Larger microconchs of *H. birkelundi* tend to have relatively smaller umbilical diameters than smaller microconchs of this species. The ratio of umbilical diameter to shell diameter averages 0.12, which is significantly higher than that in the corresponding macroconchs (0.05) but not significantly different from that in microconchs of *H. nicolletii* (0.12) and *H. comprimus* (0.13).

Ribbing on the microconch varies somewhat but follows a consistent pattern. Strong, prorsiradiate ribs appear on the earliest exposed phragmocone; the number of ribs crossing the venter at this point is 6 or 7/cm,

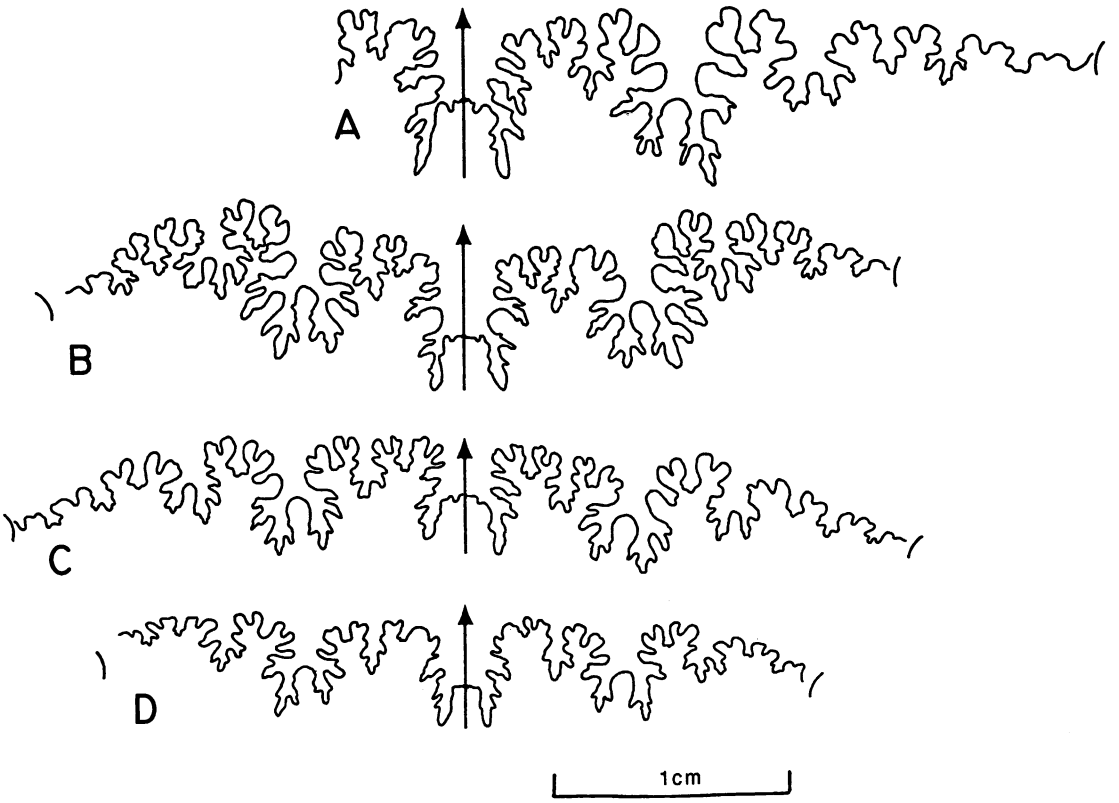

Fig. 90. Sutures of *Hoploscaphites birkelundi,* n. sp., macroconchs and microconch. **A.** Last suture of holotype, an adult macroconch, YPM 27172, loc. RB 120, bioturbated sand unit, lower Fox Hills Fm. **B.** Next to last suture of an adult macroconch, YPM 34698, loc. RB 103, bioturbated sand unit, lower Fox Hills Fm. **C.** Third from last suture of an adult macroconch, AMNH 44225, loc. 3156, bioturbated sand unit, lower Fox Hills Fm. **D.** Last suture of an adult microconch, YPM 27220, loc. RB 104, bioturbated sand unit, lower Fox Hills Fm.

TABLE 11
Adult Measurements of *H. birkelundi*[a]

	Macroconch				Microconch			
	N	$\bar{x}$	SD	Range	N	$\bar{x}$	SD	Range
LMAX (mm)	16	61.4	9.45	47.1–76.5	8	39.9	6.11	31.4–49.4
WUS (mm)	14	12.2	2.32	7.1–15.5	8	8.4	2.04	5.6–11.3
HUS (mm)	16	23.2	4.97	16.7–31.5	8	11.7	2.44	9.2–16.0
WUS/HUS	14	0.53	0.081	0.42–0.67	8	0.72	0.113	0.53–0.94
WAPT (mm)	14	16.9	1.83	13.7–19.8	8	13.1	1.40	10.4–14.5
HAPT (mm)	13	21.3	3.44	16.2–28.4	7	15.1	1.88	12.5–17.8
WAPT/HAPT	13	0.79	0.093	0.59–0.91	7	0.86	0.092	0.76–1.00
UD (mm)	16	3.1	0.45	2.4–3.9	8	4.7	0.49	4.0–5.4
UD/LMAX	16	0.05	0.014	0.03–0.08	8	0.12	0.018	0.10–0.16
A (°)	15	63.5	7.19	56.0–80.0				

[a] Abbreviations: see table 1 and figure 9.

which decreases slightly to 4 or 5/cm on the posterior half of the body chamber. About every third or fourth rib is a primary; others appear by intercalation or branching. At varying positions from the aperture, but usually on the anterior third of the body chamber, fine ribs appear abruptly at a density of 15 to more than 20/cm on the venter. The fine ventral ribs clearly show a moderate adoral projection and there is a concomitant slight projection of the ventral lip at the aperture.

Each of the strong ribs bears a ventrolateral tubercle throughout the exposed phragmocone and up to the beginning of the fine ribbing on the body chamber; rarely, a tubercle or two is found in the fine ribbing. Umbilical bullae occur on the primary ribs at the umbilical shoulder; these may or may not occur on the first few primaries of the exposed phragmocone.

In addition to the consistent nodation described, actual or incipient tubercles or bullae may locally form a short row next to that of the ventrolaterals (figs. 87I, 88A). These tubercles or bullae most commonly occur on ribs just anterior or posterior to the ultimate septum, where the ribs swing forward as they approach the venter. On smaller specimens only a few ribs may show these additional tubercles but on larger specimens they may be evident on 10 or more ribs.

The suture of microconchs, relatively simple in these small specimens, is, nevertheless, similar to that of macroconchs (fig. 90D).

DISCUSSION: Macroconchs of *H. birkelundi* differ from those of the succeeding species *H. nicolletii* in having a more compressed form, a longer, slightly tapering hook, a much smaller umbilicus, a gap between the hook and phragmocone (although a few macroconchs of *H. nicolletii* show this feature), a weaker adoral projection of ribs across the venter, and only a slight projection of the ventral lip at the aperture. The ribbing does not follow the *H. nicolletii* pattern and fine ribs may start earlier on the body chamber in *H. birkelundi* than in *H. nicolletii*. The common occurrence of tubercles other than ventrolaterals together with the more compressed form and smaller umbilicus bring *H. birkelundi* closer to *H. comprimus* than to *H. nicolletii*. These features may represent ecophenotypic characters reflecting the common habitat of *H. birkelundi* and *H. comprimus* over shallow sand substrates of the lower shore face (Landman and Waage, in press).

H. birkelundi differs from *H. melloi* in its smaller, more compressed shell, its more numerous tubercles, the lesser extent of fine ribbing on the body chamber, and the position of the umbilicus of the coil on the umbilical shoulder of the body chamber.

Elias (1933: 328) included under the name *Discoscaphites abyssinus* (Morton) a number of scaphite fragments from the Beecher Island Member of the Pierre Shale, near Beecher Island, Yuma County, Colorado. Most specimens are small microconchs, but one is a macroconch (Elias, 1933: pl. 39, fig. 3). Jeletzky (1962: 1015, pl. 141, fig. 3) refigured this specimen as *Scaphites* (*Hoploscaphites*) aff. *nicolletii* (Morton) "collected either from *Baculites grandis* or from *Baculites clinolobatus* zone" (ibid., p. 1018). Elias was not clear as to the precise horizon, but in a related publication (Elias, 1931: 124) he noted that the greater part of the fossil material was collected "from the lowest concretionary zone," which also included "casts of *Baculites grandis* and less abundant casts of *B. clinolobatus*," and "many *Discoscaphites abyssinus*."

Elias' specimen resembles *H. birkelundi* in its small umbilicus and persistent ventrolateral tubercles and umbilical bullae, features also present in small scaphites from the *Baculites grandis* Zone, as noted by Jeletzky (1962: 1015). Both Elias' specimen and complete specimens we have of very similar scaphites from the *B. grandis* Zone at the Red Bird locality differ from *H. birkelundi* in their smaller average size, less compressed form, and absence of very fine ribbing on the anterior two-thirds of the body chamber. While distinct from the *B. grandis* Zone form, *H. birkelundi* has sufficient characters in common with it to suggest a close relationship.

Macroconchs of *H. birkelundi* resemble some forms of the Eurasian species *Hoploscaphites constrictus* (Sowerby), perhaps more closely than do any other known species of *Hoploscaphites* described herein. For example, *H. birkelundi* resembles *H. constrictus anterior* described by Blaszkiewicz (1980: 36) in its general shape, small umbilicus, high apertural angle, and distribution of ventro-

TABLE 12
Measurements of *Hoploscaphites* sp.[a]

	LMAX (mm)	WUS (mm)	HUS (mm)	WAPT (mm)	HAPT (mm)	UD (mm)	A (°)
YPM 27166	49.7	11.4	17.7	15.6	17.3	4.0	46
YPM 27167	47[b]	12.0	16.6	—	—	4.0	—
YPM 27168	48[b]	12.4	16.8	—	—	5.0	—

[a] Abbreviations: see figure 9.
[b] Estimate.

lateral tubercles and umbilical bullae, but it differs in its very fine ribbing on the body chamber and in its larger overall size.

Hoploscaphites sp.?
Figure 91

DESCRIPTION: Three specimens, one entire, of *Hoploscaphites* macroconchs that differ significantly from *H. nicolletii* were found in the *H. nicolletii*-dominated concretions of the Lower *nicolletii* Assemblage Zone, each at a different locality. The specimens have the general aspect of small *H. nicolletii* and all are about the same size, averaging 48.2 mm (table 12). Dimensions of all three shells, except umbilical diameter in one specimen, fall below the average values for *H. nicolletii.* The shell also expands more gradually into the body chamber than in *H. nicolletii.*

The distinctive features of *Hoploscaphites* sp.? are an unusual rib pattern lacking any forward projection of the ventral ribs and the complete lack of tubercles. There are about 8 ventral ribs/cm at the point of exposure, which gradually increase to about 14/cm on the posterior one-quarter of the body chamber. Thereafter, the number of ribs abruptly increases to as many as 30 to 35/cm on the anterior three-quarters of the body chamber. This very fine ribbing starts earlier on the body chamber than in *H. nicolletii* and none of the other ribbing zones typical of *H. nicolletii* are apparent. However, the most striking feature of the ribbing in *Hoploscaphites* sp.? is the lack of any forward projection of the ribs across the venter. In two specimens, the ribs show a slight adapical curvature just below the umbilical shoulder, then bend forward to just above mid-flank where they become radial. In the third specimen (YPM 27168), the ribs show a more pronounced adoral swing on the flanks, extending almost to the venter, after which they curve slightly backwards across the lower flanks (fig. 91). This specimen may have some abnormality but signs of external injury are not evident. Consistent with the lack of any adoral projection of the ventral ribs in *Hoploscaphites* sp.? is the absence of any projection of the ventral lip at the aperture, typical of *H. nicolletii.*

No ventrolateral or other tubercles are present on any of the three specimens. The suture is similar to that of *H. nicolletii* and other species of *Hoploscaphites* and shows no distinctive characteristics. No microconch form with features suggesting relationship to the three macroconchs has been found.

DISCUSSION: These three specimens may be abnormalities of *H. nicolletii,* but because they are so similar to one another and share a distinctive combination of features, we recognize the possibility that they may represent a valid species within *Hoploscaphites.* Certain characteristics of *Hoploscaphites* sp.? are found in *H. melloi.* Both show a similar distribution of fine ribbing over the entire body chamber beginning from about the position of the ultimate septum. Two of the specimens of *H.* sp.?, YPM 27166 and 27168, show the offset of the umbilicus of the coil above the umbilical shoulder of the body chamber, a feature characteristic of *H. melloi. H.* sp.? lacks tubercles of any kind as do many but not all *H. melloi* specimens. But all of the *H. melloi* specimens we have are larger than those of *H.* sp.? and show a marked, although slight, adoral projection of the ventral ribs and ventral lip at the aperture.

Among other species of Western Interior *Hoploscaphites, H.* sp.? resembles the middle and upper Campanian *H. gilli* (Cobban and Jeletzky, 1965) in its fine ribbing, lack of any forward projection of the ventral ribs, and absence of tubercles. It differs chiefly in its

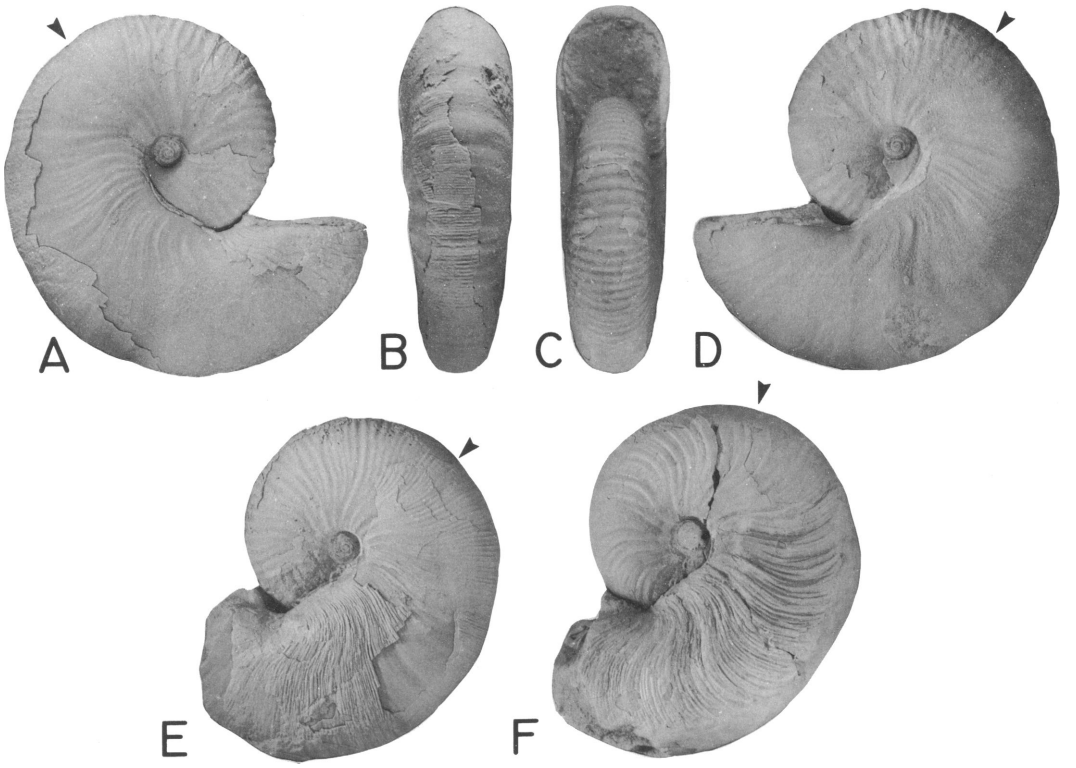

Fig. 91. *Hoploscaphites* sp.? macroconchs. **A–D.** YPM 27166, loc. 54, LNAZ. **A,** Right lateral; **B,** posterior; **C,** apertural; **D,** left lateral. **E.** Incomplete specimen, left lateral, YPM 27167, loc. 47, LNAZ. **F.** Incomplete specimen with pronounced reversal of rib direction on venter, left lateral, YPM 27168, loc. 7, LNAZ.

denser ribbing, which is restricted to the body chamber, its greater apertural angle, and its more tightly coiled last whorl. Some specimens of *H. gilli* illustrated by Cobban and Jeletzky, particularly the holotype (ibid., pl. 95, fig. 4), are as tightly coiled as our specimens, but the variable *H. gilli* more commonly has a longer hook and a pronounced gap between the hook and the phragmocone.

It is unlikely that *H. gilli* or some variant of it persisted in the Western Interior endemic basin until Trail City time without leaving more of a record. If anything, the occurrence of only three specimens among hundreds of *H. nicolletii* collected from the Lower *nicolletii* Assemblage Zone is more suggestive of rare migrants from outside the endemic basin. The Eurasian early Maastrichtian species *Hoploscaphites tenuistriatus* (Kner, 1848) has a very finely ribbed body chamber lacking tubercles as well as any forward projection of the ribs on the venter. But *H. tenuistriatus* differs in having a very small umbilicus and a high body chamber. On the other hand, the resemblance of these three specimens to the older species *H. melloi* may suggest instead atavism resulting from a growth dysfunction or genetic accident. The lack of shell asymmetry or scars that indicate injury support the possibility of an internal cause if these specimens are indeed pathologic.

Jeletzkytes Riccardi, 1983

TYPE SPECIES: *Scaphites* (*Ammonites*?) *nodosus* Owen, 1852: 581, pl. 8, fig. 4, by original designation.

DIAGNOSIS:

Relatively large scaphitids, with involute phragmocone; body chamber with short shaft extending slightly beyond the phragmocone and weakly recurved hook; whorl section remaining depressed throughout the phragmocone and body chamber, or varying from de-

pressed to slightly compressed during the ontogeny; ribs almost straight to weakly projected and flexuous; earlier representatives with stronger and sparser ribbing and bearing prominent lateral and ventrolateral tubercles on the body chamber; younger representatives with relatively finer and denser ribbing, and 2–3 rows of lateral nodes in the phragmocone, which tend to fade away on the flanks of the body chamber. Suture fairly indented, becoming more complex from older to younger species. (Riccardi, 1983: 14)

OCCURRENCE: Middle Campanian to Maastrichtian, Pierre Shale, Bearpaw Formation, and equivalents, Western Interior of North America. The species we provisionally assign to this genus are Maastrichtian and occur in the Fox Hills Formation of South Dakota, North Dakota, and Wyoming and in the Severn Formation of Maryland.

Jeletzkytes spedeni, new species
Figures 92–119

Macroconch Synonymy:

Discoscaphites conradi (Morton) Meek, Reeside, 1927: pl. 9, figs. 2–4.

Hoploscaphites nebrascensis (Owen), Landman and Waage, 1986: p. 212, 220, fig. 6.

DIAGNOSIS: Macroconch shape variable, dominantly stout with quadrate to slightly depressed aperture. Body chamber with strong, locally clavate ventrolateral tubercles, usually with bullae below umbilical shoulder and scattered flank tubercles/bullae on hook. Phragmocone with up to four rows of tubercles or none. Last whorl of microconch more loosely coiled, commonly with mid-flank row of tubercles on body chamber; phragmocone variously tuberculate.

TYPES: Holotype, YPM 27160, loc. 54, LNAZ, fig. 92A–D, 93A.

Allotype, YPM 23710, loc. 115, LGAZ, fig. 104A–D.

NAME: The species is named for Ian G. Speden, formerly a co-worker on the type Fox Hills and author (Speden, 1970a) of a systematic study of its bivalves; lately Director of the New Zealand Geological Survey.

OCCURRENCE: Trail City Member of the Fox Hills Formation and uppermost beds of Elk Butte Member of the Pierre Shale in the Missouri Valley region of north-central South Dakota and adjacent parts of North Dakota.

MATERIAL: The total number of adult specimens in the YPM collections is about 370, of which 225 are macroconchs. The number of entire or nearly entire specimens is 88 macroconchs and 65 microconchs. In addition, 9 macroconchs and 7 microconchs were borrowed from the USGS collections. The set of measured specimens consists of 61 macroconchs and 39 microconchs. All of our specimens are from the assemblage zones of the Trail City Member of the type Fox Hills Formation except for one dimorphic pair from the sideritic concretions in the uppermost Elk Butte Member of the Pierre Shale (figs. 102, 106, see p. 14); the latter were not included in the set of measured specimens.

MACROCONCH DESCRIPTION: Shells are dominantly large and robust with a rounded to somewhat compressed whorl section. Coiling is relatively tight with the dorsal part of the aperture only slightly separated from the phragmocone and the dorsal projection reflexed against it. The shaft of the body chamber is short and arcuate on the periphery and straight along the dorsal shoulder. The hook is relatively short and the apertural angle averages 42.9° (table 13). The exposed phragmocone and body chamber are each approximately 0.5 whorls in angular length.

The dimensions of the measured specimens are listed in table 13. LMAX averages 103.2 mm with two-thirds of the specimens 100 mm or more. The size distribution is bimodal with a dominant peak at 100–110 mm and a smaller peak at 120–125 mm (fig. 112). The ratio of the size of the largest specimen to that of the smallest is 1.8. The shell reaches its maximum height and width at the

→

Fig. 92. *Jeletzkytes spedeni,* n. sp., holotype, macroconch, YPM 27160, loc. 54, LNAZ. **A,** Right lateral; **B,** apertural; **C,** ventral hook; **D,** left lateral.

Fig. 93. *Jeletzkytes spedeni,* n. sp., macroconchs. **A,** Holotype, YPM 27160 (cont.), posterior; **B,** coarse ribbed macroconch, right lateral, YPM 23110, loc. 25, POAZ float. **C, D.** Compressed variant, YPM 27162, loc. 303, LNAZ. **C,** Right lateral; **D,** apertural.

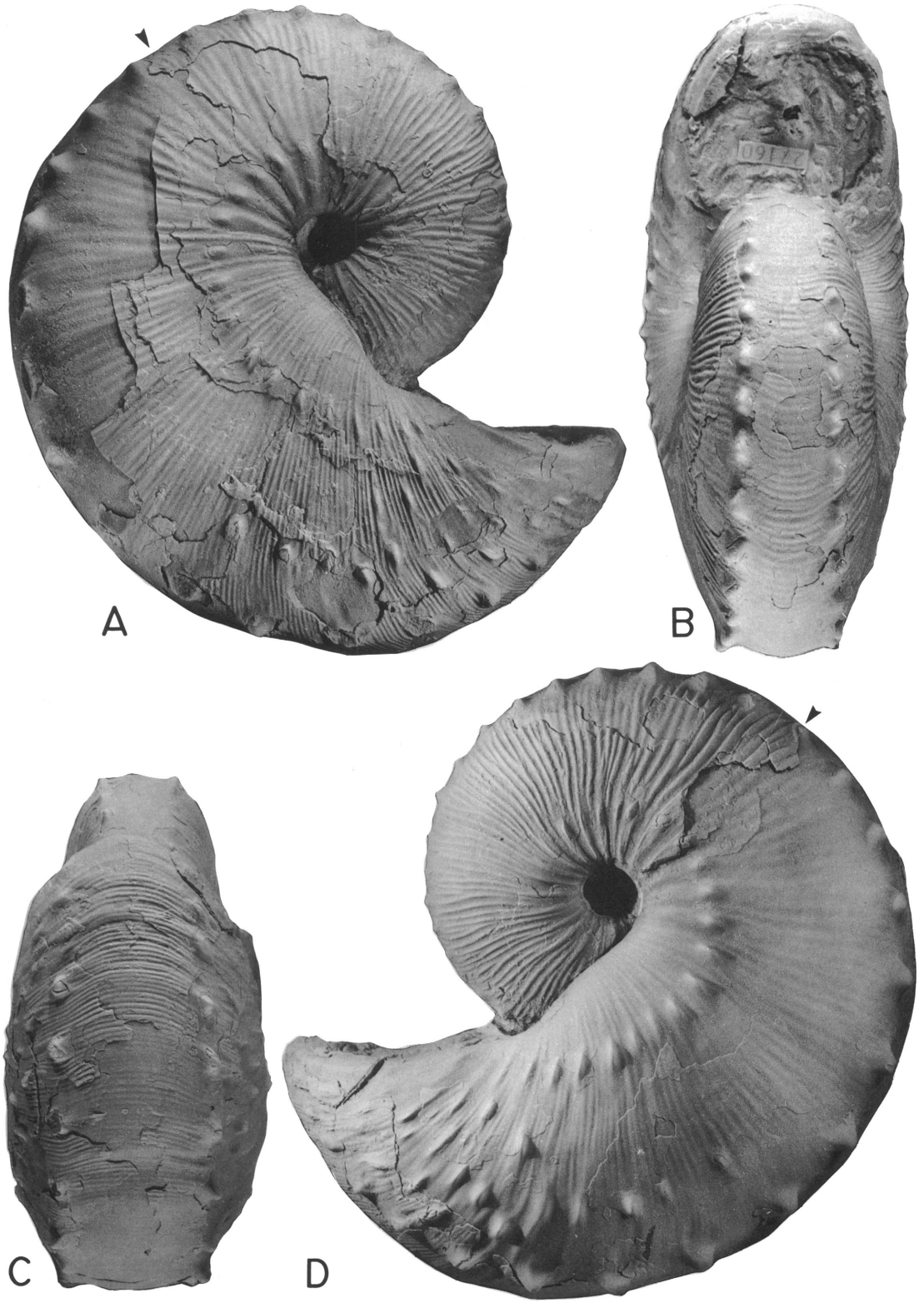

Fig. 92

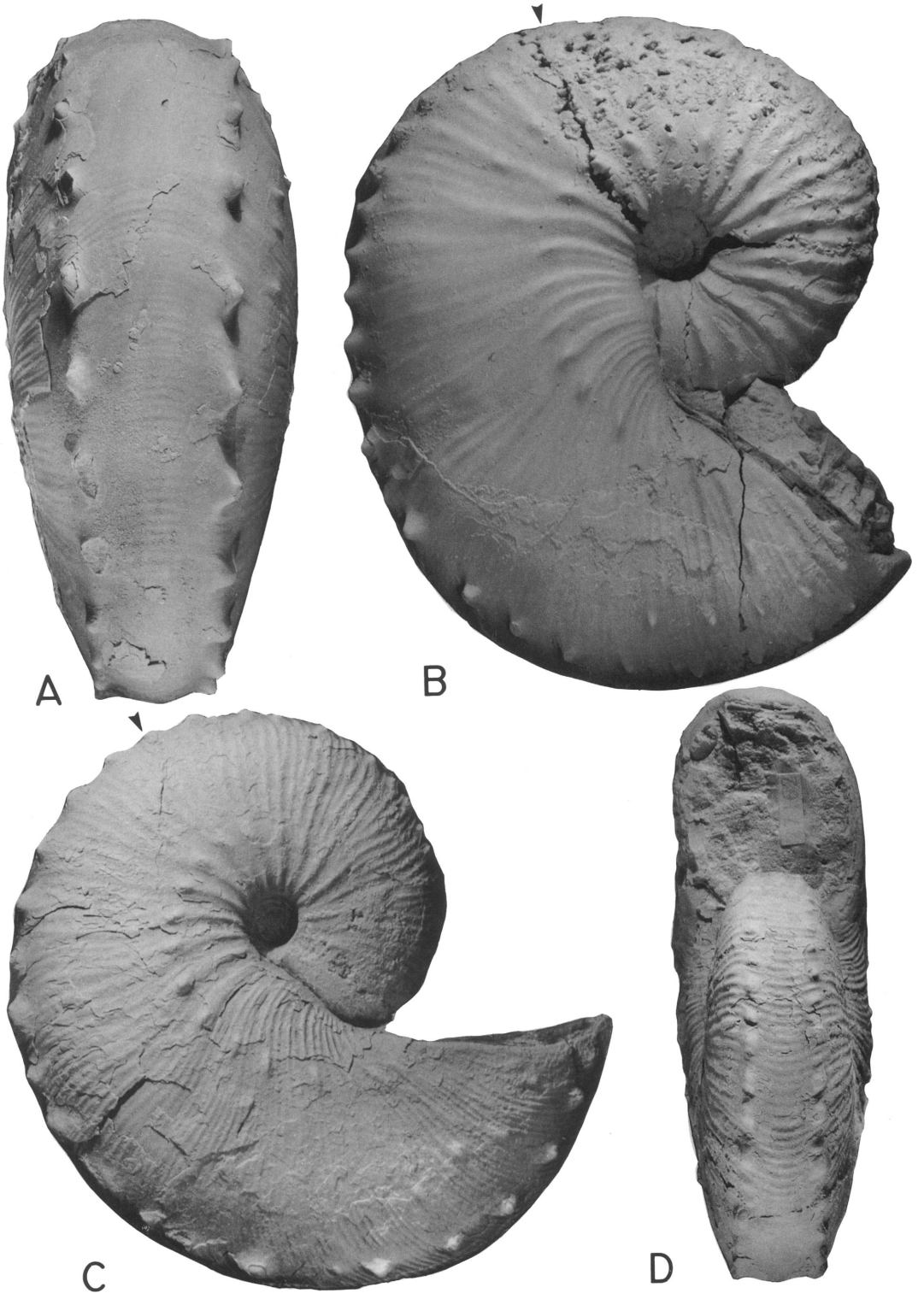

Fig. 93

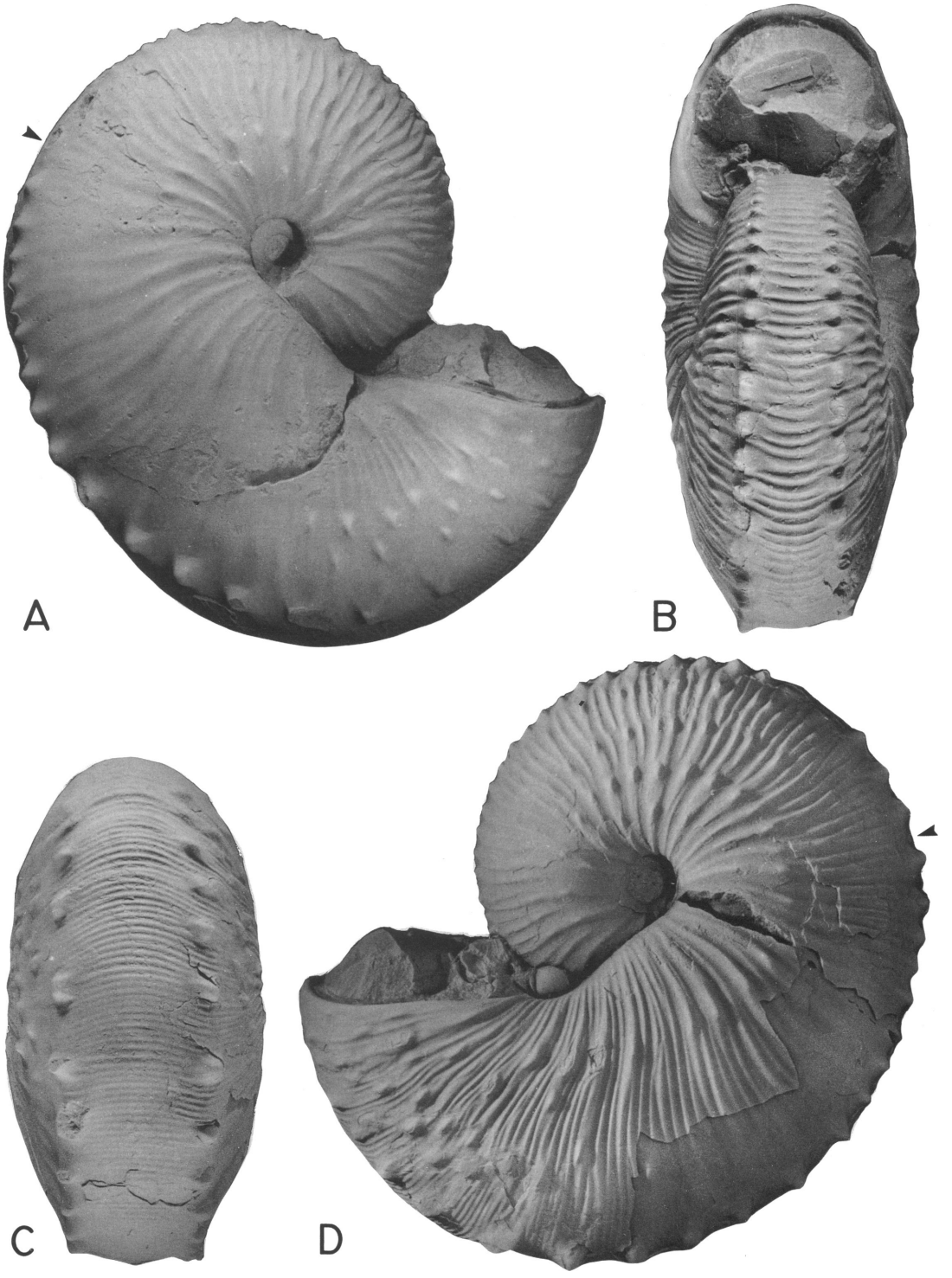

Fig. 94. *Jeletzkytes spedeni,* n. sp., macroconch, USNM 468854, loc. D2581, TCM. **A,** Right lateral; **B,** apertural; **C,** posteroventral; **D,** left lateral with most of shell; compare to right lateral (A), which lacks shell.

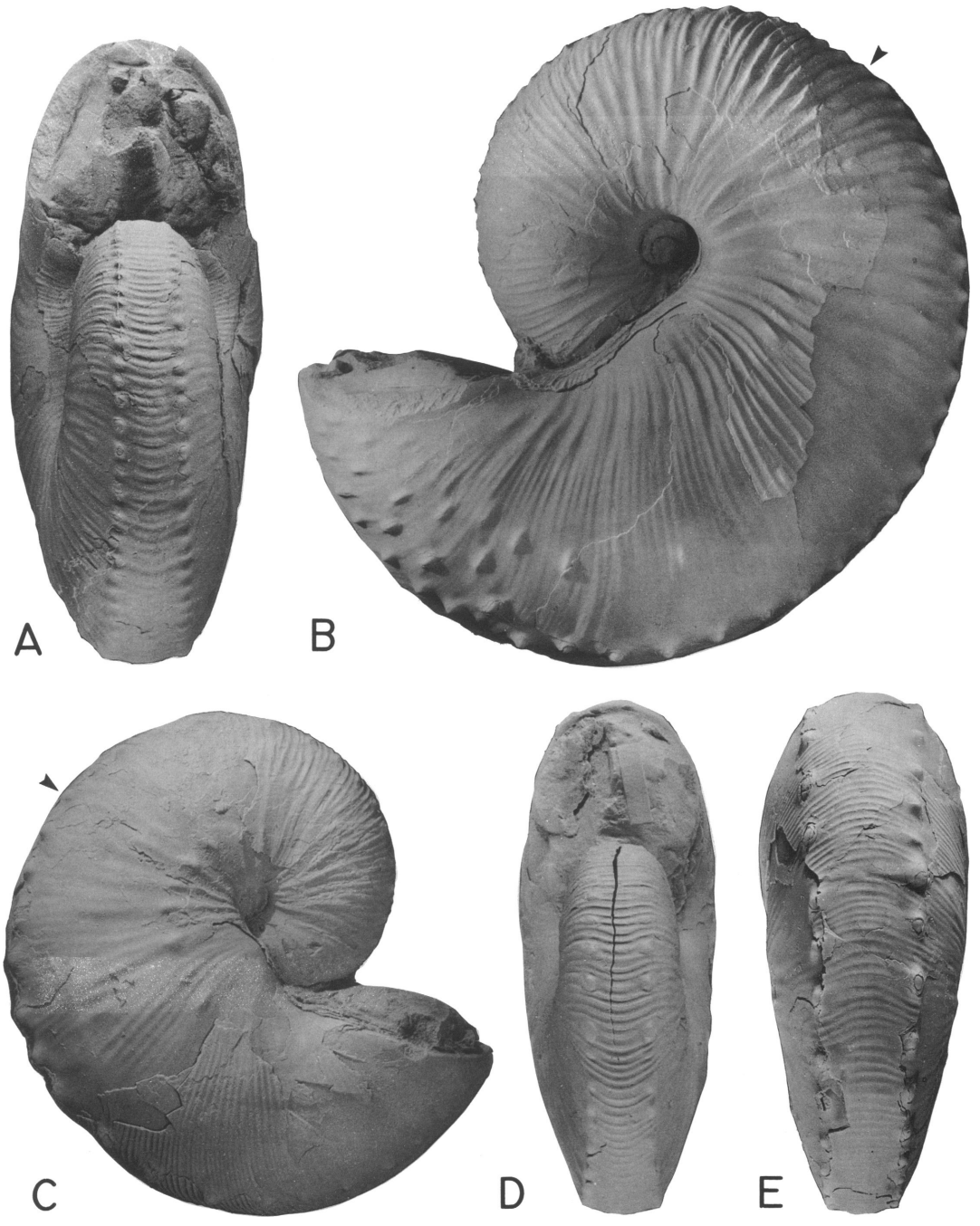

Fig. 95. *Jeletzkytes spedeni,* n. sp., macroconchs. **A, B.** YPM 23124, loc. 17, POAZ. **A,** Apertural; **B,** left lateral. **C–E.** Small specimen with subdued tuberculation, YPM 24817, loc. 17, UNAZ. **C,** Right lateral; **D,** apertural; **E,** posterior.

anterior portion of the shaft, after which it decreases abruptly in height and slowly in width to a rounded or oval aperture. The ratio of whorl width to whorl height at the ultimate septum and at the aperture averages 0.78 and 1.00, respectively (table 13). Larger specimens tend to have slightly more depressed whorl sections than smaller speci-

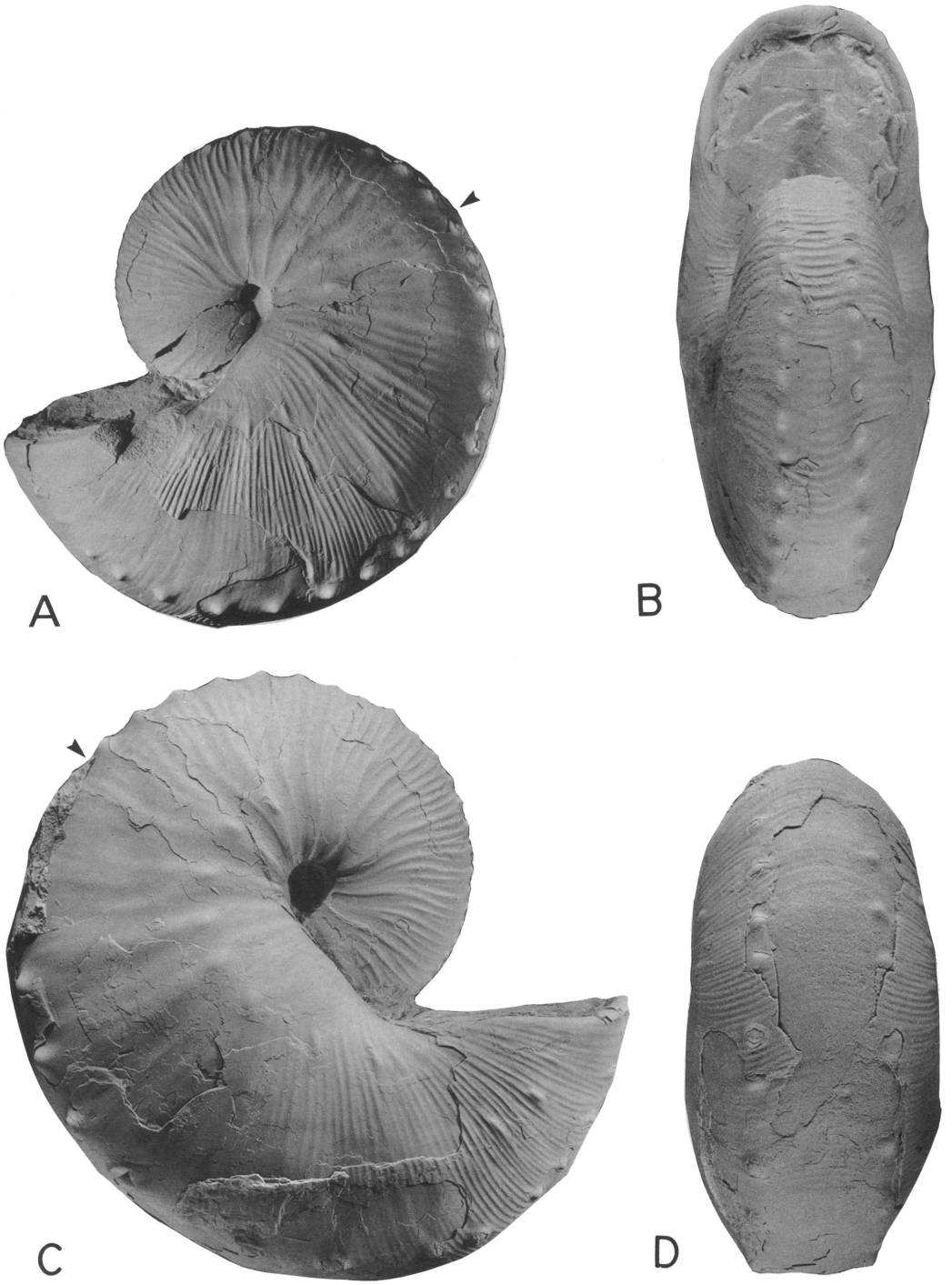

Fig. 96. *Jeletzkytes spedeni,* n. sp., macroconchs. **A.** YPM 24817 (cont.), left lateral. **B–D.** YPM 24819, loc. 17, UNAZ. **B,** Apertural; **C,** right lateral; **D,** posteroventral.

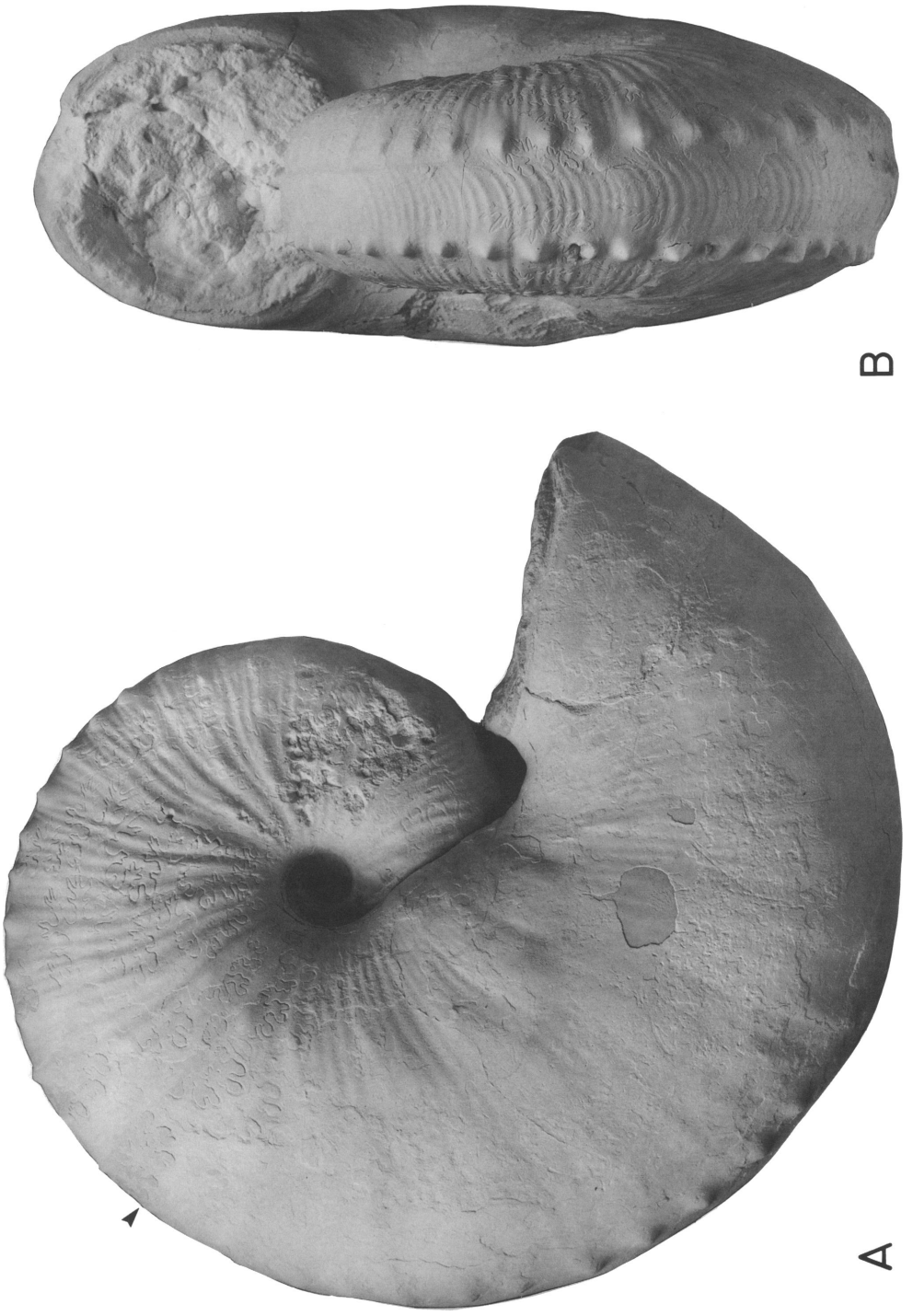

Fig. 97. *Jeletzkytes spedeni*, n. sp., large macroconch with depressed aperture; note spiral furrow from injury on ventral side of right row of ventrolateral tubercles, YPM 27156, loc. 25, POAZ float. **A**, Right lateral; **B**, apertural.

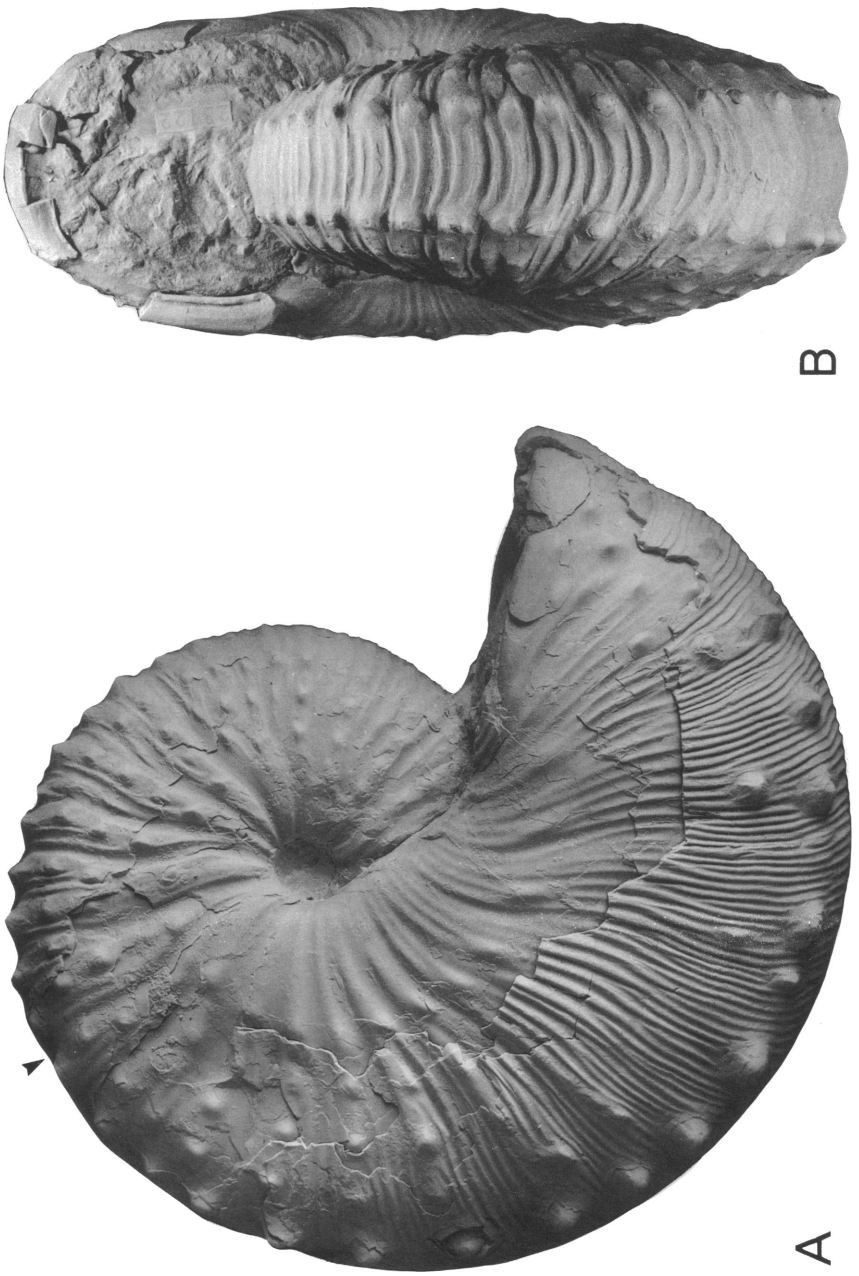

Fig. 98. *Jeletzkytes spedeni*, n. sp., macroconch, variant with broad tuberculate ribs on phragmocone, YPM 23122, loc. 200, POAZ. **A**, Right lateral; **B**, apertural.

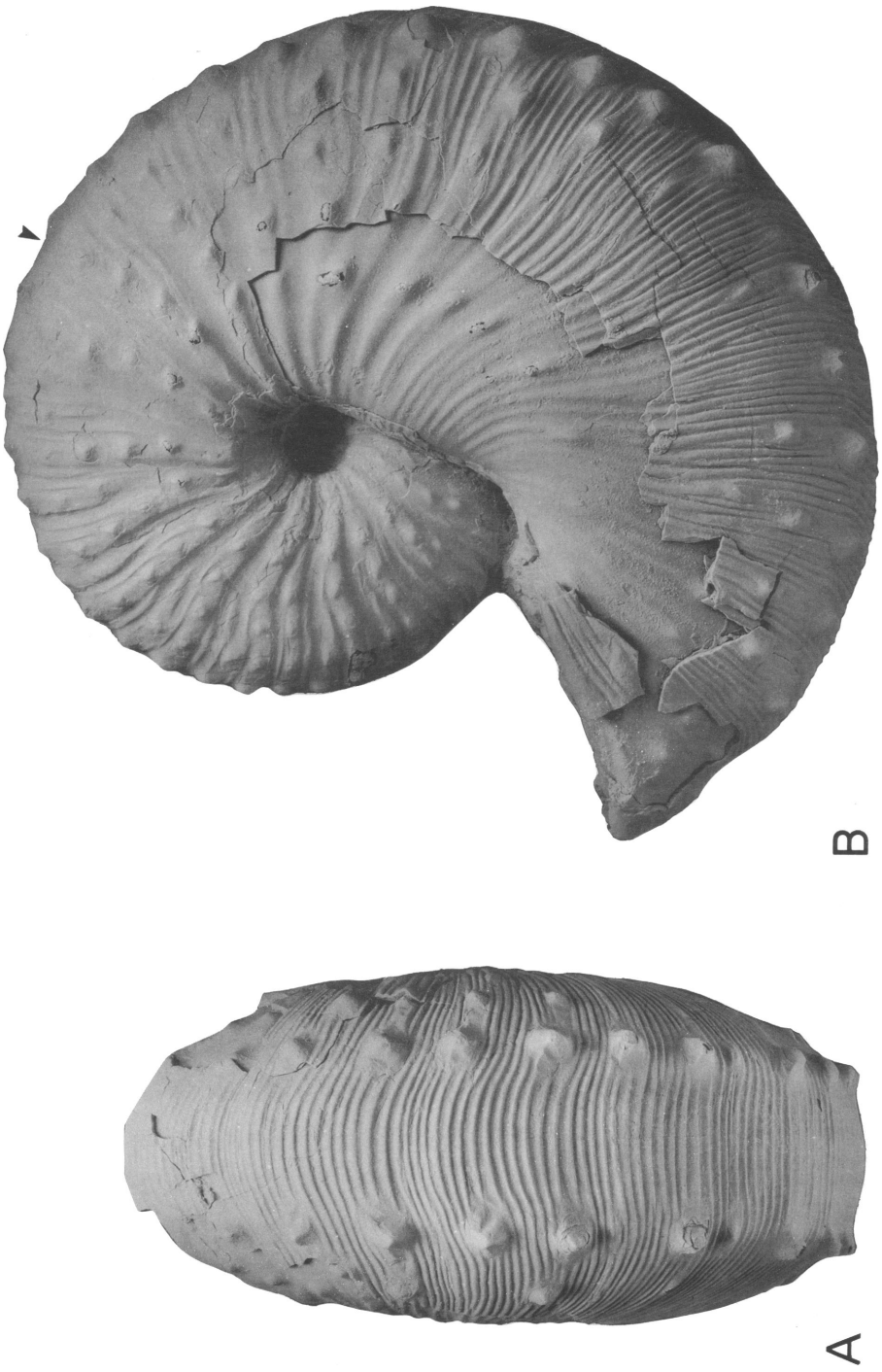

Fig. 99. *Jeletzkytes spedeni*, n. sp., macroconch, YPM 23122 (cont.). **A**, Posteroventral; **B**, left lateral.

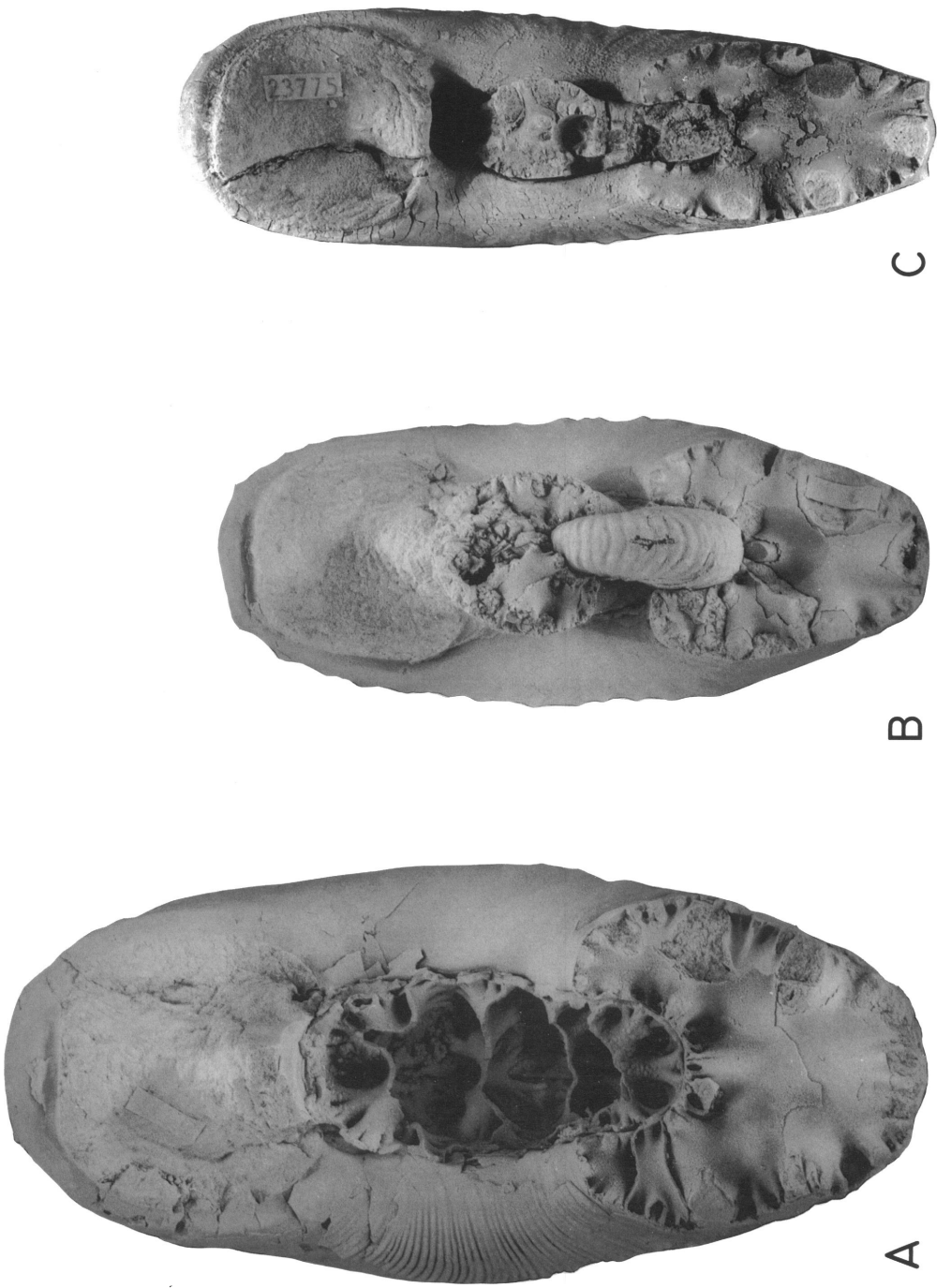

Fig. 100. *Jeletzkytes spedeni*, n. sp., apertural views of three macroconch body chambers illustrating the three principal shapes in *J. spedeni*. **A**, Large, stout variant, YPM 23206, loc. 64, LGAZ; **B**, most common intermediate form, YPM 23211, loc. 25, lower TCM float; **C**, compressed form, YPM 23775, loc. 69, LNAZ.

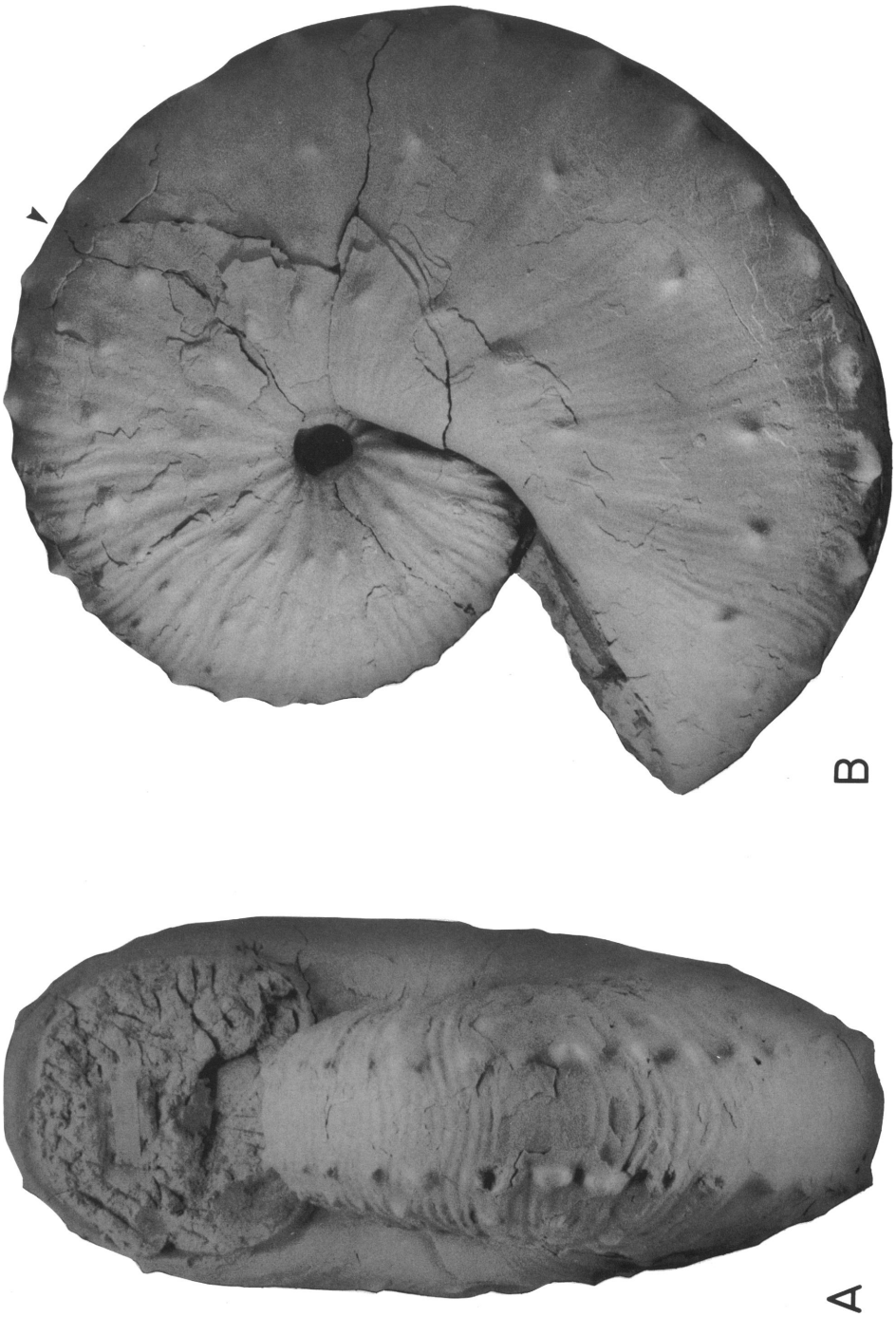

Fig. 101. *Jeletzkytes spedeni*, n. sp., large macroconch, YPM 23778, loc. 53, LGAZ. **A**, Apertural; **B**, left lateral.

Fig. 102. *Jeletzkytes spedeni,* n. sp., very large macroconch, laterally compacted in sideritic concretion, left lateral, YPM 23205, loc. 307, uppermost Elk Butte Member, Pierre Shale.

mens. Large, rotund shells with broad, rounded venters, depressed apertures, and strong ornament represent one extreme of the considerable range of variation found in this species (fig. 100A). At the other extreme are more compressed shells, generally in the lower half of the size range, with flatter flanks, narrower venters, higher-than-wide apertures, and finer, more subdued ornament (fig. 100C).

The umbilical diameter averages 7.8 mm, with larger specimens having relatively larger umbilical diameters. The ratio of umbilical diameter to shell diameter averages 0.08. The position of the umbilicus of the coiled phragmocone with respect to the umbilical shoul-

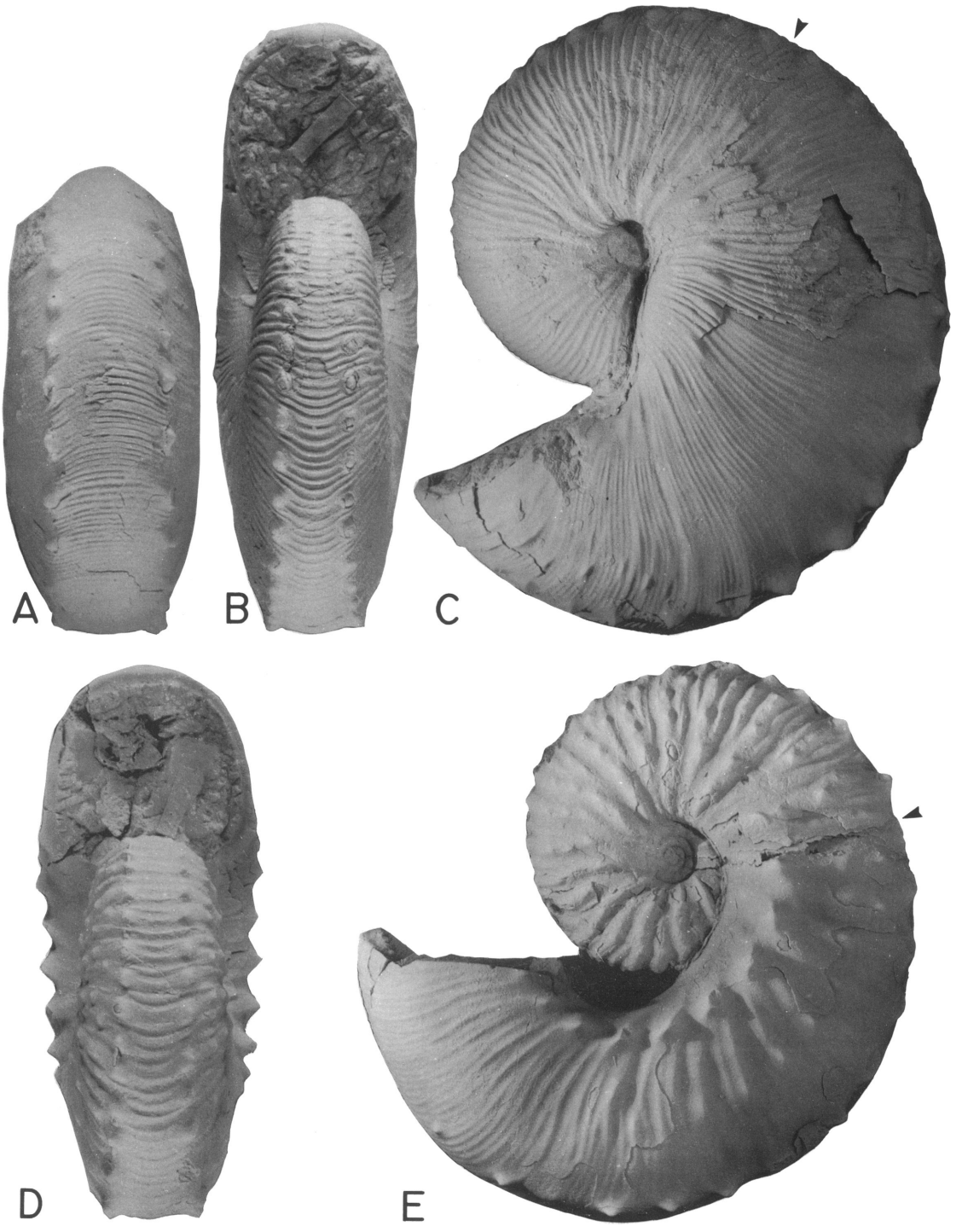

Fig. 103. *Jeletzkytes spedeni,* n. sp., macroconch and microconch. **A–C.** Compressed macroconch with fine ribbing, USNM 468855, loc. 21740, LNAZ. **A,** Posteroventral; **B,** apertural; **C,** left lateral. **D, E.** Large microconch, YPM 23704, loc. 53, LGAZ. **D,** Apertural; **E,** left lateral.

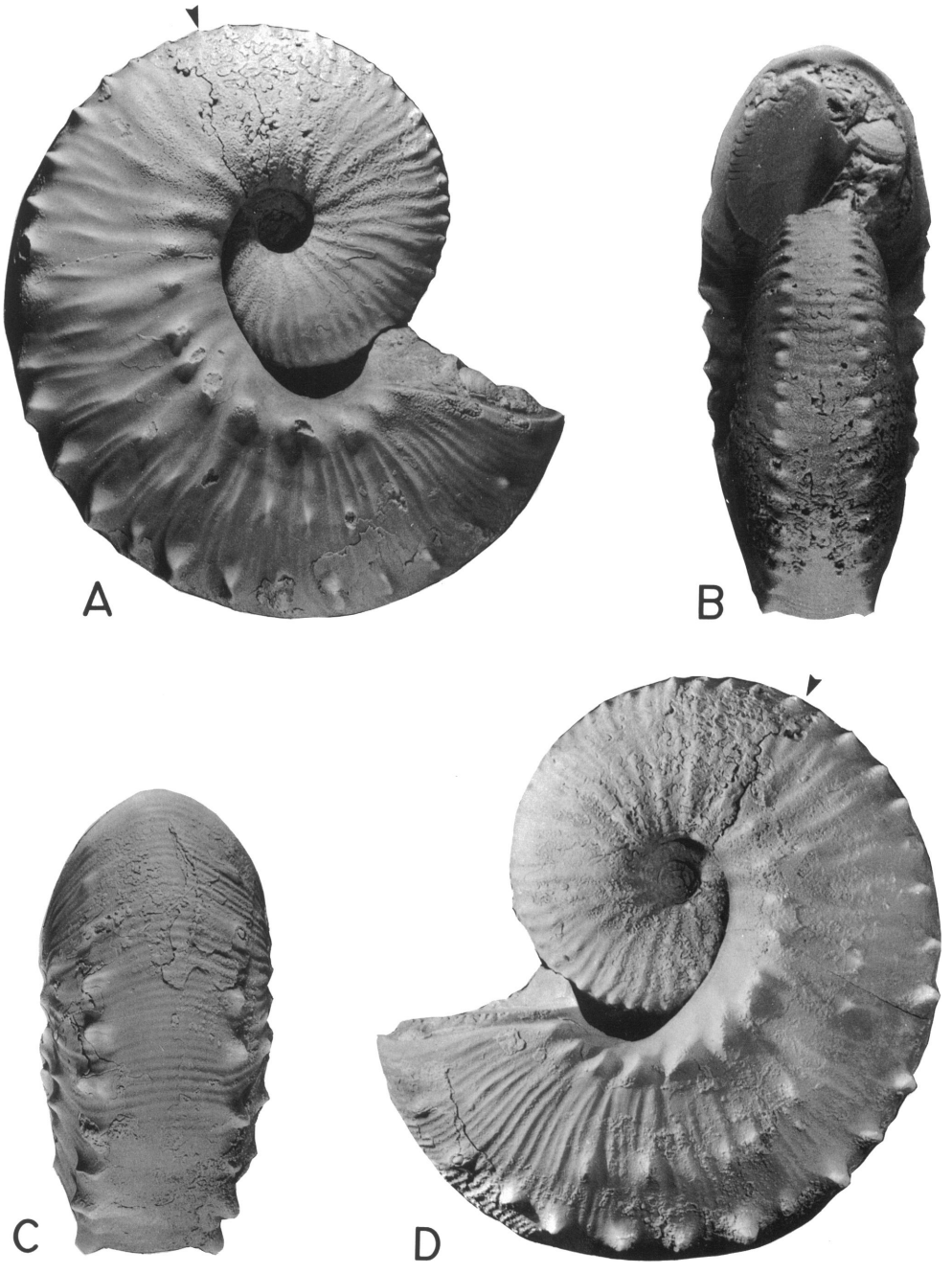

Fig. 104. *Jeletzkytes spedeni,* n. sp., microconch. Allotype, YPM 23710, loc. 115, LGAZ. **A,** Right lateral; **B,** apertural; **C,** posteroventral; **D,** left lateral.

der of the body chamber varies; in most specimens over 100 mm in size, the umbilicus of the coil lies above the umbilical shoulder of the body chamber and in most specimens under 100 mm in size it lies on the umbilical shoulder.

The ornament in *J. spedeni* macroconchs varies considerably. Smaller and more com-

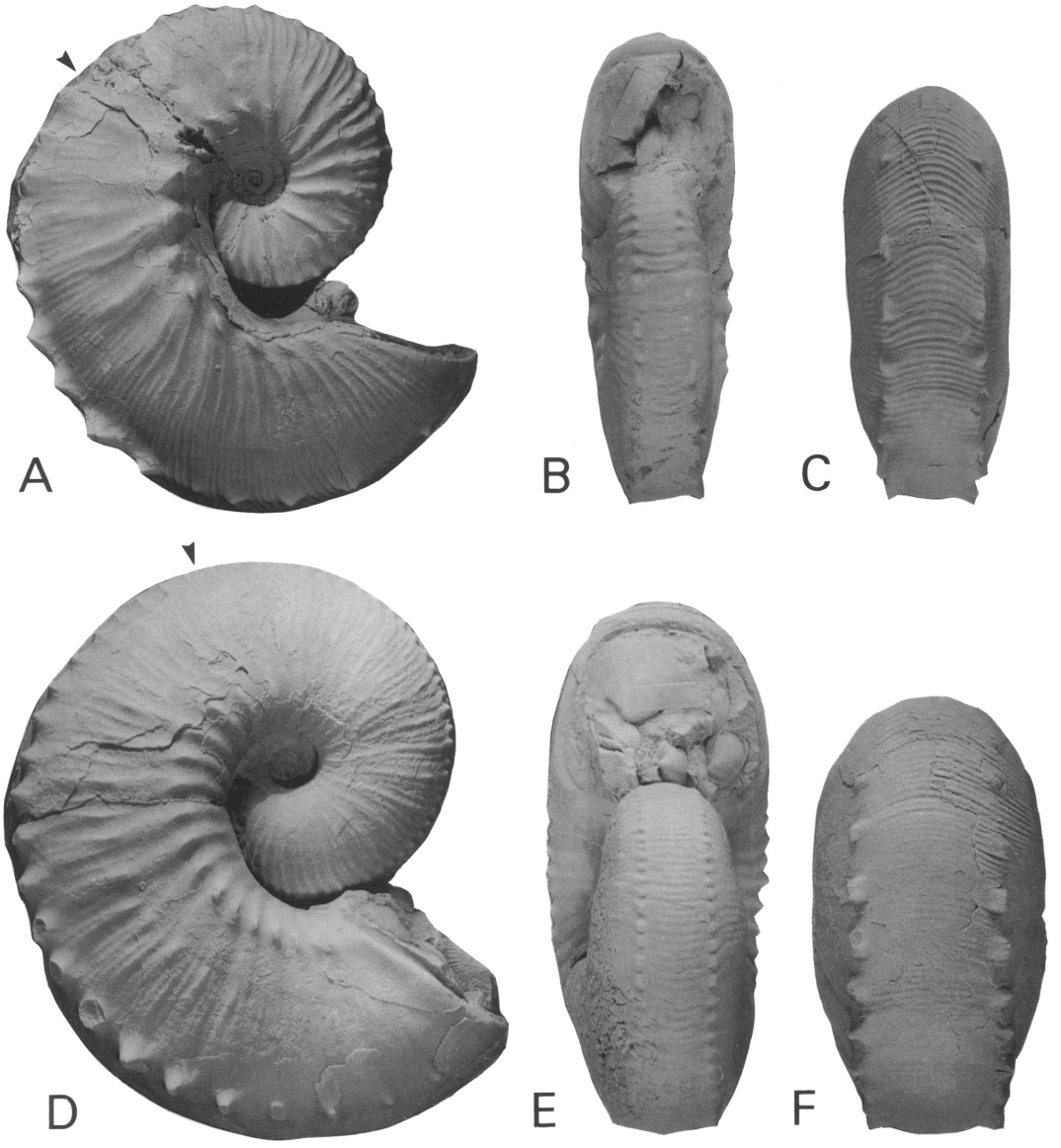

Fig. 105. *Jeletzkytes spedeni,* n. sp., microconchs. **A–C.** Compressed specimen, YPM 23199, loc. 25, POAZ. **A,** Right lateral; **B,** apertural; **C,** posteroventral. **D–F.** Stout specimen, YPM 23718, loc. 69, LGAZ float. **D,** Right lateral; **E,** apertural; **F,** posteroventral.

pressed specimens have finer ribbing and fewer tubercles and larger more rotund specimens have coarser ribbing and more tubercles. The most consistent features are the prominent ventrolateral tubercles on the exposed shell and inner whorls, and the bullae beneath the umbilical shoulder on all or part of the exposed shell.

Ribs vary from mostly rectiradiate on the phragmocone to mostly prorsiradiate on the body chamber. They show a moderate to strong adoral projection across the venter. Increase is by bifurcation and intercalation. Spacing of ventral ribs ranges from 5 to 10/cm on the phragmocone and posterior part of the body chamber. This wide range of vari-

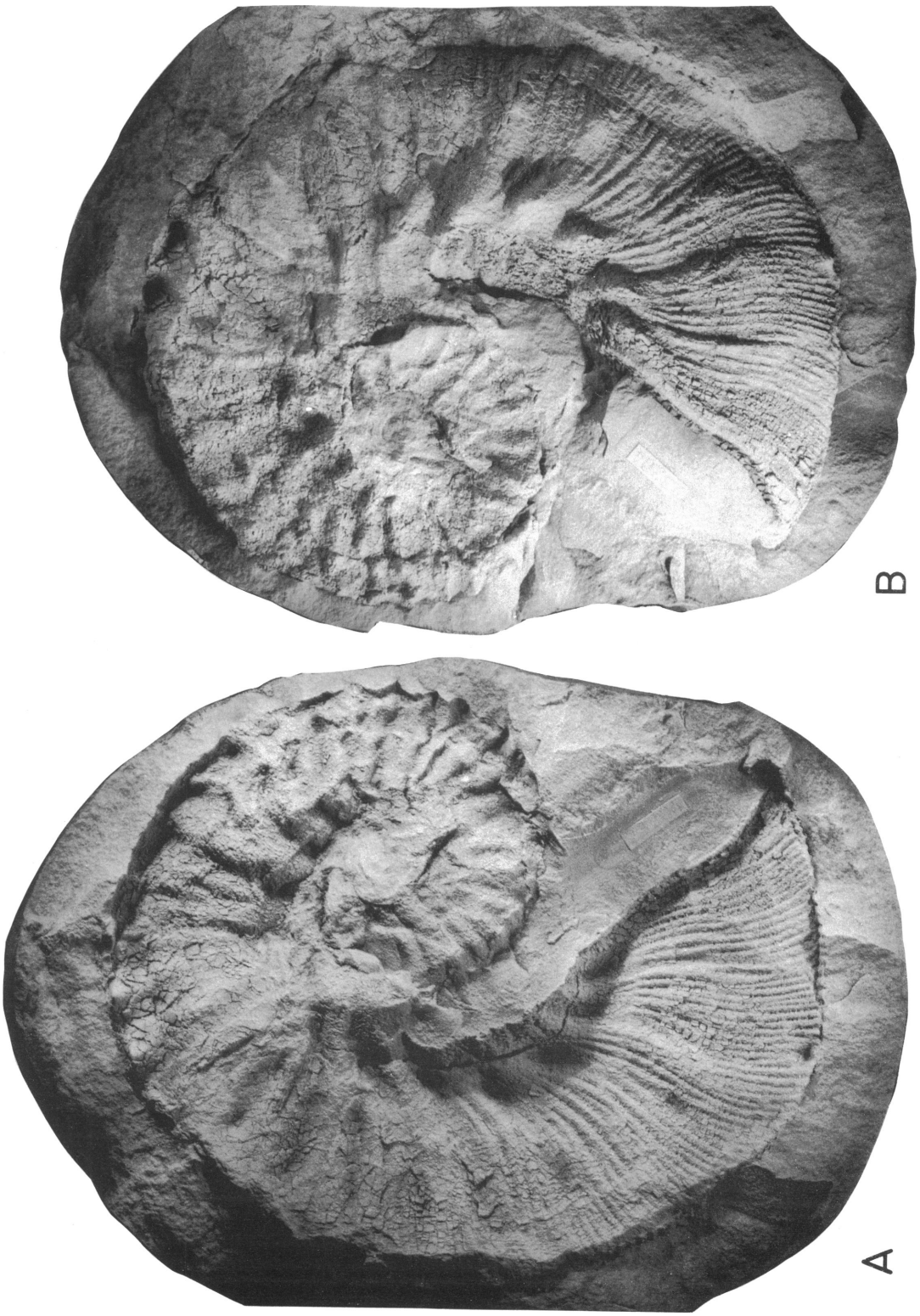

Fig. 106. *Jeletzkytes spedeni*, n. sp., very large microconch, laterally compacted in sideritic concretion, YPM 23204, loc. 307, uppermost Elk Butte Member, Pierre Shale. **A**, Left lateral impression; **B**, left lateral.

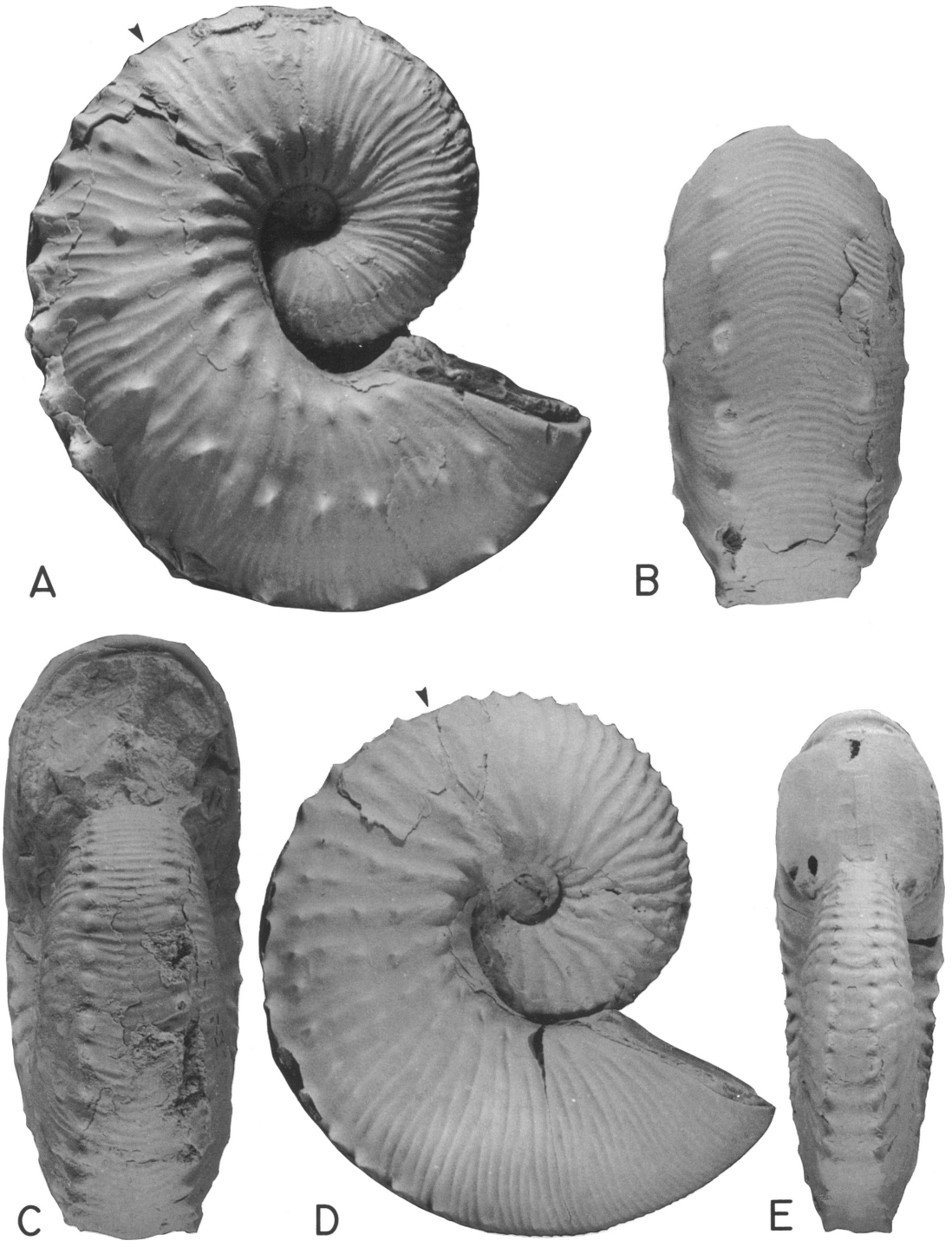

Fig. 107. *Jeletzkytes spedeni,* n. sp., microconchs. **A–C.** Stout form, YPM 23699, loc. 86, LGAZ. **A,** Right lateral; **B,** posteroventral; **C,** apertural. **D, E.** Compressed form with unusually ornate body chamber, USNM 468856, loc. D2580, top TCM, probably transition concretions. **D,** Right lateral; **E,** apertural.

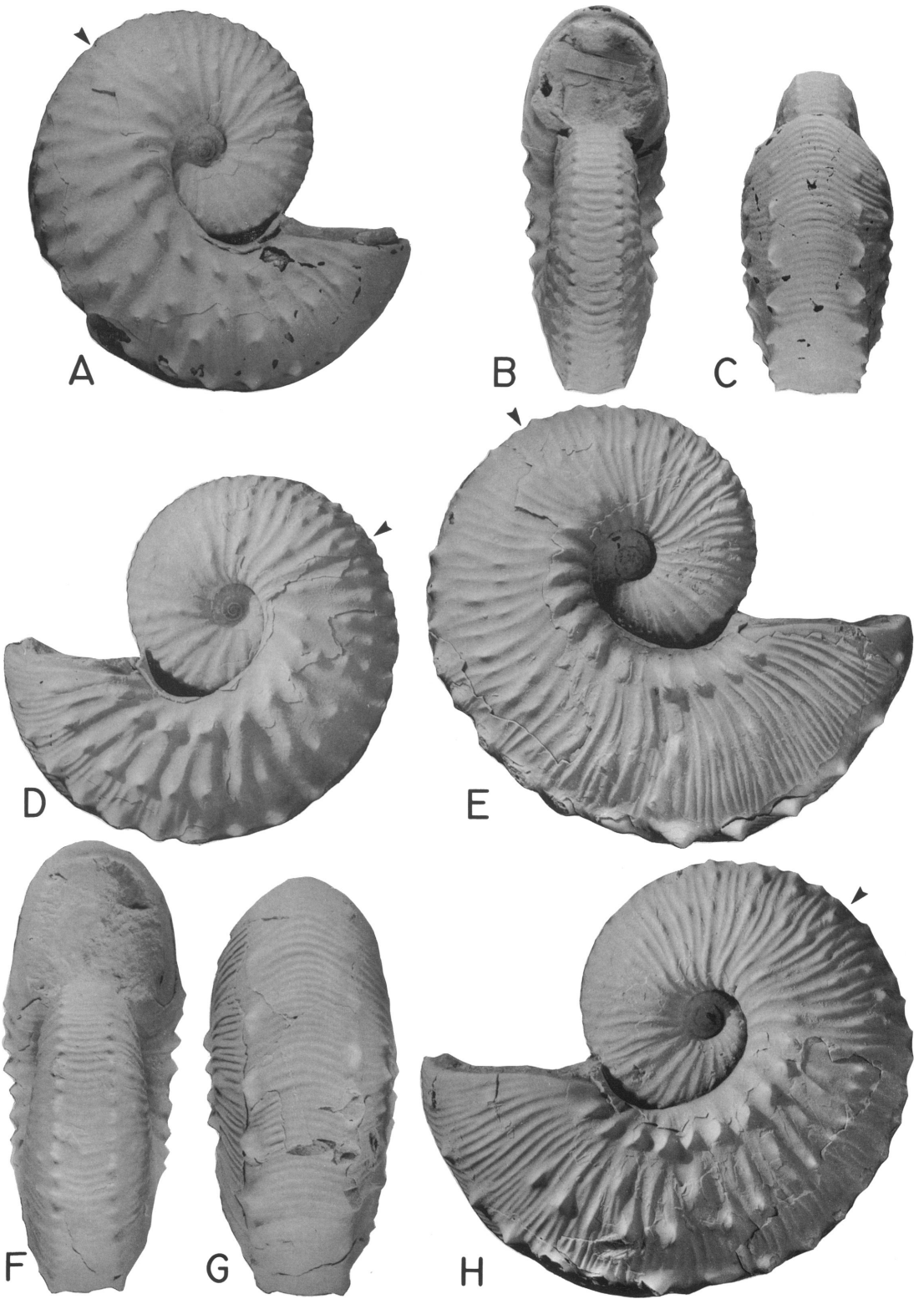
A
B
C
D
E
F
G
H

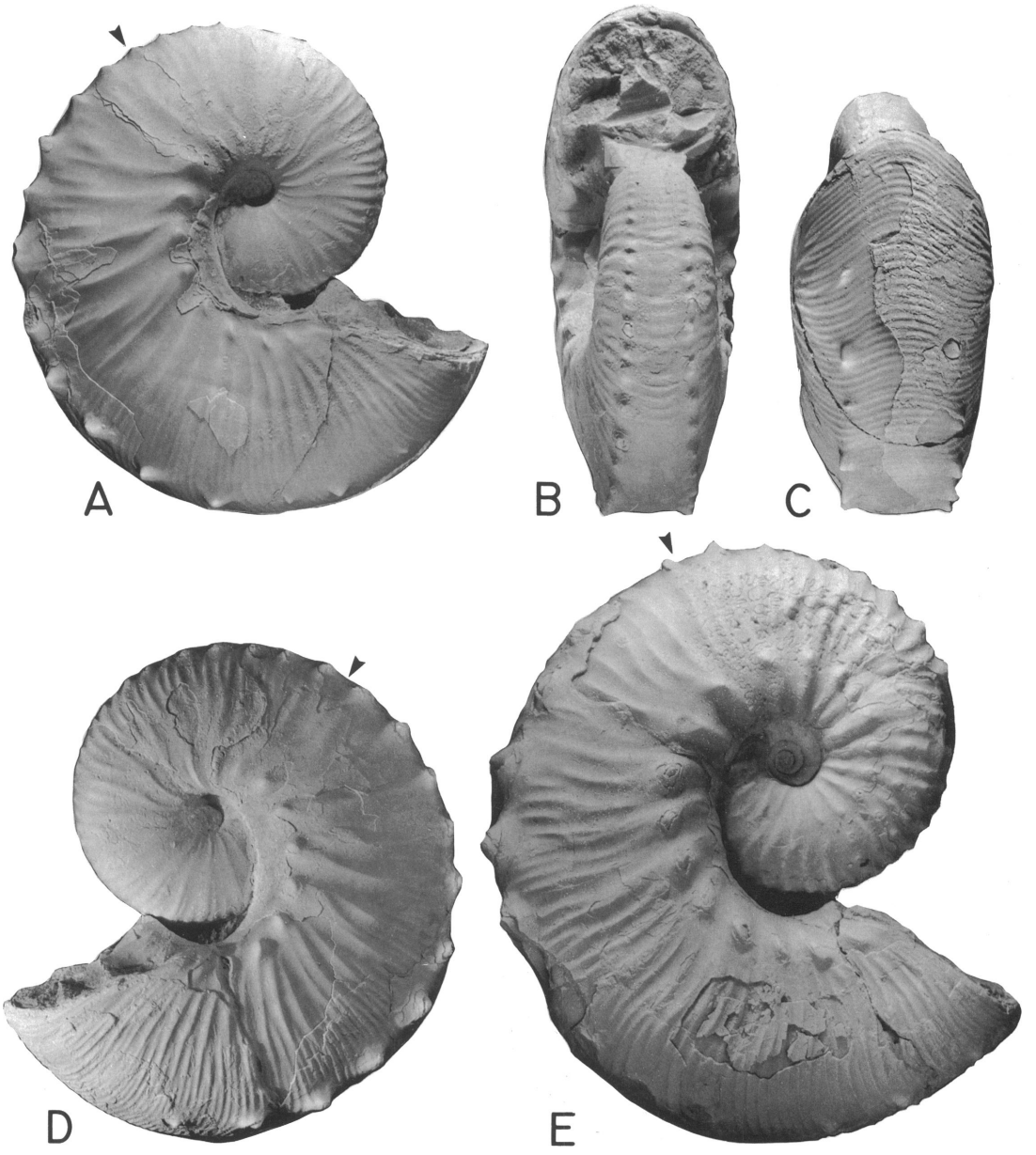

Fig. 109. *Jeletzkytes spedeni,* n. sp., microconchs. **A–D.** Weakly ornamented variant, YPM 23732, loc. 69, UNAZ. **A,** Right lateral; **B,** apertural; **C,** ventral hook; **D,** left lateral. **E.** Right lateral, YPM 23714, loc. 25, POAZ float.

←

Fig. 108. *Jeletzkytes spedeni,* n. sp., microconchs. **A–D.** YPM 23200, loc. 17, POAZ. **A,** Right lateral; **B,** apertural; **C,** ventral hook; **D,** left lateral. **E–H.** YPM 23706, loc. 200, POAZ. **E,** Right lateral; **F,** apertural; **G,** posteroventral; **H,** left lateral.

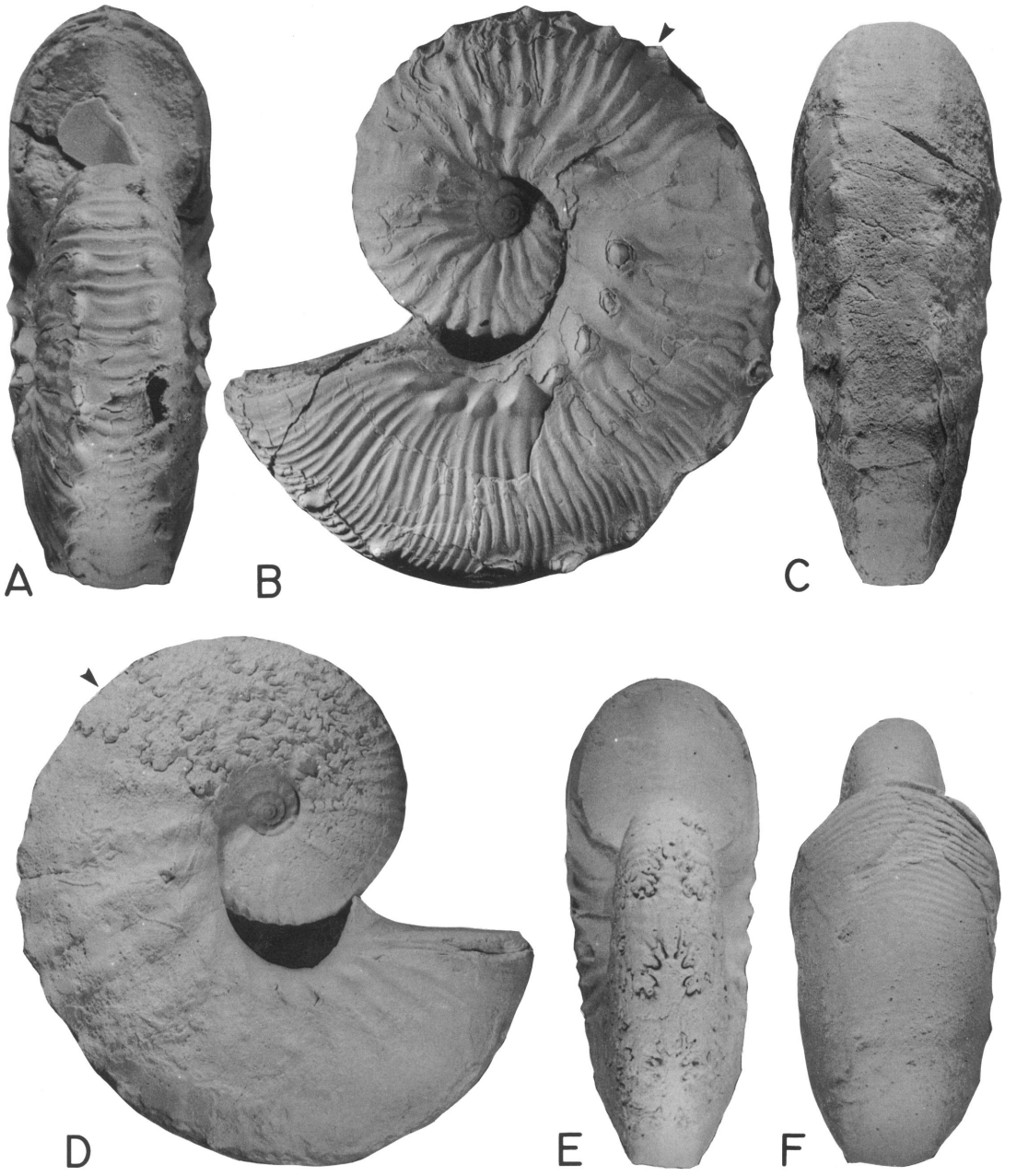

Fig. 110. *Jeletzkytes spedeni,* n. sp., microconch, YPM 23714 (cont.). **A,** Apertural; **B,** left lateral. **C–F.** Cast of *Scaphites* (*Discoscaphites*) *waagei* Birkelund, YPM 31803, West Greenland. **C,** Posterior; **D,** right lateral; **E,** apertural; **F,** ventral hook.

ation in rib spacing leads to some rather different looking phragmocones (compare figs. 99B and 103C). Where ribs are widely spaced, ventrolateral tubercles tend to occur on every rib but where ribs are closely spaced, they tend to occur on every second or third rib. Many specimens show weakening of ribbing on the flanks of the posterior part of the body

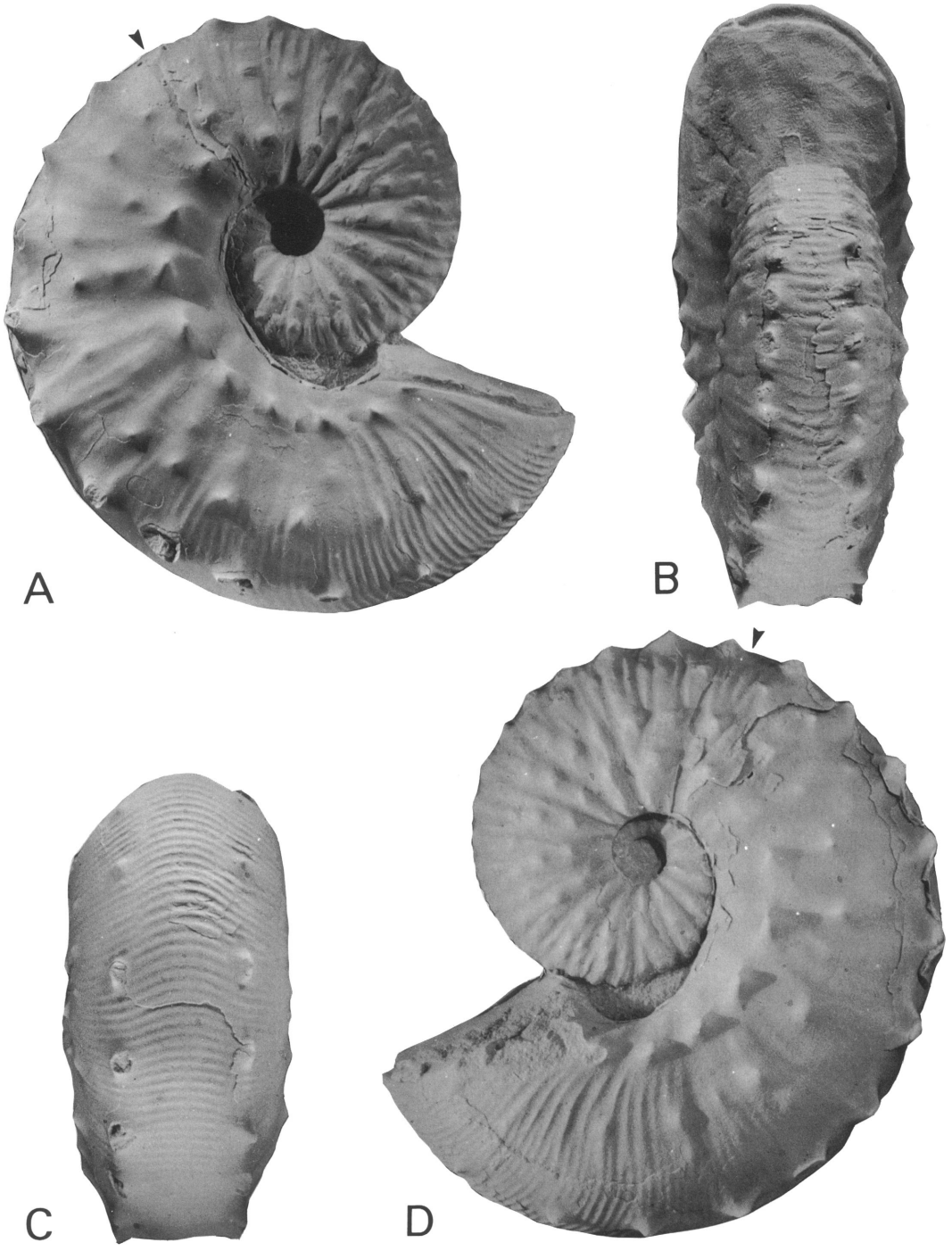

Fig. 111. *Jeletzkytes spedeni,* n. sp., large, ornate microconch, USNM 468857, loc. D2585, Fox Hills Fm. **A,** Right lateral; **B,** apertural; **C,** posteroventral; **D,** left lateral.

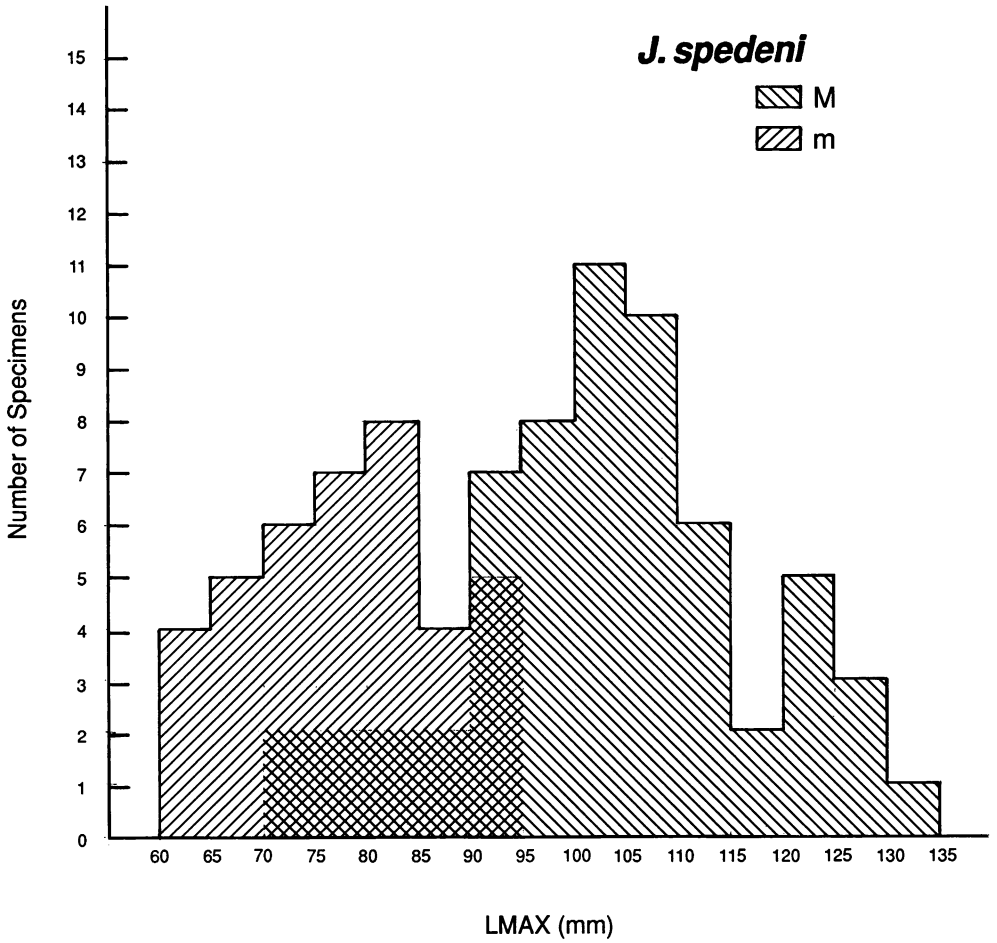

Fig. 112. Size frequency histogram of a sample of *J. spedeni,* n. sp., from the Trail City Member of the Fox Hills Formation in its type area.

TABLE 13
Adult Measurements of *J. spedeni*[a]

	Macroconch				Microconch			
	N	$\bar{x}$	SD	Range	N	$\bar{x}$	SD	Range
LMAX (mm)	61	103.2	13.81	73.0–131.7	39	77.4	8.93	62.4–94.7
WUS (mm)	60	30.3	6.36	19.6–44.5	39	21.2	3.98	14.6–28.6
HUS (mm)	60	38.6	5.69	27.9–53.2	39	25.0	3.38	18.1–32.1
WUS/HUS	60	0.78	0.089	0.62–1.00	39	0.85	0.084	0.65–1.03
WAPT (mm)	51	36.2	5.75	24.4–51.5	37	29.2	3.90	20.6–36.2
HAPT (mm)	53	35.4	4.88	24.6–48.1	38	27.8	3.22	21.0–32.8
WAPT/HAPT	48	1.00	0.078	0.84–1.18	37	1.04	0.071	0.89–1.19
UD (mm)	54	7.8	1.93	4.0–12.9	38	7.9	1.25	5.0–10.6
UD/LMAX	54	0.08	0.013	0.05–0.11	38	0.10	0.015	0.07–0.14
A (°)	57	42.9	6.52	30.0–58.0				

[a] Abbreviations: see table 1 and figure 9.

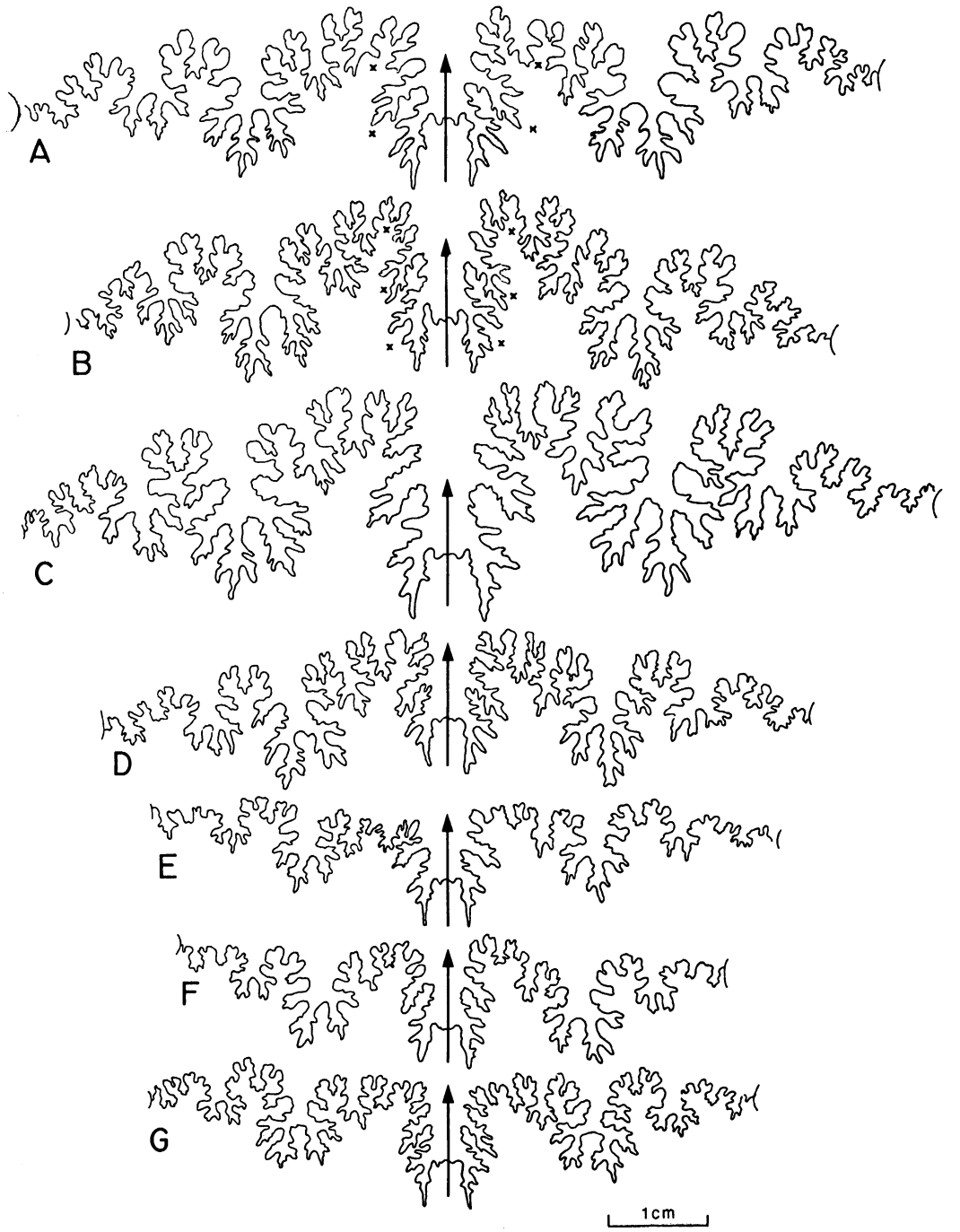

Fig. 113. Sutures of *Jeletzkytes spedeni,* n. sp., macroconchs and microconchs. **A.** Fourth from last suture of an adult macroconch, YPM 27156, loc. 25, POAZ. **B.** Sixth from last suture of an adult macroconch, YPM 27153, loc. 77, UNAZ. **C.** Seventh from last suture of an adult macroconch, YPM 27151, loc. 25, LGAZ. **D.** Fifth from last suture of an adult macroconch, YPM 27152, loc. 237, LNAZ. **E.** Third from last suture of an adult microconch, USNM 468858, loc. 21814, LGAZ and POAZ undifferentiated. **F.** Fourth from last suture of allotype, an adult microconch, YPM 23710, loc. 115, LGAZ. **G.** Fourth from last suture of an adult microconch, YPM 27091, loc. 145, LNAZ.

chamber. Ribs become finer and more closely spaced on the anterior shaft and hook, with approximately 7–14 ventral ribs/cm.

Ventrolateral tubercles are largest on the shaft of the body chamber where they are clavate in form and flare outward slightly (figs. 93, 94, 99). They diminish in size, and usually lose their clavate form, orad onto the hook and apicad onto the phragmocone. Spacing between tubercles on the shaft varies from about 0.5 to 1.5 cm. Umbilical bullae may develop into conical tubercles on specimens with coarser ornament. The umbilical bullae or tubercles vary greatly in strength, and may be entirely absent or prominent throughout the exposed shell.

Flank tubercles appear in two positions on the shell. They commonly occur on the hook where they consist of a scattering of bullae on the fine ribs (fig. 94D). In more coarsely ornamented usually larger specimens, flank tubercles also occur on the phragmocone, where they appear as bullate to nodose swellings on broad flat ribs that arise either as primaries or secondaries; these ribs are rather evenly spaced and are separated by several finer, nontuberculate ribs (fig. 98A). The tubercles on the phragmocone are spirally aligned and appear as rows on the flanks. Two to four rows appear on our specimens, in addition to the row of ventrolateral tubercles and the row that develops into the umbilical bullae on the body chamber, which usually represents the second row from the umbilicus on the phragmocone in specimens with three or four flank rows. The number of flank rows on a specimen usually reaches its maximum on the anterior half of the exposed phragmocone, after which the tubercles usually fade out rather abruptly on the posterior body chamber (fig. 99B); less commonly a single row may persist through to the aperture (fig. 101B).

A sample of 76 macroconch specimens arranged according to form and ornament, clusters into three major groups: the compressed and rotund end-forms previously noted and an intermediate form. Brief description of these forms will serve to illustrate the range of variation. Of the 76 specimens, 32 clearly fall within the intermediate group, which we identify as the typical form because it is the most common, includes the holotype, and is morphologically intermediate between the end-members.

The typical form of *J. spedeni* (fig. 100B) ranges in size from 94.5 to 116.2 mm (N = 24). The shell is stout with convex flanks and the aperture is quadrate or rounded to slightly depressed. The exposed phragmocone has closely approximated, fine ribs, strong ventrolateral tubercles, some umbilical bullae, but no flank tubercles. The body chamber has strong ventrolateral tubercles, usually conspicuous subumbilical bullae, and a scattering of bullae on the flanks of the hook and possibly on the anterior end of the shaft. In variants approaching the larger, rotund form, tuberculation on the phragmocone begins with the appearance of small bullae on the flank ribs; additional tubercles may also appear near the ventrolateral row on the flanks of the body chamber. Variants approaching the compressed form show an increase in the height of the exposed phragmocone as well as an overall decrease in the width of the shell.

The rotund form of *J. spedeni* (figs. 100A, 101) ranges in size from 103.6 to 131.7 mm (N = 15). The shell is conspicuously larger and stouter than the typical form and the aperture is usually broader than high. The exposed phragmocone usually has broad tuberculate ribs, which may or may not be separated by a few finer ribs, and which may extend onto the flanks of the posterior body chamber for varying distances. Rounded tubercles and/or bullae are also present on the flanks of the hook; rarely, a row of tubercles on the lower or middle portions of the flanks will extend across the entire body chamber (fig. 101).

The compressed form of *J. spedeni* (figs. 100C; 93C, D) ranges in size from 73.0 to 108.0 mm (N = 12). Flanks are slightly convex to nearly flat and the venter is narrower than in the other two forms although still slightly rounded. The aperture is higher than wide. Ornamentation is weak in that flank bullae on the hook are few or entirely absent, and umbilical bullae are inconspicuous or barely discernible. The ventrolaterals, however, consistently cover the exposed whorls.

The stratigraphic distribution of the three shell forms among the assemblage zones of the Trail City Member shows that in both

LNAZ and UNAZ the distribution is similar with the typical form most numerous, followed by the compressed form, and then the relatively rare rotund form. In LGAZ, the rotund form dominates and in POAZ, the rotund form is second to the typical form.

The external suture of *J. spedeni* macroconchs is typically scaphitid and essentially like those of *J. criptonodosus* as well as those of co-occurring species of *Hoploscaphites* (fig. 113A–D). The ventral lobe is somewhat broader than the lateral lobe in most specimens. The lateral lobe is slightly asymmetric, due to the relative enlargement of its inner branch, and is consistently bifid. The first auxilliary lobe is about half the size of the lateral lobe and may be bifid or trifid. The degree of incision of the suture is greater than that in *J. criptonodosus.*

The ventral muscle-attachment area in *J. spedeni* is round to teardrop shaped with its blunt end foward.

MICROCONCH DESCRIPTION: LMAX averages 77.4 mm, which is significantly lower than that in macroconchs (table 13). Macroconchs and microconchs overlap in size between 70 and 95 mm, which represents approximately one-third of their total combined range (fig. 112). The ratio of the size of the largest microconch to that of the smallest microconch is 1.52.

Shell coiling is slightly evolute with a broad umbilicus. The phragmocone and body chamber are each approximately 0.5 whorls in angular length. The shell increases gradually in size reaching its maximum height and width at the anterior end of the shaft, decreasing only very slightly through the hook to the aperture. The ratios of whorl width to whorl height at the ultimate septum and at the aperture average 0.85 and 1.04, respectively, which are significantly higher than the averages of the corresponding ratios in macroconchs. Larger microconchs tend to have slightly more depressed whorl sections than smaller microconchs. The body chamber is nearly quadrate in whorl section, tapering slightly to the venter; the aperture is quadrate or slightly compressed to depressed. The shaft of the body chamber is relatively long and arcuate. The reflexed hook is separated from the phragmocone by a small gap, which is crossed by the dorsal projection. The umbilical diameter averages 7.9 mm, which is similar to that in macroconchs (7.8 mm). The ratio of umbilical diameter to shell diameter averages 0.10, which is significantly higher than that in macroconchs.

The umbilical shoulder is broad, outwardly sloping, and bordered by strong umbilical tubercles or bullae. Strong ventrolateral tubercles are present on the exposed shell and on the inner whorls. The generally flat flanks of the body chamber converge slightly toward the ventrolateral tubercles. A single row of tubercles, or bullae, characteristically occurs about mid-flank on the phragmocone and body chamber. More coarsely ornamented specimens may show as many as three rows of flank tubercles on the phragmocone but, except for a few scattered tubercles on the flanks, the body chamber bears only ventrolateral, mid-flank, and umbilical shoulder rows of tubercles. Smaller, weakly ornamented specimens may lack all flank tubercles and the umbilicals may only be present on the end of the phragmocone and on the body chamber.

The range of variation in form and ornament in *J. spedeni* microconchs is as great as in macroconchs but clustering into groups is not as well defined. Relatively small, compressed forms with weak ornament are common (fig. 105A–C). These include specimens with only ventrolateral and umbilical tubercles as well as more ornate specimens with a mid-flank row of tubercles on the body chamber and part of the phragmocone (fig. 108A–D). One exceptional variant is a large, strongly compressed specimen with a few weak rows of flank tubercles on the exposed phragmocone and several subdued rows of flank tubercles on the body chamber in addition to a double row of umbilical tubercles (fig. 107D, E). The compressed form and small, abundant tubercles of this specimen are suggestive of the succeeding species *J. nebrascensis.* Still another variant of the smaller, more weakly ornamented form is quite stout and has a thin-ribbed phragmocone with small ventrolaterals on about every other rib (fig. 105D, F).

The most common form, found in over half of our specimens, has a quadrate to slightly depressed aperture, a body chamber cross section with flat flanks tapering slightly

to the venter, a mid-flank row of tubercles on the body chamber and part of the phragmocone, and umbilical tubercles or bullae, which first appear at the end of the phragmocone (fig. 104A–D). These typical forms grade into larger, more robust forms, some with even greater ornament on the phragmocone, and a broader body chamber, which is quadrate in cross section over most of its length and terminates in a depressed aperture (figs. 107A–C, 111A–D). These extreme forms are rare and cannot be easily distinguished on morphological grounds from larger than usual typical forms with coarser ornament.

Not only does the microconch variation series closely parallel that of the macroconch but the strong variation in rib spacing found in macroconchs is also evident in microconchs (figs. 103E, 105D–F), as is the presence of finer ribbing on the hook, and the adoral projection of ventral ribs and the ventral lip of the aperture.

The suture of microconchs is like that of macroconchs except it is more compact because of the smaller size of the shell. The ventral lobe remains slightly larger than the lateral lobe (fig. 113E–G).

The ventral muscle-attachment area in microconchs is narrower and more elongate than that in macroconchs but shows the same tapering apicad to a point just within the ventral lobe of the ultimate septum.

ONTOGENY: Dorsoventral, mostly intercostal cross sections through an adult macroconch and an adult microconch are illustrated in figure 114. The postembryonic growth of whorl width is slightly negatively allometric (slopes range from 0.8995 to 1.0133; fig. 115) whereas that of whorl height is slightly positively allometric (slopes range from 1.0859 to 1.1523; fig. 116). At comparable shell diameters, the values of whorl width and whorl height in macroconchs are approximately the same as those in microconchs. The shell whorls up to about 5 mm diameter are depressed with the ratio of whorl width to height ranging from 1.00 to 2.0. The whorls become increasingly more compressed during ontogeny with the ratio of whorl width to height reaching a minimum near the base of the mature body chamber.

The growth of umbilical diameter is approximately isometric (fig. 117). The umbilical diameter is more or less the same in both dimorphs until approximately one whorl before the base of the mature body chamber where it begins to increase more slowly or not at all in macroconchs but continues to increase at the same rate in microconchs. The ratio of umbilical diameter to shell diameter decreases through most of postembryonic growth with the rate of decrease accelerating after about 5 mm shell diameter, reaching a minimum value near the base of the mature body chamber.

The variation in coarseness of ornament in adults of *J. spedeni* is also apparent in ontogeny (fig. 118). The more coarsely ornamented forms of both dimorphs are described first. Fairly prominent primaries and secondaries appear at approximately 4 mm shell diameter. These ribs remain coarse throughout growth. Primaries are rectiradiate to slightly prorsiradiate and secondaries originate near the ventral margin. All ribs cross the venter with a slight forward projection. The ratio of the number of dorsal to ventral ribs ranges from 1:2 to 1:3 up to the point of exposure. Whorl flanks are initially convex. Ventrolateral tubercles appear on every rib at approximately 15 mm shell diameter (approximately 1.0 whorl before the point of exposure). Flank tubercles appear soon thereafter with a row just dorsal of the ventrolaterals. Secondaries begin to originate dorsal of mid-flank; some specimens show a bundling pattern of secondaries branching from a single row of tubercles. A maximum of four rows of flank tubercles and one row of umbilical tubercles or bullae may eventually develop on the exposed phragmocone. These tubercles appear sporadically on broad, straight primaries as well as on stronger secondaries. Tubercles may die out at the end of the phragmocone but generally some continue onto the body chamber. Ventrolateral tubercles may occur on every rib but more commonly occur at the juncture of two or three flank ribs. Two ventral ribs loop between pairs of ventrolaterals on either side of the venter and show a slight forward projection. The ratio of the number of dorsal to ventral ribs on the exposed phragmocone ranges from 1:4 to 1:6.

In more finely ornamented forms, the ornamentation is initially weak with rectira-

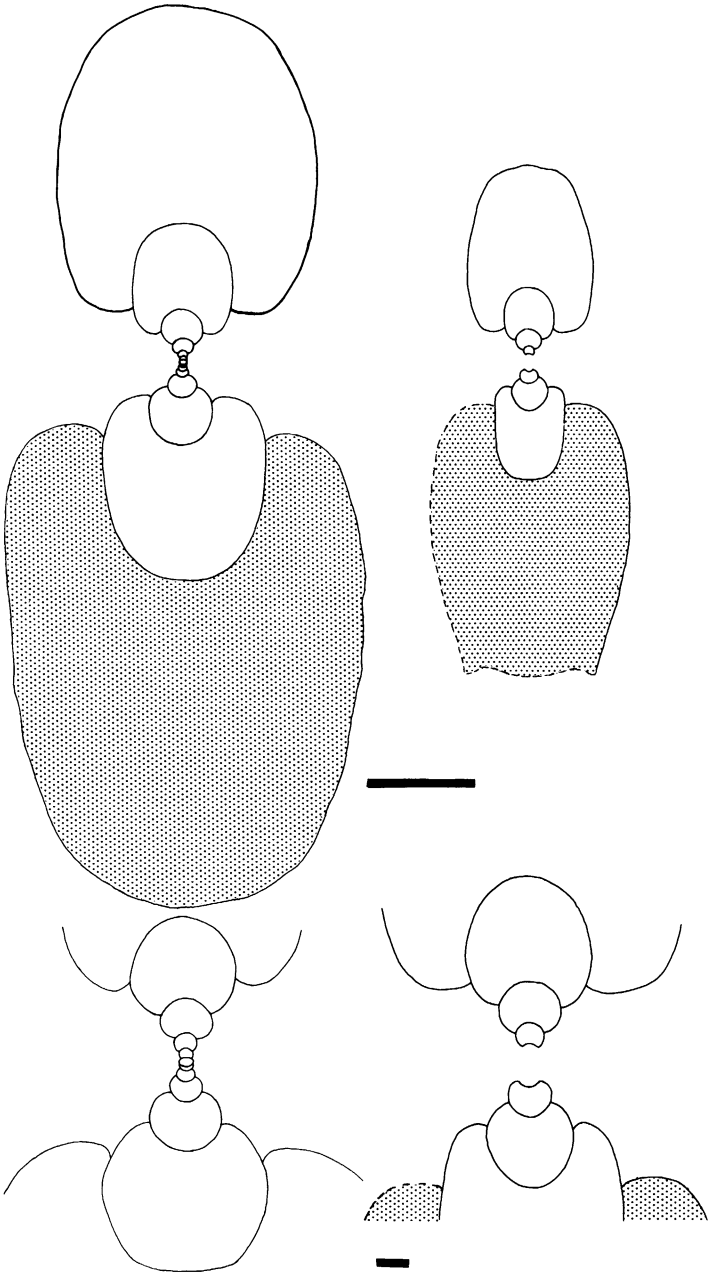

Fig. 114. Dorsoventral, mostly intercostal cross sections through adult dimorphs of *Jeletzkytes spedeni,* n. sp. **Left.** Macroconch, YPM 23062, loc. 86, LGAZ. **Right.** Microconch, YPM 32061, loc. 17, UNAZ. Shaded area demarcates mature body chamber. Upper scale bar = 1 cm; lower scale bar = 1 mm.

diate to prorsiradiate primaries. In general, ventral ribs show a more pronounced forward projection than do those on more coarsely ornamented forms. The ratio of the number of dorsal to ventral ribs is 1:2, which remains more or less constant until the point of exposure. Ribs become more prominent during ontogeny but never as prominent as

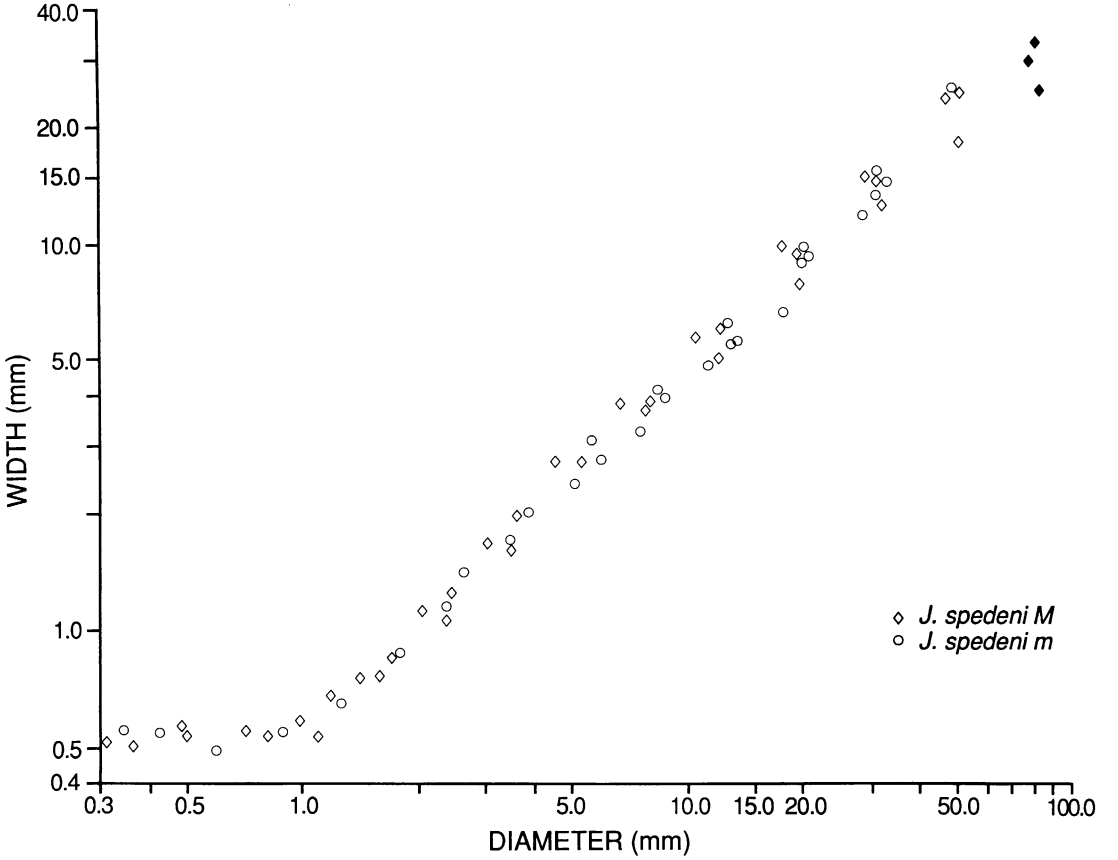

Fig. 115. Plot of whorl width versus shell diameter through the ontogeny of seven adults (three macroconchs and four microconchs) of *Jeletzkytes spedeni,* n. sp. Black symbols indicate measurements near the base of or in the mature body chamber. Measurements listed in Appendix II.

those on more coarsely ornamented forms. Secondaries arise initially near the ventral margin but may later also originate dorsal of mid-flank. Ventrolateral tubercles appear on every rib at approximately 20 mm shell diameter (approximately 1.0 whorl before the point of exposure); later they may appear at the junction of two flank ribs. Primaries and secondaries are fairly prominent on the exposed phragmocone but are less conspicuous and thinner than those on more coarsely ornamented forms. Ventral ribs are thin and show a weak forward projection. Two ventral ribs join pairs of ventrolateral tubercles on either side of the venter. There are no flank tubercles but the primaries develop umbilical bullae toward the end of the phragmocone, which commonly persist onto the body chamber. The ratio of the number of dorsal to ventral ribs ranges from 1:4 to 1:7 on the exposed phragmocone.

Thirteen macroconchs and ten microconchs of *J. spedeni* were examined for evidence of septal approximation. Interseptal distances of as many as the last six chambers were measured. The number of chambers over which septal approximation occurs varies broadly in both dimorphs (table 14): over as many as the last five chambers or over as few as the last one or two chambers. Based on this sample, the patterns of septal approximation are similar in both dimorphs. In general, the decrease in septal spacing is monotonic (fig. 119). The ratio, expressed as a percentage, of the interseptal distance of the last chamber to that of the last "normal" chamber averages 55 percent in macroconchs and 53 percent in microconchs, indicating an

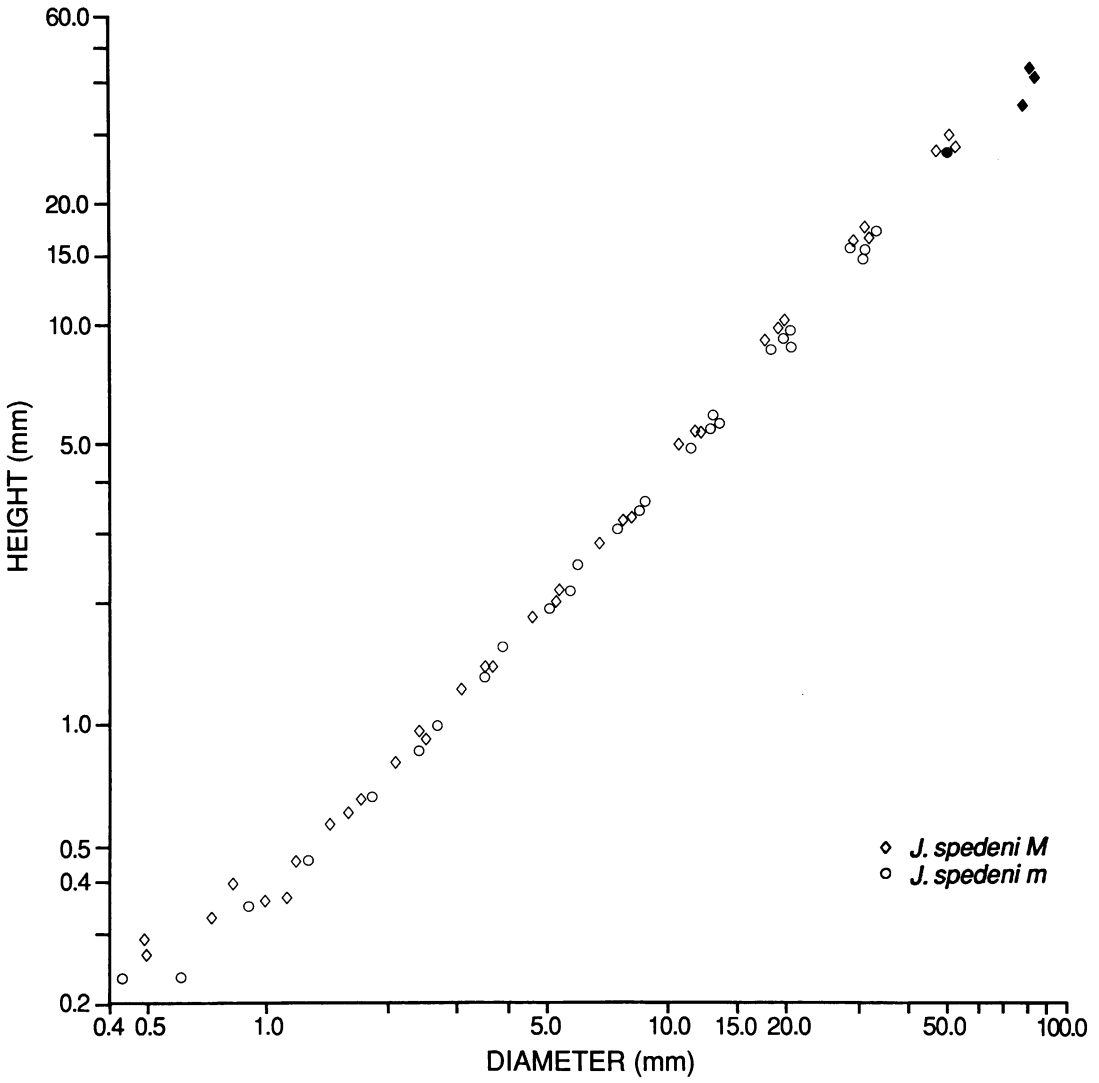

Fig. 116. Plot of whorl height versus shell diameter through the ontogeny of seven adults (three macroconchs and four microconchs) of *Jeletzkytes spedeni*, n. sp. Black symbols indicate measurements near the base of or in the mature body chamber. Measurements listed in Appendix II.

average reduction in septal spacing of about one-half in both dimorphs.

DISCUSSION: The highly variable macroconchs of *J. spedeni* show affinities with those of *J. cryptonodosus* Riccardi and *J. plenus* (Meek), both of which have incipient flank tuberculation on parts of the exposed phragmocone and both of whose general body forms are within the range of variation of that of *J. spedeni* macroconchs. There are also similar undescribed large scaphites in the strata intervening between *J. spedeni* and *J. plenus* and *J. cryptonodosus*. These scaphites occur in the *Baculites grandis* Zone in the Lance Creek–Red Bird area of Wyoming, in the *B. clinolobatus* Zone in the Mobridge Member of the Pierre Shale in South Dakota, and in the top of the Mobridge Member in association with *Hoploscaphites melloi*, n. sp. (p. 112).

In the Fox Hills Formation, *J. spedeni* approaches *H. nicolletii* with respect to two features, the adoral projection of the ventral ribs and the overall pattern of ribbing on the body

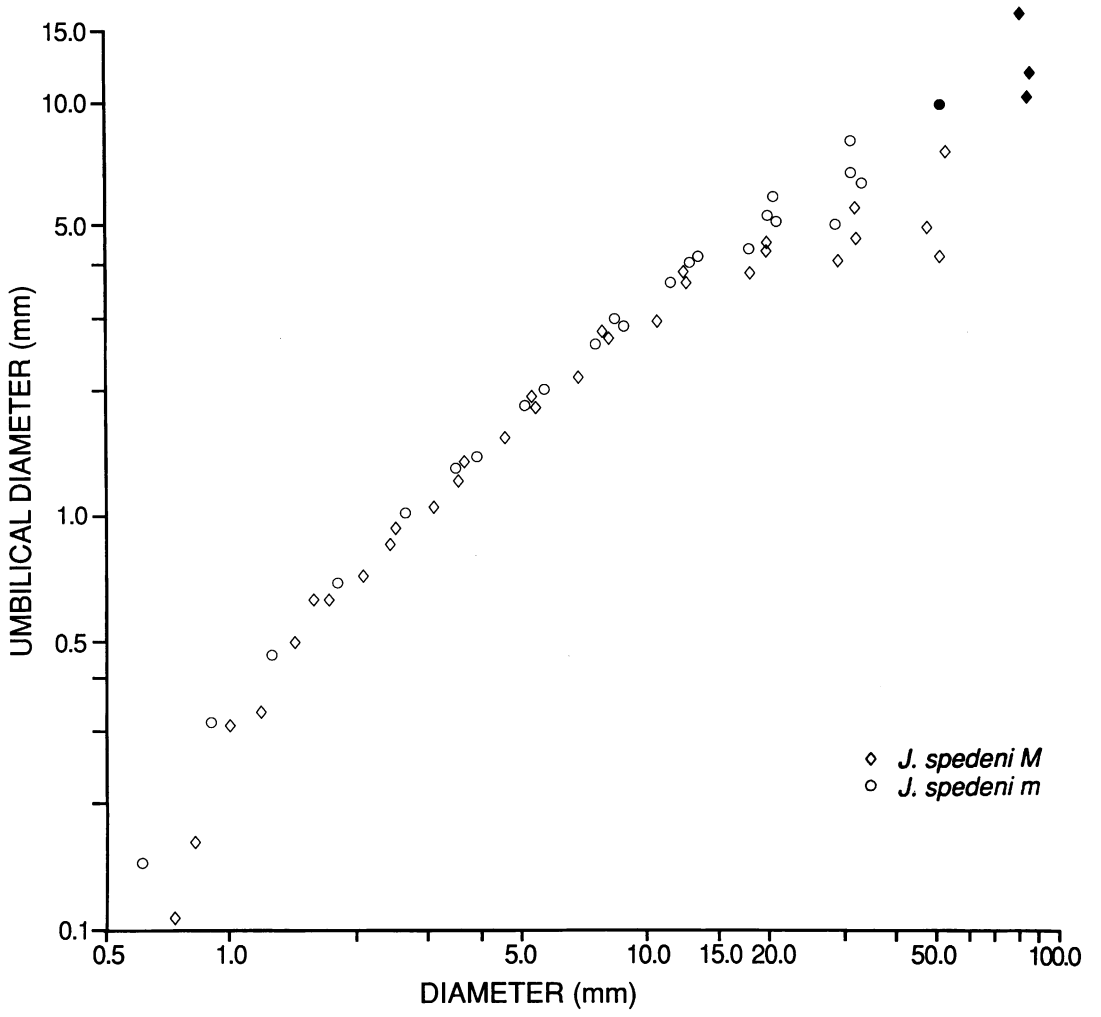

Fig. 117. Plot of umbilical diameter versus shell diameter through the ontogeny of seven adults (three macroconchs and four microconchs) of *Jeletzkytes spedeni,* n. sp. Black symbols indicate measurements near the base of or in the mature body chamber. Measurements listed in Appendix II.

chamber. The adoral projection of the ventral ribs in *J. spedeni* is a conspicuous feature but not as pronounced as that in *H. nicolletii.* This is probably because of the much greater shell compression in *H. nicolletii* which tends to accentuate the projection in this species. The fining-forward rib pattern on the body chamber of *J. spedeni* is similar to that on the body chamber of *H. nicolletii.* However, the ribbing on the phragmocone is much more variable in *J. spedeni* than in *H. nicolletii.*

Stephenson (1941: pl. 90, fig. 9) described *Scaphites yorkensis,* a microconch, from a single incomplete and distorted external mold found in the Kemp Clay of Texas. This specimen superficially resembles *J. spedeni* microconchs in its shell proportions, strong ventrolateral tubercles that extend to the aperture, and the presence on the phragmocone of two rows of flank tubercles between the ventrolaterals and umbilicals. *Scaphites yorkensis* falls at the lowest end of the size range of *J. spedeni* and differs from the latter species in that fine, closely approximated ribs appear to extend throughout the body chamber and lack any evidence of a forward projection on the venter. *S. yorkensis* also lacks the mid-flank row of tubercles usually present on body chambers of *J. spedeni* microconchs.

From the Maastrichtian Oyster-Ammo-

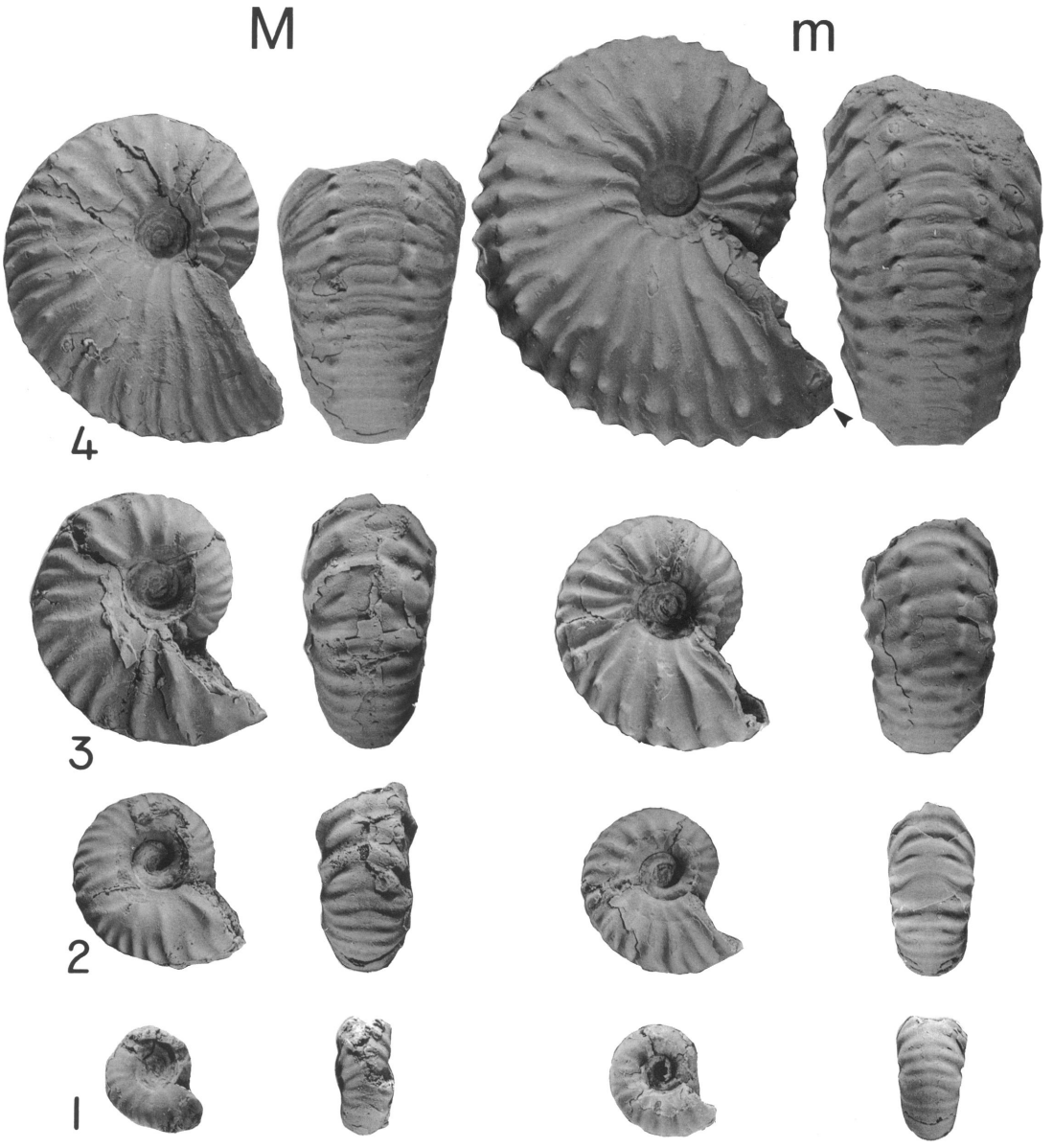

Fig. 118. Dissections of adult dimorphs (macroconch, YPM 32593, loc. 3, LGAZ, and microconch, YPM 32602, loc. 25, LGAZ and LNAZ undifferentiated) of *Jeletzkytes spedeni,* n. sp., showing four sizes through ontogeny in lateral and ventral view. 1. ×3. 2. ×2. 3. ×2. 4. ×1.5. Arrow indicates base of mature body chamber.

nite Conglomerate of West Greenland, Birkelund (1965: 117–129, pls. 35–45) described *Scaphites (Discoscaphites) angmartussutensis,* a macroconch and *S. (Discoscaphites) waagei,* a microconch, and related them to the large scaphites of the type Fox Hills that we are including in *Jeletzkytes.* As she noted, there are some conspicuous differences as well as similarities. The Greenland forms, while similar in their overall size, are generally much more compressed than the Western Interior *Jeletzkytes,* and also have far fewer tubercles. The two Greenland species are clearly a dimorphic pair and are collectively referred to

TABLE 14
Pattern of Septal Approximation in *J. spedeni*[a]

Di-morph	N	Number of chambers				
		1	2	3	4	5
M	13	1	2	2	4	4
m	10	—	2	2	3	3

[a] This table compares the number of chambers over which septal approximation occurs in a specimen versus the number of specimens within each dimorph. "N" equals the total number of specimens in which septal spacing was measured. Chambers are numbered starting with the last, most recently formed, chamber of the phragmocone (1).

here as *S. (D.) angmartussutensis.* Birkelund's (1965) generic assignment of this species followed that applied to the large Fox Hills scaphites at that time, but it cannot be inferred that she would have included *S. (D.) angmartussutensis* under *Jeletzkytes.* Indeed, she clearly pointed out differences (1965: 123) that she regarded as significant between the Greenland and North American forms, namely, the greater development of flank and ventrolateral tubercles in the North American forms.

On the other hand, the Greenland species is undeniably closer to *Jeletzkytes* than it is to any other scaphite genus. It has the very fine ribbing on the anterior body chamber and the moderate to strong adoral projection of ventral ribs typical of the type Fox Hills species of *Jeletzkytes* (see Birkelund, 1965: pl. 39, fig. 1 and pl. 40, fig. 1). Compressed variants of *J. spedeni* with weakly developed ornament include specimens very similar to some specimens of *S. (D.) angmartussutensis,* indicating some degree of overlap between the two species. A particularly good likeness between microconchs is illustrated on figure 110 where a Greenland microconch (*Scaphites (Discoscaphites) waagei*) from the Oyster-Ammonite Conglomerate is shown with a microconch of *J. spedeni* from the Trail City Member of the type Fox Hills. The holotype of the macroconch *S. (D.) angmartussutensis* (Birkelund, 1965: pls. 39 and 40) is very similar in its proportions, although slightly smaller in size, to *J. spedeni* macroconchs shown on our figure 93C, D. The degree of compression of the shells is nearly

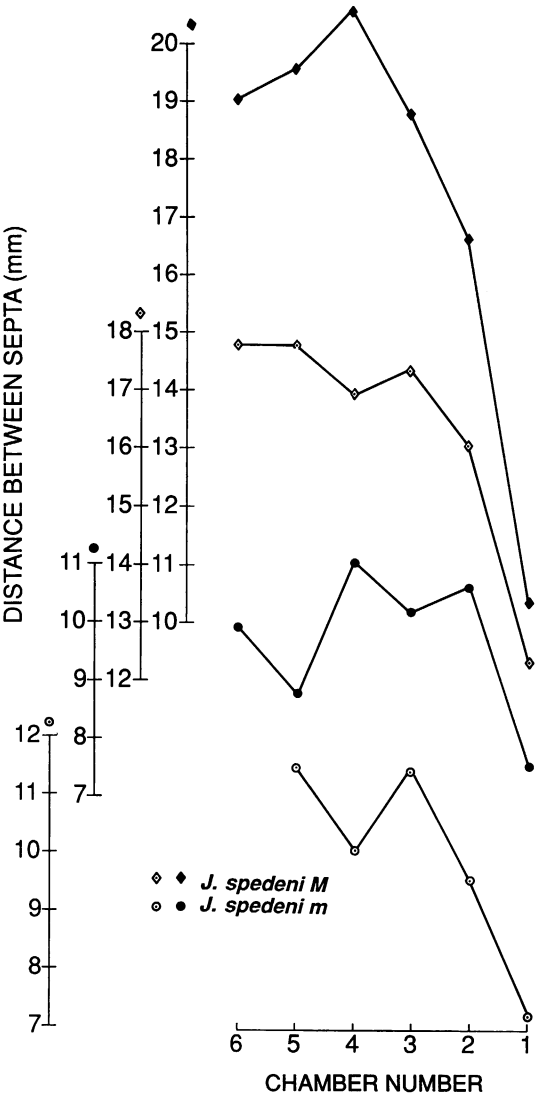

Fig. 119. Distance between septa versus chamber number, counting from the last, most recently formed, chamber of the phragmocone (1), in two macro- and two microconchs of *Jeletzkytes spedeni,* n. sp. The pattern of septal approximation is not significantly different between dimorphs.

identical. The holotype of *S. (D.) angmartussutensis* differs from *J. spedeni* in having a larger umbilicus and longer hook and in totally lacking any ventrolateral or flank tubercles.

The similarity of Birkelund's species from the Oyster-Ammonite Conglomerate to *J. spedeni* appears to be the only possible link

between the West Greenland Maastrichtian ammonites and those of the Western Interior of North America.

Jeletzkytes nebrascensis (Owen, 1852)
Figures 120–140

Macroconch Synonymy:

Ammonites nebrascensis Owen, 1852: 577, pl. 8, fig. 3, pl. 8A, fig. 2.
Scaphites conradi Morton, Meek and Hayden, 1856b: 281.
Scaphites (*Discoscaphites*) *conradi* (Morton), Meek, 1876: 430, pl. 36, fig. 2a, b, e, ?c, d.
Discoscaphites nebrascensis (Owen), Cobban and Reeside, 1952: 1021.
Scaphites (*Discoscaphites*) *nebrascensis* (Owen), Jeletzky, 1960: 30–32, fig. 2.
Discoscaphites nebrascensis (Owen), Waage, 1968: 97, 128, pl. 7, fig. B.
Discoscaphites conradi (Meek), Kennedy and Cobban, 1976: pl. 11, fig. 7.
Discoscaphites conradi (Morton), Kauffman, 1977: pl. 32, fig. 6 (= Meek, 1876, pl. 36, fig. 2b).

Microconch Synonymy:

Ammonites cheyennensis Owen, 1852: 578, pl. 7, fig. 2.
Ammonites (*nebrascensis*?) Owen, 1852: 578, pl. 8, fig. 2.
Ammonites moreauensis Owen, 1852: 579, pl. 8, fig. 7.
Scaphites (*Discoscaphites*) *cheyennensis* (Owen), Meek, 1876: 437, pl. 35, fig. 3a–c.
Discoscaphites cheyennensis (Owen), Reeside, 1927: 28.
Discoscaphites cheyennensis (Owen), Cobban and Reeside, 1952: 1021.
Scaphites (*Discoscaphites*) *cheyennensis* (Owen) Meek, Jeletzky and Waage, 1978: 1121.
Hoploscaphites cheyennensis (Owen), Landman and Waage, 1986: figs. 2, 5A, B, 7B.

DIAGNOSIS: Macroconch compressed, last whorl markedly higher than wide, phragmocone conspicuously tuberculate with strong ventrolateral tubercles and five to seven rows of weaker flank tubercles, which commonly extend onto part or all of body chamber. Microconch variably tuberculate, commonly with double row of umbilical tubercles/bullae.

TYPES: Lectotype, USNM 20242, fig. 120D. Owen (1852: 577, pl. 8, fig. 3, pl. 8A, fig. 2) figured two specimens in illustrating his species *Ammonites nebrascensis*. Both are partial macroconchs lacking all or most of the body chamber, but the ribbing of the mature phragmocone is so distinctive that an entire specimen is not required for identification. The first of Owen's two specimens (ibid., pl. 8, fig. 3) is missing but the second (ibid., pl. 8A, fig. 2) is available and is here chosen as lectotype for Owen's species. The whole specimens of *nebrascensis* we illustrate with it are topotypes in a broad sense (fig. 120). Owen's specimens were collected for him in 1849 by John Evans who crossed the Fox Hills Formation in the heart of the type area on the divide between the Cheyenne and Moreau Rivers and also saw additional *nebrascensis*-bearing strata on the north bluffs of the Moreau (Waage, 1968: 20–21). The locality on the lectotype label is "Fox Hills, Nebraska" indicating that the specimen is probably from the Timber Lake Member of the Fox Hills Formation on the Cheyenne-Moreau divide; the area was part of the Nebraska Territory in 1849.

Allotype, USNM 402, fig. 132B–E, illustrated by Meek (1876: pl. 35, fig. 3). Owen's type of *cheyennensis* (1852: 578, pl. 7, fig. 2) is lost; it was of inner whorls only and was inadequate to represent the form although it was probably a microconch because of its large unbilicus. Owen's "*Ammonites nebrascensis*?" (ibid., p. 578, pl. 8, fig. 2), UC6379, Gurley Collection, is also a microconch (*cheyennensis*) but lacks most of the body chamber. Meek's *cheyennensis* is a complete and well-preserved specimen of the compressed variant of the microconch of *Jeletzkytes nebrascensis*. It comes from the "Fox Hills, Moreau and Cheyenne Rivers, Dakota; from the Fox Hills Group" (Meek, 1876: 441) and is in a general sense a topotype of Owen's specimens which are listed as "Fox Hills, Nebraska" (1852: pls. 7, 8).

OCCURRENCE: Common in the Timber Lake Member of the Fox Hills Formation and its lateral equivalents in the Fox Hills Formation of the Missouri Valley region of north-central South Dakota and adjacent parts of North Dakota. The only record of it to date outside this area is from the Severn Formation of Maryland (see p. 184, fig. 133).

MATERIAL: The total number of adult spec-

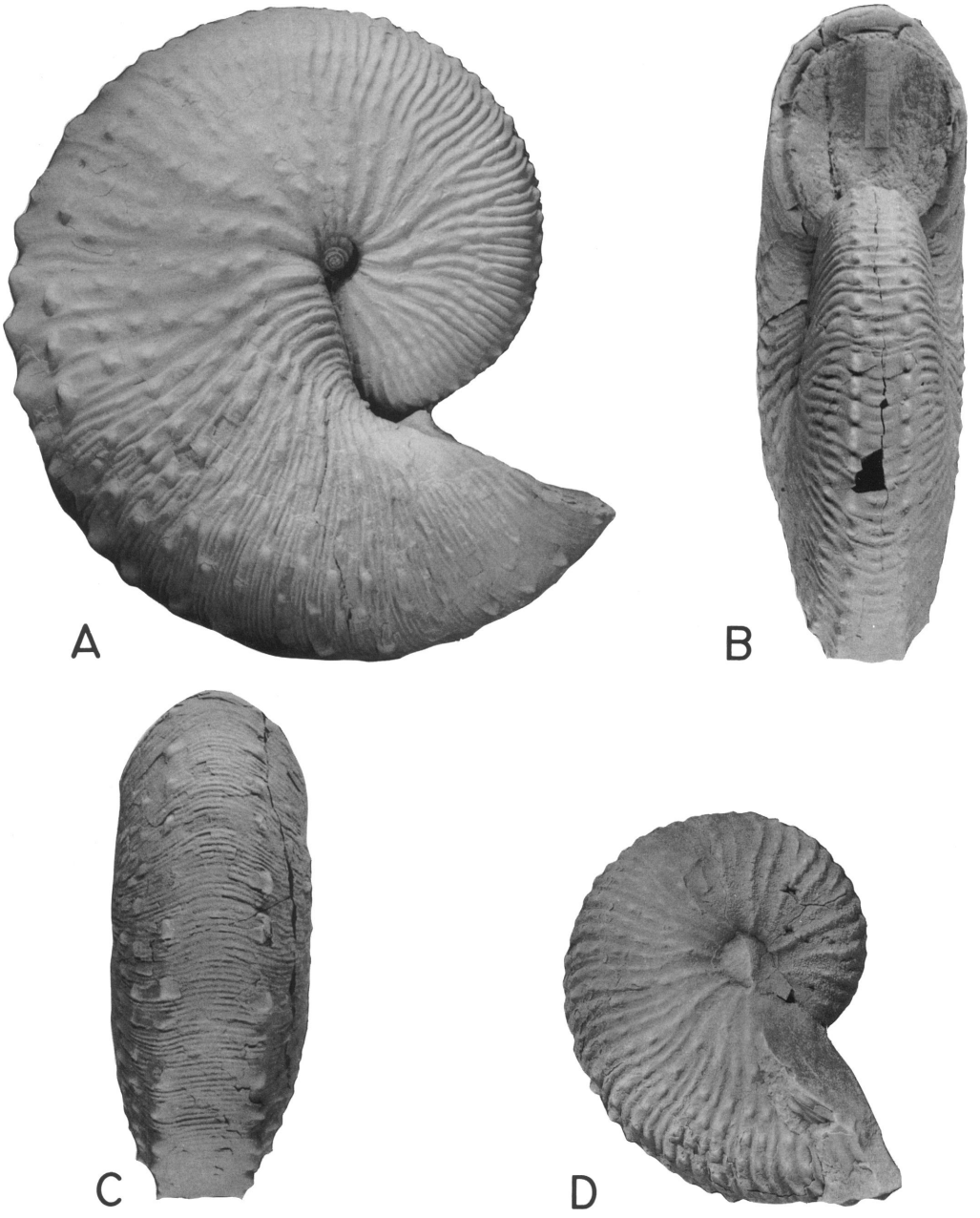

Fig. 120. *Jeletzkytes nebrascensis* (Owen) macroconchs. **A–C.** Relatively small macroconch, YPM 23146, loc. 58, TLM float. **A,** Right lateral; **B,** apertural; **C,** posteroventral. **D.** Lectotype, USNM 20242, Owen's (1852: pl. 8A, fig. 2) *Ammonites nebrascensis,* "Fox Hills, Nebraska."

imens of *Jeletzkytes nebrascensis* in the YPM collections is 180, of which 108 are macroconchs. Of the latter, 37 complete or nearly complete specimens comprise the measured suite and were supplemented by one USNM and three BHI specimens. Of the microconchs, 24 were complete enough for measurement and these were supplemented by one USNM and two BHI specimens.

MACROCONCH DESCRIPTION: Shells are me-

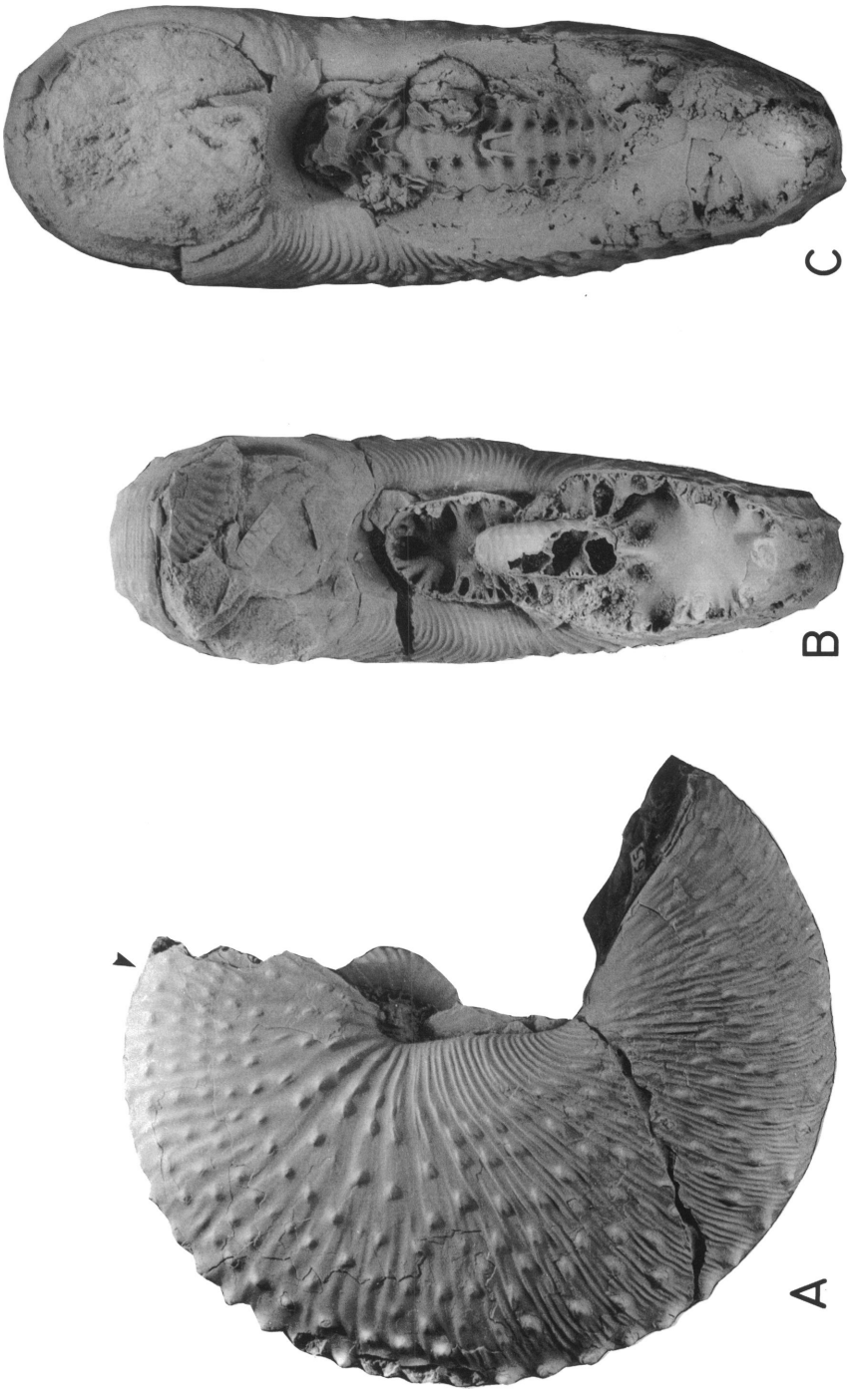

Fig. 121. *Jeletzkytes nebrascensis* (Owen) macroconchs. **A, B**, Partial specimen, YPM 23165, loc. 36, TLM float. **A**, Right lateral; **B**, apertural. **C**, Partial specimen, apertural, YPM 23210, loc. 61, upper Irish Creek lithofacies of TCM; lateral equivalent of TLM.

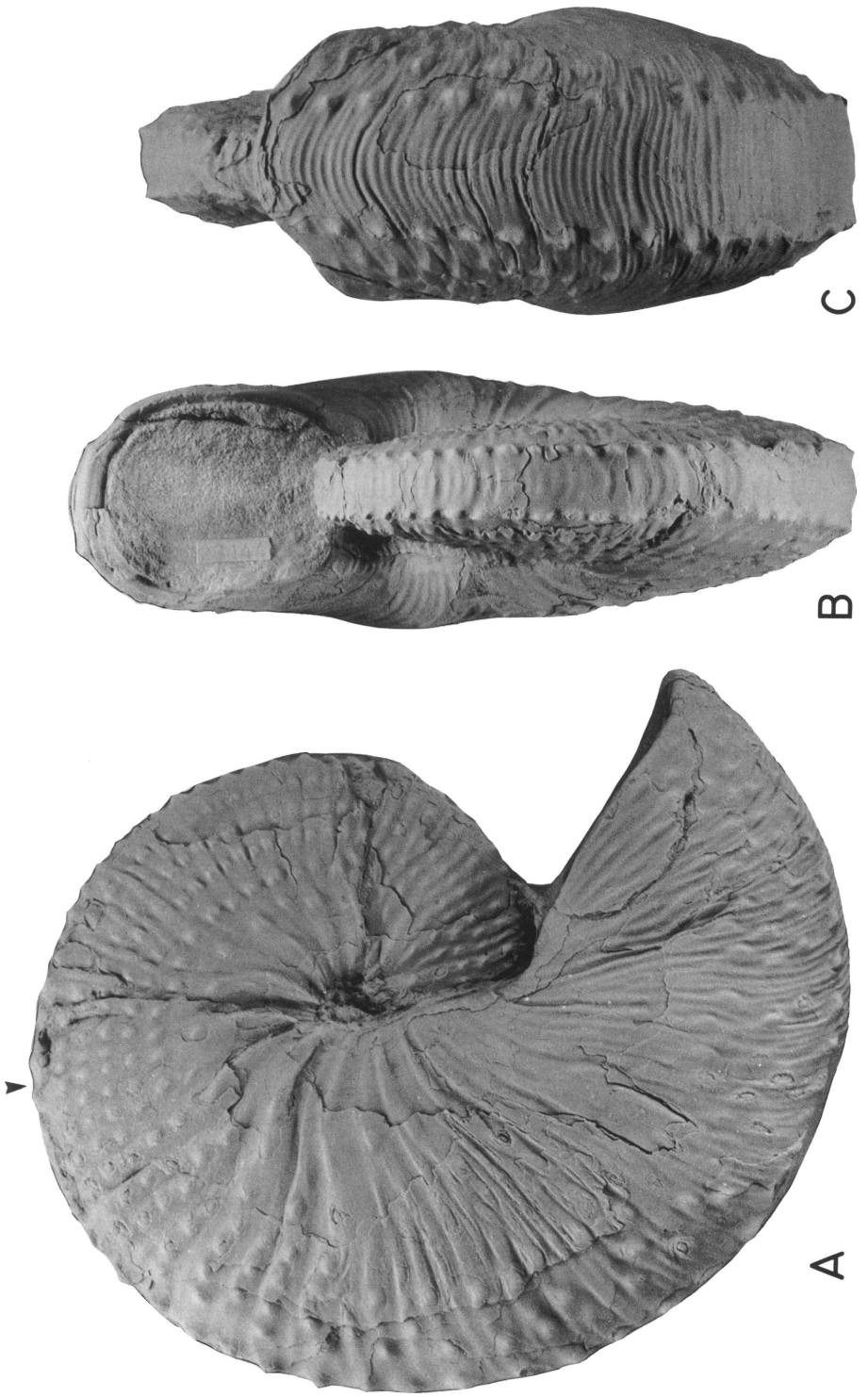

Fig. 122. *Jeletzkytes nebrascensis* (Owen) macroconch. Abrupt reduction in whorl width of terminal hook atypical, YPM 23144, loc. 35, TLM. **A**, Right lateral; **B**, apertural; **C**, ventral hook.

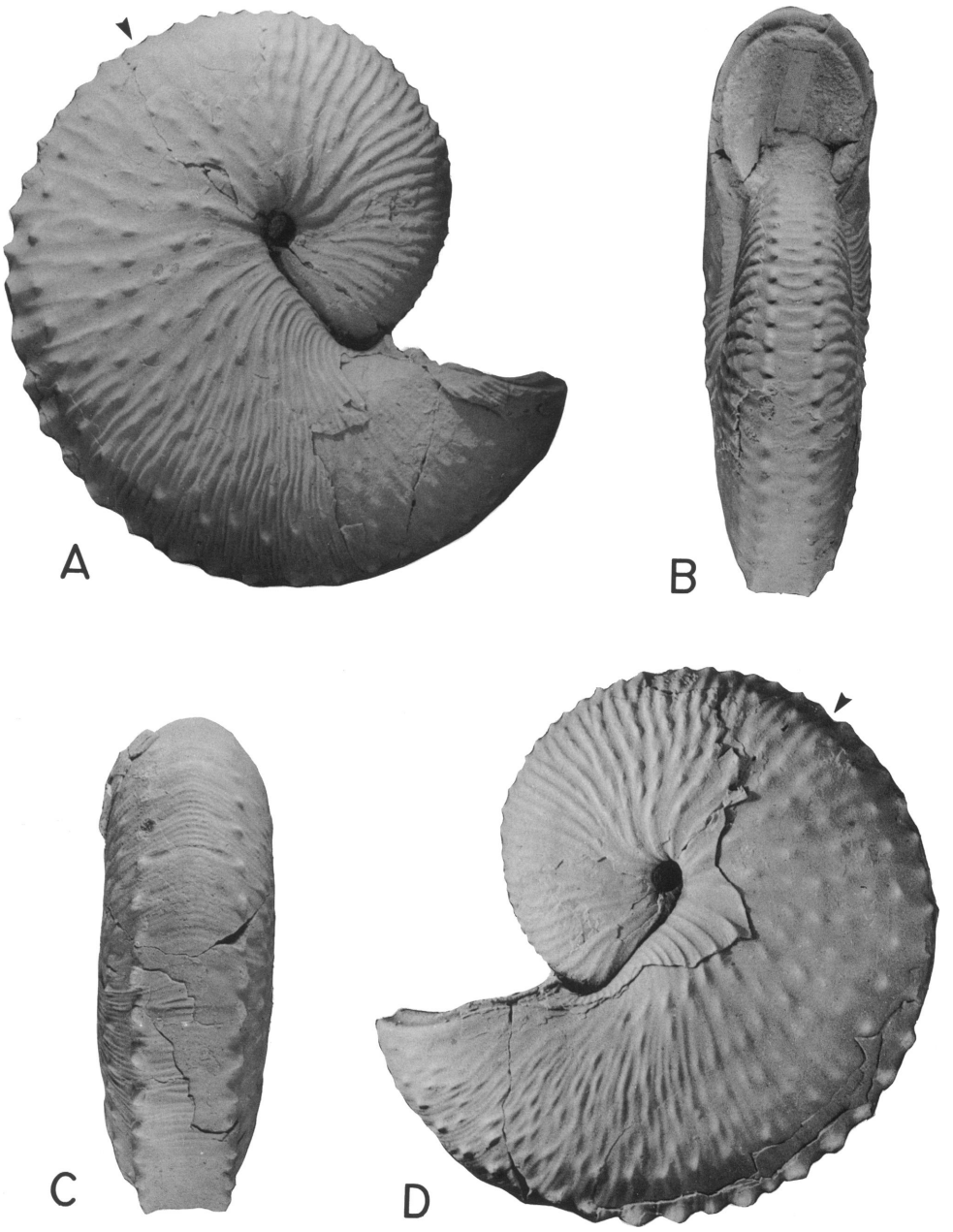

Fig. 123. *Jeletzkytes nebrascensis* (Owen) macroconch. Small specimen, YPM 23145, loc. 37, TLM. **A,** Right lateral; **B,** apertural; **C,** posteroventral; **D,** left lateral.

dium to large, compressed, and tightly coiled with the dorsal part of the aperture against or very close to the phragmocone. The whorl section up to the hook is appreciably higher than wide; the hook tapers to the aperture. The apertural angle averages 48.4° (table 15). The maximum height of the body chamber is at the midpoint of the shaft whereas the maximum width is at the anterior end of the shaft. The umbilical shoulder is straight to slightly arched.

Shells average 115.2 mm in size with three-

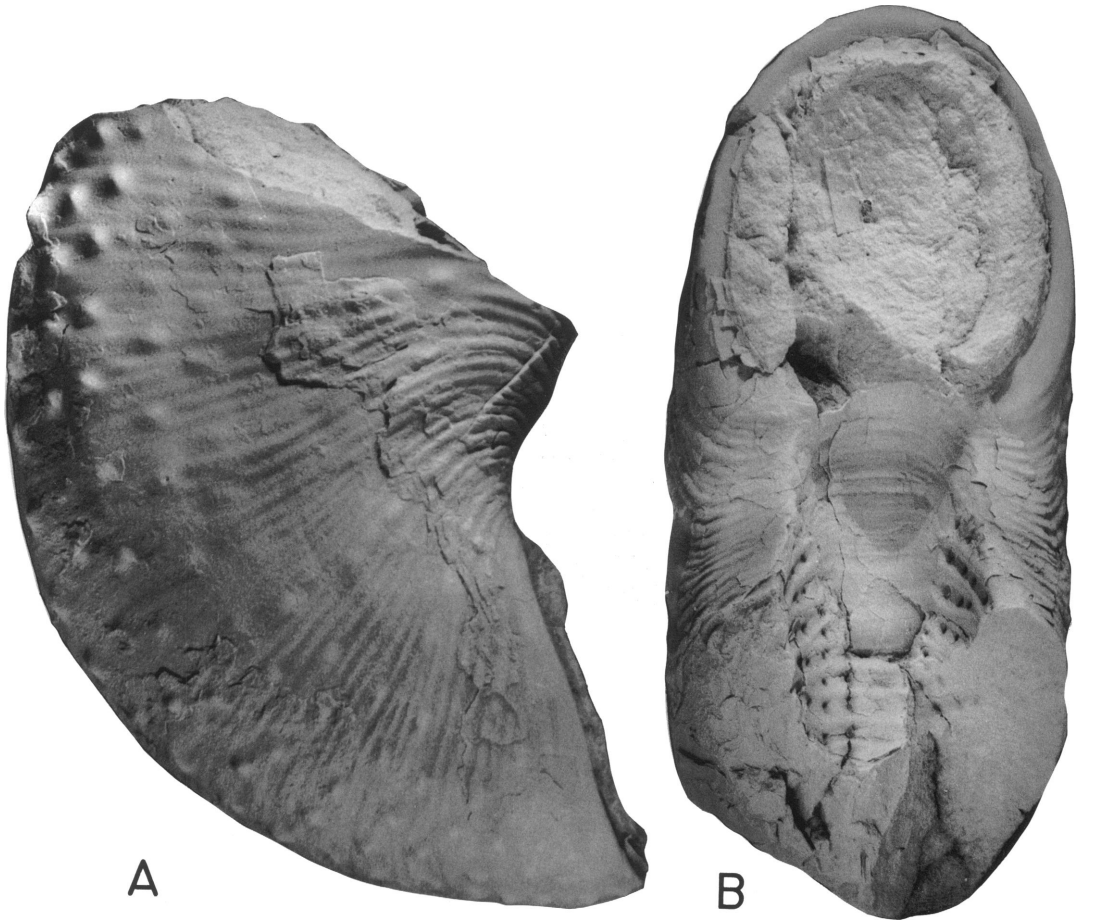

Fig. 124. *Jeletzkytes nebrascensis* (Owen) macroconch. Hook fragment of very large specimen, YPM 23172, loc. 60, TLM. **A,** Right lateral; **B,** apertural.

quarters of them over 100 mm (table 15; fig. 134). The ratio of the size of the largest specimen to that of the smallest is 2.09 (see figs. 123A and 125 for a comparison of size extremes). The shape of the shell is approximately the same in all specimens, regardless of size. The ratio of whorl width to whorl height at the aperture averages 0.91 and is significantly higher than the average of the same ratio at the ultimate septum (0.66). Shell flanks are flat to gently convex, and the venter, bordered by strong ventrolateral tubercles, is narrow and nearly flat to about midshaft after which it broadens forward and is gently rounded. A few specimens are more robust and have quadrate apertures, as wide as, or slightly wider than, high.

The umbilicus appears relatively small in these large specimens, averaging 7.1 mm in diameter; the ratio of umbilical diameter to shell diameter averages 0.06 (table 15). This ratio is approximately the same in all specimens, regardless of size.

Ribbing is dominantly rectiradiate on the exposed phragmocone becoming slightly prorsiradiate on the body chamber. Ribs vary from straight to slightly sinuous and there is a moderate adoral projection of both the ventral ribs and the ventral lip at the aperture. Spacing of the ribs on the venter ranges from 5 to 10/cm on the phragmocone and posterior part of the body chamber and from 7 to 14/cm on the anterior part of the body chamber.

Broad, tuberculate ribs dominate the ex-

Fig. 125. *Jeletzkytes nebrascensis* (Owen) macroconch. Cast of large specimen figured by Meek (1876: pl. 36, fig. 2e) as *Scaphites conradi,* USNM 398, right lateral, Fox Hills Fm., "Fox Hills, Long Lake, . . . Dakota."

posed phragmocone of most large specimens of *J. nebrascensis* (figs. 125, 128C). All ribs on the phragmocone have tubercles and/or bullae; even rare thin ribs show incipient bullae. Ribs increase by branching and intercalation. On the venter, pairs of simple ribs are looped between ventrolateral tubercles. On phragmocones of smaller specimens, under 100 mm in size, ribbing is commonly finer and more closely approximated with only a few broad tuberculate ribs and incipient bullae near the base of the body chamber (fig. 123).

Body chamber ornament is commonly

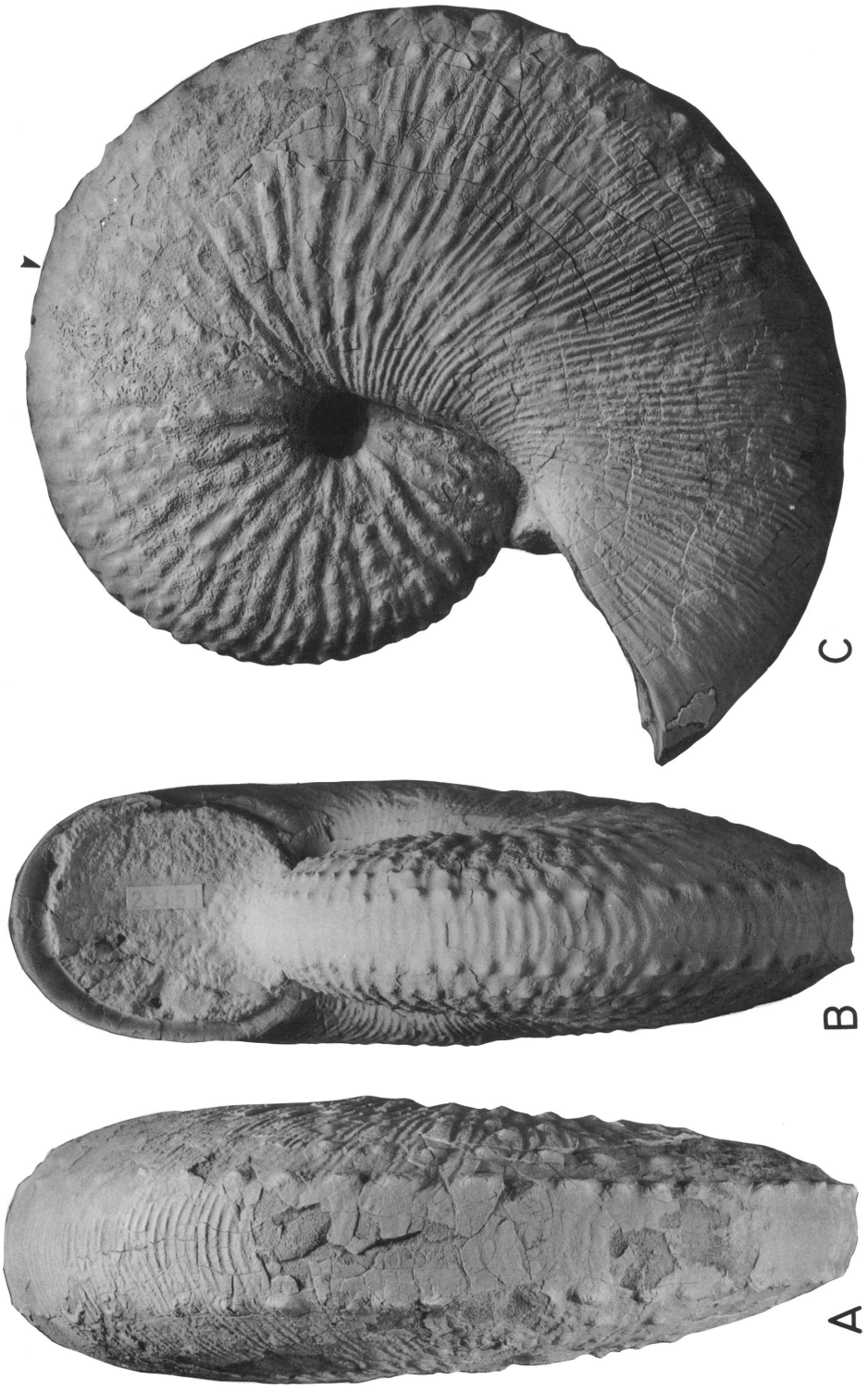

Fig. 126. *Jeletzkytes nebrascensis* (Owen) macroconch. Specimen with weak ornament on anterior body chamber, YPM 23151, loc. 158, TLM. **A**, Posterior; **B**, apertural; **C**, left lateral.

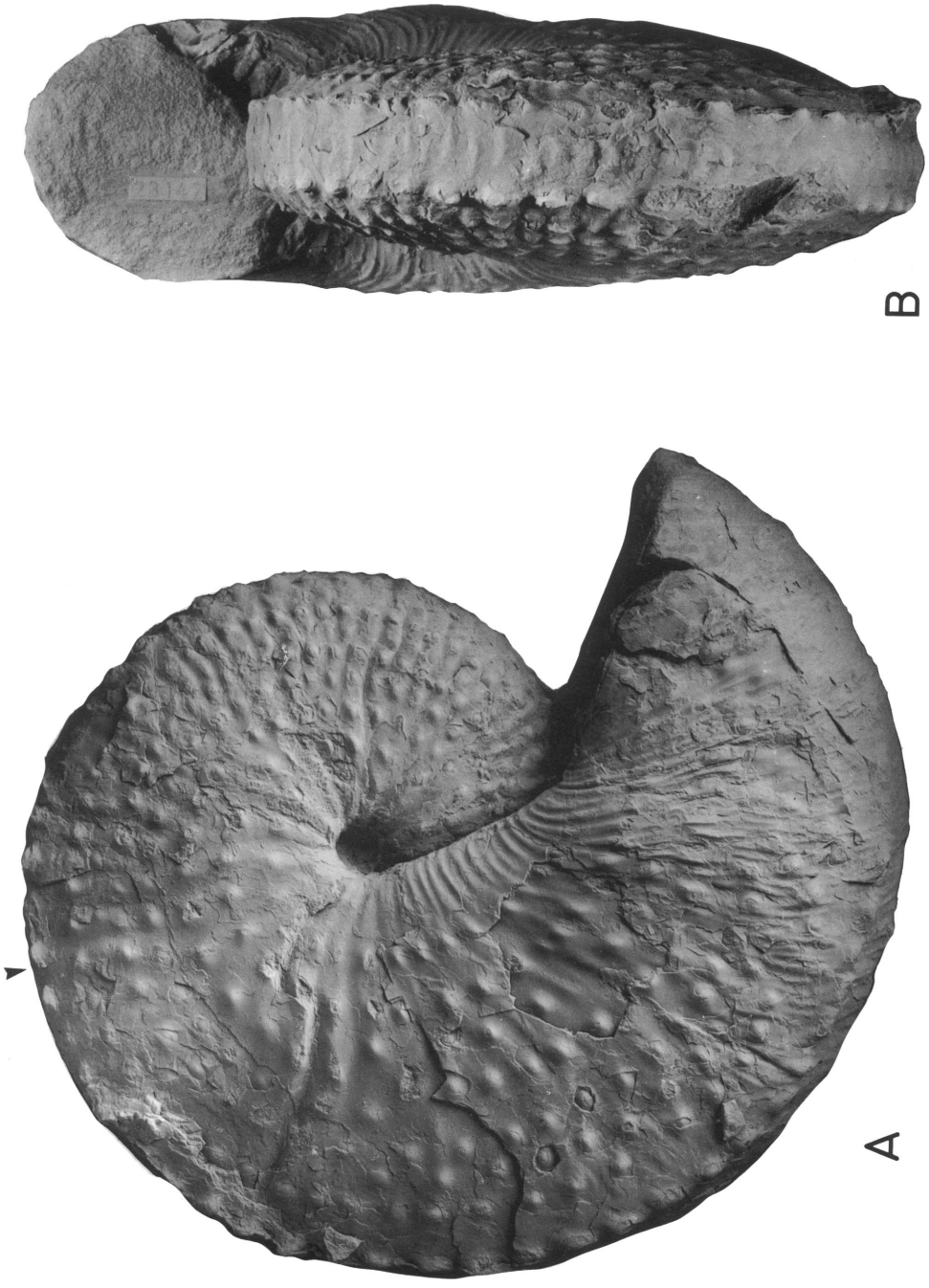

Fig. 127. *Jeletzkytes nebrascensis* (Owen) macroconch. Specimen with tubercles extending to aperture, YPM 23147, loc. 37, TLM. **A,** Right lateral; **B,** apertural.

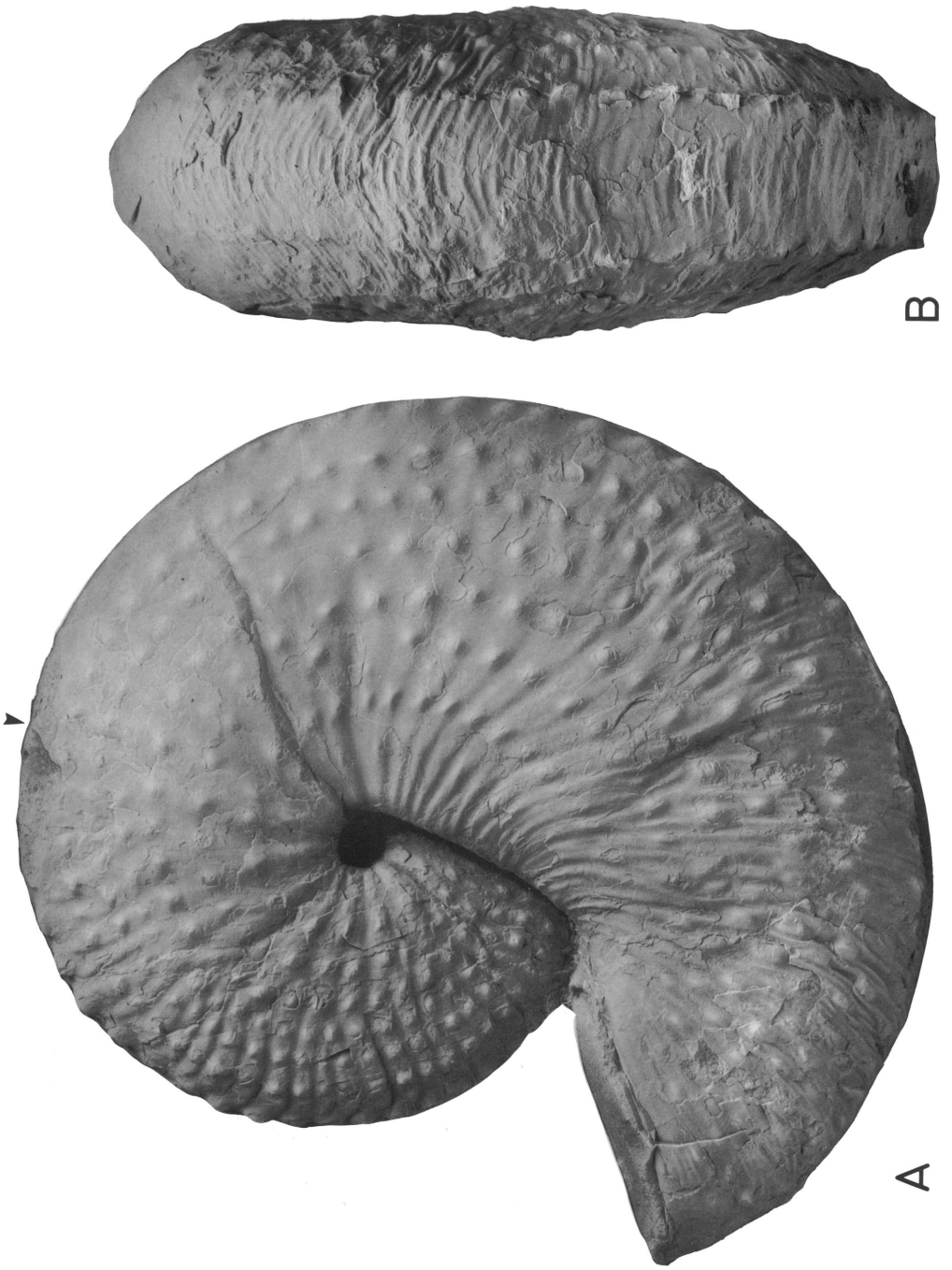

Fig. 128. *Jeletzkytes nebrascensis* (Owen) macroconch. YPM 23147 (cont.). **A**, left lateral; **B**, posteroventral.

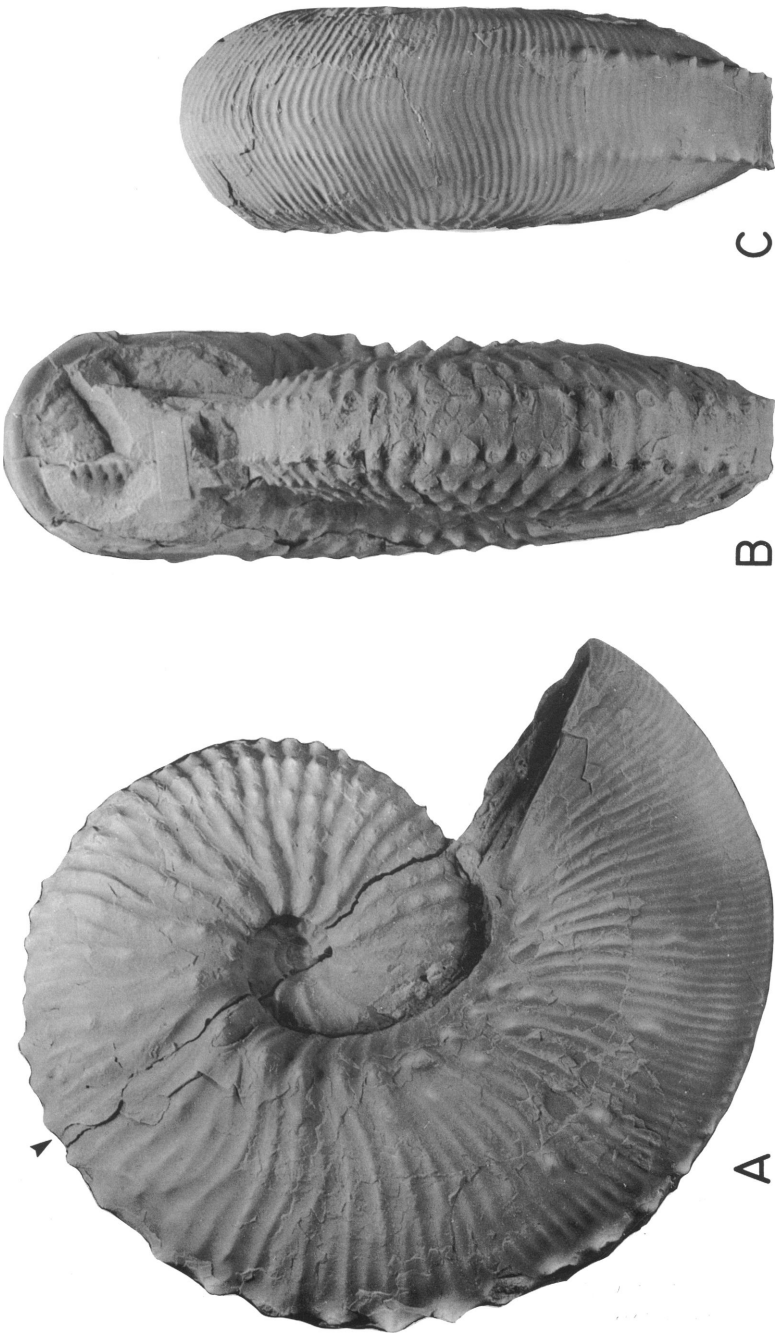

Fig. 129. *Jeletzkytes nebrascensis* (Owen) microconch. Large specimen, YPM 23687, loc. 36, TLM. **A,** Right lateral; **B,** apertural; **C,** posteroventral.

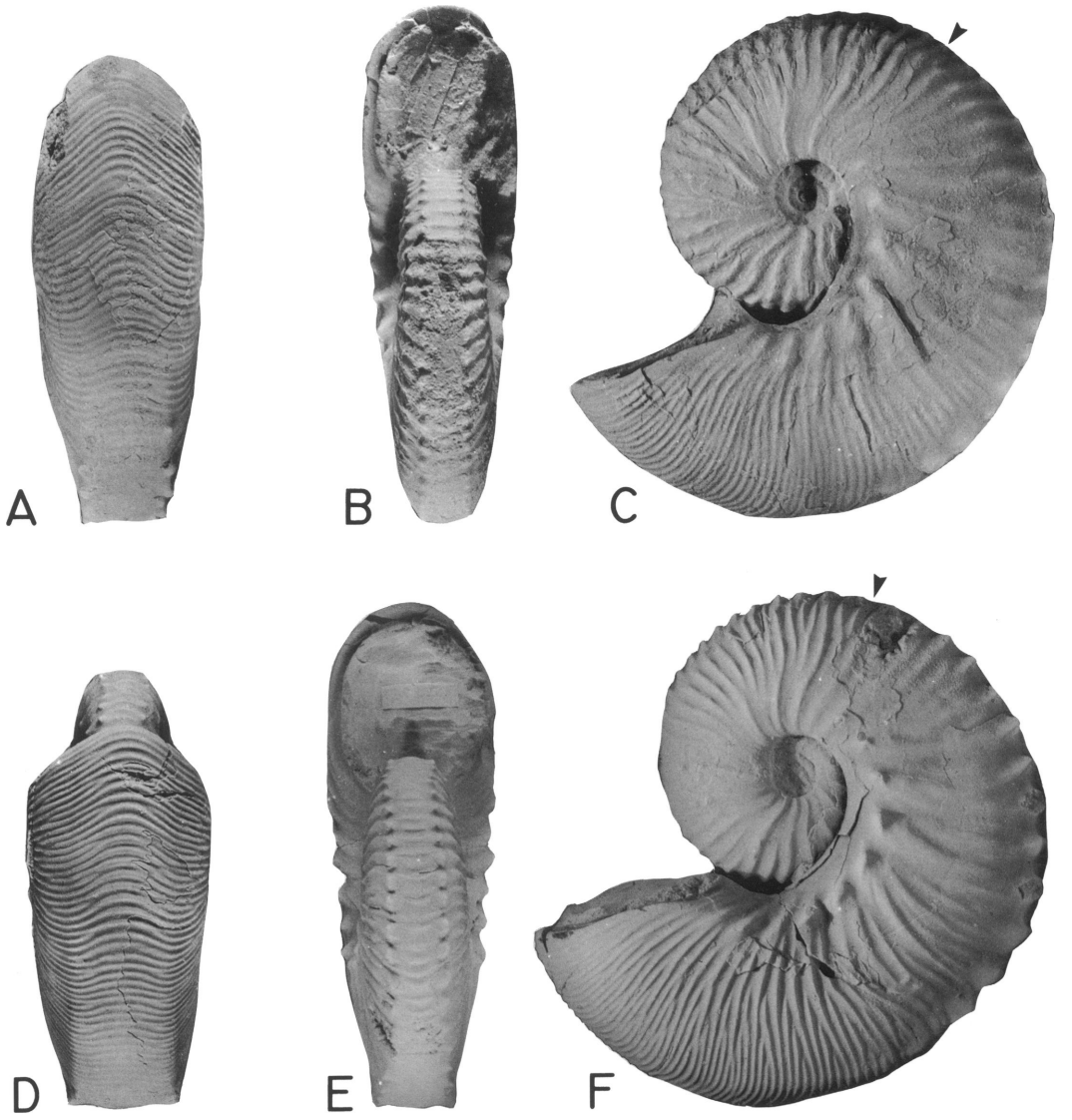

Fig. 130. *Jeletzkytes nebrascensis* (Owen) microconchs. **A–C.** Small specimen with incipient doubling of umbilical bullae, YPM 23198, loc. 37, TLM float. **A,** Posteroventral; **B,** apertural; **C,** left lateral. **D–F.** Small specimen, YPM 23195, loc. 37, TLM. **D,** Ventral hook; **E,** apertural; **F,** left lateral.

more variable than that on the phragmocone. One persistent feature is the fining and closer approximation of ribbing on the anterior end of the shaft and on the hook. The broad tuberculate ribbing characteristic of the phragmocone extends at least onto the posterior end of the body chamber, but more commonly onto its anterior end, up to the onset of fine ribbing (fig. 126C). Ribs and tubercles become considerably subdued at the appearance of fine ribbing; some of the rows of tubercles on the flanks, particularly on the dorsal flanks, may even disappear. On strongly ornamented specimens, the tubercles continue up to the onset of fine ribbing where they change to bullae; these bullae may continue as rows or become irregularly distributed. One or two of the flank rows of tubercles nearest the ventrolaterals may persist to the aperture.

The extensive tuberculation of the shell is

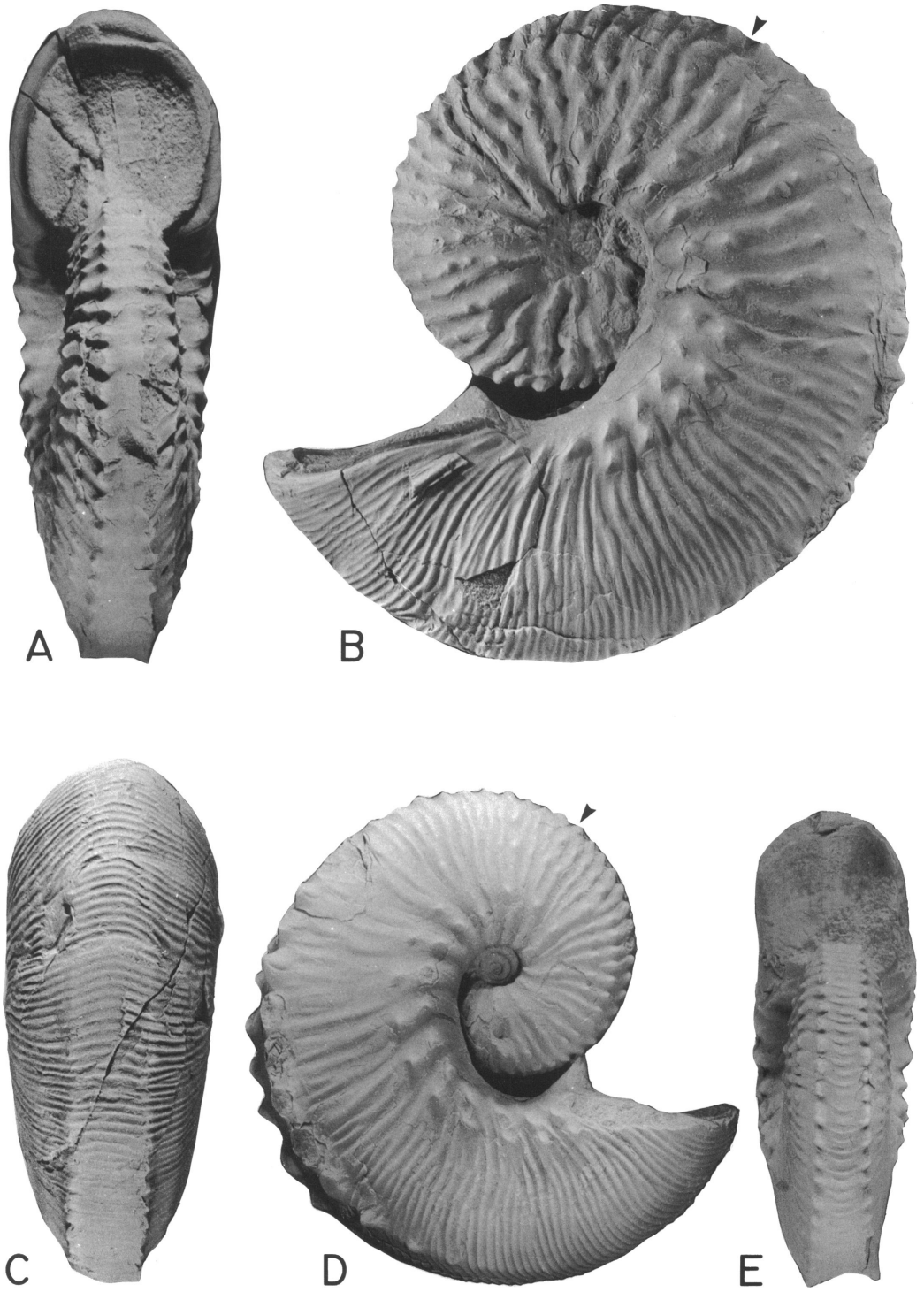

Fig. 131. *Jeletzkytes nebrascensis* (Owen) microconchs. **A–C.** Large microconch with raised venter and double row of umbilical bullae, YPM 23697, loc. 35, TLM. **A,** Apertural; **B,** left lateral; **C,** posteroventral. **D, E.** YPM 23735, loc. 227, TLM. **D,** Right lateral; **E,** apertural.

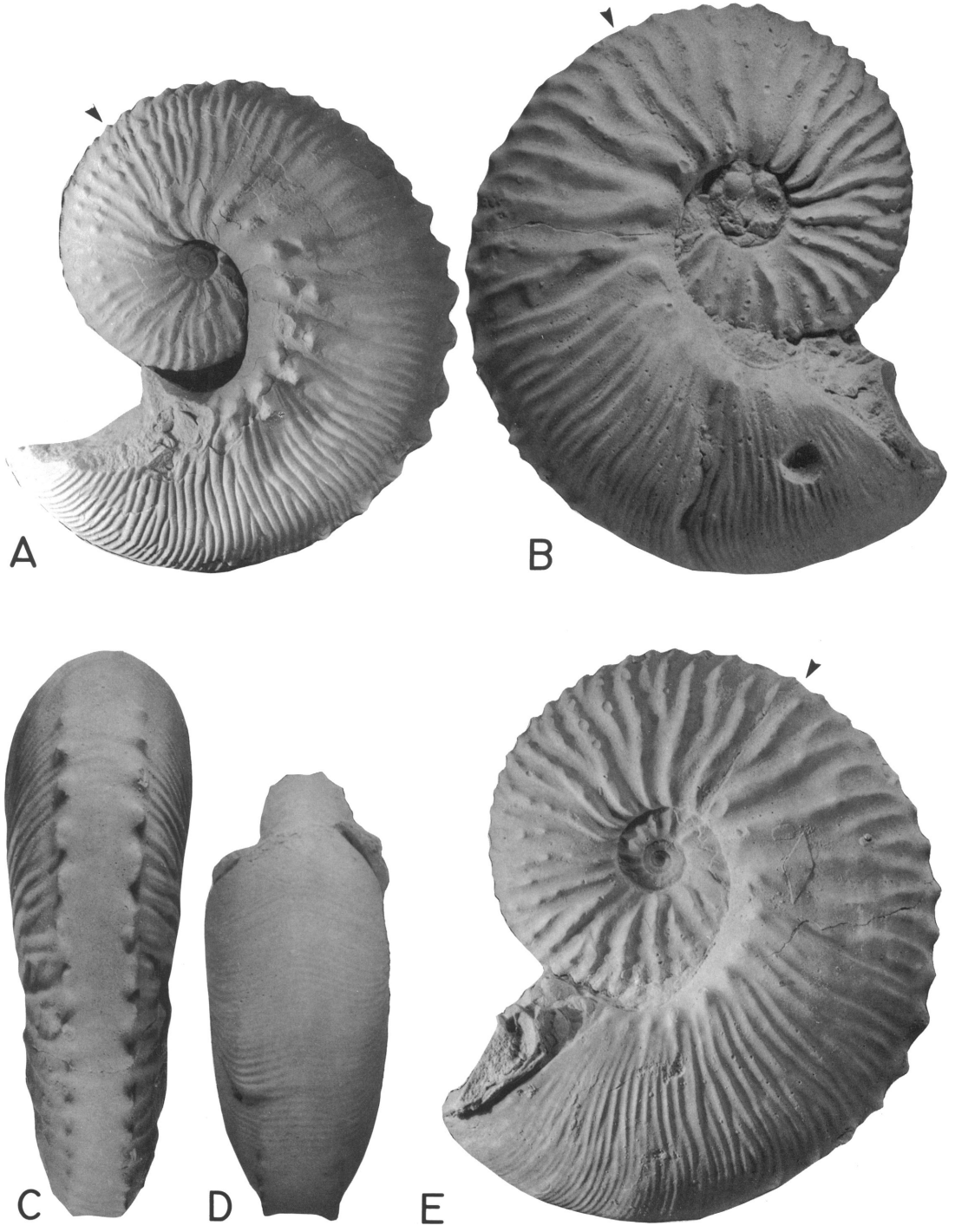

Fig. 132. *Jeletzkytes nebrascensis* (Owen) microconchs. **A.** YPM 23735 (cont.), left lateral. **B–E.** Allotype, microconch, cast of USNM 402, Meek's (1876: 437, pl. 35, fig. 3a–c) *Scaphites cheyennensis,* Fox Hills Fm., "Fox Hills, Moreau and Cheyenne Rivers, Dakota." **B,** Right lateral; **C,** posterior; **D,** ventral hook; **E,** left lateral.

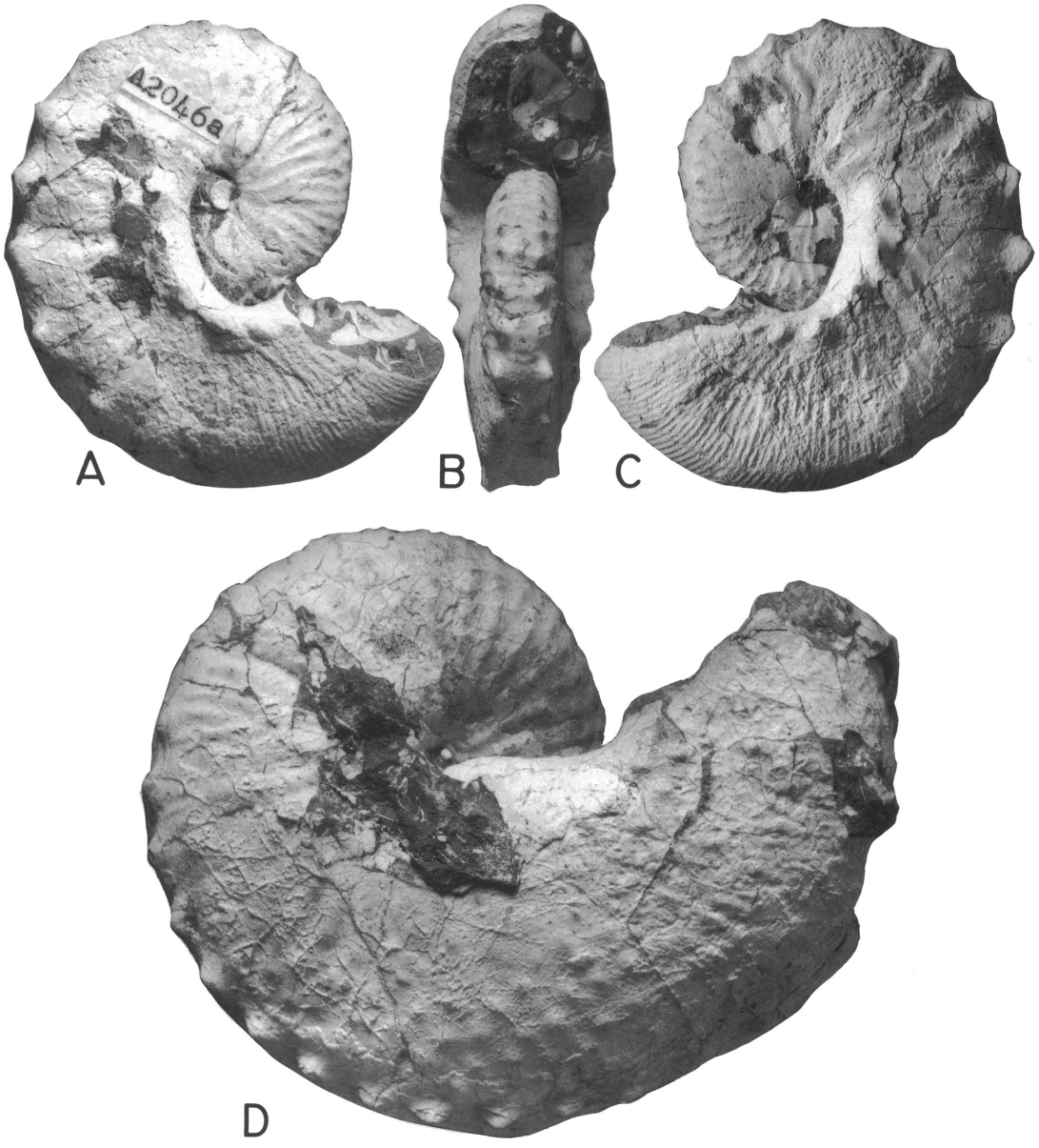

Fig. 133. *Jeletzkytes nebrascensis* (Owen) macroconch and microconch. **A–C.** Microconch, MAPS A2046a, loc. 123, Severn Fm. **A,** Right lateral; **B,** apertural; **C,** left lateral. **D.** Macroconch, right lateral, MAPS A2026a, loc. 123, Severn Fm.

the most conspicuous characteristic of *Jeletzkytes nebrascensis.* The ventrolaterals dominate in size, usually being largest on the shaft of the body chamber and diminishing on the hook; they may be clavate throughout or mostly so on the body chamber and usually are bent slightly outward. The strong ventrolaterals give rise to a bicarinate costal whorl section, which, particularly on the adapical half of the body chamber, is slightly concave above the ventrolaterals and imparts a pinched look to the narrow venter. The umbilical row of tubercales or bullae is distinguishable from flank rows largely by its po-

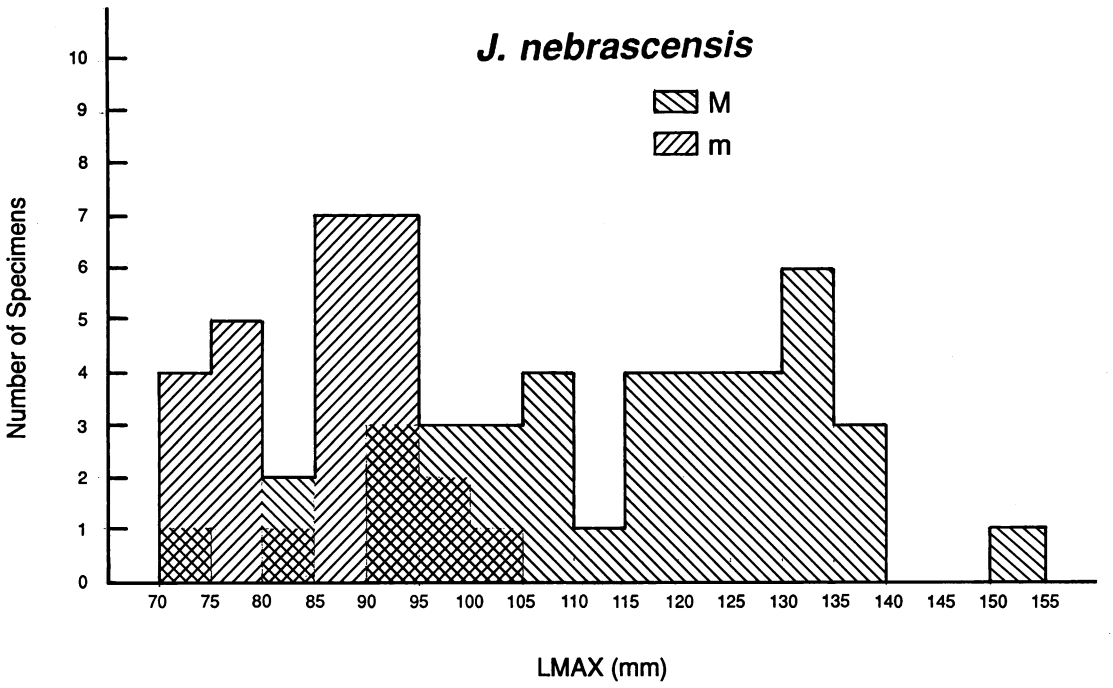

Fig. 134. Size frequency histogram of a sample of *Jeletzkytes nebrascensis* (Owen) from the Fox Hills Formation in its type area.

sition and by the fact that it is commonly less prominent than flank rows. In most of our specimens there are five or six flank rows, plus the umbilicals, depending on specimen size.

The suture of *J. nebrascensis* macroconchs is like that of *J. spedeni* macroconchs (fig. 135A–C). Fewer sutures of *J. nebrascensis* macroconchs are available for study because of the greater induration of shell and matrix. However, in these more compressed shells the ventral and lateral lobes appear more equal in size and the lateral lobe appears less asymmetrical than in *J. spedeni.*

MICROCONCH DESCRIPTION: Shells are medium size and compressed with the last whorl increasing gradually in size through the arcuate shaft of the body chamber, then de-

TABLE 15
Adult Measurements of *J. nebrascensis*[a]

	Macroconch				Microconch			
	N	$\bar{x}$	SD	Range	N	$\bar{x}$	SD	Range
LMAX (mm)	39	115.2	18.08	71.7–150.2	27	85.8	9.25	70.4–103.4
WUS (mm)	30	27.5	4.57	19.8–36.7	27	18.7	3.08	14.3–25.1
HUS (mm)	35	43.3	7.02	29.6–58.9	27	27.6	3.39	21.5–33.4
WUS/HUS	29	0.66	0.058	0.56–0.76	27	0.68	0.068	0.48–0.79
WAPT (mm)	28	35.3	6.51	21.0–47.3	27	27.6	3.70	18.4–33.6
HAPT (mm)	28	39.0	7.59	26.7–57.5	27	30.7	2.79	25.1–35.2
WAPT/HAPT	24	0.91	0.059	0.79–1.02	27	0.89	0.073	0.67–0.99
UD (mm)	31	7.1	1.58	4.0–11.6	24	8.9	1.77	6.3–12.0
UD/LMAX	31	0.06	0.011	0.05–0.08	24	0.10	0.013	0.08–0.14
A (°)	34	48.4	7.43	34.0–63.0				

[a] Abbreviations: see table 1 and figure 9.

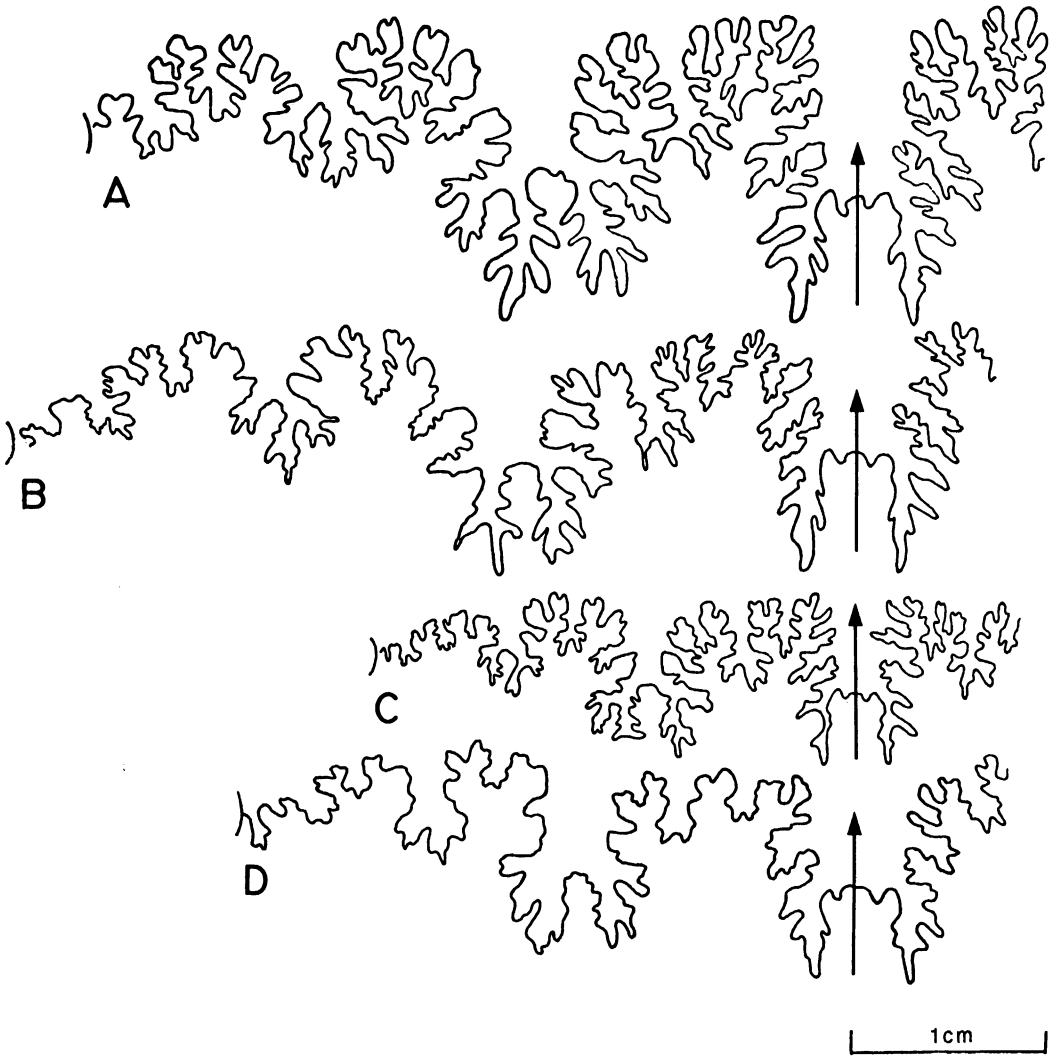

Fig. 135. Sutures of *Jeletzkytes nebrascensis* (Owen) macroconchs and microconchs. **A.** Fourth from last suture of an adult macroconch, YPM 27078, loc. 35, TLM. **B.** Third from last suture of an adult macroconch, YPM 27073, loc. 37, TLM. **C.** Fifth from last suture of an adult macroconch, YPM 27072, loc. 37, TLM. **D.** Third from last suture of an adult microconch, YPM 27092, loc. 282, CAZ.

creasing very slightly through the hook to the aperture. The shaft of the body chamber extends slightly beyond the phragmocone leaving a small gap between it and the reflexed hook. The exposed phragmocone and body chamber are each approximately 0.5 whorls in angular length. A relatively large umbilicus exposes parts of all the inner whorls. The umbilical shoulder of the body chamber is broad, slopes slightly outward, and is bordered by umbilical bullae. The venter of the body chamber is narrow and flat and bordered by strong ventrolateral clavi up to the hook where the venter broadens and the clavi disappear.

The dimensions of the measured specimens are listed in table 15. LMAX averages 85.8 mm, which is significantly smaller than that in macroconchs (115.2 mm). The size distribution is bimodal with a dominant peak at 85–95 mm and a smaller peak at 75–80 mm (fig. 134). The ratio of the size of the

largest specimen to that of the smallest is 1.47. The ratios of whorl width to height at the ultimate septum and at the aperture average 0.68 and 0.89, respectively, which are similar to the averages of the corresponding ratios in macroconchs (0.66 and 0.91, respectively). As in macroconchs, the whorl section is significantly more depressed at the aperture than at the ultimate septum. Larger microconchs tend to have slightly more depressed apertures than smaller microconchs.

The whorl section of the shell changes from essentially flat-sided for most of the exposed phragmocone to markedly wedge-shaped for the shaft of the body chamber as the umbilical shoulder increases more rapidly in width than the venter. The ventral region of the shell is bicarinate, usually with a slight concavity just above the ventrolateral clavi that accentuates the narrowness of the venter. On specimens with little or no shell remaining on the venter, a narrow, very low, mid-ventral keel is evident.

Beginning with the hook, or adoral end of the shaft, the venter broadens and the shell profile once again becomes flat-sided. As the ventrolateral clavi disappear, a very slight bevel on the rounded venter marks their projected position right up to the aperture on many specimens.

The umbilical diameter averages 8.9 mm, with larger specimens having relatively larger umbilical diameters than smaller specimens. The average umbilical diameter is significantly larger than that in macroconchs (7.1 mm). The ratio of umbilical diameter to shell diameter averages 0.10, which is also significantly larger than that in macroconchs (0.06). The curved umbilical shoulder begins to broaden near the ultimate septum, forming a shelf that extends to the aperture. Ribs cross this shelf with a backward projection, then swing somewhat forward onto the flanks.

Ribbing is dominantly rectiradiate on the phragmocone and slightly prorsiradiate on the body chamber; ribs are straight to slightly sinuous and show a weak to moderate adoral projection on the venter. They increase gradually in size and spacing through the exposed phragmocone and onto the adapical third of the body chamber; then this trend reverses itself through an abrupt gradation to fine, closely spaced ribs on the hook. On phragmocones of most specimens larger than 75 mm, flank ribs are tuberculate or at least incipiently tuberculate with two to four rows of flank tubercles between the ventrolaterals and umbilicals. These rows of tubercles extend partially onto the body chamber, most disappearing on its adapical half, although on more coarsely ornamented specimens some rows may extend nearly to the aperture. Particularly characteristic of *J. nebrascensis* microconchs is a second row of tubercles or bullae closely paralleling the umbilical row on the body chamber (fig. 131B, D). These may remain distinct from the umbilicals or become yoked to them, gradually merging with them into single bullae.

The pattern of ornamentation on smaller specimens differs from that on larger specimens in that there are no tubercles other than umbilicals and ventrolaterals on the body chamber and at most a single weak row of flank tubercles situated just above the ventrolaterals on the phragmocone (fig. 130C, F).

The suture in microconchs is like that in macroconchs (fig. 135D).

ONTOGENY: Dorsoventral, mostly costal cross sections of macro- and microconchs are illustrated in figure 136. Initially, the whorl flanks are convex and the umbilical shoulder slopes gently outward. During the course of ontogeny, the flanks become slightly less convex and the umbilical shoulder becomes steeper. The postembryonic growth of whorl width is slightly negatively allometric to isometric (slopes range from 0.8943 to 0.9844; fig. 137) whereas that of whorl height is positively allometric (slopes range from 1.0668 to 1.1437; fig. 138). At comparable shell diameters, the values of whorl width and whorl height in macroconchs are approximately the same as those in microconchs. The whorl shape becomes relatively more compressed during ontogeny; the ratio of whorl width to height ranges from 1.0 to 2.0 in early ontogeny, decreasing to a minimum near the base of the mature body chamber.

The growth of umbilical diameter is nearly isometric through most of ontogeny (fig. 139). At comparable shell diameters, umbilical diameters more or less overlap between dimorphs. However, at approximately one whorl before the base of the mature body chamber, the umbilical diameter begins to

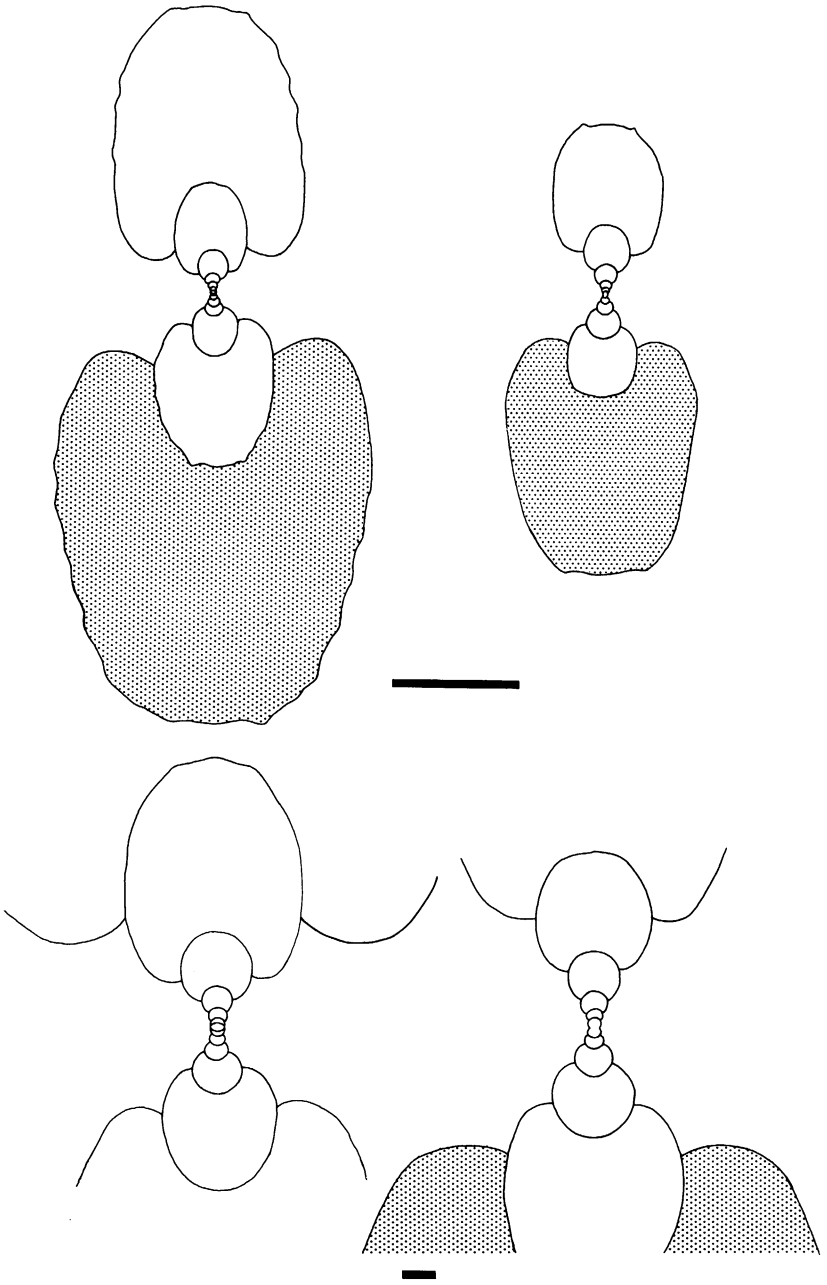

Fig. 136. Dorsoventral, mostly costal cross sections through adult dimorphs of *Jeletzkytes nebrascensis* (Owen). **Left.** Macroconch, YPM 32595, loc. 36, TLM. **Right.** Microconch, YPM 32599, loc. 73, TLM. Shaded area demarcates mature body chamber. Upper scale bar = 1 cm; lower scale bar = 1 mm.

increase more slowly or not at all in macroconchs whereas it continues to increase at the same rate in microconchs. The ratio of umbilical diameter to shell diameter decreases through most of postembryonic growth but the rate of decrease accelerates after approximately 5 mm shell diameter, reaching a minimum value near the base of the mature body chamber.

The development of ornamentation in *J.*

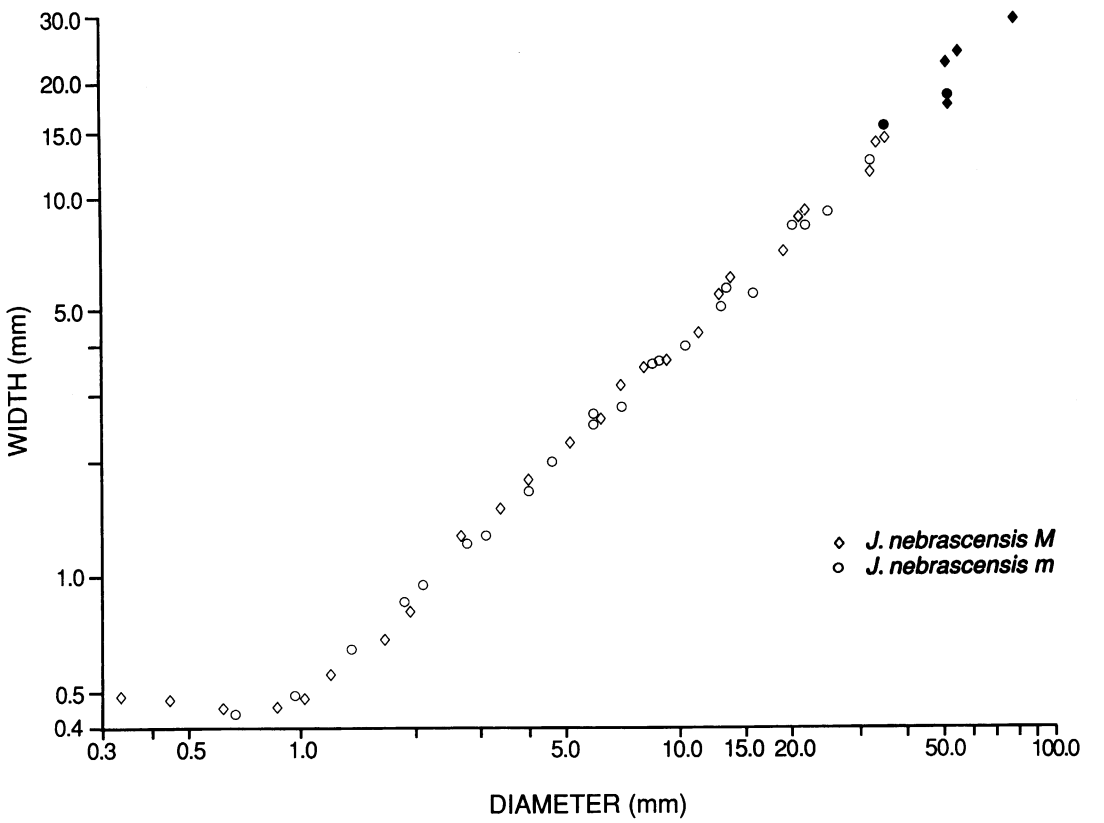

Fig. 137. Plot of whorl width versus shell diameter through the ontogeny of six adults (three macroconchs and three microconchs) of *Jeletzkytes nebrascensis* (Owen). Black symbols indicate measurements near the base of or in the mature body chamber. Measurements listed in Appendix II.

nebrascensis is illustrated in figure 140. At approximately 4 mm shell diameter, ribs appear on the venter with a forward projection and bullate ribs (primaries) appear on the flanks. The ratio of the number of dorsal to ventral ribs is 1:2, which remains the same up to the point of exposure. Most secondaries originate near the ventral margin. However, as whorl height increases, the point of origination extends from anywhere between dorsal of mid-flank to near the ventral margin. At approximately 1.0–1.5 whorls before the base of the mature body chamber (about 0.5–1.0 whorls before the point of exposure, about 15–20 mm shell diameter), ventrolateral tubercles appear on every flank rib. With the appearance of ventrolateral tubercles, the forward projection of the ventral ribs weakens. Soon thereafter, near the point of exposure in microconchs, multiple rows of flank tubercles develop; commonly the first row appears just dorsal of the ventrolaterals. The tubercles of the first row are nearly the same size as or slightly smaller than the ventrolaterals but this size difference increases during ontogeny. Flank tubercles occur on primaries and most secondaries. On the mature phragmocone, primaries are strong, broad, rectiradiate to weakly prorsiradiate, multituberculate, and slightly sinuous. They usually become bullate near the umbilicus at the end of the phragmocone. As many as seven rows of flank and umbilical tubercles appear in macroconchs, five in microconchs. The greatest numbers occur on primaries because these ribs are longer; fewer numbers of tubercles occur on the shorter secondaries.

Ventrolateral tubercles usually occur on every flank rib but may also occur at the junction of two flank ribs. Ribs cross the venter

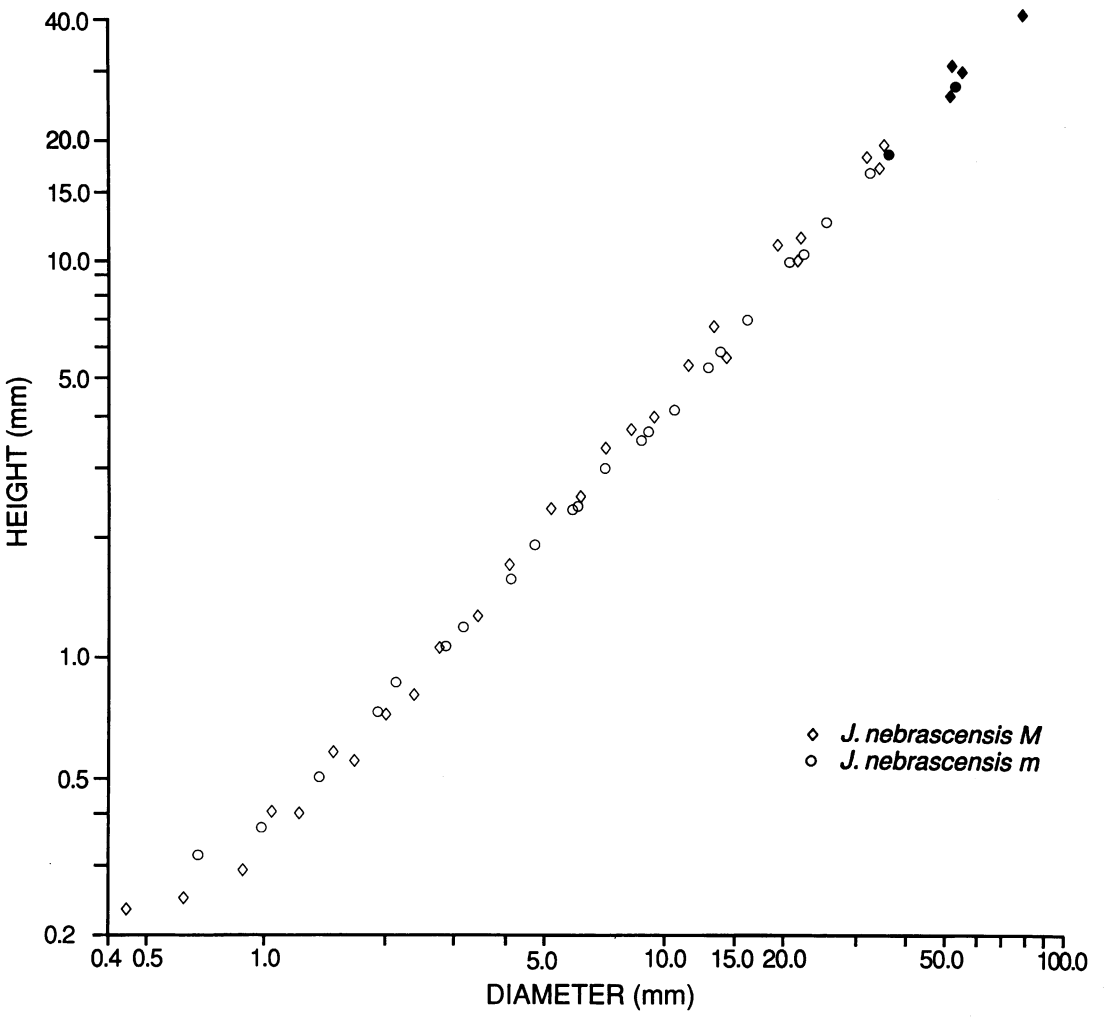

Fig. 138. Plot of whorl height versus shell diameter through the ontogeny of six adults (three macroconchs and three microconchs) of *Jeletzkytes nebrascensis* (Owen). Black symbols indicate measurements near the base of or in the mature body chamber. Measurements listed in Appendix II.

of the mature phragmocone with a slight adoral projection. Commonly, two ventral ribs loop between opposite pairs of ventrolateral tubercles. Alternatively, one of the two ventral ribs may join an adjacent ventrolateral if the ventrolaterals are offset relative to one another. The ratio of the number of dorsal to ventral ribs on the exposed phragmocone ranges from 1:4 to 1:8, averaging 1:5, in macroconchs, and 1:2.5 to 1:5, averaging 1:3, in microconchs.

DISCUSSION: *Jeletzkytes nebrascensis* macroconchs differ distinctly from those of *J. spedeni* in a number of ways. *J. nebrascensis* macroconchs are larger and more compressed, with consistently higher than wide whorl sections throughout the exposed shell. The maximum height of the body chamber is at the midpoint of the shaft rather than near its anterior end. *J. nebrascensis* macroconchs have a higher apertural angle and lower ratio of umbilical diameter to shell diameter. Tubercles are also much more common in *J. nebrascensis* with broad tuberculate ribs covering the exposed phragmocone and part or all of the body chamber.

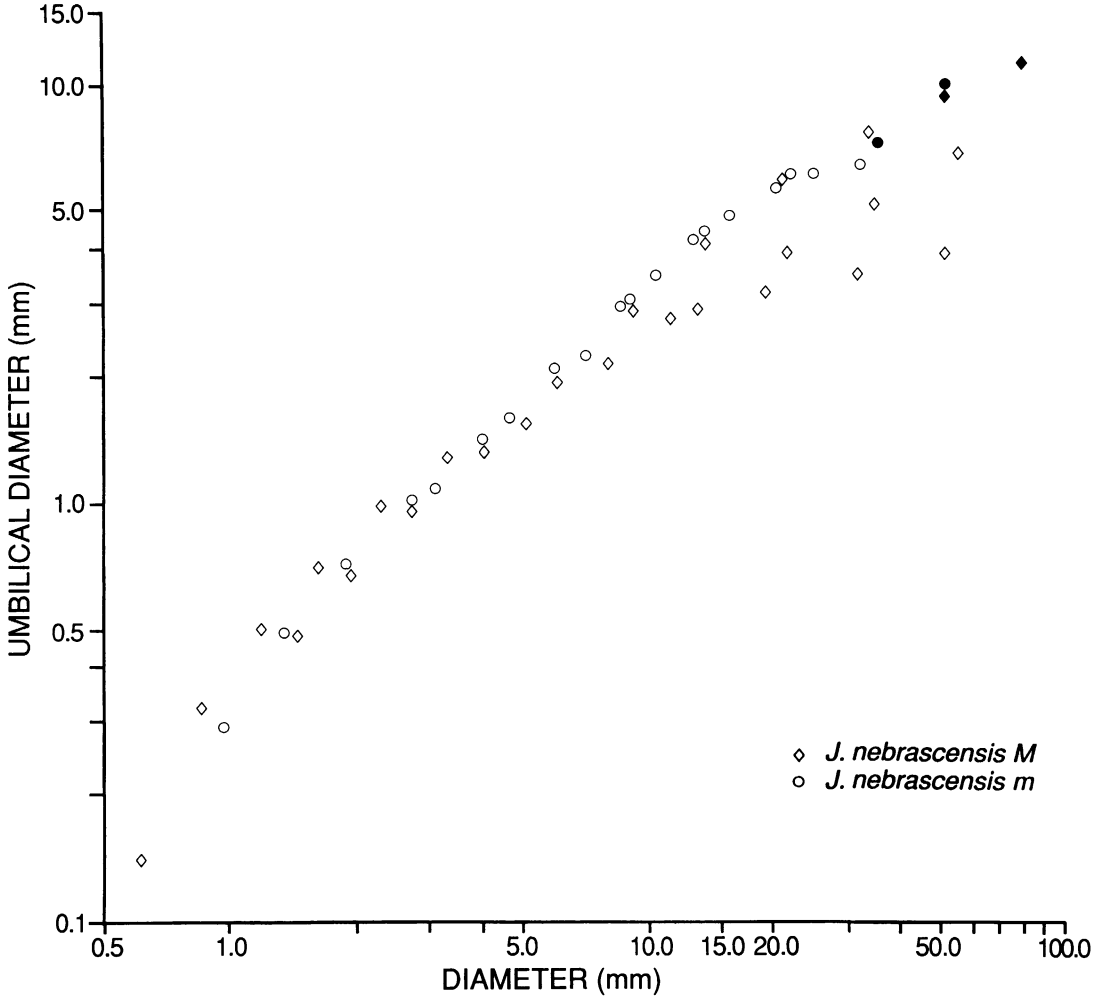

Fig. 139. Plot of umbilical diameter versus shell diameter through the ontogeny of six adults (three macroconchs and three microconchs) of *Jeletzkytes nebrascensis* (Owen). Black symbols indicate measurements near the base of or in the mature body chamber. Measurements listed in Appendix II.

Unlike the variable *J. spedeni, J. nebrascensis* shows relatively little variation in its general form and ornament.

Microconchs of *J. nebrascensis,* while not as conspicuously different from those of *J. spedeni* can, nevertheless, be distinguished by their larger size, their more compressed shells with whorl sections generally higher than wide, and the disappearance of ventrolateral tubercles in the area of fine ribbing on the hook and anterior shaft of the body chamber. The umbilical diameter also tends to be larger in *J. nebrascensis* microconchs than in those of *J. spedeni.* The median row of tubercles/bullae present on most specimens of *J. spedeni* is rarely found on specimens of *J. nebrascensis.* Microconchs of *J. nebrascensis,* especially large specimens, commonly show the distinctive tuberculate ribbing on the phragmocone characteristic of macroconchs; they also show the characteristic double row of umbilical tubercles or bullae on the body chamber.

J. nebrascensis is hard to confuse with any other co-occurring scaphite, with its predecessor *J. spedeni,* or with older species of *Jeletzkytes.* It is most closely related to the more compressed variants of *J. spedeni.* Outside

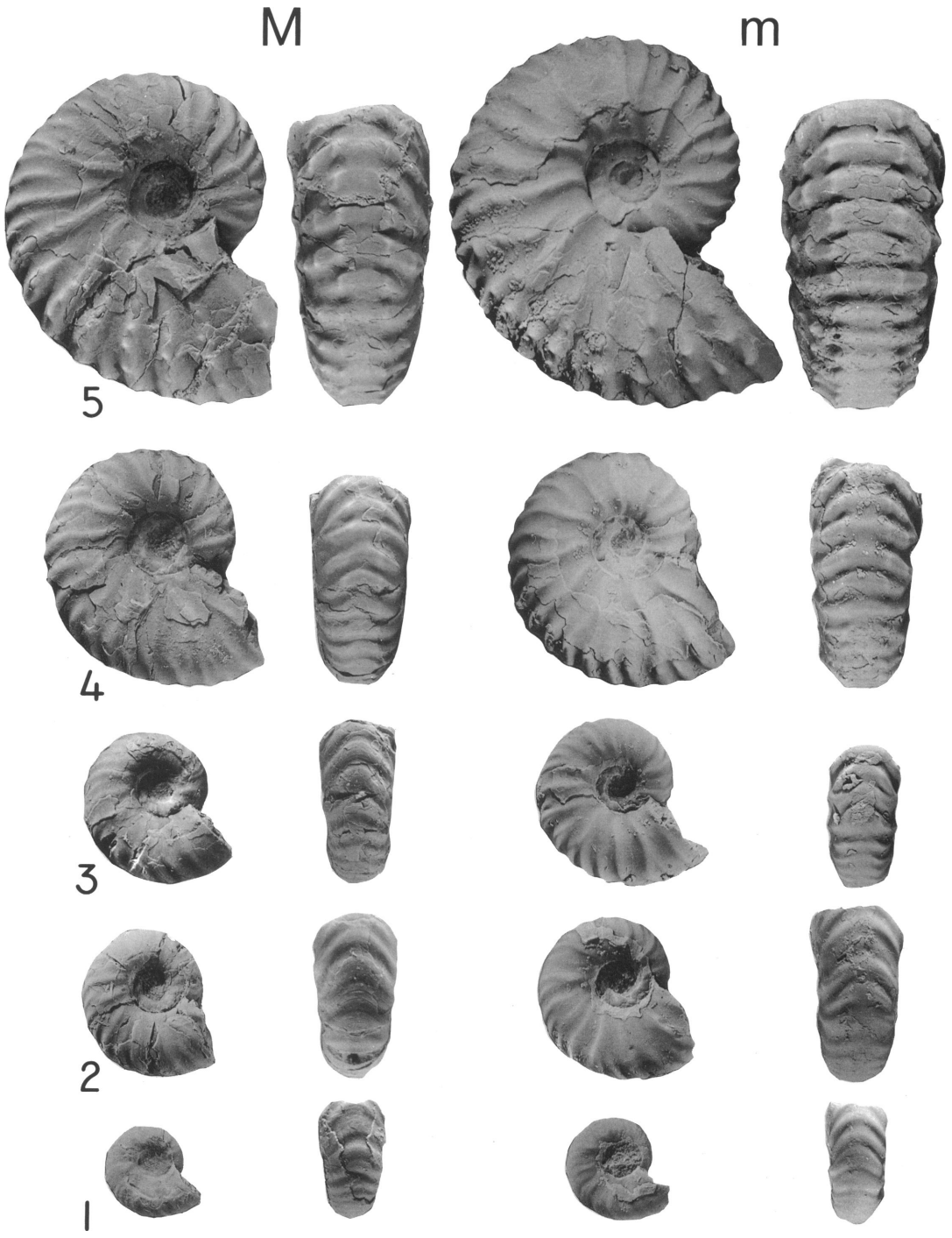

Fig. 140. Dissections of adult dimorphs (macroconch, YPM 32591, loc. 212, TLM, and microconch, YPM 32597, loc. 73, TLM) of *Jeletzkytes nebrascensis* (Owen) showing five sizes through ontogeny in lateral and ventral view. 1. ×3. 2. ×3. 3. ×2. 4. ×2. 5. ×2.

the United States Western Interior, *J. nebrascensis* is known only from the Severn Formation of Maryland; a macroconch and probable microconch were kindly loaned to us for study from the collections of the Monmouth Amateur Paleontologist's Society by Ralph Johnson (fig. 133). *J. nebrascensis* under one generic name or another has long served to mark the youngest marine zone in the Western Interior Cretaceous (see p. 17).

Jeletzkytes dorfi, new species
Figures 141–148

Macroconch Synonymy:

Discoscaphites conradi (Morton) var. *intermedius* Meek, Kellum, 1962: pl. 6, figs. 3, 5.

DIAGNOSIS: Macroconchs mostly medium size, sturdy, somewhat compressed with relatively long, tapering hook, and high apertural angle. Ribs strong, relatively widely spaced to mid-shaft, becoming finer and more closely spaced on hook; adoral projection of ventral ribs slight to moderate. Flank tubercles largely restricted to phragmocone where up to six rows may occur. Microconchs with mostly quadrate whorl section, strong ribs that arch conspicuously forward on flanks of shaft, and strong ventrolateral and umbilical tubercles; flank tubercles present on phragmocone or not.

TYPES: Holotype, YPM 23175, loc. RB 103, bluff-forming bioturbated sandstone, Fox Hills Formation, fig. 141A–E.

Allotype, YPM 23212, loc. RB 114, bluff-forming bioturbated sandstone, Fox Hills Formation, fig. 144D–H.

NAME: This species is named in honor of the late Erling Dorf, Professor and paleobotanist at Princeton University who, during his study of the flora of the type Lance Formation, introduced one of us (KMW) to the Fox Hills Formation of the Lance Creek–Red Bird area.

OCCURRENCE: The species is common in the Fox Hills Formation throughout its continuous exposure from just north of the town of Lance Creek to where the outcrop crosses the Cheyenne River, in northern Niobrara County, Wyoming. We have also identified it in BHI collections from localities in the uppermost Pierre Shale just east of the Black Hills in the vicinity of Pedro and Wall, South Dakota. In the type area of the Fox Hills, some fragments of *Jeletzkytes* occur sparingly associated with *Hoploscaphites melloi* in the upper Mobridge Member of the Pierre Shale but are not well enough preserved to identify with certainty.

Throughout the occurrences cited above, *J. dorfi* consistently lies below the *Hoploscaphites nicolletii* Zone and above the *Baculites clinolobatus* Zone; in the Lance Creek–Red Bird area it helps define the *Hoploscaphites birkelundi* Zone. The possibility exists that *J. dorfi* also occurs with *B. clinolobatus*; somewhat similar scaphites occur with *B. clinolobatus* in the Mobridge Member of the Pierre Shale in the Missouri Valley, South Dakota, but the few partial specimens in our collections appear to differ from *J. dorfi.*

MATERIAL: Study of *J. dorfi* is based on 66 specimens in the YPM and AMNH collections from the Lance Creek–Red Bird area; they include 30 macroconchs and 36 microconchs, supplemented by numerous fragments. Few specimens, mostly microconchs, are entire; the majority show postmortem breakage or deformation.

MACROCONCH DESCRIPTION: Shells are stout, mostly medium size with compressed whorls. The phragmocone is tightly coiled and the exposed whorls are higher than wide and generally flat-sided. The body chamber is arcuate on the periphery and the umbilical shoulder is straight to slightly arched. The aperture is commonly slightly separated from the phragmocone with the dorsal projection reflexed against it. The hook is relatively long with a high apertural angle.

The dimensions of the measured specimens are listed in table 16. LMAX averages 78.9 mm. Only one specimen is more than 84 mm and only one is less than 70 mm (fig. 147). The ratio of the size of the largest specimen to that of the smallest is 1.57. Maximum height of the body chamber lies approximately along a line drawn perpendicular to the umbilical shoulder at its midpoint; adorally the body chamber decreases rapidly in height to the aperture but the width of the shell, which reaches its maximum at about the base of the hook, decreases only very slightly, if at all, to the aperture. The shape

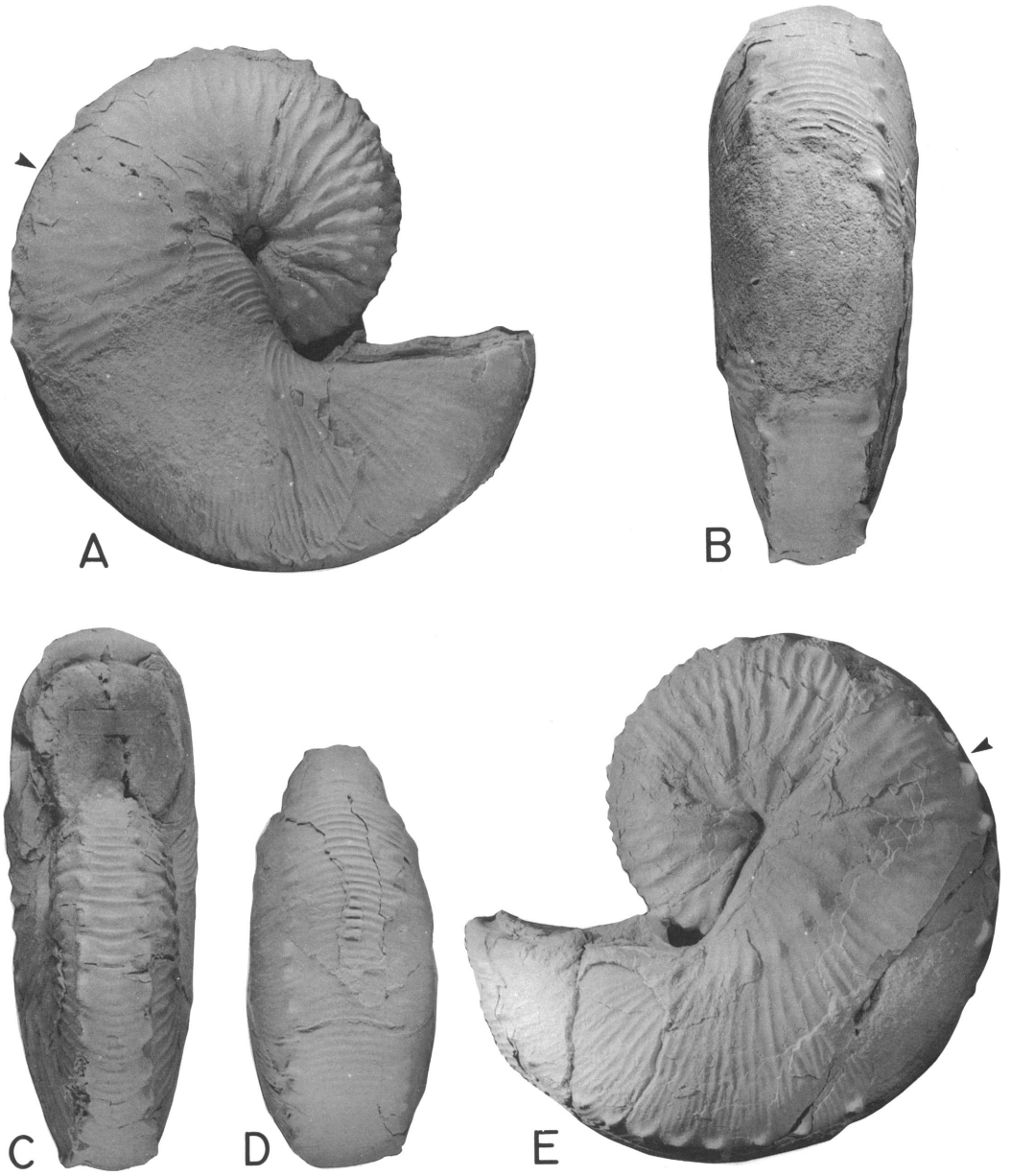

Fig. 141. *Jeletzkytes dorfi,* n. sp., macroconchs. **A–E.** Holotype, YPM 23175, loc. RB 117, bioturbated sand unit, lower Fox Hills Fm. **A,** Right lateral; **B,** posterior; **C,** apertural; **D,** ventral hook; **E,** left lateral.

of the shell is similar in all specimens, regardless of size. The ratios of whorl width to whorl height at the ultimate septum and at the aperture average 0.70 and 0.93, respectively, indicating a significantly more depressed whorl section at the aperture than at the ultimate septum.

The umbilical diameter and ratio of umbilical diameter to shell diameter average 3.9 mm and 0.08, respectively (table 16); the ratio of umbilical diameter to shell diameter does not vary consistently with adult size. The umbilicus of the coil lies on the umbilical shoulder of the mature body chamber.

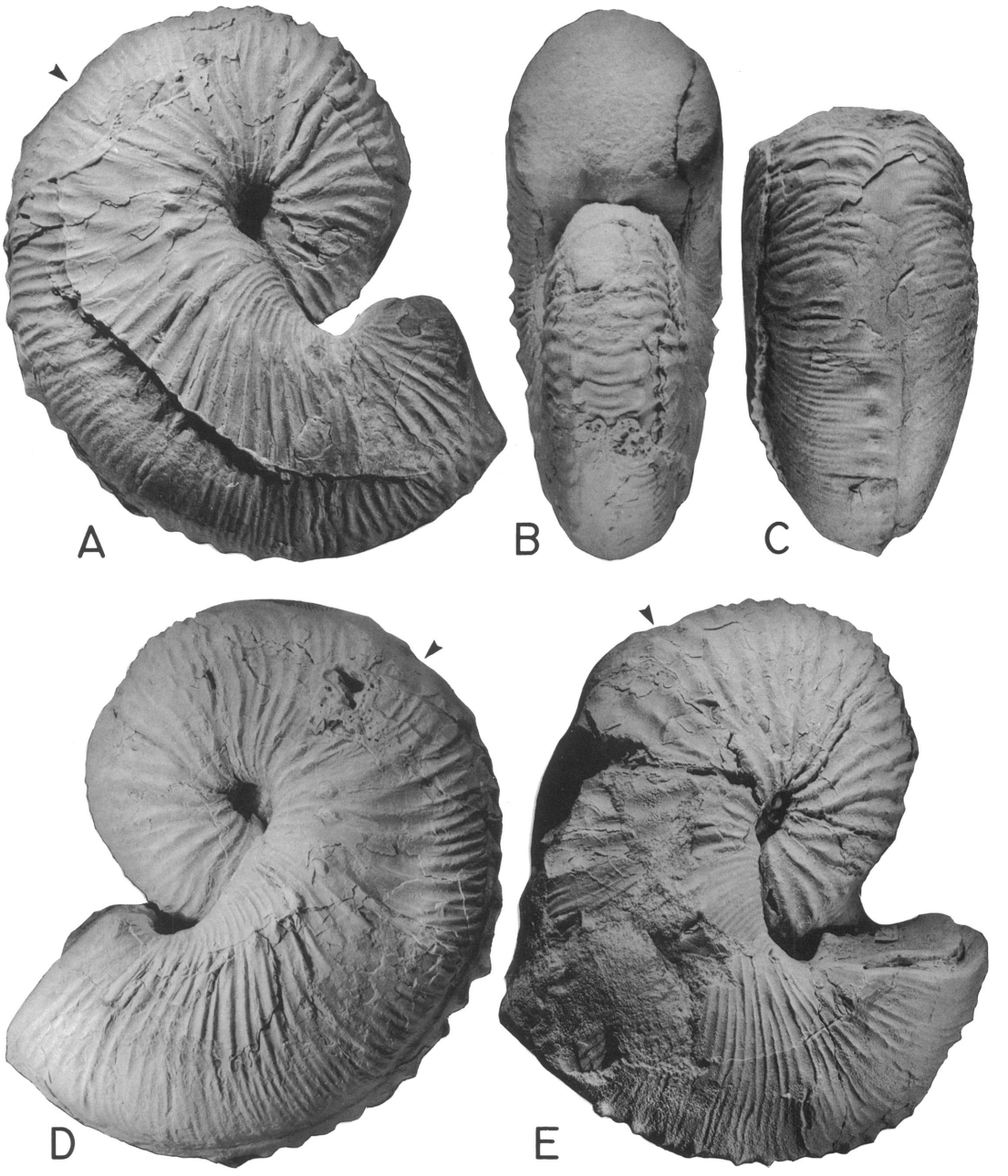

Fig. 142. *Jeletzkytes dorfi,* n. sp., macroconchs. **A–D.** Partial specimen lacking termination of hook. Injury at midbody chamber marked by loss of left row of ventrolateral tubercles and migration of right row of ventrolateral tubercles to mid-venter bordering spiral furrow, YPM 23176, loc. RB 116, upper part of bioturbated sand unit, lower Fox Hills Fm. **A,** Right lateral; **B,** apertural; **C,** posteroventral, note spiral furrow; **D,** left lateral. **E.** Secondarily deformed specimen, right lateral, YPM 23183, loc. RB 117, bioturbated sand unit, lower Fox Hills Fm.

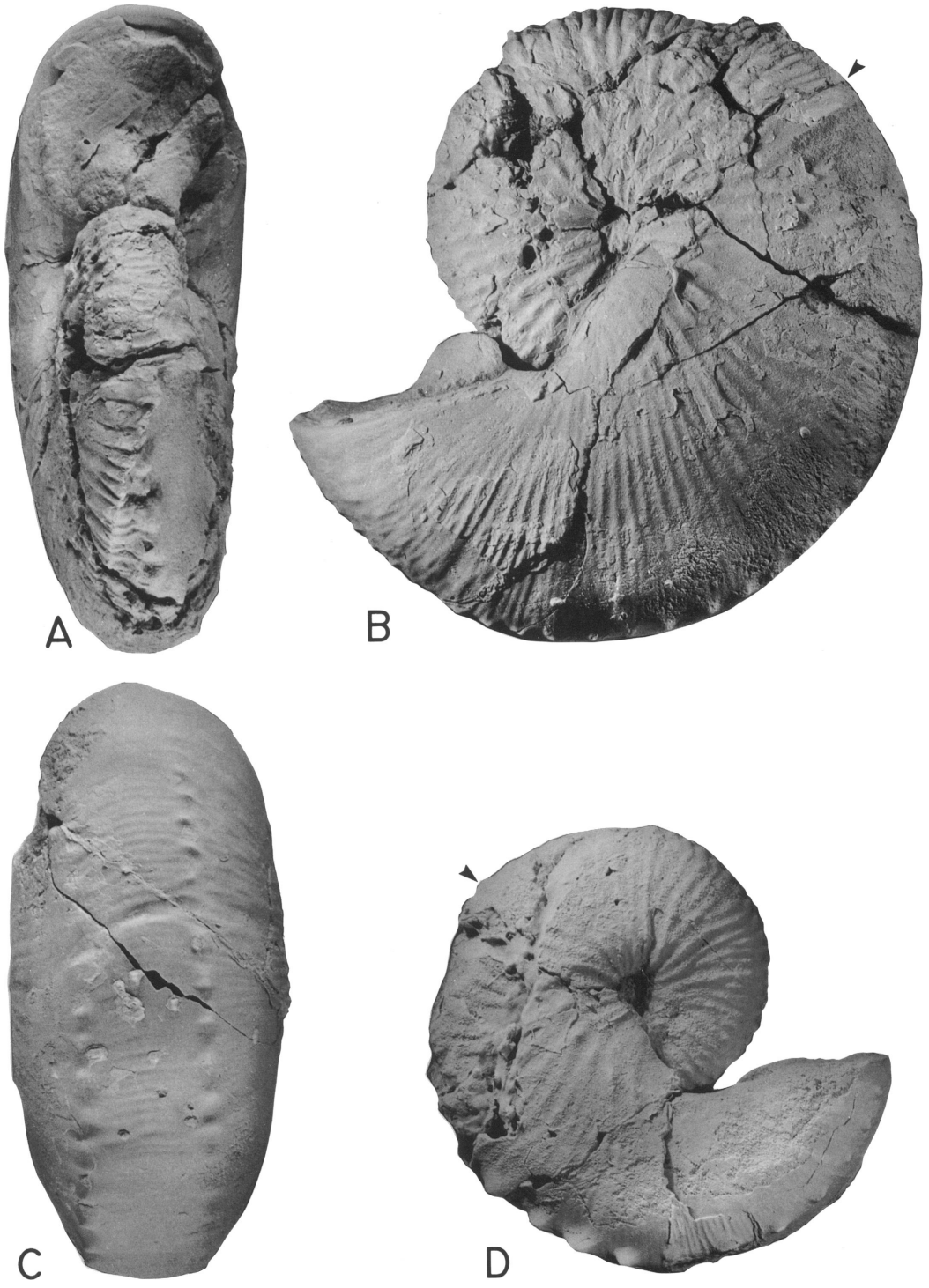

Fig. 143. *Jeletzkytes dorfi,* n. sp., macroconchs. **A–C.** Largest macroconch in collection, YPM 23174, loc. RB 103, bioturbated sand unit, lower Fox Hills Fm. **A,** Apertural; **B,** left lateral; **C,** posteroventral. **D.** Smallest macroconch in collection, right lateral, YPM 23177, loc. RB 104, upper part of bioturbated sand unit, lower Fox Hills Fm.

Shell ornament consists of relatively prominent, fairly widely spaced ribs, straight to slightly curved forward on the mid-flanks and curved backward near the umbilicus and ventral margin. Ventral ribs show a slight to moderate adoral projection, as does the ventral lip at the aperture. There are 5 to 6 ventral ribs/cm on the exposed phragmocone and 8 to 10/cm on the anterior shaft and hook; the finer ribbing begins about mid-shaft, just anterior to maximum height.

Ventrolateral tubercles extend throughout the exposed shell, and are strongest on the posterior part of the body chamber and adjacent one-quarter whorl of the phragmocone. A row of bullae lies about one-quarter of the height of the whorl below the umbilical shoulder on the anterior part of the phragmocone and body chamber. Flank tubercles are commonly restricted to the phragmocone but may continue just past the ultimate septum. Flank tuberculation is variable, ranging from one to four rows of tubercles and/or bullae covering part or most of the exposed phragmocone.

The suture is typically scaphitid with the ventral and lateral lobes subequal in width (fig. 148A, B). The first auxiliary lobe may be either bifid or trifid. None of our specimens preserves the ventral muscle attachment area.

MICROCONCH DESCRIPTION: Shells are mostly medium size; LMAX averages 57.2 mm, which is significantly smaller than that in macroconchs (table 16). The coil of the shell is tight through the exposed phragmocone, then loosens, with the shaft of the body chamber forming a broad arc that extends slightly beyond the phragmocone. The body chamber is reflexed back toward the coil in a relatively long hook. The broad, outwardly sloping umbilical shoulder of the body chamber begins at the ultimate septum. Whorl width increases more rapidly on the dorsal than on the ventral part of the body chamber, resulting in a trapezoidal cross section. The ventral part of the body chamber broadens in the hook culminating in a nearly quadrate aperture that is only fractionally higher than wide. The ratios of whorl width to whorl height at the ultimate septum and at the aperture average 0.78 and 0.96, respectively, and are similar to the averages of the corresponding ratios in macroconchs (0.70 and 0.93, respectively). As in macroconchs, the whorl section at the aperture is significantly more depressed than that at the ultimate septum. The umbilical diameter averages 4.8 mm, which is not significantly different from that in macroconchs (3.9 mm). However, the ratio of umbilical diameter to shell diameter averages 0.09, which is significantly higher than that in macroconchs (0.05).

Prominent primary ribs are straight on the

→

Fig. 144. *Jeletzkytes dorfi,* n. sp., macroconch and microconchs. **A–C.** Macroconch, AMNH 44337, loc. 3156, bioturbated sand unit, lower Fox Hills Fm. **A,** Right lateral; **B,** apertural; **C,** posteroventral. **D–H.** Allotype, microconch, strongly tuberculate body chamber, YPM 23212, loc. RB 114, bioturbated sand unit, lower Fox Hills Fm. **D,** Right lateral; **E,** ventral hook; **F,** posterior; **G,** apertural; **H,** left lateral. **I, J.** Microconch, YPM 27215, loc. RB 123, bioturbated sand unit, lower Fox Hills Fm. **I,** Posteroventral; **J,** left lateral.

Fig. 145. *Jeletzkytes dorfi,* n. sp., macroconch and microconch. **A, B.** Weakly ornamented macroconch, YPM 23185, loc. RB 117, top of transitional silty sand, lower Fox Hills Fm. **A,** Right lateral; **B,** posteroventral. **C–H.** Microconch with well-preserved dorsal projection, YPM 27212, loc. RB 106, bioturbated sand unit, lower Fox Hills Fm. **C,** Posteroventral; **D,** left lateral; **E,** left lateral, hook removed to show dorsal projection (arrow); **F,** anterior view of dorsal projection, hook removed. **G,** close-up of dorsal projection preserved as a cast developed against the venter of the phragmocone. The actual shell is retained on the body chamber, ×2.7; **H,** uncoated venter showing ventral muscle attachment area (arrow), ×3.

Fig. 146. *Jeletzkytes dorfi,* n. sp., microconchs. **A–E.** AMNH 44224, loc. 3156, bioturbated sand unit, lower Fox Hills Fm. **A,** Right lateral; **B,** apertural; **C,** posterior; **D,** ventral hook; **E,** left lateral. **F, G.** Large, strongly tuberculate variant, AMNH 44339, loc. 3156, bioturbated sand unit, lower Fox Hills Fm. **F,** Right lateral; **G,** apertural. **H–J.** YPM 27216, loc. RB 107, bioturbated sand unit, lower Fox Hills Fm. **H,** Ventral hook; **I,** apertural; **J,** left lateral.

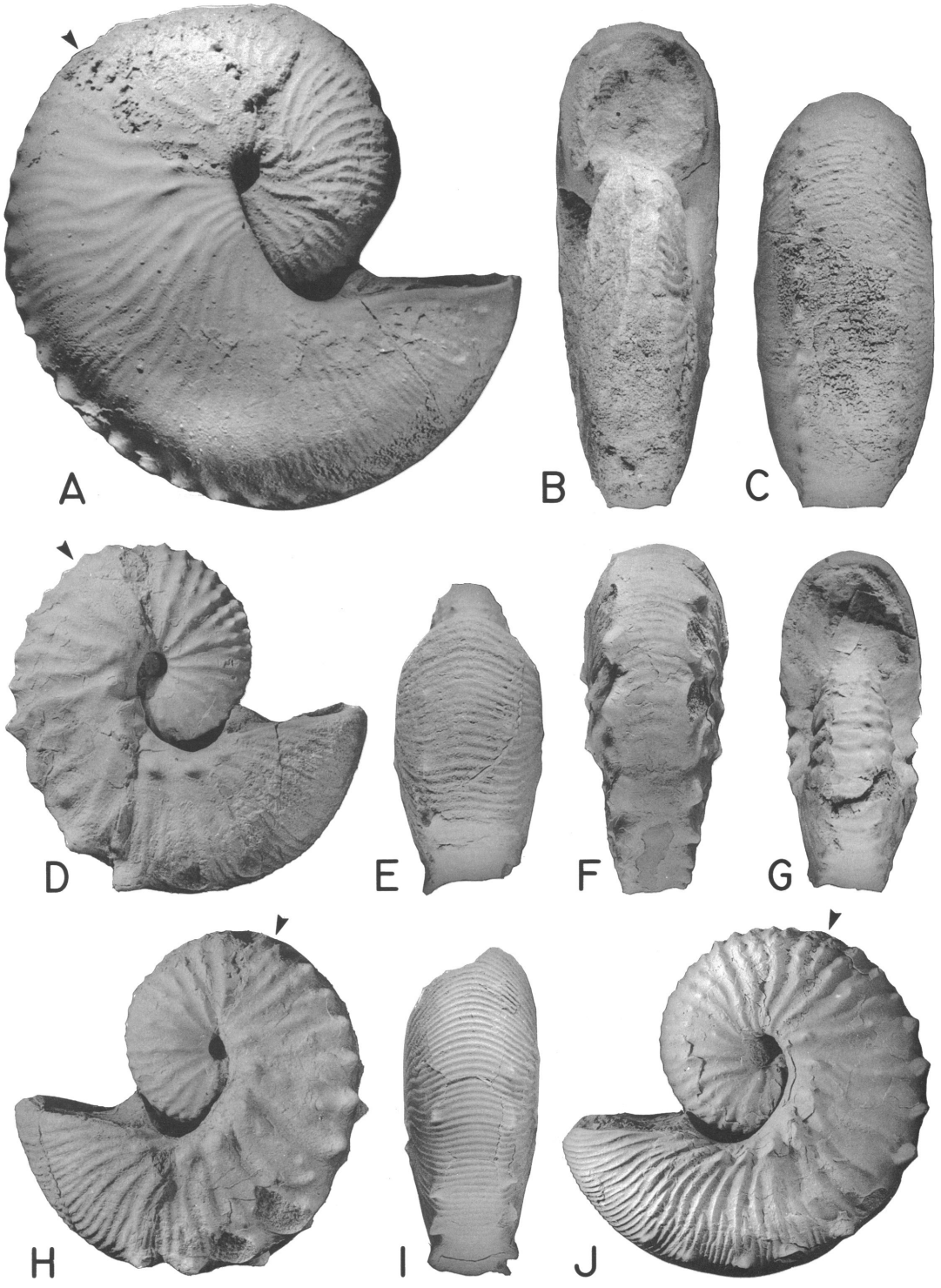
A
B
C
D
E
F
G
H
I
J

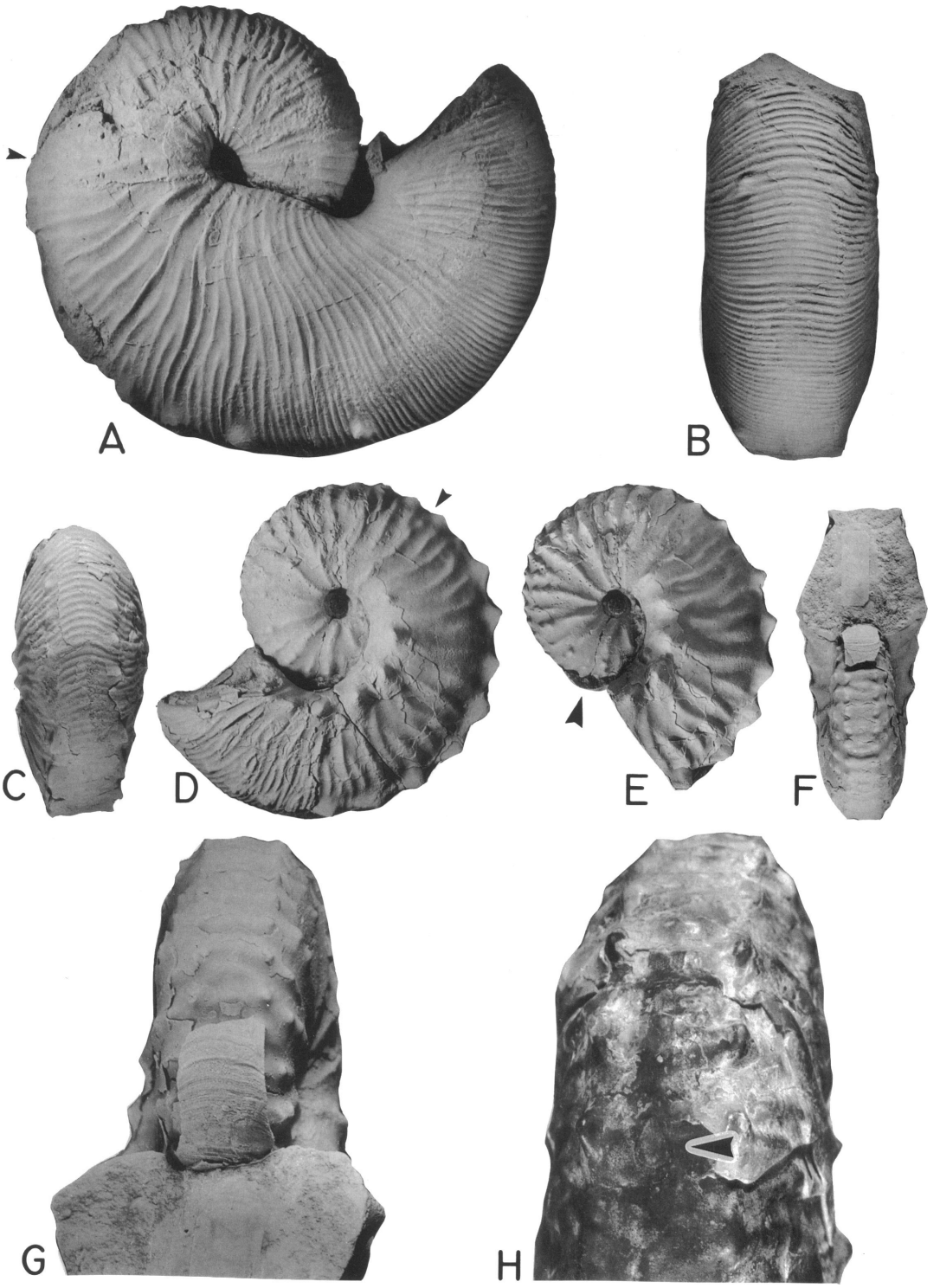

Fig. 145

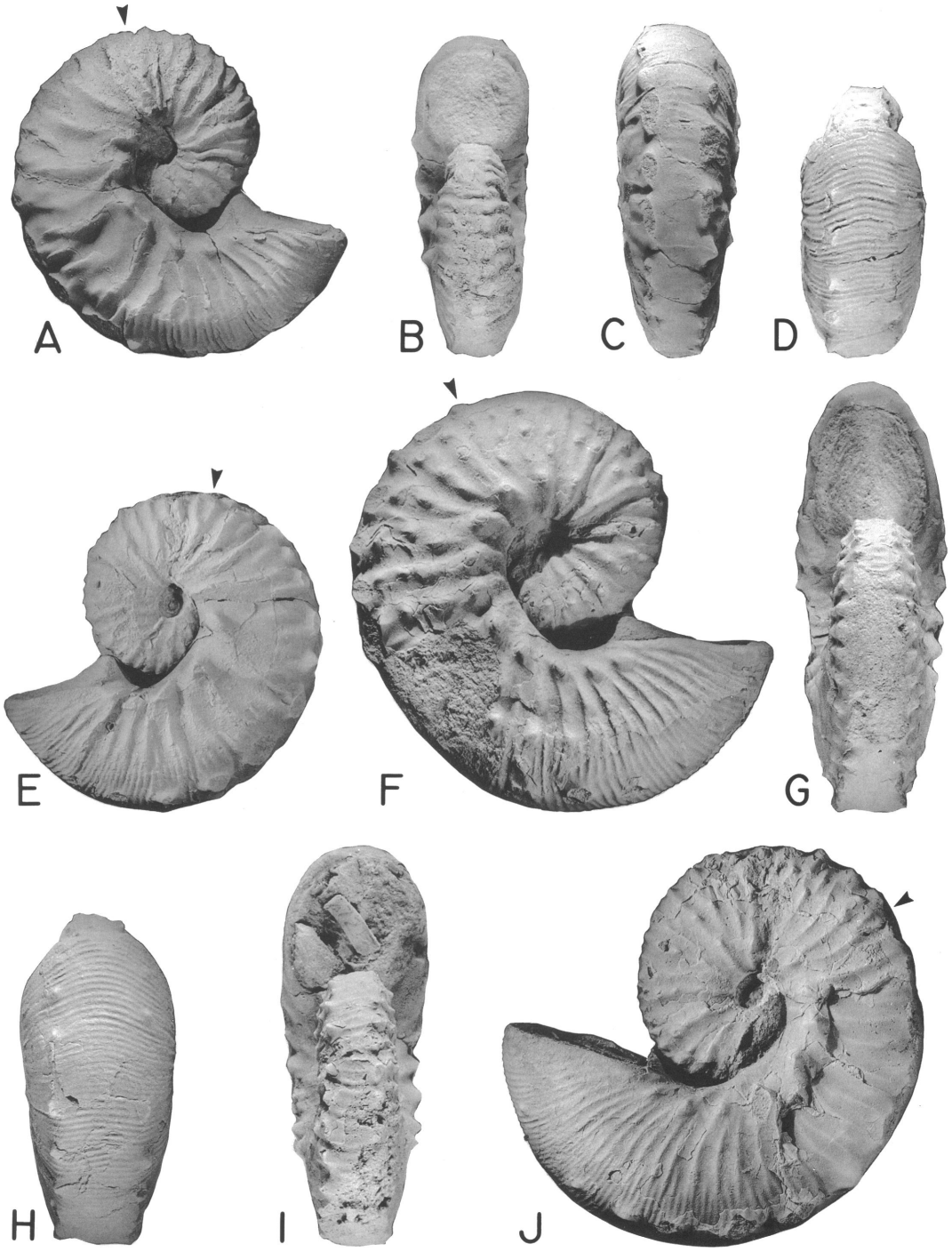

Fig. 146

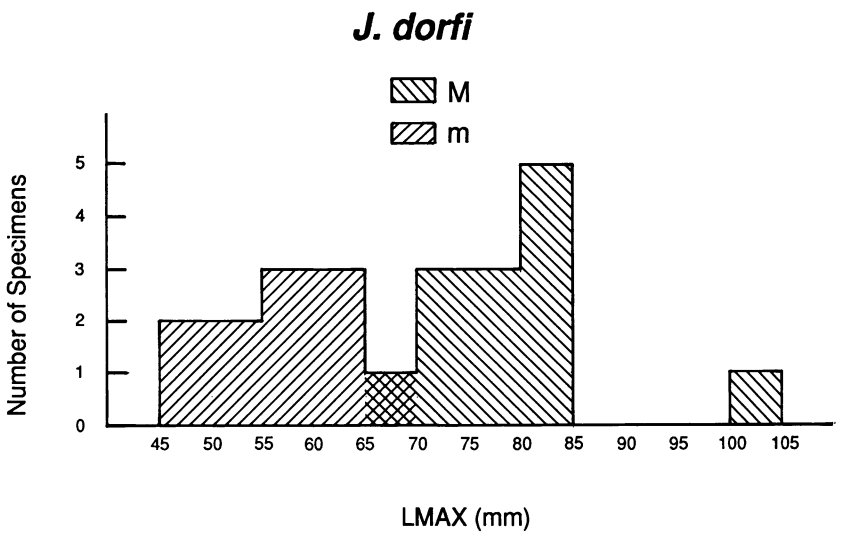

Fig. 147. Size frequency histogram of a sample of *Jeletezkytes dorfi,* n. sp., from the Fox Hills Formation in the Lance Creek–Red Bird area, Wyoming.

phragmocone and conspicuously arched forward on the flanks of the shaft; they increase by intercalation on the dorsal part of the flanks. Ventral ribs show a slight adoral projection. Ribbing is consistently finer on the hook where there are 9 to 10 ventral ribs/cm compared with 5 to 7/cm on the body chamber shaft and phragmocone.

Ventrolateral tubercles are present on the inner whorls and throughout the exposed shell. They are most prominent on the body chamber where they are clavate and projected downward and outward. Almost equally prominent are the bullae that border the umbilical shoulder of the body chamber. Well-defined flank tubercles are not common on the body chamber but do occur, either as an extension of the tubercle rows on the phragmocone (fig. 146F is an example of this) or as incipient bullae on strong ribs. Presence of flank tubercles on the phragmocone is highly variable; commonly one to three rows are present between the ventrolateral and umbilical rows of tubercles. The first flank row to appear is situated next to the ventrolaterals; it is also the most persistent of the

TABLE 16
Adult Measurements of *J. dorfi*[a]

	Macroconch				Microconch			
	N	$\bar{x}$	SD	Range	N	$\bar{x}$	SD	Range
LMAX (mm)	13	78.9	9.27	66.6–104.6	11	57.2	6.04	48.9–65.5
WUS (mm)	7	21.2	3.87	17.2–28.0	8	14.0	1.25	11.7–15.2
HUS (mm)	10	29.4	4.57	23.8–41.0	10	18.4	2.22	15.5–20.9
WUS/HUS	7	0.70	0.101	0.57–0.85	8	0.78	0.076	0.72–0.96
WAPT (mm)	10	26.0	5.2	19.8–36.9	9	20.1	1.87	17.5–23.4
HAPT (mm)	9	27.2	4.58	22.8–37.4	10	21.0	2.27	16.9–23.8
WAPT/HAPT	9	0.93	0.051	0.86–0.99	9	0.96	0.039	0.91–1.04
UD (mm)	10	3.9	1.17	2.5–5.8	8	4.8	0.817	3.5–6.0
UD/LMAX	10	0.05	0.011	0.03–0.07	8	0.09	0.013	0.06–0.10
A (°)	10	66.8	7.72	53.0–81.0				

[a] Abbreviations: see table 1 and figure 9.

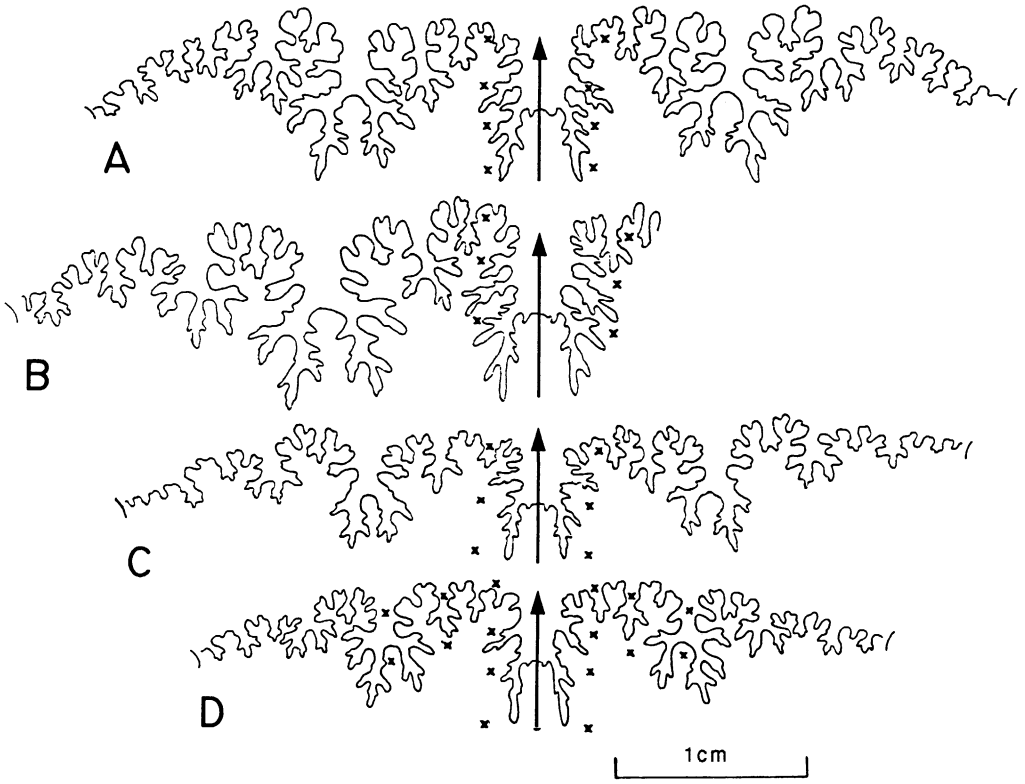

Fig. 148. Sutures of *Jeletzkytes dorfi,* n. sp., macroconchs and microconchs. **A.** Last suture of an adult macroconch, YPM 23179, loc. RB 103, bioturbated sand unit, Fox Hills Fm. **B.** Sixth from last suture of an adult macroconch, YPM 23180, loc. RB 107, bioturbated sand unit, Fox Hills Fm. **C.** Next to last suture of an adult microconch, YPM 27214, loc. RB 103, bioturbated sand unit, Fox Hills Fm. **D.** Fifth from last suture of allotype, an adult microconch, YPM 23212, loc. RB 114, bioturbated sand unit, Fox Hills Fm. Crosses indicate position of tubercles.

flank rows. Flank tubercles are more likely to be present on larger specimens and absent on smaller specimens.

The suture of microconchs is similar to that of macroconchs (fig. 148C, D); narrower lobes reflect the crowding of the suture into the smaller whorl height of the microconch shell. The ventral muscle attachment area is illustrated in figure 145H.

DISCUSSION: All macroconch specimens except one come from concretions in the bluff-forming bioturbated sandstone bed of the Fox Hills Formation (fig. 5). The one exception is from a concretion in clayey siltstone about 50 ft above the base of the Fox Hills relative to the section published by Gill and Cobban (1966: A50). This specimen (YPM 23185, fig. 145A, B) falls within 2 mm of the average size of *J. dorfi*; it is similar to this species in form but not in ornament, having no tubercles on the exposed whorl other than relatively weak ventrolaterals. We include it tentatively under *J. dorfi.*

Jeletzkytes dorfi macroconchs are smaller and generally less robust than those of *J. spedeni*; they also have a slightly longer shaft and hook which result, respectively, in a small (0.5 cm) gap between the hook and phragmocone, not commonly found in *J. spedeni* macroconchs, and in a higher apertural angle. The average umbilical diameter and average ratio of umbilical diameter to shell diameter in *J. dorfi* macroconchs are significantly smaller than the corresponding averages in *J.*

spedeni macroconchs. In their general form, macroconchs of *J. dorfi* are most like compressed macroconchs of *J. spedeni*. However, *J. dorfi* macroconchs differ from compressed *J. spedeni* macroconchs in having more widely spaced primary ribs on the phragmocone and body chamber, and in lacking scattered tubercles on the flanks of the hook. *J. dorfi* macroconchs are readily distinguished from the similarly compressed macroconchs of *J. nebrascensis* by their smaller size, larger apertural angle, smaller umbilicus, smaller whorl height, and much less tuberculate ornamentation. *J. dorfi* microconchs differ from those of *J. spedeni* and *J. nebrascensis* chiefly in their smaller size, smaller umbilicus, and fewer tubercles.

Jeletzkytes dorfi resembles *J. criptonodosus* from the Bearpaw Shale of Canada (Riccardi, 1983) and is morphologically intermediate between this earlier species and *J. spedeni* in the type Fox Hills. *J. dorfi* is similar in size to *J. criptonodosus* but somewhat more compressed. Flank tubercles in *J. criptonodosus* are few and incipient, in contrast to the obvious tuberculation in most *J. dorfi*.

GENUS DISCOSCAPHITES MEEK, 1870 (sensu Jeletzky and Waage, 1978)

TYPE SPECIES: *Ammonites conradi* Morton, 1834: 39, pl. 16, fig. 3, by original designation (see also Meek, 1876: 415; Reeside, 1927: 21–22; Jeletzky and Waage, 1978: 1120–1121).

DIAGNOSIS: Small to medium size, compressed to inflated, highly involute, strongly dimorphic, tuberculate scaphites with one or more rows of flank tubercles in addition to ventrolaterals and umbilicals; ventrolaterals subequal in size to flank tubercles; one or more umbilicals commonly enlarged. Ribs straight to slightly flexed with little or no adoral projection on venter, weaker and more widely spaced on body chamber. Ammonitella ellipsoidal in shape, protoconch somewhat depressed. Ventral muscle attachment area elongate (revised from Jeletzky and Waage, 1978: 1122).

OCCURRENCE: Maastrichtian, probably Upper only, USA Atlantic and Gulf Coastal Plain; Western Interior only in Missouri Valley region of Central Dakotas; possibly south Saskatchewan, Canada.

Discoscaphites conradi (Morton, 1834)

Figures 149–166

Macroconch Synonymy:

Ammonites conradi Morton, 1834: 39, pl. 16, fig. 3.
Discoscaphites roanensis Stephenson, 1941: 428, pl. 90, figs. 1–4.
Discoscaphites conradi conradi (Morton), Jeletzky and Waage, 1978: 1125–1129, pl. 1, figs. 1–6, 14–20.

Microconch Synonymy:

Discoscaphites conradi conradi (Morton), Jeletzky and Waage, 1978: 1125–1129, pl. 1, figs. 9–13.

DIAGNOSIS: Macroconchs compressed, flat-sided with subdued ornament; usually with six to eight rows of tubercles; one or two umbilicals on body chamber commonly enlarged. Microconchs with four to seven rows of tubercles.

TYPES: Holotype, by monotypy, Morton's figured specimen of *Ammonites conradi* (1834: pl. 16, fig. 3), a macroconch. It is in the collections of the Academy of Natural Sciences of Philadelphia (ANSP 51551) and was refigured by Jeletzky and Waage (1978: pl. 1, figs. 1–4).

Allotype, What remains of Morton's small collection at ANSP includes no microconchs of this species. Jeletzky and Waage (1978: 1129, pl. 1, figs. 10–13) selected specimen USNM 250603 from the Prairie Bluff Chalk of Alabama as a typical microconch of *D. conradi*. We consider this specimen the allotype of the species. It is from the same formation as Morton's holotype, but not the same locality.

OCCURRENCE: In the type Fox Hills Formation *Discoscaphites conradi* occurs almost entirely within the Trail City Member, being present in its four assemblage zones and most common in the upper three. In the scantily fossiliferous Upper Elk Butte Member of the Pierre Shale it occurs in the small, local fauna of exceptionally large specimens preserved in sideritic concretions. Relatively few *D. conradi* specimens have been found in the Timber Lake Member.

No other occurrences of *D. conradi* are known from the Western Interior of the United States, and this species appears to be restricted to the Fox Hills Formation in north-central South Dakota and adjacent parts of North Dakota. Jeletzky (1968: 54) reported

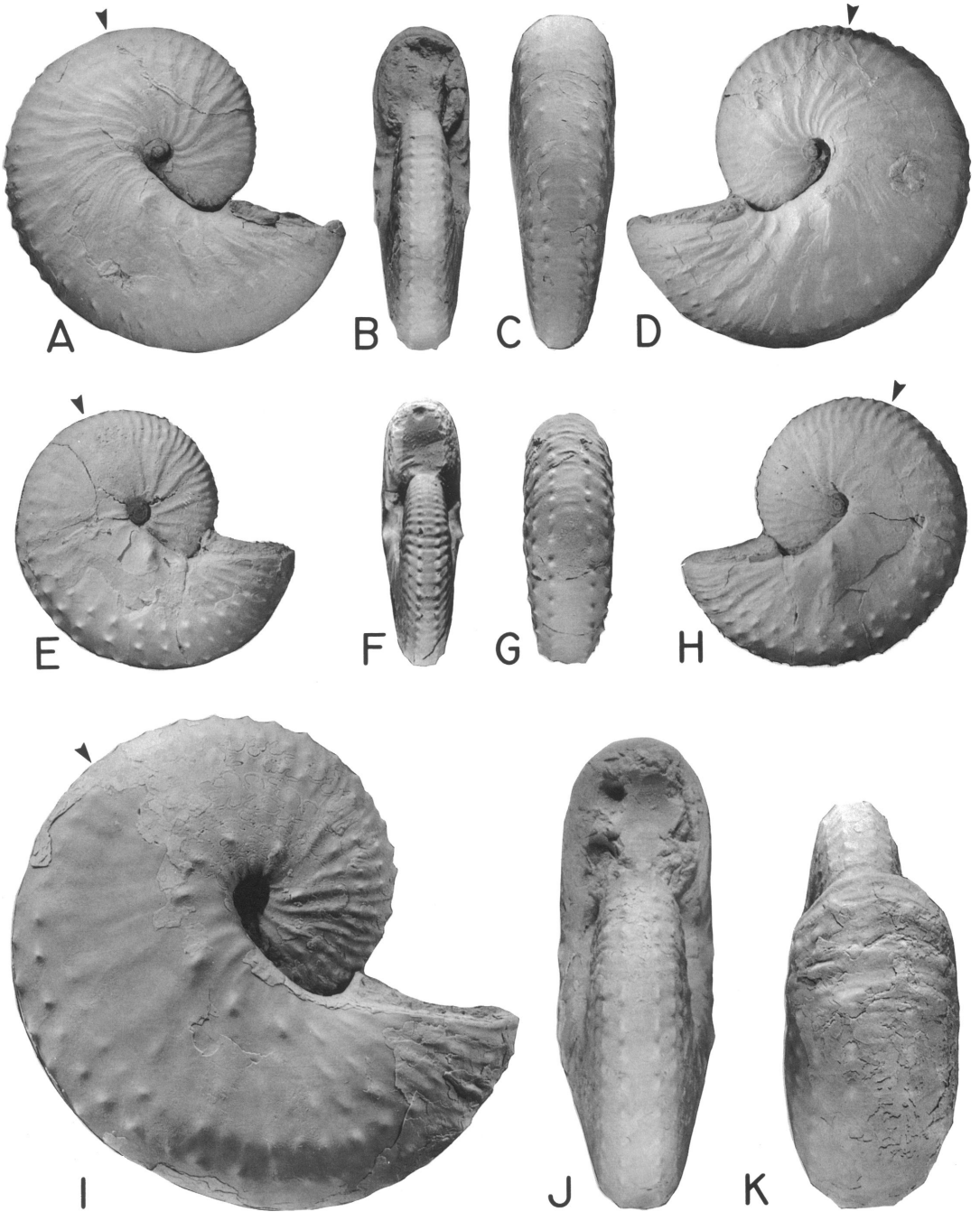

Fig. 149. *Discoscaphites conradi* (Morton) macroconchs. **A–D.** YPM 27182, loc. 25, POAZ. **A,** Right lateral; **B,** apertural; **C,** posterior; **D,** left lateral. **E–H.** YPM 27104, loc. 25, lower TCM float. **E,** Right lateral; **F,** apertural; **G,** posterior; **H,** left lateral. **I–K.** Large variant, YPM 27132, loc. 21, LGAZ. **I,** Right lateral; **J,** apertural; **K,** ventral hook.

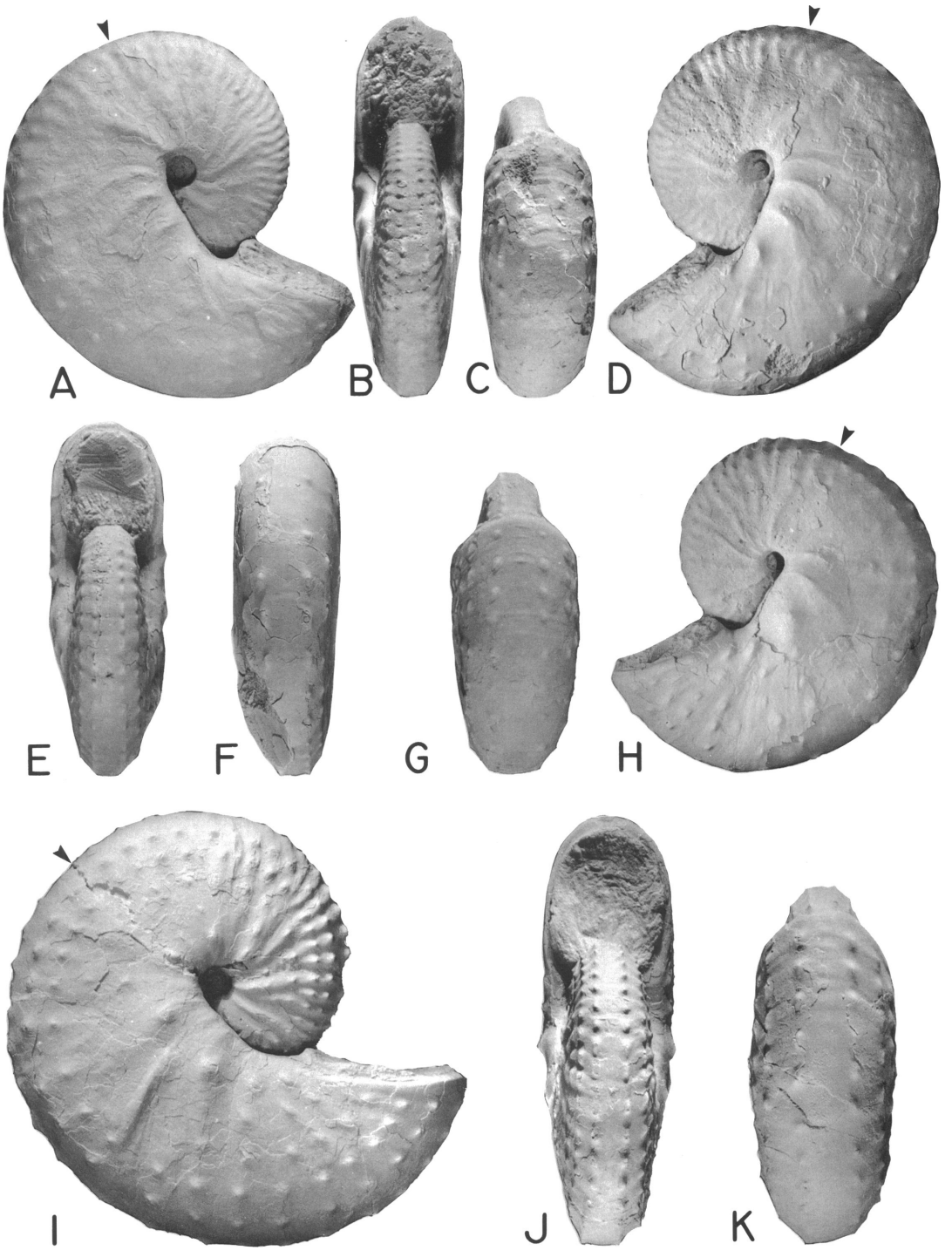

Fig. 150. *Discoscaphites conradi* (Morton) macroconchs. **A–D.** YPM 27185, loc. 62, POAZ. **A,** Right lateral; **B,** apertural; **C,** ventral hook; **D,** left lateral. **E–H.** YPM 27183, loc. 25, LGAZ. **E,** Apertural; **F,** posterior; **G,** ventral hook; **H,** left lateral. **I–K.** YPM 27188, loc. 25, LGAZ. **I,** Right lateral; **J,** apertural; **K,** ventral hook.

"a specimen of *Scaphites* (*Discoscaphites*) ex gr. *roanensis* Stephenson from an unknown locality in southern Saskatchewan . . . presumably collected from the rocks of the *Baculites grandis* Zone." This specimen, later illustrated (Jeletzky, 1970: 661, pl. 27, fig. 10a, b), is a fragment preserving adjoining parts of the phragmocone and body chamber. It resembles *D. conradi* in its compressed form and distribution of ribs and tubercles but it is too incomplete for positive identification. If it is a discoscaphite, it is unlikely to have come from strata of the *Baculites grandis* Zone.

The occurrence of *D. conradi* in the Prairie Bluff Chalk of the Mississippi embayment has already been noted. It is present also, but apparently not common, in the Kemp Clay and Corsicana Marl of the Gulf Coastal Plain in Texas (Stephenson, 1941: 429–430, pl. 90, figs. 1–4; pl. 91, fig. 6). *D. conradi* also occurs in the Severn Formation of the Monmouth Group in the Atlantic Coastal Plain of Maryland. A single small fragment in the YPM collections is either part of the inner whorls of *D. conradi,* or a specimen of *D. rossi,* n. sp., lacking the body chamber. The generally co-occurring species *D. gulosus* is also present in the Severn Formation.

The Severn specimens referred to by Jeletzky and Waage (1978: 1120) from Brightseat, Maryland, are *D. gulosus* as here defined. The specimen figured by Gardner (1916: pl. 12, fig. 1) as *D. conradi* from Brightseat is a *Jeletzkytes* fragment.

MATERIAL: Over 400 specimens of *Discoscaphites conradi* were collected from the Fox Hills Formation in its type area, most of them from the Trail City Member. Of these 213 are macroconchs and 189 are microconchs; about 100 of each of the dimorphs are complete or nearly complete. Of these, 31 macroconchs and 30 microconchs comprise the set of measured specimens. The collection was supplemented by about 30 specimens borrowed from the USNM and Denver Branch of the USGS, and by 12 specimens borrowed from BHI.

MACROCONCH DESCRIPTION: Dimensions of the measured specimens are listed in table 17. LMAX averages 60.0 mm. The size distribution is approximately normal with a peak at 50–55 mm (fig. 155). The ratio of the size of the largest specimen to that of the smallest is 2.55. In general, a variation series exists from small, weakly ornamented forms to larger, more coarsely ornamented ones. Large end-members approach *D. gulosus* and a few specimens may appear intermediate between the two species among Western Interior *Discoscaphites* as well as among those in the Prairie Bluff Chalk (Jeletzky and Waage, 1978: 1125). However, *D. conradi* macroconchs are characterized by a number of features that distinguish them from the stout and more strongly ornamented macroconchs of *D. gulosus.* These features persist throughout their joint stratigraphic range and we therefore consider *D. conradi* and *D. gulosus* as separate species.

D. conradi macroconchs are tightly coiled, with a short shaft, which is arcuate on the venter, and a hook in contact with the phragmocone. The dorsal lip and its projection are pressed tightly against the venter of the adjacent phragmocone and commonly wrapped around it as far as the first row of flank tubercles. The body chamber and exposed phragmocone are approximately 0.6 whorls and 0.45 whorls in angular length, respectively.

The umbilical diameter and ratio of umbilical diameter to shell diameter average 3.8 mm and 0.06, respectively (table 17). The

→

Fig. 151. *Discoscaphites conradi* (Morton) macroconchs. **A–E.** USNM 468859, loc. D2578, LGAZ. **A,** Right lateral; **B,** left lateral; **C,** apertural; **D,** posterior; **E,** ventral hook. **F–H.** YPM 27187, loc. 200, POAZ. **F,** Right lateral; **G,** posterior; **H,** ventral hook.

Fig. 152. *Discoscaphites conradi* (Morton) macroconchs and microconchs. **A, C, D.** Macroconch, large variant, YPM 27186, loc. 25, LGAZ. **A,** Right lateral; **C,** left lateral; **D,** apertural. **B, E.** Macroconch, YPM 27184, loc. 21, LGAZ. **B,** Right lateral; **E,** uncoated venter showing ventral muscle attachment area (arrow), ×1.75. **F, G.** Very small microconch, YPM 27195, loc. 25, LGAZ. **F,** Right lateral; **G,** apertural. **H–J.** Microconch, YPM 27129, loc. 86, POAZ. **H,** Right lateral; **I,** apertural; **J,** left lateral. **K–M.** Microconch, YPM 27198, loc. 25, lower TCM float. **K,** Apertural; **L,** ventral hook; **M,** left lateral.

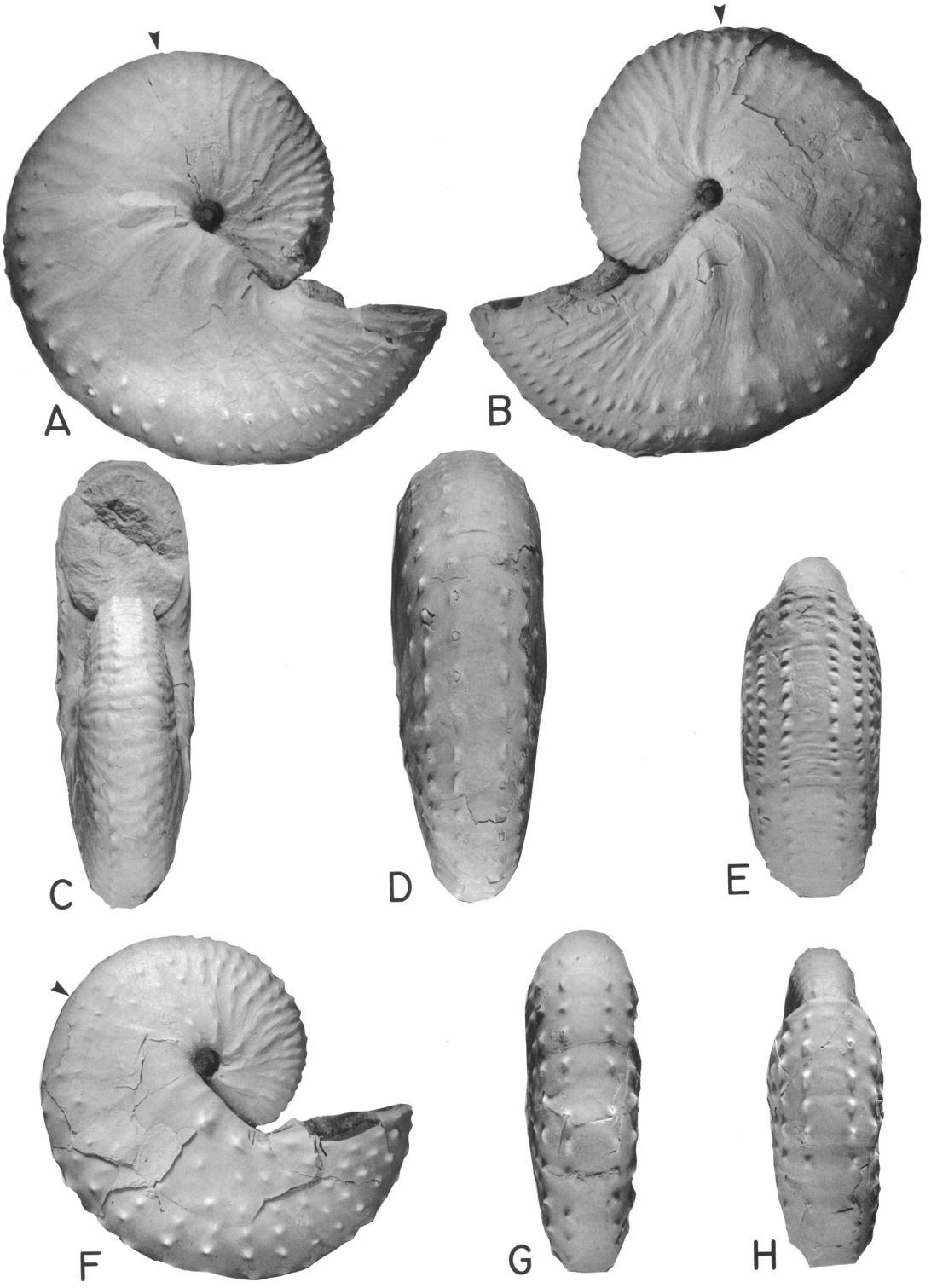

Fig. 151

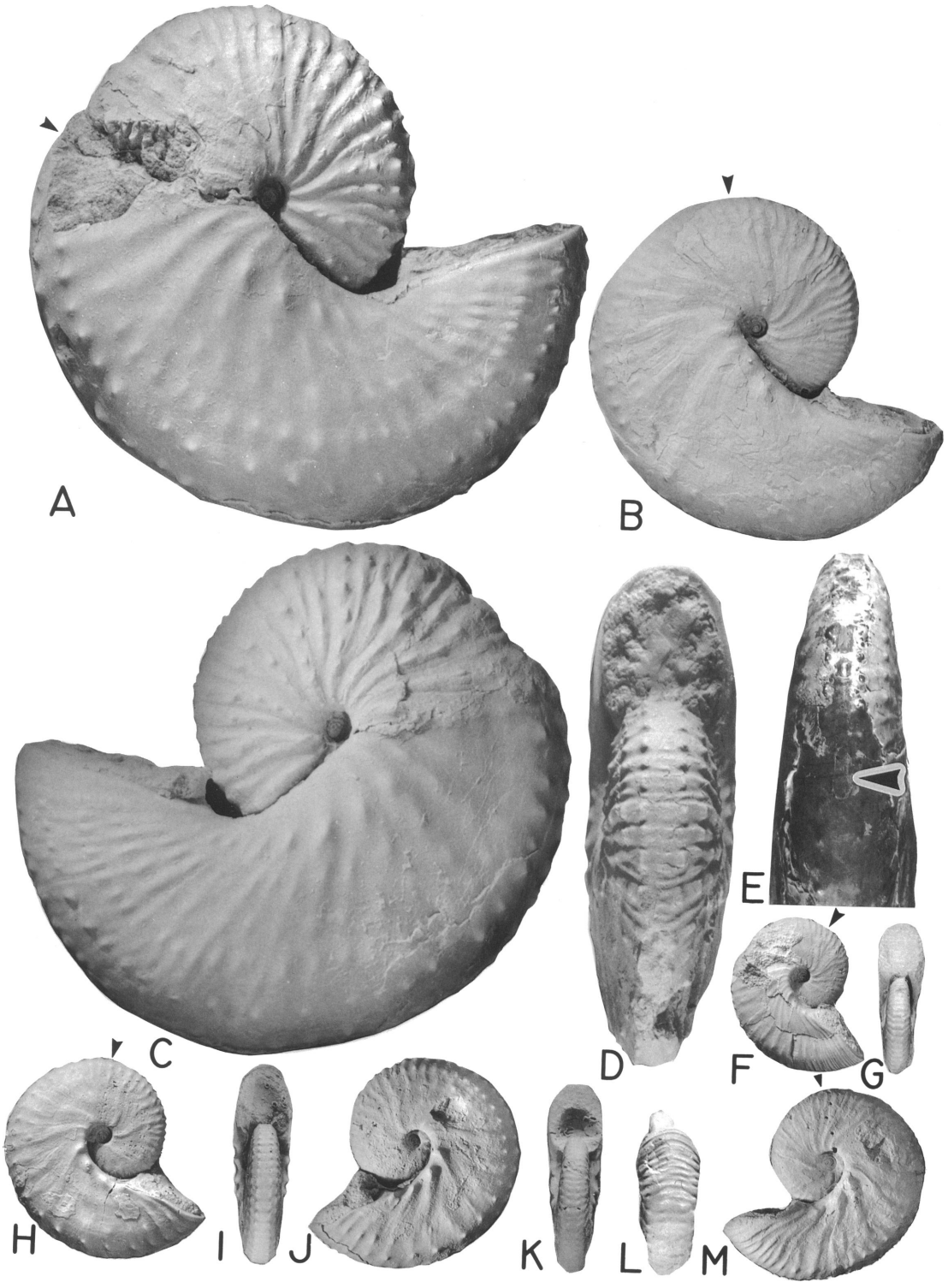

Fig. 152

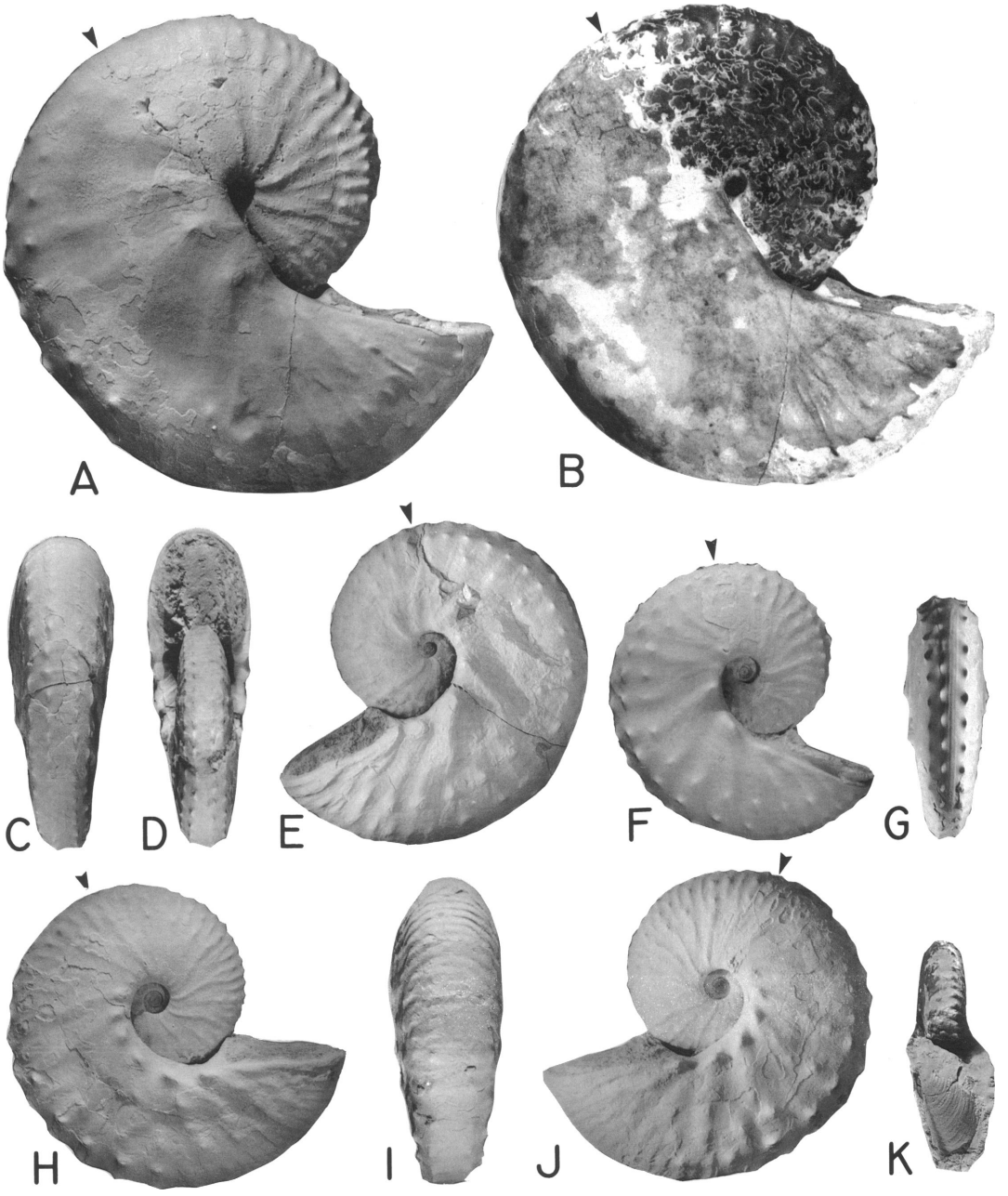

Fig. 153. *Discoscaphites conradi* (Morton) macroconch and microconchs. **A, B.** Macroconch, YPM 27128, loc. 256, LGAZ. **A,** Right lateral; **B,** same, uncoated to show sutures. **C–E.** Microconch, YPM 27219, loc. 25, POAZ float. **C,** Posterior; **D,** apertural; **E,** left lateral. **F, G.** Microconch, YPM 27106, loc. 216, LGAZ float. **F,** Right lateral; **G,** posterodorsal showing fine ventral ridges. **H–J.** Microconch, YPM 27127, loc. 25, LGAZ. **H,** Right lateral; **I,** posterior; **J,** left lateral. **K.** Incomplete microconch, hook removed to reveal lower mandible in body chamber, YPM 27133, loc. 25, LNAZ.

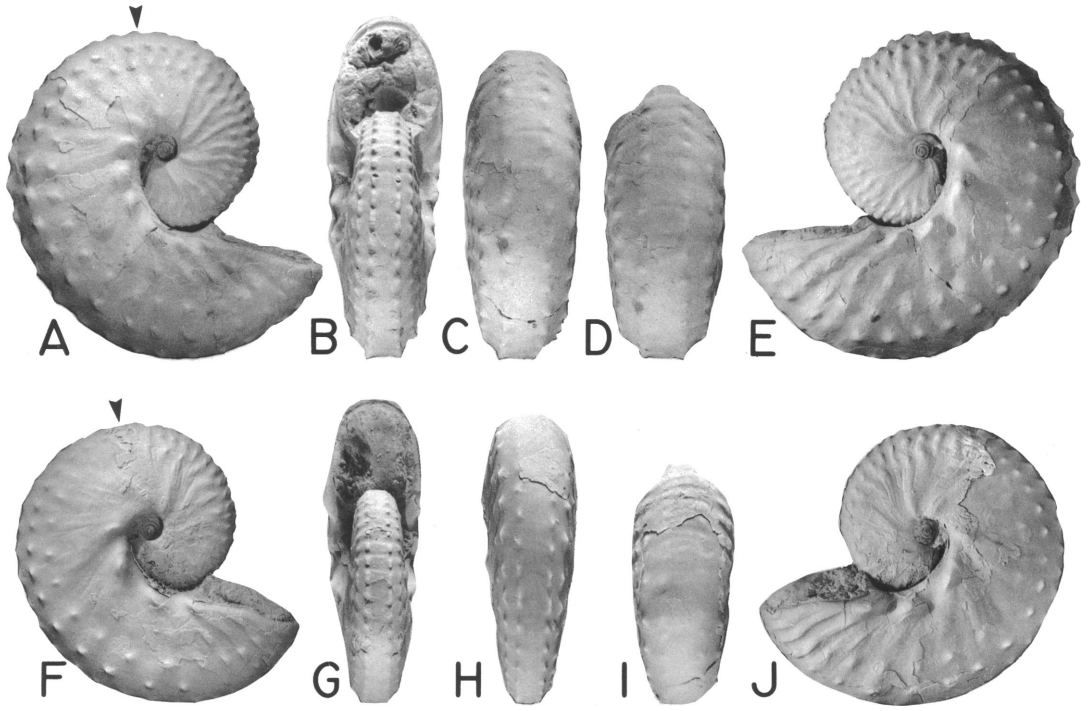

Fig. 154. *Discoscaphites conradi* (Morton) microconchs. **A–E.** Relatively stout specimen, YPM 27197, loc. 25, lower TCM float. **A,** Right lateral; **B,** apertural; **C,** posteroventral; **D,** ventral hook; **E,** left lateral. **F–J.** YPM 27196, loc. 62, LNAZ. **F,** Right lateral; **G,** apertural; **H,** posterior; **I,** ventral hook; **J,** left lateral.

ratio of umbilical diameter to shell diameter does not vary consistently with adult size. Both the exposed phragmocone and body chamber are compressed and essentially flat-sided. The ratios of whorl width to whorl height at the ultimate septum and at the aperture average 0.63 and 0.84, respectively, indicating a significantly more depressed whorl section at the aperture than at the ultimate septum. The degree of compression of the shell is approximately the same in all specimens, regardless of size (figs. 156, 157).

TABLE 17
Adult Measurements of *D. conradi*[a]

	Macroconch				Microconch			
	N	$\bar{x}$	SD	Range	N	$\bar{x}$	SD	Range
LMAX (mm)	31	60.0	13.32	35.5–90.7	30	39.4	7.27	25.3–53.4
WUS (mm)	31	13.8	3.82	7.5–22.1	30	8.3	2.09	4.5–11.7
HUS (mm)	31	21.8	5.57	11.5–34.2	30	12.6	2.69	7.2–17.4
WUS/HUS	31	0.63	0.060	0.55–0.84	30	0.66	0.058	0.55–0.82
WAPT (mm)	30	18.4	4.23	10.1–29.2	30	12.4	2.56	7.8–17.2
HAPT (mm)	30	21.9	4.29	12.4–30.7	30	15.2	2.51	11.1–20.1
WAPT/HAPT	30	0.84	0.068	0.63–1.00	30	0.82	0.089	0.51–0.99
UD (mm)	30	3.8	0.83	1.9–5.0	29	3.5	0.56	2.3–4.8
UD/LMAX	30	0.06	0.011	0.04–0.08	29	0.09	0.008	0.07–0.11
A (°)	19	47.2	6.25	37.0–56.0				

[a] Abbreviations: see table 1 and figure 9.

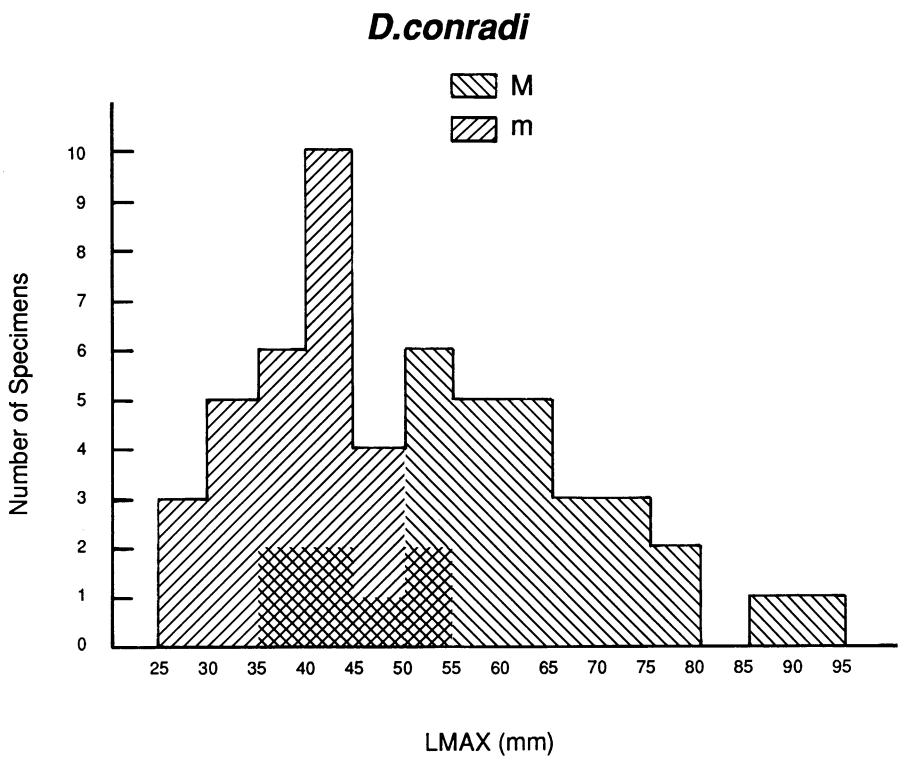

Fig. 155. Size frequency histogram of a sample of *Discoscaphites conradi* (Morton) from the Fox Hills Formation in its type area.

Ribbing on the exposed phragmocone and body chamber is slightly prorsiradiate, straight to weakly sinuous, and increases both by branching and intercalation, mostly on the ventral half of the whorl. The ratio of the number of dorsal to ventral ribs is about 1:4. Rib spacing is approximated except on the shaft of the body chamber where ribs are more widely spaced, and on the apertural part of the hook where they are finer and more closely spaced. However, the very fine, closely spaced ribbing found on the anterior part of the body chamber in *Hoploscaphites* and *Jeletzkytes* does not appear in *Discoscaphites.* Where ribs cross the venter, they subdivide into two smaller ribs, which join opposite ventrolateral tubercles. Additional small ribs may develop between these rib pairs. Ribs show a very slight adoral projection on the venter of the hook, but rarely elsewhere.

Tubercles occur on ribs in distinct rows parallel to the venter, and are usually present on every rib throughout the extent of the row. Tubercles are commonly bullate on the anterior part of the body chamber if the ribbing is well defined there (fig. 151A, B). The ventrolateral tubercle row and the first row of flank tubercles adjacent to it are also present on the inner whorls (see ontogeny of *D. conradi,* p. 209, for a more complete description of the ornament of the inner whorls). The row of umbilical tubercles is generally restricted to the end of the phragmocone and body chamber. These three rows, umbilical, ventrolateral, and first flank, usually occur on all macroconchs except for very small specimens with subdued sculpture in which the first row of flank tubercles may only first appear near the end of the phragmocone. In weakly ornamented specimens from the Western Interior, only the ventrolateral tubercle row and adjacent row of flank tubercles are present on the body chamber and exposed phragmocone; in more strongly ornamented specimens there are at least two additional rows of flank tubercles. The number of rows appears to increase with whorl height and large specimens may show as many as four.

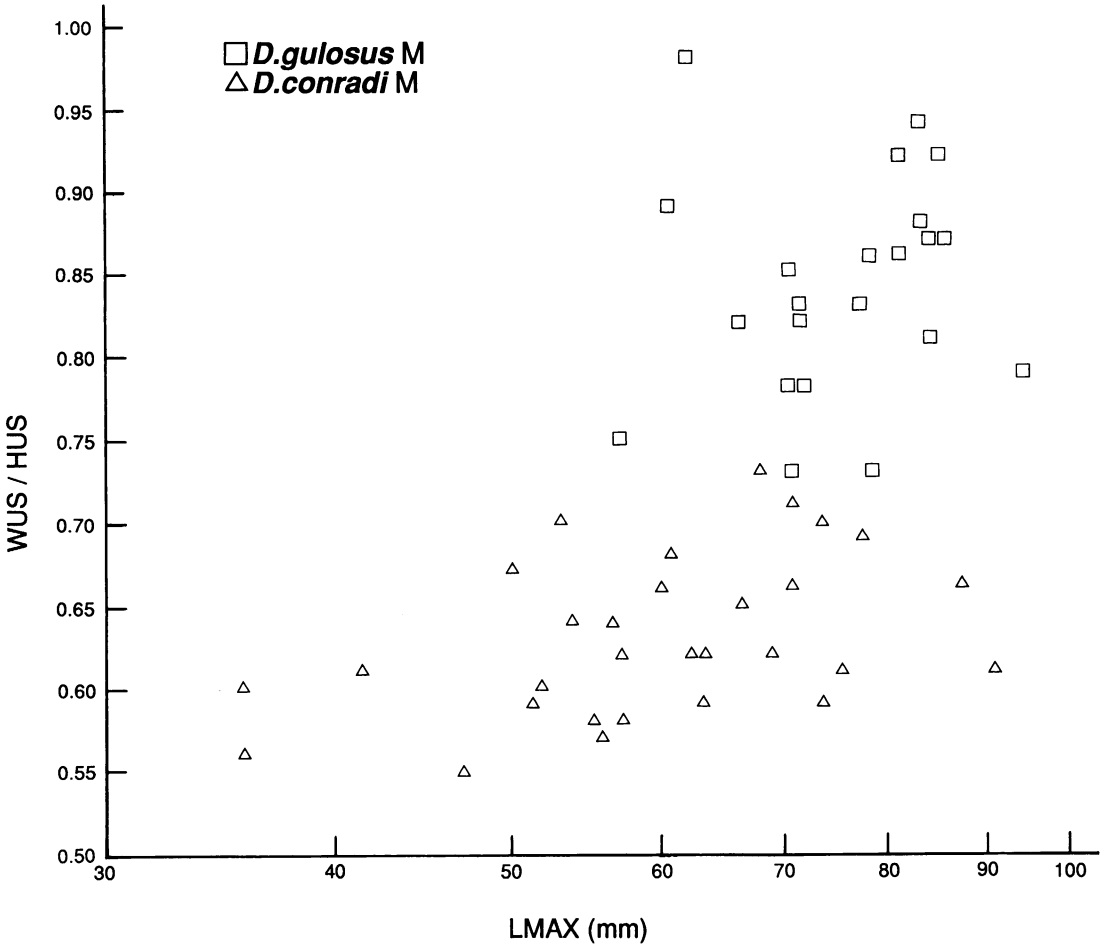

Fig. 156. Scatter plot of the ratio of whorl width to whorl height at the ultimate septum (WUS/HUS) versus maximum length (LMAX) in adult macroconchs of *Discoscaphites conradi* (Morton) and *D. gulosus* (Morton).

Umbilical tubercles are commonly bullate, and include an enlarged tubercle, usually the second or third from the aperture, which is characteristic of the species. In sharp contrast with *Hoploscaphites* and *Jeletzkytes,* ventrolateral tubercles in *Discoscaphites* are only slightly larger than flank tubercles. Flank tubercles of the row just adjacent to that of the ventrolaterals are generally subequal in size to the ventrolaterals. Tubercles of both these latter rows may be clavate in form on some specimens (fig. 151F–H) and bullate on others (fig. 152A, C).

The suture of *D. conradi* macroconchs is typically scaphitid and has an asymmetric first lateral lobe, resulting from enlargement of the inner of its two branches (fig. 158A–C). However, this character varies and in some specimens, the two branches are approximately equal and the lobe is more symmetric. The lateral lobe is commonly almost as large as or larger than the ventral lobe, whereas in most scaphitid sutures, the ventral lobe is larger than the first lateral lobe. Folioles of sutures of species of *Discoscaphites* appear slightly more inflated than those of *Hoploscaphites* and *Jeletzkytes.*

The ventral muscle attachment area just adoral of the ultimate septum is narrow and elongate with bluntly rounded ends (fig. 152E). Internal molds also commonly show a very faint, low, rounded ridge, usually tri-

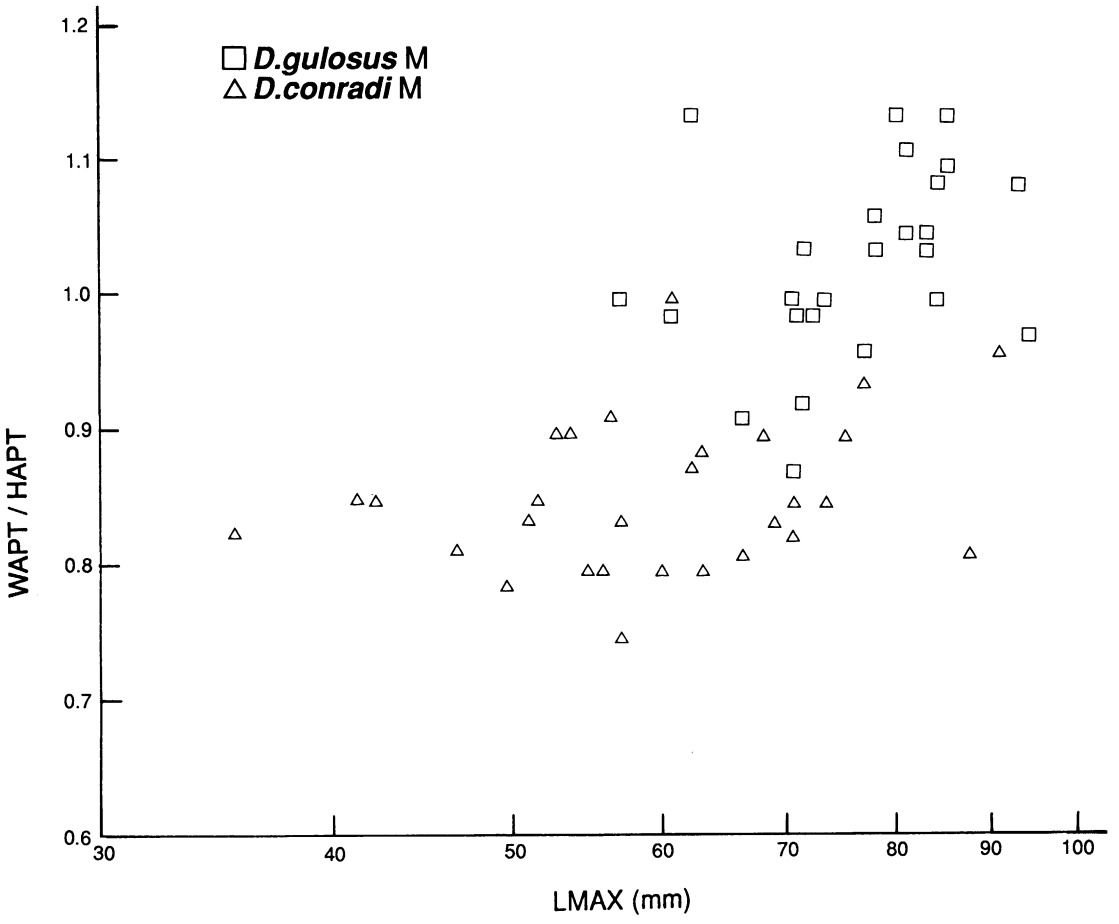

Fig. 157. Scatter plot of the ratio of whorl width to whorl height at the aperture (WAPT/HAPT) versus maximum length (LMAX) in adult macroconchs of *Discoscaphites conradi* and *D. gulosus* (Morton).

partite, running longitudinally along the venter of the body chamber and extending to or close to the aperture (fig. 153G). This feature, which must correspond to a groove on the internal shell surface, was first noted in Morton's (1834: 39) original description of *Ammonites conradi.*

MICROCONCH DESCRIPTION: Adult microconchs average 39.4 mm in size and approximately conform to a normal distribution (table 17, fig. 155). The ratio of the size of the largest specimen to that of the smallest is 2.11. The average size is significantly smaller than that in macroconchs; the ratio of the average size of macroconchs to that of microconchs is 1.54. Dimorphs overlap in size between 35 and 55 mm. As in macroconchs, there is a slight variation series from smaller forms with subdued ornament to larger forms with stronger ornament. Larger microconchs appear transitional to microconchs of *D. gulosus,* their separation being somewhat less marked than that in macroconchs. However, *D. conradi* microconchs have a number of distinct features, notably a compressed whorl section, that distinguish them from microconchs of *D. gulosus.* The ratios of whorl width to whorl height at the ultimate septum and at the aperture average 0.66 and 0.82, respectively, and are not significantly different from the averages of the corresponding ratios in *D. conradi* macroconchs, which are 0.63 and 0.84, respectively (table 17). The degree of compression of the shell in micro-

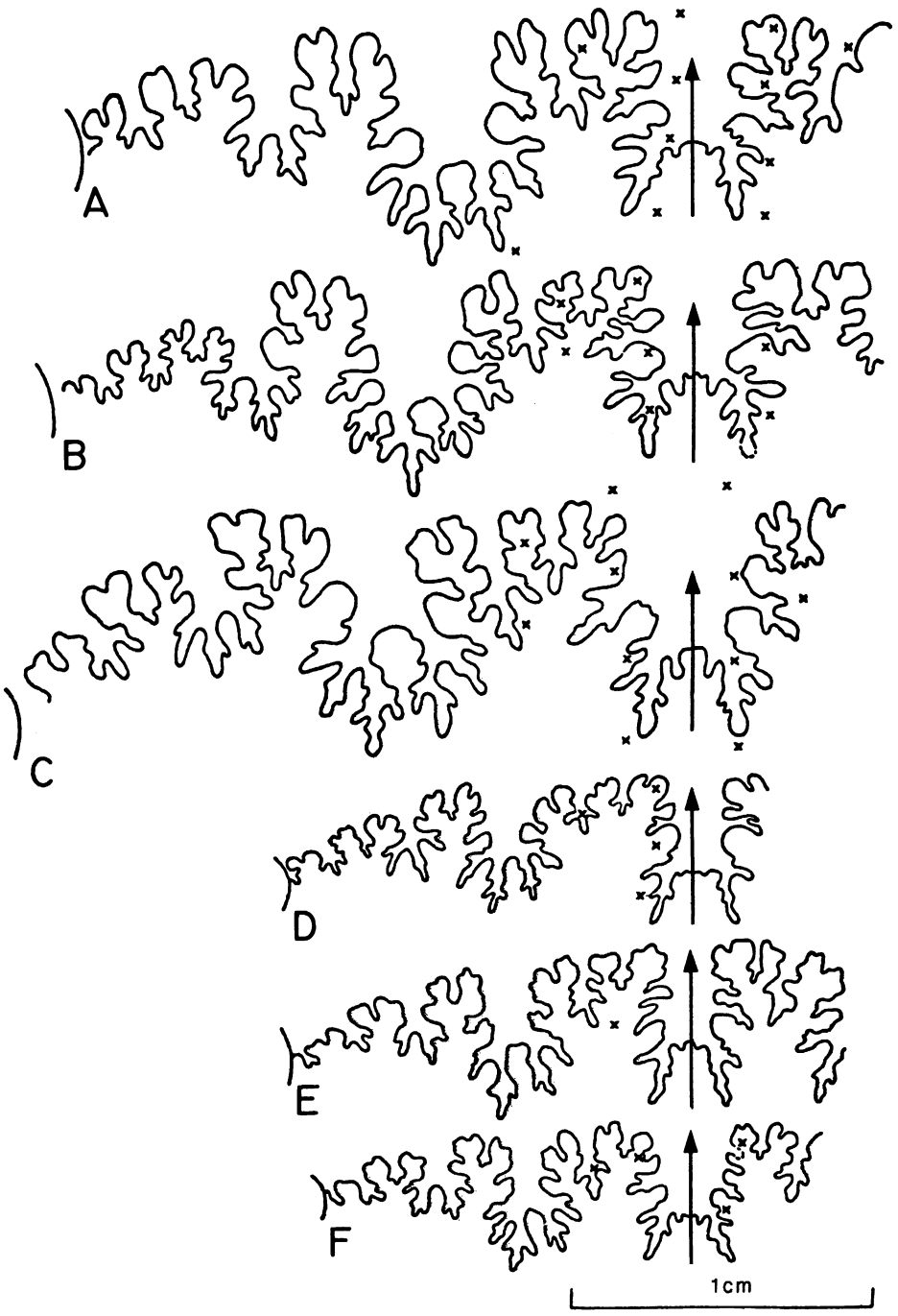

Fig. 158. Sutures of *Discoscaphites conradi* (Morton) macroconchs and microconchs. **A.** Third from last suture of an adult macroconch, YPM 27103, loc. 25, TCM. **B.** Third from last suture of an adult macroconch, YPM 27120, loc. 50, LGAZ. **C.** Fourth or fifth from last suture of an adult macroconch, YPM 27115, loc. 53, LGAZ. **D.** Fifth from last suture of an adult microconch, YPM 27112, loc. 19, TCM. **E.** Fourth from last suture of an adult microconch, YPM 27102, loc. 25, POAZ. **F.** Fourth from last suture of an adult microconch, YPM 27111, loc. 25, LGAZ. Crosses indicate position of tubercles.

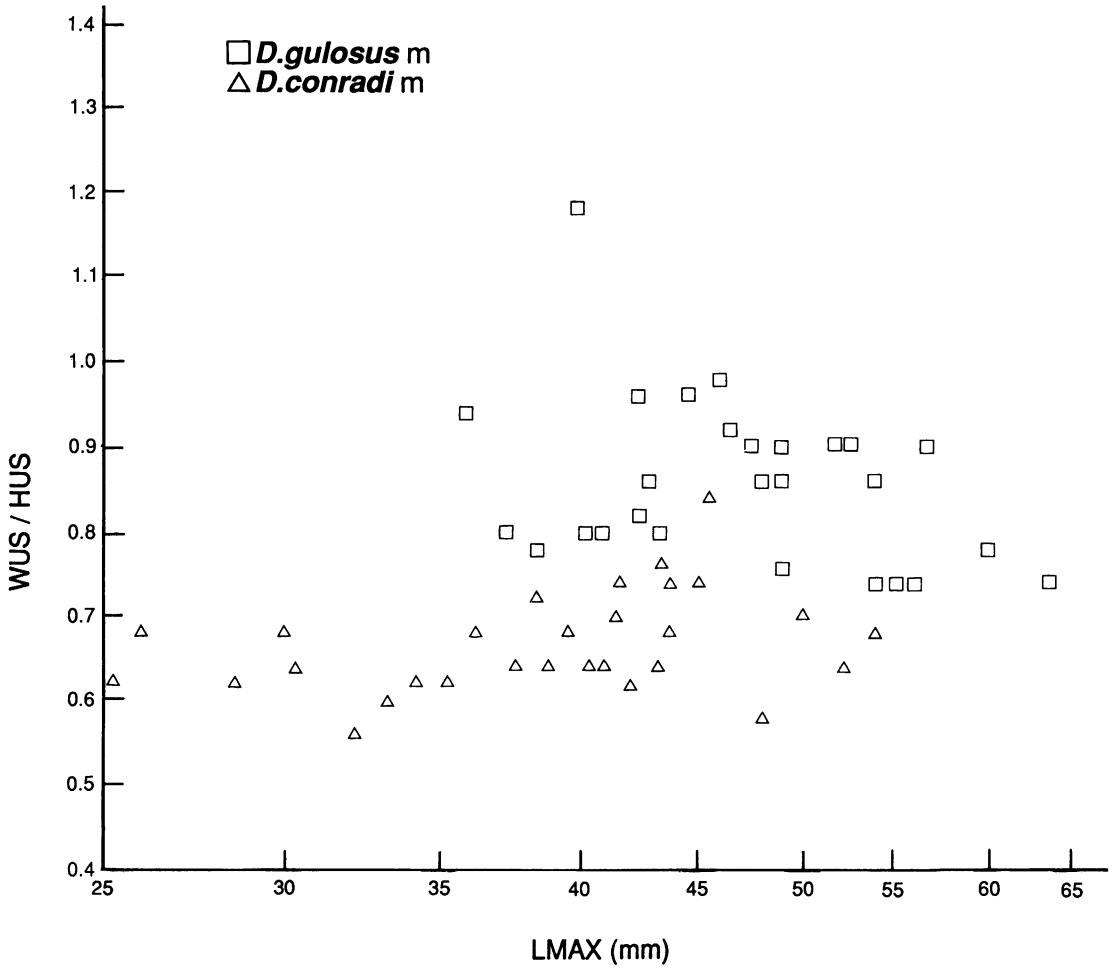

Fig. 159. Plot of the ratio of whorl width to whorl height at the ultimate septum (WUS/HUS) versus maximum length (LMAX) in adult microconchs of *D. conradi* (Morton) and *D. gulosus* (Morton).

conchs is approximately the same in all specimens, regardless of size (figs. 159, 160).

Microconchs are as tightly coiled as macroconchs with the hook in close contact with the phragmocone. The body chamber and exposed phragmocone are approximately 0.65 and 0.40 whorls in angular length, respectively. The umbilical diameter averages 3.5 mm, which is not significantly different from that in macroconchs (3.8 mm). Larger microconchs have relatively smaller umbilical diameters than smaller microconchs. The ratio of umbilical diameter to shell diameter averages 0.09, which is significantly higher than that in macroconchs (0.06). The umbilical shoulder of the body chamber in microconchs follows the curve of the venter and forms a flat dorsal shelf, nearly normal to the flanks, inside the row of umbilical bullae.

The pattern and distribution of ribs and tubercles in microconchs is similar to that in macroconchs. Rows of flank tubercles seldom exceed three; the enlarged umbilical tubercle is not consistently present; when present, it is not always near the aperture. The suture of microconchs is like that of macroconchs (fig. 158D–F).

ONTOGENY: Measurements of the ammonitella of *D. conradi* are listed in table 3. The low average of the protoconch angle (54°) reflects the depressed protoconch and ellipsoidal ammonitella characteristic of this ge-

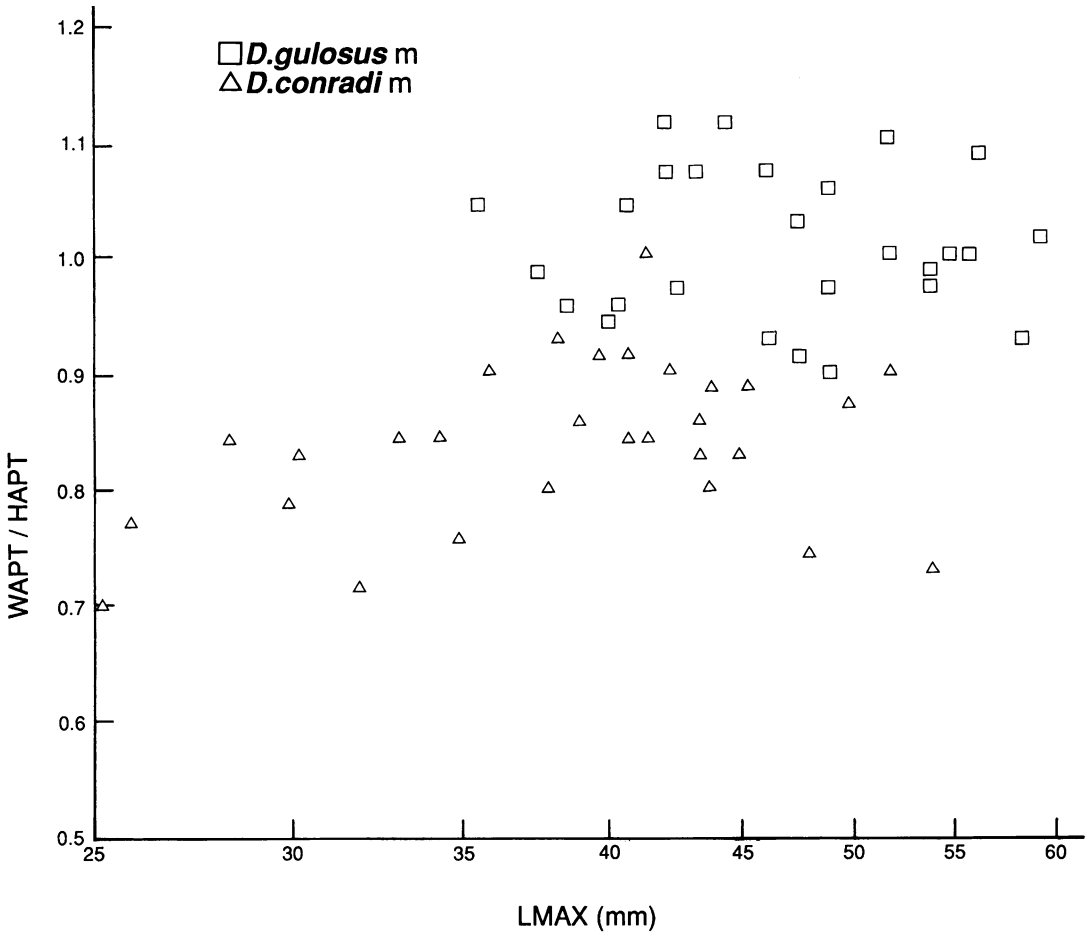

Fig. 160. Plot of the ratio of whorl width to whorl height at the aperture (WAPT/HAPT) versus maximum length (LMAX) in adult microconchs of *Discoscaphites conradi* (Morton) and *D. gulosus* (Morton).

nus. The ammonitella diameter averages 738 μm in macroconchs, which is similar to that in microconchs (746 μm). The size of the ammonitella in *D. conradi* is similar to that in other scaphite species (Landman, 1987).

Dorsoventral, mostly intercostal cross sections of macro- and microconchs are illustrated in figure 161. The shell flanks are initially flat and slant inward toward the umbilicus. The postembryonic growth of whorl width is negatively allometric in both dimorphs (slopes range from 0.7242 to 0.8642) and shows a slight change at approximately 5 mm shell diameter (fig. 162). In contrast, the postembryonic growth of whorl height is positively allometric in both dimorphs (slopes range from 1.1236 to 1.1857; fig. 163). At comparable shell diameters, the values of whorl width and whorl height in macroconchs are approximately the same as those in microconchs. The whorls become increasingly more compressed during ontogeny in both dimorphs; the ratio of whorl width to whorl height ranges from 1.0 to 2.0 up to approximately 5 mm shell diameter and decreases to a minimum of 0.6 to 0.7 near the base of the mature body chamber.

The growth of umbilical diameter is negatively allometric (fig. 164). Until the onset of maturity, the values of umbilical diameter at the same shell diameter are similar in both

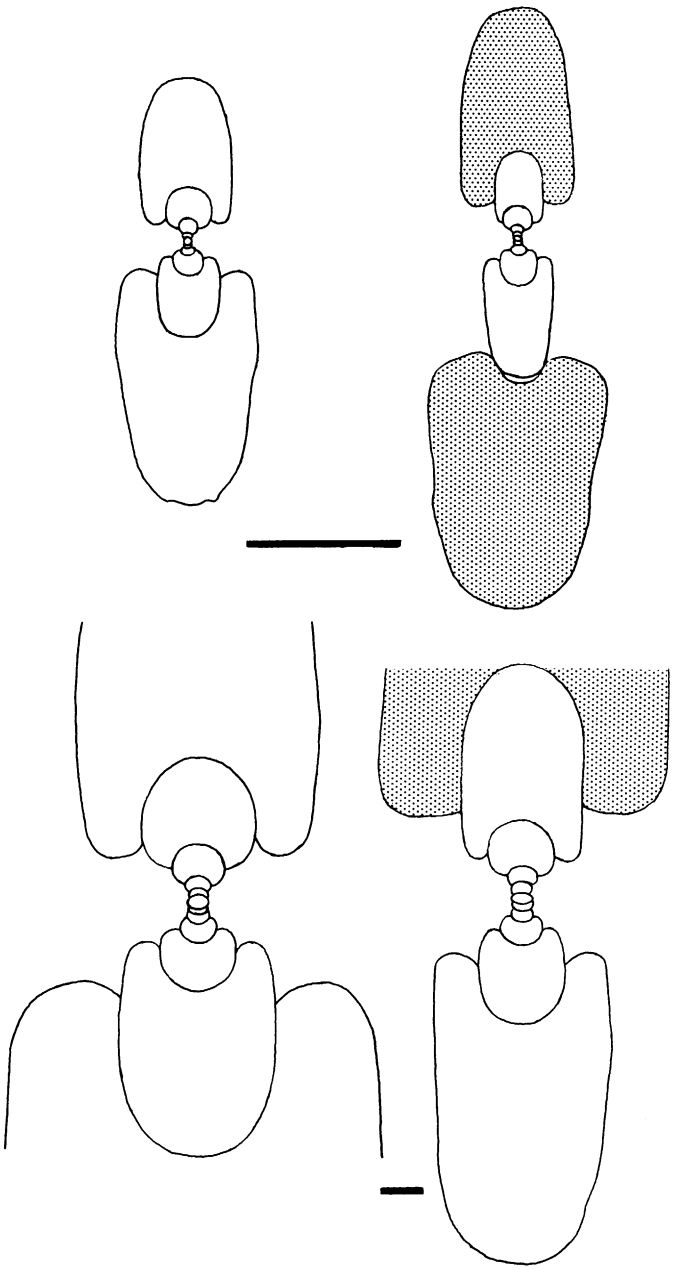

Fig. 161. Dorsoventral, mostly intercostal cross sections through adult dimorphs of *Discoscaphites conradi* (Morton). **Left.** Macroconch, YPM 34100, loc. 197, TCM. **Right.** Microconch, AMNH 44232, loc. 3158, Fox Hills Fm. Shaded area demarcates mature body chamber. Upper scale bar = 1 cm; lower scale bar = 1 mm.

dimorphs. However, at approximately one whorl before the base of the mature body chamber, the umbilical diameter in macroconchs begins to increase more slowly than that in microconchs. The ratio of umbilical diameter to shell diameter steadily decreases throughout most of postembryonic growth and reaches a minimum near the base of the mature body chamber of 0.14 to 0.18 in microconchs and 0.08 to 0.11 in macroconchs.

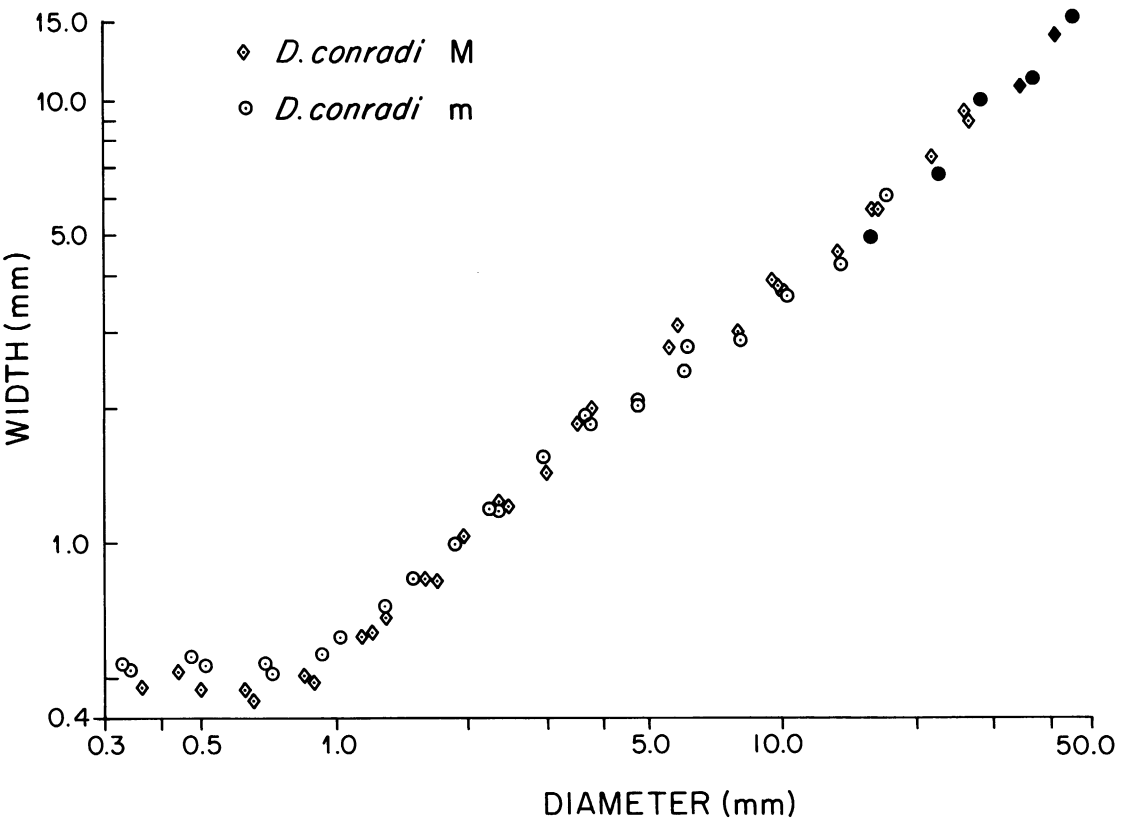

Fig. 162. Plot of whorl width versus shell diameter through the ontogeny of six adults (three macroconchs and three microconchs) of *Discoscaphites conradi* (Morton). Black symbols indicate measurements near the base of or in the mature body chamber. Measurements listed in Appendix II.

The ontogenetic development of ornament in *D. conradi* is illustrated in figure 165 and is more or less the same in both dimorphs. Ribs appear on the venter and on the flanks (primaries) at approximately 4 mm shell diameter. The primary ribs are weak to strong and prorsiradiate. They become slightly flexuous during ontogeny and are accompanied by long, flexuous lirae. The ventral ribs are weak, becoming stronger during growth, and show only a slight forward projection. Secondaries develop by both intercalation and branching. The ratio of the number of dorsal to ventral ribs is approximately 1:3 up to the point of exposure.

Small ventrolateral tubercles appear on every rib at approximately 10–15 mm shell diameter (approximately 0.25 whorls before the point of exposure). Coincident with the appearance of these tubercles is a weakening of the adoral projection of the ventral ribs. Flank tubercles, which are subequal in size to ventrolaterals, may also appear before the point of exposure, imparting an angular aspect to the costal whorl section. The flank tubercles occur in spiral rows, but unlike ventrolaterals, they may not be present on every rib. Both ventrolaterals and flank tubercles may first appear only on the exposed phragmocone of smaller specimens, mainly microconchs.

Primaries on the exposed phragmocone are weak to strong, prorsiradiate, slightly flexuous, and accompanied by thin flexuous lirae. Primaries may become bullate near the umbilicus toward the end of the phragmocone. Secondaries develop by both intercalation and branching and seem to arise more commonly on the ventral half of the flanks. The ratio of the number of dorsal to ventral ribs is ap-

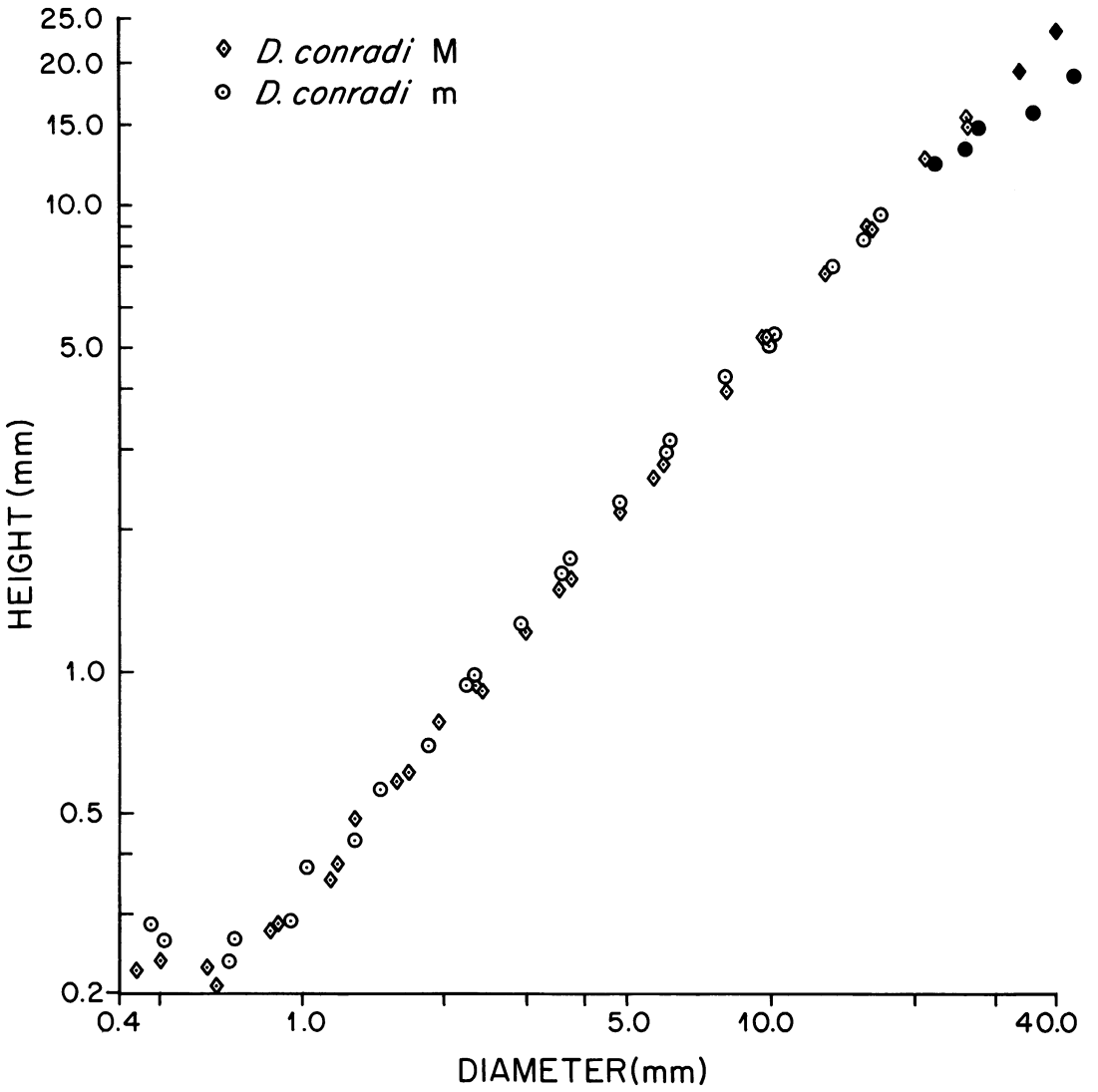

Fig. 163. Plot of whorl height versus shell diameter through the ontogeny of six adults (three macroconchs and three microconchs) of *Discoscaphites conradi* (Morton). Black symbols indicate measurements near the base of or in the mature body chamber. Measurements listed in Appendix II.

proximately 1:4 on the exposed phragmocone of macroconchs, slightly less on that of microconchs.

The pattern of septal approximation was examined in six macroconchs and nine microconchs of *D. conradi* (table 18). Interseptal distances of as many as the last six chambers were measured in both dimorphs. Septal approximation in macroconchs most commonly occurs over the last three or four chambers, whereas it most commonly occurs over the last two chambers in microconchs (table 18). In general, the decrease in septal spacing is monotonic (fig. 166). The ratio, expressed as a percentage of the interseptal distance of the last chamber to that of the last "normal" chamber, averages approximately 43% in both dimorphs, indicating an average reduction in septal spacing of a little more than one-half.

DISCUSSION: Entire specimens of *Discoscaphites conradi* are not likely to be confused with other multituberculate scaphites except

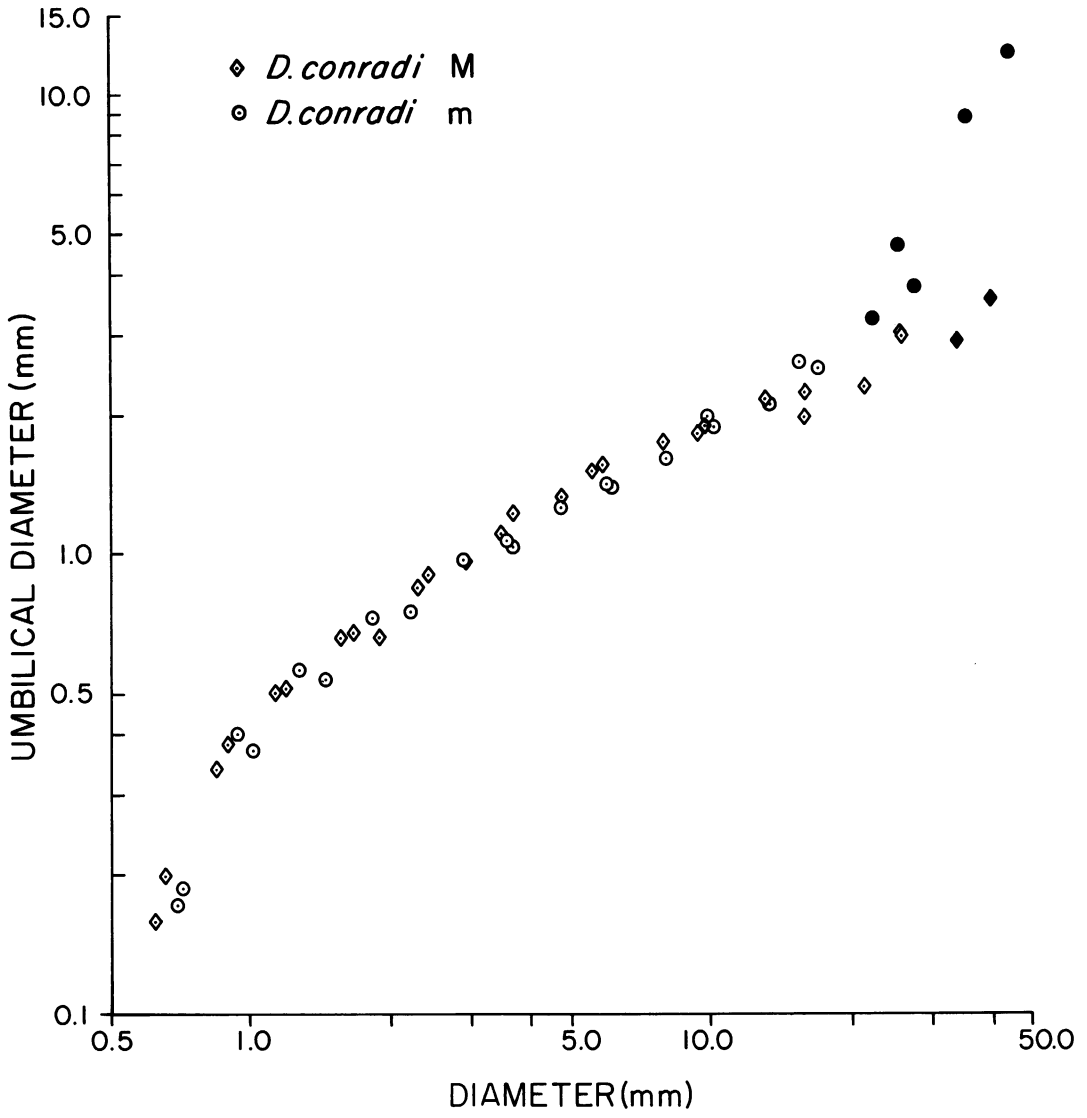

Fig. 164. Plot of umbilical diameter versus shell diameter through the ontogeny of six adults (three macroconchs and three microconchs) of *Discoscaphites conradi* (Morton). Black symbols indicate measurements near the base of or in the mature body chamber. Measurements listed in Appendix II.

possibly *D. gulosus*. The latter species is stouter and more strongly ornamented (see p. 230). Superficial resemblance to other Late Cretaceous multituberculate scaphites can be resolved using mostly generic characters. Compared with coexisting species of *Jeletzkytes, D. conradi* differs in its smaller, more compressed, and delicate shell, tighter coil, lack of an adoral projection of the ventral ribs, more widely spaced ribbing on the body chamber, subequal size of flank tubercles relative to ventrolateral tubercles, and more consistent tubercle pattern. The late Early Campanian *Trachyscaphites*, as described by Cobban and Scott (1964: E7), is a much more robust genus with the terminal part of the body chamber clearly separated from the septate coil and with a distinctly different tubercle pattern in which the ventrolaterals are consistently offset rather than opposite.

TABLE 18
Pattern of Septal Approximation in *D. conradi*[a]

Di-morph	N	Number of chambers			
		1	2	3	4
M	6	—	1	3	2
m	9	—	5	3	1

[a] This table compares the number of chambers over which septal approximation occurs in a specimen versus the number of specimens within each dimorph. "N" equals the total number of specimens in which septal spacing was measured. Chambers are numbered starting with the last, most recently formed chamber, of the phragmocone (1).

Before the ontogenetic appearance of flank tubercles, *D. conradi* juveniles resemble those of *H. nicolletii.* They have a similar whorl section but the ventral ribs of *D. conradi* are smaller and project forward less than those of *H. nicolletii.* This difference persists even after the appearance of ventrolateral tubercles. The ventral ribs joining opposite ventrolateral tubercles are more or less straight in *D. conradi,* whereas these ribs are still projected forward in *H. nicolletii,* albeit somewhat less strongly. In addition, at comparable shell diameters, the distance between a pair of ventrolateral tubercles on either side of the venter is generally smaller in *D. conradi* than in *H. nicolletii.*

In many morphological features, *Discoscaphites conradi* resembles the European species *Hoploscaphites constrictus.* This is particularly striking in examining specimens of *D. conradi* from the Prairie Bluff Chalk, which are both similar in size to specimens of *H. constrictus* and, like them, are preserved as internal molds of chalk. However, *D. conradi* has a completely different pattern of tuberculation than that of *H. constrictus.*

Specimens of *Discoscaphites* from the Western Interior are noticeably larger in average size than those from the Prairie Bluff Chalk fauna of Alabama and Mississippi, from which Morton's type lot came (see Jeletzky and Waage, 1978). *D. conradi,* in the Prairie Bluff fauna is, in addition, more varied and includes a form with mid-ventral tubercles and more than five rows of flank tubercles (Jeletzky and Waage, 1978: pl. 1, figs. 19, 20). Stephenson (1941: pl. 90, fig. 6) figured this same variety from the Corsicana Marl of Texas. No *D. conradi* with mid-ventral tubercles has yet been found in the Fox Hills Formation. However, the species is relatively rare in the Timber Lake Member where the related species *D. gulosus* is more common and includes forms with mid-ventral tubercles, which do not occur on *D. gulosus* from the underlying Trail City Member. This suggests that the possession of mid-ventral tubercles may indicate younger forms or reflect the environmental change from one member to the other. In the arenaceous chalk of the Prairie Bluff, *D. conradi* and *D. gulosus* both occur with and without mid-ventral tubercles. Unfortunately, no microstratigraphic study of the fossil distribution of this formation has been made and nothing is known of the relative stratigraphic position of the species of *Discoscaphites.* The presumably younger variety of *D. conradi* with mid-ventral tubercles apparently did not reach the Western Interior fauna.

Discoscaphites gulosus (Morton, 1834)
Figures 156, 157, 159, 160, 167–180

Macroconch Synonymy:

Ammonites conradi var. *petechialis* Morton, 1834: 39–40, pl. 16, fig. 1.
Scaphites (*Discoscaphites*) conradi var. *gulosus* (Morton), Meek, 1876: 432, pl. 36, fig. 1.
Discoscaphites sp. Stephenson, 1941: 430, pl. 90, figs. 5, 6.
Discoscaphites conradi gulosus (Morton), Jeletzky and Waage, 1978: 1129, pl. 2, figs. 8–10, 16–19 (Morton's *petechialis*), pl. 3, figs. 1–3.
Discoscaphites conradi gulosus (Morton), Landman and Waage, 1986: fig. 7A.

Microconch Synonymy:

Ammonites conradi var. *gulosus* Morton, 1834: 39, pl. 16, fig. 2.
Ammonites conradi var. *navicularis* Morton, 1834: 40, pl. 19, fig. 4.
Discoscaphites conradi gulosus (Morton), Jeletzky and Waage, 1978: 1129, pl. 2, figs. 1–4.

DIAGNOSIS: Macroconchs robust with strong ornament, usually five or six rows of tubercles. Microconchs with four or five rows of tubercles. Stratigraphically younger forms of both dimorphs may or may not develop mid-ventral tubercles on body chamber.

TYPES: Holotype, by monotypy, a micro-

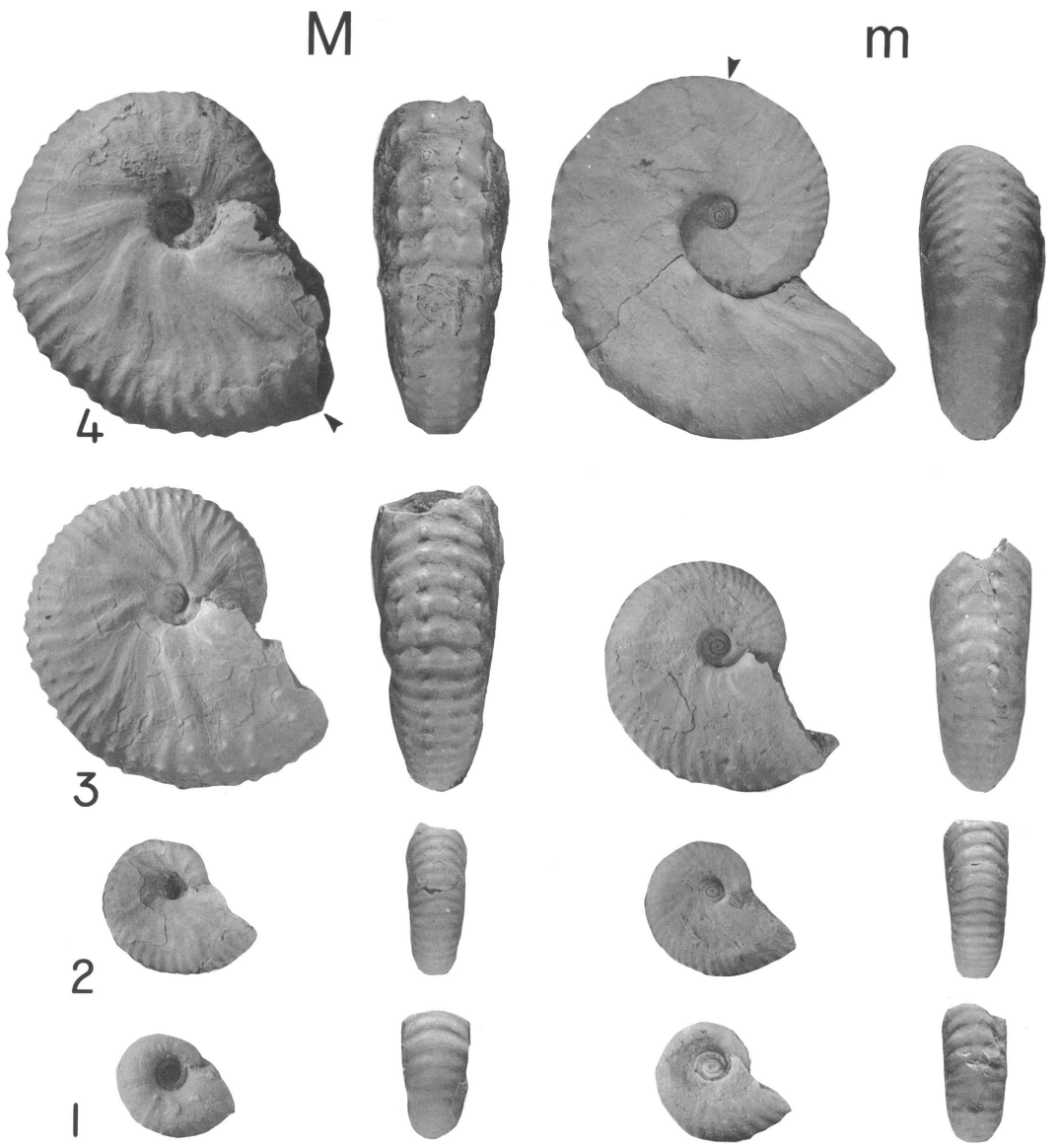

Fig. 165. Dissections of adult dimorphs (macroconch, YPM 23048, loc. 64, LGAZ, and microconch, AMNH 44677, loc. 3158, Fox Hills Fm.) of *Discoscaphites conradi* (Morton) showing four sizes through ontogeny in lateral and ventral view. 1. ×3. 2. ×2. 3. ×2. 4. ×1.5. Arrows indicate base of mature body chamber.

conch, ANSP 51552, Prairie Bluff Chalk, Alabama.

Allotype, a macroconch, YPM 2086, Prairie Bluff Chalk, Alabama.

Morton (1834: 41, 42) described and figured varieties A, B, and C as distinct forms of his *Ammonites conradi,* suggesting for each the names *A. gulosus, A. petechialis,* and *A. navicularis,* respectively. Of his specimens of *gulosus* and *navicularis,* only the microconchs are complete; of *petechialis,* the only specimen is a fragment of a macroconch lacking the body chamber. Jeletzky and Waage (1978: 1129–1130) included all three in their subspecies *Discoscaphites conradi gulosus*; Morton's (1834: 116, fig. 2) figured specimen

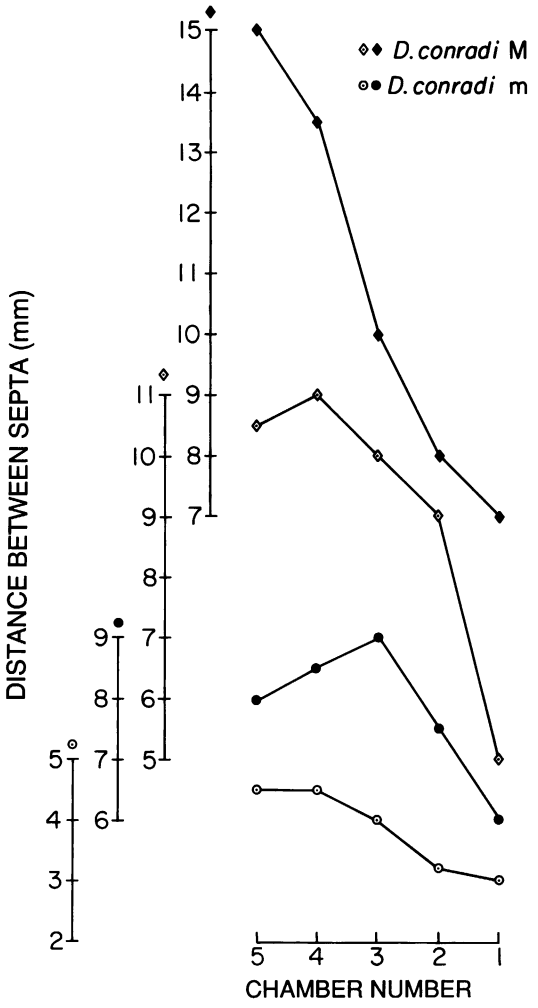

Fig. 166. Distance between septa versus chamber number counting from the last, most recently formed, chamber of the phragmocone (1), in two macro- and two microconchs of *Discoscaphites conradi* (Morton). Septal approximation occurs over more chambers in macroconchs than in microconchs.

of *gulosus* (ANSP 51552) is the holotype of the subspecies by monotypy. This microconch specimen is the holotype of *Discoscaphites gulosus* as described herein; it has been refigured by Jeletzky and Waage (1978: pl. 2, figs. 1–4), as have Morton's *petechialis* (ibid., pl. 2, figs. 16–19) and *navicularis* (ibid., pl. 3, figs. 4–6).

Jeletzky and Waage (1978: 1130, pl. 2, figs. 8–11) chose a complete specimen of a macroconch from the Prairie Bluff Chalk of Alabama in the Yale Peabody Museum collections (YPM 2086) as typical of the macroconch of *D. conradi gulosus* in place of Morton's *petechialis,* which lacked the body chamber and was the only macroconch of this form in Morton's suite of specimens. The macroconch YPM 2086 is accepted here as the allotype of *D. gulosus.*

The particular circumstances under which the taxonomy of this species has developed preclude the use of a macroconch as holotype. In spite of the importance we attach to the consistent use of macroconchs as holotypes in dimorphic species of scaphites, the possibility of using Morton's *petechialis* as the name and holotype for this species is rejected because of the even greater importance we attach to using complete specimens as types for scaphitid ammonites.

OCCURRENCE: Within the Fox Hills Formation of the type area, *D. gulosus* occurs throughout the assemblage zones of the Trail City Member and, less commonly, in the Timber Lake Member. Specimens with midventral tubercles are found only in the Timber Lake Member. *D. gulosus* is not known to occur elsewhere in the Western Interior of North America outside north-central South Dakota and adjacent parts of North Dakota.

On the Gulf Coastal Plain, dimorphs of *D. gulosus* are present in the Prairie Bluff Chalk of Alabama and Mississippi (see Jeletzky and Waage, 1978) and a single macroconch fragment was figured by Stephenson (1941: pl. 90, figs. 5 and 6) as *Discoscaphites* sp. from the Corsicana Marl of Bowie County, Texas. On the Atlantic Coastal Plain, dimorphs of *D. gulosus* have been found in the Severn Formation at Brightseat, Maryland. Casts of

→

Fig. 167. *Discoscaphites gulosus* (Morton) macroconch and microconchs. **A–D.** Macroconch, YPM 27190, loc. 57, POAZ. **A,** Right lateral; **B,** apertural; **C,** posterior; **D,** ventral hook. **E–I.** Microconch with lower mandible exposed in body chamber, USNM 468860, loc. D2578, LGAZ. **E,** Right lateral; **F,** apertural; **G,** posterior; **H,** posteroventral; **I,** left lateral. **J, K.** Microconch, YPM 27110, loc. 26, LGAZ. **J.** Right lateral; **K,** apertural.

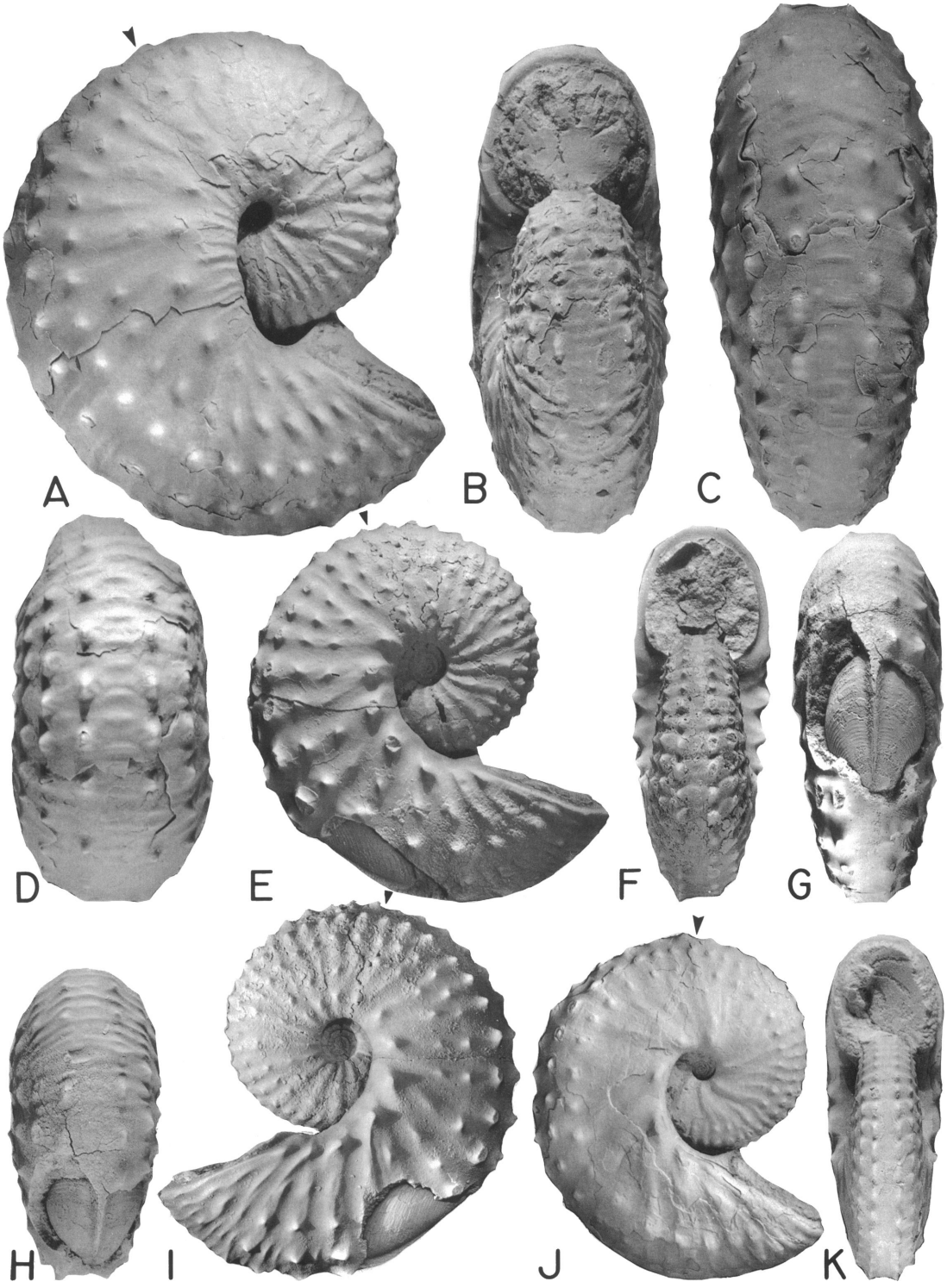
A
B
C
D
E
F
G
H
I
J
K

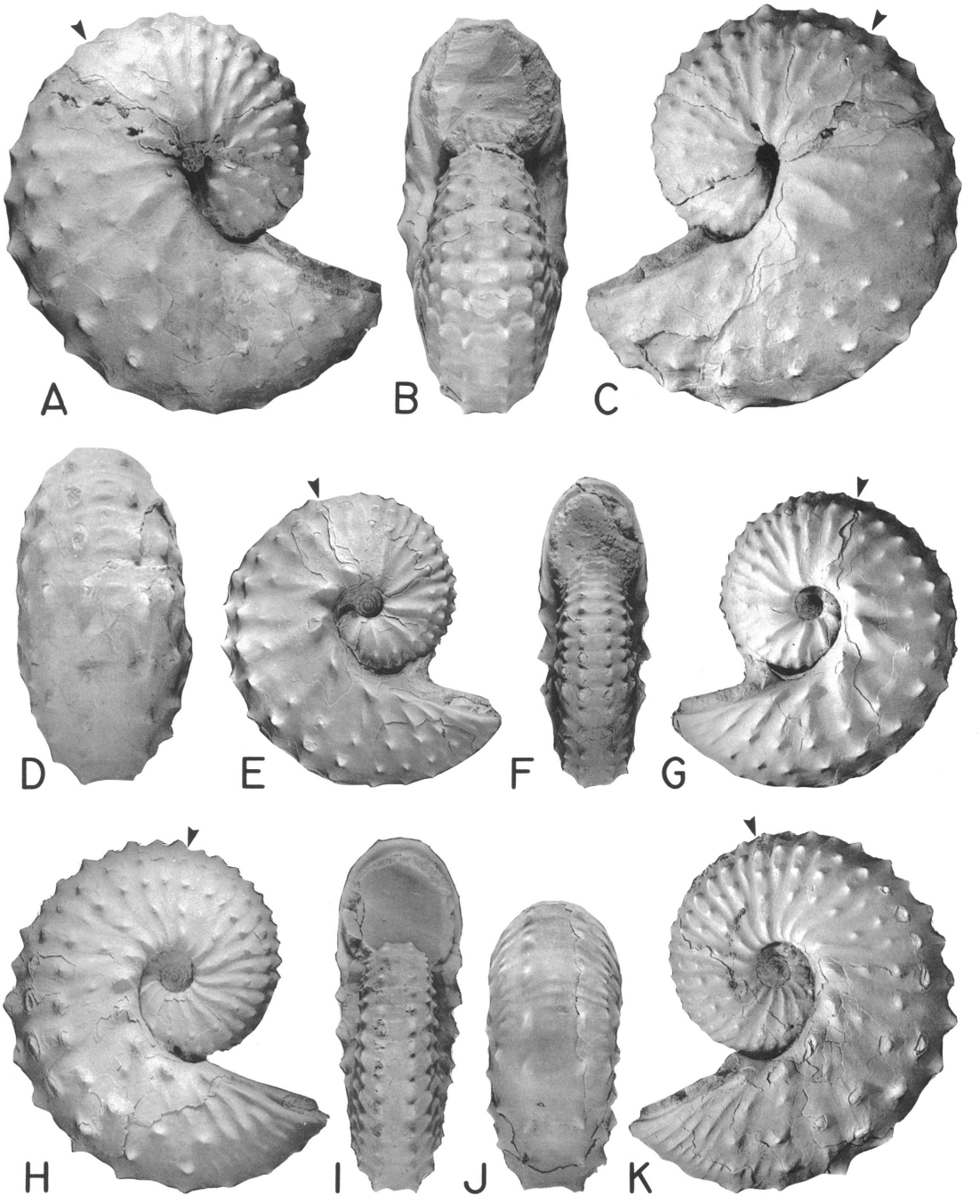

Fig. 168. *Discoscaphites gulosus* (Morton) macroconch and microconchs. **A–D.** Macroconch, YPM 27191, loc. 8, POAZ. **A,** Right lateral; **B,** apertural; **C,** left lateral; **D,** posteroventral. **E–G.** Microconch, YPM 27200, loc. 51, UNAZ. **E,** Right lateral; **F,** apertural; **G,** left lateral. **H–K.** Microconch, YPM 27199, loc. 62, POAZ. **H,** Right lateral; **I,** apertural; **J,** posteroventral; **K,** left lateral.

TABLE 19
Adult Measurements of *D. gulosus*[a]

	Macroconch				Microconch			
	N	$\bar{x}$	SD	Range	N	$\bar{x}$	SD	Range
LMAX (mm)	25	77.0	9.30	57.6–94.1	30	47.7	6.95	35.7–63.4
WUS (mm)	23	22.3	3.56	15.5–28.9	29	12.6	1.96	9.0–17.1
HUS (mm)	24	26.9	3.57	20.8–32.2	29	14.9	2.75	8.1–20.4
WUS/HUS	23	0.83	0.072	0.70–0.98	29	0.86	0.137	0.62–1.33
WAPT (mm)	25	27.0	4.30	19.8–36.0	30	17.7	2.72	12.7–23.0
HAPT (mm)	25	26.3	3.21	20.0–33.4	29	17.8	2.44	13.5–22.6
WAPT/HAPT	25	1.02	0.070	0.87–1.13	29	0.99	0.077	0.78–1.10
UD (mm)	25	4.5	0.77	3.2–7.2	30	4.4	0.83	2.8–6.6
UD/LMAX	25	0.06	0.009	0.05–0.08	30	0.09	0.011	0.08–0.12
A (°)	7	46.3	8.24	33.0–55.0				

[a] Abbreviations: see table 1 and figure 9.

partial specimens of a macroconch and a microconch, kindly given to us by W. A. Cobban, show five and four rows of flank tubercles, respectively. We were shown these and other fragmental specimens of *D. gulosus* by Ralph Johnson of the Monmouth Amateur Paleontologist's Society of New Jersey (MAPS), who is in charge of the Society's excellent collection of Monmouth Group fossils. The macroconch and microconch of *D. gulosus* noted are MAPS A2025a and A2025b, respectively.

D. gulosus is not known outside North America.

MATERIAL: About 250 specimens of *Discoscaphites gulosus* were collected from the type area of the Fox Hills Formation. Of these 98 are macroconchs and 155 are microconchs. About 40 macroconchs and 75 microconchs are complete or nearly complete, and about 30 of each dimorph constitute the set of measured specimens. Additional specimens used in the study include 7 macroconchs and 19 microconchs from the Denver Branch of the USGS and two specimens of each dimorph from BHI.

MACROCONCH DESCRIPTION: Dimensions of the measured specimens are listed in table 19. LMAX averages 77.0 mm; the size distribution is approximately normal (fig. 173). The ratio of the size of the largest specimen to that of the smallest is 1.63. Ornament is generally coarse in all specimens, regardless of size, so that a gradation series involving size and ornament is less apparent than in *D. conradi* macroconchs. The shaft of the body chamber is arcuate; it is short in small specimens bringing the dorsal lip in contact with, or slightly embracing, the phragmocone. In specimens above average size, the shaft is commonly slightly longer so that a small gap exists between the dorsal lip and phragmocone (fig. 169F). However, the dorsal projection is always in contact with the phragmocone. The body chamber and exposed phragmocone are each approximately 0.5 whorls in angular length. The umbilical diameter averages 4.5 mm. The ratio of umbilical diameter to shell diameter averages 0.06, and does not vary consistently with adult size.

The ventral half of the shell is rounded and semicircular in intercostal cross section; the flanks flatten dorsally then turn sharply into the umbilicus. The ratio of whorl width to whorl height at the ultimate septum averages 0.83 and does not vary consistently with adult size (table 19, fig. 156). The ratio of whorl width to whorl height at the aperture averages 1.02, with larger specimens having slightly more depressed apertures than smaller specimens (table 19, fig. 157).

Ribbing is radiate to slightly prorsiradiate, and mostly straight; it increases both by branching and intercalation. Ribs are strong on the exposed phragmocone where their spacing is approximated. They become gradually more widely spaced on the younger part of the phragmocone. On the shaft of the body chamber ribs are very weak and widely spaced but tend to become stronger and more closely spaced on the hook. The pattern of ribs on

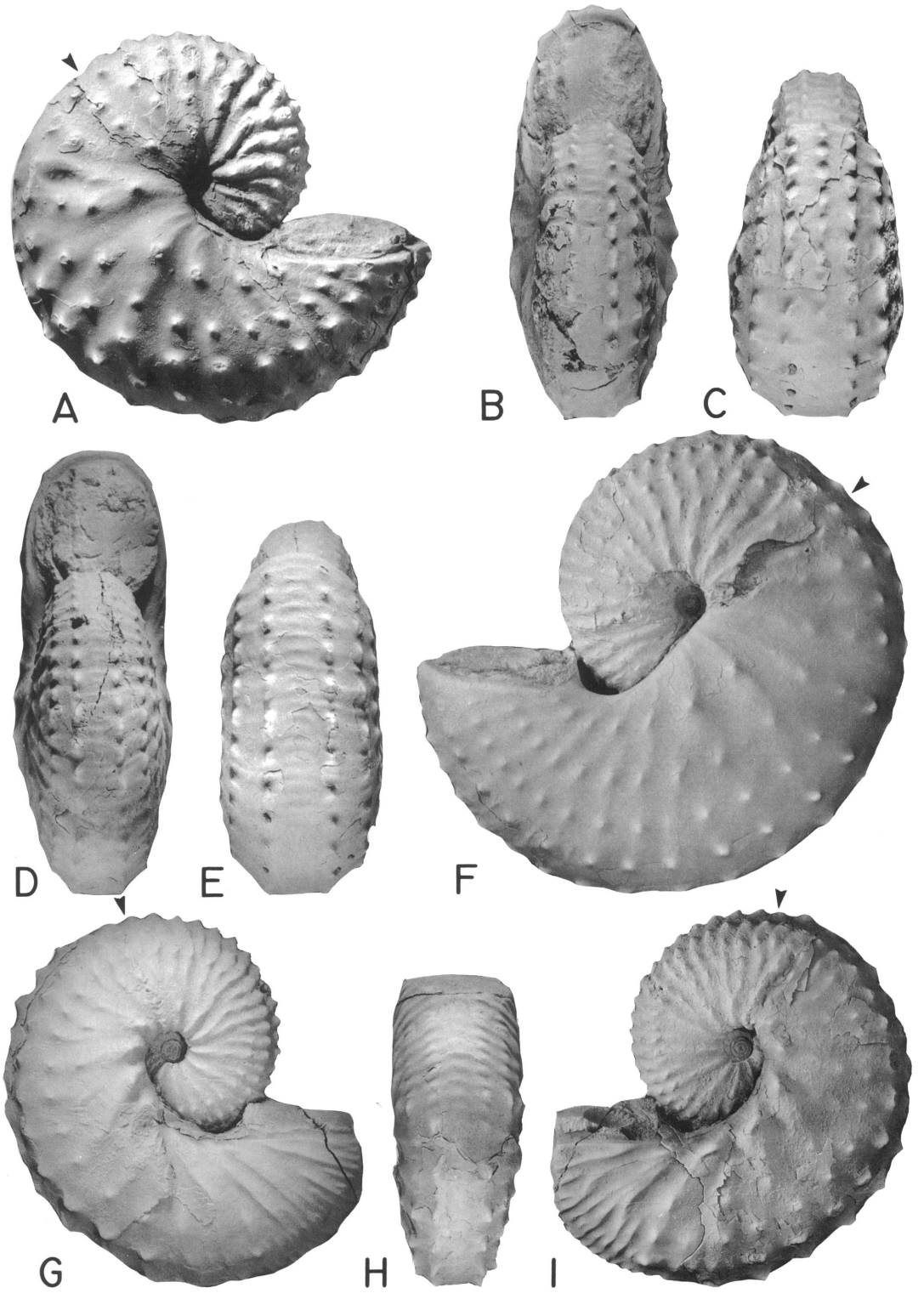

Fig. 169. *Discoscaphites gulosus* (Morton) macroconchs and microconch. **A–C.** Macroconch with mid-ventral row of tubercles on hook, YPM 27193, loc. 314, TLM. **A,** Right lateral; **B,** apertural; **C,** ventral hook. **D–F.** Compressed macroconch, YPM 27126, loc. 53, LGAZ. **D,** Apertural; **E,** ventral hook; **F,** left lateral. **G–I.** Large microconch, YPM 27114, loc. 20, LNAZ. **G,** Right lateral; **H,** postero-ventral; **I,** left lateral.

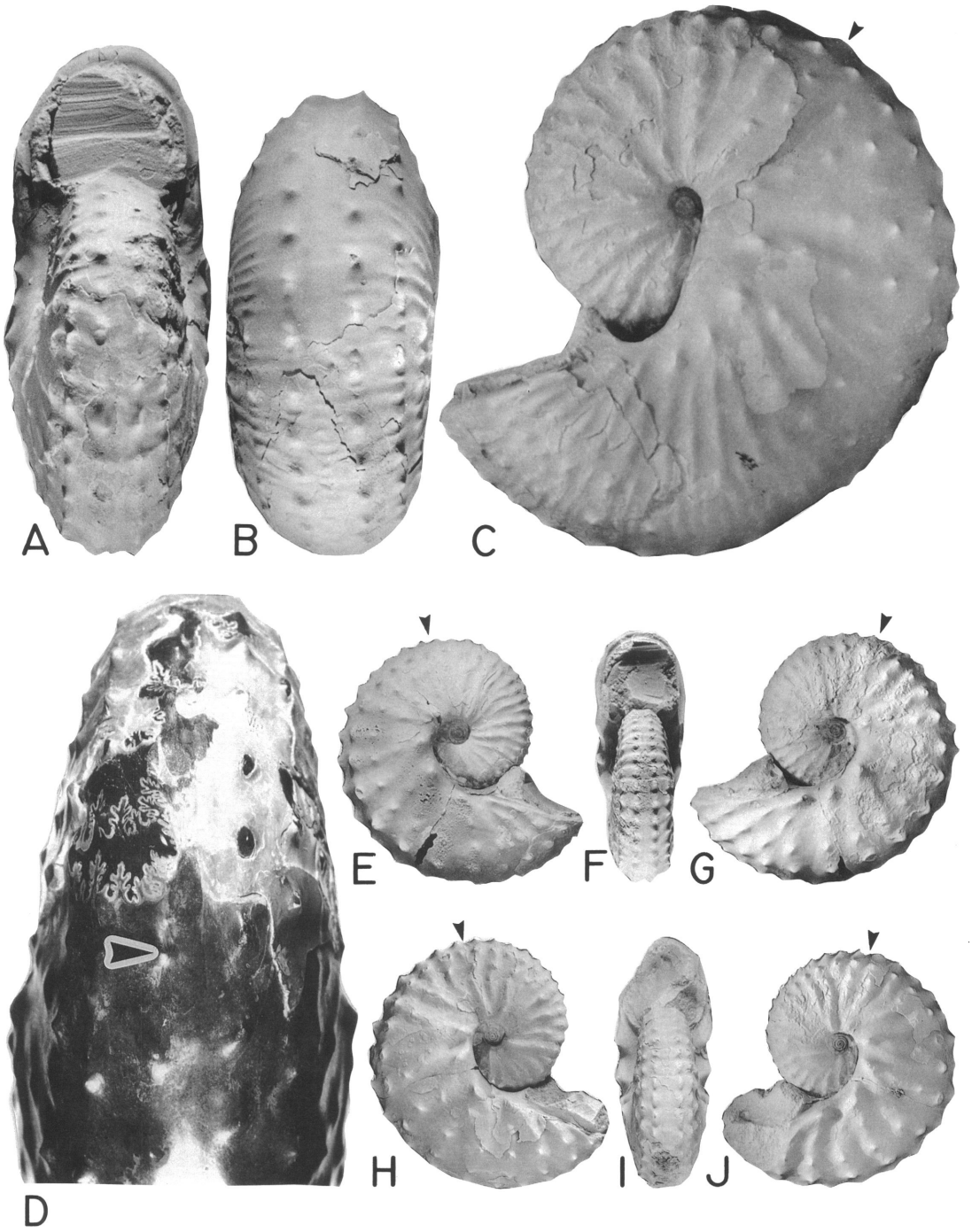

Fig. 170. *Discoscaphites gulosus* (Morton) macroconch and microconchs. **A–D.** Macroconch, YPM 27189, loc. 82, UNAZ. **A,** Apertural; **B,** posteroventral; **C,** left lateral; **D,** uncoated venter showing ventral muscle attachment area (arrow), ×1.75. **E–G.** Microconch, YPM 27202, loc. 115, LGAZ. **E,** Right lateral; **F,** apertural; **G,** left lateral. **H–J.** Microconch, YPM 27204, loc. 110, POAZ. **H,** Right lateral; **I,** apertural; **J,** left lateral.

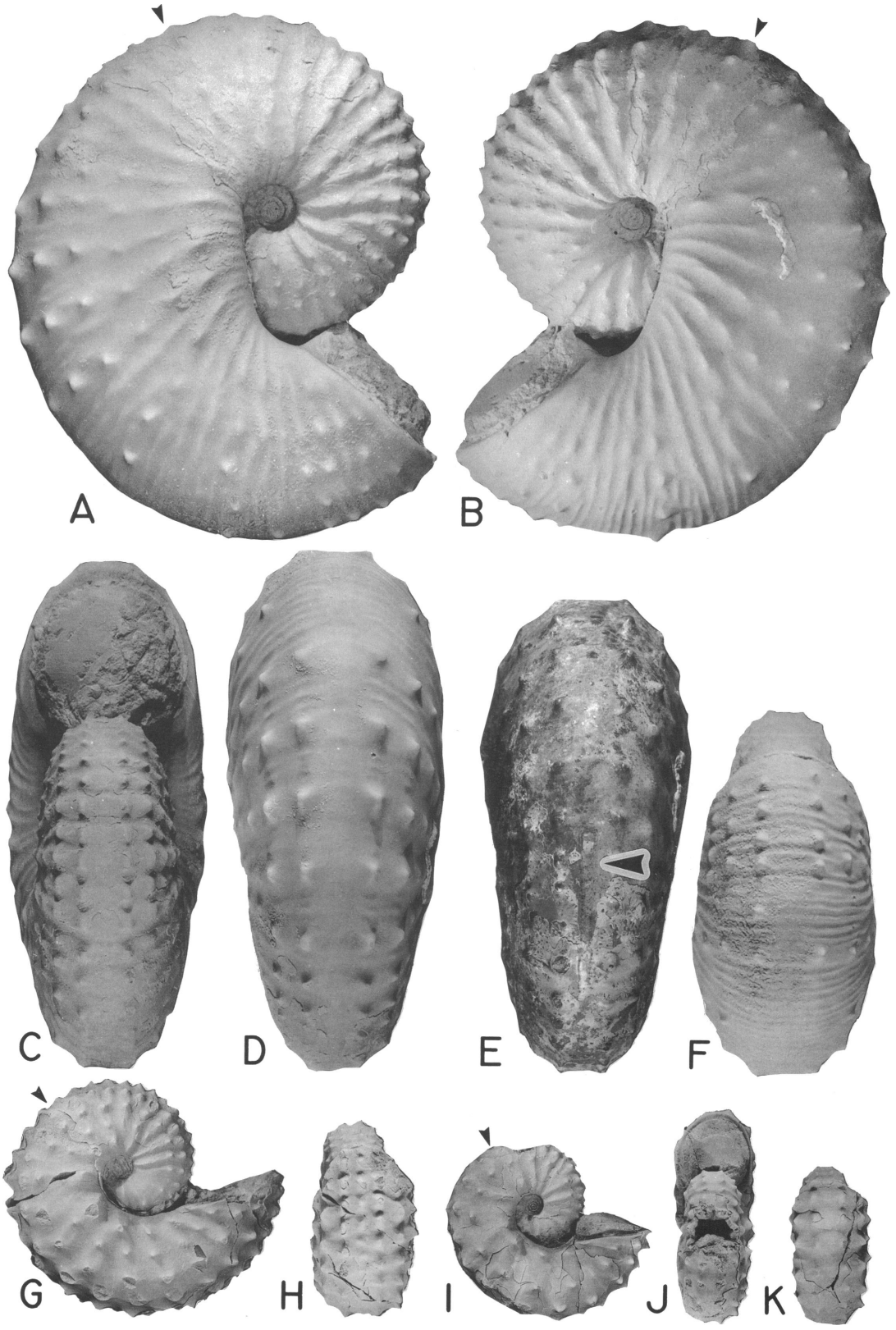
A
B
C
D
E
F
G
H
I
J
K

the venter is like that in *D. conradi*. The ratio of the number of dorsal to ventral ribs is about 1:5 or 1:6 where the ventral ribs are small and about 1:2 or 1:3 where the ventral ribs are weak and the venter nearly smooth. Neither the ventral ribs nor the ventral lip at the aperture shows more than a very slight adoral projection.

Tubercles are prominent on the ribs of *D. gulosus* and occur in well-defined rows including the ventrolaterals, three or four rows of flank tubercles, and a row of umbilical bullae. The row of ventrolateral tubercles and adjacent row of flank tubercles are more or less subequal in size and are usually the most prominent and persistent of all the tubercle rows. The umbilical tubercles/bullae on the body chamber may be as large as the ventrolaterals but are smaller or nonexistent on the exposed phragmocone. Unlike those on *D. conradi*, umbilicals on *D. gulosus* are seldom noticeably enlarged. Most of the tubercles on *D. gulosus* are conical in shape except for the bullate umbilicals and occasional flank bullae near the aperture. All tubercle rows usually extend to the aperture.

A mid-ventral row of tubercles appears commonly on *D. gulosus* macroconchs from the Timber Lake Member of the Fox Hills Formation, but has not been found on specimens from the underlying Trail City Member. The mid-ventrals may appear only on the hook or may occur on the entire exposed shell.

The suture of *D. gulosus* macroconchs is typically scaphitid and similar to that of *D. conradi* macroconchs (fig. 174A–C). In larger *D. gulosus* macroconchs the lobules tend to be more intricately divided and the folioles less expanded than the corresponding elements in *D. conradi* macroconchs.

The ventral muscle attachment area is narrow and elongate as in other discoscaphites. Internal molds and inner shell layers commonly reflect the shallow median groove along the mid-venter of the body chamber; it is usually tripartite but may be single.

MICROCONCH DESCRIPTION: Adult microconchs average 47.7 mm in size and approximately conform to a normal distribution with a right-sided tail (table 19, fig. 173). The ratio of the size of the largest specimen to that of the smallest is 1.73. The average size of microconchs is significantly smaller than that of macroconchs (77.0 mm). The ratio of the average size of macroconchs to that of microconchs is 1.61. Dimorphs overlap in size between 55 and 65 mm, which represents approximately one-sixth of their total combined size range (fig. 173). The shape and ornament of the shell are approximately the same in all microconchs, regardless of size; consequently, no gradational series exists such as that in microconchs of *D. conradi*.

The arcuate shaft of the body chamber is short and the reflexion of the hook brings the dorsal lip of the aperture into contact with the phragmocone in most specimens, although it leaves a slight gap in some. The angular length of the body chamber and exposed phragmocone average approximately 0.6 whorls and 0.4 whorls, respectively.

The ratios of whorl width to whorl height at the ultimate septum and at the aperture average 0.86 and 0.99, respectively, and do not vary consistently with adult size (figs. 159, 160). The averages of these ratios are similar to those of the corresponding ratios in macroconchs (0.83 and 1.02, respectively; table 19). As in macroconchs, the ventral half of the shell is rounded in intercostal cross section, but dorsally the flanks flatten up to the umbilical margin where they bend abruptly into the umbilicus. This sharp bend forms a broad, nearly flat shoulder with a slight outward slope bordered at the edge by a row of umbilical bullae.

The umbilical diameter averages 4.4 mm, which is similar to that in macroconchs (4.5 mm). The ratio of umbilical diameter to shell

←

Fig. 171. *Discoscaphites gulosus* (Morton) macroconch and microconchs. **A–F.** Macroconch, YPM 27194, loc. 62, LGAZ. **A,** Right lateral; **B,** left lateral; **C,** apertural; **D,** posterior; **E,** uncoated posterodorsal showing elongate ventral muscle attachment area; **F,** ventral hook. **G, H.** Microconch, YPM 27206, loc. 312, TLM. **G,** Right lateral; **H,** ventral hook showing mid-ventral row of tubercles. **I–K.** Microconch, YPM 27205, loc. 279, lower TLM transition concretions. **I,** Right lateral; **J,** apertural; **K,** ventral hook.

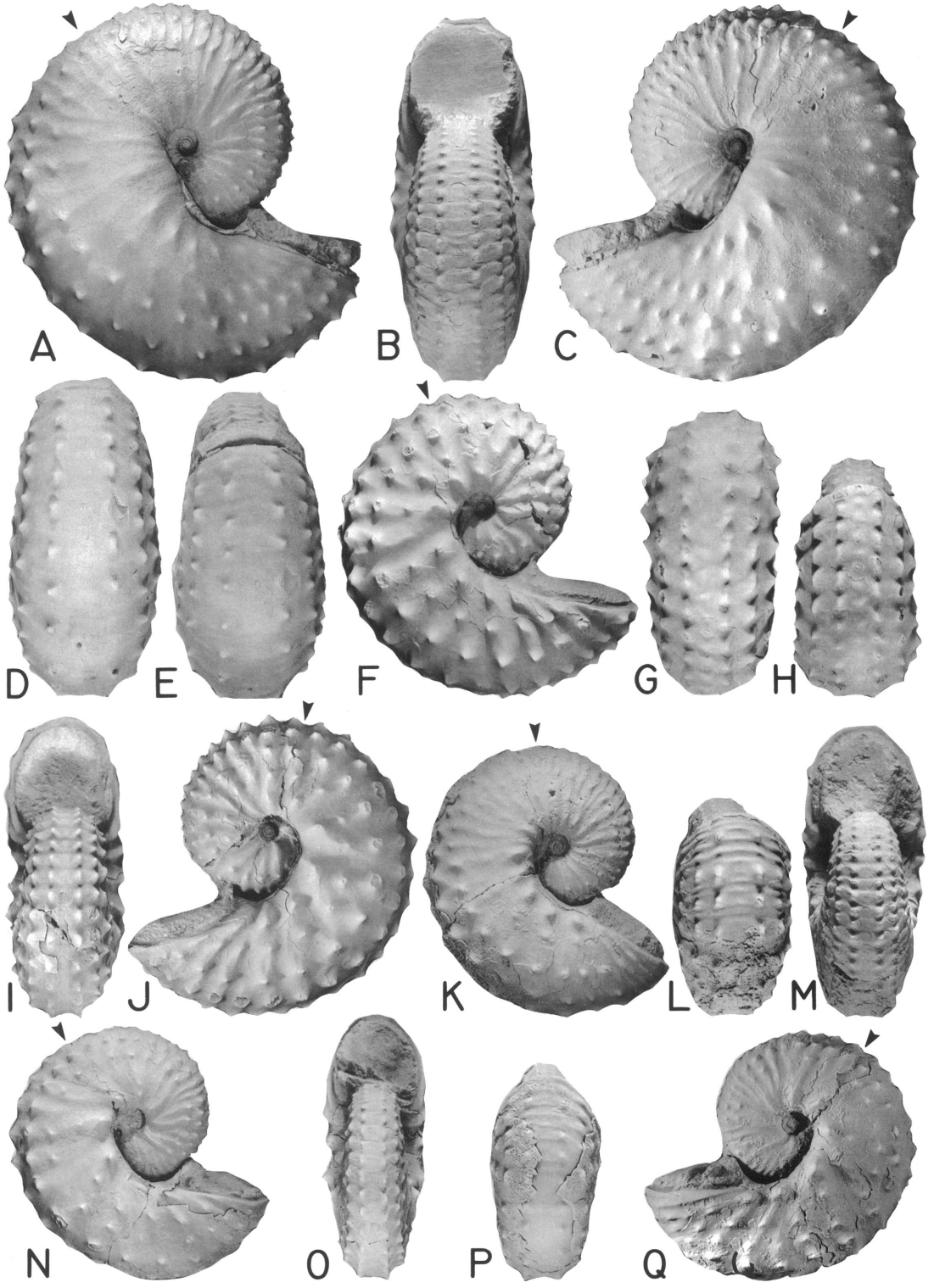
A
B
C
D
E
F
G
H
I
J
K
L
M
N
O
P
Q

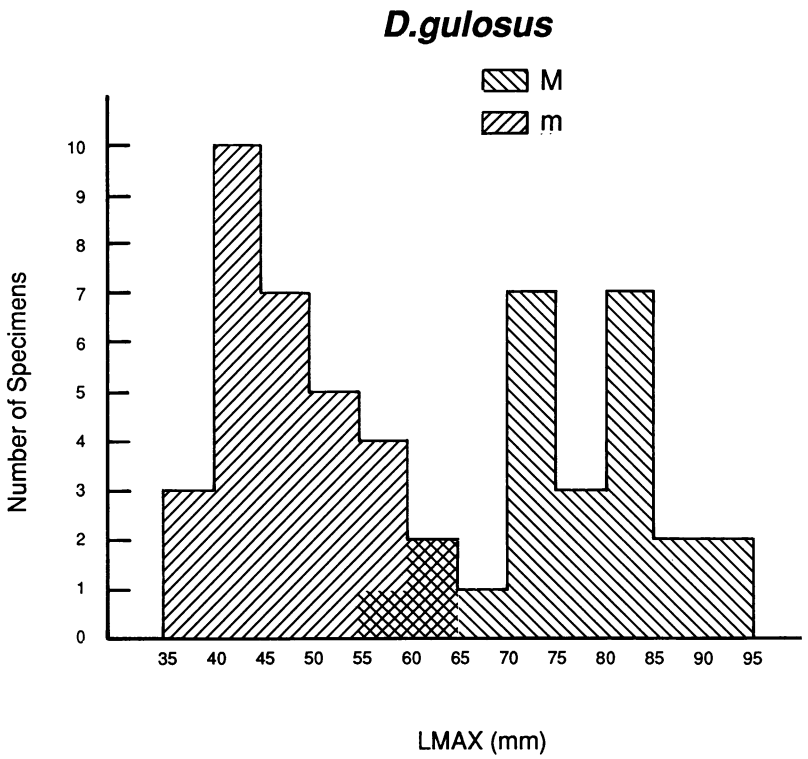

Fig. 173. Size frequency histogram of a sample of *Discoscaphites gulosus* (Morton) from the Fox Hills Formation in its type area.

diameter averages 0.09 and does not vary consistently with adult size. The average is significantly higher than that in macroconchs (0.06; table 19).

Ribbing, as in macroconchs, is radiate to slightly prorsiradiate. Ribs are more widely spaced on the body chamber except on the terminal part of the hook, where they are finer and more closely spaced, at least on the venter. On the exposed phragmocone, the ratio of the number of dorsal to ventral ribs is about 1:3, or, less commonly, 1:4. A slight, adoral projection of the ventral ribs appears confined to the anterior part of the body chamber; it is most noticeable near the aperture. Two or three rows of flank tubercles are present in addition to the ventrolateral tubercles and umbilical bullae. The first row of flank tubercles is usually subequal in size to the adjacent row of ventrolaterals, and both these rows persist throughout the exposed shell, although the first row of flank tubercles may fade out a few ribs short of the aperture in forms with conspicuously finer ribbing on the hook. Four or five strong umbilical bullae occur on the body chamber but they are small or absent on the adjacent phragmocone. On a few specimens one or two enlarged bullae

←

Fig. 172. *Discoscaphites gulosus* (Morton) macroconch and microconchs. **A–E.** Macroconch, YPM 27192, loc. 64, LGAZ. **A,** Right lateral; **B,** apertural; **C,** left lateral; **D,** posteroventral; **E,** ventral hook. **F–J.** Microconch with strong ornament, narrow venter, and incipient row of mid-ventral tubercles on hook, YPM 23736, loc. 312, TLM. **F,** Right lateral; **G,** posterior; **H,** ventral hook; **I,** apertural; **J,** left lateral. **K–M.** Microconch, YPM 27201, loc. 50, LGAZ. **K,** Right lateral; **L,** ventral hook; **M,** apertural. **N–Q.** Microconch, YPM 27203, loc. 120, LGAZ. **N,** Right lateral; **O,** apertural; **P,** ventral hook; **Q,** left lateral.

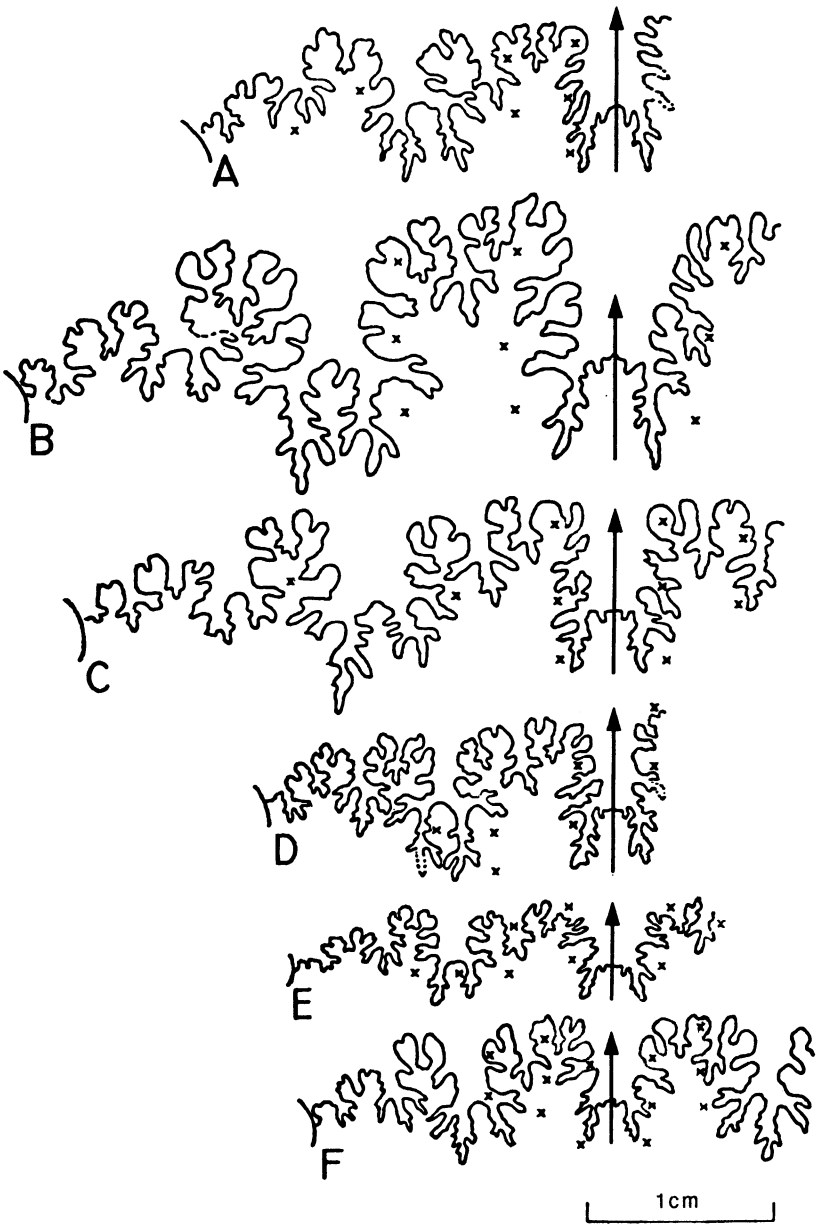

Fig. 174. Sutures of *Discoscaphites gulosus* (Morton) macroconchs and microconchs. **A.** Last suture of an adult macroconch, YPM 27097, loc. 20, LGAZ. **B.** Sixth from last suture of an adult macroconch, YPM 27121, loc. 25, POAZ. **C.** Sixth from last suture of an adult macroconch, YPM 27117, loc. 25, POAZ. **D.** Fifth from last suture of an adult microconch, YPM 27124, loc. 17, UNAZ. **E.** Next to last suture of an adult microconch, YPM 27095, loc. 52, UNAZ. **F.** Fourth from last suture of an adult microconch, YPM 27110, loc. 26, LGAZ. Crosses indicate position of tubercles.

may be present but in most microconchs the umbilical bullae are about equally strong. A mid-ventral row of tubercles is sometimes present on the hook on specimens from the Timber Lake Member.

The suture of microconchs is similar to that of macroconchs but the primary and secondary lobules and folioles are less divided (fig. 174D–F). The ventral muscle attachment area is elongate and a faint ridge along

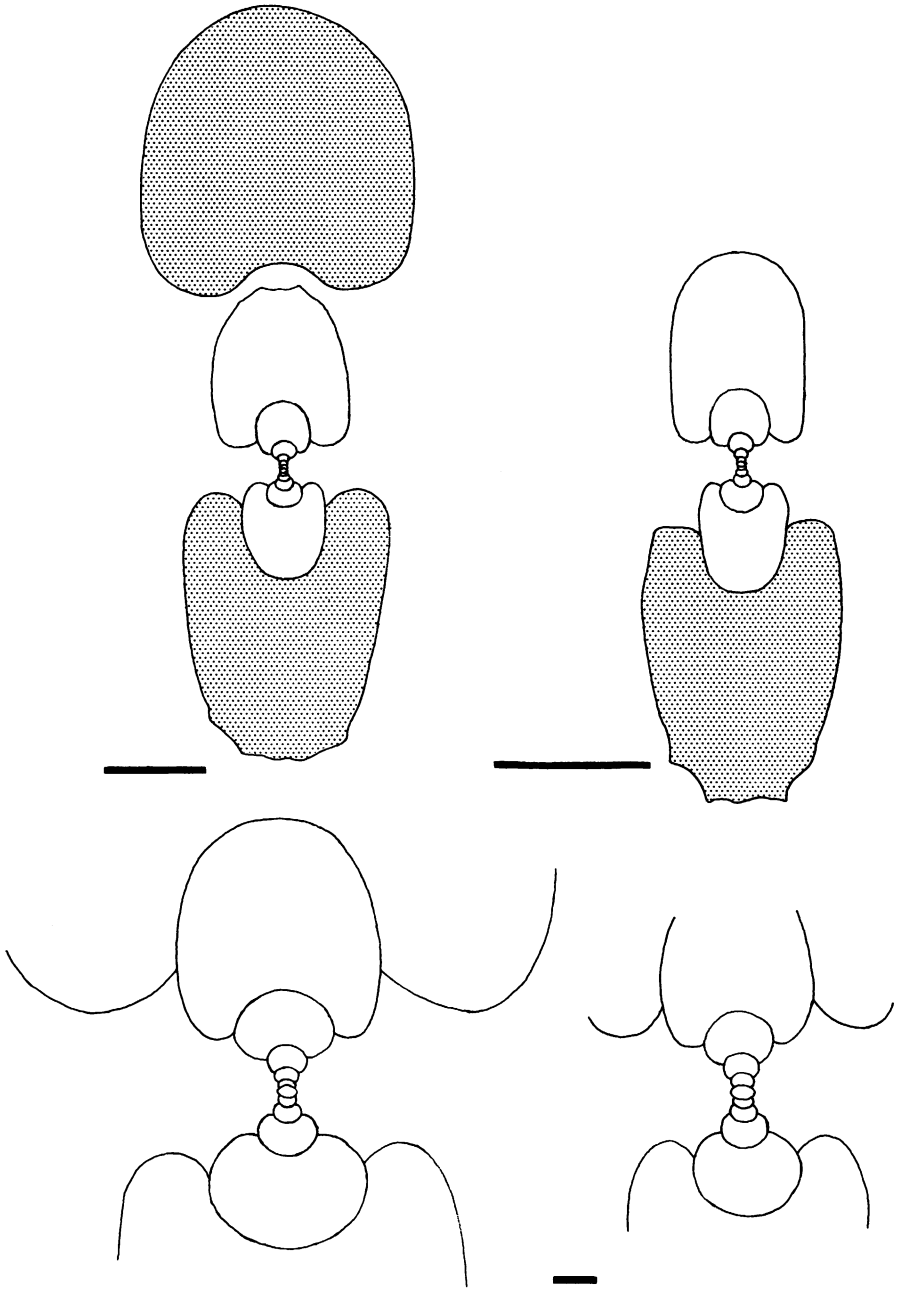

Fig. 175. Dorsoventral, mostly costal cross sections through adult dimorphs of *Discoscaphites gulosus* (Morton). **Left.** Macroconch, YPM 34106, loc. 214, POAZ. **Right.** Microconch, YPM 34107, loc. 17, UNAZ. Shaded area demarcates mature body chamber. Upper scale bars = 1 cm; lower scale bar = 1 mm.

the mid-venter of the body chamber is present and usually tripartite.

ONTOGENY: Measurements of the ammonitella are listed in table 3. The ammonitella diameter averages 695 and 692 μm in macroconchs and microconchs, respectively. The protoconch angle averages 52° and reflects the depressed protoconch and ellipsoidal ammonitella of *Discoscaphites*.

Dorsoventral, mostly costal cross sections

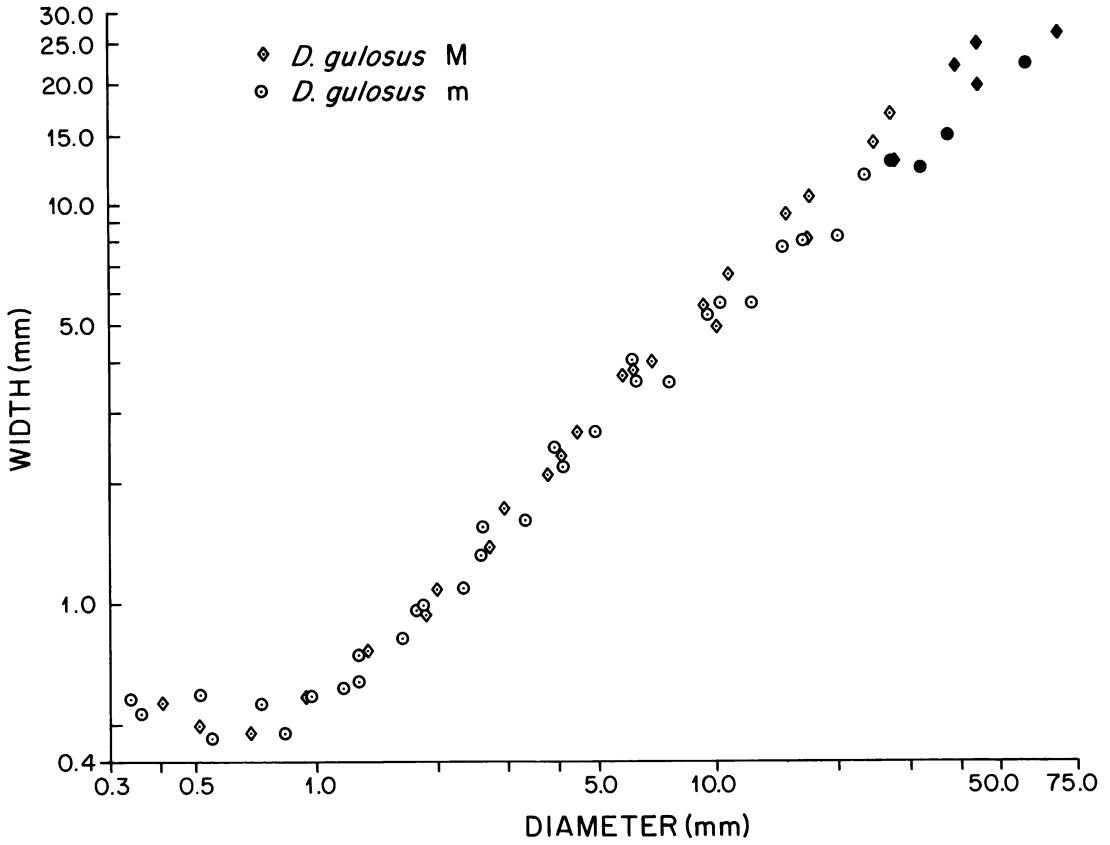

Fig. 176. Plot of whorl width versus shell diameter through the ontogeny of six adults (three macroconchs and three microconchs) of *Discoscaphites gulosus* (Morton). Black symbols indicate measurements near the base of or in the mature body chamber. Measurements listed in Appendix II.

of macro- and microconchs are illustrated in figure 175. The whorl section is robust. The postembryonic growth of whorl width is isometric to slightly negatively allometric in both dimorphs (slopes range from 0.9092 to 1.007) and shows a slight change at approximately 5 mm shell diameter (fig. 176). In contrast, the postembryonic growth of whorl height is positively allometric in both dimorphs (slopes range from 1.1029 to 1.1613; fig. 177). At comparable shell diameters, the values of whorl width and whorl height in macroconchs are approximately the same as those in microconchs. The whorls become increasingly more compressed during ontogeny in both dimorphs. The ratio of whorl width to whorl height ranges from 1.0 to 2.0 up to approximately 5 mm shell diameter and decreases to a minimum near the base of the mature body chamber of 0.7 to 1.0 in macroconchs and 0.6 to 1.3 in microconchs.

The growth of umbilical diameter is negatively allometric (fig. 178). The values of umbilical diameter at the same shell diameter are more or less the same in both dimorphs, but at approximately one whorl before the base of the mature body chamber, the umbilical diameter in macroconchs begins to increase more slowly than that in microconchs. The ratio of umbilical diameter to shell diameter steadily decreases throughout most of postembryonic growth and reaches a minimum near the base of the mature body chamber of 0.14 to 0.18 in microconchs and 0.09 to 0.11 in macroconchs.

The ontogenetic development of ornamentation is similar in both dimorphs (fig. 179). Ribs appear on the venter and on the flanks

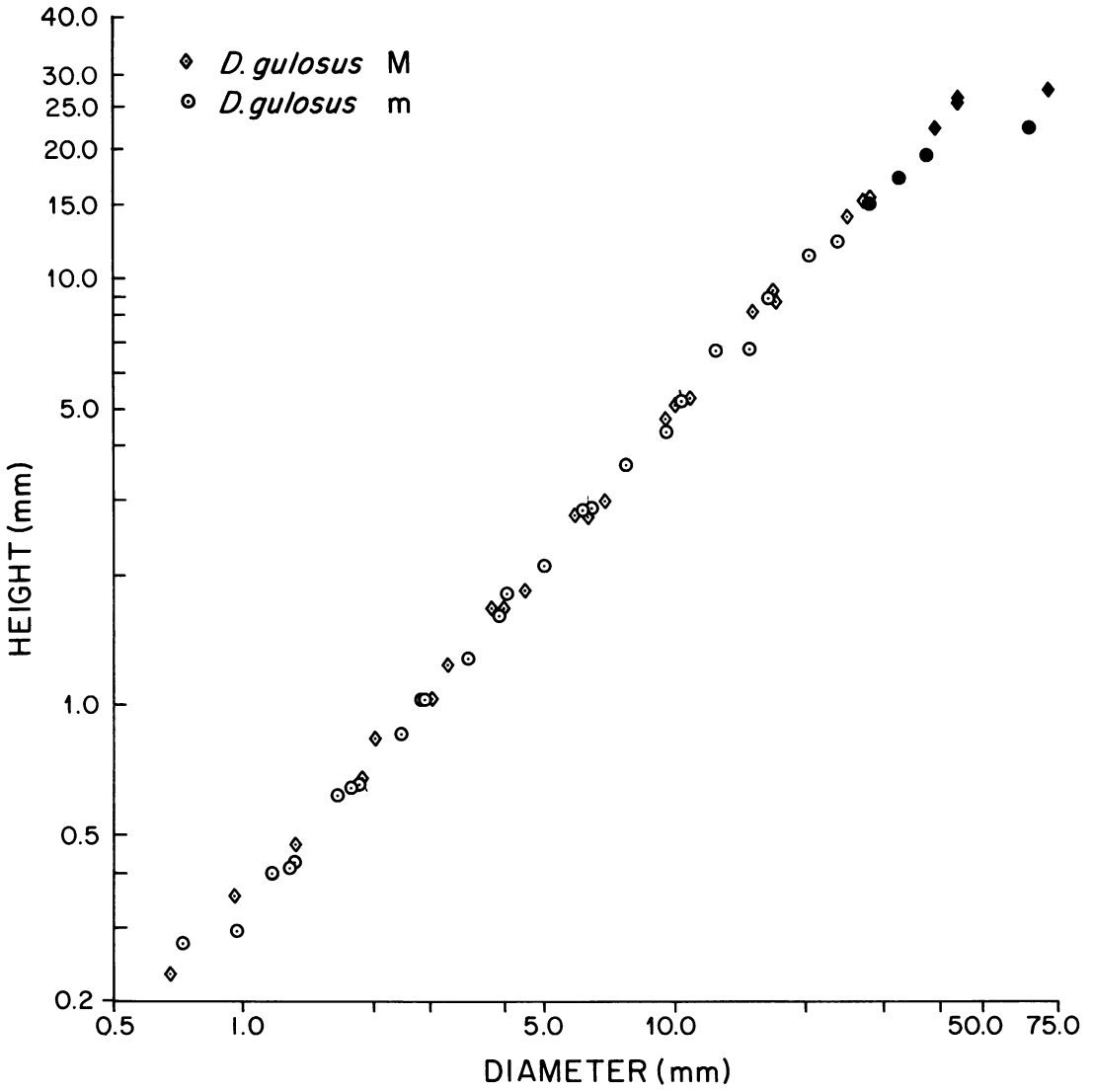

Fig. 177. Plot of whorl height versus shell diameter through the ontogeny of six adults (three macroconchs and three microconchs) of *Discoscaphites gulosus* (Morton). Black symbols indicate measurements near the base of or in the mature body chamber. Measurements listed in Appendix II.

(primaries) at approximately 4 mm shell diameter, and become stronger thereafter. The ventral ribs show a slight forward projection, which they maintain until the appearance of ventrolateral tubercles. Primaries are strong, prorsiradiate to rectiradiate, and very slightly flexuous to straight. Secondaries develop by both intercalation and branching but the ratio of the number of dorsal to ventral ribs is low, approximately 1:2 to 1:3.

At approximately 10–15 mm shell diameter (about 0.75–1.50 whorls before the point of exposure in macroconchs and about 0.5 whorls before the point of exposure in microconchs) small ventrolateral tubercles appear on every rib. One to three rows of flank tubercles also appear at approximately the same shell diameter or slightly larger. Unlike the ventrolaterals, flank tubercles may not occur on every rib. Ribs cross the venter with,

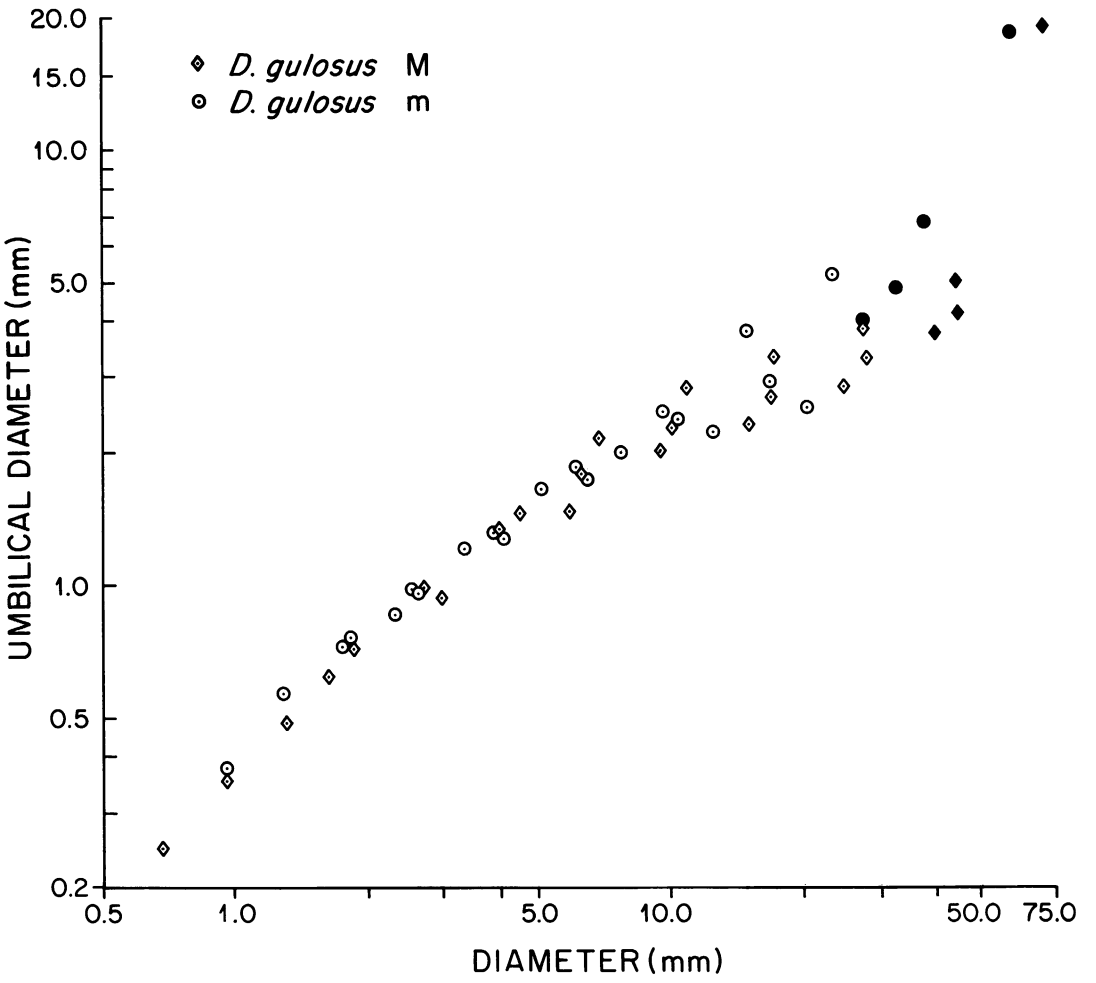

Fig. 178. Plot of umbilical diameter versus shell diameter through the ontogeny of six adults (three macroconchs and three microconchs) of *Discoscaphites gulosus* (Morton). Black symbols indicate measurements near the base of or in the mature body chamber. Measurements listed in Appendix II.

at most, a weak adoral projection. Primaries are strong, prorsiradiate to rectiradiate, and straight to slightly flexuous. The ratio of the number of dorsal to ventral ribs is approximately the same as that on earlier whorls. The presence of ventrolateral and flank tubercles imparts an angular aspect to the costal whorl section.

Additional rows of flank tubercles may develop on the exposed phragmocone. Two ventral ribs commonly join pairs of ventrolaterals on either side of the venter. These ribs become weaker toward the end of the phragmocone. As on earlier whorls, primaries are strong, rectiradiate to prorsiradiate, and only slightly flexuous to straight. Umbilical bullae develop near the anterior end of the phragmocone. The ratio of the number of dorsal to ventral ribs is approximately 1:5.

The pattern of septal approximation was examined in seven macroconchs and six microconchs (table 20). Interseptal distances of up to eight chambers were measured in macroconchs and up to six chambers in microconchs. Septal approximation most commonly occurs over the last four chambers in macroconchs whereas it most commonly occurs over the last three chambers in microconchs. In general, the decrease in septal spacing is monotonic (fig. 180). The ratio,

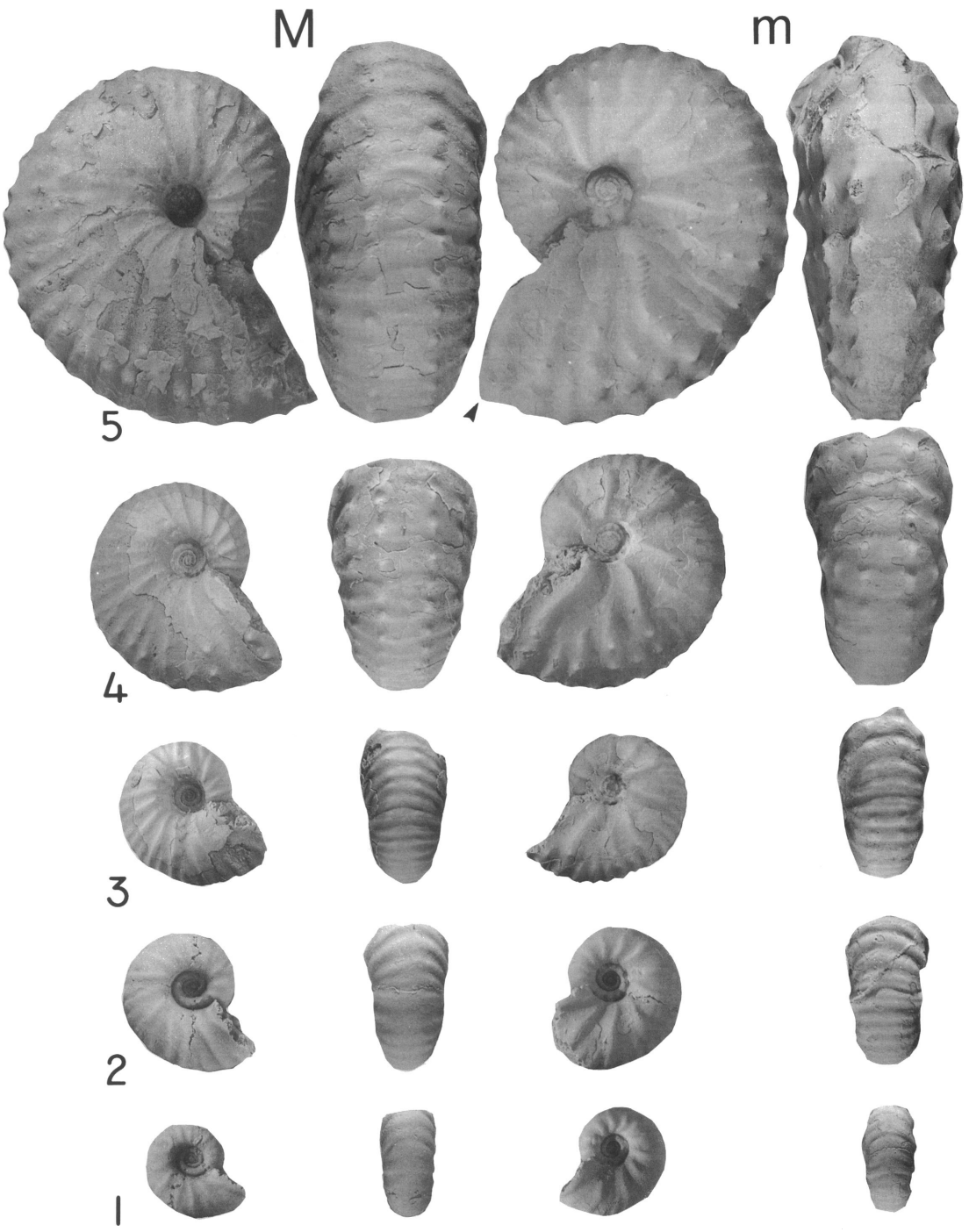

Fig. 179. Dissections of adult dimorphs (macroconch, YPM 23050, loc. 312, Fox Hills Fm., and microconch, YPM 23051, loc. 53, LNAZ) of *Discoscaphites gulosus* (Morton) showing five sizes through ontogeny in lateral and ventral view. 1. ×3. 2. ×3. 3. ×2. 4. ×2. 5. ×2. Arrow indicates base of mature body chamber.

TABLE 20
Pattern of Septal Approximation in *D. gulosus*[a]

Di-morph	N	Number of chambers				
		1	2	3	4	5
M	7	—	1	1	3	2
m	6	—	1	3	2	—

[a] This table compares the number of chambers over which septal approximation occurs in a specimen versus the number of specimens within each dimorph. "N" equals the total number of specimens in which septal spacing was measured. Chambers are numbered starting with the last, most recently formed, chamber of the phragmocone (1).

expressed as a percentage, of the interseptal distance of the last chamber to that of the last "normal" chamber averages approximately 44% in both dimorphs, similar to that in *D. conradi.*

DISCUSSION: *D. gulosus* differs from *D. conradi* in having a more robust whorl section, a significantly more quadrate aperture, and a consistently stronger ornamentation. In addition, flank tubercles on the body chamber of *D. gulosus* extend to the aperture whereas they commonly terminate farther back on the body chamber in *D. conradi.* A few microconchs of *D. gulosus* approach some of the more strongly sculptured microconchs of *D. conradi,* but no populations of the two species show a morphological continuum at any level in the Fox Hills Formation.

With respect to macroconchs, the average values of the ratios of whorl width to whorl height at the ultimate septum and at the aperture are significantly higher in *D. gulosus* than in *D. conradi.* Scatter plots of WUS/HUS versus LMAX and WAPT/HAPT versus LMAX reveal a fairly clear separation between macroconchs of these two species (figs. 156, 157). The average size of macroconchs of *D. gulosus* is also significantly larger than that of macroconchs of *D. conradi,* although the two species overlap between 55 and 95 mm. The average umbilical diameter is also larger in macroconchs of *D. gulosus* than in those of *D. conradi.* In addition, ribs on *D. gulosus* macroconchs are stronger and less numerous than those on *D. conradi* macroconchs.

Microconchs of *D. gulosus* also differ, in many of the same ways, from those of *D. conradi.* The average values of the ratios of whorl width to whorl height at the ultimate septum and at the aperture are significantly higher in microconchs of *D. gulosus* (figs. 159, 160). The average size of microconchs of *D. gulosus* is also significantly larger than that of microconchs of *D. conradi,* although the two species overlap between 35 and 55 mm. As in macroconchs, the average umbilical diameter is larger in microconchs of *D. gulosus* than in those of *D. conradi.*

The distinction between these two species is evident throughout ontogeny. The growth of whorl width is more strongly negatively allometric and the growth of whorl height is more strongly positively allometric in *D. conradi* than in *D. gulosus.* As a result, the whorl section is relatively more compressed and flat-sided in *D. conradi* whereas it is relatively more depressed and robust in *D. gulosus. D. gulosus* also has coarser ornament throughout ontogeny. In contrast to *D. conradi,* primaries in *D. gulosus* are generally straight or at most slightly flexuous, and are not accompanied by long, flexuous lirae.

D. gulosus differs from the robust macroconchs of the co-occurring, multituberculate species of *Jeletzkytes* in its tighter coil and its pattern of ornamentation. Species of *Jeletzkytes* are marked by more abundant ribs and conspicuously larger ventrolateral tubercles. At comparable shell diameters, e.g., at 15 mm shell diameter, juveniles of *D. gulosus* differ from those of *J. spedeni* in having finer ornament and a smaller umbilicus. As noted under *D. conradi,* generic differences adequately distinguish the species of *Discoscaphites* from those of other Late Cretaceous multituberculate scaphites.

D. gulosus specimens from the Prairie Bluff Chalk, like those of *D. conradi,* are strikingly smaller than their counterparts in the Western Interior; the specimens described by Jeletzky and Waage (1978: 1129) range from 38.8 to 56.2 mm in size, which falls entirely below the size range of the Fox Hills specimens (57.6 to 94.1 mm). Unlike the Fox Hills population of *D. gulosus,* the Prairie Bluff Chalk specimens show little size difference between macroconchs and microconchs. Differences other than size between these faunas from different regions appear to be minor and may in part be due to the possible age difference previously noted (p. 21).

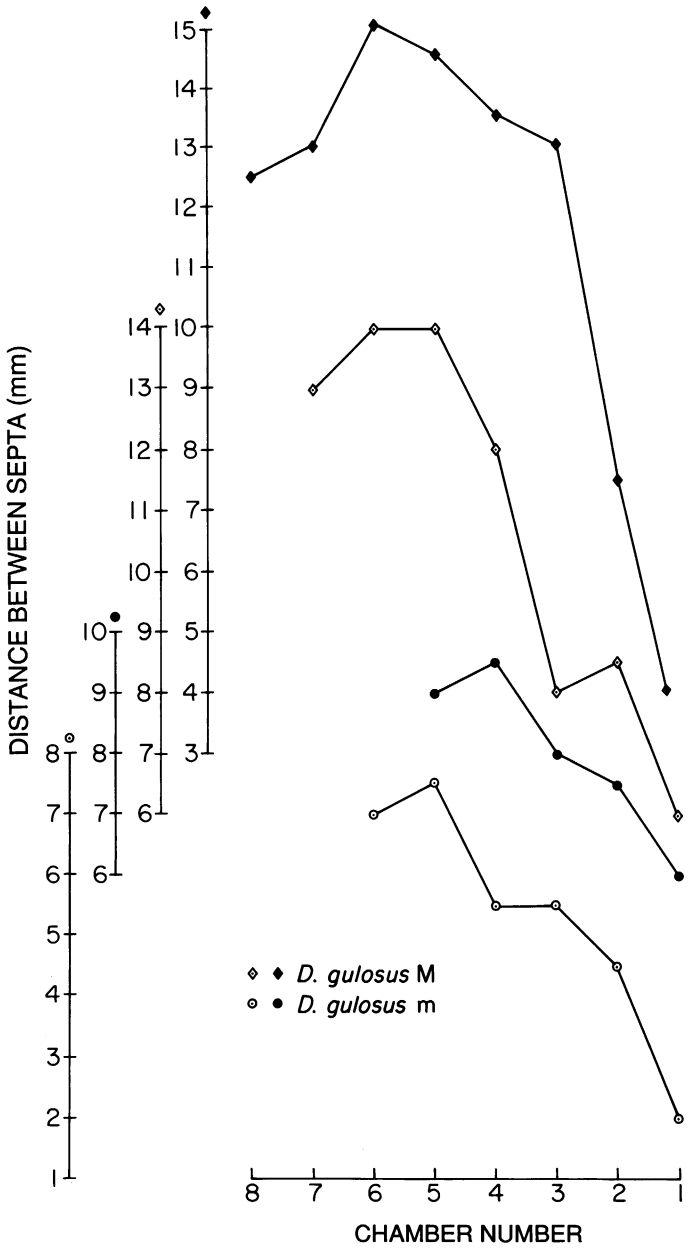

Fig. 180. Distance between septa versus chamber number, counting from the last, most recently formed, chamber of the phragmocone (1), in two macro- and two microconchs of *Discoscaphites gulosus* (Morton). Septal approximation occurs over more chambers in macroconchs than in microconchs.

Discoscaphites rossi, new species
Figures 181–189

DIAGNOSIS: Macroconchs micromorphic, highly compressed, thin-shelled with very short hooks; flanks flat, weakly ribbed, bevelled at margins of venter; venter narrow with ventrolateral tubercles on every rib, row of flank tubercles on dorsal margin of bevel present or not. Microconchs similar except smaller and with less expanded body chamber.

TABLE 21
Adult Measurements of *D. rossi*[a]

	Macroconch				Microconch			
	N	$\bar{x}$	SD	Range	N	$\bar{x}$	SD	Range
LMAX (mm)	7	25.6	4.52	21.0–33.5	18	20.4	3.71	13.8–28.3
WUS (mm)	6	4.3	1.04	3.3–6.1	21	3.7	0.58	2.8–5.0
HUS (mm)	6	7.1	1.58	5.5–9.1	21	5.4	1.13	3.5–8.1
WUS/HUS	6	0.61	0.063	0.50–0.69	21	0.68	0.066	0.60–0.81
WAPT (mm)	4	7.9	1.23	7.0–9.7	16	6.9	1.20	4.5–9.2
HAPT (mm)	4	10.1	1.65	8.6–12.3	16	7.9	1.84	5.0–12.6
WAPT/HAPT	4	0.79	0.018	0.77–0.81	15	0.88	0.086	0.73–1.06
UD (mm)	7	2.5	0.24	2.2–2.8	22	2.2	0.25	1.6–2.7
UD/LMAX	5	0.09	0.014	0.08–0.11	17	0.11	0.023	0.08–0.16
A (°)	5	15.4	5.26	8.9–21.5				

[a] Abbreviations: see table 1 and figure 9.

TYPES: Holotype, macroconch, YPM 23052, loc. 305, TLM, fig. 181A–E.

Allotype, microconch, YPM 23090, loc. 316, TLM, fig. 181Q–T.

NAME: Named in honor of Mrs. Helen Ross of Timber Lake, South Dakota, fossil hunter and friend of fossil hunters.

OCCURRENCE: All specimens studied are from the Timber Lake Member of the Fox Hills Formation on the Cheyenne-Moreau divide and bluffs on the north side of the Moreau River, Dewey County, South Dakota. A number of these specimens come from pits in terrace gravels in which Timber Lake concretions, identifiable by their lithology and associated fauna, are a common constituent.

MATERIAL: Shells representing about 100 individuals, most of them fragmental, yielded a study set of 52 specimens of which 32 were complete enough for measurement. Macroconchs appear to be less common than microconchs; of the 32 most complete specimens, only 9 are macroconchs. Because the shell wall is very thin, crushed and partial specimens are much more common than entire specimens. We were fortunate in having our own collection supplemented by gifts of these tiny scaphites from BHI of Hill City, Don Parsons of Rapid City, and Helen and Brad Ross of Timber Lake, South Dakota.

MACROCONCH DESCRIPTION: Dimensions of the measured specimens are listed in table 21. LMAX averages 25.6 mm and ranges from 21.0 to 33.5 mm (fig. 183). The ratio of the size of the largest specimen to that of the smallest is 1.60. There are approximately 5.0 whorls in the tightly coiled shell, of which 0.75 whorls represent the body chamber. The body chamber is arcuate on the venter with a short hook that slightly overlaps the phragmocone at the aperture. The umbilical diameter averages 2.5 mm and ranges from 2.2 to 2.8 mm; the ratio of umbilical diameter to shell diameter averages 0.09 (table 21). The apertural angle is difficult to determine because the aperture is rarely preserved; it is estimated to vary between 10 and 20°; as these values indicate, the hook is exceptionally short.

Dimorphs of this micromorphic species are not as clearly defined as they are in other species of *Discoscaphites* although they are still recognizable. In general, because the hook is shorter, both dimorphs deviate less from the normal coil as the shell changes into its scaphitoid form than do dimorphs of larger species. Moreover, there tends to be more variation within dimorphs and, as a consequence, it is more difficult to distinguish between them. That they are indeed mature scaphites and not juveniles is shown both by the uncoiling itself and by the close spacing of the last two septa. However, some small specimens lack a constriction at the aperture and may not be fully mature.

Macroconchs of *D. rossi* are similar to those of other scaphites in that the body chamber increases markedly in height and the umbilical shoulder is straight or shows a dorsal swelling. The umbilicus of the coil rests on

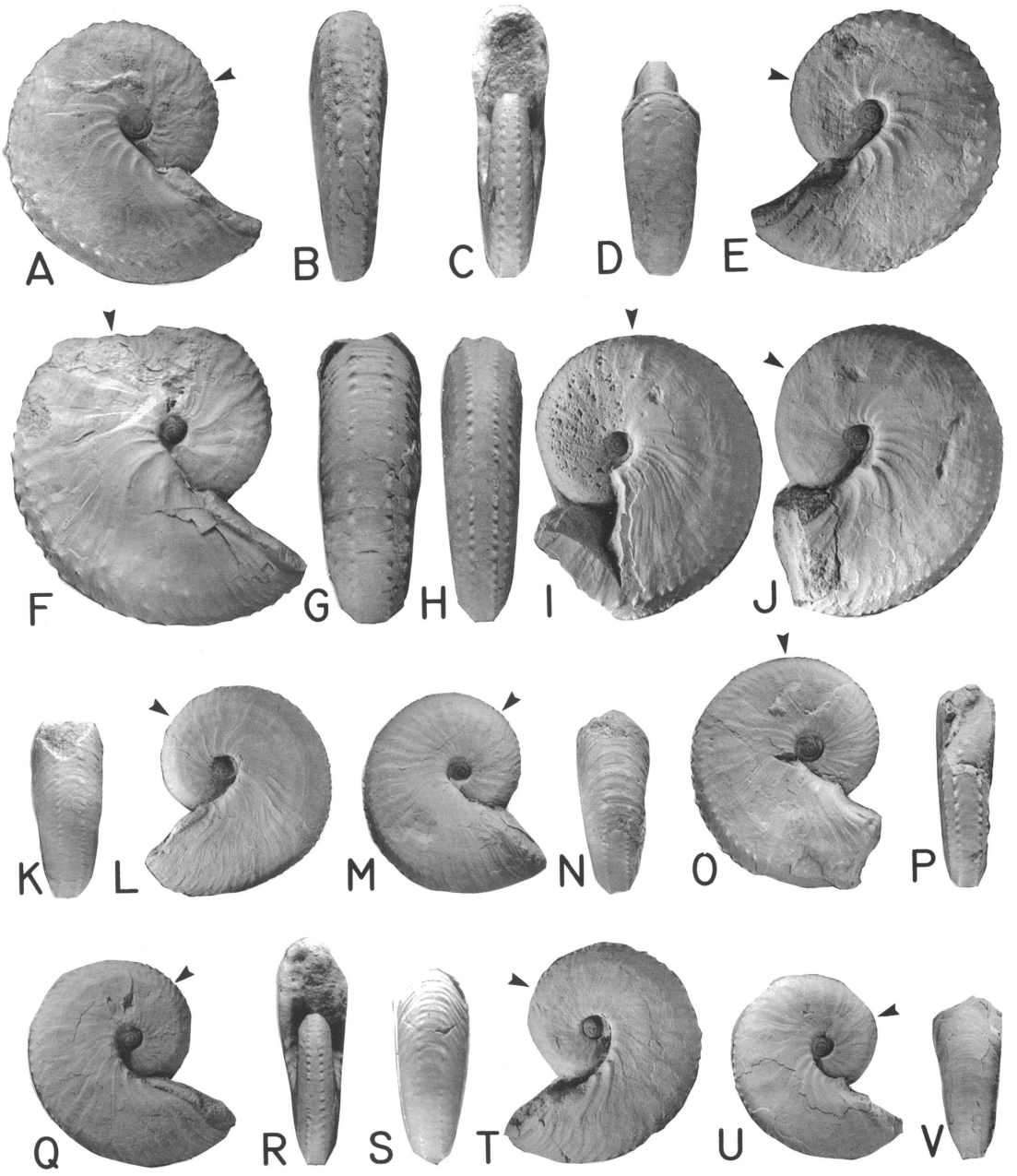

Fig. 181. *Discoscaphites rossi,* n. sp., macroconchs and microconchs. All figures ×1.5 unless noted. **A–E.** Holotype, macroconch, YPM 23052, loc. 305, TLM. **A,** Right lateral; **B,** posterior; **C,** apertural; **D,** ventral hook; **E,** left lateral. **F, G.** Macroconch, ×2, AMNH 44335, loc. 3161, TLM. **F,** Right lateral; **G,** posteroventral. **H, I.** Incomplete macroconch, YPM 27084, loc. 33, TLM. **H,** posterior; **I,** left lateral. **J.** Incomplete macroconch, left lateral, YPM 23085, loc. 316, TLM. **K, L.** Small macroconch, YPM 23095, loc. 227, TLM. **K,** Posteroventral; **L,** left lateral. **M, N.** Small macroconch, YPM 23108, loc. 316, TLM. **M,** Right lateral; **N,** posteroventral. **O, P.** Incomplete macroconch, YPM 23096, loc. 33, TLM. **O,** Right lateral; **P,** posteroventral. **Q–T.** Allotype, microconch, YPM 23090, loc. 316, TLM. **Q,** Right lateral; **R,** apertural; **S,** posteroventral; **T,** left lateral. **U, V.** Microconch, YPM 23094, loc. 33, TLM. **U,** Right lateral; **V,** posteroventral.

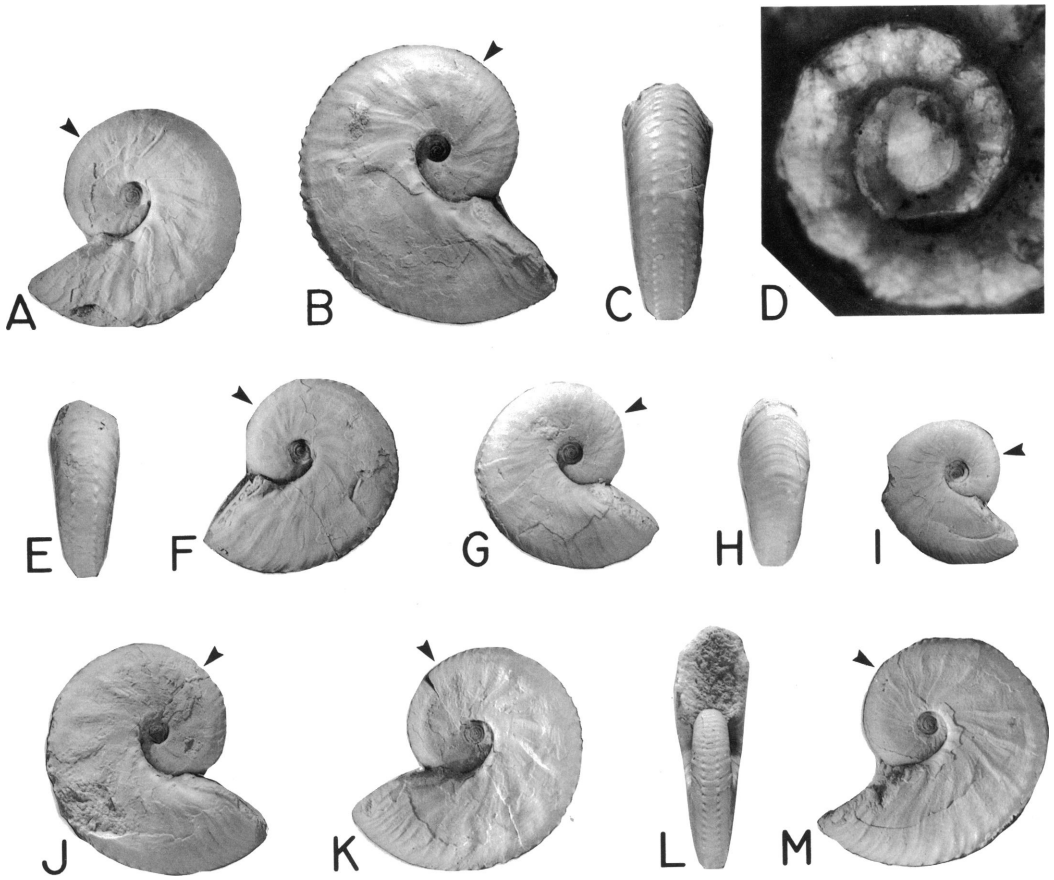

Fig. 182. *Discoscaphites rossi,* n. sp., microconchs. D is ×30, all others ×1.5. **A.** Left lateral, YPM 23097, loc. 30, TLM float. **B–D.** YPM 27081, loc. 37, TLM. **B,** Right lateral; **C,** posteroventral; **D,** early whorls in transmitted light showing ellipsoidal shape of ammonitella typical of *Discoscaphites.* **E, F.** YPM 23100, loc. 88, TLM. **E,** posteroventral; **F,** left lateral. **G, H.** YPM 23083, loc. 316, TLM. **G,** Right lateral; **H,** posteroventral. **I.** Smallest microconch, right lateral, YPM 23105, loc. 41, TLM. **J, K.** YPM 23093, loc. 305, TLM. **J,** Right lateral; **K,** left lateral. **L, M.** AMNH 44336, loc. 3161, TLM. **L,** Apertural; **M,** left lateral.

the umbilical shoulder of the body chamber. The ratios of whorl width to whorl height at the ultimate septum and at the aperture average 0.61 and 0.79, respectively (table 21).

The highly compressed whorls of *D. rossi* macroconchs have flat flanks which, near their outer edge, bend abruptly in a short bevel to a narrow, flattened venter. The juncture of the flanks and bevel commonly shows as a faint ridge on the shell, on the dorsal side of which a band of well-developed feather structure occurs. Lirae follow growth lines across the flanks from the umbilicus to the venter as do fairly widely spaced primary ribs. Ribs and lirae bend gradually forward to about mid-flank, become radial into the feather structure, then swing forward again across the feather structure and the bevel, and cross the venter with a slight adoral projection. This slight but well-defined adoral projection of the ventral ribs is an evident feature in all *D. rossi* macroconchs.

Ribbing is commonly weak and on some specimens the primaries are locally obliterated by the band of feather structure. On the other hand, a few shells show strong primaries that are enlarged and bullate on the outer part of the flanks. Secondary ribs may appear by intercalation on the flanks but more commonly are visible only on the bevel or in the

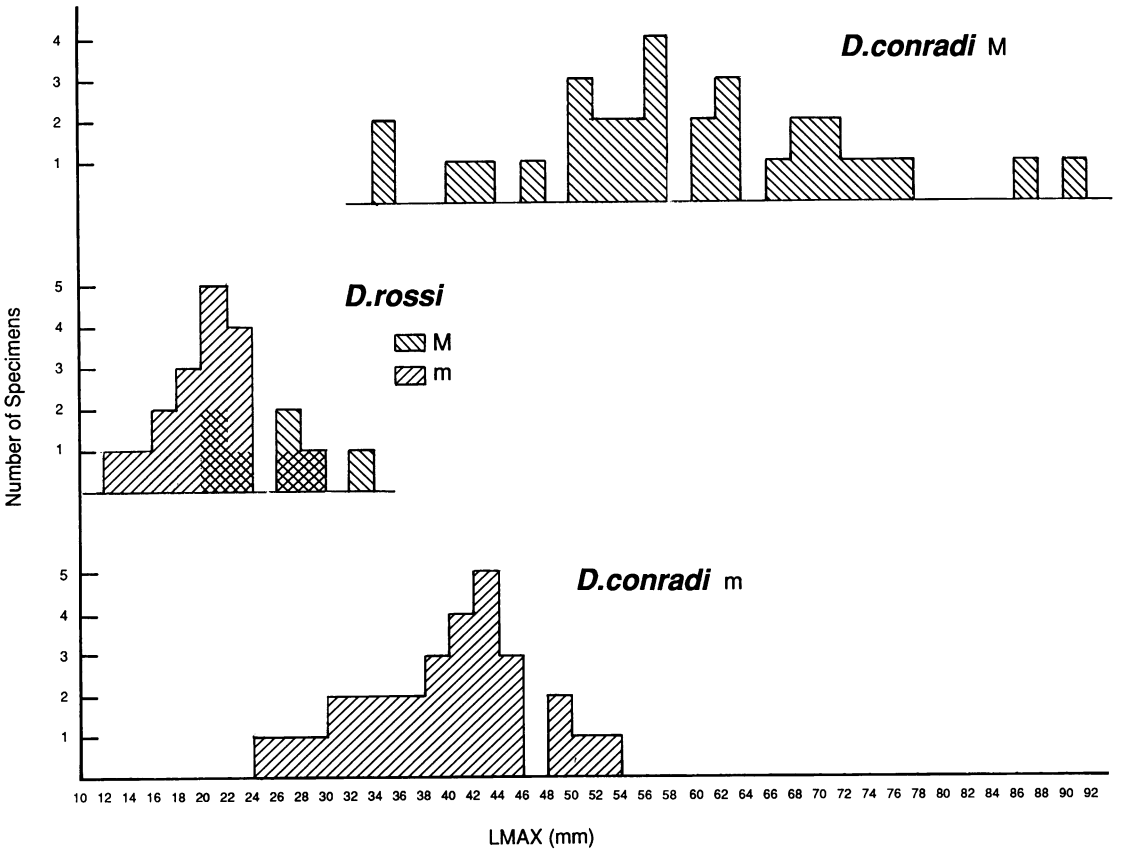

Fig. 183. Size frequency histograms of samples of *Discoscaphites rossi*, n. sp., and *D. conradi* (Morton) from the Fox Hills Formation in its type area. Dimorphs of *D. conradi* are plotted separately.

feather structure. In small specimens, secondaries may not develop, and commonly no ribs, only lirae, may be present on the flat venter. Where visible on the venter, ribs are closely approximated, slightly less than one millimeter apart, averaging about 14/cm. The ratio of the number of dorsal to ventral ribs is approximately 1:2 to 1:3.

A conspicuous character of macroconchs is the presence of tiny ventrolateral tubercles that occur on every rib of the body chamber except on the terminal part of the hook; commonly these tubercles also occur on the exposed phragmocone. They develop from bullate swellings on the ribs at the juncture of the bevel and the flat venter. On most macroconchs, a second row of tubercles may form at the juncture of the bevel and the flanks, clearly defining the bevel (fig. 181F, G); these are usually not as extensive as the ventrolaterals. Bullae may also be present on the body chamber where the ribs cross the umbilical shoulder.

The suture of macroconchs is similar to that of macroconchs of other species of *Discoscaphites* although at this small shell size the outline of the saddles and lobes is square rather than elongate; the suture is not as finely divided as in *D. conradi* (fig. 184A).

MICROCONCH DESCRIPTION: Microconchs average 20.4 mm in size; the ratio of the largest specimen to that of the smallest is 2.0 (table 21). The average size of microconchs is slightly less than that of macroconchs (25.6 mm). The ratio of the average size of macroconchs to that of microconchs is 1.25. Dimorphs overlap between about 21 and 28 mm, which represents a little more than one-third of their total combined range (fig. 183).

The body chamber of microconchs is ap-

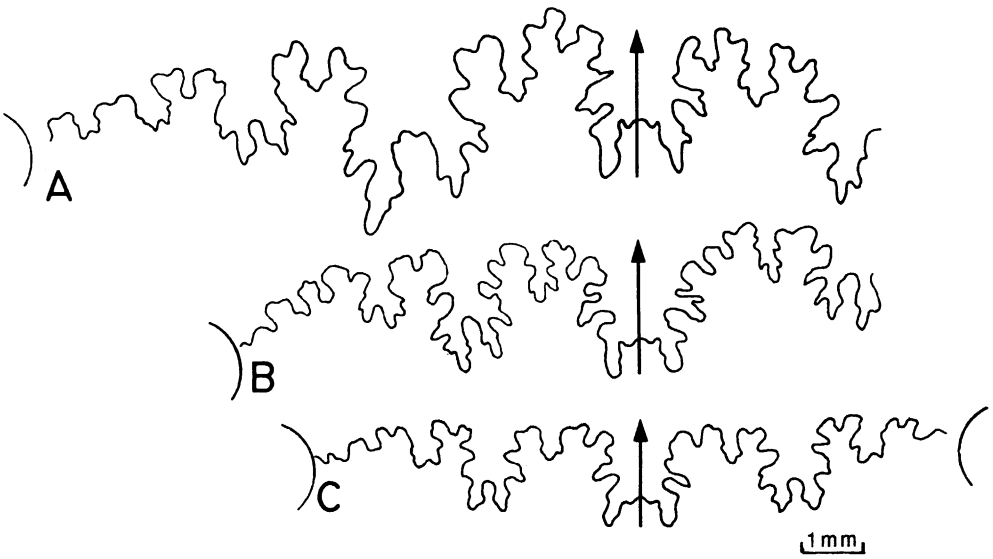

Fig. 184. Sutures of *Discoscaphites rossi,* n. sp., macroconch and microconchs. **A.** Third from last suture of an adult macroconch, YPM 27084, loc. 33, TLM. **B.** Approximately fifth from last suture (10.1 mm shell diameter) of a broken adult, probably a microconch, AMNH 44679, loc. 3161, TLM. **C.** Next to last suture (7.4 mm shell diameter) of a broken adult, probably a microconch, AMNH 44680, loc. 3161, TLM.

proximately 0.75 whorls in angular length. The total number of whorls in the shell ranges from 4.75 to 5.25 and averages 4.88 (N = 6). The shell increases only gradually in size through the arcuate shaft of the body chamber and then decreases very slightly toward the aperture. The ratios of whorl width to whorl height at the ultimate septum and at the aperture average 0.68 and 0.88, respectively. The degree of shell compression does not vary consistently with adult size. The averages of these ratios are not significantly different from those of the corresponding ratios in macroconchs (0.61 and 0.79, respectively).

The umbilical diameter averages 2.2 mm, with larger specimens having relatively smaller umbilical diameters than smaller specimens (table 2). The average is slightly smaller than that in macroconchs (2.5 mm). The ratio of umbilical diameter to shell diameter averages 0.11, which is not significantly different from that in macroconchs (0.09).

The umbilical shoulder of the body chamber is gently curved and not in contact with the umbilicus of the coiled phragmocone. The hook of the body chamber slightly overlaps the phragmocone at the aperture. The size of the hook varies with adult size; larger shells appear to have a relatively longer hook, which is less impressed on the phragmocone at the aperture than is the hook of smaller shells. This results in a gradational series of microconch shapes from very small individuals with short, tightly impressed hooks that give the shell a round appearance in side view (fig. 182G) to larger individuals with longer, less impressed hooks that give the shell a more elongate appearance in side view (fig. 182B).

Microconch ornament differs little from that of macroconchs. A well-defined second row of tubercles at the junction of the bevel and the flank is less common on the body chambers of microconchs and is mostly confined to large specimens (fig. 182B, C).

The suture of microconchs is similar to that of macroconchs (fig. 184B, C).

ONTOGENY: The ammonitella diameter averages 683 μm and the ammonitella angle averages 305° (table 3). The protoconch angle ranges from 57 to 60° and averages 58°, which reflects the depressed protoconch and ellipsoidal ammonitella of *Discoscaphites.*

Dorsoventral, intercostal cross sections of

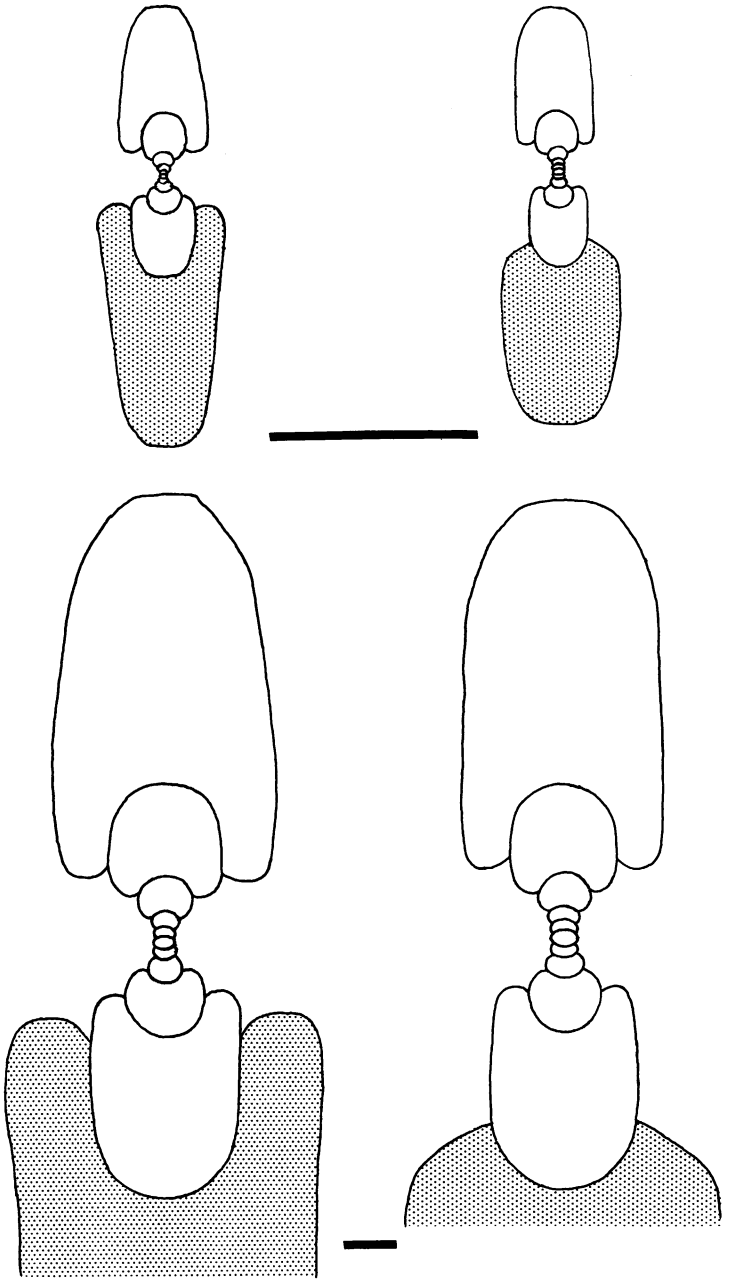

Fig. 185. Dorsoventral intercostal cross sections through adult dimorphs of *Discoscaphites rossi,* n. sp. **Left.** Macroconch, AMNH 44340, loc. 3161, TLM. **Right.** Microconch, AMNH 44344, loc. 3161, TLM. Shaded area demarcates mature body chamber. Upper scale bar = 1 cm; lower scale bar = 1 mm.

macro- and microconchs are illustrated in figure 185. The postembryonic growth of whorl width is strongly negatively allometric and shows a slight change at approximately 3–4 mm shell diameter (slopes range from 0.7315 to 0.8328; fig. 185). The allometry is similar to that in *D. conradi.* In contrast, the postembryonic growth of whorl height is positively allometric in both dimorphs (slopes range from 1.1304 to 1.1868; fig. 187). At

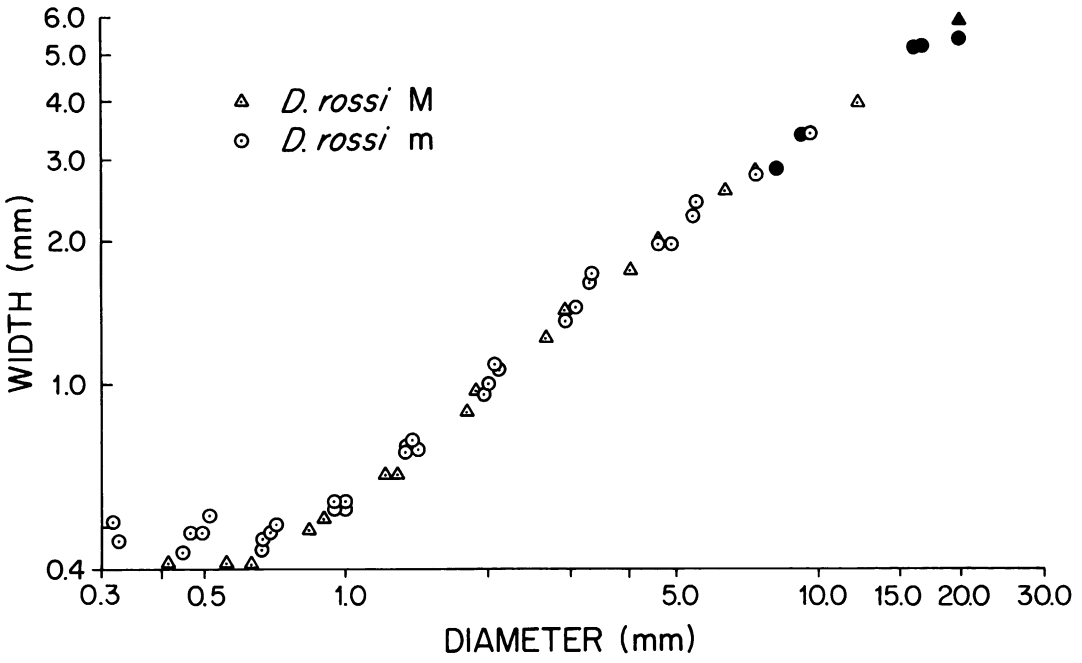

Fig. 186. Plot of whorl width versus shell diameter through the ontogeny of six adults (two macroconchs and four microconchs) of *Discoscaphites rossi,* n. sp. Black symbols indicate measurements near the base of or in the mature body chamber. Measurements listed in Appendix II.

comparable shell diameters, the values of whorl width and whorl height in macroconchs are approximately the same as those in microconchs. The whorls become increasingly more compressed during ontogeny in both dimorphs; the ratio of whorl width to whorl height ranges from 1.0 to 2.0 up to approximately 5 mm shell diameter, decreasing to a minimum of 0.6 to 0.7 near the base of the mature body chamber.

The growth of umbilical diameter is negatively allometric throughout most of postembryonic growth (fig. 188). At the same shell diameter, the values of umbilical diameter are similar in both dimorphs. The ratio of umbilical diameter to shell diameter decreases throughout most of postembryonic growth and reaches a minimum near the base of the mature body chamber of 0.12 to 0.21 in both dimorphs.

The ontogenetic development of ornamentation is illustrated in figure 189 and is more or less the same in both dimorphs. The shell flanks are initially covered with fine, prorsiradiate, flexuous growth lines that bend forward on the venter. At approximately 4 mm shell diameter, very weak flank ribs (primaries) appear. They are prorsiradiate, flexuous, and accompanied by fine growth lines and lirae. Soon thereafter, at approximately 5–6 mm shell diameter, a bevel develops between the flat flanks and narrow venter. A band of feather structure may accentuate the dorsal edge of this bevel. The flanks themselves tend to slope inward toward the umbilicus, similar to the flanks on the early whorls of *D. conradi.* Weak ventral ribs with an adoral projection may develop at approximately the same shell diameter as the bevel. The ratio of the number of dorsal to ventral ribs is approximately 1:2 to 1:3.

At approximately 10 mm shell diameter (0.25 whorls before the point of exposure), small ventrolateral tubercles appear. This is approximately the same shell diameter at which they appear in other species of *Discoscaphites.* Coincident with the appearance of ventrolateral tubercles, ventral ribs become less projected forward. Primaries are weak to moderately strong, flexuous, and ac-

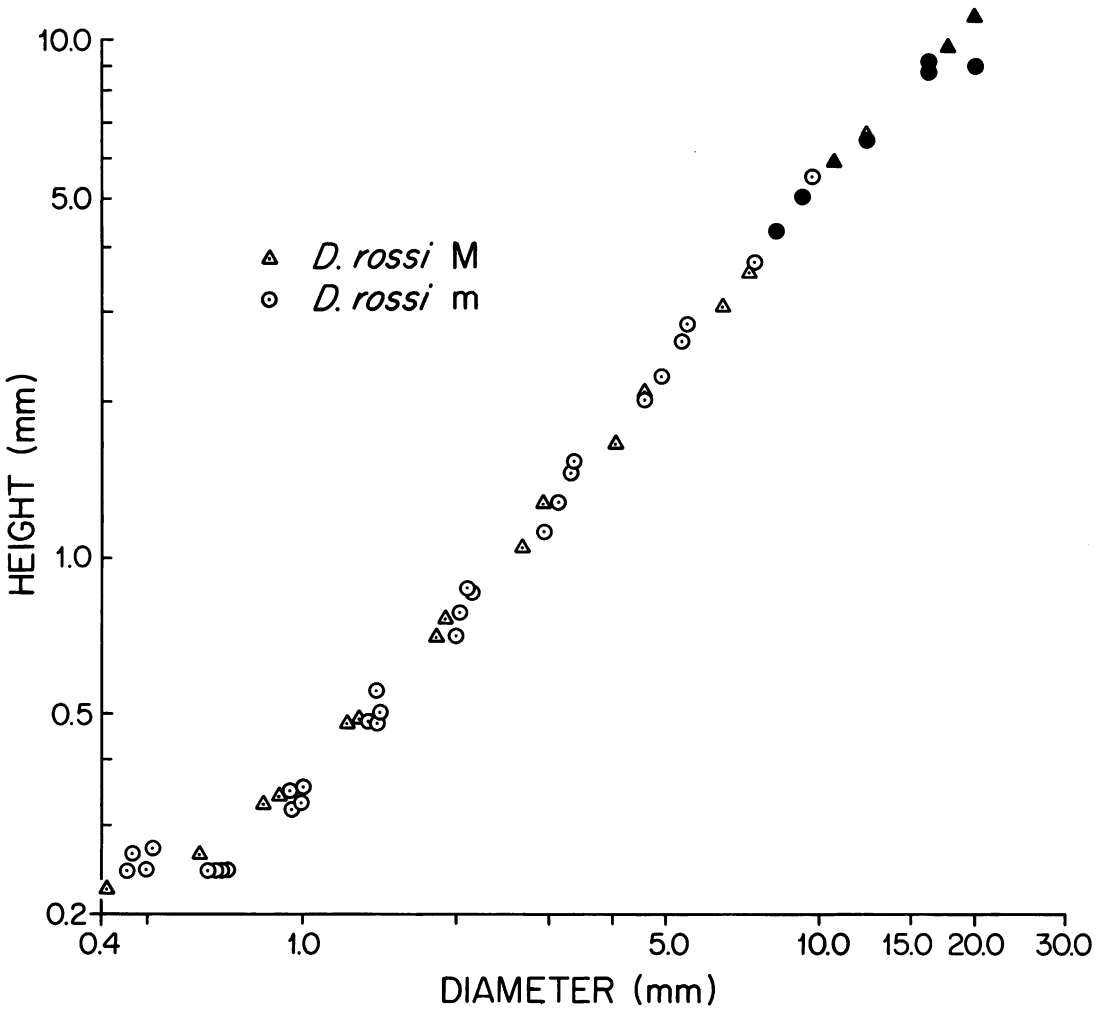

Fig. 187. Plot of whorl height versus shell diameter through the ontogeny of six adults (two macroconchs and four microconchs) of *Discoscaphites rossi,* n. sp. Black symbols indicate measurements near the base of or in the mature body chamber. Measurements listed in Appendix II.

companied by fine secondaries and lirae. Ribs and lirae bend forward to about mid-flank, become radial to the bevel, and then bend forward again across the venter. The ratio of the number of dorsal to ventral ribs is 1:2 to 1:3.

DISCUSSION: The resemblance of *D. rossi* to juveniles of *D. conradi* is marked, suggesting that *D. rossi* is a progenetic offshoot of *D. conradi.* The size distribution of *D. rossi* is compared with that of *D. conradi* in figure 183. The average size of *D. rossi* macroconchs is 25.6 mm and that of *D. conradi* macroconchs is 60.0 mm; their size ranges do not overlap. The ratios of whorl width to whorl height at the ultimate septum and at the aperture in *D. rossi* macroconchs average 0.61 and 0.79, respectively, which are not significantly different from the averages of the corresponding ratios in *D. conradi* macroconchs (0.63 and 0.84, respectively). The average size of *D. rossi* microconchs is 20.4 mm and that of *D. conradi* microconchs is 39.4 mm; their size ranges overlap between about 25 and 28 mm. The ratio of whorl width to whorl height at the ultimate septum averages 0.68 in *D. rossi* microconchs, which is similar to that in *D. conradi* microconchs (0.66).

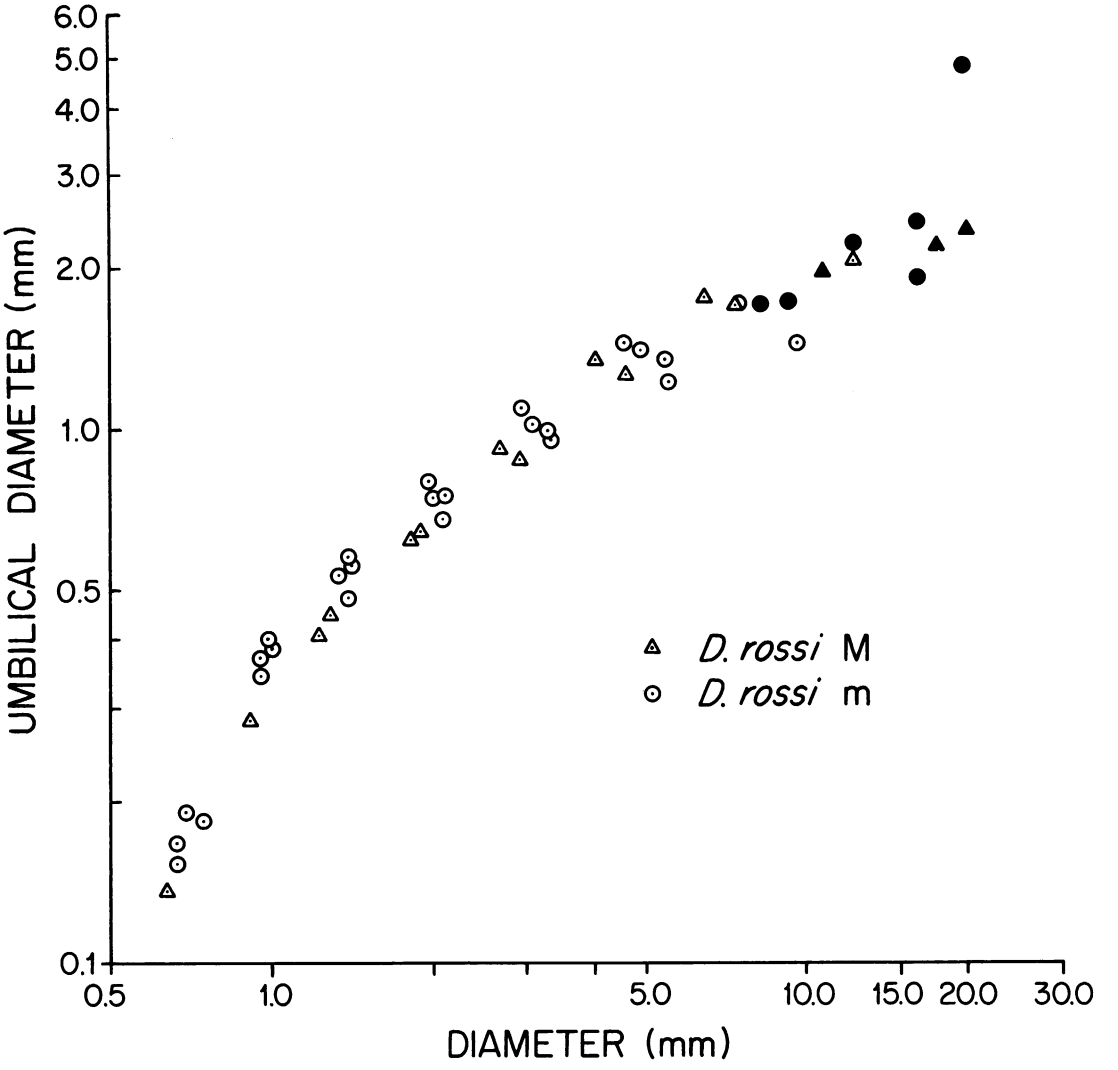

Fig. 188. Plot of umbilical diameter versus shell diameter through the ontogeny of six adults (two macroconchs and four microconchs) of *Discoscaphites rossi,* n. sp. Black symbols indicate measurements near the base of or in the mature body chamber. Measurements listed in Appendix II.

However, the ratio of whorl width to whorl height at the aperture in *D. rossi* microconchs averages 0.88, which is significantly higher than that in *D. conradi* microconchs (0.82).

D. conradi is relatively rare in the Timber Lake Member and what specimens there are tend to be large for the species. As a result, there is little chance of confusion between *D. conradi* and *D. rossi* in the Timber Lake Member. In the lower Trail City Member, small *D. conradi* microconchs are common in the *Limopsis-Gervillia* Assemblage Zone; some of these are undoubtedly *D. conradi* based on their pattern of ornamentation, but five of our specimens are indistinguishable from *D. rossi* microconchs. As in other scaphite species, microconchs are not as definitive as macroconchs, and no macroconchs of *D. rossi* have been found in the *Limopsis-Gervillia* Assemblage Zone; consequently, we cannot demonstrate the presence of *D. rossi* at this horizon, or at any other in the Trail City Member.

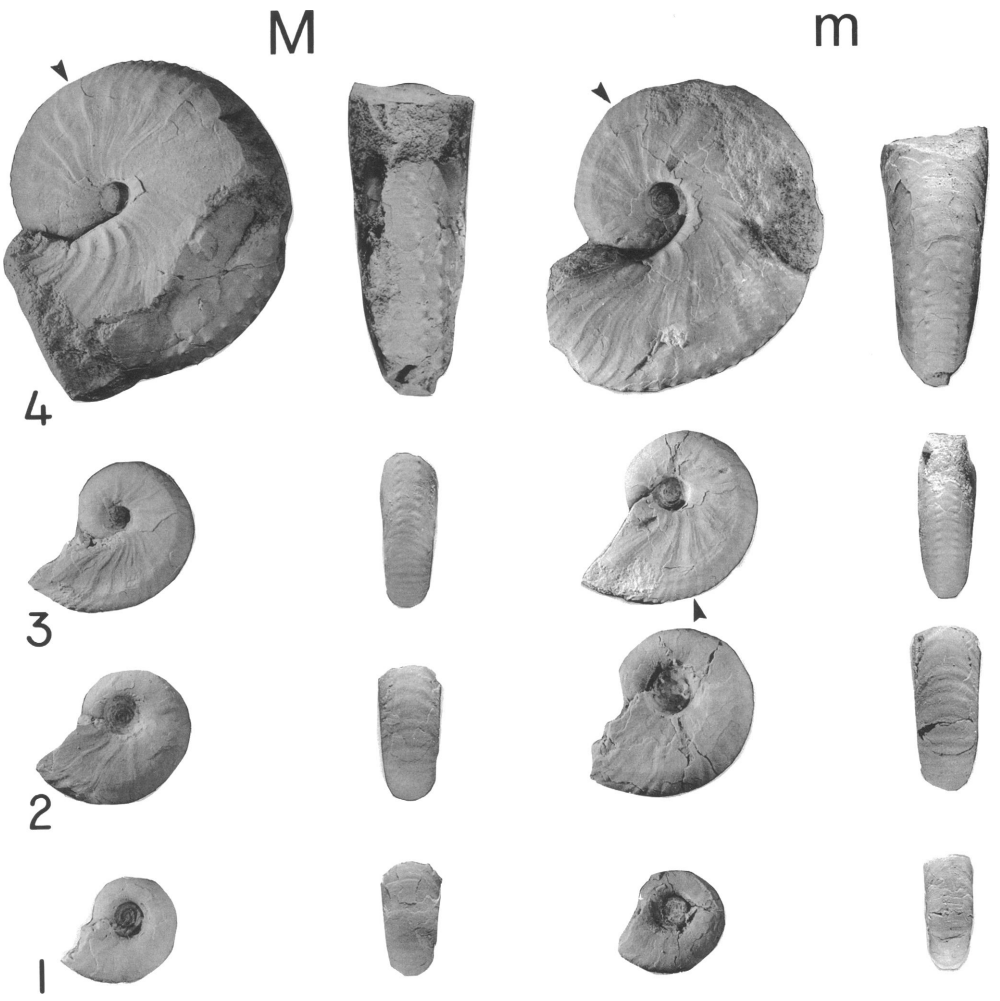

Fig. 189. Dissections of adult dimorphs (macroconch, YPM 23103, loc. 37, TLM, and microconch, AMNH 44678, loc. 3161, TLM) of *Discoscaphites rossi,* n. sp., showing four sizes through ontogeny in lateral and ventral view. 1. ×3. 2. ×3. 3. ×2. 4. ×2. Arrows indicate base of mature body chamber.

REFERENCES

Arkell, W. J.
1957. Introduction to Mesozoic Ammonoidea. *In* W. J. Arkell, B. Kummel, and C. W. Wright (eds.), Mesozoic Ammonoidea. Treatise on invert. paleontol. Pt. L, Mollusca 4: L81–L124.

Bandel, K., N. H. Landman, and K. M. Waage
1982. Micro-ornament on early whorls of Mesozoic ammonites: implications for early ontogeny. J. Paleontol. 56: 386–391.

Birkelund, T.
1965. Ammonites from the Upper Cretaceous of West Greenland. Medd. Grønland 179(7): 192 pp.
1982. Maastrichtian ammonites from Hemmoor, Niederelbe (NW Germany). Geol. Jahrb. A61: 13–33.

Birkelund, T., and H. J. Hansen
1968. Early shell growth and structures of the septa and the siphuncular tube in some

Maastrichtian ammonites. Medd. Dansk Geol. Foren. København 18: 71–78.

Blaszkiewicz, A.
1980. Campanian and Maastrichtian ammonites of the Middle Vistula River Valley, Poland: a stratigraphic-paleontological study. Proc. Inst. Geol. 92: 63 pp.

Brouwers, E. M., and J. E. Hazel
1978. Ostracoda and correlation of the Severn Formation (Navarroan; Maestrichtian) of Maryland. Soc. Econ. Paleontol. Mineral., Paleontol. Monogr. 1: 52 pp.

Callomon, J. H.
1981. Dimorphism in ammonoids. *In* M. R. House and J. R. Senior (eds.), The Ammonoidea. Syst. Assoc. Spec. Vol. 18: 251–273. London: Academic Press.

Calvert, W. R.
1912. Geology of certain lignite fields in eastern Montana. U.S. Geol. Surv. Bull. 471: 187–201.

Christensen, W. K.
1979. Maastrichtian belemnites from Denmark. *In* T. Birkelund and R. G. Bromley (eds.), Cretaceous-Tertiary Boundary Events Symposium, 1, The Maastrichtian and Danian of Denmark, pp. 42–44. Copenhagen: University of Copenhagen.

Cobban, W. A.
1951. Scaphitoid cephalopods of the Colorado Group. U.S. Geol. Surv. Prof. Pap. 239: 39 pp.
1958a. Late Cretaceous fossil zones of the Powder River Basin, Wyoming and Montana. *In* J. Strickland, F. Byrne, and J. Barlow (eds.), Wyoming Geol. Assoc. Guidebook, 13th Ann. Field Conf., Powder River Basin, pp. 114–119. Casper, WY: Wyoming Geol. Assoc.
1958b. Two new species of *Baculites* from the Western Interior Region. J. Paleontol. 32(4): 660–665.
1964. Evolution of two Upper Cretaceous mollusks. U.S. Geol. Surv., Prof. Pap. 501A: A136.
1969. The Late Cretaceous ammonites *Scaphites leei* Reeside and *Scaphites hippocrepis* (De Kay) in the Western Interior of the United States. U.S. Geol. Surv. Prof. Pap. 619: 29 pp.

Cobban, W. A., and J. A. Jeletzky
1965. A new scaphite from the Campanian rocks of the Western Interior of North America. J. Paleontol. 39(5): 794–801.

Cobban, W. A., and W. J. Kennedy
1992. The last Western Interior *Baculites* from the Fox Hills Formation of South Dakota. J. Paleontol. 66(4): 690–692.
In press. *Jeletzkytes* Riccardi, 1983, a scaphitid ammonite from the middle Campanian to lower Maastrichtian Pierre Shale and its correlatives in the Western Interior of the United States. U.S. Geol. Surv. Bull.

Cobban, W. A., and J. B. Reeside, Jr.
1952. Correlation of the Cretaceous formations of the Western Interior of the United States. Geol. Soc. Am. Bull. 63(10): 1011–1044.

Cobban, W. A., and G. R. Scott
1964. Multinodose scaphitid cephalopods from the lower part of the Pierre Shale and equivalent rocks in the conterminous United States. U.S. Geol. Surv. Prof. Pap. 483E: E1–E13.

Cooper, M. R.
1990. A revision of the Scaphitidae (Cretaceous Ammonoidea) from the Cambridge Greensand. N. Jahrb. Geol. Paläont. Abh. 178(3): 285–308.

Crick, R. E.
1978. Morphological variations in the ammonite *Scaphites* of the Blue Hill Member, Carlile Shale, Upper Cretaceous, Kansas. Univ. Kansas Paleontol. Contrib. 88: 28 pp.

Dane, C. H., W. G. Pierce, and J. B. Reeside, Jr.
1937. The stratigraphy of the Upper Cretaceous rocks north of the Arkansas River in eastern Colorado. U.S. Geol. Surv. Prof. Pap. 186K: 207–232.

Dhondt, A. V.
1979. *Tenuiptaria geulemensis* (Mollusca: Bivalvia) an inoceramid species from the upper Maastrichtian of the Sint Pietersberg area, the Netherlands. Ann. Soc. R. Zool. Belgique 108: 141–149.
1983a. Tegulated inoceramids and Maastrichtian biostratigraphy. Newsl. Stratigr. 12(1): 43–53.
1983b. Campanian and Maastrichtian inoceramids: a review. Zitteliana 10: 689–701.

Diener, C.
1916. Bemerkungen zur Nomenclatur der Gattung *Scaphites* Park. Zentbl. Miner. Geol. Paläont.: 525–558.

Dobbin, C. E., and J. B. Reeside
1929. The contact of the Fox Hills and Lance Formations. U.S. Geol. Surv. Prof. Pap. 158B: 9–25.

Donovan, D. T.
1953. The Jurassic and Cretaceous stratigraphy and paleontology of Traill Ø, East

Greenland. Medd. Grønland 3(4): 150 pp.

Druschits, V. V., and N. Khiami
1970. Structure of the septa, protoconch walls and initial whorls in Early Cretaceous ammonites. Paleontol. J. (Engl. Transl. Paleontol. Zh.) 4(1): 26–38.

Druschits, V. V., L. A. Doguzhayeva, and I. A. Mikhaylova
1977. The structure of the ammonitella and the direct development of ammonites. Paleontol. J. (Engl. Transl. Paleontol. Zh.) 11(2): 188–199.

Elias, M. K.
1931. The geology of Wallace County, Kansas. Kansas Geol. Surv. Bull. 18: 254 pp.
1933. Cephalopods of the Pierre Formation of Wallace County, Kansas, and adjacent area. Univ. Kansas Bull. 34(5): 289–363.

Frech, F.
1915. Über *Scaphites*. I. Die Bedeutung von *Scaphites* für die Gliederung der Oberkreide. Zentrabl. Mineral. Geol. Paläont. 18: 553–568.

Gardner, J. A.
1916. Mollusca. *In* B. W. Clark (ed.), The Upper Cretaceous deposits of Maryland, pp. 371–733. Baltimore: Johns Hopkins Press.

Gill, J. R., and W. A. Cobban
1966. The Red Bird section of the Upper Cretaceous Pierre Shale in Wyoming. U.S. Geol. Surv. Prof. Pap. 393-A: 73 pp.

Gill, T.
1871. Arrangement of the families of mollusks. Smithson. Misc. Coll. 227: 49 pp.

Goetzmann, W. H.
1959. Army exploration in the American West 1803–1863. New Haven: Yale Univ. Press.

Hall, J., and F. B. Meek
1856. Descriptions of new species of fossils, from the Cretaceous formations of Nebraska, with observations upon *Baculites ovatus* and *B. compressus,* and the progressive development of the septa in baculites, ammonites, and scaphites. Am. Acad. Arts Sci. Mem. (n. ser.) 5(2): 379–411.

Hayami, I., and A. Matsukuma
1970. Variation of bivariate characters from the standpoint of allometry. Palaeontology (London) 13(4): 588–605.

Hayden. F. V.
1862. On the geology and natural history of the Upper Missouri. Am. Philos. Soc. Trans. 12: 218 pp.

Imbrie, J.
1956. Biometrical methods in the study of invertebrate fossils. Bull. Am. Mus. Nat. Hist. 108: 215–252.

International Commission on Zoological Nomenclature
1985. International code of zoological nomenclature, 3rd ed. London: Int. Trust for Zool. Nomenclat. and British Mus. Nat. Hist.

Jeletzky, J. A.
1952. Annotations, Note 1. *In* W. A. Cobban and J. B. Reeside, Jr. Correlation of the Cretaceous formations of the Western Interior of the United States. Geol. Soc. Am. Bull. 63(10): 1026–1028.
1960. Youngest marine rocks in the Western Interior of North America and the age of the *Triceratops*-beds, with remarks on comparable dinosaur-bearing beds outside North America. 21st Int. Geol. Congr., Copenhagen, Rpt. 5: 25–40.
1962. The allegedly Danian dinosaur-bearing rocks of the globe and the problem of the Mesozoic-Cenozoic boundary. J. Paleontol. 36(5): 1005–1018.
1968. Macrofossil zones of the marine Cretaceous of the Western Interior of Canada and their correlation with the zones and stages of Europe and the Western Interior of the United States. Geol. Surv. Can. Pap. 67–72: 66 pp.
1970. Cretaceous paleontology. *In* Geology and economic minerals of Canada. Geol. Surv. Can., Econ. Geol. Rep. 1: 649–662.

Jeletzky, J. A., and K. M. Waage
1978. Revision of *Ammonites conradi* Morton 1834, and the concept of *Discoscaphites* Meek 1870. J. Paleontol. 52(5): 1119–1132.

Kauffman, E. G.
1977. Illustrated guide to biostratigraphically important Cretaceous macrofossils, Western Interior Basin, U.S.A. Mountain Geol. 14: 225–274.

Kellum, L. B.
1962. Upper Cretaceous Mollusca from Niobrara County, Wyoming. Michigan Acad. Sci. Arts Lett. 47: 37–70.

Kennedy, W. J.
1986a. The ammonite fauna of the Calcaire à *Baculites* (Upper Maastrichtian) of the Cotentin Peninsula (Manche, France). Palaeontology (London) 29(1): 25–83.
1986b. The ammonite fauna of the type Maastrichtian with a revision of *Ammonites*

colligatus Binkhorst, 1861. Bull. Inst. R. Sci. Nat. Belgique 56: 151–267.

Kennedy, W. J., and W. A. Cobban
1976. Aspects of ammonite biology, biogeography, and biostratigraphy. Spec. Pap. Palaeont. 17: 94 pp.

Kennedy, W. J., and H. Summesberger
1987. Lower Maastrichtian ammonites from Nagoryanÿ (Ukranian SSR). Beitr. Paläont. Öster. 13: 25–78.

Kennedy, W. J., W. A. Cobban, and G. R. Scott
1992. Ammonite correlation of the uppermost Campanian of Western Europe, the U.S. Gulf Coast, Atlantic Seaboard and Western Interior, and the numerical age of the base of the Maastrichtian. Geol. Mag. 129(4): 497–500.

Kner, R.
1848. Versteinerungen des Kreidemergels von Lemberg und seiner Umgebung. Haidingers Naturwiss. Abh. 3(2): 1–42.

Kulicki, C.
1974. Remarks on the embryogeny and postembryonal development of ammonites. Acta Palaeontol. Polonica 20: 201–224.
1979. The ammonite shell: its structure, development and biological significance. Acta Palaeontol. Polonica 39: 97–142.

Laird, W. M., and R. H. Mitchell
1942. The geology of the southern part of Morton County, North Dakota. N. Dak. Geol. Surv. Bull. 14: 42 pp.

Landman, N. H.
1987. Ontogeny of Upper Cretaceous (Turonian-Santonian) scaphitid ammonites from the Western Interior of North America: systematics, developmental patterns, and life history. Bull. Am. Mus. Nat. Hist. 185: 117–241.

Landman, N. H., and K. Bandel
1985. Internal structures in the early whorls of Mesozoic ammonites. Am. Mus. Novitates 2823: 21 pp.

Landman, N. H., and K. M. Waage
1986. Shell abnormalities in scaphitid ammonites. Lethaia 19: 211–224.
In press. Morphology and environment of Upper Cretaceous (Maastrichtian) scaphites. Geobios.

Lehmann, U.
1971. Jaws, radula, and crop of *Arnioceras* (Ammonoidea). Palaeontology (London) 14: 338–341.
1972. Aptychen als Kieferelemente der Ammoniten. Paläont. Z. 46: 34–48.
1981a. Ammonite jaw apparatus and soft parts. *In* M. R. House and J. R. Senior (eds.), The Ammonoidea. Syst. Assoc. Spec. Vol. 18: 275–287. London: Academic Press.
1981b. The ammonites: their life and their world. New York: Cambridge Univ. Press.

Lehmann, U., and C. Kulicki
1990. Double function of aptychi (Ammonoidea) as jaw elements and opercula. Lethaia 23: 325–331.

Maddison, W. P., M. J. Donoghue, and D. R. Maddison
1984. Outgroup analysis and parsimony. Syst. Zool. 33: 83–103.

Makowski, H.
1962. Problems of sexual dimorphism in ammonites. Palaeontol. Polonica 12: 92 pp.

May, F. E.
1980. Dinoflagellate-acritarch palynology. *In* J. H. Minard (ed.), Geology of the Round Bay quadrangle, Anne Arundel County, Maryland. U.S. Geol. Surv. Prof. Pap. 1109: 17–20.

Meek, F. B.
1870. A preliminary list of fossils collected by Dr. Hayden in Colorado, New Mexico and California with brief descriptions of . . . new species. Proc. Am. Philos. Soc. 11: 425–431.
1876. Invertebrate Cretaceous and Tertiary fossils of the Upper Missouri country. U.S. Geol. Surv. Terr. 9: 629 pp.

Meek, F. B., and F. V. Hayden
1856a. Description of new fossil species of Gastropoda from the Cretaceous formations of Nebraska Territory. Proc. Acad. Nat. Sci. Philadelphia 8: 63–69.
1856b. Description of new fossil species of Mollusca collected by Dr. F. V. Hayden, in Nebraska Territory; together with a complete catalogue of all the remains of Invertebrata hitherto described and identified from the Cretaceous and Tertiary formations of that region. Proc. Acad. Nat. Sci. Philadelphia 8: 265–286.
1861. Descriptions of new Lower Silurian (Primordial), Jurassic, Cretaceous, and Tertiary fossils, collected in Nebraska by the exploring expedition under the command of Capt. Wm. F. Raynolds, U.S. Top. Engrs., with some remarks on the rocks from which they were obtained. Proc. Acad. Nat. Sci. Philadelphia 13: 415–447.
1864. Paleontology of the Upper Missouri. Smithson. Contrib. Knowledge 172: 135 pp.

Mello, J. F.
1969. Foraminifera and stratigraphy of the upper part of the Pierre Shale and lower

part of the Fox Hills sandstone (Cretaceous) north-central South Dakota. U.S. Geol. Surv. Prof. Pap. 611: 121 pp.

Morgan, R. E., and B. C. Petsch
1945. A geological survey in Dewey and Corson Counties, South Dakota. South Dakota Geol. Surv. Rept. Inv. 49: 45 pp.

Morrow, A. L.
1935. Cephalopods from the Upper Cretaceous of Kansas. J. Paleontol. 9(6): 463–473.

Morton, N.
1981. Aptychi: the myth of the ammonite operculum. Lethaia 14: 57–61.

Morton, S. G.
1834. Synopsis of the organic remains of the Cretaceous Group of the United States. Philadelphia: W. P. Gibbons.
1842. Description of some new species of organic remains of the Cretaceous Group of the United States with a tabular view of the fossils hitherto discovered in this formation. J. Acad. Nat. Sci. Philadelphia 8(2): 207–227.

Nowak, J.
1911. Untersuchungen über die Cephalopoden der oberen Kreide in Polen. II. Teil. Die Skaphiten. Bull. Acad. Sci. Cracovie, Ser. B 7: 547–589.
1916. Zur Bedeutung von *Scaphites* für die Gliederung der Oberkreide. Verh. K. K. Geol. Reichsanst. Wien 3: 55–67.

Obradovich, J. D., and W. A. Cobban
1975. A time-scale for the Late Cretaceous of the Western Interior of North America. Geol. Assoc. Can. Spec. Pap. 13: 31–54.

Orbigny, A. d'
1840–42 Paléontologie Française: Terrains Crétacés, I, Céphalopodes (texte et atlas). Paris: G. Masson, 662 pp., 148 pl.

Owen, D. D.
1852. Description of new and imperfectly known genera and species of organic remains, collected during the geological surveys of Wisconsin, Iowa, and Minnesota. *In* Report of a geological survey of Wisconsin, Iowa, and Minnesota; and incidentally of a portion of Nebraska Territory, pp. 573–587. Philadelphia: Lippincott.

Parkinson, J.
1811. Organic remains of a former world. 3: 479 pp. London: Sherwood.

Pessagno, E. A.
1969. Upper Cretaceous stratigraphy of the western Gulf Coast area of Mexico, Texas, and Arkansas. Geol. Soc. Am. Mem. 111: 139 pp.

Ravn, J. P. J.
1918. De Marine Kridtaflejringer i Vest-Grønland og deres Fauna. Medd. Grønland 56(9): 309–366.

Reeside, J. B., Jr.
1927. The scaphites, an Upper Cretaceous ammonite group. U.S. Geol. Surv. Prof. Pap. 150B: 21–40.

Rhoads, D. C., I. G. Speden, and K. M. Waage
1972. Trophic group analysis of Upper Cretaceous (Maestrichtian) bivalve assemblages from South Dakota. AAPG Bull. 56: 1100–1113.

Riccardi, A. C.
1983. Scaphitids from the Upper Campanian-Lower Maastrichtian Bearpaw Formation of the Western Interior of Canada. Geol. Surv. Can. Bull. 354: 51 pp.

Rosenkrantz, A.
1942. The marine Cretaceous sediments at Umîvik. Medd. Grønland 135(3): 37–42.

Russell, L. S., and R. W. Landes
1940. Geology of the southern Alberta Plains. Geol. Surv. Can. Mem. 221: 223 pp.

Schönfeld, J., and J. Burnett
1991. Biostratigraphical correlation: Lägerdorf-Hemmoor (northwestern Germany), DSDP Sites 548A, 549 and 551 (eastern North Atlantic) with palaeobiogeographical and palaeoceanographical implications. Geol. Mag. 128(5): 479–503.

Scott, G. R., and W. A. Cobban
1965. Geologic and biostratigraphic map of the Pierre Shale between Jarre Creek and Loveland, Colorado. U.S. Geol. Surv. Misc. Geol. Invest. Map I-439: 4 pp.

Smith, C. C., and E. A. Mancini
1983. Biostratigraphy. *In* E. E. Russell, D. M. Keady, E. A. Mancini, and C. E. Smith (eds.), Upper Cretaceous in the lower Mississippi Embayment of Tennessee and Mississippi: field trip guidebook: 15–26. Geol. Soc. Am. Ann. Mtng, New Orleans, LA, 1982.

Smith, W. D.
1905. The development of *Scaphites*. J. Geol. 13: 635–654.

Sohl, N. F., and J. F. Mello
1970. Biostratigraphic analysis. *In* J. P. Owens, J. P. Minard, N. F. Sohl, and J. F. Mello (eds.), Stratigraphy of the outcropping post-Magothy Upper Cretaceous formations in southern New Jersey and northern Delmarva Peninsula, Delaware and Maryland. U.S. Geol. Surv. Prof. Pap. 674: 28–54.

Speden, I. G.
1970a. The type Fox Hills Formation, Cretaceous (Maestrichtian), South Dakota: Pt. 2. Systematics of the Bivalvia. Peabody Mus. Nat. Hist. Bull. 33: 222 pp.
1970b. Generic status of the *Inoceramus*? *tegulatus* species group (Bivalvia) of the latest Cretaceous of North America and Europe. Peabody Mus. Nat. Hist. Postilla 145: 45 pp.

Sowerby, J.
1817. The mineral conchology of Great Britain 2: 186 pp. London: the author.

Stephenson, L. W.
1941. The larger invertebrate fossils of the Navarro Group of Texas exclusive of corals and crustaceans and exclusive of the fauna of the Escondido Formation. Univ. Texas Publ. 4101: 641 pp.

Stephenson, L. A., and W. H. Monroe
1940. The Upper Cretaceous deposits (Mississippi). Mississippi State Geol. Surv. Bull. 40: 296 pp.

Swofford, D. L.
1990. Phylogenetic analysis using parsimony (PAUP). Version 3.0. Users Manual. Illinois Natural History Survey: 121 pp. Champaign, IL.

Swofford, D. L., and W. P. Maddison
1987. Reconstructing ancestral character states under Wagner parsimony. Math Biosci. 87: 199–229.

Tanabe, K.
1983. The jaw apparatuses of Cretaceous desmoceratid ammonites. Palaeontology (London) 26(3): 677–686.

Tanabe, K., I. Obata, Y. Fukuda, and M. Futakami
1979. Early shell growth in some Upper Cretaceous ammonites and its implications to major taxonomy. Bull. Natl. Sci. Mus. Ser. C (Geol.) 5: 153–176.

Tanabe, K., I. Obata, and M. Futakama
1981. Early shell morphology in some Upper Cretaceous heteromorph ammonites. Trans. Proc. Palaeontol. Soc. Japan 124: 215–234.

Tanabe, K., and Y. Ohtsuka
1985. Ammonoid early internal shell structure: its bearing on early life history. Paleobiology 11: 310–322.

Waage, K. M.
1964. Origin of repeated fossiliferous concretion layers in the Fox Hills Formation. Kansas Geol. Surv. Bull. 169: 541–563.
1968. The type Fox Hills Formation, Cretaceous (Maestrichtian), South Dakota. Pt. I, stratigraphy and paleoenvironments. Peabody Mus. Nat. Hist. Bull. 27: 175 pp.

Westermann, G. E. G. (ed.)
1969. Sexual dimorphism in fossil metazoa and taxonomic implications. Int. Union Geol. Sci., Ser A 1: 251 pp. Stuttgart: Schweizerbart.

Whitney, B. L.
1984. Dinoflagellate biostratigraphy of the Maestrichtian-Danian section in southern Maryland. *In* N. O. Frederiksen and K. Krafft (eds.), Cretaceous and Tertiary stratigraphy, paleontology, and structure, southwestern Maryland and northeastern Virginia. Am. Assoc. Stratig. Palynol. Inc. Guidebook, 1984: 123–136.

Whittaker, S. G., T. K. Kyser, and W. G. E. Caldwell
1987. Paleoenvironmental geochemistry of the Claggett marine cyclothem in south-central Saskatchewan. Can. J. Earth Sci. 24(5): 967–984.

Wiedmann, J., and J. Kullmann
1981. Ammonoid sutures in ontogeny and phylogeny. *In* M. R. House and J. R. Senior (eds.), The Ammonoidea. Syst. Assoc. Spec. Vol. 18: 215–256. London: Academic Press.

Wright, C. W.
1953. Notes on Cretaceous ammonites. I. Scaphitidae. Ann. Mag. Nat. Hist. (12)6: 473–476.

Wright, C. W., and E. V. Wright
1951. A survey of the fossil Cephalopoda of the Chalk of Great Britain. Palaeontogr. Soc. Monogr. 1: 40 pp.

Wright, E. K.
1981. Evolutionary patterns in the Cretaceous bivalve genus *Tenuipteria*. Masters thesis, on file Univ. Colorado.
1987. Stratification and paleocirculation of the Late Cretaceous Western Interior seaway of North America. Geol. Soc. Am. Bull. 99(4): 480–490.

Zittel, K. A. von
1884. Handbuch der Palaeontologie . . . Abt. 1, 2, (Lief 3), Cephalopoda, pp. 329–522. Munich: Oldenbourg.

APPENDIX I

Key to the Fox Hills Scaphites

> We find it exceedingly difficult to define limits between species amongst these Nebraska [Territory] *Scaphites*. The position and relative size of nodes and costae, as well as the more or less compressed form of the shell and relative size of the umbilicus, are not, within a considerable range of limits, characters that can always be relied upon. (F. B. Meek, *in* Meek and Hayden, 1856b: 281).

In spite of this perceptive observation, we offer this key to the Fox Hills scaphites. This key applies only to adult macroconchs, which are identified by the fact that in side view, the umbilical shoulder of the body chamber is straight rather than curved parallel to the venter. The ornament on microconchs within the same species is similar. However, microconchs of closely related species are difficult to distinguish except by their direct association with the corresponding macroconchs. Species from the type area of the Fox Hills Formation are indicated by an asterisk. *H. melloi* is included in this key although it occurs only in the upper part of the Pierre Shale in the type area of the Fox Hills Formation.

1. Flank tubercles[2] present (fig. 149I) 2
– Flank tubercles absent (fig. 48A) 6
2. Flank tubercles smaller than ventrolateral tubercles (fig. 92D) 3
– Flank tubercles approximately equal in size to ventrolateral tubercles (fig. 151D) .. 10

[2] Flank tubercles are defined by their position on the shell flanks and are distinguished from umbilical/subumbilical and ventrolateral tubercles.

3. Numerous flank tubercles on entire shell (fig. 120A) ..... *J. nebrascensis**
– Few flank tubercles (fig. 92D) 4
4. Flank tubercles present at least on hook (fig. 92D) ..... *J. spedeni**
– Flank tubercles rare or absent on hook (fig. 71A) 5
5. Flank tubercles on phragmocone, which may extend onto body chamber (fig. 141A) ... . *J. dorfi*
– Flank tubercles scattered on body chamber (fig. 71A) 9
6. Inflated whorl section (fig. 97A, B) .... *J. spedeni**
– Compressed whorl section (fig. 48A, B) .. 7
7. Strong adoral projection of ventral margin of aperture (fig. 48A) ..... *H. nicolletii**
– Weak to moderate adoral projection of ventral margin of aperture (fig. 72D) 8
8. Fine, dense ribbing on venter of entire body chamber (fig. 82A, B) ..... *H. melloi*
– Fine, dense ribbing on venter of portion of body chamber (fig. 71 F, I) 9
9. Fine, dense ribbing on anterior two-thirds of body chamber, apertural angle high (figs. 86A, 87A) ..... *H. birkelundi*
– Fine, dense ribbing on anterior one-third of body chamber, apertural angle low (figs. 69F, 71A) ..... *H. comprimus**
10. Inflated whorl section (fig. 169A, B) .... *D. gulosus**
– Compressed whorl section (fig. 149A, B) 11
11. Medium to large shell, at least one row of flank tubercles (fig. 149A) ..... *D. conradi**
– Very small shell, maximum of one row of flank tubercles (fig. 181A) ..... *D. rossi**

APPENDIX II

Ontogenetic Measurements

Measurements through the ontogeny of adult dimorphs of seven species of Fox Hills scaphites plotted in figures 64–66, 78–80, 115–117, 137–139, 162–164, 176–178, 186–188.

1. *H. nicolletii* macroconch (YPM 23054, loc. 44, LNAZ).

D	W	H	W/H	UD	UD/D
0.29	0.52	-	-	-	-
0.50	0.52	0.29	1.80	-	-
0.76	0.52	0.35	1.50	0.12	0.16
1.13	0.69	0.47	1.46	0.31	0.27
1.69	0.90	0.69	1.31	0.53	0.31
2.65	1.34	1.12	1.19	0.83	0.32
4.12	1.95	1.77	1.10	1.23	0.30
6.34	2.69	2.58	1.04	1.99	0.31
9.73	3.76	4.08	0.92	3.06	0.32
15.43	5.70	7.42	0.77	3.92	0.25
25.05	8.98	13.68	0.66	3.95	0.16
40.53	14.19[b]	22.85[b]	0.62[b]	4.00[b]	0.10[b]

2. *H. nicolletii* macroconch (YPM 23055, loc. 44, LNAZ).

D	W	H	W/H	UD	UD/D
0.40	0.60	-	-	-	-
0.54	0.59	0.32	1.83	-	-
0.75	0.54	0.27	2.00	0.16	0.21
1.06	0.64	0.40	1.62	0.39	0.37
1.56	0.85	0.59	1.44	0.57	0.36
2.36	1.21	0.92	1.32	0.83	0.35
3.64	1.75	1.59	1.10	1.13	0.31
5.72	2.53	2.42	1.04	1.70	0.30
8.92	3.64	3.76	0.97	2.73	0.31
14.51	5.44	6.99	0.78	3.76	0.26
23.76	8.55	12.58	0.68	4.19	0.18
38.01[b]	12.26[b]	21.07[b]	0.58[b]	4.37[b]	0.12[b]

3. *H. nicolletii* macroconch (YPM 23053, loc. 44, LNAZ).

D	W	H	W/H	UD	UD/D
0.36	0.56	-	-	-	-
0.53	0.55	0.31	1.78	-	-
0.77	0.52	0.29	1.80	0.16	0.22
1.12	0.68	0.45	1.52	0.39	0.34
1.66	0.85	0.64	1.33	0.57	0.34
2.50	1.24	0.99	1.26	0.87	0.35
3.80	1.78	1.50	1.18	1.30	0.34
5.84	2.48	2.39	1.04	1.94	0.33
8.98	3.71	3.76	0.99	2.82	0.31
13.92	5.43	6.47	0.84	3.69	0.26
22.66	8.01	12.07	0.66	4.12	0.18
36.86[b]	11.13[b]	20.80[b]	0.54	3.99[b]	0.11[b]

4. *H. nicolletii* macroconch (YPM 23056, loc. 44, LNAZ).

D	W	H	W/H	UD	UD/D
0.45	0.58	-	-	-	-
0.62	0.58	0.30	1.97	-	-
0.88	0.56	0.33	1.68	0.25	0.29
1.29	0.70	0.51	1.37	0.45	0.35
1.93	1.01	0.78	1.29	0.64	0.33
2.93	1.47	1.20	1.23	0.94	0.32
4.57	2.19	2.14	1.02	1.23	0.27
7.17	3.04	3.13	0.97	1.90	0.26
11.07	4.30	4.84	0.89	3.17	0.29
17.20	6.26	8.17	0.77	4.19	0.24
27.84[b]	9.35[b]	15.05[b]	0.62[b]	4.62[b]	0.17[b]

5. *H. nicolletii* microconch (AMNH 44226, loc. 3157, TCM).

D	W	H	W/H	UD	UD/D
0.31	0.46	-	-	-	-
0.46	0.46	0.24	1.93	-	-
0.64	0.44	0.25	1.79	0.16	0.24
0.88	0.48	0.32	1.51	0.32	0.36
1.25	0.60	0.46	1.32	0.48	0.38
1.80	0.80	0.67	1.20	0.67	0.37
2.68	1.13	1.04	1.09	0.96	0.36
4.00	1.62	1.57	1.03	1.38	0.35
6.08	2.52	2.43	1.04	2.08	0.34
9.43	3.62	4.06	0.89	2.94	0.31
15.04	4.74	7.09	0.67	3.89	0.26
24.91	7.89	12.70	0.62	5.12	0.21

6. *H. nicolletii* microconch (AMNH 44227, loc. 3157, TCM).

D	W	H	W/H	UD	UD/D
0.28	0.45	-	-	-	-
0.42	0.43	0.22	1.92	-	-
0.60	0.42	0.23	1.84	0.14	0.24
0.83	0.48	0.30	1.59	0.30	0.36
1.16	0.58	0.44	1.32	0.42	0.36
1.63	0.72	0.58	1.24	0.61	0.37
2.44	1.06	0.96	1.10	0.90	0.37
3.72	1.58	1.49	1.06	1.26	0.34
5.65	2.35	2.34	1.00	1.82	0.32
8.73	3.30	3.72	0.88	2.67	0.30
13.77	4.66	6.22	0.75	3.82	0.28
22.40[c]	6.82[c]	10.94[c]	0.62[c]	5.24[c]	0.23[c]

7. *H. comprimus* macroconch (YPM 23057, loc. 35, TLM).

D	W	H	W/H	UD	UD/D
0.88	0.46	0.33	1.38	-	-
1.29	0.62	0.51	1.22	0.44	0.34
1.95	0.92	0.81	1.14	0.64	0.32
2.98	1.36	1.23	1.11	0.94	0.32
4.58	1.93	1.95	0.99	1.39	0.30
7.33	2.86	3.30	0.87	2.07	0.28
11.84	4.10	5.67	0.72	2.86	0.24
19.28	6.27	10.12	0.62	3.48	0.18
32.56	10.99	18.78	0.58	3.65	0.11

8. *H. comprimus* macroconch (YPM 23058, loc. 37, TLM).

D	W	H	W/H	UD	UD/D
0.58	0.40	0.25	1.65	-	-
0.89	0.53	0.37	1.42	0.27	0.30
1.32	0.65	0.53	1.23	0.42	0.32
2.07	1.00	0.91	1.10	0.63	0.30
3.29	1.51	1.46	1.04	0.92	0.28
5.10	2.33	2.18	1.07	1.46	0.29
8.16	3.26	3.70	0.88	2.29	0.28
13.30	4.70	6.48	0.72	3.13	0.24
22.01	7.41	11.91	0.62	3.62	0.16
35.92[b]	10.69[b]	20.32[b]	0.53[b]	3.68	0.10[b]

9. *H. comprimus* macroconch (YPM 23059, loc. 282, TLM).

D	W	H	W/H	UD	UD/D
3.14	1.45	1.37	1.06	-	-
4.92	2.15	2.16	1.00	1.39	0.28
7.82	2.97	3.53	0.84	2.13	0.27
12.50	4.32	6.14	0.70	2.83	0.23
20.14	6.56	10.78	0.61	3.23	0.16
32.40[c]	9.90[c]	18.59[c]	0.53[c]	3.03[c]	0.09[c]

10. *H. comprimus* microconch (YPM 23060, loc. 4, TLM).

D	W	H	W/H	UD	UD/D
0.66	0.42	0.26	1.60	-	-
0.93	0.47	0.34	1.36	0.32	0.35
1.25	0.56	0.41	1.35	0.50	0.40
1.73	0.74	0.60	1.23	0.72	0.42
2.49	1.02	0.92	1.10	0.96	0.39
3.66	1.58	1.45	1.09	1.28	0.35
5.41	2.23	2.20	1.02	1.76	0.33
8.17	3.06	3.43	0.89	2.55	0.31
12.14	4.31	5.10	0.85	3.61	0.30
18.35	5.84	8.13	0.72	5.12	0.28
28.90[c]	8.19[c]	13.85[c]	0.59[c]	6.92[c]	0.24[c]

11. *H. comprimus* microconch (AMNH 44228, loc. 3160, TLM).

D	W	H	W/H	UD	UD/D
0.24	0.43	-	-	-	-
0.41	0.42	0.26[a]	1.66[a]	-	-
0.67	0.42	0.33[a]	1.26[a]	0.08[a]	0.12[a]
0.98	0.54	0.39	1.38	0.25[a]	0.26[a]
1.42	0.65	0.55	1.18	0.48	0.34
2.06	0.92	0.77	1.18	0.74	0.36
3.05	1.21	1.18	1.02	1.10	0.36
4.48	1.86	1.73	1.07	1.56	0.35
6.63	2.86	2.64	1.08	2.26	0.34
10.19	3.80	4.32	0.88	3.22	0.32
16.19	5.35	7.54	0.71	4.33	0.27
26.31[c]	8.21[c]	12.77[c]	0.64[c]	6.00[c]	0.23[c]

12. *H. comprimus* microconch (AMNH 44229, loc. 3160, TLM).

D	W	H	W/H	UD	UD/D
0.30	0.46	-	-	-	-
0.40	0.42	0.21	2.06	-	-
0.55	0.41	0.22	1.93	0.13	0.24
0.78	0.46	0.28	1.63	0.28	0.36
1.11	0.58	0.43	1.37	0.40	0.36
1.67	0.81	0.69	1.18	0.55	0.33
2.54	1.12	1.04	1.07	0.81	0.32
3.84	1.69	1.54	1.10	1.26	0.33
5.93	2.54	2.53	1.00	1.86	0.31
9.49	3.46	4.31	0.80	2.65	0.28
15.28	5.16	7.19	0.72	3.78	0.25
25.70	8.06	13.24	0.61	5.27	0.20

Abbreviations: LNAZ, Lower *nicolletii* Assemblage Zone; LGAZ, *Limopsis-Gervillia* Assemblage Zone; UNAZ, Upper *nicolletii* Assemblage Zone; POAZ, *Protocardia-Oxytoma* Assemblage Zone; TCM, Trail City Member; TLM, Timber Lake Member; FH, Fox Hills Formation undifferentiated; D, shell diameter; W, whorl width; H, whorl height; W/H, ratio of whorl width to whorl height; UD, umbilical diameter; UD/D, ratio of umbilical diameter to shell diameter; a, estimate; b, near base of mature body chamber; c, in mature body chamber; d, near aperture. All measurements in millimeters.

13. *J. spedeni* macroconch (YPM 23061, loc. 57, POAZ).

D	W	H	W/H	UD	UD/D
0.37	0.50	-	-	-	-
0.49	0.56	0.29[a]	1.90	-	-
0.72	0.55	0.33[a]	1.68[a]	0.11[a]	0.15[a]
1.00	0.58	0.36	1.61	0.31	0.31[a]
1.42	0.74	0.56	1.33	0.49	0.35
2.08	1.10	0.80	1.38	0.72	0.34
3.07	1.65	1.22	1.35	1.05	0.34
4.58	2.71	1.84	1.47	1.52	0.33
6.81	3.80	2.84	1.34	2.13	0.31
10.69	5.64	4.94	1.14	2.91	0.27
17.78	9.66	9.06	1.07	3.77	0.21
29.00	14.51	15.86	0.92	4.08	0.14
47.34	23.06	26.57	0.87	4.91	0.10
77.42[c]	28.71[c]	34.82[c]	0.82[c]	16.03[c]	0.21[c]

14. *J. spedeni* macroconch (YPM 23062, loc. 86, LGAZ).

D	W	H	W/H	UD	UD/D
0.31	0.52	-	-	-	-
0.50	0.53	0.26	2.00	-	-
0.82	0.52	0.40	1.31	0.16	0.20
1.19	0.67	0.45	1.47	0.33	0.28
1.73	0.84	0.65	1.30	0.63	0.36
2.49	1.24	0.92	1.36	0.93	0.37
3.66	1.95	1.40	1.40	1.35	0.37
5.37	2.67	2.16	1.24	1.82	0.34
8.10	3.84	3.25	1.18	2.70	0.33
12.40	5.90	5.32	1.11	3.83	0.31
19.56	9.14	9.70	0.94	4.55	0.23
31.93	14.30	16.79	0.85	5.43	0.17
51.38	23.70	27.20	0.87	7.40	0.14
80.57[b]	32.04[b]	43.16[b]	0.74[b]	10.21[b]	0.13[b]

15. *J. spedeni* macroconch (AMNH 44230, loc. 3159, TCM).

D	W	H	W/H	UD	UD/D
1.11	0.53	0.37	1.43	-	-
1.59	0.76	0.60	1.26	0.62	0.39
2.41	1.07	0.96	1.11	0.85	0.35
3.56	1.62	1.39	1.17	1.21	0.34
5.30	-	2.02	-	1.90	0.36
7.96	3.65	3.22	1.13	2.72	0.34
12.24	4.96	5.34	0.93	3.68	0.30
19.77	7.74	10.09	0.77	4.34	0.22
32.08	12.28	17.40	0.70	4.58	0.14
51.01	17.59	29.47	0.60	4.14	0.08
82.62[c]	23.70[c]	41.37[c]	0.57[c]	11.78[c]	0.14[c]

16. *J. spedeni* microconch (YPM 23063, loc. 3, LGAZ).

D	W	H	W/H	UD	UD/D
13.28	5.42	5.80	0.93	-	-
20.61	9.24	9.73	0.95	5.08	0.25
32.94	14.20	16.98	0.84	6.23	0.19

17. *J. spedeni* microconch (YPM 32842, loc. 248, POAZ).

D	W	H	W/H	UD	UD/D
0.35	0.54	-	-	-	-
0.43	0.54	0.23	2.36	-	-
0.61	0.48	0.23	2.08	0.14	0.24
0.90	0.54	0.35	1.56	0.31	0.35
1.26	0.64	0.46	1.40	0.46	0.36
1.81	0.87	0.66	1.32	0.69	0.38
2.66	1.40	0.99	1.41	1.00	0.38
3.92	2.00	1.55	1.29	1.37	0.35
5.72	3.04	2.16	1.41	2.01	0.35
8.49	4.16	3.40	1.22	2.92	0.34
12.78	6.02	5.39	1.12	3.98	0.31
19.73	8.92	9.16	0.97	5.18	0.26
31.13	14.65	15.35	0.95	6.61	0.21

18. *J. spedeni* microconch (YPM 32601, loc. 17, UNAZ).

D	W	H	W/H	UD	UD/D
2.40	1.14	0.87	1.32	-	-
3.50	1.68	1.33	1.26	1.30	0.37
5.14	2.38	1.96	1.21	1.84	0.36
7.61	3.22	3.06	1.05	2.59	0.34
11.48	4.78	4.86	0.98	3.56	0.31
17.93	6.56	8.75	0.75	4.32	0.24
28.90	11.54	15.18	0.76	4.96	0.17

19. *J. spedeni* microconch (YPM 32600, loc. 69, POAZ).

D	W	H	W/H	UD	UD/D
5.98	2.69	2.48	1.08	-	-
8.87	3.91	3.57	1.10	2.82	0.32
13.38	5.43	5.69	0.96	4.13	0.31
20.28	9.35	8.79	1.06	5.80	0.29
31.06	12.92	14.33	0.90	7.93	0.26
50.74[b]	23.69[b]	26.67[b]	0.89[b]	9.74[b]	0.19[b]

20. *J. nebrascensis* macroconch (YPM 23064, loc. 80, TLM).

D	W	H	W/H	UD	UD/D
1.03	0.47	0.41	1.15	-	-
1.46[a]	-	0.58[a]	-	0.48[a]	0.33[a]
1.96	0.82	0.72	1.14	0.67[a]	0.34[a]
2.72	1.32	1.06	1.24	0.95	0.35
4.08	1.80	1.71	1.05	1.32	0.32
6.13[a]	2.66[a]	2.52[a]	1.06[a]	1.91[a]	0.31[a]
9.31[a]	3.76[a]	3.98[a]	0.94[a]	2.82[a]	0.30[a]
13.88	6.15	5.80	1.06	4.10[a]	0.30[a]
21.44	8.74	9.82	0.89	5.82	0.27
34.06	13.98	16.75	0.83	7.50	0.22
51.77[b]	22.58[b]	25.99[b]	0.87[b]	9.03[b]	0.17[b]
77.78[c]	29.46[c]	40.93[c]	0.72[c]	10.86[c]	0.14[c]

21. *J. nebrascensis* macroconch (YPM 32824, loc. 58, TLM).

D	W	H	W/H	UD	UD/D
7.16	3.25	3.33	0.97	-	-
11.38	4.41	5.35	0.82	2.70	0.24
19.07	7.27	10.59	0.69	3.13	0.16
31.84	12.02	17.81	0.68	3.44	0.11
51.89[b]	18.20[b]	30.26[b]	0.60[b]	3.82[b]	0.07[b]

22. *J. nebrascensis* macroconch (YPM 32595, loc. 36, TLM).

D	W	H	W/H	UD	UD/D
0.33	0.49	-	-	-	-
0.44	0.48	0.23	2.06	-	-
0.62	0.46	0.25	1.84	0.14	0.23
0.86	0.46	0.29	1.57	0.32	0.38
1.20	0.56	0.40	1.39	0.50	0.42
1.65	0.69	0.55	1.26[a]	0.70	0.42
2.32[a]	-	0.80[a]	-	0.97[a]	0.42[a]
3.36[a]	1.53	1.28	1.20	1.28[a]	0.38[a]
5.14	2.29[a]	2.34[a]	0.98[a]	1.52[a]	0.30[a]
8.16[a]	3.62	3.70[a]	0.98[a]	2.11[a]	0.26[a]
13.27	5.59	6.75	0.83	2.82[a]	0.21[a]
21.82	9.28	11.16	0.83	3.91	0.18
35.14	14.54	18.93	0.77	5.05	0.14
54.96[b]	24.23[b]	29.40[b]	0.82[b]	6.64[b]	0.12[b]

23. *J. nebrascensis* microconch (YPM 23065, loc. 37, TLM).

D	W	H	W/H	UD	UD/D
5.91	2.58	2.36	1.09	-	-
8.75	3.70	3.50	1.06	2.88	0.33
12.95	5.16	5.32	0.97	4.12	0.32
20.53	8.60	9.73	0.88	5.48	0.27
32.57	12.63	16.32	0.77	6.23	0.19
52.03[b]	18.49[b]	26.28[b]	0.70[b]	9.43[b]	0.18[b]

24. *J. nebrascensis* microconch (AMNH 44231, loc. 3160, TLM).

D	W	H	W/H	UD	UD/D
2.09	0.98[a]	0.86	1.15[a]	-	-
3.12	1.30[a]	1.18	1.10[a]	1.07	0.34
4.67	2.05	1.92	1.07	1.57	0.34
7.10	2.84[a]	2.97	0.96[a]	2.21	0.31
10.51	4.13	4.14	1.00	3.40	0.32
15.92	5.64	6.98	0.81	4.80	0.30
25.17	9.28	12.19	0.76	6.00	0.24

25. *J. nebrascensis* microconch (YPM 32599, loc. 88, TLM).

D	W	H	W/H	UD	UD/D
0.67	0.44	0.32	1.39	-	-
0.98	0.49	0.37	1.33	0.29	0.30
1.35	0.65	0.49	1.32	0.49	0.36
1.91	0.85	0.72	1.19	0.70	0.37
2.77	1.24	1.06	1.17	0.99	0.36
4.05	1.73	1.58	1.10	1.41	0.35
6.03	2.72	2.40	1.13	2.06	0.34
9.05	3.76	3.67	1.02	2.98	0.33
13.71	5.84	5.75	1.02	4.29	0.31
21.76	8.57	10.12	0.85	5.90	0.27
35.52[c]	15.37[c]	18.38[c]	0.84[c]	7.02[c]	0.20[c]

26. *D. conradi* macroconch (YPM 34100, loc. 197, TCM).

D	W	H	W/H	UD	UD/D
0.36	-	-	-	-	-
0.44	0.52	0.23	2.27	-	-
0.62	0.47	0.23	2.04	0.16	0.26
0.85	0.50	0.28	1.82	0.34	0.40
1.13	0.62	0.36	1.72	0.50	0.44
1.58	0.85	0.56	1.50	0.66	0.42
2.33	1.23	0.93	1.33	0.84	0.36
3.55	1.85	1.52	1.22	1.10	0.31
5.61	2.76	2.60	1.06	1.50	0.27
9.52	3.82	5.12	0.75	1.80	0.19
15.93	5.61	8.86	0.63	1.95	0.12
26.13	8.82	14.31	0.62	2.97	0.11

27. *D. conradi* macroconch (YPM 34101, loc. 19, LGAZ).

D	W	H	W/H	UD	UD/D
0.37	0.48	-	-	-	-
0.49	0.47	0.24	1.98	-	-
0.65	0.44	0.21	2.10	0.20	0.31
0.88	0.49	0.29	1.69	0.38	0.43
1.18	0.64	0.39	1.64	0.51	0.43
1.67	0.83	0.61	1.36	0.67	0.40
2.42	1.22	0.91	1.33	0.90	0.37
3.70	2.00	1.58	1.27	1.22	0.33
5.89	3.08	2.76	1.12	1.55	0.26
9.81	3.75	5.14	0.73	1.91	0.20
16.17	5.59	8.82	0.63	2.21	0.14
25.93	9.35	14.17	0.66	2.95	0.11
40.58[b]	13.81[b]	22.89[b]	0.60[b]	3.53[b]	0.09[b]

28. *D. conradi* macroconch (YPM 34102, loc. 212, LNAZ).

D	W	H	W/H	UD	UD/D
1.28	0.69	0.48	1.42	-	-
1.93	1.05	0.78	1.34	0.66	0.34
2.96	1.44	1.22	1.17	0.95	0.32
4.76	2.07	2.22	0.93	1.32	0.28
7.96	2.94	4.01	0.73	1.74	0.22
13.22	4.47	7.06	0.63	2.14	0.16
21.56	7.42	12.22	0.61	2.28	0.11
34.06[b]	10.64[b]	18.97[b]	0.56[b]	2.86[b]	0.08[b]

29. *D. conradi* microconch (YPM 34103, loc. 242, LGAZ).

D	W	H	W/H	UD	UD/D
2.30	1.18	0.97	1.22	-	-
3.70	1.82	1.72	1.06	1.02	0.28
6.03	2.41	2.91	0.83	1.40	0.23
9.87	3.61	4.98	0.72	1.98	0.20
15.83	4.84	8.28	0.58	2.57	0.16
25.88[c]	-	13.01[c]	-	4.60[c]	0.18[c]

30. *D. conradi* microconch (AMNH 44232, loc. 3158, FH).

D	W	H	W/H	UD	UD/D
0.33	0.54	-	-	-	-
0.48	0.56	0.28	1.96	-	-
0.69	0.53	0.24[a]	2.25[a]	0.17[a]	0.25[a]
0.93	0.56	0.29	1.93	0.40[a]	0.44[a]
1.28	0.72	0.43	1.67	0.56	0.44
1.84	0.99	0.69	1.44	0.72	0.39
2.91	1.55	1.26	1.23	0.96	0.33
4.78	2.10	2.28	0.92	1.25	0.26
8.10	2.86	4.23	0.68	1.59	0.20
13.54	4.19	7.25	0.58	2.07	0.15
22.47[b]	6.66[b]	12.03[b]	0.55[b]	3.19[b]	0.14[b]
36.12[d]	10.96[d]	15.45[d]	0.71[d]	8.64[d]	0.24[d]

31. *D. conradi* microconch (YPM 34104, loc. 19, LGAZ).

D	W	H	W/H	UD	UD/D
0.34	0.52	-	-	-	-
0.34	0.52	0.18	2.80	-	-
0.50	0.53	0.26	2.02	0.58	0.12
0.72	0.51	0.27	1.92	0.19	0.26
1.01	0.62	0.38	1.65	0.37	0.37
1.46	0.83	0.55	1.50	0.53	0.36
2.23	1.20	0.94	1.28	0.74	0.33
3.62	1.92	1.62	1.18	1.07	0.29
6.11	2.73	3.10	0.88	1.39	0.23
10.20	3.63	5.24	0.69	1.86	0.18
17.20	6.02	9.47	0.64	2.49	0.14
27.67[ab]	9.74[b]	14.45[ab]	0.67[ab]	3.75[ab]	0.14[ab]
44.66[ad]	15.05[d]	18.28[ad]	0.82[ad]	11.93[ad]	0.27[ad]

32. *D. gulosus* macroconch (YPM 34105, loc. 85, POAZ).

D	W	H	W/H	UD	UD/D
2.00	1.08	0.83	1.29	-	-
3.00	1.73	1.24	1.39	0.92	0.31
4.51	2.68	1.84	1.45	1.43	0.32
6.90	3.96	2.94	1.35	2.12	0.31
10.88	6.49	5.14	1.26	2.80	0.26
17.20	10.19	8.76	1.16	3.30	0.19
27.52	16.45	14.89	1.10	3.87	0.14
44.88[b]	24.40[b]	25.02[b]	0.98[b]	4.97[b]	0.11[b]

33. *D. gulosus* macroconch (AMNH 44233, loc. 3158, FH).

D	W	H	W/H	UD	UD/D
3.76	2.08	1.69	1.24	-	-
5.89	3.68	2.76	1.34	1.45	0.25
9.38	5.49	4.62	1.19	2.00	0.21
15.11	9.19	8.19	1.12	2.30	0.15
24.76	14.08	13.75	1.02	2.82	0.11
39.59[b]	21.65[b]	22.05[b]	0.98[b]	3.80[b]	0.10[b]

34. *D. gulosus* macroconch (YPM 34106, loc. 214, POAZ).

D	W	H	W/H	UD	UD/D
0.40	0.56	-	-	-	-
0.50	0.49[a]	0.20	2.44[a]	-	-
0.68	0.48	0.23	2.05	0.24	0.36
0.95	0.59	0.36	1.63	0.36	0.38
1.31	0.75	0.47	1.59	0.48	0.37
1.86	0.95	0.67	1.41	0.71	0.38
2.68	1.38	1.02	1.34	0.98	0.37
4.02	2.31	1.67	1.39	1.33	0.33
6.21	3.83	2.77	1.38	1.77	0.29
10.05	4.86	5.00	0.97	2.28	0.23
16.91	8.11	9.23	0.88	2.67	0.16
27.76	12.79	15.19	0.84	3.34	0.12
45.06[b]	19.56[b]	25.67[b]	0.76[b]	4.20[b]	0.09[b]
71.79[d]	25.81[d]	27.18[d]	0.95[d]	18.94[d]	0.26[d]

35. *D. gulosus* microconch (YPM 34107, loc. 17, UNAZ).

D	W	H	W/H	UD	UD/D
0.36	0.53	-	-	-	-
0.55	0.46	-	-	-	-
0.83	0.48	-	-	-	-
1.16	0.62	0.40	1.52	-	-
1.63	0.81	0.61	1.32	0.61	0.38
2.31	1.10	0.85	1.29	0.85	0.37
3.32	1.62	1.27	1.28	1.20	0.36
5.01	2.66	2.11	1.26	1.63	0.33
7.72	3.54	3.61	0.98	2.00	0.26
12.47	5.59	6.66	0.84	2.20	0.18
20.32	8.17	11.13	0.73	2.53	0.12
32.90[c]	12.15[c]	16.98[c]	0.72[c]	4.78[c]	0.14[c]

36. *D. gulosus* microconch (AMNH 44338, loc. 3158, FH).

D	W	H	W/H	UD	UD/D
1.28	0.64	0.42	1.55	-	-
1.77	0.95	0.63	1.50	0.72	0.41
2.60	1.32	1.03	1.28	0.94	0.36
4.10	2.17	1.80	1.20	1.26	0.31
6.39	3.56	2.86	1.24	1.72	0.27
10.28	5.52	5.06	1.09	2.35	0.23
16.76	7.98	8.80	0.91	2.89	0.17
27.55[b]	12.47[b]	14.75[b]	0.84[b]	4.00[b]	0.14[b]

37. *D. gulosus* microconch (YPM 34108, loc. 3, POAZ).

D	W	H	W/H	UD	UD/D
0.34	0.58	-	-	-	-
0.51	0.59	0.31	1.92	-	-
0.72	0.56	0.28	2.03	0.14	0.19
0.95	0.58	0.30	1.97	0.38	0.40
1.28	0.74	0.42	1.74	0.56	0.44
1.82	0.99	0.65	1.52	0.74	0.41
2.63	1.55	1.03	1.51	0.95	0.36
3.95	2.42	1.62	1.50	1.30	0.33
6.22	4.02	2.81	1.43	1.79	0.29
9.61	5.21	4.33	1.20	2.46	0.26
14.87	7.66	6.72	1.14	3.81	0.26
23.76	11.50	11.94	0.96	5.10	0.21
37.90[b]	14.74[b]	19.18[b]	0.77[b]	6.78[b]	0.18[b]
59.74[d]	21.78[d]	22.00[d]	0.99[d]	18.56[d]	0.31[d]

38. *D. rossi* macroconch (AMNH 44340, loc. 3161, TLM).

D	W	H	W/H	UD	UD/D
0.24	0.40	-	-	-	-
0.42	0.41	0.23	1.82	-	-
0.63	0.41	0.26	1.57	0.14	0.22
0.90	0.53	0.35	1.51	0.28	0.32
1.28	0.65	0.48	1.34	0.45	0.35
1.88	0.98	0.76	1.28	0.64	0.34
2.91	1.42	1.26	1.12	0.88	0.30
4.59	2.00	2.07	0.97	1.26	0.27
7.42	2.74	3.65	0.75	1.70	0.23
12.28	3.92	6.59	0.60	2.05	0.17
20.08[c]	5.80[c]	11.15[c]	0.52[c]	2.35[c]	0.12[c]

39. *D. rossi* macroconch (YPM 32291, loc. 37, TLM).

D	W	H	W/H	UD	UD/D
0.55	0.42	-	-	-	-
0.83	0.49	0.33	1.48	-	-
1.22	0.65	0.48	1.36	0.41	0.34
1.80	0.87	0.70	1.25	0.62	0.35
2.66	1.24	1.04	1.19	0.91	0.34
4.04	1.76	1.65	1.06	1.34	0.33
6.46	2.54	3.05	0.83	1.76	0.27
10.78[b]	-	5.76[b]	-	1.96[b]	0.18[b]
17.66[c]	-	9.74[c]	-	2.17[c]	0.12[c]

40. *D. rossi* microconch (AMNH 44341, loc. 3161, TLM).

D	W	H	W/H	UD	UD/D
0.28	0.44	-	-	-	-
0.45	0.44	0.25	1.79	-	-
0.66	0.44	0.25[a]	1.80[a]	0.17[a]	0.25[a]
0.94	0.56	0.35	1.60	0.34[a]	0.36[a]
1.38	0.74[a]	0.55[a]	1.34[a]	0.48[a]	0.35[a]
2.09	1.09	0.86	1.27	0.67[a]	0.32[a]
3.34	1.71	1.53	1.12	0.94	0.28
5.57	2.39	2.82	0.85	1.21	0.22
9.66	3.37	5.41	0.62	1.43	0.15
16.37[b]	5.14[b]	9.06[b]	0.57[b]	1.90[b]	0.12[b]

41. *D. rossi* microconch (AMNH 44342, loc.3161, TLM).

D	W	H	W/H	UD	UD/D
0.33	0.46	-	-	-	-
0.46	0.48	0.26	1.83	-	-
0.66	0.47	0.24	1.94	0.15	0.23
0.94	0.54	0.32	1.68	0.37	0.40
1.33	0.72	0.48	1.50	0.53	0.40
1.99	1.01	0.78	1.29	0.73	0.37
3.06	1.46	1.28	1.14	1.00	0.33
4.91	1.96	2.23	0.88	1.40	0.28
8.22[b]	2.83[b]	4.29[b]	0.66[b]	1.71[b]	0.21[b]

42. *D. rossi* microconch (AMNH 44343, loc.3161, TLM).

D	W	H	W/H	UD	UD/D
0.32	0.51	-	-	-	-
0.49	0.49	0.25	1.96	-	-
0.68	0.49	0.24	1.99	0.19	0.28
0.99	0.57	0.36	1.59	0.39	0.39
1.40	0.73	0.50	1.47	0.55	0.39
2.10	1.08	0.86	1.25	0.74	0.35
3.31	1.64	1.46	1.12	0.99	0.30
5.42	2.25	2.62	0.86	1.34	0.25
9.32[b]	3.37[b]	4.99[b]	0.68[b]	1.71[b]	0.18[b]
16.10[c]	5.14[c]	8.72[c]	0.59[c]	2.39[c]	0.15[c]

43. *D. rossi* microconch (AMNH 44344, loc.3161, TLM).

D	W	H	W/H	UD	UD/D
0.35	0.51	-	-	-	-
0.51	0.53	0.27	1.93	-	-
0.71	0.51	0.25	2.06	0.19	0.27
0.98	0.57	0.33	1.71	0.40	0.41
1.38	0.74	0.48	1.55	0.57	0.41
1.97	0.96	0.70	1.36	0.78	0.40
2.91	1.36	1.12	1.22	1.09	0.37
4.58	1.98	2.02	0.98	1.44	0.32
7.47	2.74	3.72	0.74	1.74	0.23
12.39[b]	-	6.49[b]	-	2.19[b]	0.18[b]
19.99[c]	5.27[ac]	8.89[ac]	0.59[ac]	4.61[ac]	0.23[ac]

APPENDIX III

List of Localities

YPM specimens

Locality numbers of YPM specimens listed below and referred to in the text were assigned by KMW. They represent an informal numbering system but are tied in with official locality numbers registered at the Yale Peabody Museum.

3. SW¼SW¼NW¼ sec. 30, T. 16 N, R. 26 E, Whitehorse quad., Dewey County, South Dakota.

4. SE¼NW¼NW¼ sec. 30, T. 16 N, R. 26 E, Whitehorse quad., Dewey County, South Dakota.

7. About 300 ft north of center SW¼ sec. 20, T. 16 N, R. 26 E, Whitehorse quad., Dewey County, South Dakota.

8. About in center west side SW¼SW¼ sec. 20, T. 16 N, R. 26 E, Whitehorse quad., Dewey County, South Dakota.

17. Along section line west side SW¼SW¼ sec. 9, T. 19 N, R. 27 E, Little Eagle SE quad., Corson County, South Dakota.

19. Southeast corner SW¼SE¼ sec. 19, T. 19 N, R. 26 E, Little Eagle SW quad., Corson County, South Dakota.

20. SE¼NE¼NE¼ sec. 8, T. 20 N, R. 27 E, Little Eagle quad., Corson County, South Dakota.

21. Center E½SE¼ sec. 5, T. 20 N, R. 27 E, Little Eagle quad., Corson County, South Dakota.

25. S½S½NW¼ sec. 24, T. 21 N, R. 24 E, Bullhead quad., Corson County, South Dakota.

26. Center NW¼ sec. 6, T. 20 N, R. 25 E, Miscol NE quad., Corson County, South Dakota.

27. NW¼SW¼ and southwest corner NW¼ sec. 15, T. 20 N, R. 28 E, Wakpala NW quad., Corson County, South Dakota.

30. NE¼SW¼NW¼ sec. 32, T. 15 N, R. 24 E, Parade NW quad., Dewey County, South Dakota.

31. NW¼NE¼SE¼ sec. 6, T. 14 N, R. 24 E, Parade NW quad., Dewey County, South Dakota.

32. N½SE¼SE¼ sec. 7, T. 14 N, R. 24 E, Parade NW quad., Dewey County, South Dakota.

33. From E½SW¼ sec. 32, T. 12 N, R. 24 E, to northwest corner NE¼ sec. 5, T. 11 N, R. 24 E, Herbert Creek quad., Ziebach County, South Dakota.

34. Center NE¼SW¼ and E½NE¼SW¼ and S½SE¼ sec. 27, T. 15 N, R. 23 E, Lantry NE quad., Dewey County, South Dakota.

35. Center SW¼SW¼ sec. 4, T. 12 N, R. 22 E, Lantry quad., Dewey County, South Dakota.

36. Northwest corner SE¼ sec. 3, T. 14 N, R. 21 E, Dupree NE quad., Ziebach County, South Dakota.

37. Southwest corner SW¼ and along west edge SW¼ sec. 12, T. 11 N, R. 23 E, High Elk Hill quad., Ziebach County, South Dakota.

41. Along south ½ of section line between NW¼ sec. 29 and NE¼ sec. 30, T. 15 N, R. 24 E, Parade NW quad., Dewey County, South Dakota.

44. Along section line, south part of SE¼ sec. 17 and north part of NE¼ sec. 20, T. 132 N, R. 76 W, Strasburg quad., Emmons County, North Dakota.

47. Center E½NW¼ sec. 13, T. 19 N, R. 26 E, Little Eagle SE quad., Corson County, South Dakota.

50. SW¼ sec. 26, T. 20 N, R. 26 E, Little Eagle NW quad., Corson County, South Dakota.

51. SW¼SE¼NE¼ sec. 7, T. 19 N, R. 27 E, Little Eagle quad., Corson County, South Dakota.

52. SE¼SW¼ sec. 5 and NW¼NE¼NW¼ sec. 8, T. 19 N, R. 27 E, Little Eagle quad., Corson County, South Dakota.

53. From center of south line sec. 13 to center NE¼ sec 24, T. 20 N, R. 26 E, Little Eagle quad., Corson County, South Dakota.

54. From E½SE¼SW¼ sec. 18 to NW¼NE¼-NE¼ sec. 19, T. 20 N, R. 27 E, Little Eagle quad., Corson County, South Dakota.

55. SE¼NE¼SE¼ and northeast corner SE¼SE¼ sec. 11, T. 19 N, R. 26 E, Little Eagle SW quad. and Little Eagle SE quad., Corson County, South Dakota.

57. Southwest corner sec. 29, T. 15 N, R. 25 E, Parade NE quad., Dewey County, South Dakota.

58. From southeast corner NW¼SW¼ southeastward through N½SE¼SW¼ sec. 31, T. 15 N, R. 23 E, Lantry NE quad., Dewey County, South Dakota.

60. Southeast corner SE¼ sec. 36, T. 15 N, R. 21 E, and northeast corner NE¼ sec. 1, T. 14 N, R. 21 E, and southwest corner SW¼ sec. 31, T. 15 N, R. 22 E, Lantry NW quad., Ziebach County and Dewey County, South Dakota.

61. Center NE¼ sec. 1, T. 14 N, R. 21 E, Lantry NW quad., Dewey County, South Dakota.

62. Center E½SE¼ sec. 15, T. 20 N, R. 25 E, Miscol NE quad., Corson County, South Dakota.

64. From SE¼NE¼SW¼ sec. 20 to northwest corner sec. 28, T. 16 N, R. 26 E, Whitehorse quad., Dewey County, South Dakota.

67. NE¼SW¼ sec. 36, T. 15 N, R. 21 E, Lantry NW quad., Ziebach County, South Dakota.

69. Northwest corner NE¼NW¼ sec. 29, T. 19 N, R. 27 E, Little Eagle SE quad., Corson County, South Dakota.

73. Center and E½ sec. 3, T. 14 N, R. 20 E,

Thunder Butte quad., Ziebach County, South Dakota.

77. SW¼ sec. 27, T. 14 N, R. 24 E, Parade NW quad., Dewey County, South Dakota.

80. Southeast corner sec. 25, T. 15 N, R. 20 E and southwest corner sec. 30 and northwest corner sec. 31, T. 15 N, R. 21 E, Dupree NE quad., Ziebach County, South Dakota.

82. Northeast corner SW¼SE¼ sec. 30, T. 19 N, R. 27 E, Little Eagle SE quad., Corson County, South Dakota.

85. Center W½SW¼ and center E½SW¼ sec. 24, T. 20 N, R. 25 E, Little Eagle NW quad., Corson County, South Dakota.

86. East side NE¼ sec. 33, T. 20 N, R. 26 E, Little Eagle NW quad., Corson County, South Dakota.

88. E½NE¼ sec. 27 and northwest corner sec. 26, T. 14 N, R. 23 E, Lantry NE quad., Dewey County, South Dakota.

89. SE¼SW¼ sec. 22, T. 14 N, R. 23 E, Lantry NE quad., Dewey County, South Dakota.

90. NE¼SE¼ sec. 21, T. 14 N, R. 23 E, Lantry NE quad., Dewey County, South Dakota.

100. Center sec. 32, T. 15 N, R. 21 E, Dupree NE quad., Ziebach County, South Dakota.

104. Northwest corner NE¼ and northeast corner NW¼ sec. 18, T. 20 N, R. 27 E, Little Eagle quad., Corson County, South Dakota.

110. Northeast corner SW¼NE¼NW¼ sec. 17, T. 20 N, R. 25 E, Miscol NE quad., Corson County, South Dakota.

115. E½NW¼SW¼ sec. 11, T. 19 N, R. 27 E, Little Eagle SE quad., Corson County, South Dakota.

120. N½NE¼NE¼NE¼ and SE¼NE¼NE¼-NE¼ sec. 15 and center west side NW¼NW¼ sec. 14, T. 19 N, R. 26 E, Little Eagle SW quad., Corson County, South Dakota.

145. Northwest corner NW¼SW¼ sec. 8, T. 13 N, R. 25 E, Parade quad., Dewey County, South Dakota.

158. Center SE¼SE¼ and E½SW¼SE¼ sec. 14, T. 14 N, R. 27 E, Ridgeview NE quad., Dewey County, South Dakota.

177. Northeast corner SE¼NE¼ sec. 15, T. 19 N, R. 26 E, Little Eagle SW quad., Corson County, South Dakota.

193. Center NW¼ sec. 9, T. 20 N, R. 27 E, Little Eagle quad., Corson County, South Dakota.

195. At and within 0.1 mi of junction of sec. 29, 30, 31, and 32, T. 15 N, R. 24 E, Parade NW quad., Dewey County, South Dakota.

197. W½SW¼NW¼ sec. 32, T. 15 N, R. 24 E, Parade NW quad., Dewey County, South Dakota.

200. NE¼SW¼SE¼ sec. 32, T. 15 N, R. 24 E, Parade NW quad., Dewey County, South Dakota.

209. Center NW¼SE¼ and center NE¼SW¼ and NW¼NW¼SE¼ sec. 7, T. 19 N, R. 27 E, Little Eagle SE quad., Corson County, South Dakota.

212. Center west side SW¼NE¼ and center N½SW¼NE¼ and E½NW¼ sec. 26, T. 15 N, R. 21 E, Dupree NE quad., Ziebach County, South Dakota.

214. Center W½E½NW¼ and center S½N½ sec. 32, T. 15 N, R. 25 E, Parade NE quad., Dewey County, South Dakota.

216. Southeast corner SW¼SW¼ sec. 14, T. 20 N, R. 25 E, Miscol NE quad., Corson County, South Dakota.

222. SE¼NW¼ sec. 30, T. 16 N, R. 26 E, Whitehorse quad., Dewey County, South Dakota.

227. Center W½W½NE¼ sec. 27, T. 14 N, R. 23 E, Lantry NE quad., Dewey County, South Dakota.

237. Southwest corner SW¼NE¼SW¼ sec. 13, T. 15 N, R. 25 E, Little Moreau Lake quad., Dewey County, South Dakota.

241. NW¼NE¼NE¼SW¼ sec. 14, T. 15 N, R. 25 E, Little Moreau Lake quad., Dewey County, South Dakota.

242. SW¼NE¼SE¼SE¼ sec. 15 and SE¼NW¼-SW¼SW¼ sec. 14, T. 15 N, R. 25 E, Little Moreau Lake quad., Dewey County, South Dakota.

248. SW¼SW¼NE¼SW¼ sec. 14, T. 15 N, R. 25 E, Little Moreau Lake quad., Dewey County, South Dakota.

256. Center east side NW¼ and center west side NE¼ sec. 25, T. 19 N, R. 25 E, Little Eagle SW quad., Corson County, South Dakota.

279. Center north side NE¼ sec. 19 and center south edge SE¼ sec. 18, T. 20 N, R. 25 E, Miscol NE quad., Corson County, South Dakota.

282. Along middle part section line west side SW¼ sec. 4, T. 15 N, R. 23 E, Peach Lake quad., Dewey County, South Dakota.

302. Center section line between sec. 16 and sec. 17, T. 19 N, R. 27 E, Little Eagle SE quad., Corson County, South Dakota.

303. NE¼NE¼NE¼ sec. 8, T. 19 N, R. 27 E, Little Eagle quad., Corson County, South Dakota.

305. Center W½SW¼SW¼ sec. 31, T. 12 N, R. 24 E, High Elk Hill quad., Ziebach County, South Dakota.

307. Center E⅓NE¼NW¼ sec. 3, T. 14 N, R. 21 E, Dupree NE quad., Ziebach County, South Dakota.

312. Dewey County, Corson County, and north half of Ziebach County, South Dakota.

314. Moreau River Valley, Dewey County, South Dakota.

316. Near Eagle Butte, Dewey County, South Dakota.

RB103. From SE¼SW¼ to W½SE¼SE¼ sec. 18, T. 37 N, R. 62 W, Redbird quad., Niobrara County, Wyoming.

RB104. From center NW¼ sec. 20 to southeast corner sec. 18, and on to NE¼SW¼ sec. 17, T. 37 N, R. 62 W, Redbird quad., Niobrara County, Wyoming.

RB106. From NE¼SW¼NW¼ sec. 27 to center S½SE¼SE¼ sec. 28, and center W½E½ sec. 33, T. 38 N, R. 62 W, Redbird quad., Niobrara County, Wyoming.

RB107. From S½NE¼SE¼ sec. 8 to center sec. 17, T. 37 N, R. 62 W, Redbird quad., Niobrara County, Wyoming.

RB114. From northwest corner to southeast corner NE¼ sec. 13, T. 37 N, R. 63 W, Redbird quad., Niobrara County, Wyoming.

RB116. NW¼NE¼ sec. 14 and SW¼SE¼ sec. 11, T. 38 N, R. 62 W, Bowen Flat quad., Niobrara County, Wyoming.

RB117. S½SW¼ sec. 14 and northwest corner sec. 23, T. 38 N, R. 62 W, Bowen Flat quad., Niobrara County, Wyoming.

RB118. N½SE¼ sec. 12, T. 37 N, R. 63 W, Redbird quad., Niobrara County, Wyoming.

RB120. E½NE¼ sec. 11, T. 38 N, R. 62 W, Bowen Flat quad., Niobrara County, Wyoming.

RB121. S½SE¼ sec. 12, T. 37 N, R. 63 W, Redbird quad., Niobrara County, Wyoming.

RB123. SW¼SW¼ and south side NW¼SW¼ sec. 18, T. 37 N, R. 62 W, Redbird quad., Niobrara County, Wyoming.

AMNH specimens

3156. E½ sec. 13 and SE¼ sec. 12, T. 37 N, R. 65 W, Redbird quad., Niobrara County, Wyoming, bioturbated sand unit, lower Fox Hills Formation.

3157. Bluffs of Grand River, just west of Bullhead, Corson County, South Dakota, Trail City Member, Fox Hills Formation.

3158. Dewey County, Corson County, and north half of Ziebach County, South Dakota, Fox Hills Formation.

3159. Dewey County, Corson County, and north half of Ziebach County, South Dakota, Trail City Member, Fox Hills Formation.

3160. Dewey County, Corson County, and north half of Ziebach County, South Dakota, Timber Lake Member, Fox Hills Formation.

3161. Vicinity of Eagle Butte, Dewey County, South Dakota, Timber Lake Member, Fox Hills Formation.

USGS specimens

21740. East side of Little Eagle road, 2 mi south of turnoff from highway 12, Corson county, South Dakota, LNAZ, Fox Hills Formation.

21814. East side of Grand River, NW¼SW¼ sec. 30, T. 21 N, R. 25 E, Corson County, South Dakota, LGAZ and POAZ undifferentiated, Fox Hills Formation.

D2578. Hillsides, SE¼SE¼ sec. 15 and SW¼ sec. 14, T. 20 N, R. 25 E, Corson County, South Dakota, LGAZ, Fox Hills Formation.

D2580. North side of Grand River, NW¼SW¼ sec. 5, T. 20 N, R. 24 E, Corson County, South Dakota, top TCM, probably transition concretions, Fox Hills Formation.

D2581. Along Grand River, Corson County, South Dakota, Trail City Member, Fox Hills Formation.

D2585. Along Grand River, Corson County, South Dakota, Fox Hills Formation.

MAPS specimens

123. Excavation for sports arena just east of Washington, D.C. Beltway (Rt. 195-I 95), approximately 1 mi northwest of Largo, Maryland, and excavation for industrial park just north of arena at intersection of Rt. 195 and Landover Rd., Lanham quad., Maryland.